2nd Ni/Co/Cu Event

CYTEC

Delivering Technology Beyond
Our Customers' Imagination™

ALTA 2011
NICKEL/COBALT/COPPER
CONFERENCE

MAY 23-25, 2011
BURSWOOD CONVENTION CENTRE
PERTH, AUSTRALIA

**ALTA Metallurgical Services
Castlemaine, Victoria,
Australia**

PROCEEDINGS OF
NICKEL-COBALT-COPPER SESSIONS AT ALTA 2011
MAY 23-25, 2011, PERTH, AUSTRALIA

To purchase a copy of this or other publications visit
http://www.altamet.com.au/publications.htm

CONTENTS

ALTA 2011
NICKEL/COBALT/COPPER

TREATMENT OF LATERITES

THE DIRECT NICKEL PROCESS
CONTINUED PROGRESS ON THE PATHWAY TO COMMERCIALISATION

By

Fiona McCarthy and Graham Brock

Direct Nickel Pty Ltd, Australia

Presenters and Corresponding Authors

Fiona McCarthy and Graham Brock
fiona@directnickel.com
graham@directnickel.com

ABSTRACT

Over the past 12 months Direct Nickel has successfully demonstrated the reagent recycle process, which is fundamental to the DNi Process. Details of this programme and results are presented. In mid May 2011 a Demonstration Plant in Perth is 80% complete and should be operating before the end of calendar 2011. The Company is also drilling the Mambare project in PNG. Progress is both rapid and successful

INTRODUCTION

At this conference last year I presented the first public technical presentation on the Direct Nickel Process.

Over the past 12 months we have;

- Completed a successful commercial scale demonstration of our patented reagent recycle process

- Commenced construction of a 1 tpd Demonstration Plant

- Commenced drill the Mambare Project in PNG and

- Continued Process development work in our Perth laboratory.

This paper will refresh you on the DNi Process and then focus on the first two items.

THE DIRECT NICKEL PROCESS

The Direct Nickel (DNi) Process is an atmospheric hydrometallurgical process that treats the full laterite profile (from limonitic to saprolitic ores), believed to be the only process capable of doing so. (Figure 1). This ability to treat the full lateritic profile promises lower risks for investors, better return on money invested and the ability to commercialise deposits that are currently uneconomic.
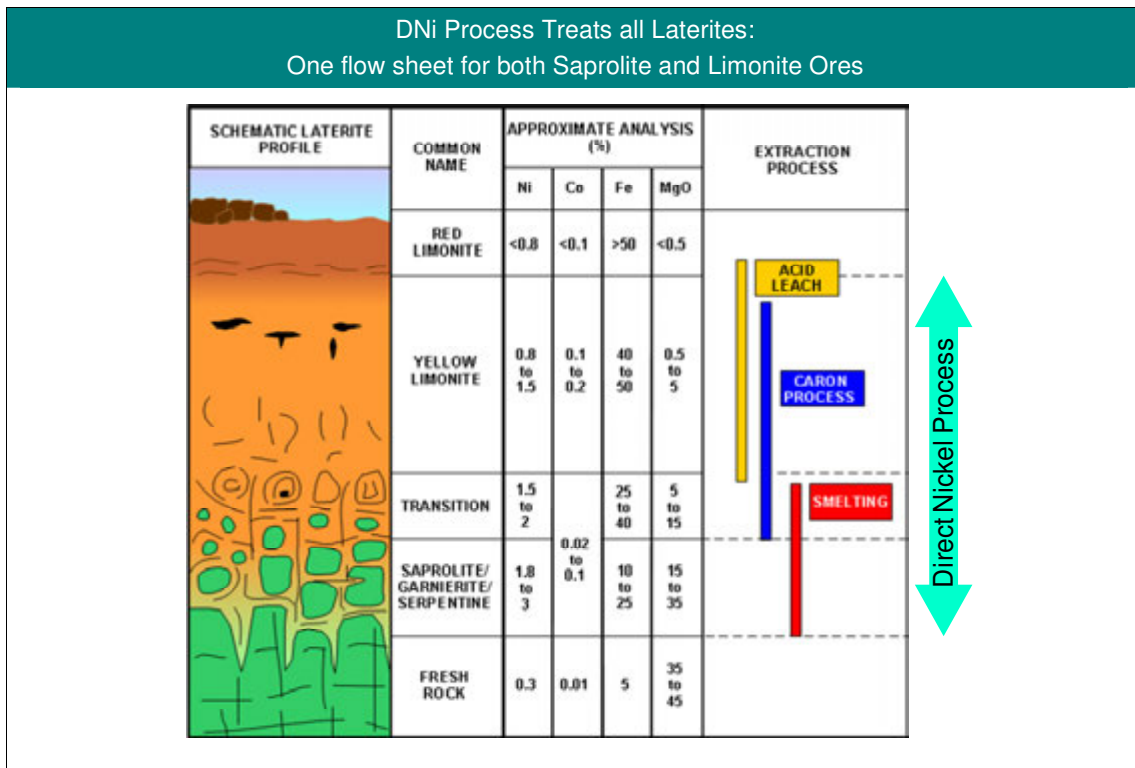
Figure 1: DNi Process Versatility

The DNi Process (Figure 2) uses nitric acid to leach nickel laterite ores to take most metals into solution leaving a silicate leach residue. One unique feature of the DNi Process is the ability to recover over 95% of the reagents for re-use in the process, significantly reducing operating costs, whilst extracting the majority of the nickel and cobalt from the deposit. Nitric acid is also unique due to the high solubility of its metal salts compared to sulphuric and hydrochloric acids. This high metals carrying capacity can translate into less capital for an equivalent metal extraction compared

to the other two acids. With some elements, for example calcium, the nitrate is soluble but the sulphate forms as gypsum, often causing scaling and build up, which in turn, results in more downtime and maintenance costs.

Leaching takes place in closed tanks generally in less than 5 hours at a temperature just over 100°C. Extraction of +90% of Ni, Co, Mn, Mg and other base metals occurs. Leaching of Fe, Al and Cr depends largely on the mineralogy of the samples. The PLS is separated from the insoluble residue by a train of CCD thickeners.

The PLS is concentrated by evaporation followed by thermal hydrolysis where +99% of the iron and chromium are precipitated into a haematite form. The pH of the iron-free solution can be raised with recycled MgO to precipitate an intermediate product, which contains the Ni, Co, Mn, Al and other base metals leaving a barren solution of mainly magnesium nitrate. The Intermediate Precipitate is separated from the barren solution by filtering and thickening and then re-leached.

The re-leach PLS is heated to remove aluminium by thermal hydrolysis and the pH of the remaining Al-free solution is raised with MgO to produce a high quality Ni/Co hydroxide as a final product. When required the nickel and cobalt hydroxide can be readily converted to oxide or sulphide to meet specific market conditions. Resulting nickel products are high grade and can be fed into existing ferro-nickel plants to increase output and drastically reduce operating costs.

The barren solution is evaporated to form a nitrate melt with between 1 and 2 moles of water. The melt is fed to a thermal decomposition unit in which the NOx gases are liberated and MgO powder is formed. NOx gases are recovered through a series of absorbers and scrubbers, which recovers 99% of the NOx into a 55% strength nitric acid. The acid and MgO are re-cycled to the Process.
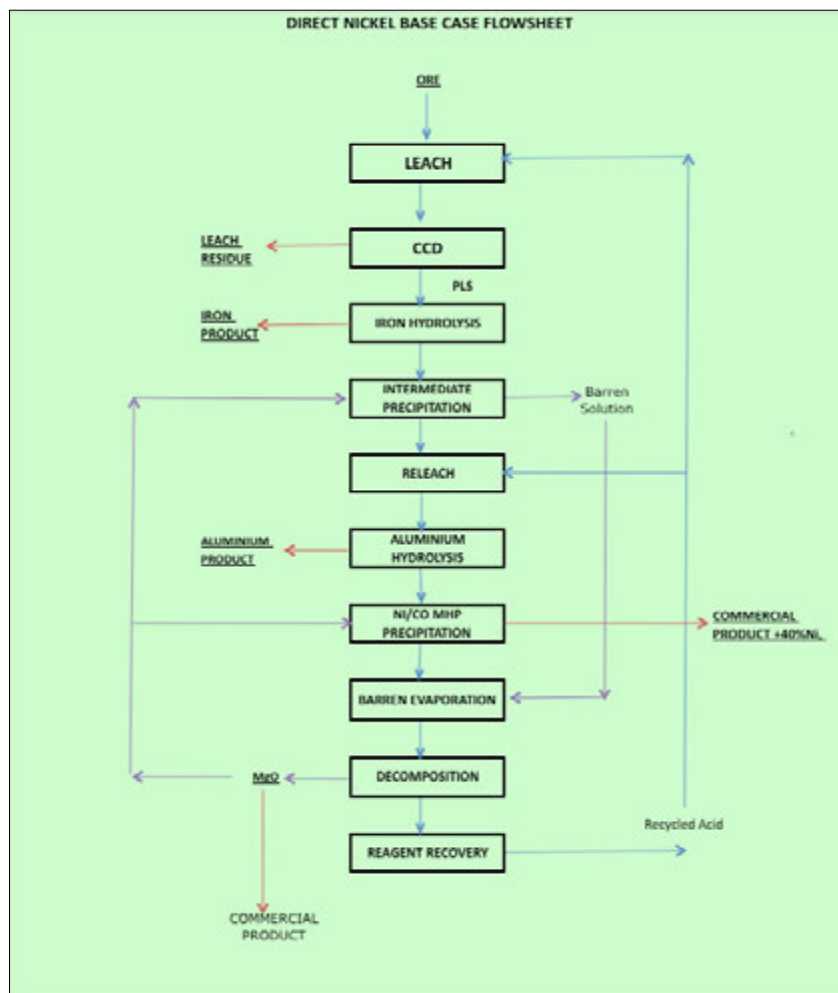
Figure 2: The DNi Process Flowsheet

Key Advantages of the DNi Process:

- A highly efficient, tank leach, atmospheric hydrometallurgy process

- The first single flowsheet to efficiently treat the full laterite profile, limonite through to saprolite

- Consistently high extractions of nickel and cobalt, > 90%

- Recycles key reagents (+95%) for enhanced economy producing more environmentally benign tailings

- Acid consumption 20-40 kg/t of ore

- Materials of construction are mainly 304 stainless steels

- The disposal of magnesium is solved rather than producing wasteful gypsum

- Reagent recycle leads to low operating, maintenance and environmental costs

- Process lends itself to significant reductions in capital costs

- A degree of operating simplicity less than the competitor

REAGENT RECYCLE DEMONSTRATION

Direct Nickel (DNi), holds the world wide rights to use Drinkard Metalox Inc (DMI) intellectual property for the treatment of nickel laterites using nitric acid (the DNi Process). A key part of the DNi Process is the thermal decomposition of a barren solution, primarily magnesium nitrate, and the regeneration of nitric acid from the off gases produced using DMI's U.S. Patent No. 6,264,909, "Nitric Acid Production and Recycle". Where required, this technology can also be used to produce nitric acid from ammonia and a large amount of waste heat can be recovered from this reaction.

Early in 2010 DNi commissioned DMI to conduct a large scale trial of the nitric recycle process at its Charlotte facilities using equipment DMI had available and a rather old thermal decomposition unit that we were able to hire.

Process Description

The goal of the process was to evaporate and decompose a barren solution, the magnesium nitrate hexahydrate solution, similar to that produced during the processing of nickel laterite ores. The resulting products were MgO, used in the DNi Process and in other applications, and NO_X vapor, captured in the nitric acid regeneration equipment and re-used in the leaching stage of the Process.
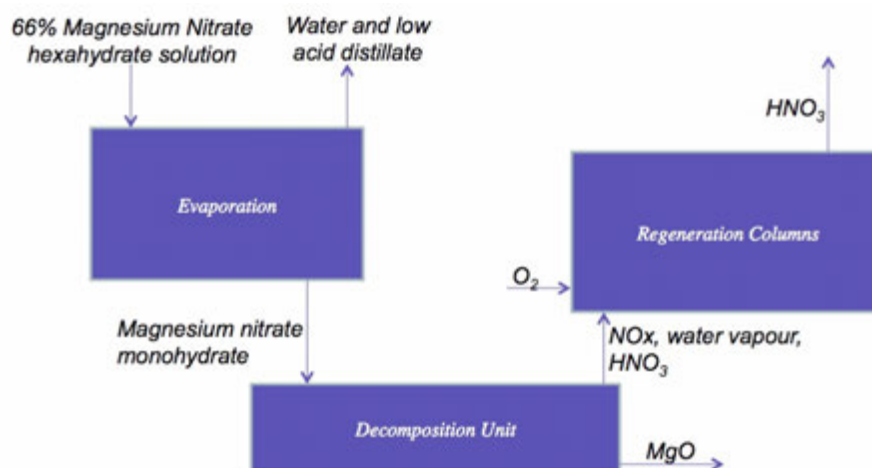
Figure 3: Reagent Re-Cycle Demonstration Simplified Flowsheet

The barren solution created in the DNi Process for treating nickel laterite ores contains in the order of 66%-69% magnesium nitrate hexahydrate. The synthetic barren solution was heated to 200°C-215°C to evaporate as much water as possible without drastically affecting the viscosity of the molten salt. Evaporation was demonstrated on both a continuous basis and a batch basis. To assist with mass balancing the batch method was used.

The molten salt obtained during evaporation was fed into the decomposition unit. Above temperatures of 300°C the molten salt decomposed into MgO and NO_X vapor. The solid MgO was discharged from the unit and collected in a 200 litre stainless steel drum while the NO_X vapor was directed through the nitric acid regeneration system to be recovered as nitric acid.

The acid regeneration system captured NO_X vapor converting the contained nitrogen into nitric acid. The hot NO_X vapor was cooled allowing any water vapor and nitric acid to condense. The gas was then drawn into the absorber train via a slight vacuum created from an eductor. In the absorber train the NO_X vapor was absorbed in varying strengths of nitric acid and regenerated in the presence of oxygen.

The off-gas from the absorber train was drawn into a scrubbing system via an eductor. The scrubbing system consisted of two columns and an effluent tank, the first column contained low concentrations of dissolved MgO and hydrogen peroxide (H_2O_2) while the second and effluent tank contained water. An on-line nitric oxide (NO), nitrogen dioxide (NO_2) and nitrogen oxides (NO_X) analyzer was used to monitor emissions, the results from which were confirmed with readings from personal hand held monitors.

Operations and Results

Following an 18 week construction and assembly period 13 Trials were run during July and August. The first six trials were by way of commissioning of the equipment and training followed by Trials 7 to 13, which were conducted under rigorous conditions to allow full mass balancing to be attempted.

The two main variables were the screw temperature (the element temperature) and the cooling system. It was anticipated that increased screw temperature would result in more throughput at the same % decomposition or the same throughput with better decomposition. The solubility of NO in nitric acid increases with falling temperature and this was tested by chilling the cooling water.

Table 1: Trials 7 to 13 Test Conditions

Trial No	Screw Temp	Feed	Hrs Run	Feed Rate	Cooling System
7	649	Pulsed	14.3	7.3	Tower
8	649	Pulsed/Continuous	17.2	9.9	Chiller
9	649	Continuous	12.4	9.3	Chiller
10	704	Continuous	10.0	9.7	Chiller
11	760	Continuous	10.8	9.7	Chiller
12	760	Continuous	11.8	5.5	Chiller
13	760	Continuous	8.8	10.3	Tower

Results and Comments

The temperatures around the decomposition unit and condenser were monitored continuously and Figure 4 shows the plot over the duration of Trial 11 with the element temperature set at the maximum we went to at 760 °C
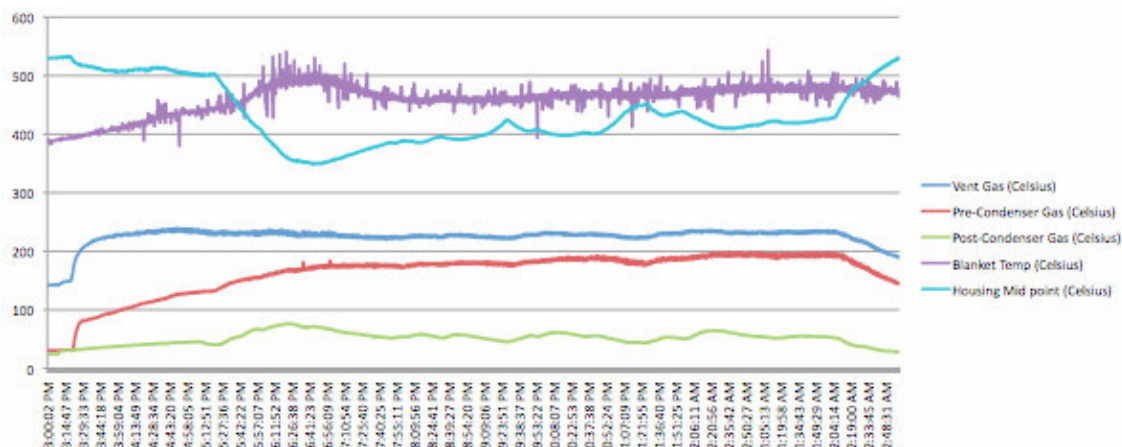
Figure 4: Process Temperatures during Trial 11

The first acid recovery step results from cooling the gas that exits the decomposition unit. In all the Trials except Trial 13 the concentration in the condensate collector was greater at the end of the trial than the beginning. This indicates the acid concentration being produced was greater than the starting concentration. Generally the impact of the chiller was to produce recovered acid at >60% concentration.
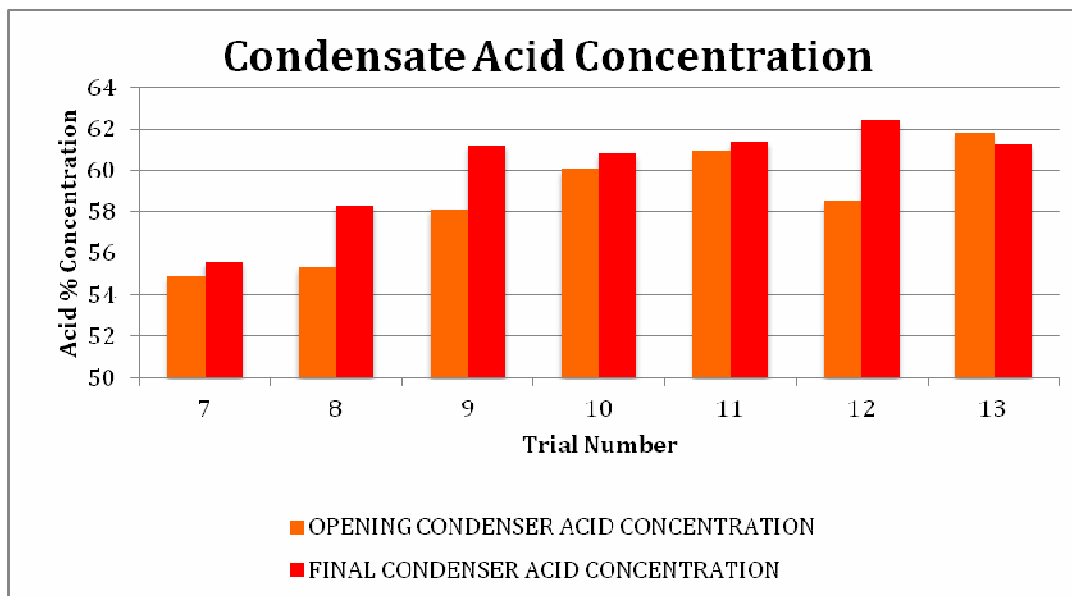
Figure 5: Produced Acid Concentration in the Collector

The amount of acid recovered to the condenser as a percentage of the total nitric acid recovered varied from 30-60 % with the highest result in trial 9 when the decomposition temperature was at the lowest setting and the chiller was running.
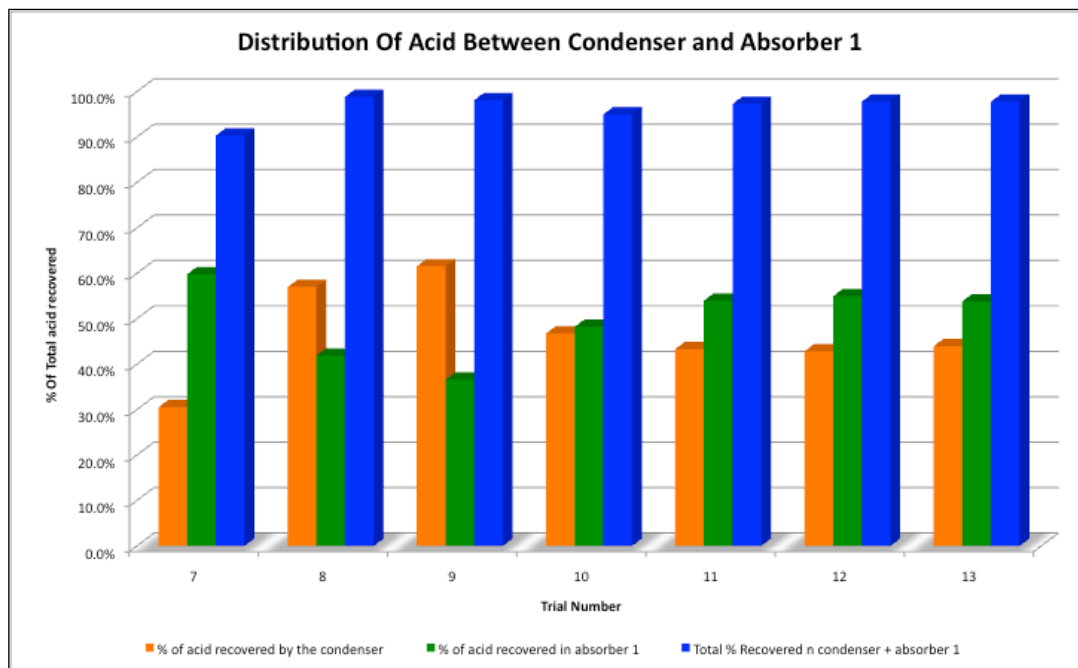
Figure 6: Distribution of Acid Between Condenser and Absorber 1

The second stage of acid recovery was absorber 1 where the gas exiting the condenser was mixed with cool acid at around 45% concentration. Generally the % recovered to the condenser was inversely related to the % reporting to absorber 1

Based on the results shown above and below Absorbers 2 and 3 and the Scrubbers played a very small role in the generation of acid and were mainly capturing any residual NO_X vapor exiting Absorber 1. The increases attributed to Absorber 3 in Trials 11, 12 and 13 are the result of the failure of the pump on Absorber 2.
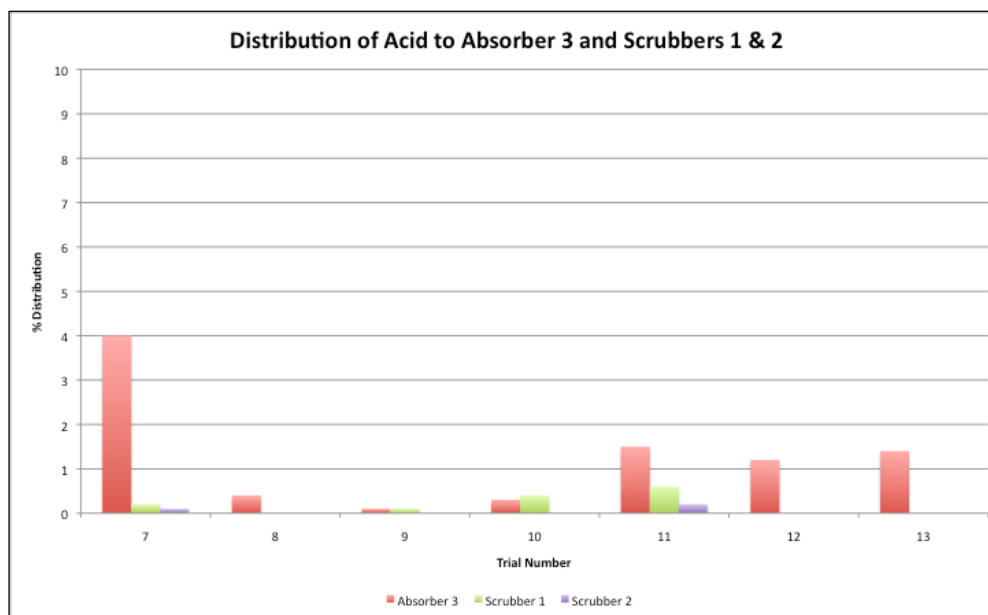
Figure 7: Acid Recovery in Gas Train Tail

The gas train discharge was monitored for NO and NO_2 by the Chemiluminescence NO-NO_2-NO_X Analyzer, (NO_x Box). During Trials 3-6 it was found that if too much moisture was taken up by the system false highs were recorded. For the remainder of the Trials a water trap was kept in place. The personal hand-held ToxiRae II Monitors (NO Model: 045-0514, NO_2 Model: 045-0516) were held into the final effluent tank head space and the values were comparable to those observed on the NO_x Box.

Conclusions

The trial, which is considered an essential step in the commercialization of the DNi Process provided significant information as described in the table below.

Highlights of the trial included:

- Demonstration of a commercial unit able to decompose the molten salt
- High standard of mass balance achieved during Trial 7 to13
- 99.8% recovery of NO_x gases to acid
- Production of nitric acid at a strength greater than 55% without the use of evaporation
- Up to 99.2% decomposition of the magnesium nitrate
- A significant learning experience.

The Trials were able to address a variety of topics, which are important to the commercialisation of the DNi Process.

Table 2: Reagent Recycle Outcomes

TOPIC INVESTIGATED	TRIAL OUTCOMES
Assess the NO_x gas recovery to nitric acid.	NO_x gas recovery to the acid collection units averaged 99.8% of the gas discharged from decomposition. The remaining 0.2% was collected in the scrubbers.
Assess the degree of magnesium nitrate decomposition and review results collected during the trial.	Decomposition of nitrates averaged 95.5%, with Trial 11, under optimized conditions, giving 99.2% decomposition
Assess the acid strength produced	An overall acid strength of >55% HNO_3 was produced.
Assess the overall nitrate balance accounting around the circuit	Nitrate balance averaged 101.2%, very acceptable for the scale of equipment being used.
Assess the decomposition energy used compared to other values used in previous work and studies	The measured decomposition energy compares well with previous estimates
Review data relating to the effectiveness of the MgO produced for use in the DNi Process	The MgO produced in the trial proved reactive and effective for pH adjustment in the DNi Process.
Assess the physical behavior of the decomposing magnesium nitrate to see if there is any hindrance to satisfactory operation of the decomposition unit.	The decomposition unit had no serious problems handling the metal nitrate melt. There was no build up of coarse material and minimal coating of the heated surfaces. Future designs can further improve on performance.
Assess carry-over of solids in the gas train.	No significant carry-over observed.
Assess the issues of handling a molten salt.	Following learning experiences in the early trials the melt proved very easy to handle.
Assess corrosion issues	No obvious signs of corrosion on the 304 stainless components of the equipment.
Make suggestions for incorporation in future demonstration or commercial plants.	Many valuable lessons learned. A range of efficiencies can be introduced in the future

Overall the trial was a success confirming the robustness of the Drinkard acid recovery process and the applicability and efficiency of the commercial decomposition unit.

DEMONSTRATION PLANT

Whilst the DNi Process precursor technology has been demonstrated at pilot scale on EAF dust in S. Carolina and a North American nickel producer conducted extensive tests on laterites in the 1990s, we plan to demonstrate the process in Perth, including the many refinements that have been developed over the last four years.

Through a funding mechanism known as the Australian Growth Partnership CSIRO has become an investor in DNi (the company) and we are building Stage 1 of a demonstration plant at the CSIRO Minerals facility at Waterford. Stage 2 will be added later in the year.

Stage 1 will allow us to demonstrate, on a continuous basis, the leaching, CCD, and reagent recycle steps. The PLS will be precipitated in Stage 1 with MgO produced from barren decomposition. Taking out the metals. in this way allows us to produce a barren solution.
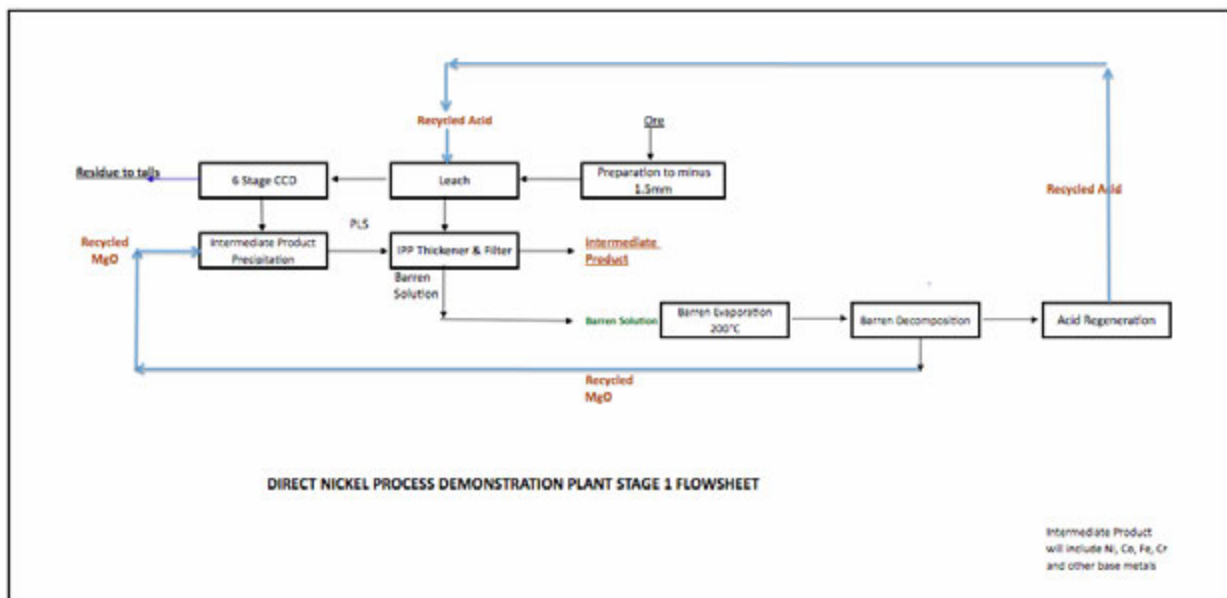
Figure 8: Stage 1 Flowsheet

The project is being jointly managed by CSIRO and DNi, whilst GR Engineering Services is providing the design and construction management. Target date for completion is the end of June. A new thermal decomposition unit is being built in USA and delivery of this unit will be in November. Our operating team is being assembled by RMDSTEM and provides a good blend of hydrometallurgical experience and youthful exuberance. We are very fortunate to have the vast knowledge of the CSIRO to draw on. We will also be welcoming some of the Teck/CESL engineers into the team.

The Demonstration plant is designed for one tonne per day and we have 9, 10 day campaigns, planned. This may change depending on results and the timing of Stage 2. Stage 2 will include iron and aluminium removal and the production of high grade MHP. We will also test the production of an MSP.

WHERE TO OVER THE NEXT TWELVE MONTHS?

Rapid and thorough progress has been achieved since last year, we have learned a great deal and chalked up the reagent re-cycle milestone. Over the next 12 months we will see the Stage 1 flowsheet running and I dare say Stage 2 built and in operation. And I can guarantee we will have learned a whole lot more.

I have the greatest respect for the fund-raisers in our small organization. They have managed to fund our technical programme. We are building on the strong foundation laid by our North American

partners, DMI, who in various industrial applications have successfully and economically handled a great deal of nitric acid and metal nitrates

ACKNOWLEDMENTS

RECENT DEVELOPMENTS IN THE CHLORIDE PROCESSING
OF NICKEL LATERITES

By

Bryn Harris and Carl White

Neomet Technologies Inc., Canada

Presenter and Corresponding Author

Bryn Harris
bryn@neomet.com

ABSTRACT

The concept of chloride processing for nickel laterite ores is one that has been promoted over the past several years as a viable method for treating both the limonite and saprolite fractions of a laterite profile. This paper reviews the recent developments in the chloride-based flowsheet, with particular emphasis on the key breakthrough acid recovery and iron precipitation unit operation developed by Neomet Technologies Inc. It is shown that the use of an inert matrix significantly improves the kinetics and flexibility of acid recovery compared to earlier flowsheets, thereby opening up the whole flowsheet. Results of leaching several different laterites are presented, and of continuous operation of the acid recovery unit operation. Preliminary capital and operating costs are presented showing that the chloride process is very attractive economically. The ability of the flowsheet to recover valuable by-products such as hematite, alumina and magnesia, along with minor elements, in particular scandium which is often associated with laterites, is highlighted.

INTRODUCTION

Despite the fact that the concept of using high-strength chloride solutions for the recovery of nickel and cobalt from all horizons of a nickel laterite profile has been introduced and discussed in some detail over the past few years[1][2][3][4][5], this approach is still being treated with caution. Apart from the economic downturn at the end of 2008, which halted much of the development work at the time, the primary reason for this has been the lack of definition in the chloride regeneration process.

The key unit operations in any chloride-based flowsheet are the recovery and regeneration of the chloride lixiviant, usually hydrochloric acid, and the control and elimination of iron within the process[6]. In many hydrometallurgical flowsheets, these are separate circuits, but increasingly, they are being considered together. Conventionally, pyrohydrolysis has been, and largely remains, the method of choice, as practiced in the steel pickling industry[7][8][9][10], and by QIT in its UGS Process[11]. Inco (now Vale) has also chosen this method for producing nickel oxide from its Goro flowsheet[12]. However, as has often been stated, pyrohydrolysis is both energy-intensive and costly to operate[13][14], although recent attempts to use oxygen enrichment have resulted in some improvements[15].

As a consequence, alternative methods to pyrohydrolysis are now being investigated for the recovery and recycle of hydrochloric acid, such as the addition of sulphuric acid (a nominally cheaper reagent, but highly dependent on the price of sulphur) to spent calcium chloride solutions[16], and the PORI Process which operated briefly during the 1970s[17][18][19][20]. More recent variations on the PORI Process have been developed by SMS Siemag[21], McGill University[22], and Starfield Resources[23]. Queen's University has very recently proposed a method of recovering HCl via precipitation of magnesium hydroxychloride followed by calcination[24].

Consideration has also been given to hybrid chloride-sulphate processes, in an attempt to marry the most attractive features of each into a technically and economically-viable flowsheet. Intec Limited published a flowsheet at ALTA 2006, describing a process wherein the limonite fraction of a laterite is leached by hydrochloric acid in a solution of calcium and sodium chlorides[25]. The process can be operated in either one or two stages, the first stage being an atmospheric leach at 100 -110°C and the second, or if it is just a single-stage process, at 150-220°C in an autoclave. In this process, both dissolved iron and magnesium are precipitated via the use of lime, iron as hematite and magnesium as magnesia. The process requires the substantial addition of sulphuric acid to regenerate the hydrochloric acid from the resulting calcium chloride solution, with the sulphate balance being controlled by the further addition of lime. The use of an autoclave and the large requirements for both sulphuric acid and lime seem to mitigate against the use of this process, and there have been no further updates.

Harris et al. evaluated concepts of the hybrid option in 2009, and concluded that it was not as cost-effective as a straight chloride flowsheet[5]. On the other hand, Anglo American has announced a different hybrid concept, wherein sulphate is used to control magnesium in the leaching circuit by taking advantage of the reduced solubility of magnesium sulphate in magnesium chloride solutions[26]. The circuit viability appears ultimately to depend on the magnesium sulphate being thermally decomposed to generate sulphur dioxide and magnesia, with both of these reagents being recycled for use in the flowsheet. The thermal decomposition of magnesium sulphate is not easy, requiring temperatures as high as 1100°C, and to be economical, it is likely that crystallisation of the monohydrate, rather than the more common heptahydrate will be required. In its 2010 Annual Report, Anglo has announced the building and commissioning in January, 2011, of a 30 kg/hr pilot plant to treat a Brazilian laterite (from the Jacaré deposit in Pará state)[27]. Anglo has not published any costs relating to the process. Further, the process produces a mixed nickel-cobalt hydroxide product (MHP), which experience shows is prone to atmospheric oxidation, especially the cobalt content, and therefore poses problems in terms of storage and shipping. Anglo has not indicated whether it intends to process the MHP internally (at Rustenburg, for example) or to sell it, where a logical destination within Brazil would likely be Tocantins in São Paolo.

Neomet Technologies Inc. (Neomet) has developed a suite of chloride-based processes, all of which have as their core technology a patented, unique hydrochloric acid recovery and regeneration process. This paper describes the application of this technology to nickel laterite processing, showing how the flowsheet is considerably simplified, and that value-added by-products such as hematite and alumina can be recovered where warranted.

THE NEOMET LATERITE PROCESS

Leaching

Neomet has tested a number of laterite ores from various parts of the world, and all of them dissolve to a greater or lesser degree in hydrochloric acid/metal chloride systems. Leaching, however, is usually not the most difficult part of any flowsheet, as opposed to separation and recovery of the dissolved metals and more especially the recovery and regeneration of hydrochloric acid. Nevertheless, it is the leaching characteristics which primarily determine whether or not an ore can be treated economically. Table 1 presents some data from different laterites leached at 30% solids and 105-110°C.

Table 1: Leach Tests on Different Laterite Samples

Laterite	HCl, kg/tonne	Time, h	Residue Fall, %	Metal Extraction, %						
				Ni	Co	Fe	Al	Mg	Ca	Mn
1 (head)				1.42	0.042	24.6	1.98	2.53	0.10	-
	200	1		39.4	55.0	27.3	37.9	51.1	83.7	-
	400	2		62.5	80.4	68.2	58.0	66.2	84.8	-
	600	3		90.1	97.1	94.7	81.8	85.5	89.7	-
	800	4	48.3	99.7	98.7	99.6	93.8	97.9	91.6	-
2 (head)				1.20	0.037	18.2	1.98	3.50	0.19	-
	200	1		46.9	66.7	33.6	46.8	54.7	95.4	-
	400	2		78.1	93.4	71.0	74.4	74.6	97.1	-
	600	3		97.5	99.0	76.4	93.7	95.4	97.3	-
	800	4	48.3	99.5	98.8	99.6	96.5	97.0	95.6	-
3 (head)	600			1.72	0.03	15.6	0.72	9.37	0.10	-
		0.5		99.2	91.2	96.1	50.2	81.9	7.4	-
		2		999.7	83.0	96.4	46.9	85.1	6.9	-
		4		99.7	91.9	96.5	48.5	86.5	6.4	-
		6	48.9	99.4	83.9	94.9	45.8	84.7	9.0	-
4 (head)				0.63	0.082	17.9	4.22	10.2	-	0.30
FeCl$_2$	200	1		61.3	100	65.0	19.6	22.6	-	100
	400	2		82.9	100	81.2	40.9	38.4	-	100
	600	3	55.5	95.5	100	91.9	50.4	71.4	-	100
5 (head)				0.63	0.082	17.9	4.22	10.2	-	0.30
FeCl$_3$	200	1		52.5	81.0	47.9	18.6	20.2	-	84.8
	400	2		79.5	100	73.4	37.5	35.8	-	94.4
	600	3	59.2	92.4	100	89.6	52.2	47.3	-	100

Note – the values for the head are chemical composition, not extraction.

The data show generally high extractions of Ni, Co, Fe, Mn and Mg, and ~50% extraction of the Al. The rate at which these metals dissolved was dependent on the nature of the laterite, some reacting much faster than others. In all cases, approximately 50% of the mass was lost during leaching. Of note is that in the chloride leaching system, the leach solids settle and filter very well, with vacuum belt filtration rates measured by vendors being of the order 300 kg/h/m^2 for dry solids. This is in contrast to the very difficult liquid/solid separation experienced with HPAL slurries, and is due to the ability of the high chloride liquor to dehydrate the leach residue. In addition, the residue fall is 50% of the mass input, thus leading to lower capital costs and a significantly smaller footprint than that required for HPAL.

Tests 4 and 5, carried out on a very low-grade laterite, had either ferrous or ferric chloride added as a background matrix for a total chloride content of 280 g/L. The intent here was to build up the overall iron concentration in order to facilitate the subsequent acid regeneration step, and to minimize the amount of water that had to be evaporated per unit of chloride. As can be seen, having a high concentration of background chloride had little impact on the efficiency of the leach reaction.

Hydrochloric Acid Regeneration

Background

The key step in the Neomet Laterite Process is the unit operation whereby hydrochloric acid is regenerated for recycle to the leaching step. As noted earlier, pyrohydrolysis, and more recently, variations of the PORI Process, have been used to achieve this. Neither of these is satisfactory, the former not only due to the high energy cost, but also because of the completely indiscriminate nature of the process, as all metals in solution end up in the metal oxide powder produced, and it is thus not possible to simply recover nickel and cobalt.

The PORI Process and its variants is more discriminating in this respect, selectively precipitating hematite and leaving the other metals in solution. However, work by Neomet (as yet unpublished) has shown that as these metals increase in solution, the liquidus temperature of the ferric chloride starts to decrease, such that when there is about 30% of other metals present in relation to ferric chloride, the system freezes and becomes inoperable without a significant bleed[28]. The recent publication by Starfield[23] demonstrates this problem. This paper describes work on a single pass, wherein 30% of the feed ferric chloride was hydrolysed, with the base metals and magnesium content of the solution increasing in the hydrolysis bath to a constant level consistent with the amount of iron being removed. The paper notes that in commercial practice, the hematite solids would be filtered and the filtrate returned to the bath. Thus, it can be expected that the base metals and magnesium content would increase with each pass. Starfield has apparently recognized this with the introduction of an iron solvent extraction step, so that only pure ferric chloride proceeds to the hydrolysis reactor. The downside of this approach is that the iron strip liquor generated from the loaded solvent is relatively dilute compared to the rest of the process, requiring more water to be removed during hydrolysis, and thus increasing the costs[23].

The Neomet "Atmospheric Autoclave"

Given these constraints, but knowing that the hydrolysis of ferric chloride by water alone at elevated temperatures is perfectly possible, Neomet returned to the fundamentals and searched for an alternative to the above approaches. Dutrizac and Riveros[29][30] demonstrated that it is possible to form hematite from ferric chloride solutions with water alone in a rigorous series of experiments conducted in an autoclave. Their experimental data suggest that although hematite readily forms, the reaction terminates after the conversion of approximately 0.3M Fe, generating 0.6M free HCl. The papers further suggested that adding chloride salts to increase the net chloride concentration had a detrimental effect on the amount of hematite formed. Although not explained in the paper, this was due to the high chloride concentration significantly increasing the activity of the proton, and thereby promoting the back reaction. It was also shown that by removing HCl acid by neutralisation with a base that the reaction continued. Thus, it is logical to assume that had they been able to strip the acid from the system as it formed, then the reaction would also have proceeded.

The unique and revolutionary Neomet "atmospheric autoclave" system is able to achieve this. The system makes use of an inert solvent matrix which remains fluid at temperatures up to 200-250°C (i.e. autoclave temperatures), but which also remains open to the atmosphere, thereby allowing the formed HCl to be removed from the system. In this way, injection of the leach solution into the solvent matrix at 180-200°C allows for:

- The advantage of high temperature to effect an instantaneous chemical reaction, thus forming hematite and HCl gas.

- Rapid removal of the HCl gas and unreacted associated water vapour, which can then be either condensed to hydrochloric acid, or recycled as-is back to the leach if the additional heat is required in the leaching step. The strength of the acid so-formed is determined entirely by the concentration of the feed ferric chloride solution, e.g. 4M $FeCl_3$ will yield 12 12M HCl.

- Formation of crystalline hematite, particle size being determined by the residence time in the reactor. The hematite filters extremely rapidly, and since the matrix solution remains fluid, it can be filtered in-situ.

- Other metals in the feed solution dissolve into the matrix. Thus, an immediate, efficient and selective separation is achieved of iron from the base metals. Hence, there are no problems associated with a build-up of metals into the ferric chloride, since a bleed of the matrix can be taken in order to recover the value metals therefrom.

The selection of a suitable matrix was crucial to the development of the acid regeneration process. It had to be sufficiently ionic at elevated temperatures to allow the chemical reaction to proceed, had to be capable of acting as a solvent for base and other metals, as well as remaining fluid at temperatures over 200°C. The background chemistry and experimentation to identify the matrix material will form the subject of a scholarly journal article currently being prepared, and due for future publication. A number of materials, each with differing properties, have been identified, and these, together with the reactor and filtration system are the subject of a PCT (Patent Co-Operation Treaty) application[31].

Practical Example

A number of real and simulated laterite leach solutions have been tested by injecting into the matrix solution in the Neomet miniplant. The nature of the process is such that simple laboratory batch tests cannot be carried out and either semi-continuous (continuous addition of feed, but no removal of formed solids) or continuous operation is required. Figure 1 shows the results of one such test, using a feed solution analyzing in g/L 40.1 Fe(III), 8.6 Fe(II), 15 Al, 5.1 Ni, 1.07 Na, 1.06 Co.
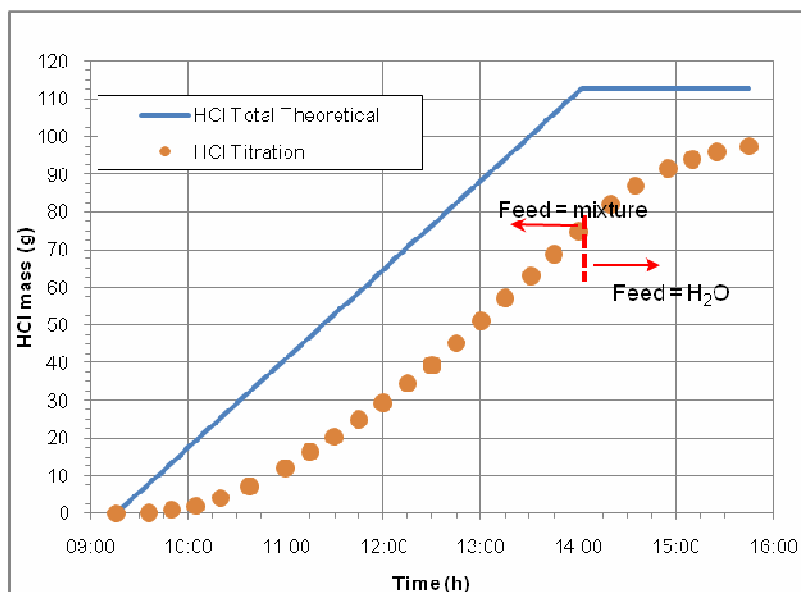
Figure 1: Results of Semi-Continuous Acid Regeneration Test (Complex Feed) at 195°C

It can be seen from this graph that once the system stabilized, the acid produced followed the input of the feed solution. Due to the relatively dilute nature of the feed solution, the acid recovered reached a steady concentration of only 160 g/L shortly after start-up. The difference between the theoretical amount of acid to be produced and that recovered is due to the other chloride salts in the feed which dissolved in the matrix solution. Earlier work had indicated aluminium would precipitate as a gel-like material at a temperature of 150-165°C, or as a more crystalline hydroxy-chloride at >225°C. However, when present with ferric chloride, both hydrolysed simultaneously to form their respective oxides, hematite as a crystalline material and alumina as a more amorphous material. An XRD of the final solids showed highly crystalline hematite, but was not able to fully define the alumina phase. The solids settle and filter very well, with liquor retention being as low as 4%, but typically in the 5-10% range. Surprisingly, and beneficially, the alumina component is very easily removed by a simple wash with sodium hydroxide, yielding a solution of sodium aluminate, which can be used as a precursor to the formation of smelter-grade alumina. The hematite contained <2% alumina.

Table 2 shows the deportment of the elements during the test. It can be seen that essentially, all of the iron and aluminium reported to the solids phase, with all other elements reporting to the matrix solution filtrate. A small amount of carryover into the recovered acid was also seen.

Table 2: Deportment of Elements During Acid Regeneration

Element	Deportment, %			Test Mass
	Filtrate	Solid	Acid	Balance, %
Al	0.0	99.99	0.009	102.3
Co	99.99	0.0	0.010	96.8
Fe	0.33	99.63	0.033	89.3
Na	99.74	0.25	0.010	102.2
Ni	99.82	0.17	0.011	87.2

The ratio of Fe:Al in the final solids matched that of the feed solution. Analysis of similar solids carried out by an independent third party laboratory has shown an average chloride content of 0.07%.

Copper, Nickel and Cobalt Chlorides

As noted above, the base metals dissolve into the matrix solution as the ferric iron and aluminium hydrolyse to form their oxides. Previous testwork has been reported showing that individual solutions of 10 g/L for each of copper, nickel and cobalt chlorides dissolved in a magnesium chloride matrix can be hydrolysed with water at 180°C[32]. It should be noted that magnesium is but one of several matrices that can be used, but because of its tendency to spontaneously hydrolyse at 195-200°C, its use is somewhat limited. The copper and cobalt precipitates were highly crystalline and filtered extremely well. The solids formed were not the oxide as observed with iron and aluminium. Chemical analyses and XRD scans indicated that the basic chlorides, with a generic formula of $Me(OH)_2 \cdot Me(OH)Cl \cdot nH_2O$, where Me is Ni, Cu or Co, had formed. The analysis of the copper precipitate was 48.3% Cu, which corresponds to $Cu(OH)_2 \cdot Cu(OH)Cl \cdot 3H_2O$.

XRD analysis of the copper precipitate solids indicated a very close resemblance to the natural mineral paratacamite. Similar, though less defined, XRD patterns were observed for the nickel and cobalt precipitates. Paratacamite has the basic formula of $(Cu,Zn)_2(OH)_3Cl$, with the Cu/Zn ratio being 3:1. Figure 2, Figure 3 and Figure 4 show the precipitates of nickel, copper and cobalt respectively. The colour of the cobalt precipitate, especially, being lilac, indicates that the solids are clearly not the hydroxide, which would have been expected to be a blue colour similar to that of the copper precipitate solids.

Figure 2: Basic Nickel Chloride Precipitate

Figure 3: Basic Copper Chloride Precipitate

Figure 4: Basic Cobalt Chloride Precipitate

Each of the solids was taken and gently heated in a crucible, where they readily decomposed at 200-300°C to the respective metal oxides, with fumes of HCl being evolved. The resultant oxides were very reactive, and readily dissolved in dilute sulphuric acid.

NEOMET PROCESS FLOWSHEET

Based on the results of testing carried out over the past two years, the flowsheet depicted in Figure 5 has been conceived. This particular version of the flowsheet, and the associated costs which follow, have been based on head sample 1 shown in Table 1. This sample had 30 g/tonne of scandium, which was recovered 100%, and hence is included to show the flexibility of the Neomet Process and the opportunities it presents.

The salient points of the flowsheet are as follows:

- Saprolite, limonite or a mixture thereof is leached at 100-110°C under atmospheric conditions with recycled HCl. The leach is aggressive in order to affect maximum dissolution of pay-metals. This has the advantage that minor value metals, such as scandium in this case, dissolve and can be recovered. The leach slurry filters well and solid/liquid separation is effected on a vacuum belt filter. The leach residue is predominantly silica, which could be used as a furnace flux if so desired.

- Scandium can be recovered directly from the leach solution by either of two methods that have been developed, and which are currently the subject of a patent filing. The basis of these recovery methods is that the scandium can be recovered directly from solutions with high ferric iron content without either having to remove the iron or to reduce it to ferrous. Pure scandium oxide is produced.

- Iron and aluminium are then removed as oxides at 180-190°C during the primary acid regeneration process, and the concentrated HCl recovered is recycled back to the leaching stage. The only other metal which hydrolyses under these conditions is chromium, but the levels are usually so low as to not have an impact on the product quality. Base metals and magnesium dissolve into the solvent matrix, and are allowed to concentrate to a reasonable level to facilitate their subsequent recovery. The level of concentration can be anywhere between 10 and 30%, depending upon the make-up of the leach liquor.

- If desired, the oxide solids can be washed with caustic soda solution to remove the alumina. This then forms two valuable and marketable by-products, namely hematite and alumina.

- Following S/L separation, a bleed of the solvent matrix is taken and water or steam injected to affect the recovery of the base metals as the tri-basic chloride. If copper is present, an effective separation of copper from nickel and cobalt can be achieved, since copper hydrolyses preferentially, and a two-stage process can be employed. The solids again filter well on a vacuum filter, and they can be re-dissolved in dilute acid for further processing, or calcined at 200-400°C to metal oxides, with the recovered HCl being recycled to the leaching stage.

- Finally, a further bleed is taken to affect the recovery of magnesia.

The Neomet Process is a flexible and basically simple flowsheet. Being chloride-based, high solubilities are possible which reduce the volumetric flowrate, and hence equipment size. Working at high temperatures facilitates rapid reaction times, which leads to short residence times and again to reduced equipment size. A further advantage of the hot, high chloride background is that solids are either crystalline or generally dehydrated, making them amenable to both rapid solid/liquid separation and also to having low liquor retention. This again reduces equipment size, and also has a major beneficial impact on the water, and hence energy, balance, since wash water requirements are minimised.

The process also allows for the recovery of valuable by-products. It is fair to say that the mining and base metals extraction industry has largely focused on only one or two pay metals in a deposit. Metals such as iron, aluminium and magnesium have been regarded as nuisances rather than opportunities, and other metals such as scandium, gallium, indium, germanium, etc. have only received attention if present in significant concentrations. The Neomet Process is capable of generating pure oxides of all of these, thereby potentially adding considerably to the revenue stream. At the very worst, all are present in an environmentally-benign form that can be safely disposed of.
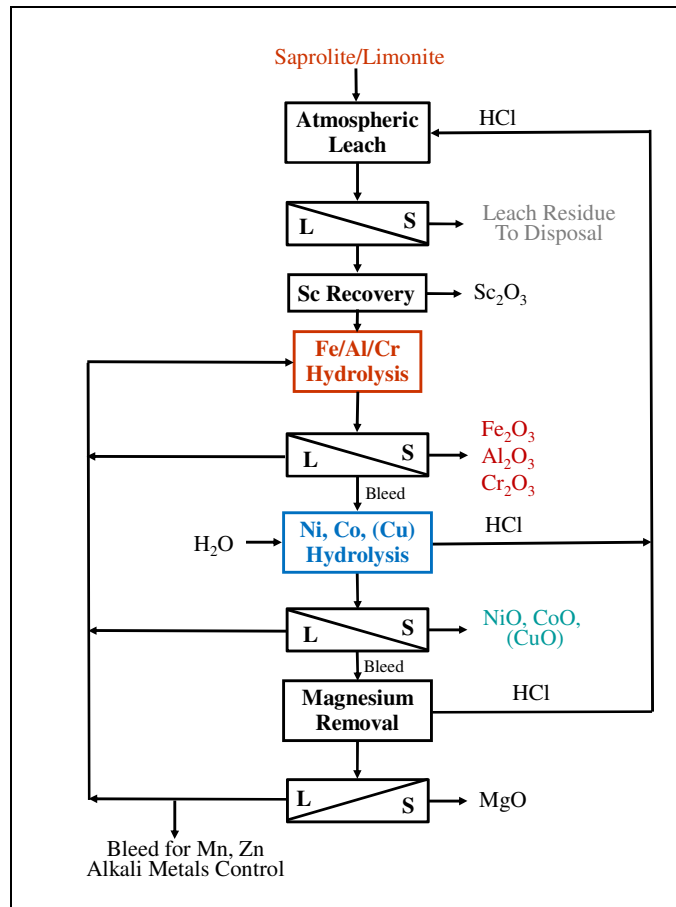
Figure 5: Generic Laterite Processing Flowsheet

Costs

Order of magnitude capital and operating costs have been estimated to see if the Neomet Laterite Process is competitive with other options. At present, more rigorous costing is planned to be carried out in conjunction with a miniplant run later in 2011.

Capital Costs

As noted earlier, Head Sample 1 in Table 1 was used as the basis for the costing exercise. A nominal 50 kilotonnes of nickel production was arbitrarily set as a production target. Based on this, a feed rate of 12,500 tonnes/day of ore was used, and a processing plant based on the flowsheet depicted in Figure 5 was costed. The cost of the mine was not included, as this will vary from site to site, but it was assumed that the leach residue could be returned to the mine for disposal. It was further assumed that a mixed nickel/cobalt oxide would be produced. Again, specific site preferences will determine whether or not to produce separate nickel and cobalt products, and whether or not to produce metal. All of these options are possible with the Neomet Laterite Process.

Using internal cost data generated for similar projects and similar unit operations, and applying a 100% contingency, a capital cost of $650 million was estimated, with an accuracy of ±50%. As noted above, this cost represents the processing plant only, and does not include either the mine or infrastructure. This cost correlates well with that recently announced for the Baja Mining El Boleo Project in Mexico[33], a project with a similar head grade of ore and similar production rate of major metal (copper in this case), and one which also can generate appreciable by-product credits. It also correlates well with the processing plant cost estimated for Starfield Resources' Ferguson Lake Project in Nunavut, which is also a chloride-based circuit[34].

Even if doubled, this represents only 30% of the capital expenditures reported for the HPAL projects of Vale at Goro, Sherritt at Ambatovy and BHP Billiton at Ravensthorpe. Thus, compared to the

accepted industry standard of High Pressure Acid Leaching (HPAL), the Neomet Process offers a considerable economic benefit.

Operating Costs

A rigorous mass and energy balance was carried out using up-to-date data from the testwork program, using the commercial software AspenPlus®. Table 3 below summarises the variable costs as estimated by the balance. Two scenarios were considered, namely one case with a typical moisture content of 25% as might be experienced in a wet tropical location, and another situation from a dry, arid location. Included in the Table are costs for the recovery of scandium and alumina. The alumina costs were taken from published data indicating that the overall energy requirement of producing alumina by the Bayer Process is 12 GJ/tonne, of which 25% of this is required for calcining[35]. For the purposes of this exercise, 33% of the value was taken to allow for some cost in dissolving the alumina.

Table 3: Summary of Variable Costs

Variable Cost Summary	High Moisture (25%)		Low moisture (5%)	
	Cost per		Cost per	
	t feed	lb (Ni+Co)	t feed	lb (Ni+Co)
Hydrochloric acid @ $700/t HCl	$0.95	$0.03	$1.00	$0.03
Sulphuric acid @ $250/t H_2SO_4	$0.88	$0.03	$0.88	$0.03
Scandium reagents @ $500/t reagent	$0.23	$0.01	$0.23	$0.01
Natural gas @ $0.5/m³	$15.02	$0.51	$14.81	$0.50
Process water @ $1/m³	$0.00	$0.00	$0.17	$0.01
Boiler feed water @ $2/m³	$0.92	$0.03	$1.18	$0.04
Power @ $0.05/kWh	$23.51	$0.80	$22.70	$0.77
Energy for alumina extraction @ $13.3/GJ	$6.56	$0.22	$6.56	$0.22
Calculated variable cost	**$48.07**	**$1.63**	**$47.53**	**$1.61**

The results show very little dependence on the moisture content of the feed laterite, and that the costs for recovering alumina and scandium are modest. The biggest contributors to the costs are power and energy in the form of natural gas. Thus, an increase in the cost of these components would have a negative impact on the overall processing costs.

Table 4 shows the projected revenues from the feed of Head 1 in Table 1.

Table 4: Projected Revenue Summary

Revenue Summary	High Moisture (25%)		Low moisture (5%)	
	Revenue per		Revenue per	
	t feed	Year	t feed	Year
Nickel @ $8/lb	$229.62	$880m	$229.56	$880m
Cobalt @ $20/lb	$17.31	$57m	$17.30	$57m
Scandium oxide @ $70/kg	$22.23	$85m	$22.23	$85m
Hematite @ $100/t	$30.44	$117m	$30.44	$117m
Alumina @ $200/t	$24.61	$94m	$24.61	$94m
Magnesia @ $100/t	$4.96	$19m	$4.96	$19m
Projected revenue	**$329.17**	**$1253m**	**$329.10**	**$1253m**
Internal rate of return, IRR	**61%**		**61%**	

The current (April, 2011) market price of scandium is 10-20 times that used here. The lower value, in accordance with the price of rare earth oxides, has been used on the assumption that a new, large supply of scandium would significantly lower its price. However, whether this would be the case for the first project of this nature cannot be predicted. The prices for alumina and hematite are also significantly lower than current market prices, especially for a high-grade product. The IRR was calculated using a four-year ramp up period (25% per year), the capital cost indicated earlier, and a fixed cost of $7.3 million annually (based on Canadian labour rates). Ignoring the contributions of hematite, scandium, alumina and magnesia, the IRR falls to 50%, which is still very attractive.

Whilst nickel is by far the largest contributor to the net revenue stream, the revenues to be accrued from considering the by-products is, nevertheless, substantial. For a plant producing 50,000 tonnes of nickel, there is a by-production of just over 1 million tonnes of hematite and 500,000 tonnes of alumina using the feed grades chosen for this exercise. A Neomet laterite project, therefore, could be a significant supplier of both high-grade hematite and smelter-grade alumina to the primary iron and aluminium industries.

DISCUSSION AND CONCLUSIONS

This paper has presented the latest advances in the genesis of the Neomet Laterite Process, showing that the process conditions are now well-established, and that the process is economically attractive. Notably, the development of the unique "atmospheric autoclave" approach to acid regeneration has simplified the flowsheet appreciably, allowing it to handle a variety of different complex ores.

The highlights of the process can be summarized as follows:

- The process is capable of treating any or all horizons of a laterite orebody, and unlike other processes, all valuable components of the ore can be recovered if desired. In the example used, a small amount of scandium has an appreciable positive contribution to the overall IRR. Iron, aluminium and magnesium, normally regarded as nuisance elements, can all be recovered in a pure form and marketed. At the very worst, they are low-volume, benign solids that can easily be returned to the mine for disposal.

- High recoveries are achieved during leaching, and the resultant leach is amenable to vacuum filtration due to the dehydrated nature of the leach solids. This therefore requires a much lower footprint and generates more concentrated liquors than would be possible by using the CCD circuit commonly associated with HPAL circuits.

- No secondary neutralisation is required to remove residual iron and aluminium, unlike with HPAL or atmospheric sulphuric acid leaching.

- Acid regeneration is rapid and efficient, generating a much higher strength HCl than is possible by pyrohydrolysis. Simultaneously, iron and aluminium are precipitated as discrete, pure crystalline solids. If desired, the aluminium can be easily separated from the iron by a simple caustic wash. Being highly crystalline and dehydrated, the solids filter rapidly and have a very low (<10%) liquor retention, thus requiring very little wash water. This in turn helps both the water and energy balances.

- After iron removal, base metals are recovered initially as basic chlorides ($Me_2(OH)_3Cl$). It is possible to preferentially recover copper ahead of nickel and cobalt. The basic chlorides dissolve readily in dilute HCl for processing to metal, or can be calcined directly at 200-500°C to give the metal oxide.

- Magnesium is not an issue in this flowsheet. It can be recovered either as a hydroxy chloride or as magnesia at the end of the flowsheet.

- Alkali metals, if present, are easily salted out. Potassium is marketable as potash if warranted. Calcium (and lead if present) are easily controlled by addition of sulphate.

- The flowsheet is closed loop, in that there are no liquid effluents. Solids are either environmentally benign, or can be sold directly as additional revenue streams.

The Future

At the time of writing, Neomet is planning a miniplant campaign at its facilities in Montreal (Figure 6 below) in the third quarter of 2011 in order to generate sample products and engineering data for a more rigorous cost study. The miniplant is nominally 1-L capacity, capable of treating up to 1 kg/hr of feed solids, the rate depending on the reactivity of the solids in the leaching reaction. The circuit is multi-purpose, having already been used successfully for gold and vanadium ores.

Figure 6: General View of Leaching and Acid Regeneration Sections of Miniplant

Beyond, the construction a 1 tonne/day pilot plant has commenced at the same site, with the objective of demonstrating this and other processes on a larger scale.

ACKNOWLEDGEMENTS

REFERENCES

1. Bryn Harris, John Magee and Ricardo Valls, Beyond PAL: The Chesbar Option, AAL, Presented at ALTA Nickel-Cobalt-9, Perth, WA, May 18-20, 2003.

2. Bryn Harris and John Magee, Atmospheric Chloride Leaching: The Way Forward For Nickel Laterites, in Proceedings of Hydrometallurgy 2003 - International Symposium in Honor of Professor Ian Ritchie, (C.A. Young, A. Alfantazi, C. Anderson, A. James, D. Dreisinger and B. Harris, Editors), Vancouver, CIM/TMS/SME, August 2003, p. 501.

3. G.B Harris, T.J. Magee, V.I. Lakshmanan and R. Sridhar, The Jaguar Nickel Inc. Sechol Laterite Project Atmospheric Chloride Leach Process, in Proceedings of International Laterite Nickel Symposium 2004 (W.P. Imrie and D.M. Lane, Editors), TMS Annual Meeting, Charlotte, North Carolina, March 14-18, 2004, p. 219.

4. Bryn Harris, Carl White, Mal Jansen and Duncan Pursell, A New Approach to High Chloride Leaching of Nickel Laterites, Presented at ALTA Ni/Co 2006, Perth, WA, May 2006.

5. Bryn Harris, Carl White, Mike Dry and Phil Evans, Treatment of Nickel Laterites by Chloride and Hybrid Chloride Sulphate Processes, Proceedings of Hydrometallurgy of Nickel & Cobalt 2009 (J.J. Budac, R. Fraser, I. Mihaylov, V.G. Papangelakis and D.J. Robinson, Editors), 48th CIM Annual Conference of Metallurgists, 39th Annual Hydrometallurgy Meeting, Sudbury, Ontario, Canada, August 23-26, 2009, p. 523.

6. G.B. Harris, C.W. White and G.P. Demopoulos, Iron Control in High Concentration Chloride Leach Processes, in Iron Control Technologies (J.E. Dutrizac and P.A. Riveros, Editors), Proceedings of the Third International Symposium on Iron Control in Hydrometallurgy, 36th Annual CIM Hydrometallurgical Meeting, Montreal, October 1-4, 2006, p. 445.

7. R. Tang Poy, Regeneration of Hydrochloric Acid from Ferrous Chloride Using the Keramchemie/Lurgi Fluidised Bed Reactor System, in Proceedings of Iron Control and Disposal (J.E. Dutrizac and G.B. Harris, Editors), Second International Symposium on Iron Control in Hydrometallurgy, Ottawa, Canada, October 20-23, 1996, p. 471.

8. E.M.L. Peek, O.F. Goedhart and G. Van Weert, Process Evaluation of Steel Pickle Liquor Pyrohydrolysis in a Commercial Keramchemie Fluid Bed Reactor, in Proceedings of Iron Control and Disposal (J.E. Dutrizac and G.B. Harris, Editors), Second International Symposium on Iron Control in Hydrometallurgy, Ottawa, Canada, October 20-23, 1996, p. 483.

9. F. Baerhold, A. Lebl and J. Statrcevic, Recycling of Spent Acids and Iron Via Pyrohydrolysis, in Iron Control Technologies (J.E. Dutrizac and P.A. Riveros, Editors), Proceedings of the Third International Symposium on Iron Control in Hydrometallurgy, 36th Annual CIM Hydrometallurgical Meeting, Montreal, October 1-4, 2006, p. 789.

10. K. Adham, C. Lee and D. Small, Energy Consumption for Iron Chloride Pyrohydrolysis: A Comparison Between Fluid Beds and Spray Roasters, in Iron Control Technologies (J.E. Dutrizac and P.A. Riveros, Editors), Proceedings of the Third International Symposium on Iron Control in Hydrometallurgy, 36th Annual CIM Hydrometallurgical Meeting, Montreal, October 1-4, 2006, p. 815.

11. M-C. Patoine, A. De Mori, K. Borowiec and C. Coscia, Pyrohydrolysis of a Calcium and Magnesium Bearing $FeCl_2$ Leach Liquor, in Chloride Metallurgy 2002 Volume 2 (E. Peek and G. van Weert, Editors), Proceeding of the 32nd Annual CIM Hydrometallurgical Conference, CIM, Montreal, 2002, p. 699.

12. A. Vahed, D.F. Colton, J-P. Duterque, W. Karner and F. Baerhold, Development of a Fluid Bed Pyrohydrolysis Process for Inco's Goro Nickel Project, in Proceedings of International Laterite Nickel Symposium 2004 (W.P. Imrie and D.M. Lane, Editors), TMS Annual Meeting, Charlotte, North Carolina, March 14-18, 2004, p. 171.

13. W. Steinbach and F. Baerhold, Comparison of Spray Roasting and Fluid Bed Granulation for the Recovery of Hydrochloric Acid from Metallurgical Processes through Pyrohydrolysis, in Chloride Metallurgy 2002 Volume 2 (E. Peek and G. van Weert, Editors), Proceeding of the 32nd Annual CIM Hydrometallurgical Conference, CIM, Montreal, 2002, p. 643.

14. K. Adham and C. Lee, Energy Recovery in the Metal Chloride Pyrohydrolysers, in Chloride Metallurgy 2002 Volume 2 (E. Peek and G. van Weert, Editors), Proceeding of the 32nd Annual CIM Hydrometallurgical Conference, CIM, Montreal, 2002, p. 657.

15. K. Adham, C. Lee, K. O'Keefe and B. Wasmund, Application of Oxygen Enrichment for the Pyrohydrolysis of Metal Chlorides, Chloride 2011, TMS EPD Congress 2011, San Diego, CA, March 2011, p. 539.

16. G.P. Demopoulos, Z. Li, L. Becze, G. Moldoveanu, T. Cheng and G.B. Harris, New Technologies for HCl Regeneration in Chloride Hydrometallurgy, World of Metallurgy-ERZMETALL, 61(2), 2008, 84-93.

17. Jack W. Burtch, PORI Hydrochloric Acid Regeneration Process, Iron and Steel Engineer, Vol. 50(4), 1973, p. 40.

18. J.W. Burtch, PORI Hydrochloric Acid Regeneration Process, SEAISI Quarterly Vol. 2(4), 1973, p. 52.

19. Jack W. Burtch, Hydrochloric Acid from Industrial Waste Streams - the PORI Process, CIM Bulletin, Vol. 68, January 1975, p. 96.

20. J.W. Burtch, The Pori process. Regeneration of Hydrochloric Acid from Spent Pickle Liquor, Wire Journal, Vol. 9(2), 1976, p. 57.

21. SMS Siemag Process Technologies GmbH, Hydrothermal Hydrochloric Acid Regeneration. http://www.sms-siemag.at/Hydrometallurgy.html

22. L. Becze, S.J. Hock and G.P. Demopoulos, Precipitation of Hematite and Recovery of Hydrochloric Acid from Concentrated Iron Chloride Solutions by a Novel Hydrolytic Decomposition Process, Chloride 2011, TMS EPD Congress 2011, San Diego, CA, March 2011, p. 529.

23. M. Dry, N. Verbaan, E. Bourricaudy and M. Moran, Development of a Novel High-Chloride Circuit for the Starfield Resources' Ferguson Lake Project, Chloride 2011, TMS EPD Congress 2011, San Diego, CA, March 2011, p. 415.

24. J. de Bakker, J. LaMarre, V. Papangelakis and B. Davis, HCl Leaching and Acid Regeneration Using $MgCl_2$ Brines and Molten Salt Hydrates, Chloride 2011, TMS EPD Congress 2011, San Diego, CA, March 2011, p. 521.

25. A. John Moyes, The Intec Nickel Laterite Process, presented at ALTA 2005 Ni/Co 10, Perth, W. Australia, May 16-18, 2005.

26. M. Pelser, J.D.T. Steyl and J. Smit, Development of the Anglo Research Nickel (ARNi) Process for the Treatment of Laterite Ores, Proceedings of Hydrometallurgy of Nickel & Cobalt 2009 (J.J. Budac, R. Fraser, I. Mihaylov, V.G. Papangelakis and D.J. Robinson, Editors), 48th CIM Annual Conference of Metallurgists, 39th Annual Hydrometallurgy Meeting, Sudbury, Ontario, Canada, August 23-26, 2009, p. 409.

27. Anglo American plc., Annual Report 2010, p. 39.

28. Neomet Technologies Inc., internal data to be published.

29. P.A. Riveros and J.E. Dutrizac, The Precipitation of Hematite from Ferric Chloride Media, Hydrometallurgy Vol. 46, 1997, p. 85.

30. J.E. Dutrizac and P.A. Riveros, The Precipitation of Hematite from Ferric Chloride Media at Atmospheric Pressure, Metallurgical and Materials Transactions B, Vol. 30B, December 1999, p.993.

31. Bryn Harris and Carl White, Process for the Recovery of Metals and Hydrochloric Acid, PCT International Application No. PCT/CA2011/000141, February 4, 2011 (Priority Date February 18, 2010).

32 . Bryn Harris, Carl White, George Demopoulos and Levente Becze, Recovery of Metal Oxides and Associated Acid from Process Solutions Using Water as Reagent, Presented at ALTA Copper 2008, Perth, Australia, June 19-20, 2008.

33. Baja Mining Corp., Baja Signs US$858 Million of Financing Facilities for the Development of Boleo Project, September 29, 2010.

34. Scott Wilson Roscoe Postle Associates Inc., Preliminary Assessment of the Ferguson Lake Project, Nunavut Territory, Canada, Prepared For Starfield Resources Inc., NI 43-101 Report, December 15, 2008, http://www.sedar.com

35. A. Kontopoulos, D. Panias and I. Paspaliaris, Precipitation of Monohydrate Alumina in the Bayer Process, National Technical University of Athens, Université Libre de Bruxelles and Hellenic Alumina Industry, Contract Joe3-Ct95-0003, Publishable Final Report, January 1996 To June 1997. (Research Funded in Part by The European Commission In The Framework of the Non Nuclear Energy Programme Joule III.

STUDY OF CERTAIN PARAMETERS IN LABORATORY-SCALE PREREDUCTION OF SIVRIHISAR LATERITE ORES OF TURKEY

By

[1]Ender Keskinkilic, [2]Saeid Pournaderi, [2]Ahmet Geveci and [2]Yavuz A. Topkaya

[1]Atilim University, Department of Metallurgical and Materials Engineering, Turkey
[2]Middle East Technical University, Department of Metallurgical and Materials Engineering, Turkey

Presenter and Corresponding Author

Ender Keskinkilic
ekeskinkilic@atilim.edu.tr

ABSTRACT

This study investigated prereduction behavior of one of the Turkish laterite deposits, which was recently found in Sivrihisar region. Sivrihisar laterite ore (1.26% Ni) is a limonitic one with its high iron content and low MgO composition. Low arsenic content of the ore makes ferronickel smelting a suitable method for nickel extraction. In the scope of this study, calcined laterite samples were reduced with the addition of coal in a laboratory-scale horizontal tube furnace under argon atmosphere. Effect of temperature, time and the amount of coal addition on degree of reduction of nickel, iron and cobalt were studied. For the particle size used in the current work, optimum temperature, time and coal addition were determined for prereduction of Sivrihisar laterites.

INTRODUCTION

The share of laterites in world nickel production has been continuously increasing. 40% of the annual production was from laterites in 2004. It was estimated that the amount of nickel production from laterites would be the same as from sulfide type nickel ores in 2012[1]. In Turkey, there are three nickel ore deposits. Two of them are in the region of the Western Anatolia, namely Gordes and Caldag ores. The third one, located in the Central Anatolia, was found in the Sivrihisar region (Yunusemre and Mihaliccik) in the first decade of the millennium. All three ore bodies are lateritic. Various studies have been conducted for pyrometallurgical and hydrometallurgical nickel extraction from Gordes and Caldag ores[2-8]. Sivrihisar ore is characterized by its high iron content with low MgO composition. Low arsenic content of the ore makes ferronickel smelting a suitable method for nickel extraction. Laboratory-scale calcination behavior of Sivrihisar laterite ores was studied as a part of project work supported by The Scientific and Technological Research Council of Turkey (TUBITAK)[9]. In that work, the run of mine ore (ROM) sample prepared was screened at 50 mm. The oversize lumpy materials containing chiefly gangue minerals were rejected and remaining undersize particles were used for calcination experiments. The ore calcined at the optimum temperature and time was reported to have the following chemical analysis given in Table 1. Nickel content of the ore was found to upgrade from 1.41% to 1.58% after calcination.

Table 1: Chemical Composition of the Calcined Ore (%)

Ni	SiO$_2$	Fe	Cr	Co	As
1.58	31.6	37.1	1.38	0.103	0.03
Al$_2$O$_3$	**MgO**	**Fe$_2$O$_3$**	**CaO**	**MnO**	**P$_2$O$_5$**
3.48	1.44	53.0	1.65	0.85	*
K	**Pb**	**S**	**TiO$_2$**	**Zn**	**Cu**
0.1	<0.01	0.05	0.07	0.03	0.013

* not analyzed.

In the present study, prereduction behavior of Sivrihisar laterite ores of Turkey was investigated. Laterite samples calcined at the optimum conditions[9] were reduced with the addition of coal in a laboratory-scale horizontal tube furnace under argon atmosphere. Effect of temperature, time and the amount of coal addition on degree of reduction of nickel, iron and cobalt were studied. For the particle size used in the current work, optimum temperature, time and coal addition were determined for prereduction of Sivrihisar laterites. The results of these experiments provide useful information regarding the prereduction characteristics of Sivrihisar laterites, which will hopefully be treated in the ferronickel plant in the Yunusemre region within the present decade.

EXPERIMENTAL

In the prereduction experiments, coal was used as a reducing agent. Reductant coal obtained from META Nickel Cobalt Co. was in the form of lumps having an average diameter of 5 cm. Coal was subjected to crushing and grinding and its particle size was reduced below 0.5 mm. Properties of the coal are illustrated in Table 2.

Table 2: Properties of Reductant Coal Used in the Experiments

Total Moisture (%)	1.77
Ash (%)	4.20
Volatiles (%)	17.64
Total Sulfur (%)	0.33
Total Calorific Value, max. (Kcal/kg)	7,967
Net Calorific Value, min. (Kcal/kg)	7,752

Prereduction experiments were conducted in a horizontal tube furnace under an argon atmosphere. In each experiment, calcined ore and reductant coal were mixed and charged into alumina crucibles having dimensions of 50 mm length, 20 mm height and 25 mm width. In each run, the charge mixture was heated to a predetermined temperature and it was held at that temperature for a predetermined time. At the end of this period, the furnace was cooled down to room temperature using its cooling program. From the start of the experiment till the shutdown of the furnace, argon gas was sent into the system with an average rate of 10 cc/min. Although it was not given in the scope of this work, in detail, the hot zone of the tube furnace was determined using a chromel-

alumel type thermocouple, and the set temperatures were determined such that experiments were performed at the hot zone temperatures of 900, 1000 and 1100 ^{o}C, respectively.

At the beginning, it was decided to charge the stoichiometric amount of carbon necessitated by the reduction reactions for the reduction of hematite to wustite, nickel oxide to metallic nickel and cobalt oxide to metallic cobalt. Therefore, carbon to be added was calculated according to the following reactions:

1. Reduction of hematite to wustite:

$$3Fe_2O_3 + C \rightarrow 2Fe_3O_4 + CO \qquad [1]$$

$$2Fe_3O_4 + 2C \rightarrow 6FeO + 2CO \qquad [2]$$
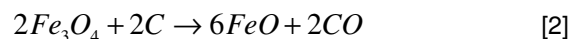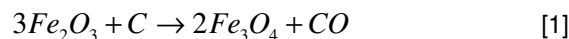
2. Reduction of nickel oxide to metallic nickel:

$$NiO + C \rightarrow Ni + CO \qquad [3]$$

3. Reduction of cobalt oxide to metallic cobalt:

$$CoO + C \rightarrow Co + CO \qquad [4]$$
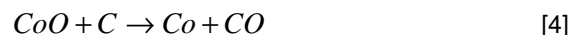
According to the calculations conducted, it was found that 5.74 g of reductant coal should be charged per 100 g of calcined ore. Therefore, a total charge of 20 g was prepared for the first experiment to satisfy this proportion. At the end of the experiments, the products in the alumina crucibles were taken out and weighed. The products were subjected to chemical analysis. Chemical analysis was performed using the bromine-methanol technique, which was described extensively in the literature[10,11]. The metallic Ni, metallic Fe and metallic Co values were determined using atomic absorption spectrometry (AAS). The degree of reduction of nickel, iron and cobalt was calculated according to the following formula:

$$\% \ REDUCTION \ of \ i = \frac{\%i \ (metallic) \ in \ prereduced \ calcine \cdot weight \ of \ prereduced \ calcine}{\%i \ in \ calcined \ ore \cdot weight \ of \ calcined \ ore}$$

where i denotes Ni, Fe and Co. \qquad [5]

The amounts of Fe^{2+} and Fe^{3+} in prereduced calcine were determined using wet methods. The amount of magnetite in prereduced material was measured using SATMAGAN.

RESULTS AND DISCUSSION

As indicated previously, experiments were conducted at 900, 1000 and 1100 ^{o}C. The effect of temperature on the degree of reduction of nickel, iron and cobalt was determined with the runs, in which coal contents were adjusted such that stoichiometric carbon (5.74%C), 50% excess carbon (8.61%C) and 100% excess carbon (11.48%C) were added to calcined ore. The reduction time in these experiments was fixed as 40 minutes. The effect of temperature and coal content on the degree of reduction of nickel is illustrated in Figure 1. The results showed that an increase in experiment temperature led to an increase in the degree of reduction of nickel, as expected. Per cent reduction of nickel could not reach 40% in the experiments conducted at 900 ^{o}C with the addition of stoichiometric and 50% excess carbon. On the other hand, it was reported to reach around 65% when the temperature was raised to 1100 ^{o}C. The experiments performed with the addition of 100% excess carbon produced higher degree of reduction: Per cent reduction of nickel was found to be higher than ~57% at all temperatures and it was reported to reach a maximum value of 87.79% at 1100 ^{o}C.
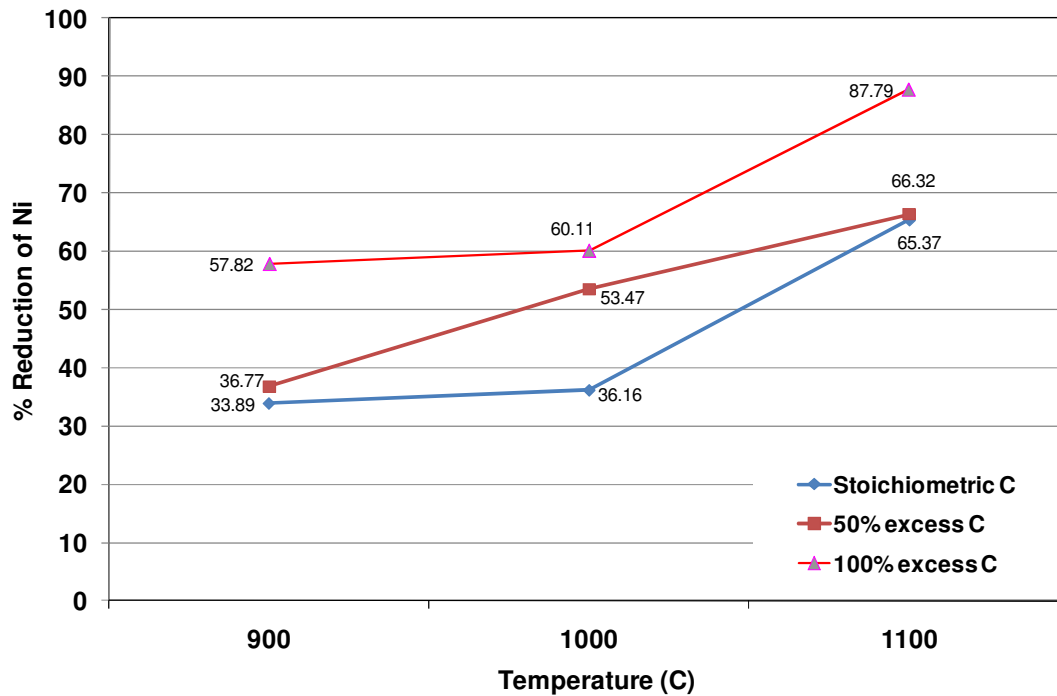
Figure 1: Variation of degree of reduction of Ni with temperature for different coal contents

Variation of degree of reduction of iron with temperature was reported to show similar behavior with that observed for nickel. On the other hand, the rate of increase was more prominent in the former. The effect of temperature and coal content on the extent of reduction of iron is given in Figure 2. The experiments conducted at 900 ^{o}C showed that the degree of reduction of iron was very small regardless of the coal content. The experiments performed at 1000 ^{o}C produced significantly higher per cent reduction values than those conducted at 900 ^{o}C. An increase in coal content also gave rise to an increase in the extent of reduction of iron: At 1000 ^{o}C, per cent reduction of iron was found as 3.24% when stoichiometric carbon was charged. These values were reported as 8.43% and 15.03% when 50% and 100% excess carbon was used, respectively. A substantial amount of increase in % reduction of Fe was reported when the temperature was raised to 1100 ^{o}C: When stoichiometric carbon was charged, the value obtained was reported as 22.24%, which was nearly 7 times greater than the one obtained at 1000 ^{o}C. Likewise, 50% excess carbon addition yielded per cent reduction value of 38.33%, which was approximately 5 times higher than that encountered at 1000 ^{o}C. The highest degree of reduction of iron was noted when 100% excess carbon was used at 1100 ^{o}C. The extent of reduction under these conditions was reported as 52.24%.

As a summary, it was found that an increase in experiment temperature led to significant increases in the degree of reduction of iron. This was more prominent when the temperature was raised to 1100 ^{o}C and excess carbon practice was applied. However, high extent of iron reduction should be prevented in the preduction stage of ferronickel smelting, since high metallic iron bearing prereduced calcine produces iron-nickel alloy, which is very rich in iron. In other words, the desired nickel content in crude ferronickel cannot be achieved.

Variation of extent of reduction of cobalt with temperature is illustrated in Figure 3 for different coal contents. The degree of reduction of cobalt was reported to increase almost linearly as the temperature increased. On the other hand, for a specific temperature, changes in coal content did not result in a significant change in the extent of reduction of cobalt. Per cent reduction of cobalt was reported to stay in 28.55-31.54% interval at 900 ^{o}C. The extent of reduction values were obtained as 38.39-42.7% for 1000 ^{o}C and 60.03-65.87% for 1100 ^{o}C.
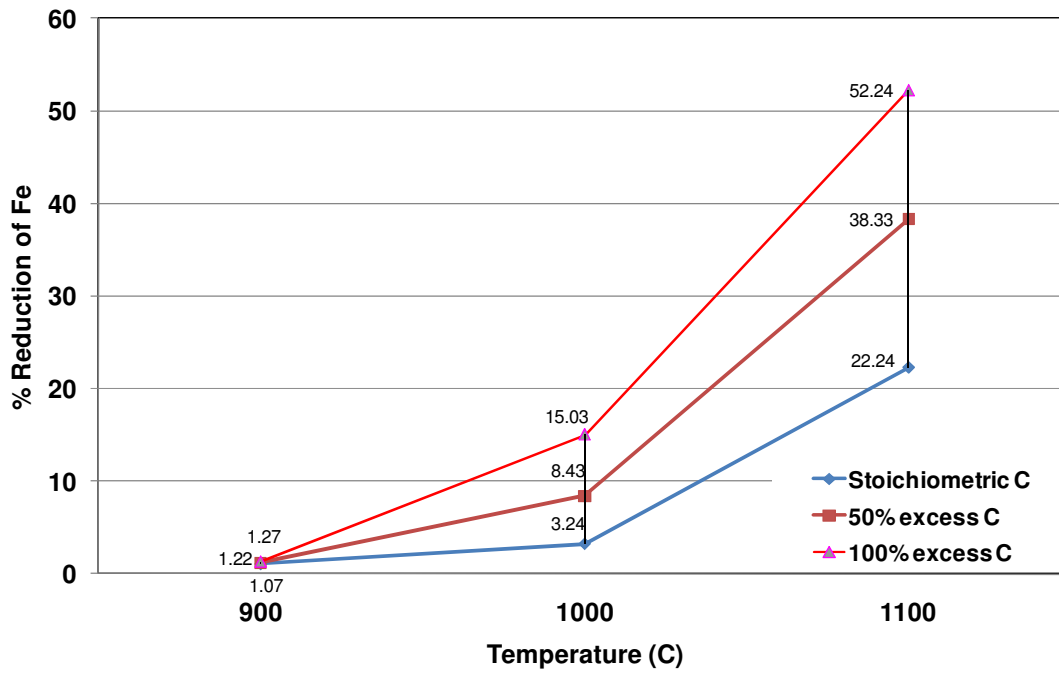
Figure 2: Variation of degree of reduction of Fe with temperature for different coal contents
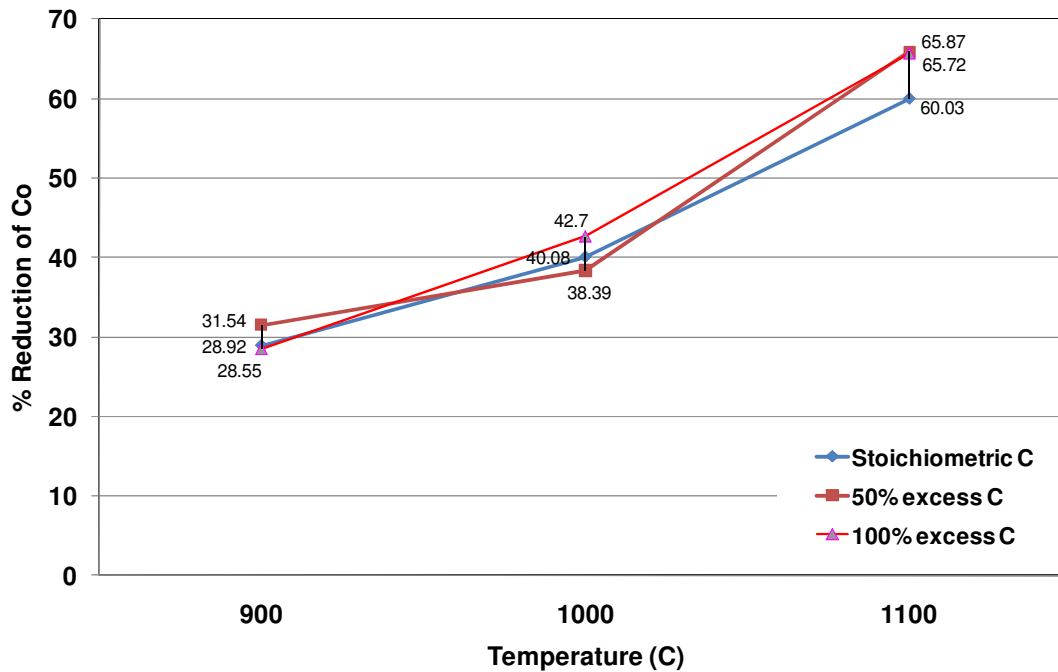
Figure 3: Variation of degree of reduction of Co with temperature for different coal contents

The effect of reduction time on the degree of reduction of nickel, iron and cobalt were investigated with the experiments conducted at 1000 and 1100 ^{o}C. The charges were reduced for 40, 60 and 80 minutes. The coal content in these experiments was fixed as 100% excess carbon. The effect of reduction time on the extent of reduction of nickel is shown in Figure 4. It was reported that a slight increase in the degree of reduction of nickel took place when the reduction period was extended. The similar trends were observed at both temperatures. At 1000 ^{o}C, a slight increase in per cent reduction of nickel was noted: %reduction value of 60.11% was obtained at the end of 40 minutes while it was reported to reach 65.78% when the time was doubled. Similarly, an increase from 87.79% to 95.66% in the extent of reduction of nickel was reported for the same increase in time at 1100 ^{o}C. These results showed that an increase in reduction time beyond 40 minutes did not produce a significant rise in %reduction of nickel as compared to that observed when temperature was increased. Therefore, it was concluded that 40-minute reduction time was almost sufficient to achieve the desired degree of reduction of nickel for the present prereduction system.
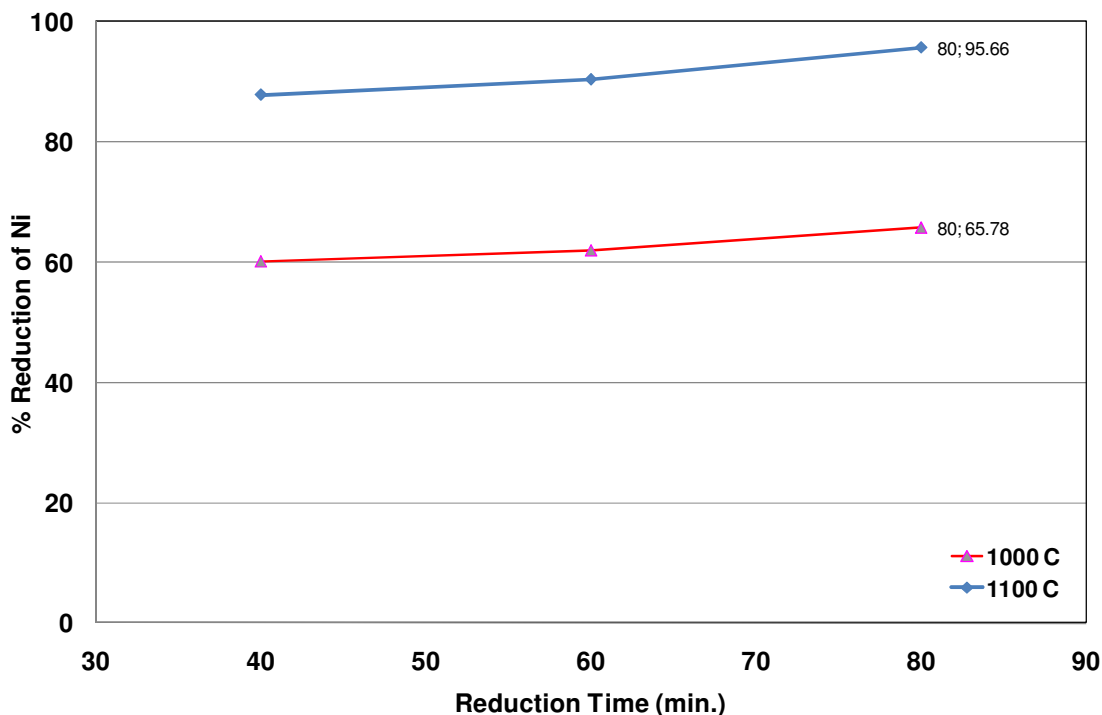
Figure 4: Variation of degree of reduction of Ni with reduction time

The degree of reduction of iron showed increasing trend with reduction time (See Figure 5.). This trend was more prominent compared to that in nickel reduction. At 1000 ^{o}C, the extent of reduction of iron was reported as 15.03% at the end of 40 minutes. Per cent reduction value increased to 38.08% while the time was doubled. A similar tendency was noted at 1100 ^{o}C, although it was not as sharp as the one at 1000 ^{o}C. According to these findings, it was inferred that the reduction time had a significant effect on the degree of reduction of iron. As indicated previously, high degree of reduction in iron is not desired in prereduction. The experiments conducted in the scope of this laboratory scale work showed that 40-minute reduction time is fairly sufficient to achieve the desired extent of reduction of iron.

The experiments performed at 1000 ^{o}C showed that the extent of reduction of cobalt was reported to increase slightly in 40-60 minutes interval, and to reach steady state afterwards. On the other hand, the runs conducted at 1100 ^{o}C produced almost the same degree of reduction of cobalt independent of the reduction time: %reduction of Co was noted as around 67% in all runs. In conclusion, the highest degree of reduction was obtained at 1100 ^{o}C and at the end of 40 minutes.
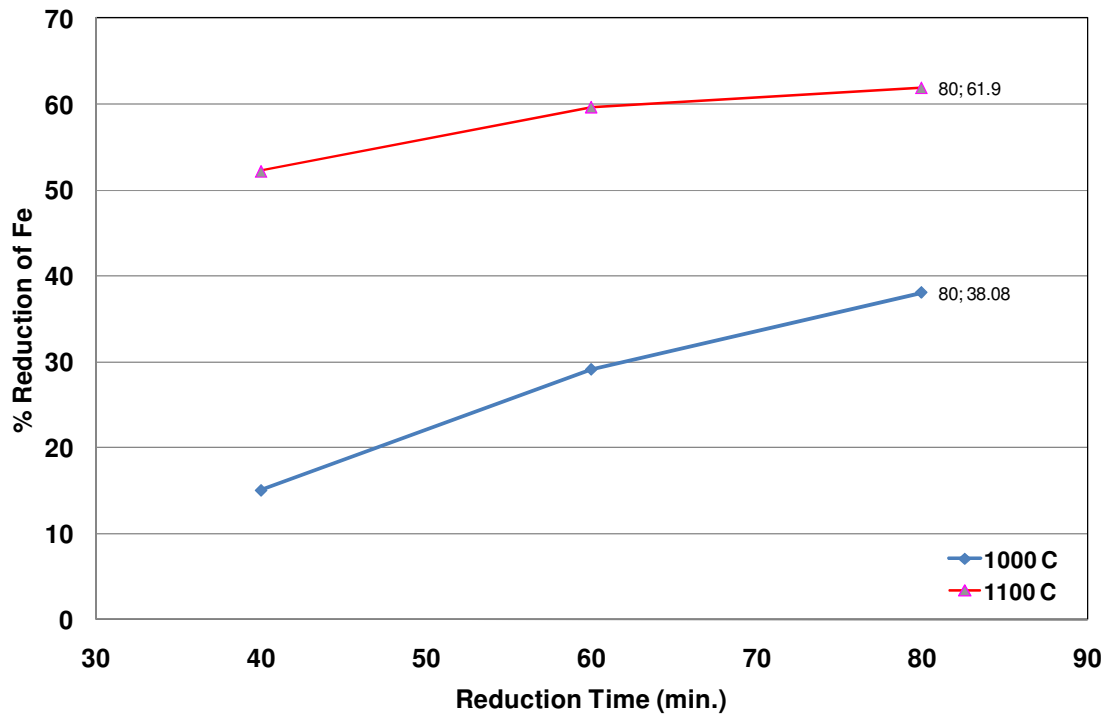
Figure 5: Variation of degree of reduction of Fe with reduction time

The effect of coal content on metallic Fe/Ni ratio of prereduced calcine is illustrated in Figure 6. Experiments performed at 900 $^{\circ}$C revealed that an increase in coal content did not produce a significant change in metallic Fe/Ni ratio. As explained previously, the extent of reduction of nickel oxide and especially iron oxides were limited at 900 $^{\circ}$C. Correspondingly, metallic Fe/Ni ratio was below 1 for all coal contents. Therefore, sufficient and effective prereduction of laterite ore could not be achieved at 900 $^{\circ}$C for the reduction system used in the current work. When the temperature was raised to 1000 $^{\circ}$C, the metallic Fe/Ni ratio increased almost linearly as the coal content was increased: A ratio of nearly 2 was obtained when stoichiometric carbon was used in the charge mixture, while the ratio approached 4 for 50% excess coal addition. The highest ratio was obtained as 5.89 when 100% excess coal was added. At the smelting stage of the conventional ferronickel process, nickel content of the crude ferronickel produced is roughly in the range of 15-25% indicating that iron content is approximately in the interval of 75-85%. These values represent that metallic the Fe/Ni ratio of crude ferronickel is between 3 and 5.67. Therefore, the corresponding ratio in prereduction product should not differentiate substantially from that to be obtained in crude ferronickel. If the ratio was significantly lower than that to be reached at the end of smelting, it would mean that the aim of prereduction could not be attained. If the other extremum was the case, the desired nickel content of the crude ferronickel would not be reached at the end of smelting. Therefore, it was inferred from the results that use of around 50% excess carbon at 1000 $^{\circ}$C was appropriate to satisfy the desired metallic Fe/Ni ratio in prereduced calcine. The highest ratios were obtained at 1100 $^{\circ}$C, given as 8.01 for stoichiometric carbon, 13.61 for 50% excess carbon and 14.02 for 100% excess carbon. These results clearly showed that iron oxides were excessively reduced to metallic iron at 1100 $^{\circ}$C. Therefore, it was definitely concluded that 1100 $^{\circ}$C was not a suitable temperature for prereduction.

It is well known that one of the most important aims in prereduction is to convert Fe^{3+} into Fe^{2+} before smelting. This is especially important to reduce the energy requirement of electric furnace smelting. In the scope of the current study, prereduced samples were also analyzed to determine Fe^{2+} and Fe^{3+}. The variation of Fe^{2+} content in reduced samples with temperature is given in Figure 7. In all experiments conducted with any one of the carbon contents indicated before, Fe^{2+} composition was reported to form a peak at 1000 $^{\circ}$C. As mentioned previously, sufficient degree of reduction could not be obtained at 900 $^{\circ}$C. Corresponding to this, Fe^{2+} content of prereduced calcine was found to be limited: In the experiment conducted with stoichiometric carbon, the Fe^{2+} value was reported as 21.30%, while it was found as 22.73% and 27.50% for 50% excess carbon and 100% excess carbon, respectively. At 1000 $^{\circ}$C, maximum Fe^{2+} values were obtained for specified carbon content. The highest values were encountered as 35.30% and 36.33% when stoichiometric carbon and 50% excess carbon were used, respectively. 100% excess carbon use

produced Fe^{2+} value of 30.85%. When the temperature was raised to 1100 ^{o}C, significant decreases were noted in Fe^{2+} values. These were more apparent for 50% and 100% excess coal additions. These decreases were mostly attributed to the increase in the extent of magnetite formation when the temperature was increased to 1100 ^{o}C, as obtained from SATMAGAN results. Therefore, 1100 ^{o}C was not an appropriate temperature to reach the desired Fe^{2+} content. The highest Fe^{2+} values were obtained at 1000 ^{o}C. Therefore, it was concluded that 1000 ^{o}C is the optimum temperature for prereduction for the system used in the present study. Although the detailed information was not given in the scope of the current work, Fe^{3+} results were found to be in an agreement with this conclusion.
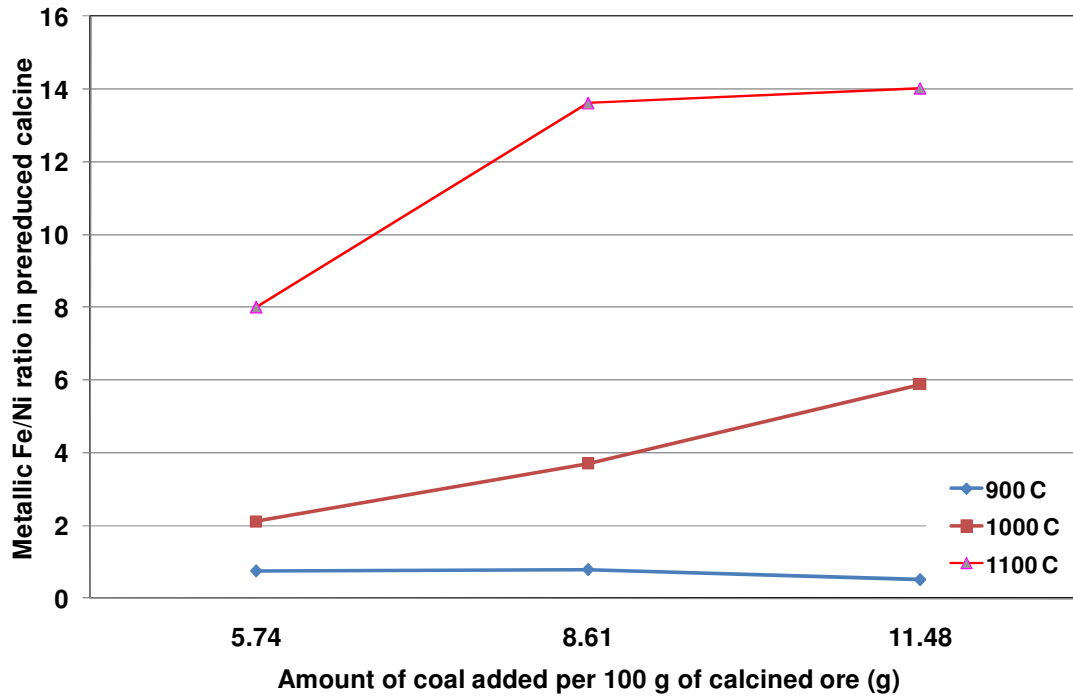
Figure 6: Variation of metallic Fe/Ni ratio in prereduced calcine with coal content
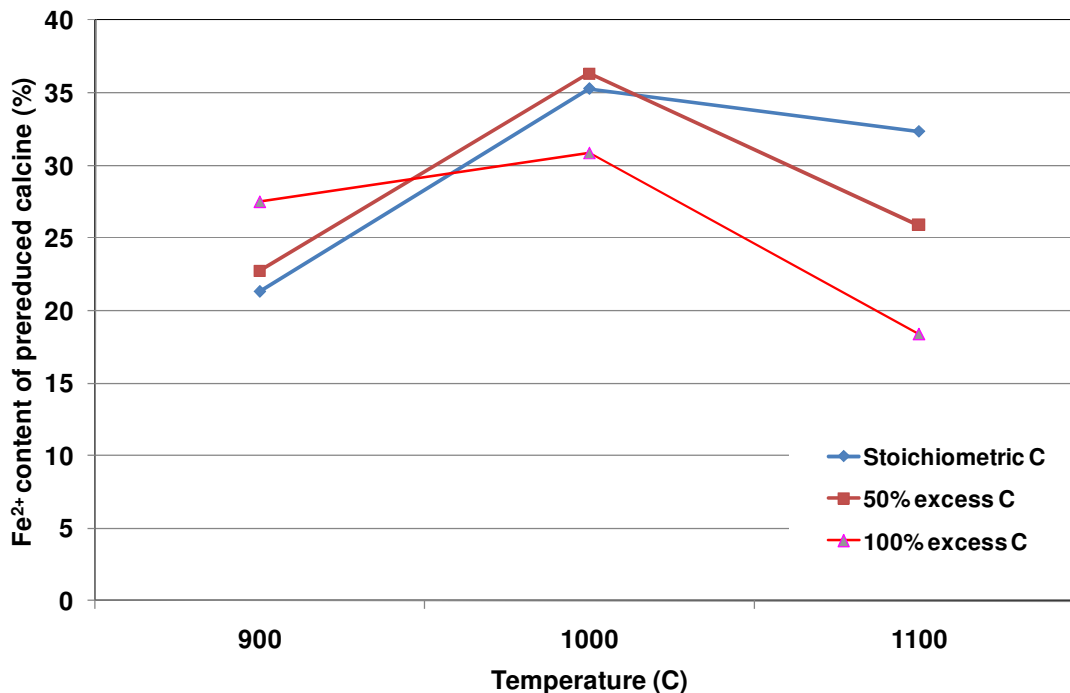
Figure 7: Variation of Fe^{2+} composition of prereduced calcine with temperature for different coal contents

As indicated previously, the amount of magnetite present in prereduced samples was measured using SATMAGAN. Although a detailed discussion was not included in the scope of the present paper, the measurements showed that the magnetite content stayed in 20-25% interval at 900 ^{o}C with a slight decrease as coal content increased. At 1100 ^{o}C, on the other hand, the magnetite composition was reported to increase linearly with the coal content. The highest magnetite values of 30.6% and 45.1% were reported when 50% excess carbon and 100% excess carbon was charged to the system, respectively. The smallest magnetite values were obtained at 1000 ^{o}C such that the magnetite content stayed in the range of 12-17%.

The effect of reduction time on magnetite composition was also investigated with the runs conducted with the addition of 100% excess carbon at 1000 and 1100 ^{o}C (See Figure 8.). SATMAGAN results showed that an increase in reduction time caused an increase in magnetite composition: At 1000 ^{o}C, the experiment performed for 40 minutes produced a calcine containing 12% magnetite. Magnetite content was found as 22.7% when the reduction time was extended to 60 minutes. This value was noted as 27.2% when the calcine was allowed to be reduced till the end of 80 minutes. Therefore, the reduction time should not be increased too much to control the magnetite content in the prereduced calcine. Similar results were obtained from the experiments conducted at 1100 ^{o}C. As mentioned previously, the optimum temperature for prereduction was determined as 1000 ^{o}C for the reduction system used in the present study. Therefore, it was further concluded that the reduction time of 40 minutes was fairly good to achieve the desired degree of reduction of nickel, iron and cobalt as well as to obtain the highest Fe^{2+} composition and the lowest magnetite content in the prereduced product.
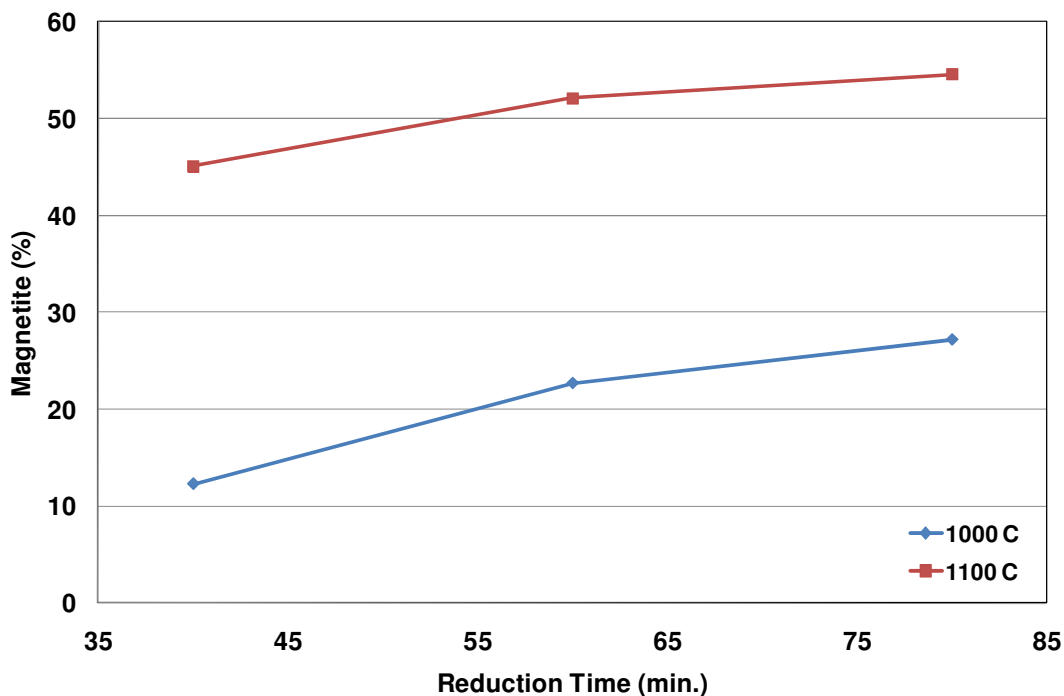
Figure 8: Variation of magnetite content with reduction time

CONCLUSIONS

Laboratory-scale prereduction of Sivrihisar laterite ores of Turkey was investigated. Effect of temperature, reduction time and the amount of coal addition on degree of reduction of nickel, iron and cobalt were studied. For the reduction system and ore particle size used in the current work, 1000 ^{o}C was determined to be the optimum temperature for prereduction. At this temperature, use of around 50% excess carbon was reported to produce the desired metallic Fe/Ni ratio in the prereduced product. It was further concluded that the reduction time of 40 minutes at 1000 ^{o}C was fairly good to achieve the desired degree of reduction of nickel, iron and cobalt as well as to obtain the highest Fe^{2+} composition and the lowest magnetite content in the prereduced calcine.

ACKNOWLEDGEMENTS

REFERENCES

1. A.D. Dalvi, W.G. Bacon, R.C. Osborne, International Laterite Symposium-2004 Roasting and Smelting, ed. W.P. Imrie et al., TMS, Warrendale, PA, p. 21, 2004.

2. M. Yuksel, "Recovery of Nickel from Lateritic Caldag Deposit", MS Thesis, Middle East Technical University, Ankara, Turkey, 1985.

3. Y.A. Topkaya, "Nickel Extraction from Lateritic Nickel Ores", TUBITAK Project, Project No: 106M079, 2009.

4. E. Buyukakinci, "Extraction of Nickel from Lateritic Ores" MS Thesis, Middle East Technical University, Ankara, Turkey, 2008.

5. E. Buyukakinci, Y.A. Topkaya, "Extraction of Nickel from Gordes Lateritic Ore with Atmospheric Leaching", ALTA 2008 Nickel/Cobalt Conference, Perth, Australia, 2008.

6. E. Buyukakinci, Y.A. Topkaya, "Extraction of Nickel from Lateritic Ores at Atmospheric Pressure with Agitation Leaching", Hydrometallurgy, 97, 33-38, 2009.

7. V. Ozdemir, "Ferronickel Production from Manisa Caldag Lateritic Ore", Report, General Directorate of Mineral Research and Exploration, 2008.

8. C. Colakoglu, "Production of Ferronickel from Domestic Lateritic Ores", MS Thesis, Istanbul Technical University, Istanbul, Turkey, 2008.

9. E. Keskinkilic, S. Pournaderi, A. Geveci, Y.A. Topkaya, "Calcination Behavior of Sivrihisar Laterite Ores of Turkey", 140th TMS 2011 Annual Meeting and Exhibition, San Diego, California, March 2011.

10. Y. Shirane, J. Min. Metal. Inst. Japan, vol. 85, 1001-07, 1969.

11. K. Kinson, J.E. Dickeson, C.B. Belcher, Anal. Chim. Acta, vol. 41, 107-112, 1968.

THE AGATA NICKEL PROJECT – PROJECT UPDATE

A POTENTIAL LOW COST NICKEL PRODUCER IN THE SURIGAO DISTRICT OF NORTHERN MINDANAO, THE PHILIPPINES

By

[1]Boyd Willis, [2]Jon Dugdale and [3]Tony Climie,

[1]Principal Consultant, Boyd Willis Hydromet Consulting, Australia
[2]Mindoro Resources Ltd, Australia
[3]Mindoro Resources Ltd, Philippines

Presenter and Corresponding Author

Boyd Willis
hydromet@boydwillis.com

ABSTRACT

Mindoro Resources Ltd (MRL) is undertaking feasibility studies into the development of an integrated nickel-cobalt laterite project at Agata in the Surigao District of Mindanao, the Philippines. The Agata deposit has a National Instrument NI 43-101 Measured and Indicated Resource of 32.6 million DMT at 1.04% nickel and 0.05% cobalt, and an Inferred Resource of 1.7 million DMT at 1.04% nickel and 0.04% cobalt. An Exploration Target of an additional 50 to 70 million DMT grading 0.9 to 1.2 percent nickel has been identified for other Surigao District tenements within 30 km north of the Agata resource.

A scoping study completed in 2010 considered processing options employing a combination of high pressure acid leach (HPAL) and atmospheric leach (AL) technologies. Preliminary metallurgical testwork has been performed on selected ore blends, demonstrating excellent leaching performance for HPAL of limonite and transition ores and AL of saprolite ores.

The project is conveniently located about 47 km northwest of Butuan City and 73 km southwest of Surigao City. The Surigao District is an historic and established mining district for copper, gold and nickel and is a politically stable and supportive jurisdiction for mining in the Philippines. These strategically located resources and exploration targets have strong competitive advantages: close proximity to established infrastructure and deep ocean port sites, no inhabitants or forest in the resource area, large regional population base, close proximity to markets, abundant limestone for acid neutralisation on site and plentiful fresh water. These attributes, combined with the quality of the resource and outstanding metallurgical characteristics, offer high potential for the establishment of a world class nickel and cobalt processing operation.

This paper reports on the findings of the scoping study, the metallurgical testwork results to date, and the selection of plant capacity and configuration for the Pre-Feasibility Study.

GENERAL

Location

The Agata Nickel Project is located within the northern part of Agusan del Norte province in North-eastern Mindanao, Republic of the Philippines. It lies within the Western Range approximately 10 km south of Lake Mainit (Figure 1) and falls within the political jurisdiction of the municipalities of Tubay, Santiago and Jabonga. The Project is located about 47 km north of Butuan City and 73 km south of Surigao City.
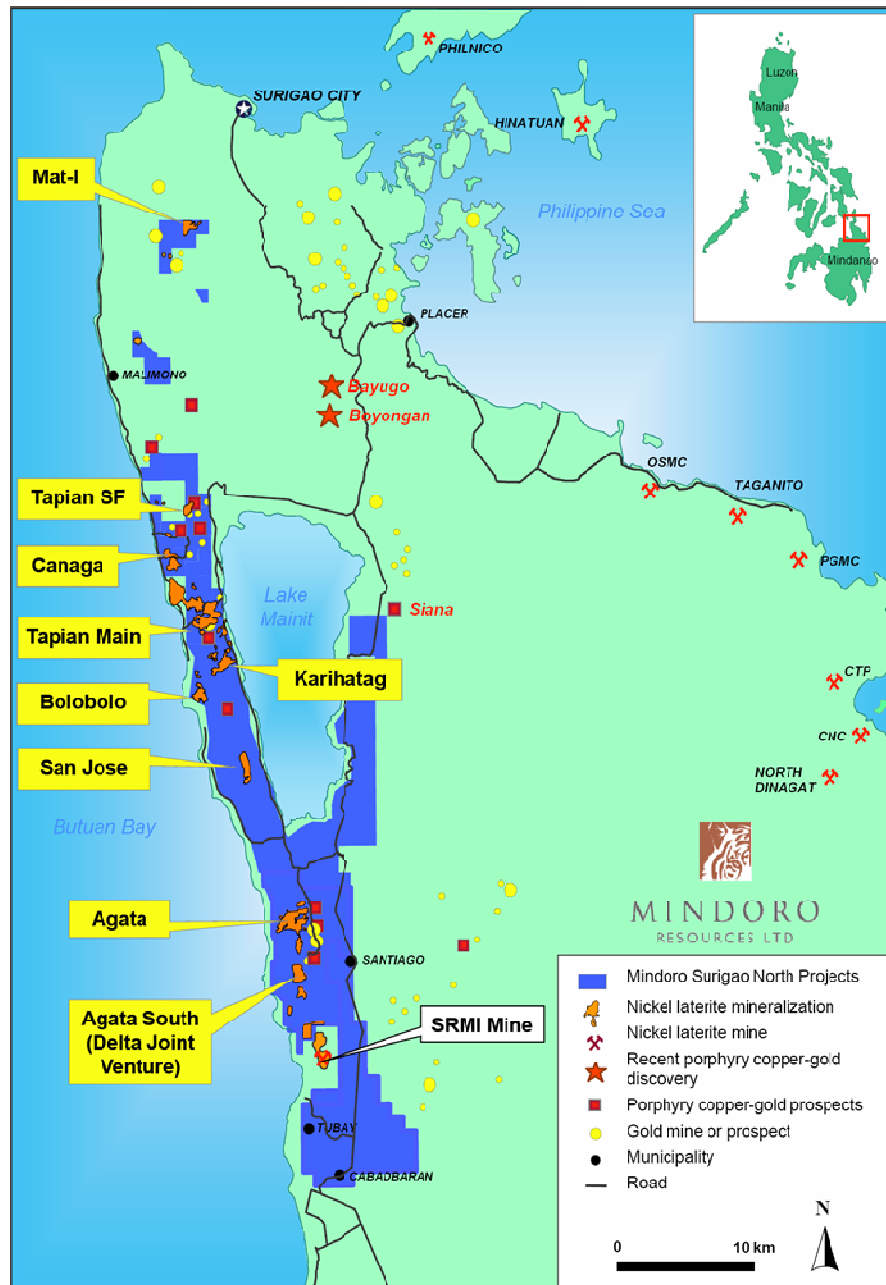
Figure 1: Location of Agata Nickel Project in Northern Mindanao

Figure 1 depicts the Agata Nickel Project's resources. The laterite resources are located in barangays Lawigan and Tinigbasan, municipality of Tubay, barangay E. Morgado (formerly Agata) and La Paz, municipality of Santiago, and barangay Colorado, municipality of Jabonga, all in the province of Agusan del Norte. The majority of MRL's exploration activities in the project area are located in barangays Lawigan and E. Morgado[1].

The Agata Nickel Project is situated within the established mining district of Surigao and the location offers several advantages, such as no population or forest in the resource area, close proximity to established infrastructure, large local population, abundant fresh water, an abundant supply of limestone on site for acid neutralisation, protected deep ocean access, and a short shipping distance to China and other potential Asian markets.

The proposed process plant and port site are situated in barangay Binuangan, municipality of Tubay, shown at the bottom of Figure 2. The Tubay river, which is about 3km from the proposed plant site, has been identified by Coffey[2] (E63511-1) as the major raw water source.

Accessibility

The Agata laterite deposit is accessible by land vehicle from either Surigao City or Butuan City or Davao City via the Pan-Philippine Highway (AH26). At the highway junction in barangay Bangonay, Jabonga, the access is through a partly sealed, gravel paved Jabonga Municipal road for approximately 4 km, then another 6 km via a farm-to-market road (FTMR) to barangay E. Morgado, Santiago (Figure 2)[1].
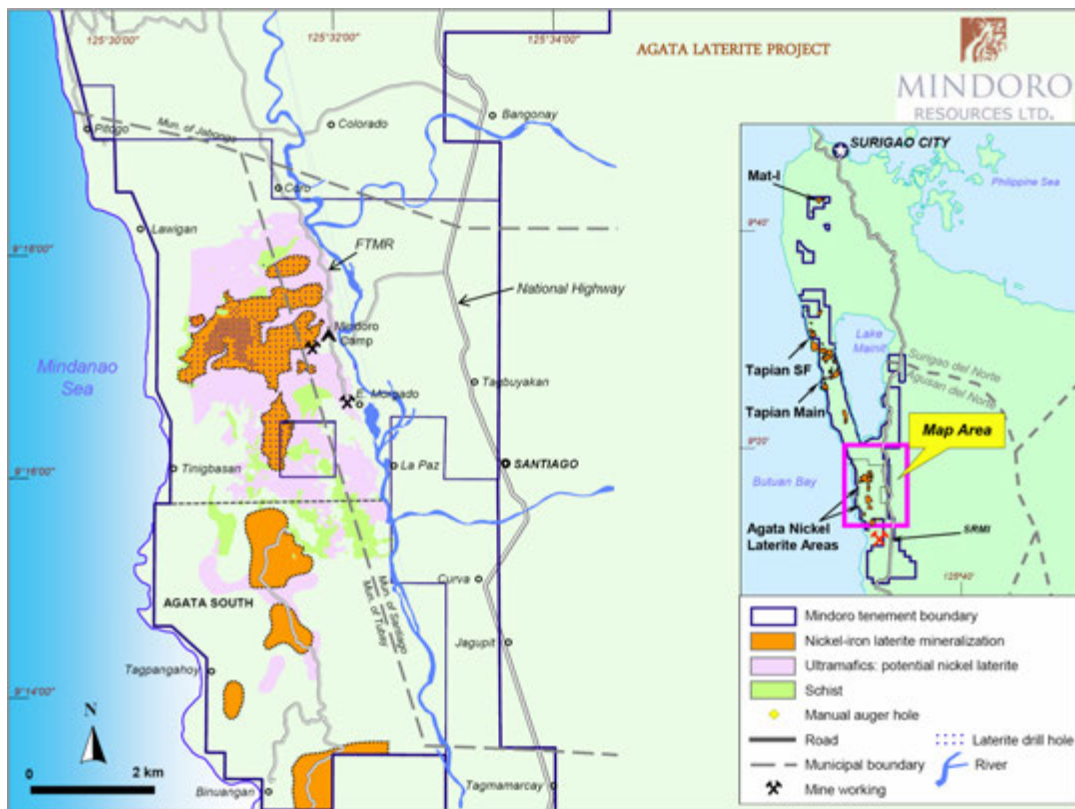
Figure 2: Agata Nickel Project Access Routes

Commercial passenger jet aircraft flights operate daily from Manila and Cebu City to Butuan City or Surigao City. Furthermore, commercial sea transport is available from Singapore, Jakarta, Manila, Batangas and Cebu to Surigao City, Cagayan de Oro (CDO) or Nasipit (west of Butuan City) ports.

An alternate road route exists from the Pan-Philippine Highway (AH26) via the municipality of Santiago. From the town proper, barangay E. Morgado can be accessed via a 1.5 km municipal-barangay road going to barangay La Paz via boat. The travel time is about 10 minutes via the Tubay River[1].

The northern portion of the Agata resource can be reached from barangay E. Morgado by hiking for about 1 hour along existing foot trails (approximately 1.5 km)[1].

The proposed process plant and port sites are situated near Binuangan, to the southwest of the Agata deposits. The location is also accessible via the Pan-Philippine Highway (AH26) and then via an existing municipal road.

Regional Population

A substantial population base exists within a short distance of the project area. The municipalities of Santiago and Jabonga, located within 10 km of the project area, each have populations of around 20,000 people. Situated about 35 km by road to the south, Cabadbaran City has a population of over 60,000. Butuan City, located about 65 km by road to the south, has a population of approximately 310,000, and Surigao City, located about 80 km by road to the northwest, has a population of approximately 132,000.

There are no inhabitants on the Agata resource area.

Climate

The climate of the Philippines is tropical and maritime. The climate in the Agusan del Norte and Surigao region, where the project is located, is categorised as Type II according to the PAGASA Modified Coronas Classification Map. Typically, there is almost no dry season with heaviest rainfall during the months of November to January (Figure 3).
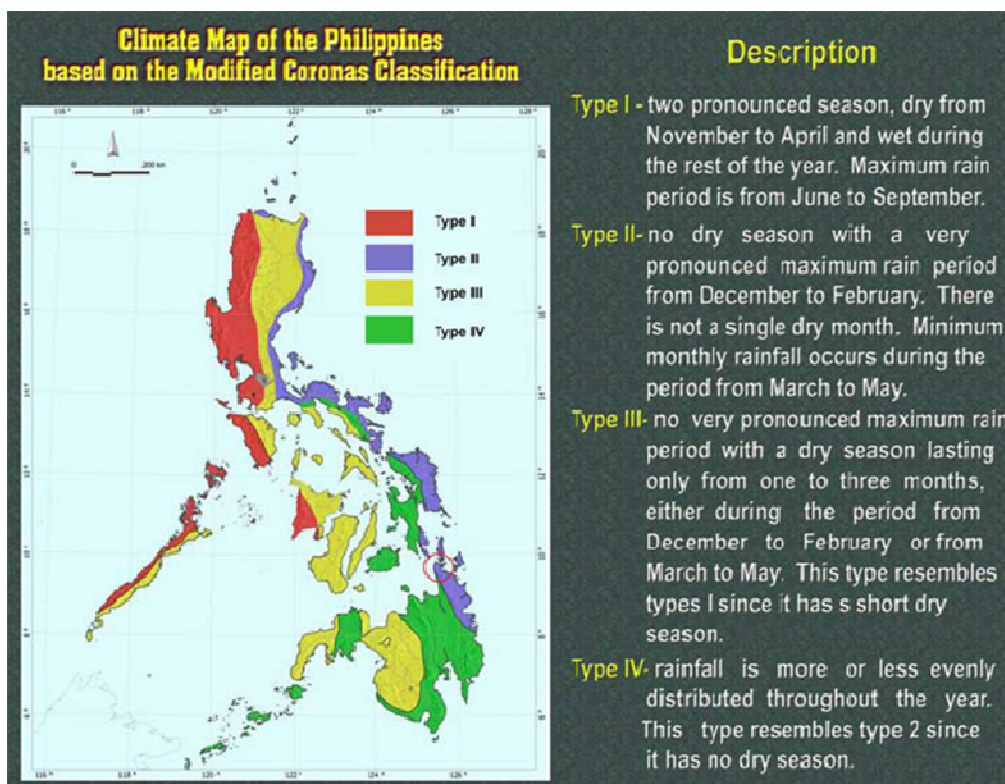
Figure 3: Climate Map of the Philippines

The mean annual temperature of the area is 27.6°C, with the coolest month in January at 26.1°C and warmest month in May at 28.8°C. The relative humidity is high and varies between 82% from April–May and 88% from December–January.

The project area is less prone to typhoons than the rest of Mindanao Island but it is not spared from the dangerous storms which often occur during the months of July to October.

Climatological records for the area from 1961 to 2000 (Table 1) show that the peak rainfall months are from October to February. The highest mean monthly rainfall is 308 mm during January and the lowest is 105 mm during May. The mean annual rainfall is 2027 mm.

Month	Rainfall		Temperature						RH %	Wind		Cloud Amt (okta)
	Amount (mm)	# of Days	Max	Min	Mean	Dry Bulb	Wet Bulb	Dew Pt.		Dir	Spd	
Jan	308.0	21	30.1	22	26.1	25.7	24.2	23.6	88	NW	1	6
Feb	211.8	15	30.8	22	26.4	26.0	24.2	23.5	86	NW	1	6
Mar	149.8	16	31.8	22.4	27.1	25.7	24.5	23.7	83	NW	1	5
Apr	107.2	12	33.1	23.1	28.1	27.7	25.2	24.3	82	ESE	1	5
May	104.8	14	33.8	23.8	28.8	28.3	25.8	25.0	82	ESE	1	6
Jun	135.1	16	33.0	23.6	28.3	27.8	25.5	24.7	83	ESE	1	6
Jul	157.5	16	32.5	23.3	27.9	27.5	25.3	24.5	84	NW	1	6
Aug	105.1	12	32.8	23.5	28.1	27.8	25.4	24.6	82	ESE	2	6
Sep	140.2	14	32.8	23.3	28.1	27.7	25.4	24.6	83	NW	2	6
Oct	195.3	17	32.3	23.2	27.8	27.4	25.3	24.6	84	NW	1	6
Nov	193.7	18	31.6	22.9	27.2	26.9	25.1	24.5	86	NW	1	6
Dec	218.4	19	30.8	22.5	26.7	26.3	24.7	24.1	88	NW	1	6
Annual	2026.9	190	32.1	23.0	27.6	27.1	25.1	24.3	84	NW	1	6

Based on Butuan City Synoptic Station

RESOURCES

The Agata Nickel deposits are situated along the southern part of the uplifted and fault-bounded Western Range of the northern end of the east Mindanao Ridge. Greenschist metamorphosed volcano-sedimentary sequences, ultramafics, limestones, andesitic volcanics and tuff, younger limestones, intrusive rocks, and alluvium underlie the area. The laterite profile, from surface to Increasing depth (up to approximately 20m), consists of ferruginous laterite, limonite and saprolite zones or horizons, and saprolitic rock. The limonite zone is characteristically iron oxide-rich where the predominant minerals are goethite, quartz, chromite, and magnetite-hematite, and with moderate nickel content (>1%), while the predominant minerals in the saprolite zone are saponite clays and serpentines, with much less iron oxide, and a slightly higher nickel content than the limonite zone[3][,5].
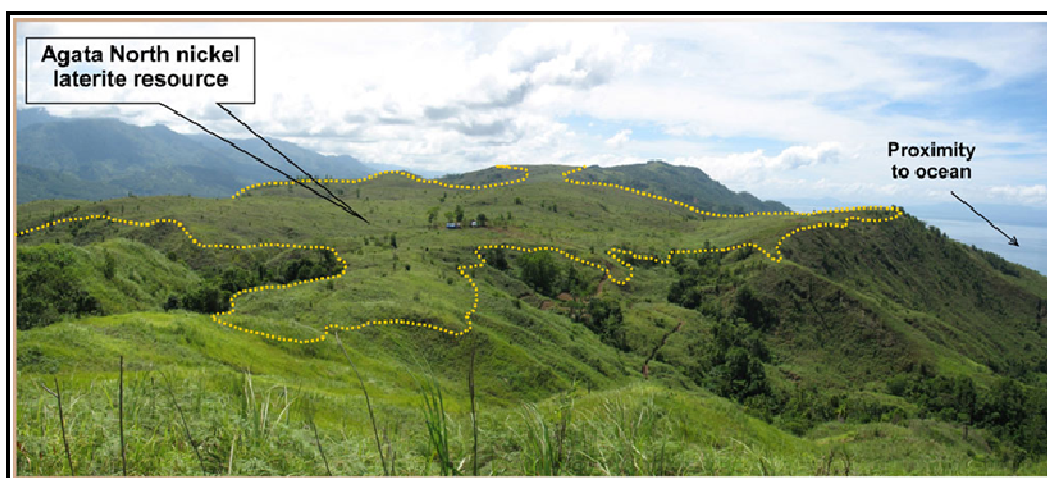
Figure 4: Photograph of the Agata Laterite Resource Area (looking south)

The Agata Nickel Project has estimated combined measured and indicated resources of 32.59 million dry metric tonnes (DMT) at 1.04% Nickel, and an inferred resource of 1.68 million DMT at 1.04% Nickel for a combined 357 500 tonnes of Nickel, as reported in MRL's NI 43-101 compliant mineral resource estimate of 9 September 2010[4], and described in a technical report published on SEDAR in October 2010, using a cut-off grade of 0.5% Ni for limonite and 0.8% Ni for saprolite. The summary of the NI 43-101 compliant mineral resource is presented in Table 2.

Table 2: Recalculated Agata North Laterite Resources (Ni 43–101), September 2010

Classification	Horizon	kT (dry)	Ni %	Co %	Fe %	Al %	Mg %	SiO$_2$ %
Measured	Limonite	247	1.01	0.12	48.26	2.94	0.98	4.70
	Saprolite	535	1.15	0.03	10.96	0.37	18.03	41.68
	Sub-Total	782	1.10	0.06	22.74	1.18	12.66	30.02
Indicated	Limonite	9,963	0.94	0.11	45.52	3.39	1.25	5.85
	Saprolite	21,847	1.09	0.03	11.47	0.51	17.04	39.90
	Sub-Total	31,811	1.04	0.05	22.74	1.41	12.09	29.24
Measured + Indicated	Limonite	10 210	0.94	0.11	45.59	3.37	1.24	5.82
	Saprolite	22 382	1.09	0.03	11.46	0.51	17.06	39.95
	Total	**32 592**	**1.04**	**0.05**	**22.15**	**1.41**	**12.11**	**29.24**
Inferred	Limonite	260	1.00	0.11	44.52	3.24	1.77	9.91
	Saprolite	1 421	1.05	0.03	11.80	0.53	17.06	40.26
	Total	**1 681**	**1.04**	**0.04**	**16.85**	**0.95**	**14.69**	**35.58**

  ∗ *Total metal contents in the reported resources represent metal in the ground and have not been adjusted for metallurgical recoveries and other factors which will be considered in a later study.*

  ∗ *Mineral resources which are not mineral reserves do not have demonstrated economic viability.*

  ∗ *The estimate of mineral resources may be materially affected by environmental, permitting, legal, title, taxation, socio-political, marketing or other relevant issues.*

A drilling program is currently being undertaken to cover the greater part of the Agata Exploration Potential (Figure 6), consisting of an area of approximately 800 hectares, based on an average projected thickness of 6m and specific gravity (SG) of 1.25. The additional Exploration Target covers approximately 80% of the total Agata deposits identified and is estimated to be in the range 50-70 million DMT at a grade of 0.9 to 1.2% Ni (Figure 7).

Recent drilling on a 50m x 50m grid pattern at Bolobolo (see Figures 1 and 7) will provide sufficient drilling density to enable calculation of indicated resources upon completion of the full regional program, and current drilling results include:

- BBL-22: Total 6.65m @ 1.23% Ni from surface including:
    Saprolite 5.15m @ 1.23% Ni from 1.50m
- BBL-38: Total 8.95m @ 1.10% Ni from surface including:
    Saprolite 5.60m @ 1.23% Ni from 3.35m
- BBL-40: Total 8.45m @ 1.22% Ni from surface including:
    Saprolite 5.95m @ 1.18% Ni from 8.45m
- BBL-52: Total 9.70m @ 1.19% Ni from surface including:
    Saprolite 8.85m @ 1.24% Ni from 0.85m
- BBL-57: Total 7.25m @ 1.10% Ni from surface including:
    Saprolite 5.30m @ 1.24% Ni from 1.95m
- BBL-65: Total 7.50m @ 1.22% Ni from surface including:
    Saprolite 5.55m @ 1.30% Ni from 1.95m
- BBL-98: Total 10.30m @ 1.01% Ni from surface including:
    Saprolite 7.50m @ 1.13% Ni from 2.80m

The reader is cautioned that the potential quantity and grade of the Exploration Target is conceptual in nature; it is uncertain if further exploration will result in the Exploration Target being delineated as a mineral resource and there is no guarantee that these resources, if delineated, will be economic or sufficient to support a commercial mining operation. The company's production objectives are intended to provide an indication of management's current expectations and are still conceptual in nature. It is uncertain that it will be established that these resources will be converted into economically viable mining reserves. Until a feasibility study has been completed, there is no certainty that these objectives will be met.

Figure 5: Drill Rig on the Agata Nickel Laterite Project
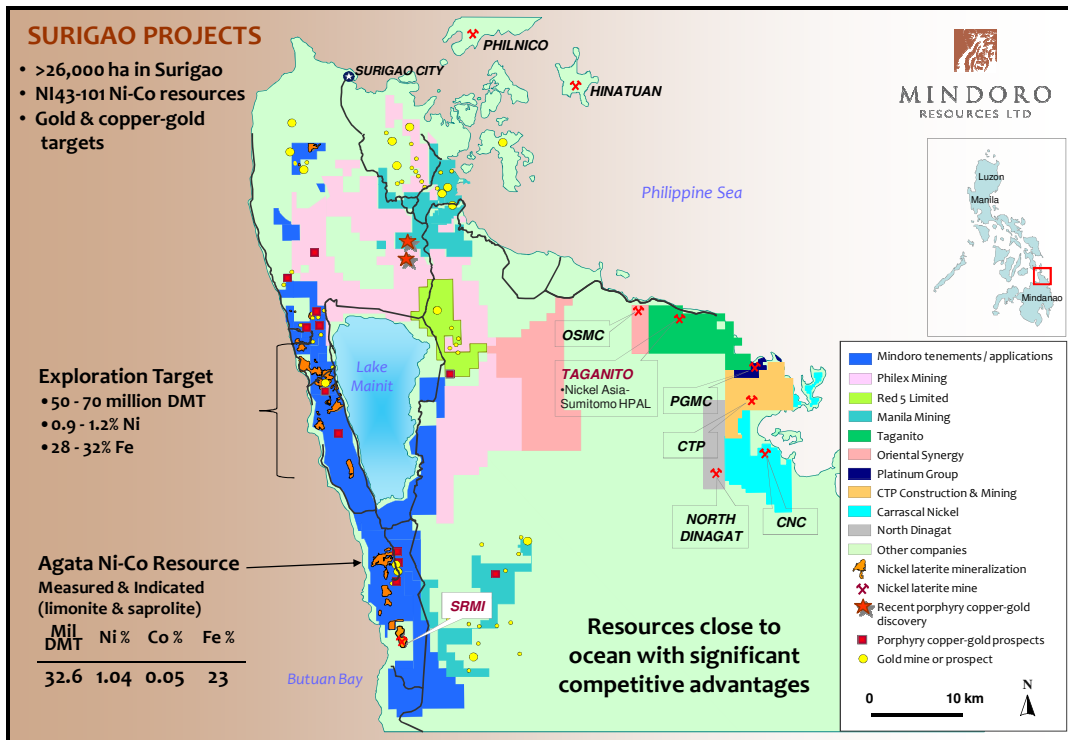
Figure 6: Agata Nickel Project Resources
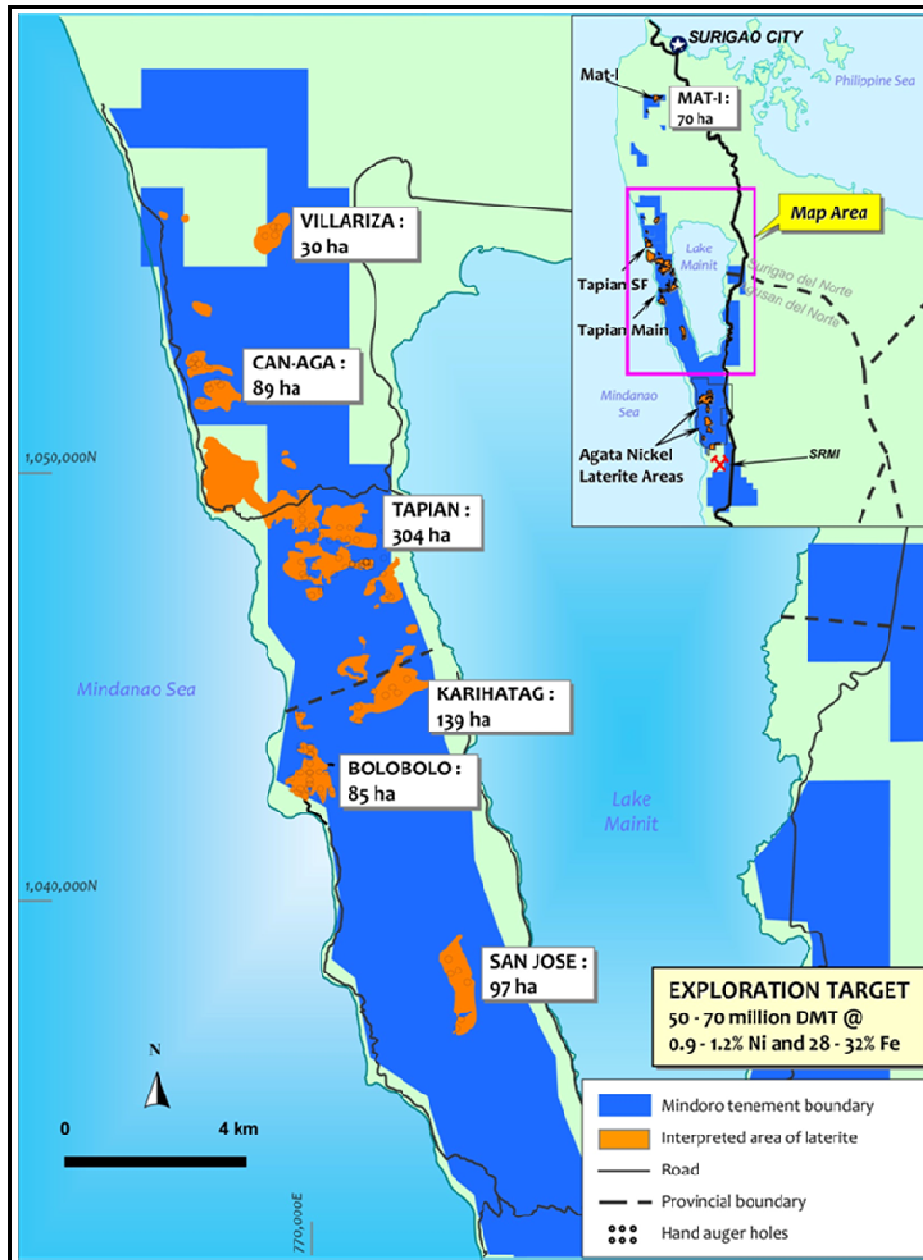
Figure 7: Agata Nickel Project Exploration Target

METALLURGICAL DEVELOPMENT

Early Testwork - Enlin Stainless Steel Corporation

A preliminary metallurgical testwork investigation for the Agata nickel laterite ores was conducted by Enlin Stainless Steel Corporation (ESSC) in the Philippines. The bench scale testwork included atmospheric leaching, HPAL, saprolite neutralisation, limestone neutralisation / iron removal and mixed hydroxide precipitation. The following points summarise the testwork performed:

- The testwork was conducted using limonite, transitional and saprolite ore.
- Particle size analysis suggested that nickel and other components were distributed throughout the size fractions of the material, however no ore scrubbing or de-agglomeration was attempted. (Subsequent preliminary scrubbing testwork at SGS Lakefield Oretest indicated that upgrading of limonite ore is possible).
- Ore slurry thickening to 50% solids was reportedly achieved without the aid of flocculant. This is questionable since laterites are typically clayey materials and hard to settle without proper

flocculation. A conservative value of 35% solids was therefore assumed for the recent scoping study.

- Approximately 90% nickel extraction was achieved in atmospheric leaching of saprolite at an acid dosage of 900 kg/t.
- 94-99% nickel extraction was achieved in HPAL with residence times of 20-40 minutes and acid dosage of 275-400 kg/t.
- Saprolite neutralisation achieved 82-95% nickel extraction in 2 hours.
- Iron removal / solution neutralisation was conducted using limestone addition and typical results were obtained.
- Mixed hydroxide precipitation was tested to recover the nickel and cobalt using caustic soda or magnesia slurry.

Testing at SGS Lakefield Oretest (SGS)

A more detailed program of metallurgical testwork was undertaken in 2010 by SGS Lakefield Oretest in Perth, Western Australia, to investigate the metallurgical characteristics of the Agata ores[5].

Testwork Samples

The samples were sourced as intervals from the walls of three metallurgical test pits located to target three ore types. The intervals used, and test pit identifications, are presented in Table 3. The samples were blended so as to target elemental composite grades similar to that of global resource values, especially those elements influencing leaching properties such as iron and magnesium.

Table 3: Source of Metallurgical Test Samples

Location ID/Pit	Zone	Pail No	Interval m	Weight kg	Total Weight kg
AGL 281	Limonite	1	1.00-1.40	42.50	
		2	1.40-1.70	35.36	
		3	1.70-2.00	40.35	118.21
AGL 373	Transition	4	1.20-1.70	32.00	
		5	1.10-1.70	36.05	
		6	1.10-1.70	40.25	109.30
AGL 300	Saprolite	7	2.00-5.00	36.36	
		8	5.00-8.00	32.69	
		9	8.00-11.00	36.52	108.57

Limonite, Transition and Saprolite composites were initially prepared, however MRL's mining group advised that transition ore would report with limonite ore as feed for HPAL processing. A fourth composite was therefore prepared as a blend of limonite and transition ore, and was identified in testwork as L/T Blend. The L/T Blend sample was mixed in the ratio of 95% limonite and 5% transition ore.

Drill samples were sourced from the Payong Payong limestone deposit near the mine and were blended by SGS to form a limestone composite sample for testwork.

Mineralogy

Mineralogical examinations of size fractions from the Limonite and Saprolite composites were undertaken by SGS South Africa. A subsample of each composite was screened into four size fractions (+212 µm down to -38 µm) for examination. The main objective of the work was to investigate mineral liberation and nickel deportment in the samples.

The investigations included qualitative XRD analysis; chemical analysis; electron microprobe analysis of the mineral phases present; and QEMSCAN analyses.
Some key observations from the work on the limonite sample fractions were:

- The ore is predominantly of made up of quartz, chromite and iron hydroxides.

- The amount of quartz in size fractions decreases with decreasing screen size. Almost all of the quartz is rimmed by iron hydroxides.
- The amount of chromite decreases with decreasing screen size. The chromite is mostly well liberated.
- The amount of iron hydroxides in screen fractions increases with decreasing screen size. The iron hydroxides are well liberated in the -75 µm fractions but relatively poorly in the +75 µm fractions. Most of the unliberated iron hydroxides in the +75 µm fractions are intergrown with Mn-wad, magnetite-hematite and/or contain silicate inclusions. Most of the nickel is hosted by the iron hydroxides.
- The Mn-wad in limonite is poorly liberated and is closely associated with the iron hydroxides. The Mn-wad contains significant nickel.

Some key observations from the work on the Saprolite sample fractions were:

- The saprolite size fractions consist primarily of altered serpentine and saponite clay (an alteration product of serpentine)
- The Mg:Si ratios of the serpentine and saponite are on average 1.1 and 0.9 respectively as the Mg is leached from the serpentine during alteration
- The iron hydroxides present in the fractions are poorly liberated in the serpentine
- Approximately 50-60% of the serpentine is liberated. The saponite is mostly well liberated. Unliberated saponite is mostly associated with iron hydroxides as rims.
- The serpentine is nickel rich

The mineralogical work suggests that moderate upgrading may be able to be achieved by rejection of quartz in coarse fractions.

SGS also considered that the saprolite ore would be amenable to atmospheric sulphuric acid leaching as none of the fractions were observed to contain excessive iron oxide/hydroxides or a high iron content.

Head Analyses

Head analyses were conducted on the four samples. The samples were subjected to a four acid digest and metal elemental compositions determined by ICP-MS. Si and Cr were determined by XRF.

The analytical results are presented in Table 4.

Table 4: Head Analyses of Metallurgical Composites

Sample	Ni %	Co %	Al %	Mg %	Si %	Cr %	Ca %	Fe %	Mn %
Limonite	1.32	0.087	2.37	1.00	7.4	1.97	0.08	42.7	0.76
Saprolite	1.29	0.024	0.40	14.7	18.1	0.61	0.16	12.9	0.18
Transition	1.52	0.048	1.08	6.78	14.4	1.42	0.41	26.6	0.41
L/T Blend	1.33	0.086	2.39	1.3	7.7	2.00	0.10		0.75

The sample blends were prepared with the main objective of achieving similar grades to the scoping study mine schedule in species significant to leach chemistry, particularly iron, magnesium and aluminium.

Ore Scrubbing and Head Sizing

A sub-sample of each composite was lightly scrubbed to assist in removing iron hydroxides from silica particles, and then wet screened to examine potential for ore beneficiation by sizing. Scrubbing was achieved by soaking a 10 kg sub-sample of ore in water overnight and then bottle rolling the slurry for one hour prior to wet screening.

The mass, grade and metal recovery in wet screening for a reject screen size of 0.25 mm is summarised in Table 5.

Table 5: Scrubbing Test Results – Limonite/Transition Blend Sample

Sample	Fraction	Mass	Nickel		Cobalt		Magnesium	
		%	Grade %	Distrib %	Grade %	Distrib %	Grade %	Distrib %
L/T Blend	Feed	100	1.65	100	0.052	100	7.19	100
	-0.25 mm	80.7	1.83	89.6	0.049	77.2	5.29	59.3

The Limonite/Transition blend sample test results showed that some upgrading of nickel could be achieved by rejection of coarse fractions. The upgrading of nickel was accompanied by rejection of magnesium. Cobalt showed a poorer response than nickel. MRL plans to undertake further larger scale scrubbing testwork in the next phase of testwork.

Saprolite ore showed no potential for upgrading by beneficiation via scrubbing and sizing.

Feed Ore Settling Testwork

Settling testwork was performed on the limonite/transition blend and saprolite samples to determine requirements for thickening of leach feed. A flocculant screening program was first undertaken resulting in selection of Magnafloc 10 for the settling trials.

The settling tests were conducted in 2m high raked columns. The key test parameters and results are presented in Table 6.

Table 6: Ore Slurry Settling - Key Parameters

Parameter		Limonite		Saprolite	
Initial Density	% Solids	4.0	4.0	4.0	4.0
Final Density (24 h)	% Solids	39.9	40.4	33.8	35.9
Floc Dosage	g/t	150	200	150	200
Thickener Requirement					
30% Solids	m^2/tonne/day	0.59	0.57	1.11	0.54
35% Solids	m^2/tonne/day	0.67	0.65		0.58

The settling tests showed that a slurry density of over 40% solids for limonite ore and over 35% solids for saprolite ore could be achieved with flocculant additions in the range 150 to 200 g/t. Thickener unit area requirements are high at around 0.6 m^2/tonne/day.

Heap Leaching Amenability Testing

Agglomeration, percolation and bottle roll acid leaching testwork was conducted on crushed -25 mm saprolite to evaluate amenability to heap leaching.

The agglomeration tests were conducted in a cement mixer with varying additions of concentrated sulphuric acid. Agglomerates were then cured for three days in columns and flooded. After a 48 hour soak period, the ore height slump and column percolation maximum drain rate were determined. Results are presented in Table 7.

Table 7: Agglomeration Test Results

Agglomeration Acid kg/t	Slump %	Drain Rate L/m^2/h
50	0.0	52 700
100	2.4	43 100
150	8.6	2 300

The results showed that agglomeration acid additions of over 100 kg/t resulted in low drainage rates.

The response of ore samples to acid heap leach conditions was investigated by acid bottle roll leaching following agglomeration at 50 kg/t acid. The tests were conducted at 30% solids and

varying target free acid concentrations in leach over a period of 50 days. The nickel extraction results with leach time for each target acidity are presented graphically in Figure 8.

High nickel extractions of 90 to 99% were achieved, but at very high acid addition requirements of 887 to 985 kg acid/ tonne of ore. Both metal extraction and acid consumption increased as target acidity was increased from 25 to 50 g/L.

Nickel Extraction v Time
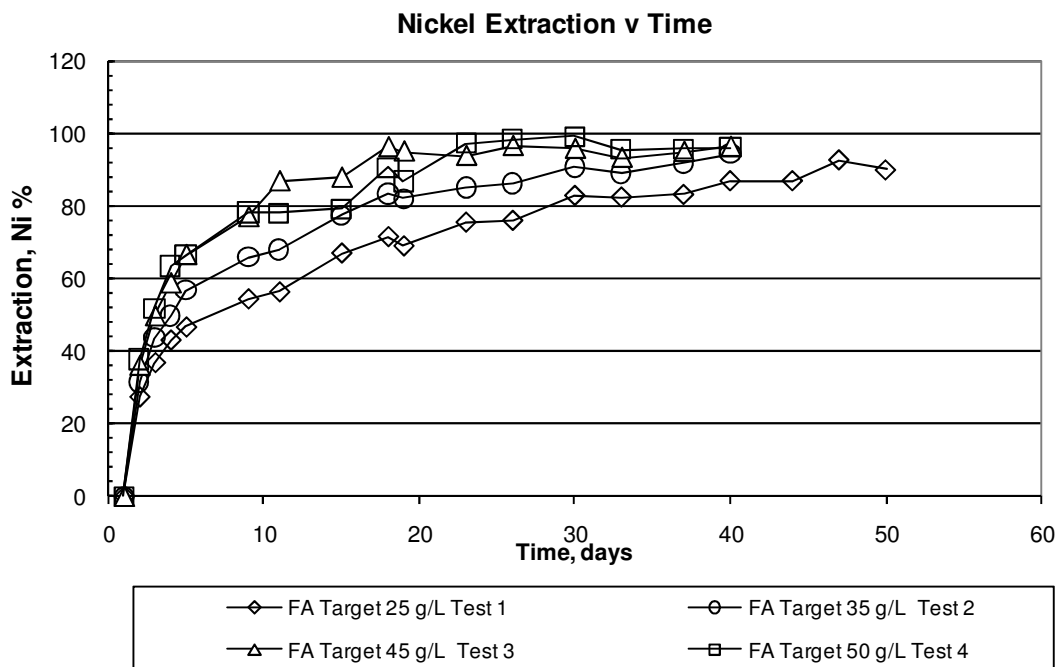
Figure 8: Acid Bottle Roll Test Results

High Pressure Acid Leach (HPAL) Testing

HPAL tests were conducted on the L/T blend sample at varying acid additions to examine extraction response with retention time and acid addition. All tests were conducted with slurry made up to 29% solids with a mix of seawater and fresh tap water blended in a ratio of 1.33 of sea to fresh. The target water blend reflects ore slurrying using seawater, adjusted for ore moisture content and process dilution by gland water, screen sprays, flocculant make-up water and condensation of live steam during slurry heating. All tests were conducted in a mechanically stirred laboratory batch autoclave at a temperature of 255 °C. Acid addition rates varied between 276 and 351 kg/t.

Some key results from the testwork program are presented in Table 8.

Table 8: HPAL Test Results on Limonite/Transition Blend Samples

Acid Dose	Over-pressure	Time	Free Acid	ORP	Extraction	
kg/t	Air, kPa	Mins	g/L	mV	Ni%	Co%
300	0	20	33.3	459	96.9	95.5
		30	36.4	466	97.4	96.0
		40	37.6	467	97.5	95.9
		60	36.8	170	97.6	96.1
325	0	20	32.9	467	98.0	95.6
		30	31.7	468	98.2	95.4
		40	33.1	468	98.4	95.7
		60	33.0	469	98.4	95.3
351	0	20	42.7	461	98.2	94.1

Acid Dose	Over-pressure	Time	Free Acid	ORP	Extraction	
kg/t	Air, kPa	Mins	g/L	mV	Ni%	Co%
		30	46.4	462	98.5	95.9
		40	42.9	472	98.7	95.9
		60	43.9	479	98.8	96.2
276	200	20	32.2	487	97.9	96.1
		30	35.7	501	98.2	94.8
		40	38.5	500	98.5	96.6
		60	38.3	496	98.7	96.4
325	250	20	42.4	486	98.4	96.1
		30	42.4	482	98.4	95.5
		40	43.0	476	98.5	95.6
		60	43.4	485	98.7	95.5
368	*	30	41.1	461	97.9	92.1
350	500	30	47.0	564	98.0	96.5
351	500	5	36.4	515	95.2	91.5
		10	37.5	493	97.1	93.4
		15	42.1	487	97.9	94.3
		20	44.9	499	98.2	94.9

* performed using MnO_2 as an oxidant instead of air

The results show that the ore exhibits very fast leaching kinetics, with approximately 97-99% of the nickel and 95-96% of the cobalt extracted within 20 minutes (Figure 9). Residual free acid levels ranged between 33 and 47 g/L. Ferrous iron concentrations in leach solution tended to be high (up to 9.6 g/L), but with air overpressure in the autoclave the concentration was decreased. Operating with air overpressure of 500 kPa resulted in a ferrous iron concentration of just 270 mg/L.
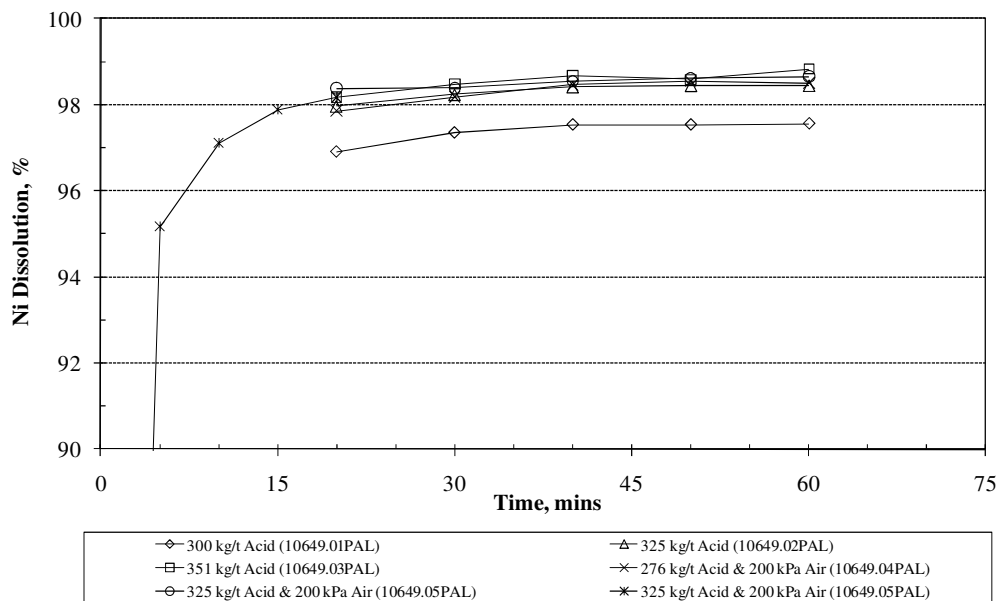
Figure 9: HPAL Nickel Extraction vs Time

47

Atmospheric Leach (AL) Testing

Atmospheric Leach (AL) tests were conducted on saprolite ore at 95°C with acid addition rates from 850 to 1000 kg/t. The samples were prepared using a sea water/fresh water mix in the ratio 3.8:1. The water blend reflects ore slurrying using seawater, adjusted for the impact of ore moisture and process dilution by gland water, screen sprays and flocculant make-up water.

The results of the AL tests are presented in Table 9.

Table 9: AL Tests on Saprolite Samples

Acid Addition	Time	Free Acid	ORP	Extraction	
kg/t	Mins	g/L	mV	Ni%	Co%
850	30	24.7	525	90.4	86.5
	60	14.1	550	92.9	86.8
	120	15.0	547	93.3	87.7
	180	15.3	544	93.5	87.8
	240	17.2	542	93.9	88.3
900	30	56.1	565	91.5	85.2
	60	40.8	558	95.7	88.0
	120	30.2	557	93.6	88.6
	180	26.3	554	94.5	89.3
	240	24.1	548	94.9	89.1
950	30	73.1	562	92.0	84.6
	60	47.6	560	93.7	89.1
	120	37.2	563	95.4	90.4
	180	32.3	558	96.3	91.5
	240	28.2	556	96.6	91.9
1000	30	78.4	547	93.7	87.6
	60	57.8	535	95.8	89.5
	120	47.4	521	96.6	91.3
	180	41.7	519	97.4	94.3
	240	39.2	509	97.6	93.6
950	240	26.9	553	97.4	94.1
	240	27.1	557	96.8	92.7
	240	29.3	561	96.4	92.7
949	240	27.1	557	96.8	92.7
950	240	29.3	561	96.4	92.7

The results indicated favourable leaching kinetics with 4 hour extractions of around 94 to 98% for nickel and 88 to 94% for cobalt. Initial leaching rates are fast, with over 90% nickel extraction in just 30 minutes. Leaching rates are illustrated in Figure 10.

Ferric and ferrous iron concentrations were shown to significantly increase with increasing acid additions. Magnesium concentrations in leach solution were very high at 65-75 g/L.
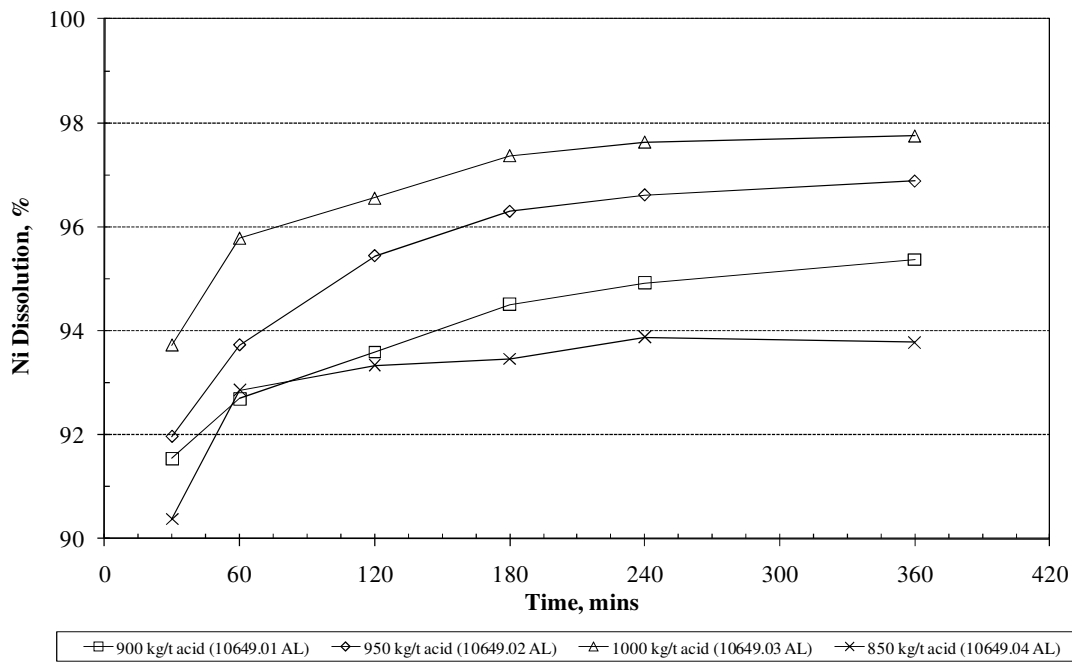
Figure 10: AL Nickel Extraction vs Time

Saprolite Neutralisation Testwork – Combined HPAL, AL Slurry

A combined leach pulp for the saprolite neutralisation testwork was prepared from two separate leach tests as follows:

- AL test on saprolite at 35% solids and 95°C for 240 minutes, with an acid addition of 950 kg/t
- HPAL test on L/T blend ore at 29% solids and 255°C for 30 minutes, at an acid addition of 350 kg/t

Saprolite ore for neutralisation was added to the combined leach pulps in varying ratios. In each test the slurry was agitated for six hours and kinetic samples taken to monitor solution acidity and elemental concentrations in liquids and solids.

Results from the saprolite neutralisation tests are summarised in Table 10.

Table 10: Saprolite Neutralisation Testing

Ratio of Feeds	Residual Acid	Residual Fe	Dissolution	
HPAL:AL:SN	g/L	g/L	Ni	Mg
1.00 : 0.79 : 0.26	19.6	8.10	87	83
1.00 : 0.79 : 0.31	10.3	6.84	80	79
1.00 : 0.79 : 0.36	11.2	5.15	82	86
1.00 : 0.79 : 0.48	7.5	4.65	79	85
1.00 : 0.79 : 0.36	**6.3**	**4.72**	**83**	**90**
1.00 : 0.79 : 0.31	**16.0**	**2.84**	**89**	**93**

A scoping test, during which saprolite ore was progressively added in the SN step to establish the optimal conditions for subsequent confirmatory tests, accounts for the first four test results shown in Table 10. The last 2 tests were confirmatory tests in which all of the SN feed ore was added at the start. The confirmatory tests demonstrated that neutralisation of a combined HPAL and AL pulp with saprolite ore resulted in the dissolution of 83-89% of the nickel and 78-87% of the cobalt contained in the neutralising saprolite. Concentrations of total iron in solution decreased with residual free acid due to precipitation of sodium jarosite, a side benefit of using seawater for ore slurrying.

The kinetics of the neutralisation reactions for the test with a HPAL:AL:SN feed ratio of 1.00:0.79:0.36 are shown in Figure 11.

Ni Extraction & Free Acid Concentration vs Time
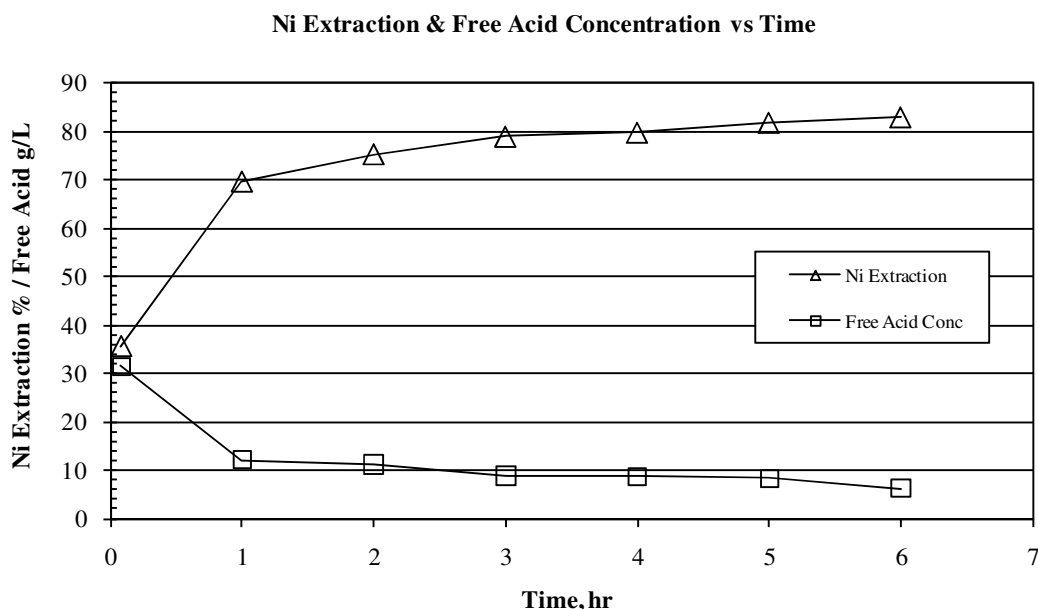
Figure 11: Saprolite Neutralisation of Combined HPAL and AL Pulps

Settling testwork on the pulp from the saprolite neutralisation confirmatory tests was performed in 2m raked columns. Test parameters and test results for the HPAL/AL/SN pulps are presented in Table 11.

Table 11: Settling Tests on Saprolite Neutralisation Slurry

Sample	Flocculant Dose g/t	Underflow Density (% w/w)	Thickener Unit Area (m^2/t/d)
SN.02 Final Pulp	80	35.7	0.24
Diluted to 4% Solids	160	38.5	0.09
SN.03 Final Pulp	100	40.2	0.09
Diluted to 4% Solids	120	38.1	0.09

The settling tests showed that a slurry density of 38-40% solids can be achieved for tests with flocculant additions in the range 100-160 g/t.

Limestone Reactivity and Calcination

Drill samples from one of the limestone deposits on the mining lease were obtained for testwork and a composite sample prepared.

A test on a sub-sample of limestone was undertaken to determine neutralisation activity. Testing involved neutralising a 48 g/L sulphuric acid solution with staged additions of dry ground limestone and pH monitoring. The neutralising capacity of the limestone was 0.94 tonnes acid per tonne limestone.

A sub-sample of the limestone was crushed to -25 mm +9 mm and then calcined in a furnace at 1050°C for varying residence times from 30 to 120 minutes. The test results showed that after 60 minutes the mass loss was 44% with an available lime of 92%. The neutralising capacity of the lime was 1.26 tonnes acid per tonne hydrated lime.

PFS Testwork Program at SGS Minerals (Lakefield, Canada)

A more comprehensive program of metallurgical testwork is currently underway at SGS Minerals in Lakefield, Canada, to provide design criteria for the Prefeasibility Study. This program will use ore blends reflecting the current mine plan and will include variability testing.

EVALUATION OF A POTENTIAL DIRECT SHIPPED ORE (DSO) OPERATION

DSO of Untreated Ore

In May 2008, an Environmental Compliance Certificate (ECC) was issued by the DENR to MRL for nickel laterite mineral production covering 600 ha within the Agata MPSA Contract area, to develop a Direct Shipped Ore (DSO) project, subject to certain lesser permit requirements, exporting 1.5 million DMT per annum (year 1) to 2 million DMT per annum (year 2 onwards). Preliminary discussions with potential offtakers have confirmed there is a market for limonite material containing >0.9% nickel and >48% iron as Nickel Pig-Iron feedstock, and for saprolite material containing >1.5% nickel for Electric Arc Furnace ferronickel production. DSO is traded on a "Wet Metric Tonnes (WMT)" basis and the ores contain approximately 35% moisture.

A scoping study, examining the potential to develop a small scale DSO operation, shipping up to 2 million wet metric tonnes (WMT) of ore per annum to destinations in the Asia Pacific region, was completed as part of the preliminary economic assessment (PEA).

The Mineral Resource estimate for the Agata Nickel Project released on the 9th September 2010, and described in a technical report published on SEDAR in October 2010, forms the basis of the mining inventory estimates for the three production scenarios below:

- Limonite Only: shipping 7.6 million WMT DSO over 3 years
- Saprolite Focus: limonite and saprolite, shipping 4.7 million WMT DSO over 2 years
- Limonite and Saprolite (optimum case), shipping 8.9 million WMT DSO over 4 years

The PEA financial modelling results for the three options are tabulated below:

Table 12: Financial Modelling Results for DSO

Parameter	Limonite	Saprolite	Limonite + Saprolite
Mine Life (years)	3	2	4
Nickel price NPV Break-even ($US/lb)	10.20	10.30	10.00
Initial Capital Cost ($US M)	8.0	8.0	8.0
Operating Cost ($US/t) Shipped	15	19	17
Mining Inventory - limonite (million WMT)	7.54	3.34	7.54
%Ni	0.92	0.98	0.92
%Fe	48	47	48
Mining Inventory - saprolite (million WMT)		1.43	1.36
%Ni		1.6	1.8
%Fe		13	13

Note 1: DSO pricing is based on generally applicable offtake, representing ~9% to 12% nickel payability.
Note 2: The potential quantity and grade of material included in the mining inventory is conceptual in nature and based solely on the Mineral Resources and includes Inferred Mineral Resources. There has been insufficient work to define a Mineral Reserve and it is uncertain if further work will result in the determination of a Mineral Reserve.

Thermally Upgraded DSO

Due to the relatively low margins and current market uncertainty associated with direct shipped ore, MRL is not planning to pursue a stand-alone DSO operation at this stage, but is examining the potential for thermal upgrading to enhance the value of the shipped product. The early results from thermal upgrading tests in progress at SGS-Lakefield in Perth, supervised by Hatch Associates Pty Ltd, are positive, and MRL has committed to further, larger scale testing at a Mines and

Geosciences Bureau (MGB) based testing facility in the Philippines. Positive results from this work and preliminary economic and marketing studies, will allow completion of a feasibility study into the early production stage of the project.

Thermal upgrading removes the moisture (including molecular water) from the material, which improves blending and handling properties. Most importantly, this dramatically reduces the shipping cost, which, in combination, achieves a premium price over unprocessed DSO material. Further upgrading of the nickel content can be achieved through optional process enhancements. If the nickel grade is increased - this is normally achieved pyrometallurgically by metallising and concentrating iron and nickel metal in the product – nickel is payable at a higher percentage of LME price, but at greater capital and operating cost.

HYDROMETALLURGICAL PROCESSING OPTIONS

Hydrometallurgical Process Options Considered in the Scoping Study

A detailed Scoping Study ([6]) by Ausenco Vector and Boyd Willis Hydromet Consulting, completed in September 2010, evaluated three potential processing options:

- Base Case – an integrated HPAL/Atmospheric Leaching (AL)/Saprolite Neutralisation (SN) project treating 2.75 million DMT of ore per annum. This option employed a Coral Bay Nickel sized autoclave (4.7 m ID). Nickel was recovered by Direct Solvent Extraction (DSX) followed by Electrowinning (EW) to produce a Ni-cathode product. The base case was designed to produce 27,400 tpa Ni as Ni-cathode.
- Option 1 - a scale-up of the base case, employing the maximum sized HPAL autoclave to date (5.4 m ID), as fabricated for Ambatovy, and treating 4.21 million DMT of ore per annum. The nickel production for this option increased to 42,000 tpa Ni as Ni-cathode.
- Option 2 – Atmospheric leaching of saprolite only, treating 1.44 million DMT of ore per annum. The nickel was recovered by hydroxide precipitation producing an intermediate Mixed Hydroxide Precipitate (MHP) product. The design capacity for this option was about 14,300 tpa Ni, contained in MHP.

The process plant costs for the three options (with the exception of the refinery area for the Base Case and Option 1) were developed from detailed estimates for similar nickel projects and locations. The applicable data were adjusted for flow or equipment capacity and currency movements. Costs for the refinery area for the Base Case and Option 1 were developed by Canopean Pty Ltd.

A contingency of 35% was applied to direct costs. The contingency reflects the state of development of the project, and allows a margin for changes to the process, and equipment selection and sizing, where specific design criteria are not yet available.

The capital cost estimates developed in the Scoping Study are summarised in Table 13.

Table 13: Capital Cost Estimates – Scoping Study Options

Description	Capital Costs (Million US$)		
	Base Case	Option 1	Option 2
Ore Preparation	34.23	43.73	15.96
Leach Section	175.28	226.57	72.17
Refinery/Products Section	161.56	208.87	13.10
Sulphuric Acid	105.81	134.95	99.32
Power Plant	77.42	98.16	45.50
Other Major Process Packages	46.30	61.44	47.47
Services and Utilities	39.26	49.34	22.05
Process Plant Infrastructure	154.75	215.15	129.70

Description	Capital Costs (Million US$)		
	Base Case	Option 1	Option 2
General Infrastructure	33.40	40.83	28.49
Other Direct Cost	9.56	12.51	4.83
Total Direct Cost	**837.56**	**1 091.54**	**478.60**
EPCM	103.53	135.83	52.82
Other Construction Services	78.64	107.64	38.22
Total Indirect Cost	**182.17**	**243.47**	**91.04**
Direct + Indirect Cost	1 019.73	1 335.01	569.63
Contingency	305.92	400.50	170.89
Total Project Cost	**1 325.65**	**1 735.51**	**740.52**
Project Cost, US$/annual lb Ni	**21.94**	**18.73**	**23.49**

The operating cost estimates developed in the Scoping Study are summarised in Table 14.

Table 14: Operating Cost Estimates – Scoping Study Options

Operating Costs (year 3 onwards)	US$ million/year		
	Base Case	Option 1	Option 2
Expense Item:			
Mining and Haulage	32.2	46.9	15.2
Labour	13.8	14.0	12.1
Reagents & Consumables	63.5	95.2	50.0
Maintenance Materials	22.9	29.4	9.7
Contract Expenses	12.1	15.7	12.2
Admin. & General Expenses	4.5	5.0	3.4
Total Operating Cost	**148.9**	**206.1**	**102.6**
Operating Cost US$/lb Ni	**2.47**	**2.22**	**3.25**
Operating Cost after Co-credits *	1.59	1.35	2.94

* Assumes a cobalt price of US$18/lb (12-month low) and 80% payable for cobalt contained in cobalt sulphide.

Preliminary Economic Assessment - March 2011

A Preliminary Economic Assessment (PEA) was completed by MRL in March 2011. The PEA evaluated an integrated HPAL/Atmospheric Leaching (AL)/Saprolite Neutralisation (SN) project treating 1.79 million DMT of ore per annum. The nickel is recovered by hydroxide precipitation producing about 18,000 tpa nickel contained in an intermediate Mixed Hydroxide Precipitate (MHP) product.

Process plant costs were developed from detailed estimates for similar nickel projects and locations. The capital cost estimates are developed using factored estimating techniques. Where applicable, an equipment scale-up/down and cost escalation is applied. Two factored estimating approaches are used in the study estimates: the model driven approach, which is applied to the direct costs, and the approach that factors the facility cost from the total equipment cost, which is applied to the project indirect costs.

The sulphuric acid plant cost was based on a recent pricing from a western supplier for a nickel laterite project in the Philippines. Other major packages such as the power plant and auxiliary boilers, the limestone and lime plant were all based on recent vendor quotations for a similar nickel project.

The residue storage facility cost was based on costing calculations by Golder, adjusted to allow for staged construction of the storage area/s.

The infrastructure costs were based on a nickel project in the Surigao region that has recently entered the construction phase.

The indirect costs were prepared on the basis of a project management team being retained to perform the services of engineering, procurement of major equipment and management of construction.

A contingency of 30% has been applied to direct costs. The contingency reflects the state of development of the project, and allows a margin for changes to the process and equipment selection and sizing where specific design criteria are not yet available.

The capital cost estimates developed in the PEA are summarised in Table 15.

Table 15: PEA Capital Cost Estimate

Description	Capital Costs (US$ Millions)
Ore Preparation	29.5
Leach Section	129.8
Products Section	10.1
Sulphuric Acid	92.8
Power Plant	48.0
Other Major Process Packages	7.5
Services and Utilities	26.5
Process Plant Infrastructure	198.3
General Infrastructure	23.8
Total Direct Cost	**566.3**
EPCM	62.8
Other Construction Services	58.8
Total Indirect Cost	**121.6**
Direct + Indirect Cost	687.9
Contingency	206.4
Total Project Cost	894.3
Project Cost, USD/annual lb Ni	**23**

A deferred capital amount of US$ 21.1 M per annum is allocated after year 6 for expansion of the residue storage facilities.

The accuracy of the capital cost estimates are aimed at ±35%.

Operating costs have been developed for each year of operation based on the projected project ramp-up. Year 3 is considered to represent full nameplate production.

Table 16 details the operating cost data for the PEA flow sheet after ramp-up in Year 3. Estimated costs are presented in February 2011 US dollar (US$) values. For Year 3 onwards (full nameplate capacity), the project operating costs are US$ 106 M per annum or US$ 2.61 per pound of nickel (excluding cobalt credits). The main operating cost items are sulphuric acid production, processing costs, and mining and haulage (in order). Operating costs (per pound of nickel) are higher in Years 1 and 2 of production due to lower metal production during project ramp-up, particularly Year 1 of the project.

Table 16: PEA Operating Cost Estimates

Description	Operating Costs in US$/lb Ni
Expense Item:	
Mining and Haulage	0.54
Labour	0.31
Sulphuric Acid Production	0.62
Processing	0.61
Utilities	0.04
Maintenance	0.31
Admin., Overheads and Marketing	0.18
Total Operating Cost	**2.61**
Operating Cost after Co-credits *	2.16

* Assumes a cobalt price of USD18/lb (12-month low) and 50% payable for cobalt contained in mixed hydroxides.

The accuracy of the operating cost estimate is considered to be ±35%.

More power is generated from acid plant surplus steam than the project requires. Approximately 106,000 MWh per year of power is available for export to the grid. Mindanao is experiencing a power crisis and power costs are high, with diesel generator cost recoveries at PhP 7–9/kWh and long-term costs forecast to be PhP 12–15/kWh. After applying a credit of PhP 8/kWh (US$ 186/MWh) for power exported to the grid, the operating cost reduces to US$ 1.65/lb nickel for Year 3 onwards.

Readers should note that the unit operating costs presented above are low in comparison with available published information from some nickel laterite operations in production. The relatively low cost of the proposed operations will need to be confirmed in more detailed studies.

The key inputs to the operating cost development were as follows:

- mining and haulage costs of US$8.50 per wet tonne, developed by MRL;
- manning levels evaluated for each project area and labour rates at different salary levels, including on-costs, sourced from Philippine based HR consultant's data;
- reagent and consumables quantities based on the process mass and energy balances and unit pricing sourced from both budget pricing and from data for recent projects;
- estimated costs of spare parts and maintenance consumables using historical ratios for similar scale plants based on the installed equipment costs;
- contract expenses estimated for a range of services provided to the project on a contract basis, including: product transport and insurance, contract maintenance, periodic metallurgical testing and consultants fees in areas such as safety and training
- administration and general expenses estimated for a range of miscellaneous expenses associated with providing services to the project, including: insurances, safety equipment and training, medical costs, community relations, vehicle operating costs, environmental costs, human relations costs, telecommunications costs, business travel, Manila and Butuan City office costs.

MINING

Mining will be carried out by industry standard open cut methods that are commonly practised in the Philippines and elsewhere. Excavators and articulated dump trucks, supported by standard auxiliary fleet (dozers, graders, watercarts) are proposed, and will be operated by an experienced Philippine mining contractor. Mining will be relatively selective on 2-3m high benches and will involve a range of grade control and stockpiling strategies. The minor amounts of overburden generated will ultimately be used in rehabilitation of the natural surface. Management of road quality and surface water flows will be the key areas of focus for the mining operation to minimise and control the sediments generated from the earthmoving activities. The haulage of ore to plant stockpiles will be carried out by the mine contractor's fleet as the haulage distance is typically less than 8 km.

A preliminary Mining and Plant Feed Schedule for the first 15 years of operations was developed for the PEA The Mining Inventory used as a basis for the schedule was subset of the resource from the September 2010 NI 43-101 compliant resource estimate.

The mining inventory production schedule has been produced based on preliminary open pit designs. The total mining inventory is summarised in Table 17

Table 17: Proposed Mining Inventory by Ore Type for Processing

Mining Inventory Type:	kT (dry)	Nickel %	Cobalt %	Iron %	Mg %
Limonite to HPAL	9,500	0.95	0.11	45.6	1.2
Low Mg Saprolite to HPAL	4,700	1.20	0.03	14.2	14.1
Medium Mg Saprolite to AL	6,000	1.15	0.03	11.6	17.1
High Mg Saprolite to SN	5,900	1.03	0.02	9.7	19.1
Total	**26,100**	**1.05**	**0.06**	**24.0**	**11.2**

Note that the potential quantity and grade of material included in the mineral inventory is conceptual in nature and based solely on the Mineral Resources and includes Inferred Mineral Resources. There has been insufficient work to define a Mineral Reserve and it is uncertain if further work will result in the determination of a Mineral Reserve.

The pit shell used to develop the Mining inventory was based on the lower Saprolite contact surface generated from available drillhole data, and is not based on a Lerchs Grossman optimised pit. The pit shell was split into 63 Mining Panels, generally 250m x 250m in lateral extents; considered adequate for the level of detail required for this preliminary schedule.

Figure 12: Stockpiling of Laterite Ore in the Vicinity of Agata

The mining panels were scheduled in several iterations (over 60 quarterly periods commencing January 2014) and sequenced to generate a Plant Feed Schedule that maximised nickel production in the early years, but also optimsed the proportions of ore feed to the HPAL, Saprolite Neutralisation and Atmospheric Leach circuits.
The Mining schedule was smoothed over quarterly periods with mine production commencing at a rate of 3,400 bcm per day, peaking in Year 10 at 6,700 bcm per day. The average mine production rate over 15 years is 5,400 bcm per day.

The schedule allows for the ramp-up of Plant Feed throughput over the first 3 years of operation to 1,786,000 dmt per annum, which is maintained for the duration of the schedule. Plant Feed was constrained by a limonite/saprolite ratio of 1:1.67 and a Saprolite Neutralisation/HPAL feed ratio of 0.35. Nickel metal production peaks at 18,500t per annum in Year 3.

Since mining activities will be conducted by parcel, the rehabilitation or reforestation program will take place progressively. This method is highly significant with respect to environmental impacts because only small areas are mined during each given period, thus minimising any potential adverse impacts on the broader environment. At least 10 hectares will be rehabilitated per year. MRL will endeavour to replant the mined-out areas with local species. Exotic species such as mangium and mahogany will be replanted as nurse species to provide shade to slow-growing premium species. Non-mineable areas that are presently fern-dominated will also be included in the reforestation programs.

PROCESS PLANT DESCRIPTION

Processing Technology

In the process plant, limonite ore is treated by conventional high pressure acid leaching (HPAL) and saprolite ore is treated by a parallel atmospheric leach (AL) circuit.

The process design for the leach plant will be based largely on the hydrometallurgical route proven at Moa Bay in Cuba for 5 decades and at the Sumitomo/Nickel Asia operated Coral Bay Nickel Project (Coral Bay) in the Philippines since 2005. The leach flowsheet incorporates high pressure acid leaching and counter-current decantation.

Limonite and low magnesium saprolite ore will be treated by conventional HPAL and medium magnesium saprolite ore will be treated by a parallel atmospheric leach (AL) circuit. The PEA design throughput has been based on one million dry tonnes per year of ore feed to HPAL (resulting in a HPAL circuit smaller in scale than that employed at Coral Bay). This was chosen because both autoclave trains at Coral Bay had very fast ramp-ups to full production. Autoclave throughput is based on 31% solids in the autoclave feed slurry (after direct steam heating).

Additionally, the recent start of construction at the Taganito Nickel Project (a sister company of CBNC) in the Surigao District, also employing the HPAL process, is considered to be a major step towards launching the region into the ranks of globally important nickel laterite processing zones.

A parallel atmospheric leaching circuit will treat about 38% of the saprolite ore fed to the process. Atmospheric acid leaching is well established technology practised in many industries over several decades. Atmospheric Leaching of nickel laterites has gained recognition recently as an alternative to the high capital cost HPAL route, and was operated in parallel to the HPAL circuit at Ravensthorpe. The process is currently being investigated by Weda Bay Nickel (Eramet) in Indonesia, Berong Mining in the Philippines and BHP Billiton nickel projects to treat their high grade saprolitic material.

An innovation in the proposed processing route will be the inclusion of saprolite neutralisation. This will involve pre-neutralisation of the residual free acid in the combined leach discharge streams using high magnesium saprolite ore. This process, performed at atmospheric pressure, will consume much of the free acid while recovering additional nickel and cobalt values from the saprolite ore. Neutralisation of the remaining acid will be achieved using limestone.

The concept of saprolite neutralisation was first investigated for laterite ores from the Surigao district in testwork conducted in 1998. Recovery of 60–65% of the nickel and cobalt contained in the high magnesium saprolite ore was achieved. In recent years much higher recoveries have been achieved in testwork for the Weda Bay (Indonesia), Sulawesi (Indonesia) and Mindoro (Philippines) nickel projects. Bench-scale testwork at SGS using Agata saprolite has demonstrated that recoveries of 83-89% are achievable. Higher recoveries may be possible and ongoing testwork on the Agata ores may improve upon the PEA assumptions.
After saprolite neutralisation, the pregnant solution will be recovered by conventional counter-current decantation (CCD), followed by limestone neutralisation of excess acid and precipitation of iron, aluminium and chromium, prior to metal recovery by mixed hydroxide precipitation (MHP).

Metal recovery will be by a two-stage MHP circuit similar to that operated for several years at the Cawse Nickel Project (Western Australia) and more recently at Ravensthorpe Nickel Operation (Western Australia).

Plant Feeds and Products

Plant feed and production data are summarised in Table 18 below.

Table 18: PEA Production Summary

Item	Description	Data
Ore Feed	Limonite + Low Mg Saprolite to HPAL (million DMT p.a.)	1.00
	Med Mg Saprolite to AL (million DMT p.a.)	0.43
	High Mg Saprolite to SN (million DMT p.a.)	0.36
	Total (million DMT p.a.)	**1.79**
Products	Mixed Hydroxide Precipitate (wet tonnes p.a.)	77,500
	(dry tonnes p.a.)	46,500
Contained Metal	**Nickel (tonnes p.a.)**	**18,000**
	Cobalt (tonnes p.a.)	930

Ore Preparation

The ore treatment plant includes separate circuits to treat limonite and saprolite ores. Ore is slurried with seawater to minimise fresh water consumption and improve the leaching chemistry. The limonite ore preparation circuit produces fully de-agglomerated limonite slurry for high pressure acid leaching (HPAL) and the saprolite circuit produces three types of ground saprolite slurry for HPAL, atmospheric leaching (AL) and saprolite neutralisation (SN). The limonite ore treatment plant comprises the following principal operations:

• primary crushing to <200 mm by roll sizer
• limonite de-agglomeration by wet rotary drum scrubbing and rejection of the coarse oversize fraction (>10 mm) by screening
• single stage, closed circuit ball milling to produce a ground limonite slurry
• HPAL feed slurry thickening.

The saprolite ore treatment plant consists of the following principal operations:

• primary crushing to <200 mm by roll sizer
• single stage, closed circuit saprolite SAG milling to produce ground saprolite slurry
• storage tanks for three types of ground saprolite slurry: low magnesium saprolite, medium magnesium saprolite and high magnesium saprolite
• thickening of the medium magnesium saprolite and high magnesium saprolite slurries for delivery to atmospheric leaching and saprolite neutralisation.

Leach Plant

HPAL feed is comprised of limonite and low magnesium saprolite ore slurries, which are combined in the required proportions in the HPAL feed thickener. The HPAL plant includes feed slurry heating, leaching of nickel and cobalt from limonite ore at high temperature (255°C) and pressure (4425 kPag), and autoclave discharge slurry pressure letdown. Atmospheric leach feed is comprised of medium magnesium saprolite slurry. In the atmospheric leach circuit nickel and cobalt are leached from saprolite ore at atmospheric conditions (95-100°C and ambient pressure). Sulphuric acid is used as the lixiviant for both HPAL and atmospheric leaching.

A recycle leach circuit utilises a small stream of sulphuric acid to re-dissolve nickel and cobalt precipitated in the downstream iron/aluminium removal and second stage MHP circuits. Discharge slurries from the HPAL, atmospheric leach and recycle leach circuits are combined and forwarded

to the saprolite neutralisation circuit where the neutralising capacity of the high magnesium saprolite ore consumes some of the excess free acid. Additional nickel and cobalt are leached from high magnesium saprolite during this process. The resultant slurry flows to the CCD circuit, to separate and wash soluble nickel and cobalt from the leach residue solids.

The recovered pregnant liquor is forwarded to two stages of iron/aluminium removal. In the first stage of iron/aluminium removal the majority of the remaining free acid in solution is neutralised with limestone slurry and most of the iron and some of the aluminium are precipitated. In the second stage of iron/aluminium removal the remaining iron and aluminium are precipitated. The pregnant liquor is separated from the precipitated solids by thickening prior to transfer to the mixed hydroxide precipitation area. The thickener underflow slurry is directed to the recycle leach circuit for recovery of co-precipitated nickel and cobalt.

The barren leach residue solids from the final stage of CCD washing along with barren solution from the mixed hydroxide precipitation circuit report to final neutralisation circuit where most of the remaining metals in solution are precipitated.

Treated residue is pumped to the residue storage facility (RSF).

Product Section

Nickel and cobalt are recovered as a Mixed Hydroxide Precipitate (MHP).

The virtually iron/aluminium-free pregnant leach solution (PLS) is forwarded to the first stage MHP reactors to precipitate the nickel and cobalt from the solution by the addition of magnesia slurry. The resulting precipitate contained in the slurry is thickened and forwarded to wash filtration where the precipitate is filtered for further dewatering and washed with demineralised water to displace the chlorides and other sea salts entrained with the precipitates. The filter cake is then repulped with demineralised water and filtered in a pressure filter to achieve the required product moisture specification. The MHP product is packaged in 2 t bulk bags and containerised for shipment and sale.

The un-precipitated nickel and cobalt values remaining in solution after first stage MHP are recovered by lime precipitation in the second stage MHP reactors. The resulting precipitate is thickened and recycled back to the recycle leach area to re-dissolve the nickel and cobalt.

Major Process Packages

Major process packages include a sulphur-burning acid plant, a limestone slurrying plant, a lime kiln and lime slaking plant, a magnesia slurrying plant and a residue storage facility.

The sulphuric acid plant provides sulphuric acid for the leaching circuit and other process consumers, and high pressure (HP) steam for power generation. The acid plant products are up to 2700 t/d of 98.5% sulphuric acid and up to 152 t/h of HP steam.

The limestone plant provides limestone in slurry form for neutralisation of acidic process liquors and crushed limestone for burnt lime production. The limestone plant consists of crushing and slurrying facilities.

The lime plant provides lime in the form of milk-of-lime slurry for neutralisation of acidic process liquors and precipitation of nickel and cobalt in the second stage MHP circuit. The plant consists of a fuel-oil fired limestone calciner and lime slaking facilities.

The magnesia slurrying plant provides magnesia slurry for the precipitation nickel and cobalt as mixed hydroxides in the first stage MHP circuit.

The Residue Storage Facility (RSF) area includes transport and storage facilities for process residue slurry. The impoundment area consists of a walled coastal valley located a short distance from the mine area. The neutralised tailings are pumped via a slurry pipeline to the RSF.

Utilities and Infrastructure

The provision of infrastructure is a significant part of the overall development of the project due to the green field nature of the proposed site.

In the immediate area of the proposed mine site there is minimal existing infrastructure, except for an existing gravel public road and the exploration camp facilities. The proposed plant and port sites are adjacent to an existing town and existing infrastructure includes sealed roads, grid power, communications and services.

Key factors affecting the layout of infrastructure for the project include:

• the location of the ore bodies
• the site topography
• access to site for equipment, operating personnel and reagents
• the position of the industrial and port sites

The facilities will be located predominantly on the coast southwest of the mine site, as the topography is relatively flat compared to the steeper inland terrain.

The infrastructure facilities to be provided for the project include:

• water supply and treatment
• power station and power reticulation
• port
• bulk materials handling
• fuel tank farm
• solid and liquid waste management
• plant control system
• plant site and service buildings and ancillary facilities
• accommodation village and facilities
• communications
• mobile equipment
• roads
• security

Sea water will be used for ore preparation and slurrying. Fresh water for other process plant requirements will be sourced from the Tubay River system.

About half of the personnel working on the project will be accommodated in a permanent company township, which will be situated about 1 km from the process plant. The balance of the workforce will come from nearby established towns and villages.

Facilities for medical services, religious and social activities, shopping and recreation are provided in the township.

ENVIRONMENTAL AND SOCIAL RESPONSIBILITY

Environmental

The Agata Nickel Project will be developed into an integrated mining and processing project which will involve potential social and environmental impacts. These will require comprehensive assessment and planning of mitigating measures to ensure they are appropriately managed. The Company shall implement this in accordance with the International Finance Corporation Performance Standards on Social and Environmental Sustainability and the requirements under Philippine law.

MRL has committed to a Health, Safety, Environment and Community Policy (HSEC) document jointly developed with IFC. The Company has also agreed on an 'Environmental & Social Action Plan' to cover all HSEC aspects related to exploration activities, feasibility work and potential future mine development. MRL, with IFC's assistance, is developing an Environmental Management System (EMS) to adequately manage, plan and document the environmental and social issues relating to their activities in the Philippines. The Company is also preparing a Stakeholder Engagement Plan which will describe their strategy and program for engaging with stakeholders in a culturally appropriate manner.

A key element is the Social and Environmental Impact Assessment (SEIA), which considers in an integrated manner the potential social and environmental (including labour, health, and safety) risks and impacts of the project. The SEIA will be based on current information, including an accurate project description, and appropriate social and environmental baseline data. The SEIA will consider all relevant social and environmental risks and impacts of the project, and those who will be affected by such risks and impacts.

MRL completed an SEIA for submission to the Environmental Management Bureau in January 2008, as part of its application for an ECC permit covering DSO operations that was granted in May 2008. Although fully compliant with Philippine regulatory requirements, this SEIA will be upgraded to meet IFC Performance Standards prior to the commencement of any mining and/or processing operations. MRL has committed to the SEIA upgrade and reaching full compliance with IFC Performance Standards.

The project will comply with other requirements as defined under: the Philippine Environmental Impact Statement System (PEISS), the Pollution Control Law (1976), the Water Code (1976), the Clean Water Act (2003), the Clean Air Act (1998), the Ecological Solid Waste Management Act (2000), the Toxic Substances and Hazardous and Nuclear Wastes Control Act (1990) and numerous other environmental and social legislations and regulations.

Social Engagement

General

MRL has been actively engaged with local communities since early exploration work conducted prior to 2004, in association with minor activities such as reconnaissance work or the implementation of drilling activities. Through several years of immersion in the community, MRL has recognised that it can only be successful if it has the support of the locals, thus a Community Relations (ComRel) Division was formally created. Several activities were undertaken to gather information on the communities and to determine their main concerns. This includes the identification of host communities, community immersion, networking, and effective Information, Communication and Education (ICE) campaigns. MRL also implements social development programs and exercises transparency to the people and other community groups and organisations. MRL's community engagement is a progressive process with a well-defined strategy and approach along with the project development stages.

In consultation with the communities themselves, MRL has launched and assisted with social development programs that focus on improving economic, education, health and social well-being of its community-partners within budget constraints and dictates.

MRL has implemented the Community Technical Working Group (CTWG) system in collaboration with local government units and non-government organisations, including representatives from business and the church. 19 CTWGs were established which comprise representatives at

Barangay (village) level from: existing village organisations, religious groups, village council, youth groups, women, local NGOs, farmers, fisherfolk, focal government agencies and vulnerable peoples. The CTWGs provide valuable input into the communities and have acted as MRL's partner in planning and implementing the company's extensive community development programs.

MRL has implemented several programs in the area of social development, including:

- Partnering with the Department of Education in the implementation of the "Adopt-a-School" Program (Figure 13), which benefits five elementary schools in the Agata Project area.
- In areas where the Department of Education cannot provide for the honorarium for volunteer teachers, MRL provides a minimal honorarium to volunteer teachers.
- A Computer Literacy Program to accommodate MRL scholars, out-of-school youth, teachers and other locals.
- Supporting host communities and local government units with small infrastructure programs, such as road construction, building barangay and municipal centres, day care and health centres, water reticulation projects, school rooms, and assistance in many socio-cultural projects.
- MRL also implements the Computer Literacy Program to accommodate MRL scholars, out-of-school youth, teachers and other locals. This is a program of which MRL is especially proud; utilising the Company's computer equipment and the education skills of its staff, MRL is able, at low-cost, to introduce these skills into remote communities with a paucity of such high technical skills and assets.

MRL has also supported its host communities and local government units with small infrastructure programs; such as road construction, building barangay and municipal centres, day care and health centres, water reticulation projects and school rooms, and has assisted in many socio-cultural projects.

Photos counterclockwise: Jon Dugdale and Tony Climie lead the ribbon-cutting ceremony for the turnover of the school building (center) built by MRL at Agata Project; Children of Agata Grade School; Dalaw-turo (teach-in) by MRL Senior Environmental Officer

Figure 13: "Adopt-a-School" Program

The possibility of future mining operations and the resultant land acquisition for the development of the mine and port in the project area has been discussed extensively with the affected landowners. MRL has undertaken demographic profiling and understands the consequences of possible future

land acquisition for each individual, and plans to incorporate this assessment and their management plan for land acquisition into a Land Acquisition and Compensation Plan.

Indigenous Peoples

There is no community of Indigenous People (IP) physically or economically displaced or otherwise directly impacted by exploration activities or by land access. One IP community is indirectly and lightly affected by the development and the use of the existing access road to the exploration camp site.

The access road passes the small village of Sitio Coro, where two IP groups (the Manobo and the Mamanwa) currently reside. The village of Coro is experiencing indirect impacts from additional 5 light vehicles per day travelling through the village. During a meeting in the village of Coro, people spoke favourably about MRL's exploration and expressed their high level support to the project's potential mining activities. The Mamanwa and Manobo are all tenants and they do not own the land on which they reside.

Free, Prior, Informed Consent

To the extent that Indigenous Peoples have been impacted by the Project, the National Commission of Indigenous Peoples (NCIP) has concluded that Free, Prior, Informed Consent (FPI Consent) has been given for the Project by the Manobo and Mamanwa of Coro. The consultation process includes on-going engagement with communities and individuals, signing of formal agreements with communities as appropriate, provision of timely information, and time for decision-making according to local cultural practices.

Identification of the local IP community was conducted in 1999 by the NCIP prior to any of MRL's activities in the areas. Neither IP nor indigenous customary lands were recognised. Interaction between the village of Coro and MRL commenced in 2005, when MRL recognised the village of Coro as an indigenous village through its extension of a 7km farm to market road. Formal engagement with Sitio Coro commenced in late 2005 with extensive consultation and community development activities. Under the Philippines Indigenous Peoples Rights Act, FPI Consent of indigenous peoples is required for a project to proceed. The NCIP therefore conducted another field-based investigation and declared the existence of the FPI Consent in early 2008.   A Memorandum of Understanding was signed between the Mamanwa, Manobo, MRL and the NCIP.

Development Benefits

The area where the village of Coro is located is not considered a Certificate of Ancestral Domain Claim/Title (CADC/T) area under Philippine law, and therefore the company is not required to pay a "1% of revenue" royalty to indigenous peoples as otherwise would be applied. MRL recognised the vulnerability of the IP groups, and is determined to maximise sharing of project benefits with the IP community. Consequently MRL will voluntarily contribute the 1% revenue royalty to the IP community in the area.

The Memorandum of Understanding and subsequent royalty agreements have been developed through Good Faith Negotiations. Once MRL starts generating revenue, the 1% royalty will be managed through an Ancestral Domain Sustainable Development and Protection Plan (ADSDPP).

Meanwhile, Coro residents were given first priority for jobs on the farm to market road construction and maintenance work which was undertaken. MRL has also assisted the village of Coro in applying for ancestral domain rights on the area. MRL established a nutritional program for children in Coro in 2006, which has now been rolled into an "Adopt a School" program. The village of Coro was also highly involved in the Medical, Surgical, Optometry and Dental Mission initiated by MRL in early 2008.

Socio-economics

The opening of the mining project will certainly have significant effects on the socio-cultural and economic situation, not only of the host villages but the neighbouring villages as well. The socio-cultural practices of the community will fundamentally change as this project changes the land use and sources out human, mineral and biological resources for project subsistence. It will provide additional wealth to the community and at the same time cause either favourable or adverse impacts to the people and the environment. More livelihood opportunities and social development

projects will be provided for the local community through the Social Development and Management Program budget.

The project will also provide employment for the locals, thereby lessening their dependency on fishing and farming. Generally the economic status of the community will improve and the project subsequently will offer growth and development of each resident as the company requires more permanent, contractual or even rotational employees. The project will improve incomes in the area so more people will be attracted to settle in the locality. Demand for basic products such as food, housing, health, and basic services will increase. This may also enhance external influences and change the values and lifestyle of the residents.

The project will bring wealth not only to the local government but to the national government as well, in the form taxes and fees. These taxes fund infrastructure, health and basic services, and development projects throughout the community. The project will also make direct contributions to the community through its Social Development and Management Program (SDMP), wherein the community shall benefit through programs such as training, livelihood, infrastructure, education and health services.

Resettlement

Physical and/or economic displacement is the most immediate and personal of all social issues in mine development. Compensation packages for loss of assets will include payment for the land and assistance to help restore the original or improve the living standards of affected landowners/occupants, along with other development benefits.

In the case of MRL's laterite mining project, only those people living near the pier yard, causeway, plant site and access roads, like communities in Sitio Payongpayong, Sitio Awasan, Sitio Coro and Barangay Lawigan, are likely to be affected by the project. Initial consultations with these people have been undertaken. Final negotiations will follow a detailed Resettlement Action Plan (RAP) in consonance with Philippines regulatory requirements and IFC guidelines.

Loss of Terrestrial Habitat and Habitat Fragmentation

No exotic faunal species are found in the project site and the density of faunal population is low. This is attributable to the predominance of bare or sparse vegetation in the area as cited in the baseline study.

Figure 14 depicts the major vegetation types encountered in the project area. As observed, the eastern slope of the Agata mountain range is mostly open area with grassland and the aggressive bracken fern (*Pteridium aquilinium*) enjoys almost complete dominance. Signs of burning are noticeable in the area as manifested by burned vegetative parts and soil surface. The forested areas are confined to the riverine areas or gullies of the micro watersheds, especially at the plateau-like, very moderately rolling ridge. The most dominant of the grasses is talahib (*Saccharum spontaneum*).

Figure 14: Extensive open areas at the eastern slope of Agata prospect.

CONCLUSIONS

The Agata Nickel Project is a potential low cost producer at production capacities as low as 18 000 tonnes per annum nickel contained in a mixed hydroxide intermediate product. The current NI 43-01 compliant resource, upon which the Preliminary Economic Assessment was based, contains sufficient resources to support a mining inventory to sustain an acid leach processing operation for 15 years. Ongoing drilling of the regional Exploration Target is expected to define sufficient resources to support a project life well in excess of 20 years.

The project has significant competitive advantages including: excellent metallurgical response, established mining precinct, no inhabitants or forest in the resource area, large regional population base, close proximity to established infrastructure and deep ocean port sites, abundant fresh water, an abundant supply of limestone on site, and a short shipping distance to China and other potential Asian markets.

MRL has an excellent environmental and social reputation in the region and has been involved in many highly regarded and award winning social engagement programs for more than 10 years.

REFERENCES

1. Cox, Dallas. "Independent Report on the Nickel Laterite Resource Estimate Upgrade at Agata North". December 22, 2009.

2. Coffey Philippines Inc., "Consulting Services for the Conduct of Preliminary Baseline Environmental Studies, Volume 3. Water", Project Ref. E63511-1, September 30, 2008.

3. Cox, Dallas. "43-101 Technical Report on the Mineral Resource Estimate for the Agata North Laterite Project of MRL". January 22, 2009.

4. Gifford, Mark. "ANLP Resource Review". September 2010.

5. SGS Lakefield Oretest Report, "Agata Nickel Bench Scale Metallurgical Testwork", Job No. 10649, 31 March 2011.

6. Ausenco Vector & Boyd Willis Hydromet Consulting, "Agata Nickel Project Scoping Study", USVC-00008-00, September 2010.

WHY MAKE MHP?

By

Tony Treasure and Harald Muller

Metals Finance Limited, Australia

Presenter and Corresponding Author

Harald Muller
harald@metalsfinance.com

Important Notice

This presentation contains certain statements which may constitute 'forward looking statements". Such statements are only predictions and are subject to inherent risks and uncertainties which could cause actual values, results, performance or achievements to differ materially from those expressed, implied or projected in any forward looking statements.

No representation or warranty, express or implied, is made by Metals Finance Limited that the material contained in this presentation will be achieved or proved to be correct. Except for statutory liability which cannot be excluded, each of Metals Finance, its officers, employees and advisers expressly disclaims any responsibility for the accuracy or completeness of the material contained in this presentation and excludes all liability whatsoever (including in negligence) for any loss or damage which may be suffered by any person as a consequence of any information in this presentation or any error or omission there from. Metals Finance accepts no responsibility to update any person regarding any inaccuracy, omission or change in information in this presentation or any other information made available to a person nor any obligation to furnish the person with any further information

Metals Finance
Specialists in Metals Recovery

- Listed on the ASX in the Industrial Sector during Dec 2007
- Metals Finance Limited has been formed for the specific purpose of providing a unique combination of finance and technical skills for the development of small to medium scale metal recovery projects around the globe.
- Primary targets are those opportunities which, even during an upturn in world metal markets, may be too small, complex or unusual to easily attract the funding and high level technical input required to ensure their successful development.

Typical Projects

- Medium sized, proven, high-grade primary resources

- Start up projects requiring demonstration of new technologies

- Mine waste dumps and tailings

- Smelter and solid industrial wastes

- Industrial waste materials and streams

Business Model

- Establishment of a suitable process flow sheet
- Preliminary financial modelling and risk assessment
- Site testing of the proposed flow sheet
- Decision to proceed with plant design and engineering
- Determination of minimum scale for positive return
- Design and engineering of treatment facility including permitting
- Determination of capital and operating costs
- Establishment of personnel requirements and availability
- Generation and independent review of project plan
- Project development: Finance, EPCM,

Recent Projects and Investments

Projects:
- Palabora
  - Recently sold to Rio Tinto
- Chambishi
- Lucky Break
- Barnes Hill

Investments:
- Bass Metals

Lucky Break Nickel Project

- Small Ni deposit in N-QLD, approximately 140km West from Townsville

- ML owned by Nornico, subsidiary of Metallica Minerals (MLM)

- JV Agreement between MLM and Metals Finance

Lucky Break Nickel Project

| Classification	Total Ore '000 t	Nickel t	Cobalt t
Measured	592.6	4866	333
Indicated	48.1	395	27
Inferred	492.7	3277	188
Total	**1133.4**	**8538**	**548**

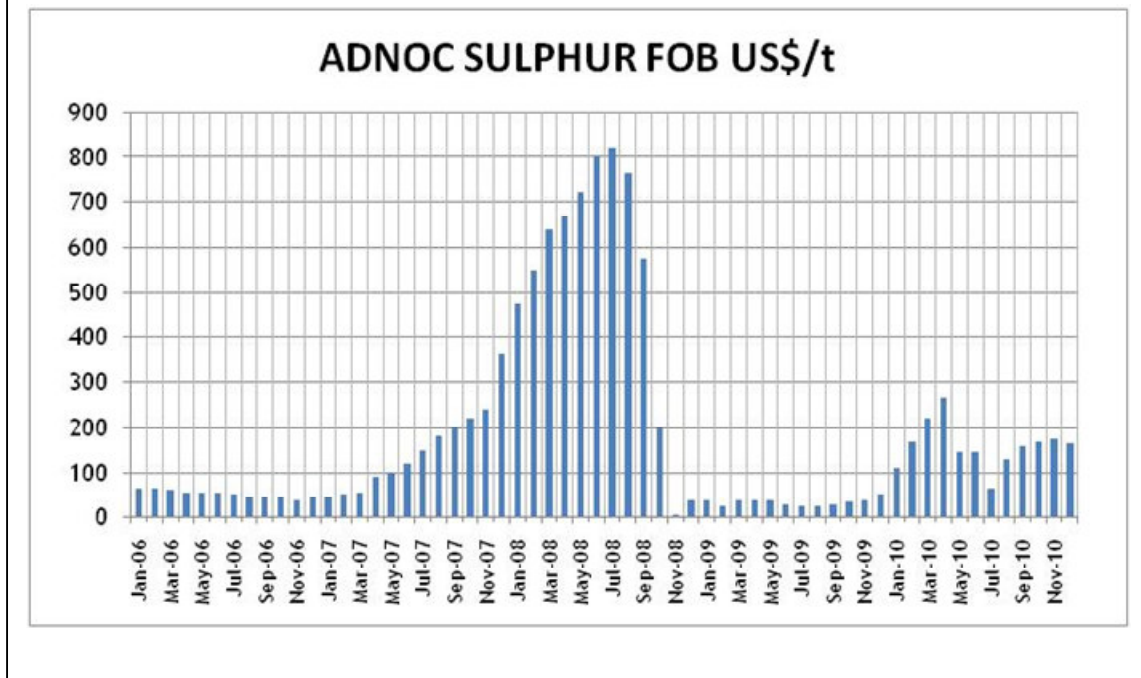# Lucky Break Project Timeline

- Initial Feasibility Study (2007)
- Ready for Implementation
  - Some contracts were already in place
  - Limited procurement started
  - Official approval was awaited

Lucky Break Nickel Project

5 Year Nickel Spot

Lucky Break Nickel Project
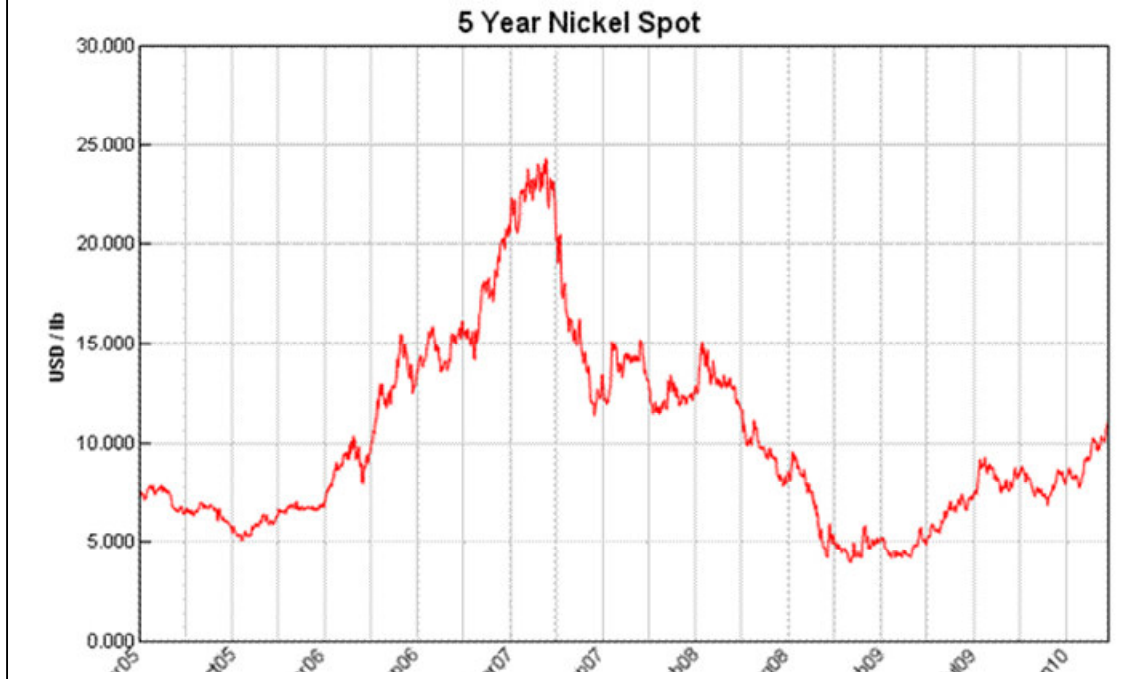
ADNOC SULPHUR FOB US$/t

Project Timeline

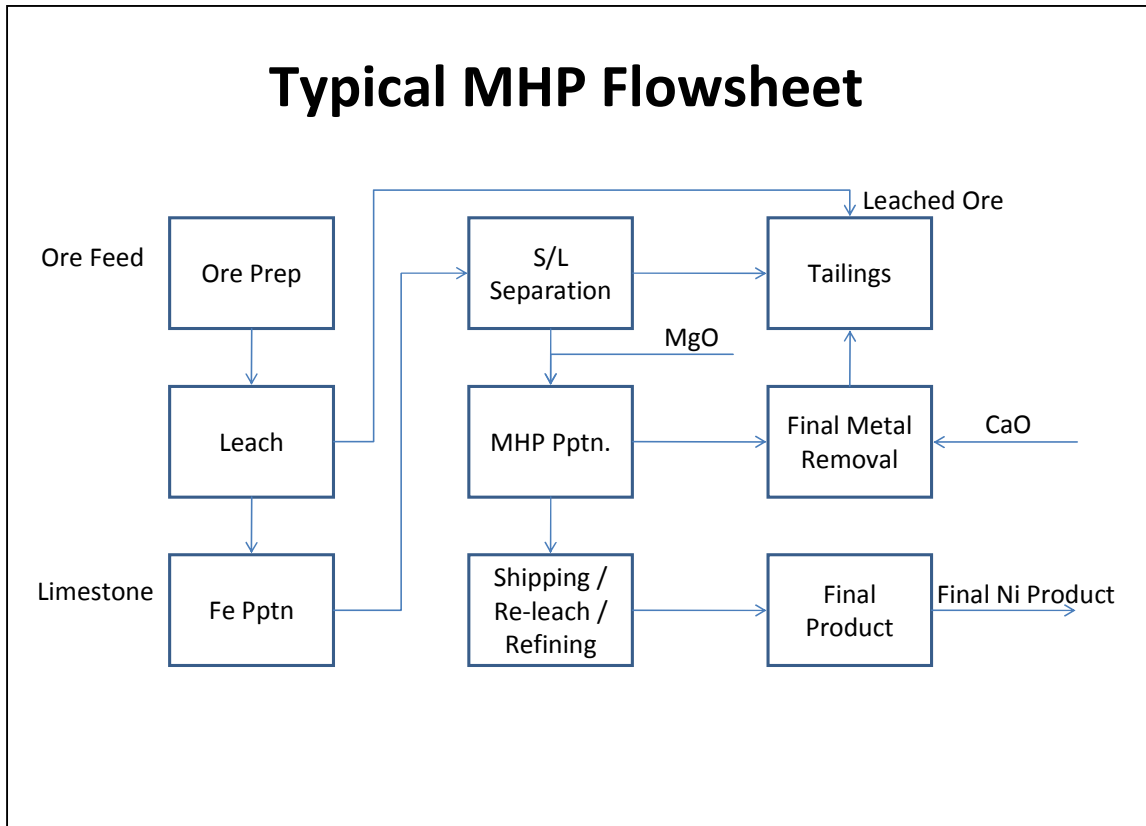- Initial Feasibility Study (2007)

- GFC

- Project Review (2008)

- Revision of Scope (2009)

- Revised Feasibility Study (2009 / 2010)
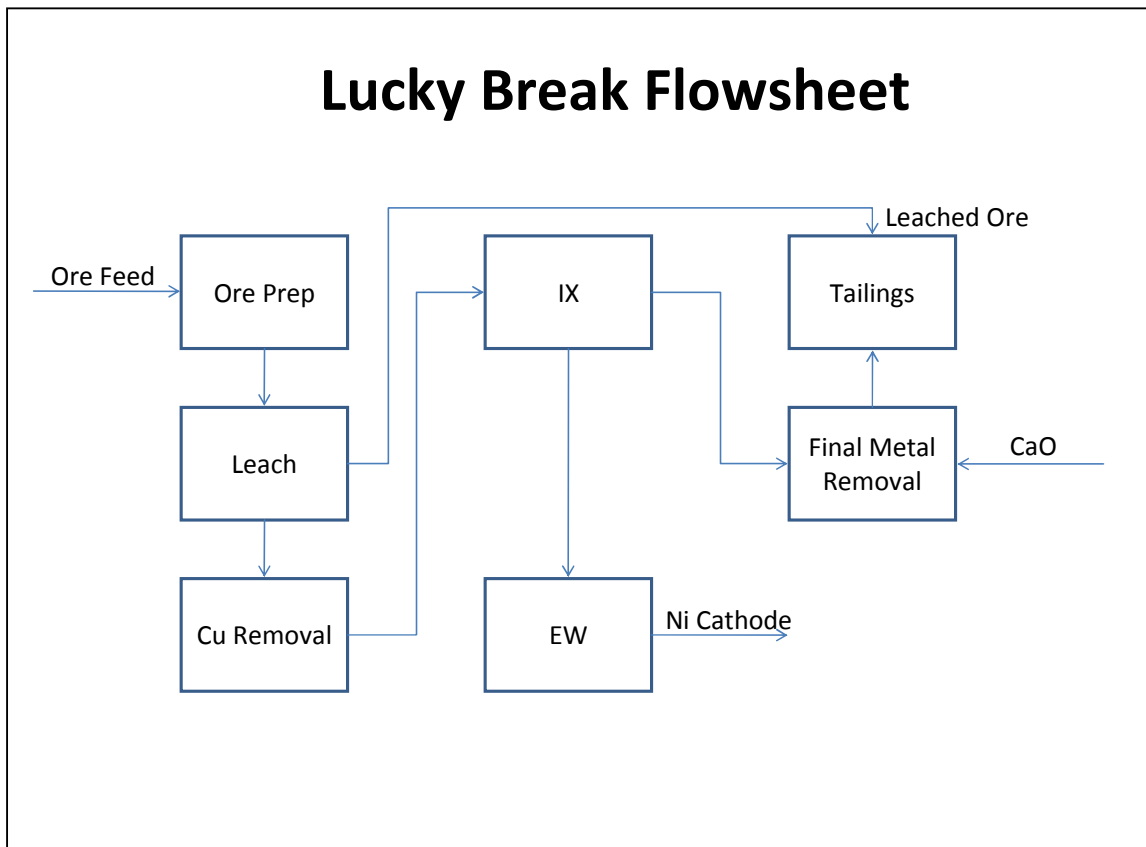
Lucky Break Nickel Project

- Initial Feasibility Study (2007)
  - 250,000 tpa ore treated
  - Ni cut-off grade: 0.3%
  - Average Ni Grade: 0.81%
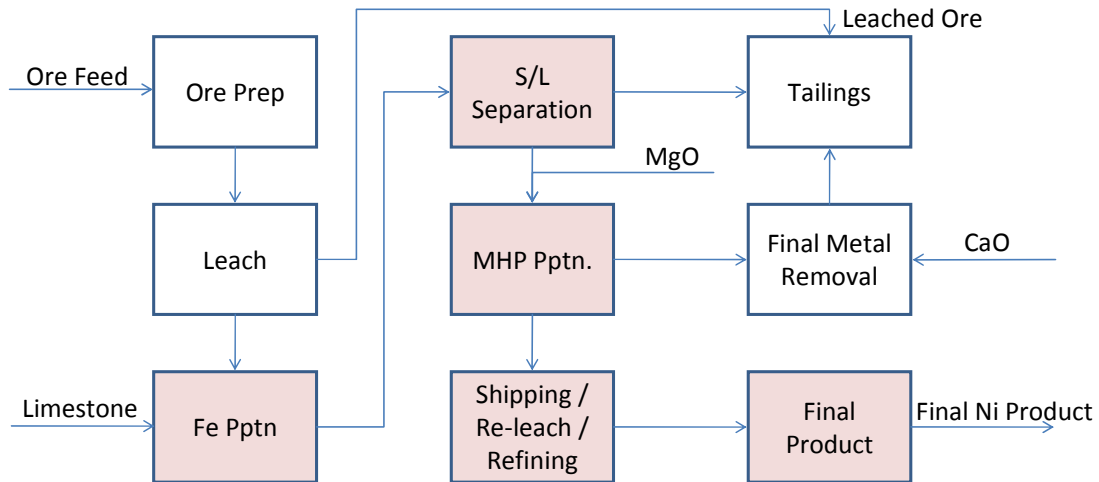 - Annual Ni Production: 1,400 tpa
  - Ni Product: Ni Carbonate

Typical MHP Flowsheet

Lucky Break Flowsheet

Differences in the Flowsheets

Comparison of Flowsheets

- What is the overall impact of the flowsheet on the Lucky Break project economics?
  - Capital Costs
  - Operating Costs
    - o Acid consumption
    - o Reagent Costs
    - o Diesel / Power Costs
  - Ni revenue

Lucky Break Feasibility Study

- 2010 Feasibility Study

    – 60,000 tpa ore treated
    – Ni cut-off grade: 1.0%
    – Average Ni Grade: 1.35%
    – Annual Ni Production: 670 tpa
    – Ni Product: Ni Cathode

Comparison of Flowsheets

- Capital Costs:

    – Typical MHP Plant costs available were for much larger plants
    – Power of 2/3 rule was used and then adjusted in line with our experience of small scale projects

Capital Costs

Capital Costs

Ore Preparation	Identical	Identical	0
Leach	Identical	Identical	0
Fe Removal	Yes	None	-$3.97M
MHP Precipitation	Yes	None	-$1.23M
IX	None	Yes	+$1.99M
Ni EW	None	Yes	+$1.94m
Final Effluent Neut.	Identical	Identical	0
Total Benefit of LB Flowsheet:			-$1.27M

Operating Costs

Operating Costs

Ore Preparation	Identical	Identical
Leach	Identical	Identical
Fe Removal	$0.52/lb	0
MHP Precipitation	$0.21/lb	0
IX	0	$0.15/lb
Ni EW	0	$0.14/lb
Final Effluent Neut.	Identical	Identical
Total Opex (Penalty)	$7.01/lb	$7.14/lb

Revenue

Revenue

Expected penalty for MHP	**-25%**	**0%**
Losses assumed during MHP Production	**-1.5%**	**0%**
Total Revenue (Benefit)	**$8.16/lb**	**$11.06/lb***

   * Ni Price as on 15 May 2011

NPV Sensitivity

NPV Sensitivity to 30% Changes in Capital Costs, Operating Costs and Revenue
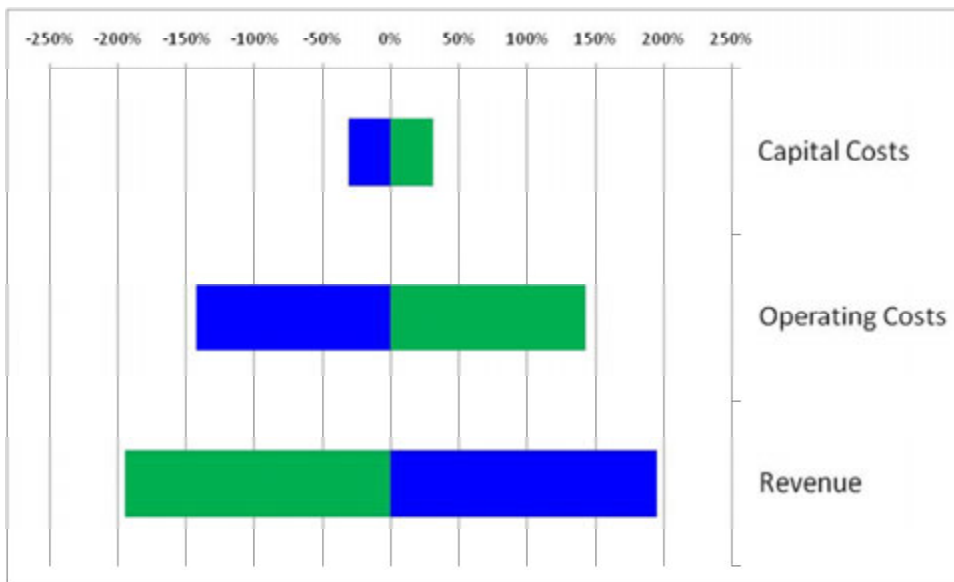
Lucky Break Nickel Project Conclusions

– Replacing a MHP Circuit with a circuit that provides Ni Cathode as final product will improve net revenue significantly

– The process route identified for the Lucky Break project shows a small benefit with regards to Capital Costs when compared with an MHP Circuit

– The IX / EW process will lead to a slight increase in Operating Costs

Conclusions

– Capital Costs

• Based on a high-level estimate for the MHP Flowsheet, the IX/EW Flowsheet will lead to small reduction in Capital Costs

• The project economics are not as sensitive to variations in Capital Costs as Operating Costs and Revenue

• Capital cost per annual pound of Ni produced:
  – MHP Circuit: ~$10.09/lb
  – IX/EW Circuit: ~$9.21/lb

Conclusions

– Operating Costs
  • Reduced acid consumption / ton of Ni produced due to high-grading of feed
  • Reduced Chemicals Required for alternative flowsheet
  • Increased power demand leads to increased diesel costs
  • Operating Costs per lb of Ni roughly on par for the two process options, however IX/EW produces cathode as final product:
    – MHP Circuit: ~$7.01/lb
    – IX/EW Circuit: ~$7.14/lb

Conclusions

– Revenue
  • Significant penalty when selling MHP vs. Ni Cathode
  • Improved revenue has most significant impact on project economics
  • Revenue based on current Ni Price:
    – MHP Circuit: ~$8.16/lb
    – IX/EW Circuit: ~$11.06/lb

Conclusions

– Does this flowsheet offer a benefit in all cases?

- Scale of the project
  - At 20,000tpa Ni the IX Carrousel would become a significant issue and may not be as beneficial as for a smaller project
  - Discussions are ongoing with vendors to optimise equipment configuration, which may benefit larger installations.
- Simplified Flowsheet tested comprehensively by DOW Chemicals
- EW Circuit is standard
- No large S/L separation equipment

Next Steps for Lucky Break Project

– Secure funding

– Implement project

CHEMICAL ASPECTS OF MIXED NICKEL-COBALT HYDROXIDE PRECIPITATION AND REFINING

By

[1]James Vaughan, [1]William Hawker, [2]David White

[1]The University of Queensland, School of Chemical Engineering, Australia
[2]Metallurgical Consultant, Perth, Australia

Presenter and Corresponding Author

James Vaughan
james.vaughan@uq.edu.au

ABSTRACT

The precipitation of mixed hydroxide is increasingly being considered as an intermediate step in the hydrometallurgical processing of nickel and cobalt, particularly from nickel laterite ores. Mixed hydroxide precipitation reaction equilibrium and kinetics are discussed. Hydrometallurgical MHP refining is briefly reviewed. A new method of leaching MHP is discussed that involves the fast and efficient separation of nickel from cobalt and manganese, yielding a concentrated nickel solution suitable for direct recovery of a nickel metal by electrowinning, hydrogen reduction, or nickel sulfate by crystallization.

INTRODUCTION

There are three practiced methods to concentrate and purify nickel and cobalt from pregnant (acid) leach solution in the hydrometallurgical processing of nickel ores. The methods are summarized in Table 1.

- Mixed Sulfide Precipitation (MSP)
- Solvent Extraction (SX)
- Mixed Hydroxide Precipitation (MHP)

Table1: Recovery of nickel and cobalt from pregnant (acid) leach solution
[Websites Accessed 10-12-2010]

Method	Operation	Production, kt/y		Comment	References
		Nickel	**Cobalt**		
MSP	Moa Nickel (Cuba)	34	3.7	2009 Production	www.sherritt.com
	Murrin Murrin (Australia)	33	2.4	2009 Production	www.minara.com.au
	Coral Bay (Philippines)	24	1.5	2009 Production	www.smm.co.jp
	Ambatovy (Madagascar)	60	5.7	Under Construction	www.sherritt.com
	Taganito (Philippines)	30	?	Under Construction	www.smm.co.jp
SX	Bulong (Australia)	9	0.5	Suspended	
	Goro (New Caledonia)	60	4	In Ramp-up	www.vale.com
	Voisey's Bay (Canada)	50	?	Under Construction	www.vale.com
MHP	Cawse (Australia)	9	2	Suspended	www.nornik.ru
	Ravensthorpe (Australia)	40	2	Suspended	www.first-quantum.com
	Ramu (P.N.G.)	31	3	Under Construction	www.ramunico.com
	Caldag (Turkey)	20	1	Under Study	www.enickel.co.uk
	Acoje & Zambales (Philippines)	24	0.9	Under Study	www.enickel.co.uk
	Northmet (U.S.A.)	7.7	0.4	Under Study	www.polymetmining.com
	Mesaba (U.S.A.)	-	-	Under Study	www.cesl.com (Mayhew, 2009)
	Gördes (Turkey)	10	0.7	Under Study	www.metanikel.com.tr (Yesil, 2010)

MIXED HYDROXIDE PRECIPITATION

Recovery of nickel in hydroxide form was considered as early as 1913, when the Madagascar Minerals Syndicate lodged a patent application for "Recovery of Nickel from its Ores" (US patent 1,091,545).

During the Moa Bay development, Freeport considered producing a hydroxide concentrate (Carlson 1961, Simons 1961), but discarded the concept on the basis of product grade and purity: "The hydroxide concentrate thus produced contains 15 to 25% nickel plus cobalt and is usually contaminated with compounds of manganese, calcium, or aluminum" (Roy, 1961).

Taylor (1995) identified some of the drivers for utilizing a mixed hydroxide processing route, stating, "This eliminated the costly and undesirable H_2S precipitation step, and yield a product readily soluble in ammonia or dilute sulfuric acid with potential for the application of SX/EW."

The industrial application of mixed nickel-cobalt hydroxide precipitation as employed at the Cawse and Ravensthorpe operations in Western Australia has been described in detail by White (2009).

The breakthrough in making a high quality mixed hydroxide product involved the understanding that:

1. Upstream solution treatment to remove iron, aluminium and chromium was critical;
2. Magnesia could be used successfully, if it were caustic calcined (not over burned) and kept dry (not hydrated) before addition to the nickel containing solution;
3. Good selectivity against magnesium and some selectivity against manganese could be achieved if only 90 to 95% of the nickel were precipitated per pass.

A typical process flowsheet (Figure 1) begins with leaching nickel and cobalt by contacting the solids with sulphuric acid. The resulting acid leach slurry is neutralised using limestone to eliminate free acid and precipitate impurities such as iron(III) from solution. The solid phase is then washed and separated from the solution phase by counter-current decantation (CCD). Iron(II), aluminium, chromium and silica are eliminated in a second neutralisation step, with the precipitated solids recycled for recovery of any contained nickel and cobalt. Nickel and cobalt are then precipitated from solution together as mixed hydroxides, using magnesia. Residual nickel and cobalt are recovered using lime with manganese eliminated in a final precipitation step. The MHP is further refined to separate nickel and cobalt.

Ore
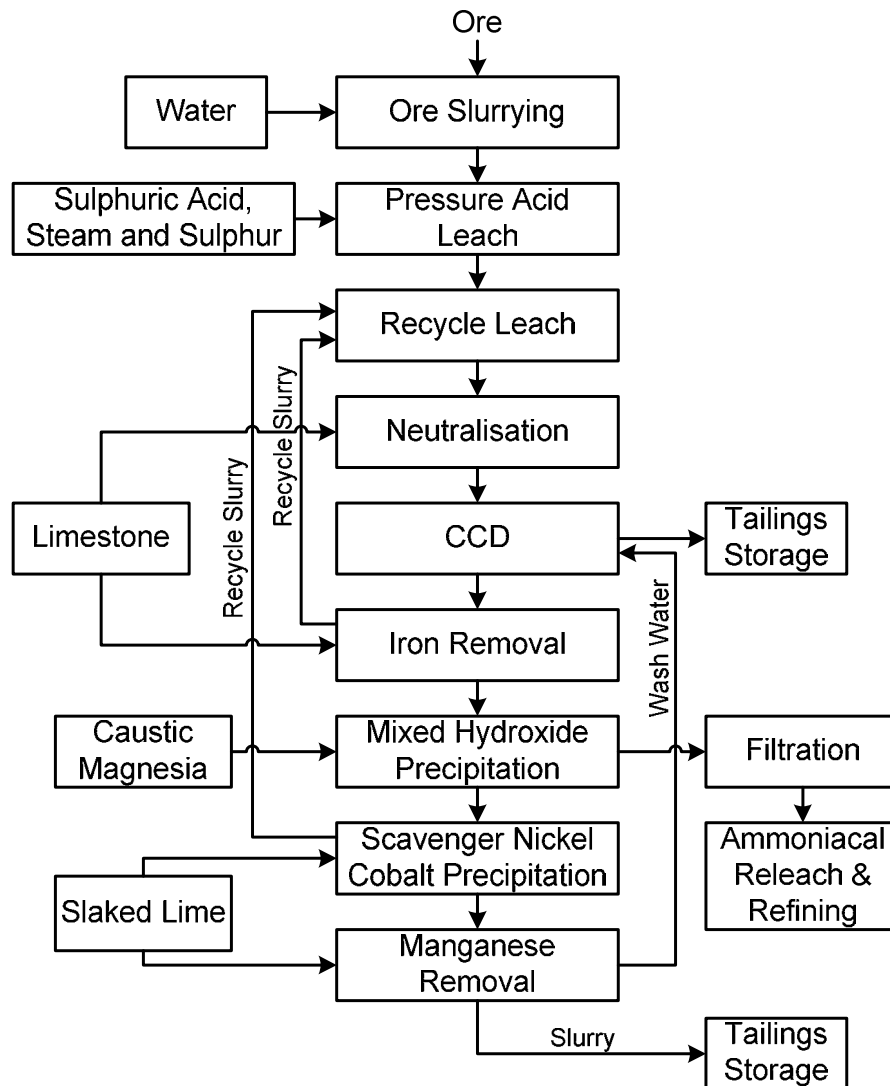
Figure 1: Generic process flowsheet

The detailed MHP circuit is shown in Figure 2. The pregnant leach solution is combined with magnesia in the first reactor. The nickel and cobalt are precipitated as mixed hydroxides at 50˚C for a single pass residence time of about 3 hours. The objective of the primary MHP stage is to selectively precipitate the majority of the nickel and cobalt, with maximum magnesia utilisation and minimum precipitation of manganese. The solids from primary precipitation are thickened and split. One of the split fractions is recycled as seed material, providing additional solids residence time, improving the precipitate handling characteristics and purity. The solids in the other split fraction are washed (not shown in figure) and filtered to remove excessive solution before being sent to refining. The remaining nickel and cobalt in the solution is recovered in the scavenger precipitation stage, where lime is used as the precipitant. This material is recycled back to the neutralisation stage (see Figure 1).
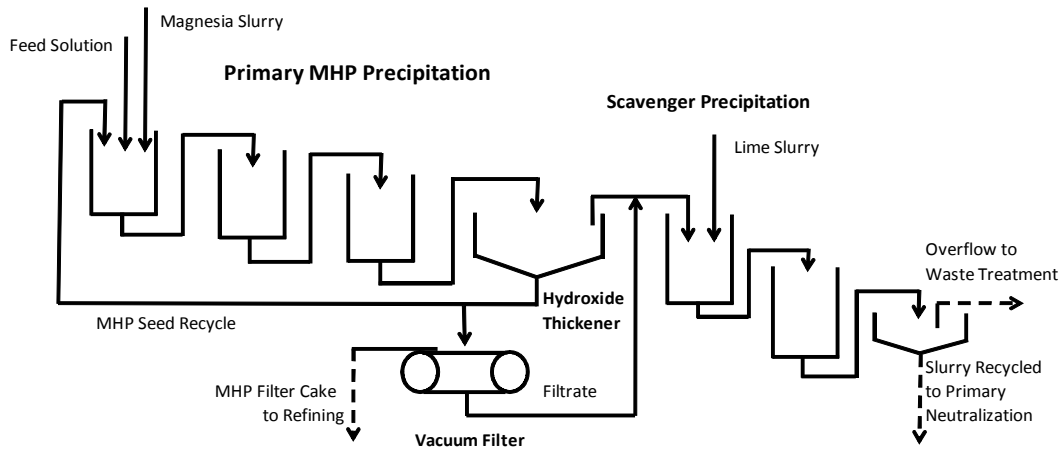
Figure 2: MHP process flow diagram

MHP EQUILIBRIUM THERMODYNAMICS

Hydrometallurgists often refer to the precipitation diagrams of Monhemius (Figure 3). The log of cation solution activity plotted on the y-axis and the pH is plotted on the x-axis. The lines describe the tendency for the metals to precipitate from solution as hydroxides. To the left of the lines the metals are stable in the solution phase and to the right the metals are stable in the solid phase. The equilibrium lines relate to Equation 1 where M is the metal cation and n is the cation charge.

$$M^{n+} + nH_2O = M(OH)_n + nH^+ \text{ (Equation 1)}$$
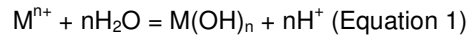
The process for treating nickel-cobalt ores, shown in Figure 1, can be reasonably accurately described by the hydroxide precipitation diagram. In general, leaching takes place to the left of the Fe(III) line, primary neutralisation takes place between the Fe(III) and Al(III) lines, secondary neutralisation takes place between the Cr(III) and Ni(II) lines, and MHP takes place in the region of the Ni(II) and Co(II) lines with primary precipitation being to the left of scavenger precipitation.
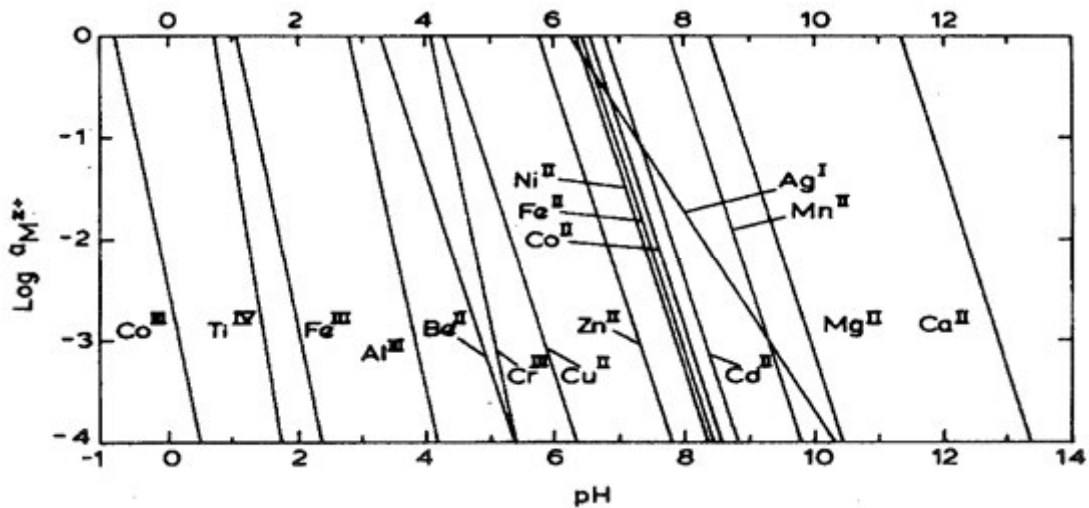

**Figure 3: Hydroxide precipitation diagram, 25°C (adapted from Monhemius, 1977)**

The diagram's predictions can be improved by carefully considering the assumptions that are made in their development. Table 2 summarises these assumptions with comments.

Table 2: Precipitation diagram assumptions

| Assumptions	Comments
Solution species activities are equal to the molar concentration. Activity of water is 1.	Data for solution species activity models (Zemaitis 1986) are increasingly available for more complex systems. Most models consider molality (moles/kg-H_2O) not molarity (moles/L-solution).
Activities in mixed solid phase (solid solution) are assumed to be 1.	When more than one solid is being precipitated at the same time, the activity of the solid in the solid solution may not be the same as the concentration. Limited fundamental data is available for these processes.
No adsorption effects.	Ions may adsorb onto the surface of solids; this is not predicted by a precipitation diagram and the effect can be substantial, especially when dealing with dilute solutions (e.g. $Au(CN)_2^-$ on carbon).
Solid phase is a simple hydroxide.	Identify solid phases and use appropriate thermodynamic data (e.g. $NaFe_3(SO_4)_2(OH)_6$ instead of $Fe(OH)_3$ to describe neutralisation at Ravensthorpe).
The precipitate solid phase and crystallinity matches that of the thermodynamic data.	In precipitation, often an amorphous or partially amorphous solid is formed initially which are less stable than the crystalline solid. Also, multiple crystal structures may be possible, each exhibiting different properties.
Oxidation states are known and constant.	Certain ions and solids can be oxidized or reduced at process conditions (e.g. Fe^{2+}/ Fe^{3+}).
Process temperatures and pressures are 25˚C and 1 atm.	Thermodynamic calculations can be adjusted to consider various temperatures and pressures provided the heat capacities functions are known. The Criss Cobble Entropy Correspondence Principle can be used for common ions.
The process reaches equilibrium.	It can take a long time to reach equilibrium which is why we must consider the reaction kinetics.

MHP PRECIPITATION KINETICS

The precipitation of mixed nickel-cobalt hydroxide was studied at simulated industrial conditions in a batch laboratory reactor (Harvey 2008). The reaction kinetics are shown in Figure 4. In this experiment, the feed solution was seeded with previously prepared MHP 30 minutes before magnesia (EMAG[®] 45) addition. A significant portion of the cobalt was precipitated upon contacting the seed. According to thermodynamic predictions (Figure 3), it is expected that nickel precipitates prior to cobalt. Contrary to this prediction, in MHP the cobalt is observed to precipitate faster and more completely than the nickel (Figure 4). This effect is believed to be caused by faster reaction kinetics along with co-precipitation. A substantial portion of the manganese also precipitated during the course of this experiment. Fast reaction kinetics relative to nickel and co-precipitation are believed to be factors with the added complication of the potential for manganese to be oxidized. The oxidative precipitation of manganese may occur at pH levels around that of divalent nickel or cobalt hydroxide precipitation (Zhang 2010).
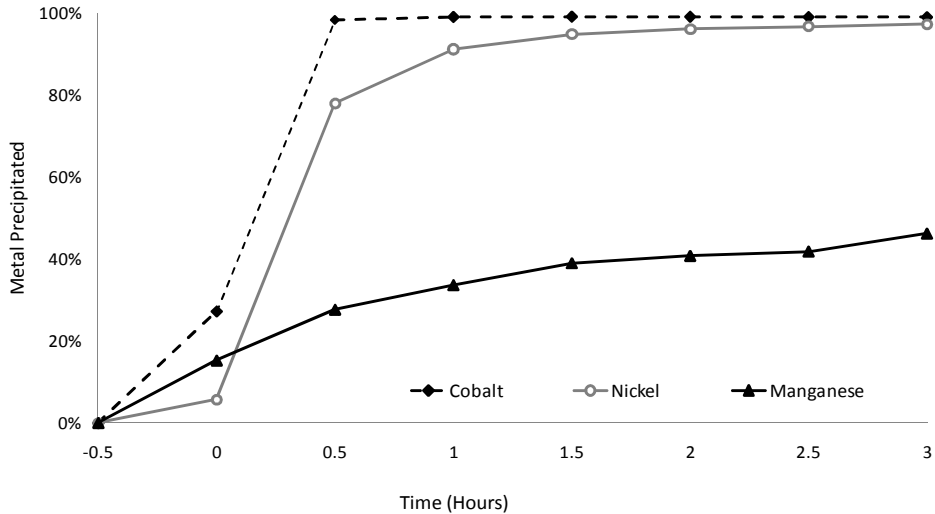
Figure 4: Kinetics of MHP precipitation, 5 g/L Ni, 1 g/L Mn, 0.2 g/L Co in initial solution, seed added at time = -0.5 hours, magnesia added at time = 0, 50 °C (adapted from Harvey 2008)

The experimental data points from the MHP precipitation kinetics study were compared with thermodynamic predictions (Figure 5). The slurry pH measurements were temperature compensated. The region local to the surface of the magnesia particles would have a relatively high pH compared with the bulk solution, resulting in high levels of supersaturation. The experimental points were taken between 0.5 and 2 hours after magnesia addition. The thermodynamic data and solution species activity coefficients at temperature were obtained from HSC Chemistry Software v7.00 (2009). The large discrepancy between the experimental cobalt points and the cobalt equilibrium line suggests that the activity of cobalt in the MHP is much lower than unity. The experimental points for nickel fall reasonably close to the thermodynamic prediction. The manganese is seen to start precipitating well before the predicted line for $Mn(OH)_2$ precipitation.
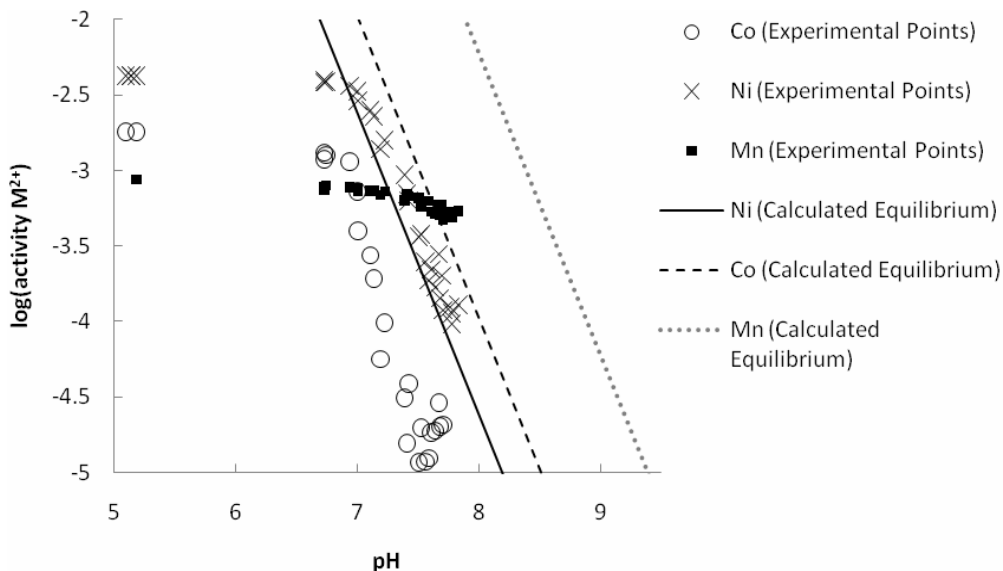
Figure 5: Hydroxide precipitation diagram at 50°C with data points from magnesia addition experiments (adapted from Harvey 2011)

While mixed nickel-cobalt hydroxide precipitation at industrial conditions is reasonably selective, impurities remain in the material. Typical composition of MHP and possible methods to help minimize contamination are suggested in Table 3. Impurities complicate the refining of MHP as they either reduce re-leach recovery, cause reactor scaling, consume ammonia, or increase the burden on impurity removal stages.

Table 3: Mixed hydroxide precipitate composition

| Element / Compound	Weight % (Dry Basis) (White 2006)	Comments on impurity form and possible methods to help minimize contamination
Ni	40	-
Co	2	-
SO_4	17	Associated with calcium. Included and occluded in the hydroxide matrix. Water/alkaline wash may help.
Cl	0.2	From leach liquors, if saline water used. Water wash.
Mn	3	Co-precipitated, partially oxidized, occluded. Precipitate contact with feed solution may help (Jones 2002).
Mg	3	Mostly unreacted magnesia. Decrease rate of MgO addition / extent of reaction. Increased seeding ratio. Precipitate contact with feed solution. Water wash.
Si	0.4	Introduced with magnesia, present as SiO_2. Also in purified leach solution. Use higher purity magnesia. Maximise pH in neutralisation steps.
Ca	0.7	Likely mostly present as $CaSO_4$. Some CaO is contained in the magnesia. Water wash.
Fe	0.1	Reduces ammonia re-leach extractions. Need to remove from solution prior to MH Precip.
Al	0.02	Reduces ammonia re-leach extractions. Need to remove from solution prior to MH Precip.
Cr(VI)	-	Contaminates refining process. Need to reduce to Cr(III) prior to neutralisation.

MHP REFINING

Mixed Ni/Co hydroxide precipitate produced at Cawse and Ravensthorpe was refined by leaching both metals into ammonia ammonium-carbonate solution (Equation 2 where M is Ni^{2+} or Co^{2+}).

$$M(OH)_2 + (NH_4)_2CO_3 + 4NH_3 \rightarrow M(NH_3)_6CO_3 + 2H_2O \text{ (Equation 2)}$$
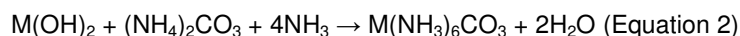
The subsequent separation of the nickel from the cobalt is effected by oxidizing the cobaltous ammine complex to cobaltic then preferentially extracting nickel into a liquid organic phase (Price 1992).

In the Cawse flowsheet (Dobson 2001), the liquid organic is stripped using sulfuric acid, resulting in a concentrated nickel sulfate solution suitable for recovery of the nickel using electrowinning as cathode (Figure 6). Operational issues during start-up included the faster than expected degradation of the organic extractant, excessive crud formation and serious problems in the electrowinning cellhouse due to organic excursions that lowered the current efficiency and damaged the cathode starter sheets.
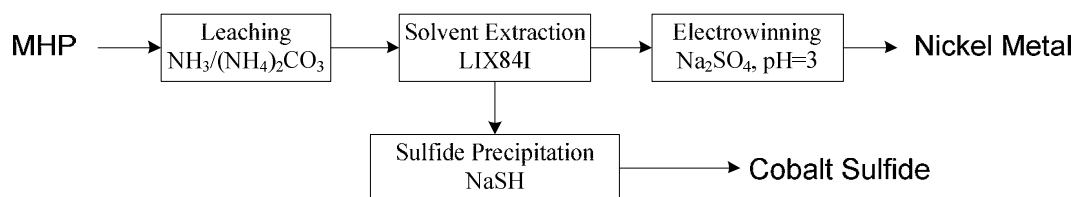
Figure 6: MHP Refining at Cawse

At Queensland Nickel (Figure 7), nickel is stripped from the loaded organic using a concentrated ammonia ammonium carbonate solution. The nickel is then recovered from that aqueous solution as nickel carbonate by steam stripping.
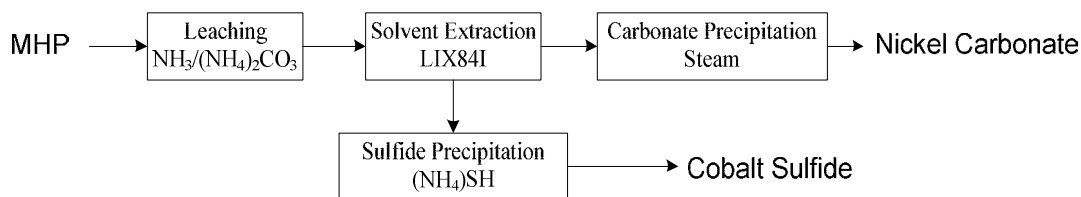
```
                  ┌──────────────┐     ┌──────────────────┐      ┌────────────────────────┐
MHP ─────────────▶│  Leaching    │────▶│Solvent Extraction│─────▶│ Carbonate Precipitation │────▶ Nickel Carbonate
                  │NH₃/(NH₄)₂CO₃  │     │      LIX84I       │      │         Steam          │
                  └──────────────┘     └──────────────────┘      └────────────────────────┘
                                                  │
                                                  ▼
                                       ┌──────────────────┐
                                       │Sulfide Precipitation│────▶ Cobalt Sulfide
                                       │      (NH₄)SH       │
                                       └──────────────────┘
```

Figure 7: MHP refining at QNI

STUDIES AT THE UNIVERSITY OF QUEENSLAND

An alternative MHP leaching process has been developed at the University of Queensland (UQ) that combines the process outcomes of leaching and solvent extraction into a single selective leaching stage. It was found that with an appropriate oxidising reagent regime, along with sulfuric acid, cobalt (and much of the manganese) remains insoluble, whilst nickel is almost completely extracted. The solid cobalt concentrate can be further treated to recover the nickel content. This selective leaching process can be advantageously combined with nickel electrowinning as the acid generated at the anode can be used in the selective leaching stage although hydrogen reduction or sulfate crystallisation could also be employed to obtain nickel products. The new refining process is described in Figure 8.
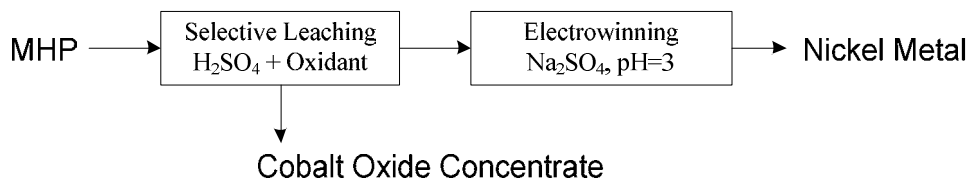
```
                  ┌──────────────────┐     ┌──────────────────┐
MHP ─────────────▶│Selective Leaching│────▶│  Electrowinning  │────▶ Nickel Metal
                  │ H₂SO₄ + Oxidant  │     │ Na₂SO₄, pH=3     │
                  └──────────────────┘     └──────────────────┘
                            │
                            ▼
                  Cobalt Oxide Concentrate
```

Figure 8: Proposed MHP refining by UQ

Provided that a sufficiently strong oxidant is employed, an effective separation of nickel from cobalt can be achieved over a wide pH range of 5.5 down to 2.3 as seen in Figures 9 and 10.
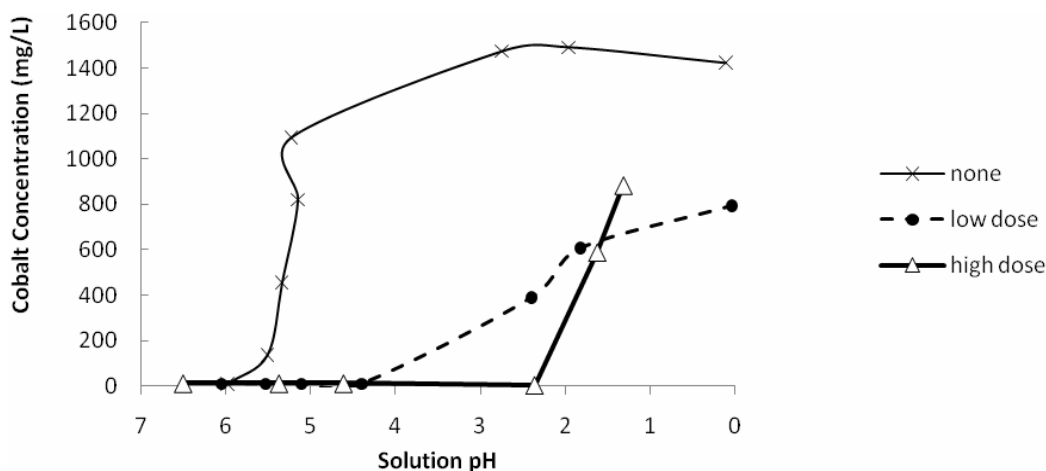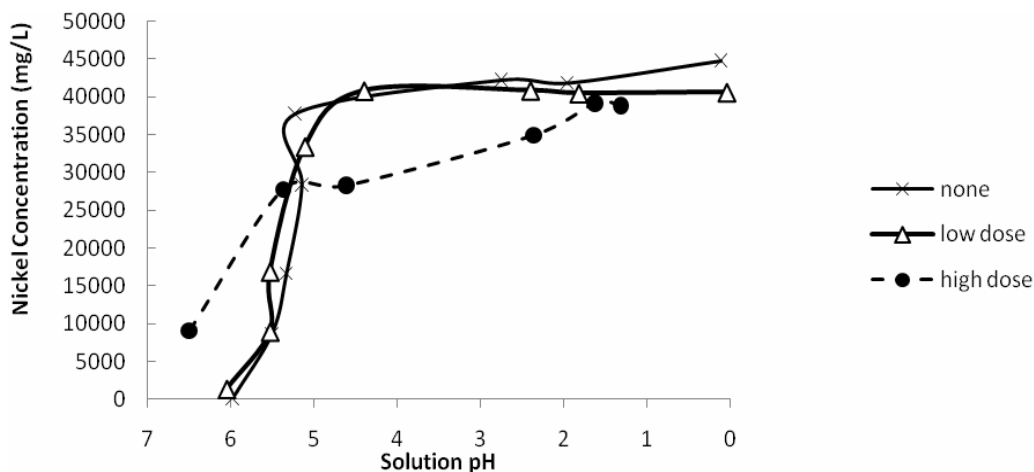
Figure 9: Extraction of cobalt from MHP as a function of reagent addition and pH in a sulfuric acid leach.

Figure 10: Extraction of nickel from MHP as a function of reagent addition and pH in a sulfuric acid leach.

An example of the extent of nickel-cobalt separation that can be achieved is shown in figure 11 (batch reactor experiment controlled to a terminal pH of 3). At these conditions, the concentrated nickel solution contains minimal cobalt, with nickel to cobalt ratios above 3600. With the correct conditions, the reaction is fast, nearing completion after only 1 hour. As for the impurities, if operating at pH 3, the silica, iron, aluminium and most of the manganese report to the cobalt concentrate whereas sodium, magnesium, calcium, copper and zinc will largely follow the nickel electrolyte. The deportment of iron and aluminium to the cobalt concentrate may have positive implications for the MHP producer as strict control of these elements to the MHP is not as critical as with the ammonia leaching process. Typically solvent extraction, ion-exchange, or selective precipitation steps will be required to manage impurities such as copper and zinc in a nickel electrowinning circuit.
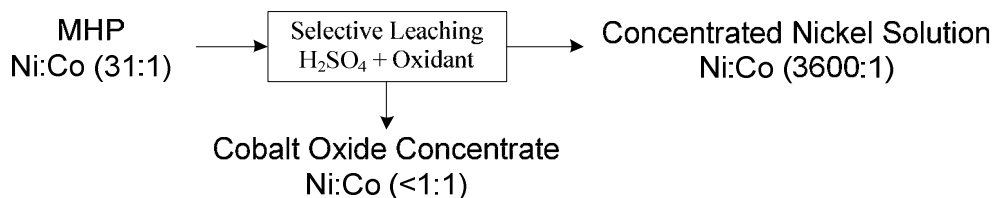
Figure 11: Example of nickel cobalt separation in the selective leaching process in a batch reactor experiment, terminal pH = 3, 2 hours.

CONCLUSIONS

Research programmes at the University of Queensland have identified a number of the thermodynamic and kinetic factors that influence the composition of mixed hydroxide precipitates, derived from nickel laterite leach liquors.

UQ staff developed a process to enable nickel to be selectively leached as nickel sulfate from mixed hydroxide precipitate, while retaining most of the cobalt and manganese in the leach residue.

REFERENCES

Carlson, E.T., and Simons C.S., 1961. Pressure Leaching of Nickeliferous Laterites with Sulfuric Acid. Extractive Metallurgy of Copper, Nickel and Cobalt, P.E. Queneau, Ed., AIME, New York, NY, U.S.A., 1961, 363-397.

Dobson T., Young R., O'Sullivan D., 2001. Commissioning under a microscope – the Cawse nickel start-up. Proceedings of the AusIMM, Vol. 306 No. 1.

Harvey R., 2008. The study and potential improvement of Ni/Co mixed hydroxide precipitate (MHP). The University of Queensland Honours Thesis, Chemical and Metallurgical Engineering Program.

Harvey R., Hannah R., Vaughan J., 2011. Selective precipitation of mixed nickel-cobalt hydroxide. Hydrometallurgy 105 222-228.

HSC Chemistry Software, 2009. Version 7.00, Outotec.

Jones E.M., Miller M.J., 2002. Hydroxide solids enrichment by precipitate contact. Patent WO2002048042.

Krebs D., Furfaro D., White D., 2010. The Mount Thirsty Process. Proceedings of the 15th Annual ALTA Nickel/Cobalt Conference. May, Perth, Australia.

Mayhew, K., Mean, R., O'Connor L., Williams, T., 2009. Nickel and Cobalt Recovery from Mesaba Concentrate. Proceedings of the 14th Annual ALTA Nickel/Cobalt Conference. May 25-27, Perth, Australia.

Monhemius A. 1977. Precipitation Diagrams for Metal Hydroxides Sulfides Arsenates and Phosphates. Transactions of the Institution of Mining and Metallurgy, 86, pp. C202.

Price M.J., Reid J.G., 1992. Separation and recovery of nickel and cobalt in ammoniacal systems. U.S. Patent 5,174,812.

Roy T.K., 1961. Preparing Nickel and Cobalt Concentrates. Industrial and Engineering Chemistry, Vol. 53, No. 7, July 1961, 559-566.

Simons, C.S., Dufour, M.F. and Carlson, E.T., 1961. Recovery of Nickel, Cobalt and Other Valuable Metals, Canadian Patent 618,826, 25 April 1961.

Sulman, H.L., Picard, H.F.K., 1914. Recovery of Nickel From Its Ores, US Patent 1,091,545.

Taylor, A., 1995. Laterites – has the time finally come? Mining Magazine, 172(3), 167-170.

White, D.T., 2002. Selective Precipitation of Nickel and Cobalt, US Patent 6,409,979.

White, D.T., Miller, M.J., Napier, A.C., 2006. Impurity Disposition and Control in the Ravensthorpe Acid Leaching Process. Proceedings of the 3rd International Symposium on Iron Control in Hydrometallurgy, CIM, October 1-4, Montreal, Canada.

White, D.T., 2009. Commercial development of the magnesia mixed hydroxide process for recovery of nickel and cobalt from laterite leach solutions. In: Hydrometallurgy of Nickel and Cobalt (Proc. 39th Annual Hydrometallurgy Meeting, Sudbury), Eds J.J. Budac, R. Fraser, I. Mihaylov, V.G. Papangelakis, D.J. Robinson, CIM, Montreal, 351-368.

Yesil M. 2010. Gordes nickel cobalt HPAL project. 2nd Euro Nickel Conference, March 18-19, London, England.

Zemaitis Jr., J.F., Clark, D.M., Rafal, M., Scrivner, N.C., 1986. Handbook of Aqueous Electrolyte Thermodynamics A.I. Chem. Eng.

Zhang W., Cheng C.Y., Pranolo Y., 2010. Investigation of methods for removal and recovery of manganese in hydrometallurgical processes. Hydrometallurgy 101 58–63.

SEQUENTIAL LEACHING OF NICKEL LATERITE ORES

By

[1,2]Nicole Botsis, [2]Wilhelm van Bronswijk and [1]Helen Watling

[1]Parker CRC for Integrated Hydrometallurgy Solutions, CSIRO Minerals Down Under National Research Flagship, CSIRO Process Science and Engineering, Australia
[2]Department of Chemistry, Curtin University, Australia

Presenter and Corresponding Author

Nicole Botsis
nicole.botsis@csiro.au

ABSTRACT

Sequential extractions are used to study element speciation in ore bodies. The extraction methodology consists of a series of successive chemical treatments of a sample and the metals removed help determine the different levels of substitution present in these minerals. This study was performed to assess whether the sequential leaching methodology could be applied to nickel laterite ores. Three samples were chosen, a saprolite, nontronite and limonite ore, and a five-step leaching protocol was developed.

In the first step, which removes the water soluble fraction, no minerals were leached from the saprolite and nontronite ores. However, for the limonite ore, the halite was completely removed and was nickel-barren. No minerals were leached in the second step, which removes the exchangeable fraction, although 40% of the magnesium present in the nontronite was removed. The crystal structure of the nontronite was altered indicating that magnesium existed between the layers of the nontronite structure. Step three, which removes the amorphous material, indicated that no mineral leached from either the nontronite or limonite ores. However, the asbolane present in the saprolite ore was leached, with 7% of the nickel associated with this mineral. There were different extents of nickel leaching in step four, which removed the adsorbed nickel on the oxides and silicates. In the final leach step, which breaks the oxide/silicate crystalline lattice, the lizardite, nontronite and goethite were completely leached along with all the remaining nickel. The only minerals remaining were nickel-barren.

Application of the leaching protocol enabled the determination of different nickel-containing and nickel-barren minerals. It also allowed for the distinction to be made between nickel in amorphous or crystalline material. The use of this technique does not allow for the leaching of goethite independently of lizardite and/or nontronite. However, the leaching methodology is rapid and uses simple solution analysis and therefore it is an affordable method to determine whether nickel is present in minerals that are difficult to leach (i.e. spinels), amorphous phases and/or leachable crystalline phases.

INTRODUCTION

Sequential extractions are used to study element speciation in ore bodies. This type of extraction process consists of a series of successive chemical treatments of a sample, each being either more aggressive in action or differing in nature from the previous treatment (Hall et al., 1996). The metals removed can then help determine the different levels of substitution present in these minerals.

Six major factors may influence the success of selective extraction analyses. These are:
(1) The chemical properties of the extractants
(2) The extraction efficiency
(3) Experimental parameter effects
(4) The sequence of the individual extractions
(5) Matrix effects
(6) The heterogeneity and physical associations (i.e. coatings) in the sample
(Kersten and Förstner, 1989).

There are many different extractant types that can be used in sequential extraction methodologies, some of which are highly specific while others are less selective. When determining which extractants to use, care and forethought are required to ensure meaningful results are produced. However, the method of sequential extraction has been criticised due to the low mineral selectivity of these leaches. In general, studies in the past have not been able to demonstrate that the extraction solutions specifically remove metals from only one component of a sample. Also, it has not been proven that different extraction solutions can leach minerals with differing crystallinity, i.e. poorly or highly crystalline goethite (McCarty et al., 1998).

This study was performed to assess whether the sequential leaching methodology could be applied to nickel laterite ores. Three samples were chosen from a typical laterite profile (Figure 1), one from the saprolitic zone (termed saprolite), one from the clay zone (termed nontronite) and one from the limonitic zone (termed limonite). A five-step leaching protocol was developed.
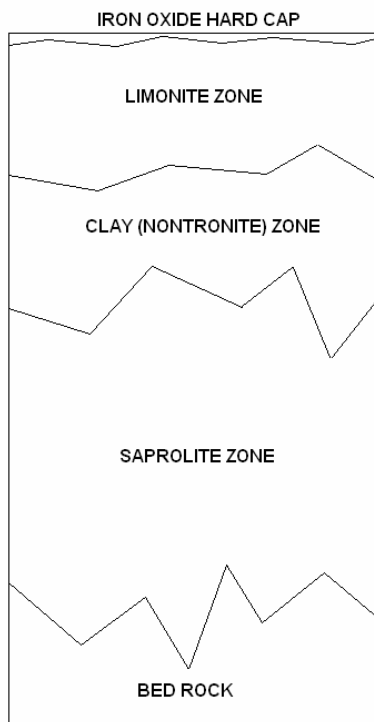
Figure 1: Typical laterite profile

CHARACTERISATION

X-ray powder diffraction (XRD) and Quantitative X-ray powder diffraction (QXRD) patterns were collected from pulverised solid samples (ball milled for 2 minutes), with 10% CaF_2 added as an internal standard, using a Philips X'Pert Automated Powder Diffractometer fitted with a Cobalt Lone Line Focus X-ray tube (6.9keV). Patterns were collected between 2Θ angles of 3°–120° (at 40 kV, 30 mA), and interpreted using Topaz (Version 3). Using the internal standard, the percentage of undetermined or amorphous content was also calculated. Elemental analysis was obtained by inductively coupled plasma-atomic emission spectrometry (ICP-AES) analysis using a Varian VISTA-PRO or 735-ES ICP-AES. Solution analysis of process water was also by ICP-AES.

Table 1: Elemental analysis

	Element (wt %)											
	Al	Ca	Co	Cr	Fe	K	Mg	Mn	Ni	Si	S	C
Limonite	1.26	0.013	0.069	1.77	45.2	0.019	1.10	0.173	1.32	2.87	0.02	0.02
Nontronite	4.21	0.008	0.043	1.31	14.1	0.052	1.90	0.026	1.37	23.1	0.17	0.07
Saprolite	0.52	0.009	0.048	0.355	15.4	0.062	13.1	0.162	1.57	18.8	0.01	0.02

Limonite

QXRD analysis of the limonite ore (Figure 2) indicates that goethite (60.6%), halite (4.9%), spinels (24.1%), quartz (0.2%), lizardite (1.1%) and unaccounted/amorphous material (9.1%) (the amorphous material comprises mainly poorly crystalline silicate phases).are present in the ore. The high level of goethite (FeOOH) is further confirmed by the elemental analysis (Table 1) as the predominant element present is iron. As there is very little silicon present, the low percentage of lizardite $(Mg_3(Si_2O_5)(OH)_4)$ present can be corroborated. The Rwp value, a goodness of fit value calculated from differences between the theoretical and actual XRD plots is 9.78%. Low Rwp values indicate a good fit and it can therefore be said that the QXRD is a good fit.
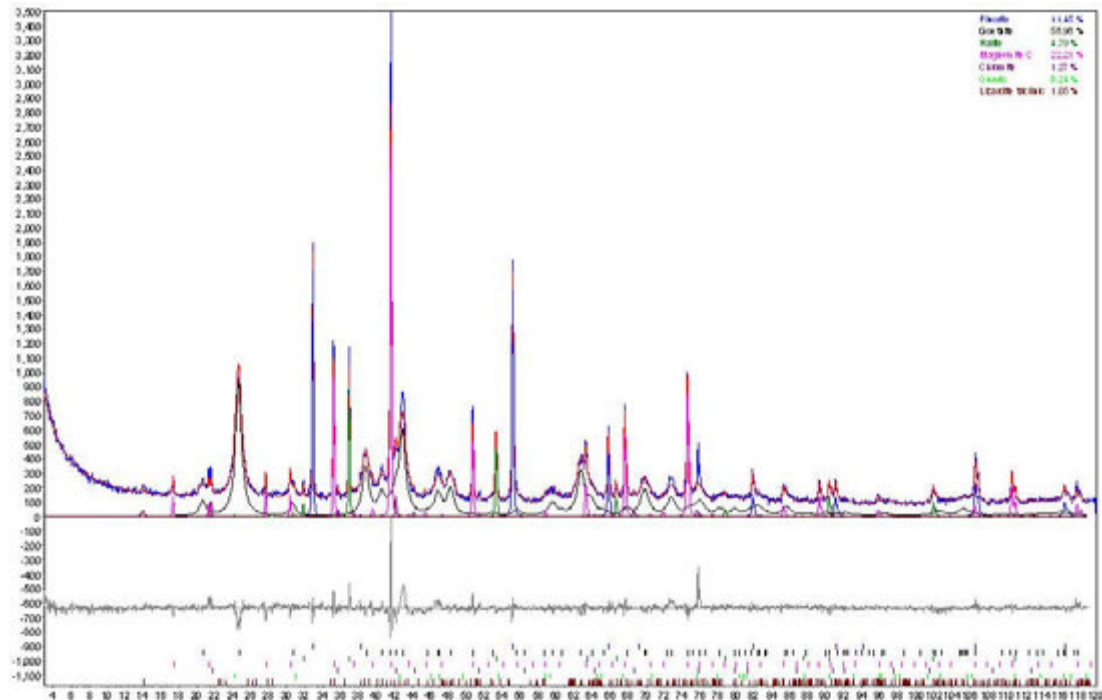
Figure 2: Limonite QXRD

Nontronite

QXRD analysis of the nontronite ore (Figure 3) indicates that there is nontronite (79.3%), quartz (5.8%), chlorite (13.1%), spinels (0.2%) and unaccounted/amorphous material (1.7%) present in the sample. The elemental analysis (Table 1) further confirms the presence of high levels of nontronite $(X_{0.3}Fe_2(Si,Al)_4O_{10}(OH)_2.nH_2O$ where X can be elements such as Na, Ca, Mg etc.) as there are relatively high levels of silicon, iron and aluminium in the sample. The Rwp value is 18.61% which is higher than that obtained for the limonite ore but can still be said to be a good fit.
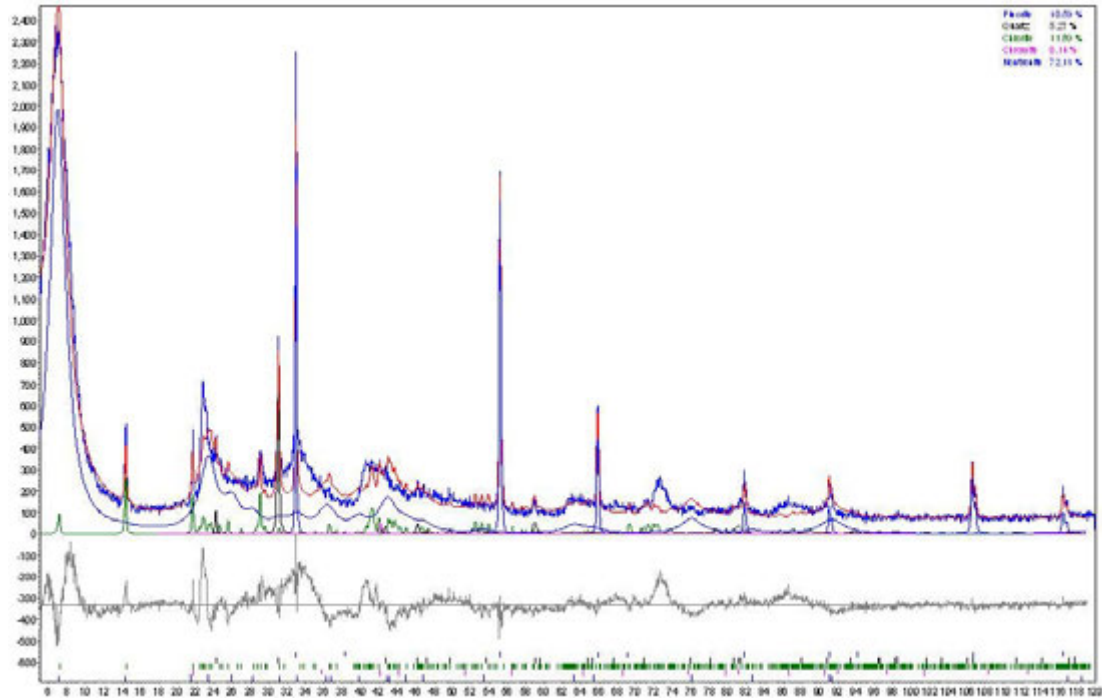

Figure 3: Nontronite QXRD

Saprolite

QXRD analysis of the saprolite ore (Figure 4) indicates the presence of lizardite (44.2%), nontronite (20.4%), quartz (0.9%), spinels (5.7%) and unaccounted/amorphous material (28.9%). The Rwp value is 21.81% which is relatively high implying that a high percentage of mineral types are unaccounted. No additional peaks can be identified and it can therefore be stated that there are no other crystalline minerals present (unless they are below detection limit). The material that is unaccounted for is most likely from amorphous minerals and accounts for the calculated XRD not fitting the real XRD well. The high percentage of lizardite $(Mg_3(Si_2O_5)(OH)_4)$ as determined from the QXRD correlates with the high levels of silicon and magnesium seen in the elemental analysis (Table 1).
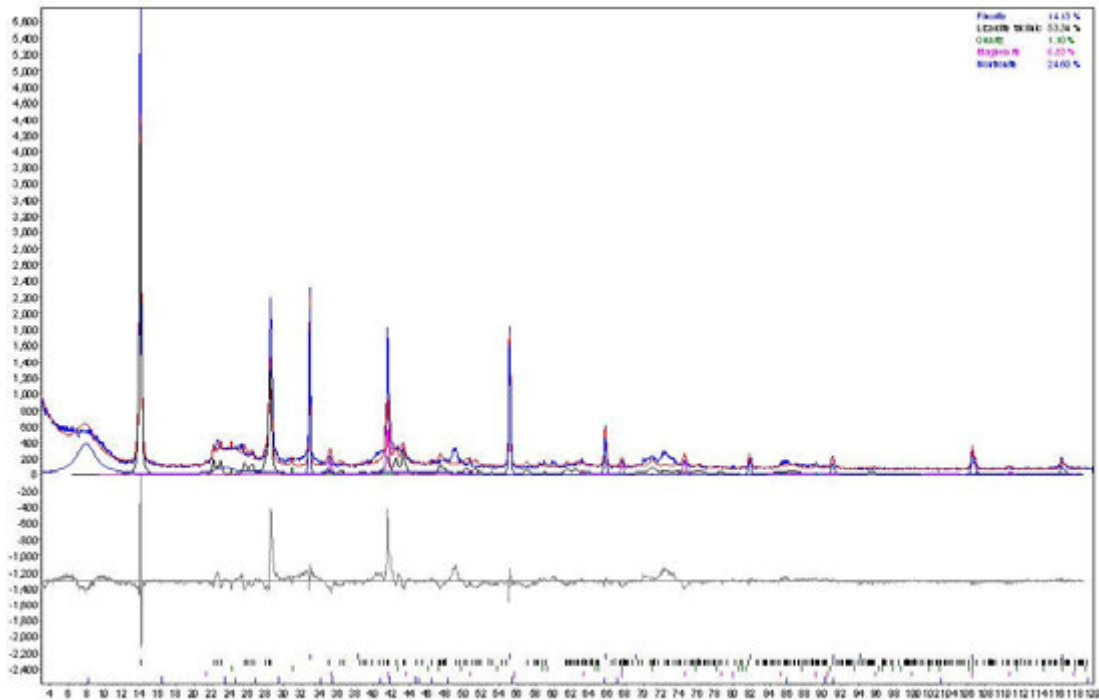
Figure 4: Saprolite QXRD

LEACHING RESULTS

Samples were milled to ensure that there were no locked minerals present in the ores.

A five stage in-house leaching protocol was used:
- Step 1: removes the water soluble fraction
- Step 2: removes the exchangeable fraction
- Step 3: removes the amorphous material
- Step 4: removes the adsorbed elements on the oxides and silicates
- Step 5: breaks the oxide/silicate crystalline lattice

A summary of the mineral formulae is given in the Appendix.

Limonite

Table 2 gives the percentage Al, Co, Fe, Mg, Mn and Ni leached from the limonite (although a complete ICP analysis was conducted, no other elements measured showed any change with these leaching steps) while Figure 5 shows the changes in limonite mineralogy (obtained by QXRD) using the sequential leaching protocol. A mineral change of ±10% or greater is considered to be noteworthy when evaluating whether leaching of that mineral has occurred.

**Table 2: Percentage element leached from limonite during the sequential leaching protocol**

	Element leached (%)					
	Al	Co	Fe	Mg	Mn	Ni
Step 1	0	0	0	36	0	0
Step 2	0	0	0	4	0	0
Step 3	0	0	0	0	0	0
Step 4	3	0	0	3	0	2
Step 5	86	43	109	50	56	110
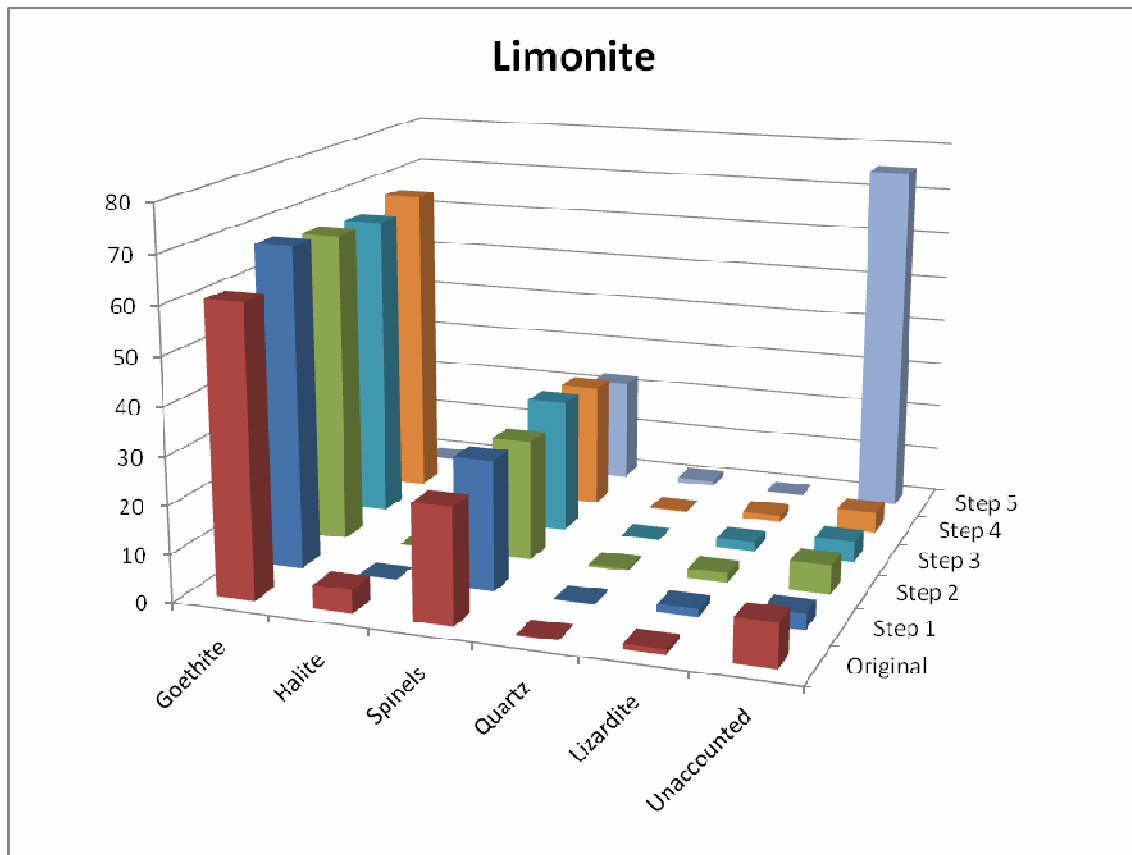
**Figure 5: Changes in limonite mineralogy during the leaching protocol
as determined by QXRD**

Step 1

The leach in Step 1 removed the halite, which was confirmed by XRD (Figure 6). This mineral was found to be nickel-barren from elemental analysis of the liquor and solid residues. From the elemental analysis (Table 2), 36% magnesium leached in this step while the QXRD (Figure 5) indicates that there was no leaching of any other minerals (i.e. the change in all other minerals is less than 10%). Because the percentage of unaccounted material decreases from 10% to 3% as compared to the original, it can be assumed that this magnesium most likely comes from a water soluble amorphous (nickel-barren) mineral.
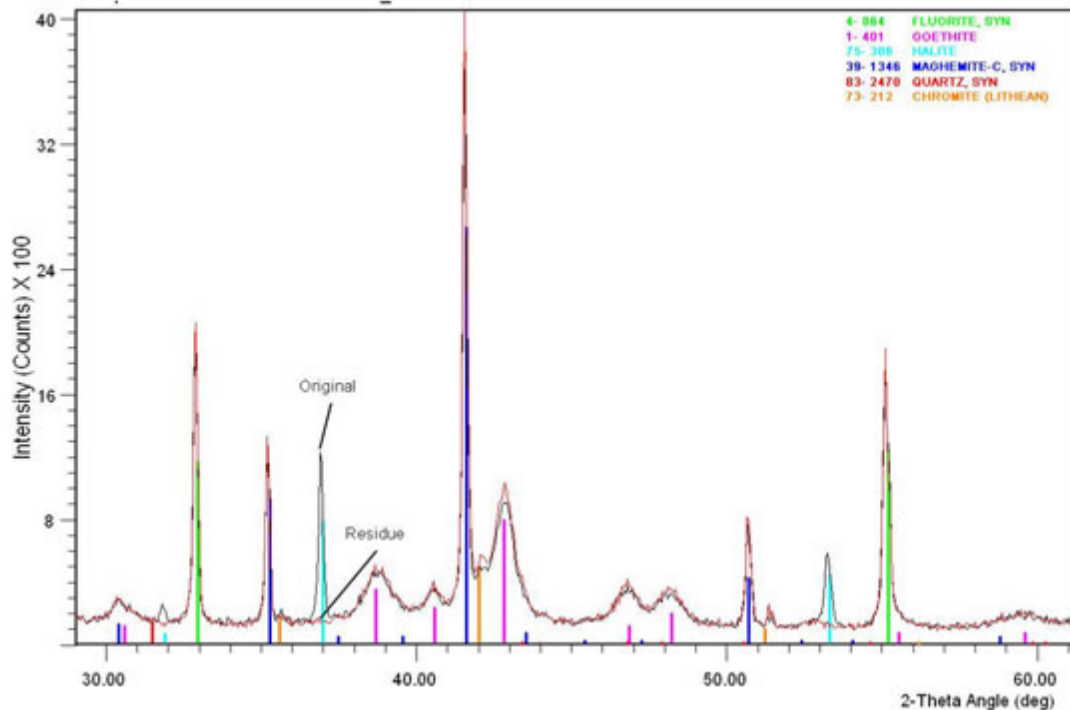
Figure 6: XRD Limonite original and leaching residue after step 1 profiles

Step 2

The QXRD analysis (Figure 5) indicated that there was no significant change in the mineralogy of the sample after this leaching step. The elemental analysis indicated that there as a small (4%) magnesium loss and this again is likely to be from the same amorphous material as was leached in Step 1.

Step 3

The QXRD analysis (Figure 5) indicated that there was no significant change in the mineralogy of the sample after it had been leached in step 3 and the elemental analysis also indicated that no leaching occurred.

Step 4

Again, QXRD analysis (Figure 5) did not show any change in the mineralogy after the sample was subjected to this leaching step. The elemental analysis indicated that a very small amount of aluminium (3%), magnesium (3%) and nickel (2%) were leached during this step. This could imply that these elements were adsorbed onto the mineral surfaces and were not actually part of the crystal phases.

Step 5

The QXRD data (Figure 5) indicated that all the goethite and the small amount of lizardite were leached. The minerals remaining were the spinels and quartz and a large percentage of amorphous material was produced. This is further confirmed by the broad "peak" in the XRD spectrum between 20° and 35° 2Θ (Figure 7). The elemental analysis indicated that all the nickel was leached in this step thereby yielding nickel-barren minerals.
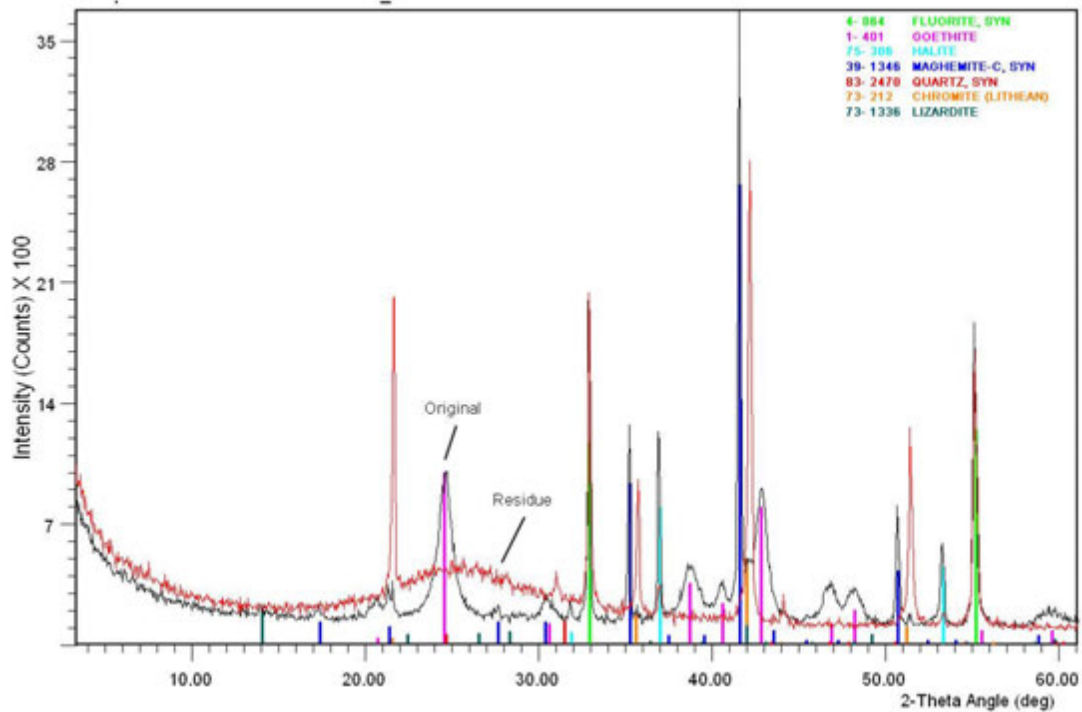
Figure 7: XRD Limonite original and leaching residue after step 5 profiles

Overall

The majority of the nickel present in the ore is associated with the goethite and/or lizardite mineral (leached in Step 5) with only a small amount of nickel adsorbed onto the mineral's surface.
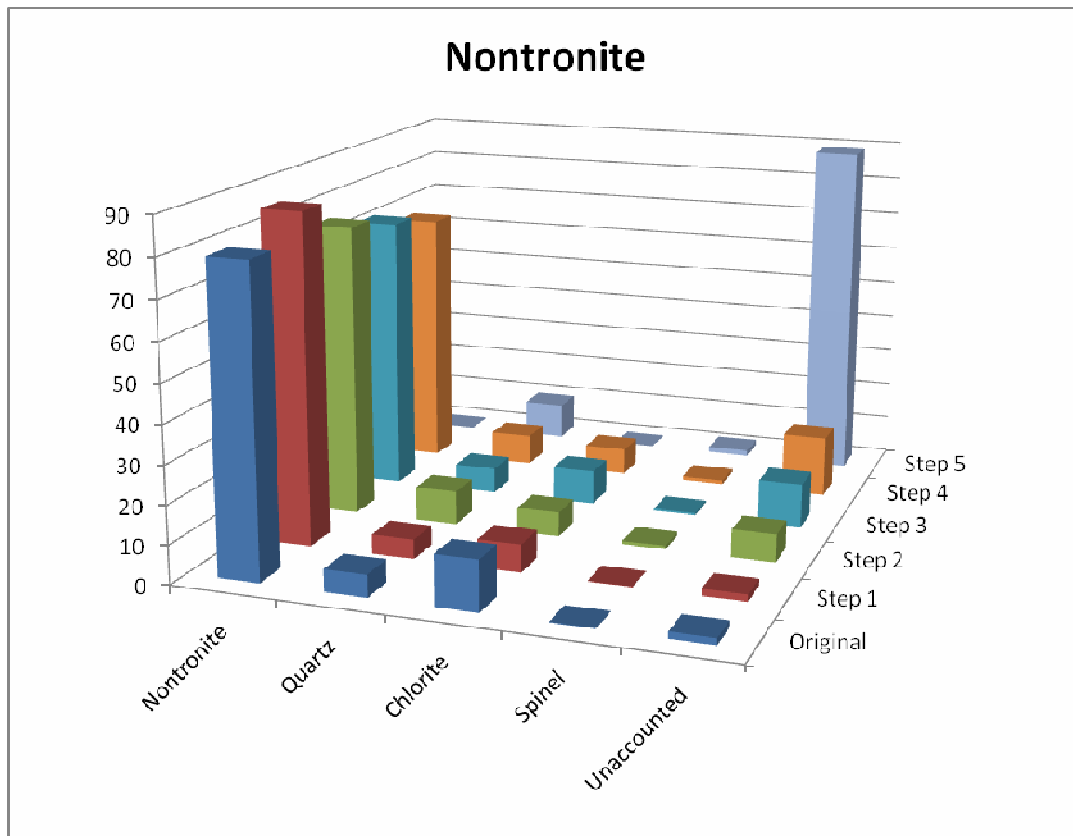
Nontronite

Table 3 gives the percentage Al, Co, Fe, Mg, Mn and Ni leached from the nontronite. All other elements measured showed no change with these leaching steps. Figure 8 shows the changes in nontronite mineralogy (obtained by QXRD). Again a mineralogical change of at least ±10% is considered to be noteworthy when using the sequential leaching protocol.

Table 3: Percentage element leached from nontronite during the sequential leaching protocol

|	Element leached (%)					
	Al	Co	Fe	Mg	Mn	Ni
Step 1	0	0	0	0	0	0
Step 2	0	0	0	43	0	0
Step 3	0	0	0	0	0	0
Step 4	3	0	0	4	0	4
Step 5	83	44	83	43	0	96

**Figure 8: Changes in nontronite mineralogy during the leaching protocol
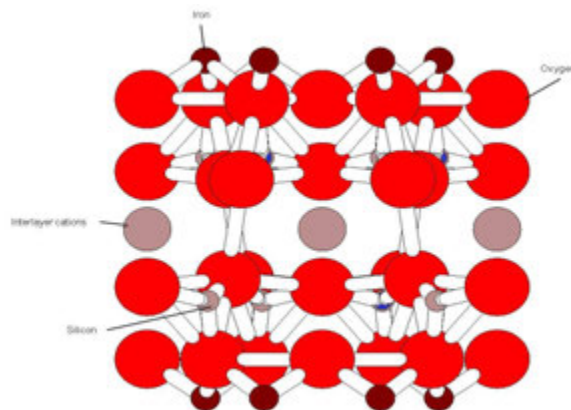as determined by QXRD**

Step 1

The QXRD analysis (Figure 8) indicated that there was no change in the mineralogy of the sample after it had been leached and the elemental analysis (Table 3) also indicated that no leaching had occurred.

Step 2

The QXRD analysis (Figure 8) did not indicate any appreciable change in the mineralogy of the ore after this leaching step. However the elemental analysis (Table 3) showed that 43% of the magnesium leached during this step. It can be seen from the XRD analysis (Figure 9) that the nontronite 001 peak has shifted significantly. This occurs because the interlayer cations present in the structure (Figure 10) are exchanged in this step, thereby changing the mineral's d-spacing. This indicates that the leached magnesium was located between the layers of the nontronite structure.
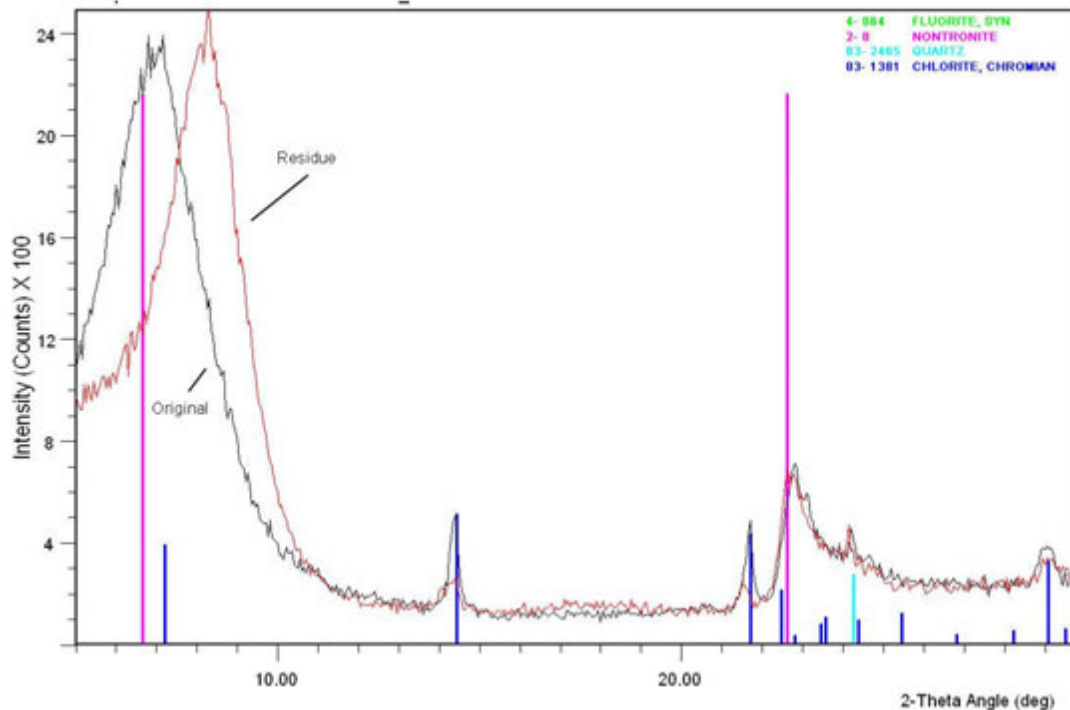
Figure 9: XRD of original nontronite sample and leaching residue after Step 2

Figure 10: Ball and stick model of nontronite

Step 3

The QXRD analysis (Figure 8) indicated that there was no change in the mineralogy of the sample after it had been leached and the elemental analysis also indicated that no leaching had occurred.

Step 4

The QXRD analysis (Figure 8) showed that there was a slight increase in the amorphous/unaccounted content after this leaching step. The elemental analysis only indicated small amounts of aluminium, magnesium and nickel were leached during this step (most likely adsorbed onto the mineral surfaces). Therefore it is likely that this increase is an issue with the QXRD analysis and there is no leaching occurring during this step.

Step 5

QXRD data (Figure 8) indicates that the nontronite was completely leached during this step together with the chlorite. The minerals remaining were the spinels and quartz with a large percentage of

amorphous material produced (Figure 11). The elemental analysis indicated that all the remaining nickel was leached in this step and therefore the remaining minerals were nickel-barren.
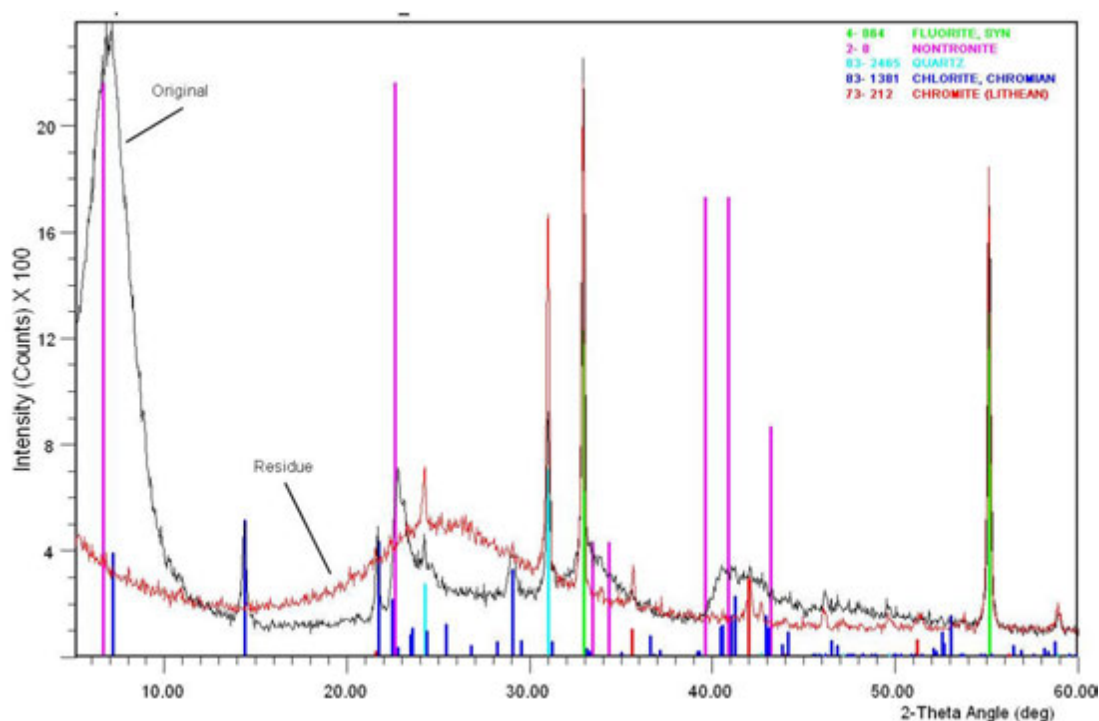

Figure 11: XRD of original nontronite sample and leaching residue after Step 5

Overall

The majority of the nickel present in the ore is associated with the nontronite and/or chlorite minerals as shown by the nickel recoveries in Step 5, with only a small amount of nickel adsorbed onto the mineral surfaces. It is impossible to determine if the chlorite mineral was nickel-rich or -barren from this leaching protocol.

Saprolite

Table 4 gives the percentage Al, Co, Fe, Mg, Mn and Ni leached from the saprolite. The other elements measured showed no change with these leaching steps. Figure 12 shows the changes in nontronite mineralogy (obtained by QXRD and where a mineralogical change of ±10% or greater is considered to be noteworthy) using the sequential leaching protocol.

Table 4: Percentage element leached from saprolite during the sequential leaching protocol

|	Element leached (%)					
	Al	**Co**	**Fe**	**Mg**	**Mn**	**Ni**
Step 1	0	0	0	0	0	0
Step 2	0	0	0	2	0	0
Step 3	0	0	1	1	38	7
Step 4	8	0	3	6	9	16
Step 5	113	0	78	99	34	87
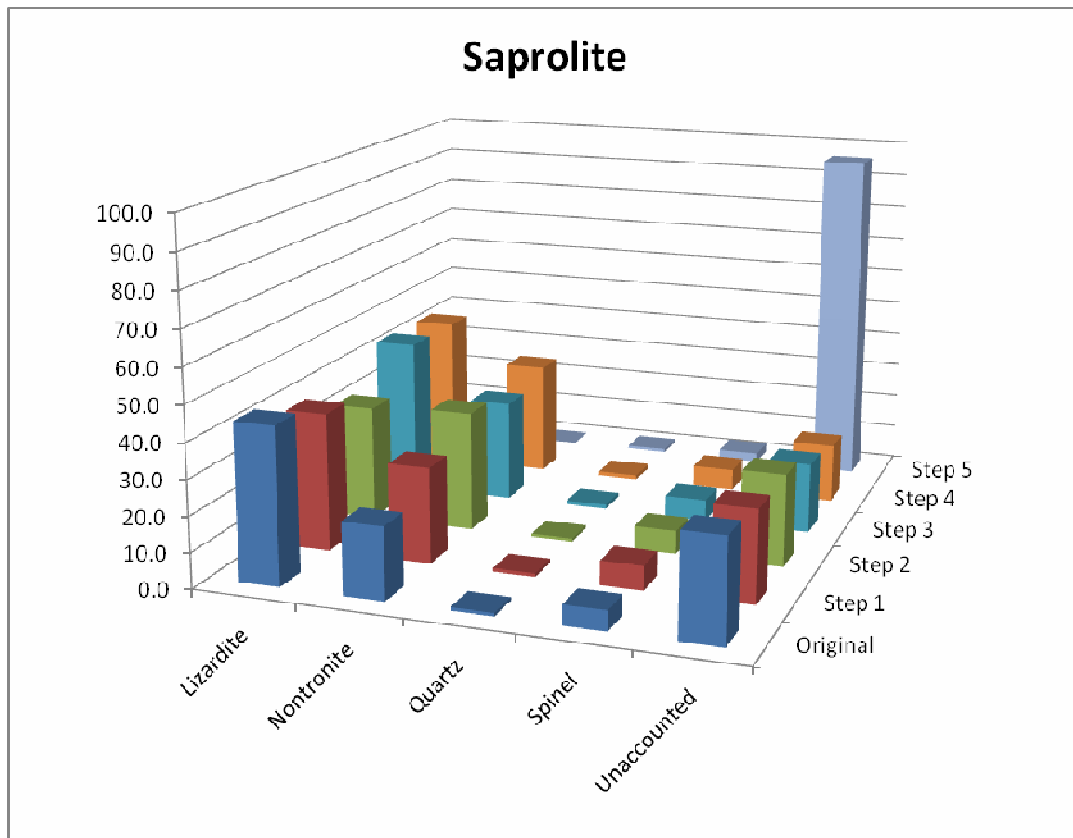
**Figure 12: Changes in saprolite mineralogy during the leaching protocol
as determined by QXRD**

Step 1

The QXRD analysis (Figure 12) indicated that there was no change (any perceived changes were within experimental error) in the mineralogy of the sample after it had been leached and the elemental analysis (Table 4) also indicated that no leaching occurred.

Step 2

The QXRD analysis (Figure 12) did not indicate any appreciable change in the mineralogy of the ore after this leaching step. The slight drop in lizardite seen is attributed to issues with the QXRD analysis of this ore. However the elemental analysis shows that 2% of the magnesium leached during this step. It can be seen from the XRD analysis (Figure 13) that the nontronite peak has changed shape and, as with the nontronite ore, this is due to the cations present within the structure being exchanged during this leaching step.
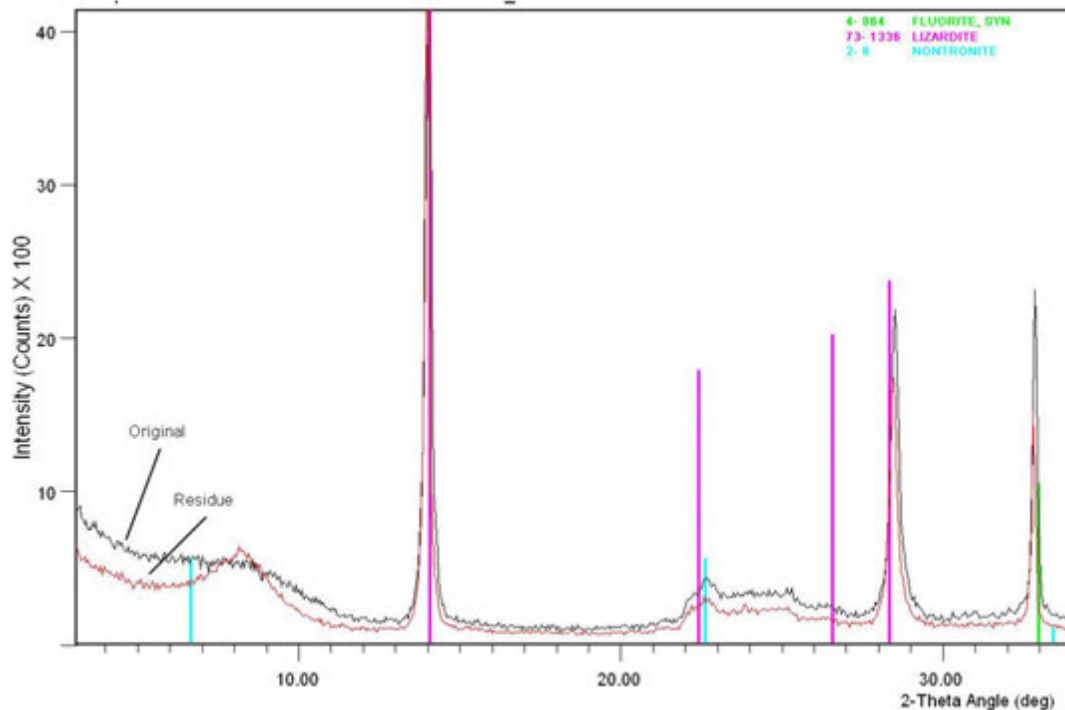
Figure 13: XRD of original saprolite sample and leaching residue after Step 2

Step 3

The QXRD analysis (Figure 12) did not indicate any change in the mineralogy of the ore after this leaching step except for a slight decrease in the unaccounted/amorphous content. The elemental analysis indicated that 38% of the manganese and 7% of the nickel leached during this step. This is most likely due to the leaching of asbolane. Asbolane $((Co,Ni)_{1-y}(MnO_2)_{2-x}(OH)_{2-2y+2x}.nH_2O)$ has a very poor XRD pattern (i.e. it is quite amorphous) and cannot be easily analysed by QXRD. No cobalt was found in the leach liquor, however, due to the low percentage of cobalt present in the ore, the amount leached could be below detection limits. To prove that asbolane has been leached during this step a SEM (or QEMSCAN) analysis would be required. However, this was not possible in this test work, as the sample had been pulverised resulting in a particle size distribution which is too small to be analysed by SEM.

Step 4

The QXRD analysis (Figure 12) did not show any change in the mineralogy after the sample was subjected to this leaching step. The elemental analysis indicated that a small amount of aluminium (8%), magnesium (6%), iron (3%), manganese (9%) and 16% nickel were leached during this step. This indicates that these elements were adsorbed onto the mineral surfaces and were not actually part of the crystal structure. Alternatively, asbolane that had not been removed completely during Step 3 could have leached in Step 4. If the assumption is made that all of the manganese leached during this step is from the asbolane mineral, using the ratio of manganese and nickel leached during Step 3, ~2% of the nickel leached during this step is associated with the asbolane mineral and the remaining ~14% was adsorbed onto the mineral surfaces.

Step 5

The QXRD (Figure 12) indicates that the lizardite and nontronite were completely leached during this step. The minerals remaining were the spinels and quartz with a large percentage of amorphous material produced (Figure 14). The elemental analysis indicated that all the remaining nickel was leached in this step, therefore the residual minerals left were nickel-barren.
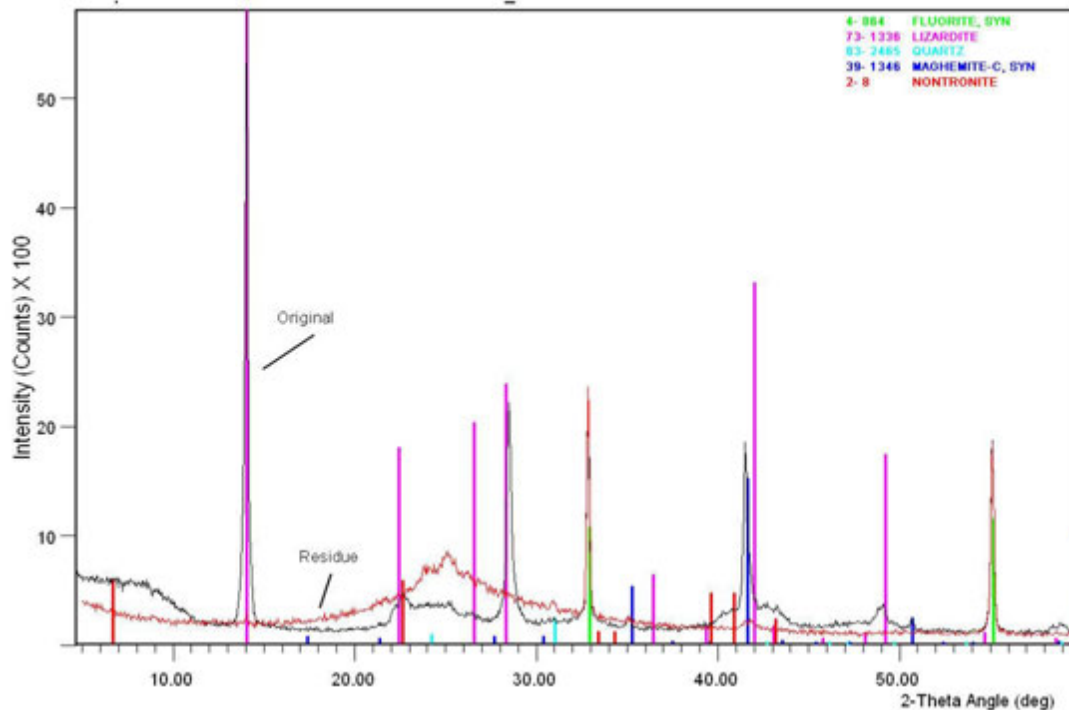
Figure 14: XRD of original saprolite sample and leaching residue after Step 5

Overall

The majority of the nickel present in the ore is associated with the lizardite and/or nontronite minerals. However, 7–9% of the nickel was associated with a manganese rich amorphous material, most likely asbolane. There was also a significant percentage of nickel (14–16%) adsorbed onto the mineral surfaces.

CONCLUSION

The application of the leaching protocol enabled the determination to be made that the spinel and quartz minerals, present in these ores, were nickel-barren. It also allowed the distinction to be made between nickel in the amorphous phases and crystalline minerals. However, use of this technique does not allow for the independent leaching of the three main minerals goethite, lizardite and nontronite. Therefore, if more than one of these minerals is present, the amount of nickel associated with each mineral cannot be determined. However, the leaching methodology is rapid and using simple solution analysis is an affordable method to determine whether nickel is present in minerals that are difficult to leach (i.e. spinels), amorphous phases and/or leachable crystalline phases.

REFERENCES

1. Hall, G. E. M., Vaive, J. E., Beer, R. & Hoashi, M. "Selective Leaches Revisited, with Emphasis on the Amorphous Fe Oxyhydroxide Phase Extraction" *Journal of Geochemical Exploration,* 56**,** 59-78, 1996.

2. Kersten, M. & Förstner, U. "Speciation of Trace Elements in Sediments", IN Batley, G. E. (Ed.) *Trace Element Speciation: Analytical Methods and Problems,* USA, CRC Press Inc., 1989.

3. McCarty, D., Moore, N. & Marcus, W. "Mineralogy and Trace Element Association in an Acid Mine Drainage Iron Oxide Precipitate; Comparison of Selective Extractions, Applied Geochemistry, 13, 165-176, 1998.

Mineral Formulae

Goethite: FeOOH

Lizardite: $Mg_3(Si_2O_5)(OH)_4$

Nontronite: $X_{0.3}Fe_2((Si,Al)_4O_{10})(OH)_2 \cdot nH_2O$ where X can be elements such as Na, Ca, Mg

Halite: NaCl

Quartz: SiO_2

Chlorite: $(Fe, Mg, Al)_6(Si, Al)_4O_{10}(OH)_8$

Spinel: Chromite $FeCr_2O4$, Maghemite Fe_2O_3

Asbolane: $(Co,Ni)_{1-y}(MnO_2)_{2-x}(OH)_{2-2y+2x} \cdot nH_2O$

ALTA 2011
NICKEL/COBALT/COPPER

HEAP & BIOLEACHING

OPTIMIZING NICKEL LATERITE AGGLOMERATION FOR ENHANCED HEAP LEACHING

By

[1]Jonas Addai-Mensah, [1]Ishmael Quaicoe, [1]Ataollah Nosrati, [2]George Franks, [2]Liza Forbes[,]
[3]Lian Liu, [4]David J. Robinson and [4]John Farrow,

[1]Ian Wark Research Institute, University of South Australia, Australia

[2]Dept. Chemical and Bimolecular Engineering, University of Melbourne, Australia

[3]School of Chemical Engineering, University of Queensland, Australia

[4]CSIRO Process Science and Engineering & Minerals Down Under National Research Flagship
Australian Minerals Research Centre, Australia

Presenter

Jonas Addai-Mensah
Jonas.addai-mensah@unisa.edu.au

ABSTRACT

Although about 60 % of the world's nickel (Ni) mineralization occurs as nickel laterite ore, processing of complex, low grade laterite ores by conventional physical unit operations (e.g. magnetic, electrostatic and flotation) is still intractable. Due to their mineralogical and chemical complexity, low grade nickel laterite ores require more aggressive chemical and hydrometallurgical techniques (e.g., acidic lixiviant heap leaching) for value metal (Ni and Co) extraction. To process such ores, agglomeration of the feed particles into robust and porous granules as a precursor to heap leaching of 4-10 m permeable bed, is desirable. In the present work, we investigate agglomeration behaviour of siliceous goethite Ni laterite ore and selected oxides and clay minerals (hematite, quartz and kaolinite) which constitute the predominant host gangue phases of typical low grade nickel laterite ores. Fundamental knowledge and understanding of the agglomeration mechanisms and kinetics which are essential for producing robust real ore granules, and pivotal to the subsequent heap leaching process, are gleaned. Isothermal, batch agglomeration tests involving 30 and 44 wt.% sulphuric acid solution as a binder indicated that 5 – 40 mm granules of differing roughness and morphologies were produced in 8-14 min.

The results clearly showed feed characteristics (such as mineralogy and primary particle size distribution) and binder content (15-25 wt.%) dependent agglomeration behaviour. Slow induction type nucleation and growth agglomeration were displayed by the kaolinite clay mineral whilst the oxides exhibited fast nucleation and growth agglomeration processes. Siliceous goethite feed ore fine/coarse ratio, H_2SO_4 binder dosage and acidity, post-agglomeration drying temperature and aging conditions, all showed significant impact on controlling agglomeration mechanism (e.g., particle wetting, nucleation and growth processes) and granule attributes (e.g., size, density and strength). Agglomerates strength and density increased with increasing fine/coarse particle ratio.

108

INTRODUCTION

Current demand for commodity metals (e.g., Ni) and depletion of high grades ores have necessitated the need to process alternative ore deposits which are often variable, complex in mineralogy and low in grade (Lee et al., 2005; Golightly, 1981; Horton, 2008). In the case of nickel, these alternative ores in recent years has been laterites (Kuck, 2009; Kim et al., 2010; Elias, 2002; Mudd, 2010). Conventional unit operations (e.g. flotation, electrostatic and magnetic) are mostly employed initially to concentrate or upgrade these ores where possible. For complete value metal recovery, aggressive chemical / hydrometallurgical techniques such as heap leaching (HL), atmospheric leaching (AL) and high pressure acid leaching (HPAL) are usually employed. Due to the cost involved in processing these complex low grade ores and environmental issues HL is relatively considered to be the most favourable, particularly, for treating complex, low-grade ores (Lewandowski and Kawatra 2008, 2009). Several scientific and technological challenges persist in making HL an effective and economically viable processing technology. Some of these are linked to poor permeability issues usually associated with finely ground feed ore bed and the presence of acid consuming clay minerals (Chamberlin, 1986; Dixon, 2003; Eisele and Pool 1984; Lewandowski and Kawatra, 2008, 2009; Kappes, 1979). Poor permeability caused by fine particles usually occurs through segregation during heaping and fine particles migration with leachate through the heap (Chamberlin, 1986; Dixon, 2003; Eisele and Pool 1984; Lewandowski and Kawatra, 2008; Kappes, 1979). The migration of fine particles clogs the natural flow channels, and form impermeable layers within the heap that restrict lixiviant percolation. Consequently, the leachate flows through paths of least resistance, leading to poor solution distribution and hence, low metal recovery. Fine mineral particles pre-treatments methods such as agglomeration are used to improve the performance of heap leaching and minimised the poor permeability issues (Chamberlin, 1986; Dixon, 2003; Eisele and Pool 1984; Lewandowski and Kawatra, 2008, 2009; Kappes, 1979).

In spite of the economic importance of agglomeration pre-treatment, its successful application to complex low grade Ni laterite ores heap leaching is limited. To date, there are only two commercial plants in minerals industry operating full-scale heap leaching of agglomerated nickel laterite ores, the Murrin Murrin (Western Australia) and Caldag (Turkey) operations. Fundamental agglomeration studies are required to understand the agglomeration behaviour which determines the geotechnical and hydrometallurgical characteristics of the heap granules of typical low grade Ni laterite (e.g., siliceous goethite, saprolite) ores.

In this study, the agglomeration behaviour of selected clay (Kaolinite) and oxide (hematite and quartz) minerals which typically constitute the predominant host gangue phases in low grade Ni laterite ores were investigated in tandem with a real nickel laterite (siliceous goethite) ore. Specifically, the effect of binder content and its composition (30% vs. 44% w/w H_2SO_4) and post-agglomeration treatment (air-drying) on agglomeration behaviour and granule properties (size, integrity, strength) were studied. Particularly, the influence of feed characteristics (chemical / mineralogical composition and primary particle size distribution) on granule growth behaviour and binder on agglomerate properties (e.g., size, morphology, density and compressive strength) was examined.

MATERIALS AND METHODS

Materials

Model Minerals

Three model polydispersed minerals: kaolinite (clay), quartz and hematite (oxide) were used. Tables 1, 2 and 3 show the properties of these powders. The specific surface area was determined by a 5 point N_2 BET (Brunauer et al., 1938) analysis (Coulter Omnisorp 100, Hialeah FI. USA). The particle size distributions (PSD) of the minerals (Figure 1) were determined by laser diffraction method using Malvern Mastersizer 2000A. X-ray fluorescence (XRF) method was also used to determine their individual minerals' chemical compositions. The measurements were conducted using a Panalytical MiniPal 4 EDXRF Spectrometer using default condition sets for 60 s for each condition. The XRF equipment was calibrated using pure oxides.

109

Nickel Laterite Material

Polydispersed, -2 mm and -150 μm siliceous goethite (SG) laterite ore (~1.0 wt.% Ni) from Western Australia were used in this study as received. Quantitative X-ray powder diffraction QEMSCAN analyses showed complex mineral associations where the quartz, goethite, nontronite and serpentine comprise the dominant and hematite, asbolane and kaolinite comprise the minor mineral phases (Tables 4 & 5). It also established the dominant, sub-dominant and minor gangue mineral phases with some size dependency in the sample, where bimodal particle size distributions of fine and coarse size fractions were displayed.

Binder

For the model minerals (hematite, quartz and kaolinite), 30 % w/w H_2SO_4 solution was used as the liquid binder for all the tests. In the case siliceous goethite (SG), 30 and 44% w/w H_2SO_4 solutions were used as the liquid binders at mass contents in the range 15 – 25 %. Due to the difference in minimum binder saturation requirement for effective agglomeration for the model minerals, as a result of their initial porosities and true densities, the binder contents used for successful agglomeration varied: 15, 18 and 30 wt. %, respectively for hematite, quartz and kaolinite.

Batch Agglomeration Equipment

The agglomeration tests were carried out batch-wise in a horizontal, stainless-steel drum granulator of 0.3 m internal diameter and length of 0.2 m (Figure 2A) operated at a constant rotational speed of 60 rpm. Within the drum are six 5 mm high baffles spaced evenly around the interior to aid in tumbling of the feed charge. To enable visual observations during the agglomeration process, Perspex material was used as cover plates both openings of the drum. Due to safety precautions, the granulator was operated in an enclosed guarded cage as shown in Figure 2B.
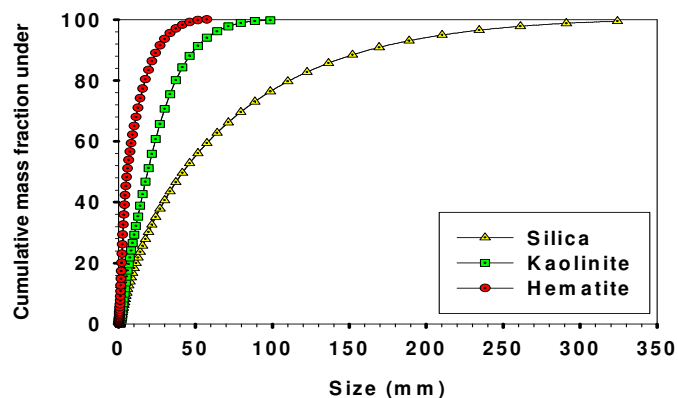

Figure 1: Primary particle size distribution of hematite, kaolinite and quartz minerals

Table 1: Specific surface area and particle mean diameters of hematite, quartz and kaolinite

Material	D_{10} (μm)	D_{50} (μm)	Mass mean – $D_{4,3}$ (μm)	BET Specific surface area (m^2/g)	Surface weighted mean – $D_{3,2}$ (μm)
Hematite	1.4	6.3	11.1	14.5	3.1
Quartz	5.2	41.9	65.6	1.0	13.5
Kaolinite	3.8	18.9	23.3	24.8	9.7

110

Table 2: Density, amount of acid used and initial bed pore volumes of hematite, quartz and kaolinite

Material	Dry mass (g)	True density (g/cm^3)	Bulk density (g/cm^3)	Mass of acid used (g)	Volume of acid used (cm^3)	Initial bed pore volume (cm^3)
Hematite	500	5.3	2.0	88.2	73.5	155.0
Quartz	500	2.7	1.7	109.8	91.5	108.8
Kaolinite	500	2.6	0.8	214.3	174.2	432.7
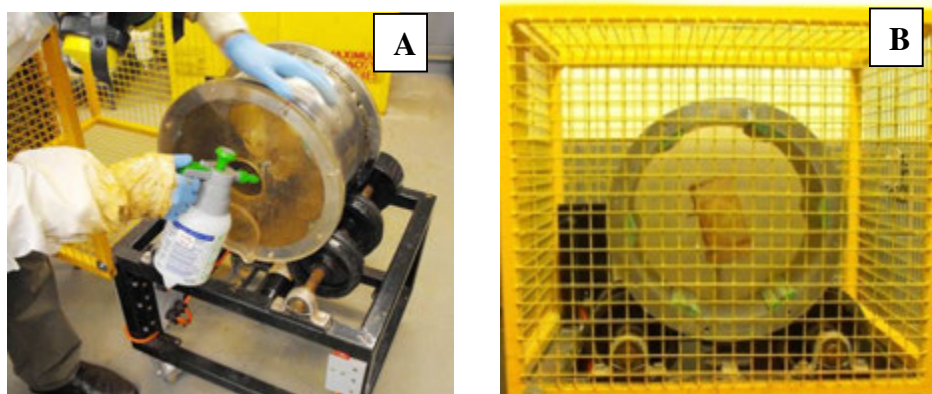
Figure 2: The laboratory scale batch drum granulator (A) without and (B) with guarded cage (for safe operation)

**Table 3: Chemical composition of hematite, kaolinite and quartz minerals**

Major oxide	Hematite	Kaolinite	Quartz
SiO_2	2.4	45.8	99.1
TiO_2	-	1.9	-
Al_2O_3	3.1	35.6	-
Fe_2O_3	93.0	1.2	-
MgO	-	0.2	-
CaO	-	0.1	-
K_2O	-	0.2	-
Na_2O	-	0.2	-
LOI*	1.5	14.8	0.9

*Loss of ignition

Table 4: Mineralogical composition of -2 mm siliceous goethite ore

Mineral phase	Mass %
Quartz	36.06
Kaolinite	0.21
Mg-bearing silicates (e.g., serpentine)	8.71
Nontronite (smectite group)	18.77
Goethite	27.43
Hematite	2.81
Asbolane	0.40
Total Nickel	1.1
LOI*	5.64

The distribution of nickel, cobalt and manganese in the SG ore based on chemical analysis is given in Figure 3. Details of the Quantitative X-Ray Diffraction data for the main components of the ore are given in Figure 4. As shown in Figure 3, the dissemination of the three elements is greater for the -1.18 to 0.038 mm and C6 and C7 size fractions than for the C1-C5 size fractions.
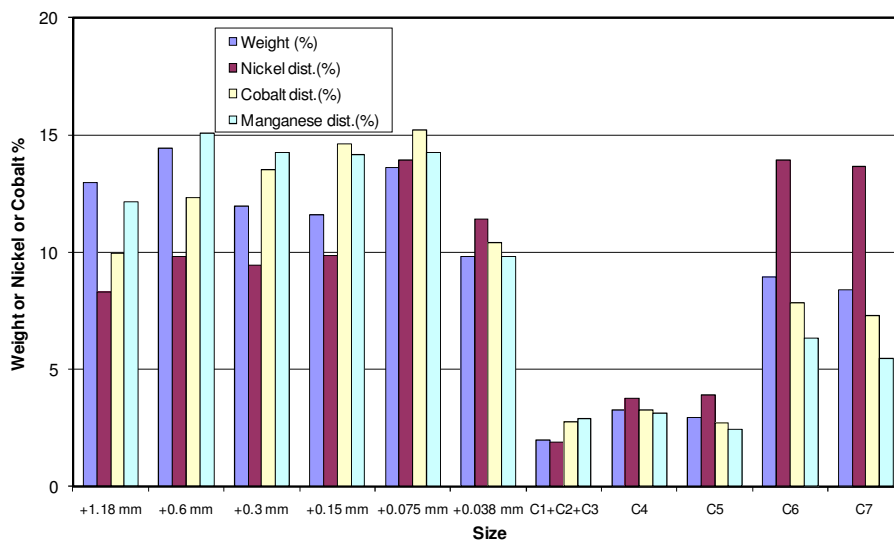
Figure 3: Sizing and metal distributions in the Siliceous Goethite sample

The dominant phases are goethite across all the sizes with quartz being the predominant phase in the coarse sizes (Figure 4). Smectite and serpentine clay minerals are indicated, with both largely showing up in the fine fractions as expected.

112
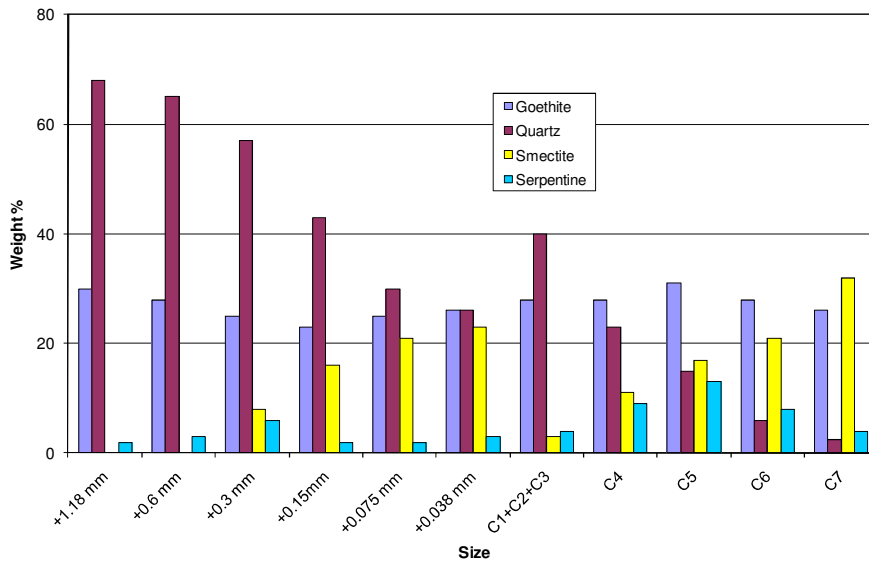
Figure 4: Quantitative X-Ray Diffraction data for major host gangue mineral species in the siliceous goethite ore sample

Agglomeration Procedure

Approximately, a feed charge consisting of 500-800 g of dry powder with a known amount of H_2SO_4 binder was used for each agglomeration test. This loading corresponds to about 4-7 % of the total effective drum volume. The weighed powder was pre-mixed with a pre-determined amount of liquid binder in an acid resistance glass ware before transferred into the drum granulator. For all the agglomeration tests, a constant drum speed of 60 rpm and maximum batch agglomeration time of 14 min were used. It is worth mentioning that due to the tendency of the wet material sticking to the drum wall, a regular scraping of the material (~ 30 s intervals) was found to be sometimes necessary for efficient tumbling and agglomeration.

Agglomerate Characterisation

After each agglomeration test the product size distribution on mass basis was determined by a sieving technique. The cumulative mass fractions under were then plotted against granule size (defined as mesh size of retaining sieve). A bench-top tensile-compressive strength machine (Hounsfield, UK) shown in Figure 5 was used to load the agglomerates in diametric compression. This was achieved by applying a load (force) to a granule held between two parallel flat surfaces, one of which is held stationary and the other attached to a constant velocity drive (Figure 5). A load cell attached to the upper drive surface enables the measurement of the resultant force at a maximum load setting of 1000 N and velocity of 10 mm/min. Based on the agglomerate diameter and the force at which breakage occurred (as measured by the machine), the tensile failure strength was calculated from equation (1).

$$\sigma_s = \frac{4P}{\pi d_g^{\ 2}} \tag{1}$$

where σ_s is tensile failure strength, d_g is granule diameter (m) and P is the applied load or force (N) Three sets of agglomerates were used for strength measurements, one set air-dried at ambient temperature (~ 22 – 25 $^{\circ}$C) or oven dried at 40 $^{\circ}$C, both for 24 h, and the other kept wet in air-tight plastic for 24 h.

113
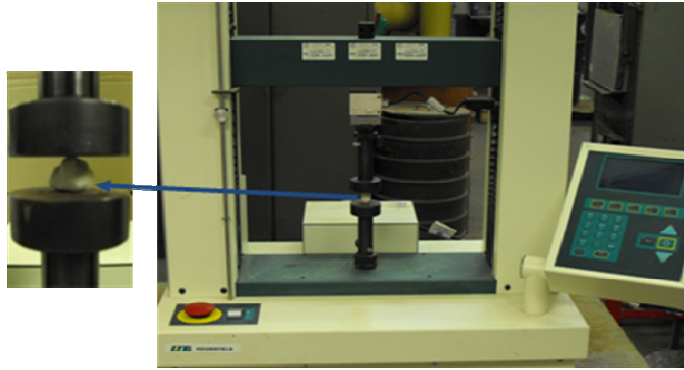
Figure 5: Apparatus for loading agglomerates in diametric compression

RESULTS AND DISCUSSION

Model Minerals Agglomeration Behaviour

The model oxides and clay minerals agglomeration behaviour was investigated by analysis of the evolution of their PSD after 2, 4, 8 and 14 min (Figures 6 and 7). The results show that kaolinite granules (Figure 6C) have irregular shape and less smooth surfaces in comparison with the smooth spherical granules of hematite (Figure 6A) and quartz (Figure 6B).

Figure 7 displays the agglomerates PSDs, reflecting marked differences. The results show that hematite nucleation was more intensive than for quartz and kaolinite. Noticeable amounts of fine (feed) particle fractions were observed in the quartz (Figure 7B) and kaolinite (Figure 7C) up until to 8 min of agglomeration. On the other hand, there was a significant shift to larger granule size with time for hematite (Figure 7A). This indicates that hematite displays shorter nucleation induction time than quartz and kaolinite, a behaviour which depends upon the time for the liquid binder to be distributed from the granules core to the surface (Iveson, 1997). The results further show that after nucleation phase at time > 2 min, quartz and kaolinite particles followed similar agglomeration sub-processes of random pseudo-layering growth between 2- 4 min, followed by non-random coalescence (4-8 min) and then random pseudo-layering growth between 8-14 min. The hematite, on the other hand, displayed non-random coalescence behaviour between 2-4 min and 8-14 min.

These growth behaviour displayed by the ores may be attributed to binder-ore interaction characteristics (Benali, 2009). Whilst constant binder surface tension and composition and drum speed were used, different binder volumes were involved. Apart from the differences due to ore mineralogy, there is a noticeable difference in the PSDs of the three samples. The mean particle sizes ($D_{3,2}$ and $D_{4,3}$) decrease as follows: quartz > kaolinite > hematite. Feed PSD has influence on granule growth, with granule dynamic strength and growth rate increasing with decreasing mean particle size at saturation (Benali, 2009). Broader PSD of feed also causes the powder bed to be more densely packed as the smaller particles easily fill the inter-granular gaps among the larger particles. Consequently, this leads to difficulty in the liquid binder distribution and wetting of particles resulting in poor or slow agglomeration growth behaviour. Therefore the difference in the growth behaviour exhibited by the ores can be attributed to the differences in feed ore characteristics such as porosity, particle density, primary particle size distribution, mineralogy and volume of binder used.

In order to ensure reliability of the observed trends, reproducibility of the agglomeration behaviour was checked. Three replicate experiments were performed at three different times for each material used. Evidently, the results (Figure 7D) showed that the agglomeration behaviour was reproducible because substantial similar size distributions were obtained after 14 min in all the three replicate agglomeration tests. The model minerals agglomeration results are useful for benchmarking our understanding of the real nickel laterite ores. The striking agreement between the behaviour of the quartz and hematite and that of siliceous goethite laterite ores shown below (Figure 10), is worth noting.
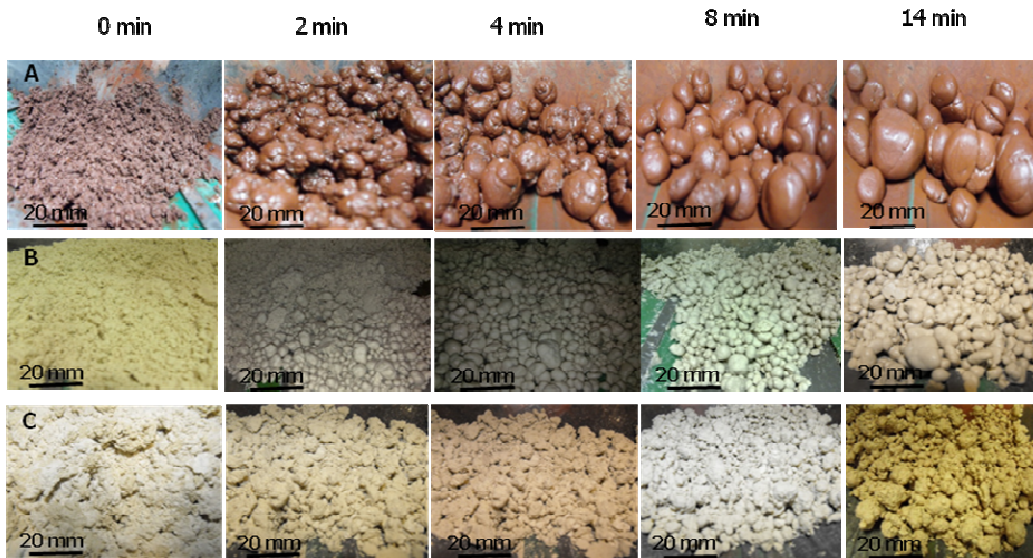
114

Figure 6: Digital images of (A) hematite (B) quartz and (C) kaolinite granules inside the drum agglomerator
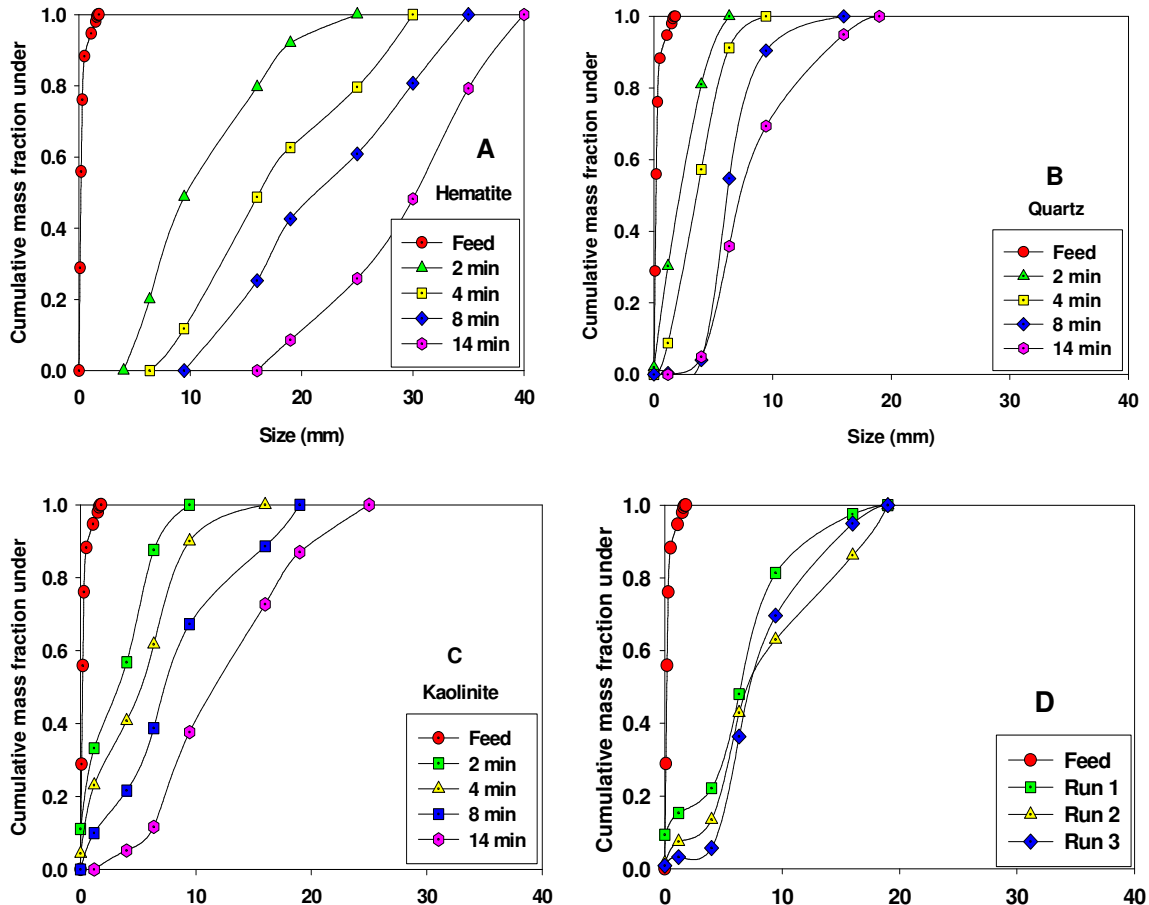

Figure 7: Granules size distribution of (A) hematite, (B) quartz and (C) kaolinite as a function of time and (D) three replicate quartz agglomeration tests at 14 min.

Model Agglomerates Strength

The tensile failure strength results (Figure 8) indicated that 24 h air-dried agglomerates have higher strength than the fresh (wet) agglomerates. This difference may be due to the type of bonding mechanisms that exist within the agglomerates. Literature indicates that fresh agglomerates

115

compression strength is controlled by liquid bridges whilst dry agglomerates compression strength is controlled by relatively strong solid bridges (McClelland and van Zyl, 1988; Lewandowski and Kawatra, 2009; Forsmo et al., 2006). These solid bridges may be formed from solidification or re-crystallization of leached acid-soluble minerals within the agglomerates as a result of drying. Kaolinite as a clay mineral is acid-soluble mineral whilst quartz is least soluble, hence the trend displayed by the strength data. In addition, the difference in strength may also be due to the difference in the feed primary particle size distribution. The broader the particle size distribution the weaker the granule strength (Capes and Danckwerts, 1965) and this is evident in Figure 8, where quartz with relative broader size distribution displayed the least strength. This means that the strength is dependent on post-agglomerate treatment (e.g., drying), ore mineralogy and primary particle size distribution. The results indicate that the clay mineral phases in laterite ores may increase the agglomerates strength.
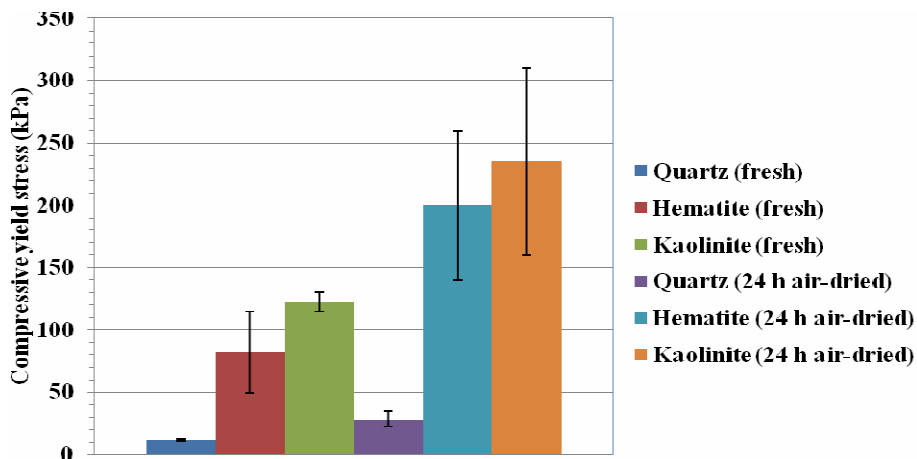

Figure 8: Tensile failure stress of wet and air-dried quartz, hematite and kaolinite agglomerates loaded in diametric compression

Nickel Laterite Agglomeration Behaviour: Effect of Binder Solution Composition/Content

To investigate the effects of binder solution composition (i.e., acidity) and content (wt.% of binder solution) on agglomeration behaviour of SG ore, two H_2SO_4 solutions (30 and 44% w/w) were used as binder liquid. For agglomeration tests conducted with 44% w/w H_2SO_4 as binder liquid (water/acid ratio: 1.27), 15% binder content led to insufficient wetting and hence, no agglomeration was observed in the course of 24 min. At 20% binder content, the added moisture was adequate to agglomerate the feed particles (Figure 9A). The data clearly indicate that despite rapid nucleation observed during first 2 min, granule size growth was slow where only ~20% of granules had size > 5 mm after 8 min. This partly was due to strong adherent tendency of the nuclei towards the drum walls, reducing the number of nuclei – granule collisions. These collisions are believed to facilitate granule size growth via mechanisms such as pseudo-layering and/or coalescence.
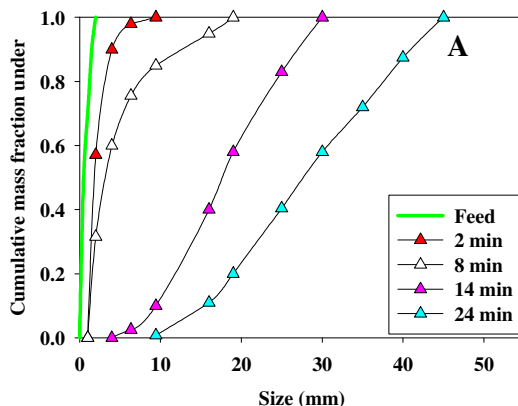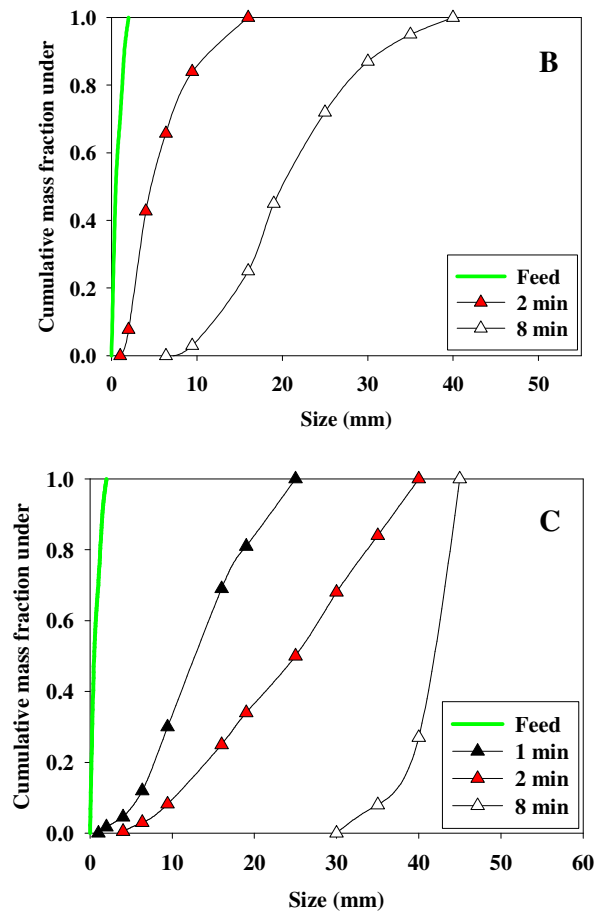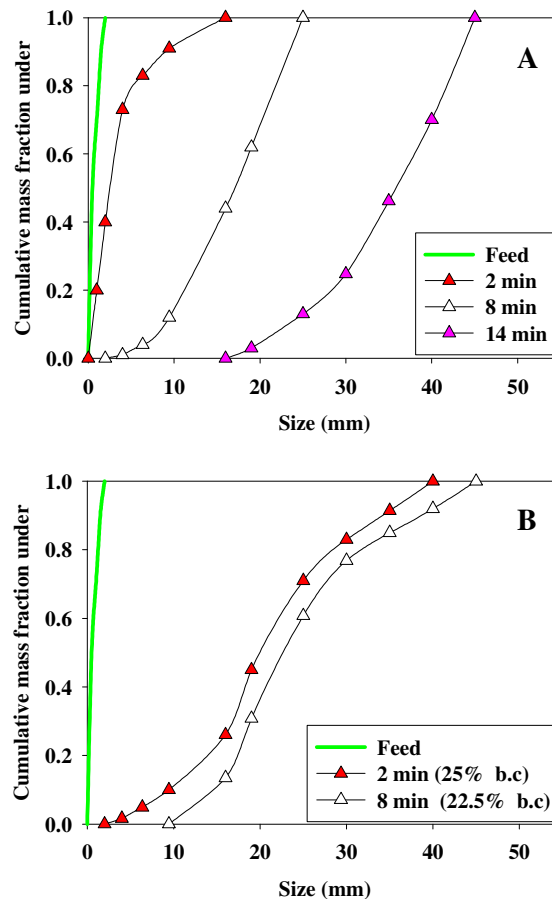
Figure 9: The granule size distribution for the SG ore as a function of agglomeration time with 44% w/w H_2SO_4 solution at 20% (A), 22.5 (B) and 25% (C) binder content

The results in Figure 9A also show that granules of 5 – 25 mm size range were produced within 8 – 14 min, whilst further agglomeration up to 24 min resulted in the formation of oversize agglomerates. The increase of the 44% w/w H_2SO_4 binder solution content from 20 to 22.5% enhanced the binder saturation of the feed ore and led to noticeably faster nucleation and growth process (Figure 9B). The data indicate that 2 – 15 mm size granules were produced after 2 min, with ~80% of 5 – 25 mm size granules formed within 8 min. A further increase of binder content to 25%, dramatically intensified the agglomeration process (Figure 9C). This led to massive nucleation which started during of dry feed and binder solution mixing and hence, formation of 5 – 15 mm size granules after 1 min and thereafter, coarse granules (5 – 40 mm). It is worth mentioning that the main mechanism for granule size growth changed from pseudo layering to coalescence upon 2.5 – 5 % binder content increase.

To better understand the effect of H_2SO_4 binder composition on agglomeration behaviour of SG ore, further tests were conducted using 30% w/w H_2SO_4 solution. Agglomeration was insignificant at 15% binder content due to poor wetting of the powder, at 20 wt.% or higher binder content however, it was effective. Figure 10A clearly shows that agglomerates in the size range 5 – 25 mm were produced within 8 min whilst longer time of 14 min led to the formation of coarser agglomerates (> 40 mm). At higher binder contents, 22.5% and 25%, larger agglomerates were produced within 8 and 2 min, respectively (Figure 10B).
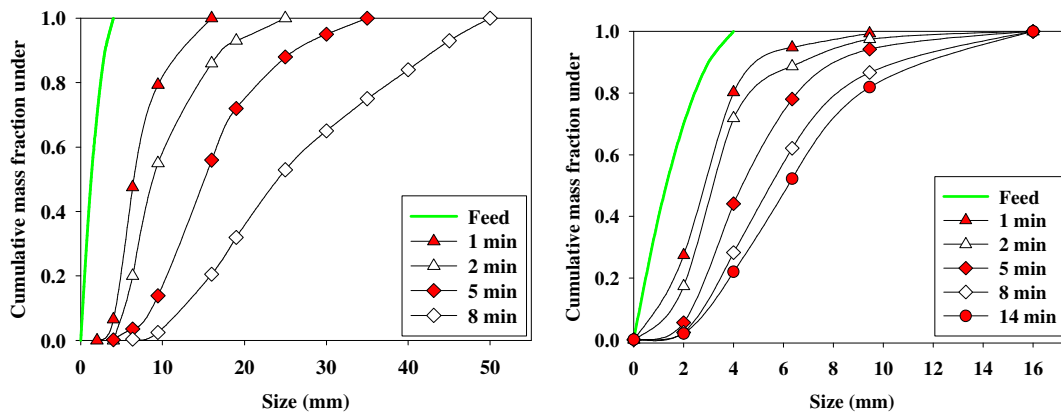
Figure 10: The granule size distribution for the SG ore as a function of agglomeration time with 30% w/w H$_2$SO$_4$ solution at 20% (A), 22.5% and 25% (B) binder content

For the latter, the agglomerates coalesced rapidly forming two or three large lumps after 3 min. The results in Figures 9 and 10 suggest that the higher the H$_2$SO$_4$ binder content, the faster the agglomeration rate at a given batch time. These observations underscore the key role of binder content in wetting the ore particles and controlling their bonding mechanisms during the agglomeration process. Strong cohesive forces (capillary forces arising from negative Laplace pressure) become increasingly dominant as the wetted particles move from pendular state through the funicular and capillary states, fostering strong agglomeration.

Nickel Laterite Agglomeration Behaviour: Effect of Fines to Coarse Particles' Ratio

Increasing the fine (F) (-150 µm)/ROM coarse (-2 mm) particles' mass ratio of the SG ore feed (at a fixed binder content):

1. slows down the overall agglomeration rate and granule size growth (Figure 11A) where smaller granules of narrower size distribution form at a given process time (Figure 10B).

2. enhances the nucleation stage, where more nuclei form per unit mass of feed ore during the initial stage, leading to larger number of smaller size of granules (Figure 10B).

3. changes the granule growth mechanism from coalescence to pseudo layering due to decreased wetting.

4. requires higher binder content to maintain faster agglomeration rate in a fixed process time.

118

Figure 11A: The granule size distribution for the SG ore with 20%F/80%ROM (A) and 60%F/40%ROM (B) produced with 25 wt.% binder content (30% w/w H$_2$SO$_4$) as a function of agglomeration time
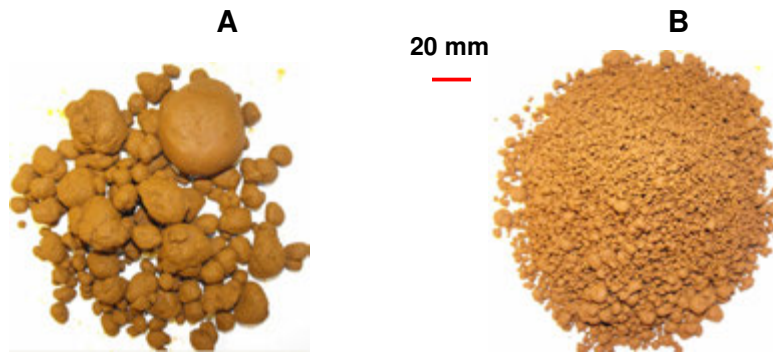
Figure 11B: Digital images of 20%F/80%ROM (A) and 60%F/40%ROM (B) SG ore after 8 min of agglomeration with 25 wt.% binder content (30%w/w H$_2$SO$_4$)

## Failure Strength of Siliceous Goethite Agglomerates

The effect of binder composition (acidity) and content on tensile failure strength (diametric loading) and integrity of agglomerate are shown in Tables 5. Prior to strength measurements, some agglomerates were air-dried at ambient temperature (~22 °C) for 24 h, whilst others, referred to as wet agglomerates, were kept in a sealed container for 24 h. The data in Table 5 indicate that the compressive strength of fresh agglomerates slightly decreased with decreasing binder acid content. This may be partly attributed to the greater density and more viscous binder liquid within the granules at higher binder acid strength (44% w/w H$_2$SO$_4$). Minor increase in binder content (e.g., 20 to 22.5%) had no significant effect on the agglomerate strength. In contrast, the strength of air-dried agglomerates was significantly higher than that of fresh agglomerates and increased slightly with increasing binder content. The higher strength observed for air-dried agglomerates is due to the stronger solid bridges which form between particles when the acid-mediated leached species solidify (crystallize) within the agglomerate with decrease in porosity upon drying.

119

Table 5: The compressive strength of fresh and air dried SG agglomerates produced with different binder liquid type and content

Binder liquid	Binder content (wt.%)	Agglomerate failure strength (kPa)	
		Wet (sealed container)	24 h air-dried (ambient)
44% w/w H_2SO_4	20%	35 ± 5	110 ± 10
	22.5%	30 ± 5	120 ± 10
	25%	35 ± 5	150 ± 10
30% w/w H_2SO_4	20%	25 ± 5	160 ± 10
	22.5%	20 ± 5	180 ± 10

Dry Siliceous Goethite Agglomerate Failure Strength and Density

The data of oven dried (40 ^{o}C 24 h) granule failure strength with increasing proportion of fines in the agglomerator feed are shown in Figure 12. The results show that agglomerates containing a lower fraction of fine material tend to be weaker than those containing a higher fraction of fines. The density of the resulting agglomerates was measured with the results presented in Figure 13. The data show that agglomerate density increases with increasing feed fine particles fraction. This may be attributed to the improved packing of the fine particles within the agglomerate matrix. The trends are quite significant within the margin of error in the measurement.
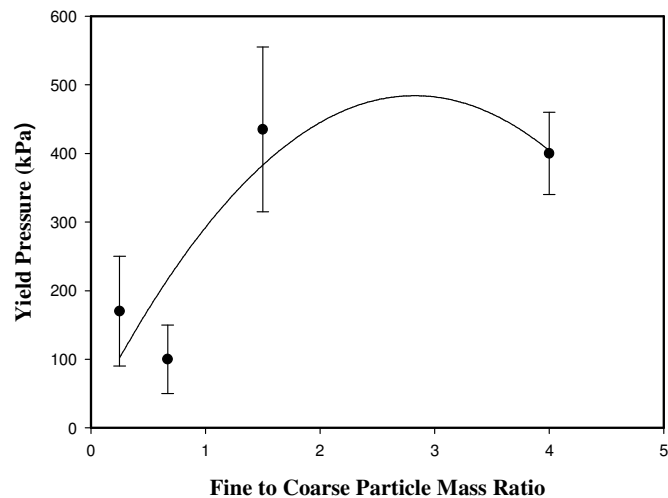
Figure 12: Dry failure strength of agglomerates as a function of the ratio of fine to coarse particles in the feed

120
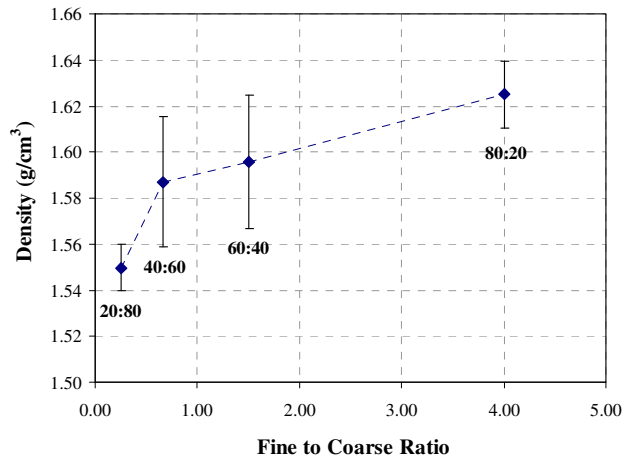
Figure 13: Bulk densities of agglomerates as a function of the ratio of fine to coarse particles in the SG feed

CONCLUSIONS

In this paper, the influence of feed and binder characteristics on agglomeration behaviour and granule properties was studied fundamentally. The results revealed that

- Model mineral hematite exhibited relatively faster nucleation and stronger agglomerate growth behaviour in comparison with quartz and kaolinite.

- Feed ore mineralogy, binder content and primary particle size distribution have a decisive impact on agglomeration behaviour and product properties (size, shape, surface morphology, density and failure strength).

- 5 – 40 mm siliceous goethite laterite ore granules with good failure strength may be readily produced within 8-14 min of agglomeration, depending upon the H_2SO_4 binder content used.

- Post-agglomeration drying enhanced the failure strength of agglomerates.

- The agglomeration growth behaviour exhibited by the mineral phases was found to be highly reproducible.

ACKNOWLEDGEMENTS

REFERENCES

1. Benali, M., Gerbaud, V.,Hemati, M., 2009. Effect of operating conditions and physico-chemical properties on the wet granulation kinetics in high shear mixer. Powder Technology, 190, 160-169.

2. Bouffard, S.C. (2005) Review of agglomeration practice and fundamentals in heap leaching. Mineral Processing and Extractive Metallurgy Review: An International Journal **26**: 233-294.

3. Butwell, J.W. (1990) Heap leaching of fine agglomerated tailings at Asamera's Gooseberry mine. Minerals Engineering **42**:1327.

4. Chamberlin, P.D. (1986) Heap leaching and pilot testing of gold and silver ores. Mining Congress Journal **67** (4): 47-52.

5. Chamberlin, P.D. (1986) Agglomeration: Cheap insurance for good recovery when heap leaching gold and silver ores", Mining Engineering **38**: 1105-1109.

6. Chamberlin, P.D., 1986. Agglomeration: cheap insurance for good recovery when heap leaching gold and silver ores. Mining Engineering, Vol. 38, No. 12, pp. 1105-1109.

7. Dixon, D., 2003. Heap leach modelling – The current state of the art. Hydrometallurgy 2003 – 5th International Conference – Volume 1 : Leaching & Solution Purification, C.A. Young, A.M. Alfantazi, C.G. Anderson, D.B. Dreisinger, B. Harris and A. James, eds., August 24-47, 2003, Vancouver, TMS.

8. Eisele, J.A. and Pool, D.L, 1987. Agglomeration heap leaching of precious metals. Metallurgy, CIM Bulletin, p. 31-34.

9. Golightly, J., 1981. Nickeliferous laterite deposits, Economic Geology 75th Anniversary Volume.

10. Forsmo, S. (2007) Influence of green pellet properties on pelletizing of magnetite iron ore, PhD thesis, Lulea University of Technology.

11. Horton, J., 2008. Integration of disparate data types for resource estimation – A nickel laterite example, Proceedings of PACRIM Congress 2008, 189-194.

12. Iveson, S. M., (1997). Fundamentals of granule consolidation and deformation. University of Queensland.

13. Lewandowski, K.A., Kawatra, S.K. (2009) Development of experimental procedures to analyze copper agglomerate stability, Minerals & Metallurgical Processing 28 (2): 110-116.

14. Lewandowski, K.A., Kawatra, S.K. (2009) Binders for heap leaching agglomeration. Minerals and Metallurgical Processing **26**: 1-24.

15. Kappes, D.W., 1979. Precious metals heap leaching: simple-why not successful. Presentation at Northwest Mining Association, Dec. 1979.

16. Kim, J., Dodbiba, G., Tanno, Hideaki, Okaya, K., Matsuo, S., Fujita, T.,2010. Calcination of low-grade laterite for concentrate of Ni by magnetic separation. Minerals Engineering 23, 282-288.

17. Kuck, P. H., 2009. US Department of Interior: US Geological Survey, http://minerals.usgs.gov

18. Lee, H. Y., Kim, S. G., Oh, J. K., 2005. Electrochemical leaching of nickel from low-grade laterites. Hydrometallurgy 77, 263-268.

19. Lewandowski, K.A. and Kawatra, S.K., 2008. Development of experimental procedures to analyse copper agglomerate stability. Minerals and Metallurgical Processing, vol. 25, no. 2.

20. Lewandowski, K.A., Kawatra, S.K., 2009. Polyacrylamid as an agglomeration additive for copper heap leaching. Int. J. Miner. Process., 91, 88-93.

21. McClelland, G.E., van Zyl, D.J.A., 1988. Ore Preparation: Crushing and Agglomeration, Chapter 5, Introduction to Evaluation, Design and Operation of Precious Metal Heap Leaching Projects, Society of Mining Engineers, Inc., Littleton, Colorado, pp. 61-67.

22. Mudd, G. M., 2010. Global trends and environmental issues in nickel mining: Sulfides versus laterites. Ore Geology Reviews 38, 9-26.

23. Nosrati, A., Addai-Mensah, J., Skinner, W. (2011) Drum agglomeration of nickel laterite ore: effect of process variables (in preparation).

24. Pietsch, W. (2002) Agglomeration Processes. Weinheim, Wiley-VCH Verlag GmbH, p. 614.

25. Rumpf, H., Engl. Ed.: F.A. Ball (Translator), Particle Technology, Chapman & Hall, London, UK (1990).

PROPHECY RESOURCES CORP. LYNN LAKE PROJECT

Nickel Bioleach Development
Mintek Laboratory Test Work Program Update

By

Andrew J. Carter

Tetra Tech , UK

Presenter and Corresponding Author

Andrew J. Carter
Andy.Carter@wardrop.com

ABSTRACT

A description of the Prophecy Resources Corp. Lynn Lake Nickel project is provided together with an update of the Nickel Bioleach laboratory test work currently underway at Mintek, Randburg, South Africa. The results achieved to date and their implications for further development are further discussed

The current test work and development program has demonstrated that bioleaching may be used to successfully extract Nickel, Copper and Cobalt from low grade Lynn Lake concentrates. Also that the costs of recovery are comparable to existent processes. Further that there are a number of options that can be further developed in order to optimise the process and significantly reduce costs

INTRODUCTION

A description of the Prophecy Resources Corp. Lynn Lake Nickel project is provided together with an update of the Nickel Bioleach laboratory test work currently underway at Mintek, Randburg, South Africa. The results achieved to date and their implications for further development are further discussed

LOCATION

The project is located in the historic mining town of Lynn Lake, in northern Manitoba approximately 320 km by road access northwest of the Thompson mining camp.
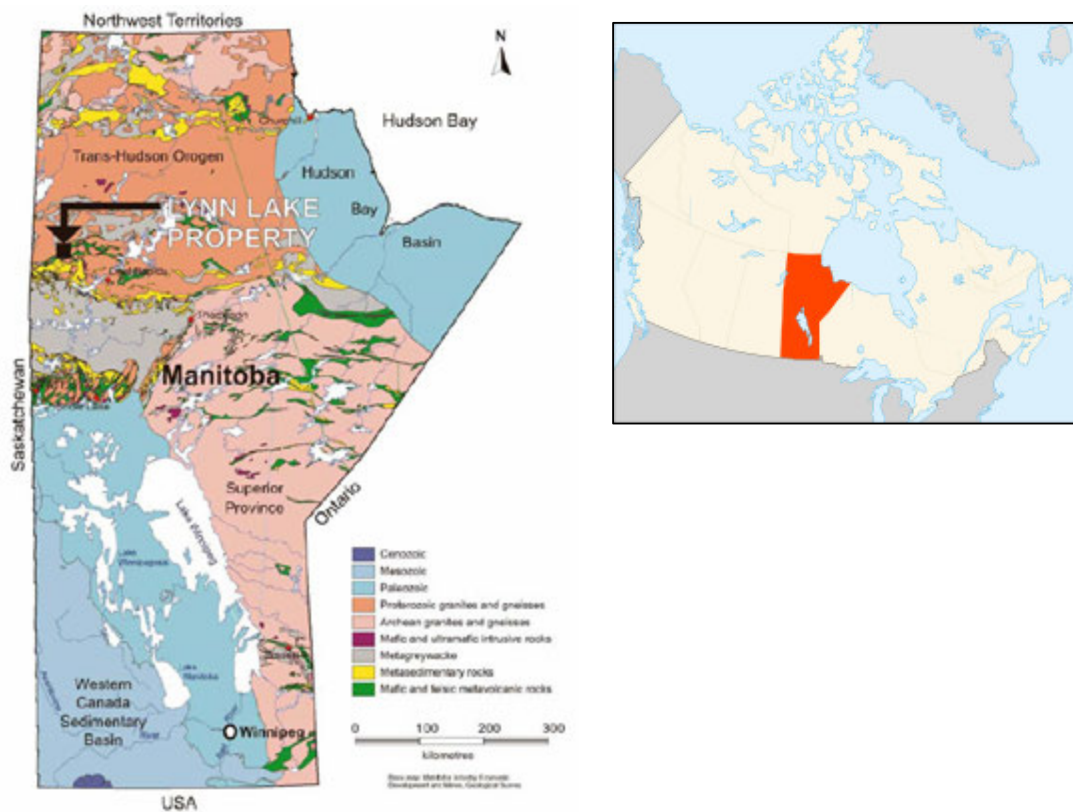
Figure1: Lynn Lake Location Map
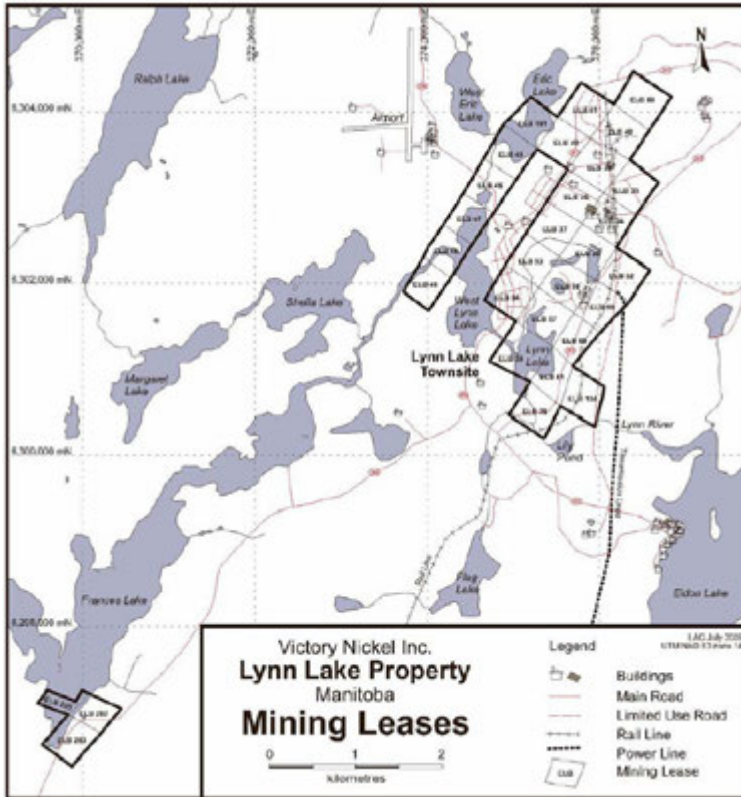
Figure 2: Lynn Lake Mining Leases

The Property is the former Sherritt producing mine site known as the Lynn Lake A mine and Farley mine. Victory Nickel Inc. holds 30 mineral leases covering an area of 590 hectares (ha). Prophecy entered into an option agreement with Victory Nickel Inc. (Victory Nickel) on October 21, 2009, whereby Prophecy has the right to acquire a 100% interest in the Lynn Lake Nickel Project. The Property contains ten mined out historic zones and other mineralized zones with exploration potential.

Figure 3: Lynn Lake Image

125

LYNN LAKE HISTORY

Historical Production

In 1953, mill feed was derived from development work at the A and EL mines. Tons milled in the first year were 13,324 averaging 1.36% nickel and 0.58% copper, 966 tons of nickel concentrate were produced at 15.9% nickel and 1.84% copper and 173 tons of copper concentrate were produced averaging 0.54% nickel and 30.55% copper.

Production reached a maximum in 1965 with a total of 1,363,583 tons of ore mined and milled at Lynn Lake. Production decreased thereafter and in 1973, 676,000 tons of ore averaging 0.84% nickel and 0.39% copper was mined and milled resulting in 7,619,000 pounds of nickel concentrate and 2,609,000 pounds of copper concentrate. To the end of 1973 a total of 21,232,474 tons of ore were mined and milled from the A and EL mines (Sherritt Gordon Annual Reports, 1953-73).

1959 marked the end of the period in which practically all of Sherritt's nickel production from Lynn Lake was sold on long term contracts with more than half of it going to the United States Government stockpile. As a result, in 1959, only 12% of the nickel production was delivered to the stockpile, the balance being sold to consumers in Canada, United States, Europe, Asia, and South America" (Sherritt Gordon Mines Limited Annual Report, 1959).

During the years 1954 to 1956, an additional 18,283,291 pounds of nickel were produced and sold in the form of concentrates. In addition 4,969,475 tons of fertilizers were produced at the refinery between 1953 and 1973.

Over the years the production at the mine was raised to 3,500 tons per day to counteract the lower grade and the refinery averaged 30,000,000 pounds of refined nickel per year. In 1973, the production rate of the mine was decreased to 1,500 tons per day and production of refined nickel was 30,262,000 pounds, well below the record level of 37,321,000 pounds in 1972 (Sherritt Gordon Mines Limited, Annual Report 1973).
 "Because of the grade of ore for nickel and copper, the Lynn Lake mine is approaching the end of its productive life. At present, nickel concentrates are shipped to Fort Saskatchewan for further processing and copper concentrates are shipped first to Hudson Bay Mining and Smelting Limited for smelting and next to Noranda Mines Limited near Montreal for refining" (Task Force Report, 1974).

Processing

In 1948, an ammonia leaching process was developed by Professor Forward and a pilot plant was built in Ottawa, followed by construction (in 1952) of a full scale chemical metallurgical plant (nickel refinery) at Fort Saskatchewan, Alberta. Initial financing of the Lynn Lake project was arranged with Newmont Mining Corporation, J.P. Morgan & Co., and eleven other banks and insurance companies (Brown, E.L., 1955).

In 1953, production started at Lynn Lake (the first nickel concentrate was loaded in November) and Sherritt Gordon's entire nickel output and 60% was sold on long term contracts to the United States Government, which ended in 1959.

After the Farley shaft began operation in 1957, two concentrates were produced. A nickel concentrate, consisting of 14% nickel, 1.5% copper and 0.35% cobalt and a copper concentrate having 30% copper and 0.60% nickel. In this circuit, 85% of the nickel, 93% of the copper and 80% of the cobalt were recovered however, as the nickel head grade dropped so did the percentage recovery.

The nickel was shipped to the Fort Saskatchewan refinery where the metal was recovered, while copper concentrate was sold to Noranda Mines Limited (Milligan, 1960) but was later diverted to Hudson Bay Mining and Smelting Company Limited in Flin Flon, with Noranda accepting any surplus. At the end of 1960 reserves stood at 1.3 million tonnes (1.43 million tons) averaging 0.92% nickel and 0.53% copper (Sherritt Gordon Mines, Annual Report 1960).

Some of the richer ores from the EL mine had produced a mill feed of over 2.2% nickel for several years beginning in 1953, however the bulk of these operating records have not been obtained.

In 1968 low grade ore was discovered in the lower N orebody and between 1969 and 1972 some test work was carried out on increasing plant throughput at a lower grade. This produced a concentrate of 5% nickel and a recovery of 83% (if no upgrading was attempted then the feed and concentrate would be the same indicating 100% recovery). However the deposit was not upgraded to reserves and the expansion did not proceed. The results below indicate normal mill operations during the final years of operation from 1972 to 1977, when the nickel concentrate typically contained 8% nickel, 2% copper and about 0.5% cobalt with some platinum group metals. By 1974 mine exploration was abandoned as the metal prices available then did not support continued mine operations. The mill operations ended in 1977.

PREVIOUS STUDIES

Laboratory Test Work

Batch Flotation Tests

Sixteen comparable batch tests were performed at PRA laboratories in Vancouver, BC. In 9 of the tests the 2nd cleaner flotation results showed higher grade than the 3rd cleaner at around 56.25%. In these batch tests the nickel grade varied between 4.73% and 13.04%, the copper grade between 5.20% and 12.85% and the cobalt grade between 0.17% and 0.43%. The iron was in the range of 40 to 45%, the sulphur about 30 to 35% and the magnesium oxide about 1.5 to 4.0%. The silver ranged within 11 to 30 grams per tonne but was gold tested in only one batch which had a grade of 2.65 grams per tone.
Based on the test results the grades were determined as follows:

• Nickel in Concentrate – 9.26%
• Copper in Concentrate – 7.54%
• Cobalt in Concentrate – 0.27%

The rougher flotation recoveries were as follows:

• Nickel – 83.46%
• Copper – 94.06%
• Cobalt – 82.45%
• Sulphur – 86.54%

Locked Cycle Tests

Two lock cycle tests were performed on the concentrates at PRA after undertaking 26 tests on reagents and grinding parameters. The reagent suite selected was,

• Sodium Isopropyl Xanthate (SIPX).
• Methyl Isobutylcarbinol (MIBC).
• Carboxymethylcellulose (CMC).
• Copper Sulphate (CuSO4).
• Sodium Sulphide (Na_2S).

The first lock cycle test was based on a flow sheet consisting of primary grinding with a size analysis report for six cycles resulting with a P_{80} passing size between 59 and 73 microns. The ground product was then feed of a rougher/scavenger bulk flotation. The rougher concentrate was then sent to regrind and subsequently to three stages of cleaners with the 1st cleaner tail going to a 1st cleaner scavenger flotation.

The final concentrate recovery and grades were:

• 5.27% nickel, recovery 79.6%
• 3.04% copper, recovery 93.7%
• 0.18% cobalt, recovery 77.5%

The second lock cycle test was conducted at a coarser grind with a size analysis report for six cycles resulting with P_{80} passing between 61 and 76 microns.

The final concentrate recovery and grades were:

- 6.37% nickel, recovery 82.1%
- 3.27% copper, recovery 92.2%
- 0.19% cobalt, recovery 81.1%

This was slightly better compared to the first lock cycle test

Bioleaching

Bioleaching was selected as a potential concentrate treatment option on the basis of the experience in the production of cobalt from pyrite concentrates at KCCL in Uganda, BHP-Billiton's success in developing the BioNIC® process and BioCOP® process in conjunction with CODELCO. KCCL was viewed as an analogue as it embodied many of the features of the anticipated process. Pressure oxidation was considered but did not appear to be a clear winner at the scale of operations being considered and the degree of technological sophistication was perceived as a potential drawback. However, it remains a potential option for future consideration.

The bio-leaching test work was performed at the PRA laboratory in Vancouver. For the test purposes PRA used thiobacillus thiooxidans adapted to the nickel concentrate. The test procedure was as follows:

- Fine grinding of the concentrate and pulp to 50 grams per litre or more depending on concentrate analyses.
- Agitate with mixer with air sparging below impeller.
- Adjust temperature to 35°C.
- Adjust to pH 2.2 with sulfuric acid and stabilize.
- Add "0"K (zero iron in it) nutrient solution (dilution is recommended)
- Add 5% inoculum by volume of adapted PRA thiobacillus thiooxidans.
- Control oxidation reduction potential (ORP), pH, ferrous and ferric iron, dissolved metals by ICP.

The preliminary test results showed approximately 92.5% nickel extraction, 81% copper extraction and 12.5% iron extraction. Leaching of chalcopyrite was incomplete, as the bacteria used had been previously adapted to a nickel concentrate.

Wardrop 2007 Pre-Feasibility Study

A pre-feasibility study was conducted by Wardrop Engineering Inc. in 2007. The study examined the reopening of the Lynn Lake mine and the re-establishment of metallurgical operations. The mine was to be dewatered and re-equipped in order to exploit known reserves of high grade mineralisation and potential lower grade zones, as indicated in Figure 4.
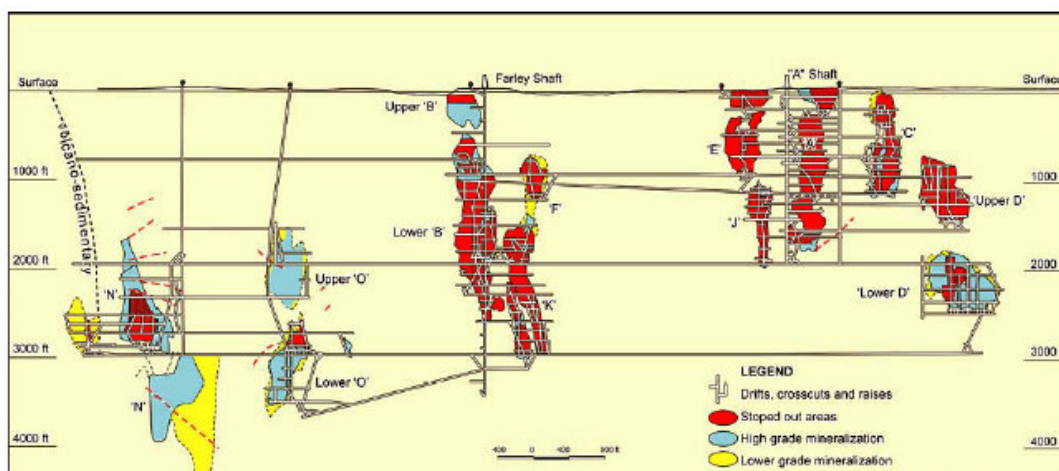
Figure 4: Lynn Lake Mine Section

Two process options were to be considered namely,

- Option1, production and toll treatment of separate nickel and copper concentrates.
- Option 2, onsite treatment of a bulk concentrate.

Simplified flow diagrams for these options are shown in Figures 5 and 6, respectively. In each case the process considers a 3,000 tpd milling and flotation plant. Option 1 is based on a sequential float of separate copper and nickel concentrates. Option 2 provides for production of a bulk sulphide concentrate, bioleaching of nickel and copper and subsequent recovery of the metals by precipitation of the hydroxides after iron removal. The study ultimately assessed the efficacy of production of finished nickel metal on site via an SX/EW process as an alternative to a hydroxide intermediate.
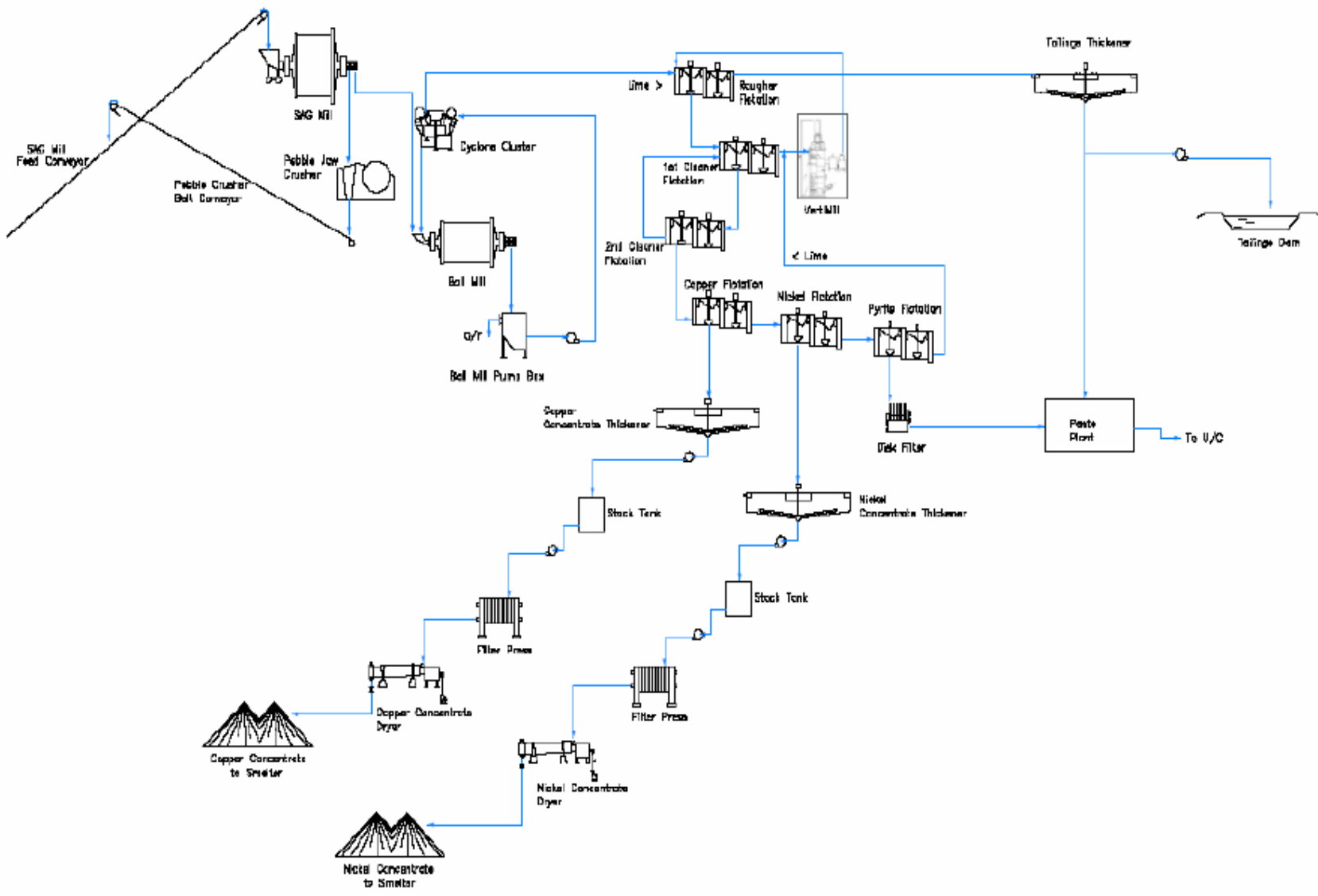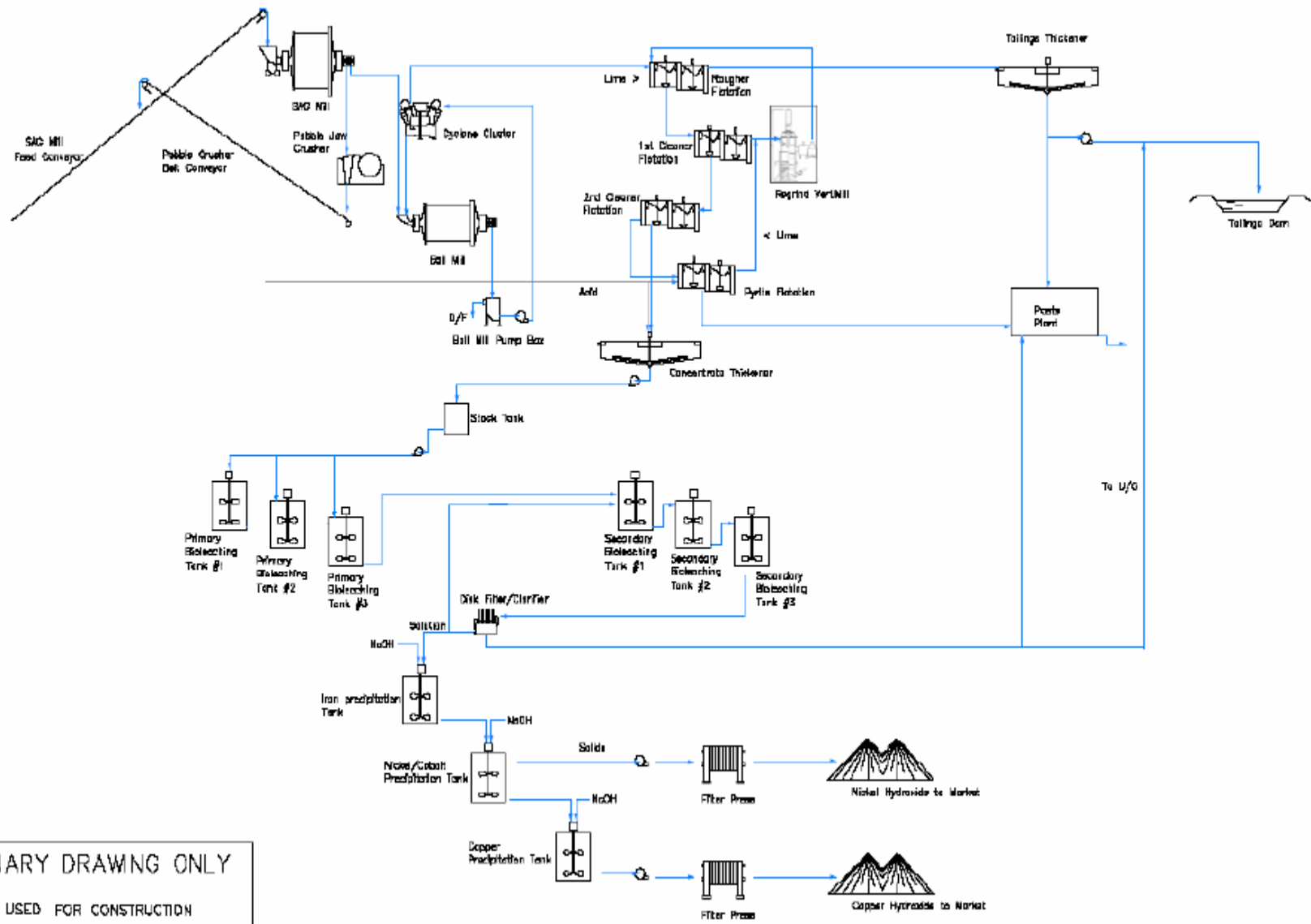
Figure 5: Nickel and Copper Concentrates Option

130

Figure 6: Bioleaching Option

The key findings of the pre-feasibility study are summarised in Tables 1 to 4.

	Units	Values
Underground (all zones)		
Underground Ore - Production	tonnes	10,737,237
Average Mined (diluted) Grades		
Nickel	%	0.64
Copper	%	0.35
Cobalt	%	0.02
Total Ore Milled	tonnes	10,737,237
Processing		
Plant Throughput	tonnes/day	3,000
	tonnes/year	1,080,000
Mill Recoveries		
Nickel	%	81.5
Copper	%	92.0
Cobalt	%	80.5
Bio-leach Plant Recovery		
SX/EW Recovery Nickel	%	92.5
SX/EW Recovery Copper	%	81.4
SX/EW Recovery Cobalt	%	85.0

Table 1: Preliminary Economic Assessment Criteria

Cost Centre	Total (CDN$)	First Three Years (CDN$)	Sustaining (CDN$)	Indirects (%)	Contingency (%)
Underground					
Equipment	$14,190,000	$6,110,000	$8,080,000	5%	10%
Shaft	$13,736,000	$13,736,000	$0	5%	15%
Development	$61,551,000	$6,798,000	$54,753,000	5%	10%
Crusher & UG Conveyor	$4,393,000	$4,393,000	$0	5%	10%
Processing					
Mill including SX/EW	$53,780,000	$53,780,000	$0	0%	24%
Paste Fill Plant	$1,750,000	$1,750,000	$0	0%	24%
Tailings Facility	$24,000,000	$6,000,000	$18,000,000	0%	24%
Surface Capital					
Infrastructure	$50,186,000	$31,290,000	$18,846,000	5%	10%
Surface Equipment	$1,020,000	$1,020,000	$0	0%	0%
Sustaining Capital	$10,000,000	$0	$10,000,000	0%	0%
Environmental	$15,000,000	$0	$15,000,000	5%	15%
Indirects	$6,589,000	$2,638,000	$3,951,000	2.9%	
Contingency	$33,285,000	$20,989,000	$12,296,000		14.8%
Total Capital	**$289,400,000**	**$148,500,000**	**$140,900,000**	17.8%	

Table 2: Wardrop Pre-feasibility Study Capital Cost Estimates

Costing Area	Unit Cost
Mining – Total Ore	$32.33
Milling – Ore	$16.06
General & Admin	$20.11
Power	$2.04
Metal Transportation	$2.56
Losses & Marketing	$0.62
Total Mining & Milling	**$73.73**

Table 3: Wardrop Pre-feasibility Study Summary Operating Cost Data

The capital costs for development of the Lynn Lake project have been summarized in Table 4. It is based on the concept of a 3,000 tonne per day processing plant, with the entire production coming from an underground operation providing mill feed.

Commodity Scenario/Variance	Option	Bio-leach OP Base Case 3 Year Average	Sudbury Smelter Base Case 3 Year Average
Nickel	US$/lb	$9.01	$9.01
Copper	US$/lb	$2.13	$2.13
Cobalt	US$/lb	$18.59	$18.59
Exchange Rate	US$:CDN$	1.15	1.15
Nickel	CDN$/lb	$10.36	$10.36
Copper	CDN$/lb	$2.45	$2.45
Cobalt	CDN$/lb	$21.37	$21.37
Discount Rate	**NPV**		
5.0%	CDN$ (millions)	$178.7	$3.5
7.0%	CDN$ (millions)	$145.7	($6.9)
8.0%	CDN$ (millions)	$131.4	($11.1)
10.0%	CDN$ (millions)	$106.5	($18.0)
12.0%	CDN$ (millions)	$85.7	($23.3)
IRR	%	28.9%	5.6%
EBITDA Cash Flow (Net of Capex $CDN millions)		295.5	44.7
Capital & Operating Cost per by-product			
Total Operating Cost/lb Nickel Produced		$6.75	$5.44
Total Capital Cost/lb Nickel Produced		$2.48	$2.06
Credit Copper, Cobalt/lb Nickel Produced		($1.85)	($1.77)
Transportation & Market/lb Nickel Produced		$0.38	$3.10
EBITDA (Net of Capex)/lb Nickel Produced		**$2.59**	**$1.53**

Table 4: Wardrop Pre-feasibility Study Preliminary Economics

The primary conclusion drawn from the economic assessment was that onsite treatment of a bulk concentrate via a process of milling, flotation, bioleaching and SX/EW for the production of nickel gave higher returns compared with production and toll treatment of separate nickel and copper concentrates.

The study provided a number or recommendations concerning further development of the project. However, with respect to the process there were four main recommendations, namely,

- Implementation of a revised sampling program reflecting the updated resource model and mine plan.
- Additional locked cycle testing including PGE + Au + Ag.
- Implementation of a comprehensive bioleach development program.
- Implement Nickel SX/EW development test work.

KCCL

As indicated earlier the Kasese Cobalt Plant in Uganda was regarded as an operating analogue of the proposed process. The Kasese cobalt plant, owned by the Kasese Cobalt Company Ltd., is located in south-west Uganda at the site of a pyrite concentrate dump which was stockpiled during operation of the now defunct Kilembe Copper Mine. The plant was designed to treat approximately 1 million tonnes of pyritic dump material, to produce approximately 10 000 tonnes of cobalt cathode over a 10 year life-span. The beneficiation process includes bio-leaching of the dump material to solubilise cobalt and other metals, followed by iron removal by neutralisation and precipitation, zinc removal by solvent extraction with D2EHPA®, copper and nickel removal by precipitation, cobalt recovery by solvent extraction with Cyanex 272® and electro winning to produce high-grade cobalt cathode. The cathode is crushed and degassed for sale.

The various features of the Kasese plant as they relate to Lynn Lake are illustrated in Figures 5. through 8.
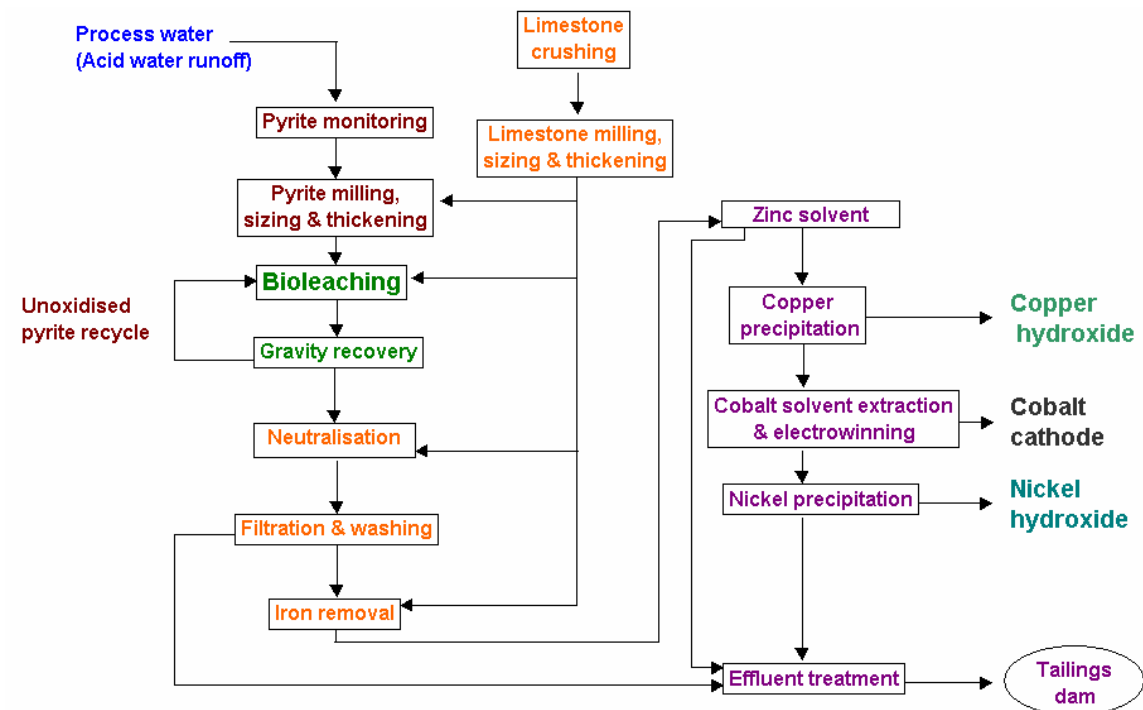

Figure 5: KCCL Bioleaching Plant

Figure 6: KCCL Process Flow Diagram

Figure 7: KCCL Nickel Circuit

Figure 8: KCCL SX/EW Plant

The success of the Kasese Cobalt project demonstrates unequivocally that bioleaching can be used for the simultaneous co-extraction of copper, nickel and cobalt and that these metals can be recovered either as intermediate hydroxide products or as finished metal.

MINTEK BIOLEACH DEVELOPMENT PROGRAM

Based on the success of the preliminary batch amenability test work, preliminary economics and the Kasese demonstration, Prophecy Resources decided to investigate the option of an on-site bioleach plant for the production of nickel and copper from a bulk flotation concentrate, which will be produced from the Lynn Lake mine. The option of an on-site flotation and bioleach plant may have certain advantages over alternative hydrometallurgical processes as it is readily able to treat low grade concentrates. The modular nature of a bioleach process would also make it possible to expand capacity in future with relative ease. Mintek was contracted to perform flotation test work and produce sufficient concentrate to be used in a series of bioleach tests.
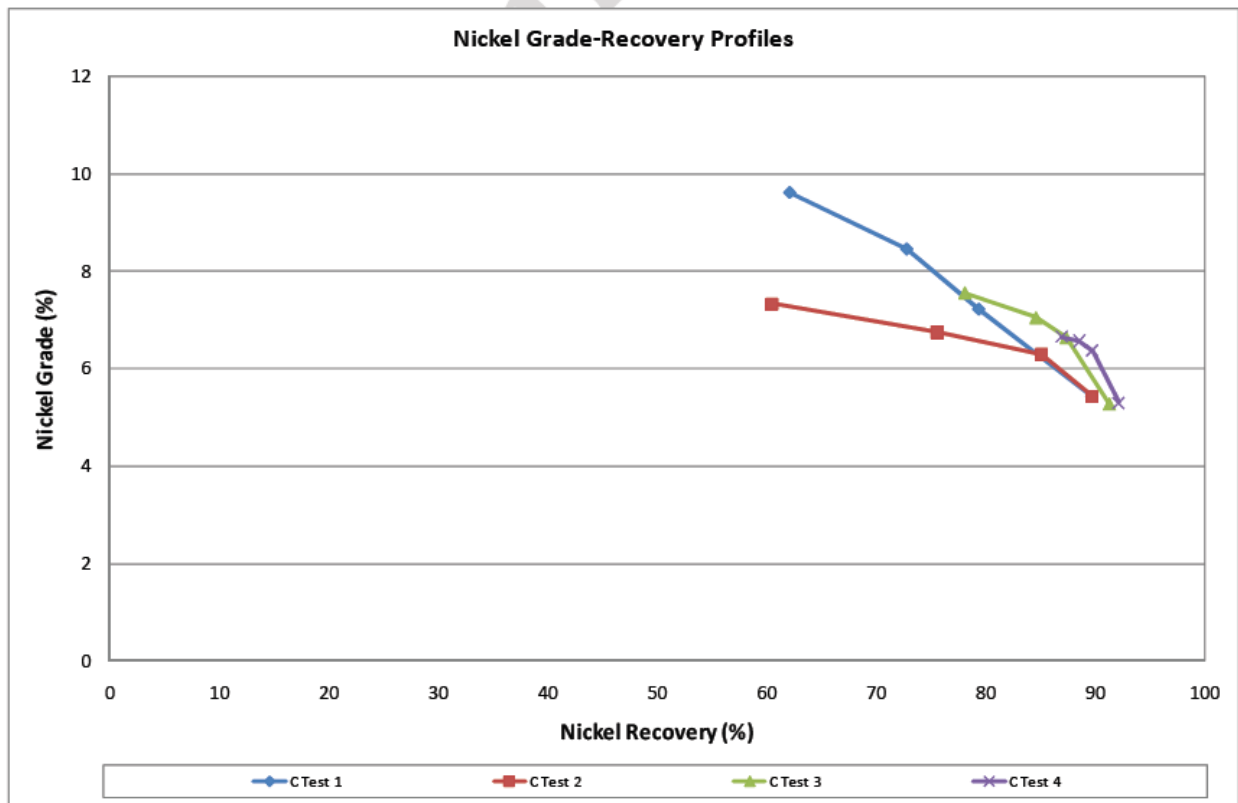
Flotation

A comparison of the Mintek bulk sample head anlalysis compared with the earlier PRA Sample is shown in Table 5. The Mintek sample was higher in total S, Ni and Cu grades. The Mg content of the PRA sample was higher at 12.8% compared to 4.7% of the Mintek sample. This may account for some of the difficulty PRA experienced with talc depression in earlier tests

Sample #	Average mintek	Analytical Method	average head PRA Method	Analytical Method
Total S	4.99	Leco	4.13	Leco
Mg	4.74	ICP1	12.81	ICPM
Al	6.82	ICP1	2.79	ICPM
Si	18.85	ICP1		
Ca	6.01	ICP1	5.11	ICPM
Ti	0.46	ICP1	0.08	ICPM
V	<0.05	ICP1	0.01	ICPM
Cr	0.05	ICP1	0.17	ICPM
Mn	0.12	ICP1	0.15	ICPM
Fe	14.59	ICP1	13.85	ICPM
Co	<0.05	ICP1	0.02	ICPM
Ni	0.97	ICP1	0.80	ICPM
NonSNi	0.12	AA		
Cu	0.61	ICP1	0.38	ICPM
Zn	0.05	ICP1	0.01	ICPM
Pb	<0.05	ICP1	0.004	ICPM
Cu	0.558	ICP16		
Ni	1.02	ICP16	0.79	AsyMuA
Co	0.026	ICP16		

Table 5: Comparison of Mintek and PRA Sample Head Analysis

A series of roughing and cleaning tests were conducted in order to verify the earlier PRA results and establish the conditions required bulk flotation. The nickel and copper grade recovery profiles for the bulk concentrate are shown in Figures 10 and 11 below.

Figure 10: Nickel Grade – Recovery Profile
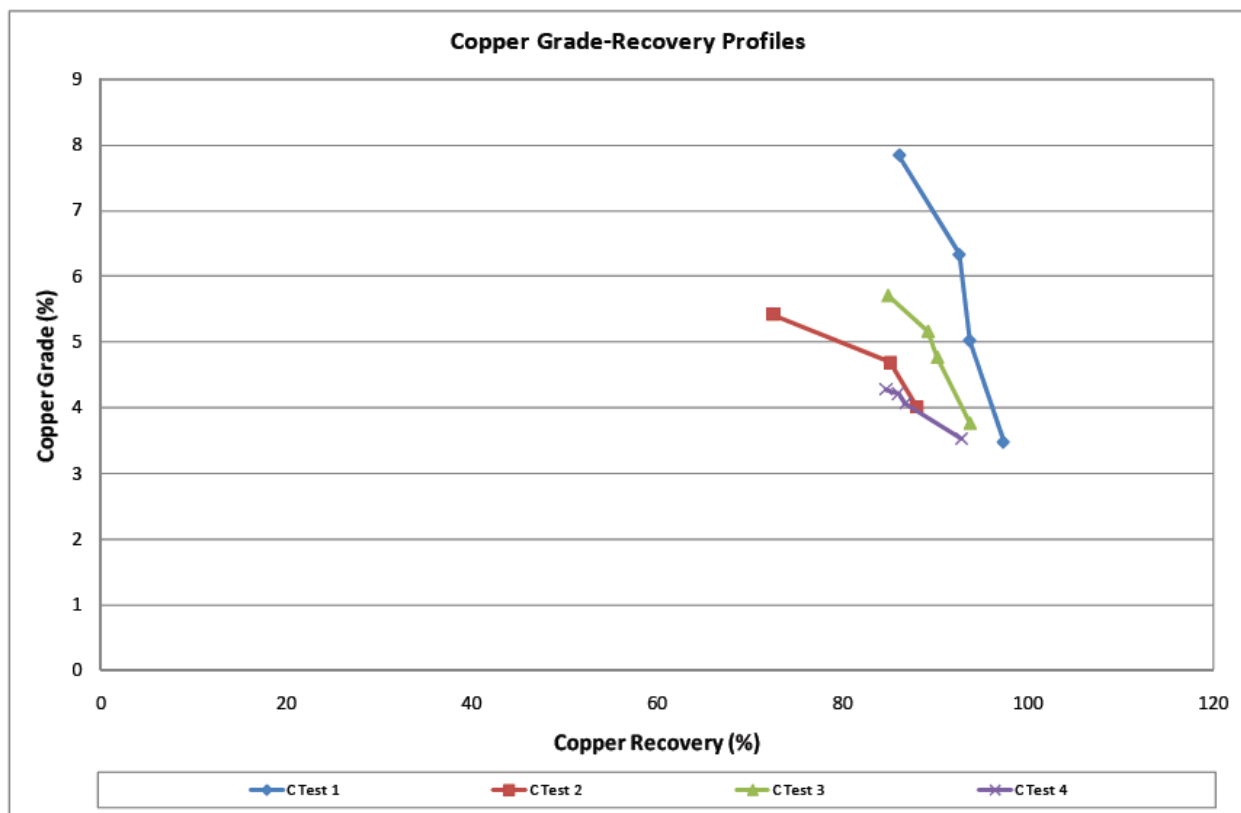
Figure 11: Copper Grade – Recovery Profile

The flotation test work confirmed that it is possible to upgrade the Lynn Lake ore by flotation from 1% Ni and 0.6% Cu at a grind of 80%-75µm to a bulk sulphide-rich product grading at 5.2% Ni and 3.1% Cu at a metal recovery of 90%. The product is high in sulphur at 28.5% and Fe at 37% with some minor dilution with Mg, Al, Si and Ca.

Once the optimal flotation conditions had been established a mini pilot flotation run was instituted in order to generate sufficient concentrate for continuous bioleaching tests.
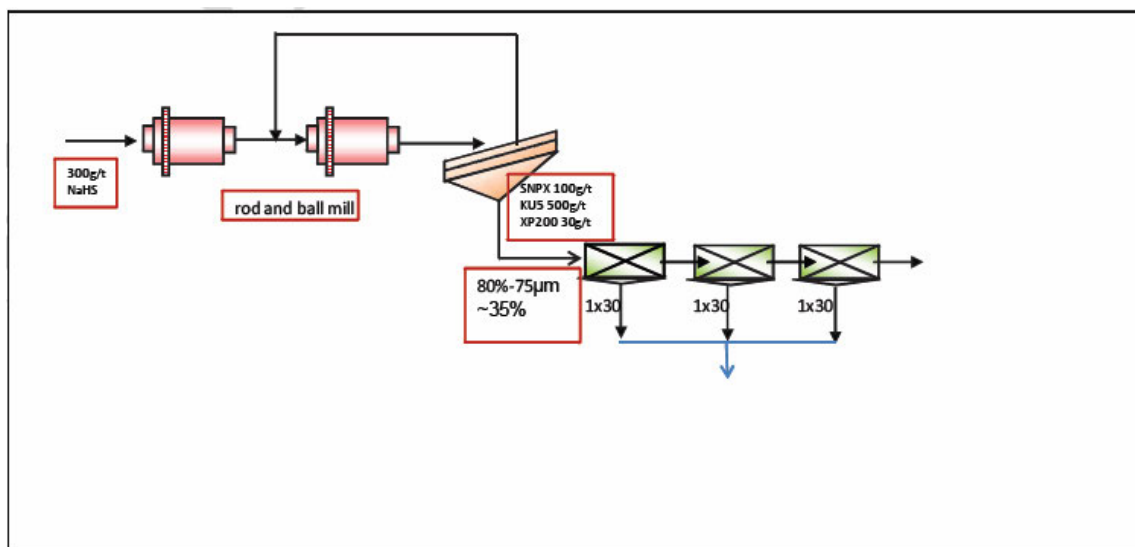
Figure 12: Bulk Concentrate Production Circuit

	Unit	Assay	Analytical Method
Total S	%	28.47	Leco
Mg	%	1.30	ICP1
Al	%	2.14	ICP1
Si	%	5.99	ICP1
Ca	%	2.05	ICP1
Ti	%	0.15	ICP1
V	%	<0.05	ICP1
Cr	%	<0.05	ICP1
Mn	%	<0.05	ICP1
Fe	%	37.05	ICP1
Co	%	0.20	ICP1
Ni	%	5.33	ICP1
Cu	%	3.39	ICP1
Zn	%	<0.05	ICP1
Pb	%	<0.05	ICP1

Table 6: Mintek Bulk Concentrate Analysis

The analysis of the bulk concentrate is shown in Table 6. above. Optical and scanning electron microscopy indicated that the Cu and Ni ore-bearing phases present in concentrate included chalcopyrite as the major Cu-bearing mineral with Pentlandite and Violarite as the major Ni-bearing ore minerals. Trace amounts of Covellite were also present. Pyrrhotite was abundant in the test sample and with trace amounts of Pyrite. The concentrate contained approximately 10.0% Chalcopyrite, 15.6% Pentlandite and 52.8% Pyrrhotite.

Bioleaching

Based on the results from the flotation test work, a decision was made to perform the bioleach tests on a bulk Ni-Cu concentrate at both 45°C and 70°C. The objectives of the test work program were as follows:

Establish baseline bioleach amenability data in a continuous reactor system while operating at a pulp density of 10% and a particle size of d90=10μm at both 45°C and 70 °C, respectively.

Optimisation of the grind size, feed solids concentration and residence time at both 45°C and 70°C.

The tests were conducted with moderately thermophilic and thermophilic cultures, which had been maintained over a number of years at 45 and 70 °C, respectively on a pentlandite-chalcopyrite containing concentrate.

The dominant microbes present in the moderate thermophile culture included *Leptospirillum ferriphilum*, *Acidithiobacillus caldus* and *Sulfobacillus spp.* The thermophile culture was dominated by *Acidianus brierleii* with lower numbers of *Metallosphaera spp* and *Sulfolobus spp.* present.

Group	Temperature °C		
	Minimum	Optimum	Maximum
Thermophiles	40 to 45	55 to 75	60 to 80
Mesophiles	10 to 15	30 to 45	35 to 47
Psychrophiles:			
Obligate	-5 to 5	15 to 18	19 to 22
Facultative	-5 to 5	25 to 30	30 to 35

Table 7: Classification of Bacterial Inocculum by Temperature Range

Figure 13: Mintek Continuous Mini Pilot Plant

Bioleach amenability test work was performed at 45 and 70 °C in fully-controlled continuously operated three- and four-stage reactor systems. The 4-stage system had a volume of 3 ℓ in the first stage reactor and 1 ℓ in each of the consecutive reactors, whereas the 3-stage system consisted of a 2 ℓ first stage reactor followed by two consecutive 1 ℓ reactors.

Each system consisted of a feed tank, bioleach reactors in series, and a container placed at the end of the series of reactors for product collection. Nutrients were added to the feed tank at the following concentrations; 1.0 g/ℓ $(NH_4)_2SO_4$, 0.5 g/ℓ $MgSO_4 \cdot 7H_2O$, 0.1 g/ℓ KCl and 0.5 g/ℓ K_2HPO_4. The feed slurry was fed from the feed tank to the first reactor via a peristaltic pump, at a feed solids concentration of 10 %. Peristaltic pumps were also used to transfer pulp between reactors at the same flow rate as the feed slurry.

The feed flow rate was set to obtain an overall residence time of six days. The air supply to the bioleach reactors was enriched with 0.35 % CO_2, which was introduced to the reactors by means of a sparger situated below the impeller. The air flow rates were controlled by means of a rotameter, and the pulp temperature was controlled via temperature probes and immersion heaters placed in the reactors.

The reactors were monitored daily for temperature, pH level, redox and oxygen uptake rates and the level of iron, nickel and copper in solution. Once steady-state conditions were reached, a set of pulp samples was collected from each reactor, and the residues were analysed for their nickel, copper, iron, elemental sulphur and sulphide sulphur content. These analyses were used to calculate the extractions of nickel and copper as well as the sulphide oxidation levels. The preliminary results are indicated in Tables 8 through 9. The effect on grind on metals extraction is illustrated in Figures 14 through 17.

|	R1	R2	R3
Temperature (°C)	70	70	70
Cumulative residence time (d)	3	4.5	6
pH level	1.47	1.40	1.43
Redox (mV vs Ag|AgCl)	635	679	691
O_2 uptake rate (kg/(m^3.d))	18.3	1.3	0.65
Soluble Fe (g/ℓ)	20.2	18.1	14.1
Soluble Ni (g/ℓ)	4.9	4.9	4.1
Soluble Cu (g/ℓ)	2.1	2.7	2.5
Fe extraction (%)	53.7	47.4	53.0
Ni extraction (%)	96.8	99.2	99.4
Cu extraction (%)	62.7	83.8	88.1
S^{2-} oxidation (%)	95.1	98.1	98.2

Table 8: Thermophile Bioleach Metals Extraction Data for Feed d_{90} = 10 µm
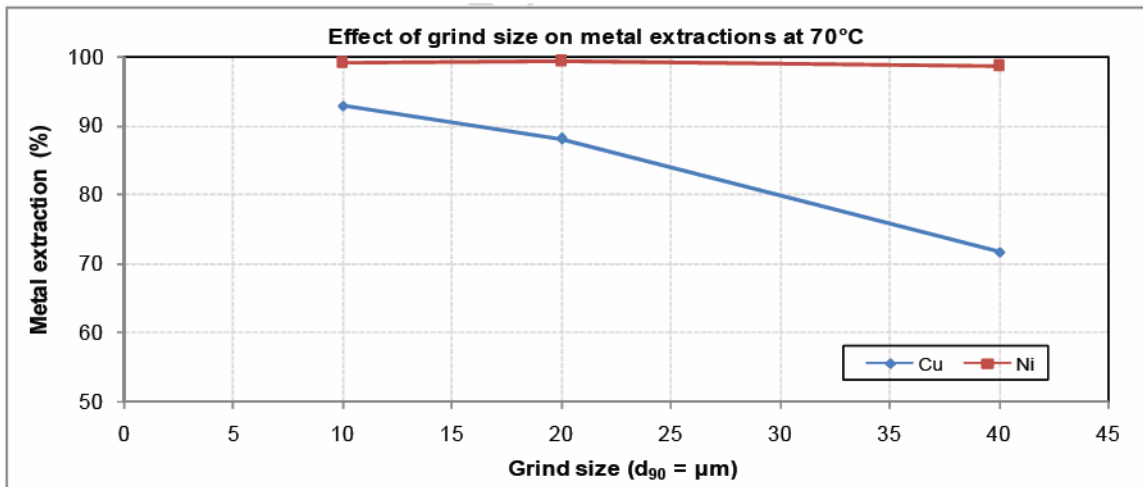
**Figure 14: Thermophile Bioleach Effect of Grind on Metals Extraction**

141

	R1	R2	R3
Temperature (°C)	45	45	45
Cumulative residence time (d)	3	4.5	6
pH level	1.65	1.57	1.58
Redox (mV vs Ag|AgCl)	680	692	705
O_2 uptake rate (kg/(m^3.d))	15.0	1.3	0.2
Soluble Fe (g/ℓ)	24.5	23.3	24.0
Soluble Ni (g/ℓ)	4.5	4.6	4.6
Soluble Cu (g/ℓ)	1.0	1.1	1.1
Fe extraction (%)	68.5	75.2	74.2
Ni extraction (%)	89.5	98.1	99.0
Cu extraction (%)	66.6	81.1	82.4
S^{2-} oxidation (%)	92.7	96.9	97.2

**Table 9: Moderate Thermophile Metals Extraction Data for Feed d90 = 10μm**
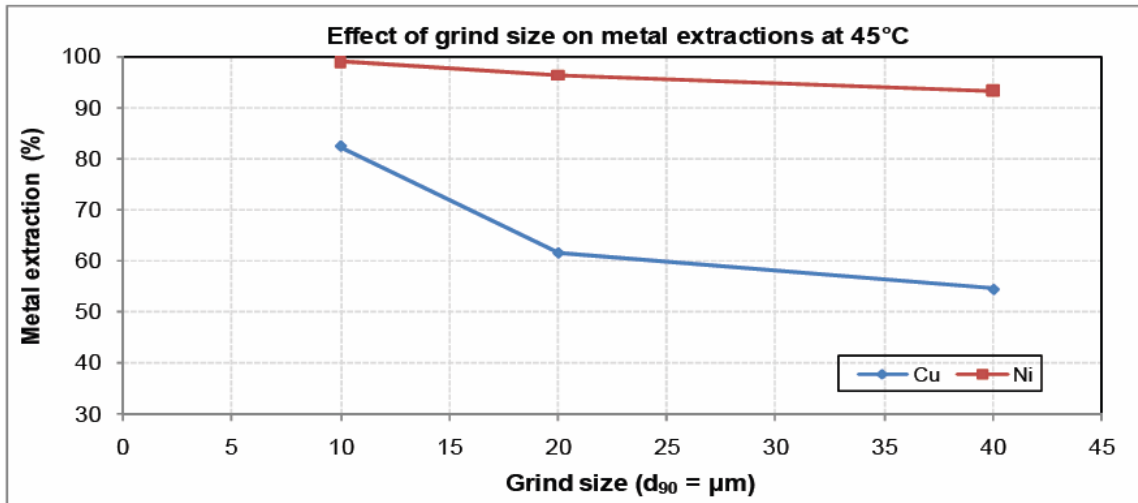
Figure 15: Moderate Thermophile Bioleach Effect of Grind on Extraction

The results show that Nickel is easily extracted and that extractions well in excess of 95% can be anticipated further, that the grind has only a limited effect on extraction. The results also show that copper extraction is heavily dependent on grind. This is owing to passivation of chalcopyrite and the relationship between mineral surface area passivated and mineral particle volume. This implies a grind vs. copper trade-off will be necessary. Nonetheless copper extractions in the mid 80's% can be expected.

MLR Cu Extraction % vs. Grind
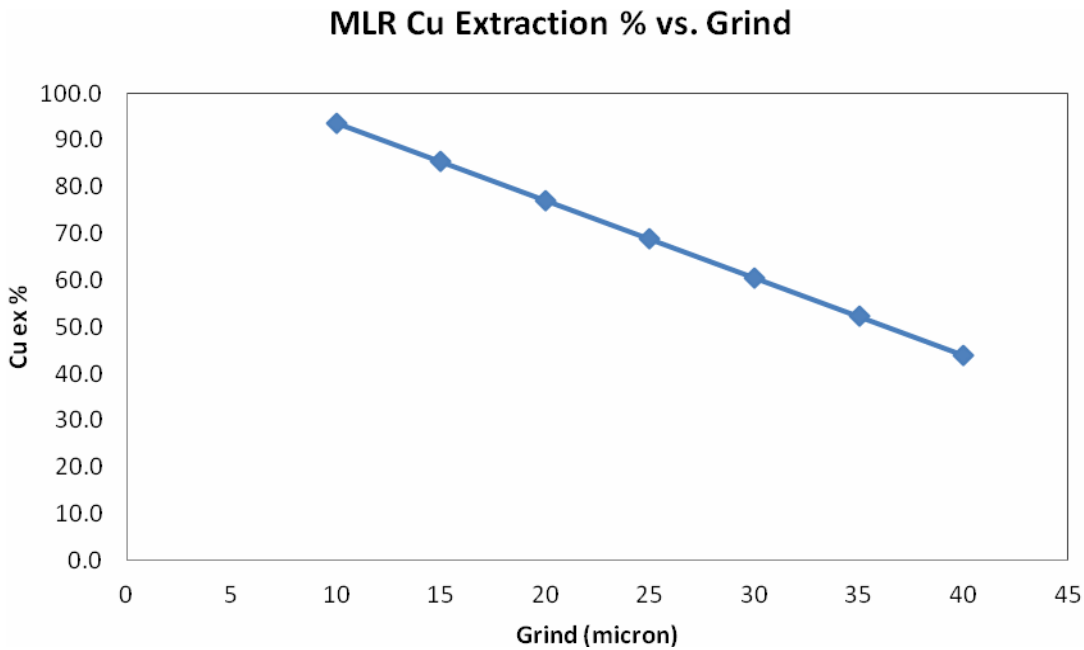
Figure 16: Multiple Linear Regression of Copper Extraction vs. Grind Data

MLR Cu Extraction Data

$R^2 = 0.9807$
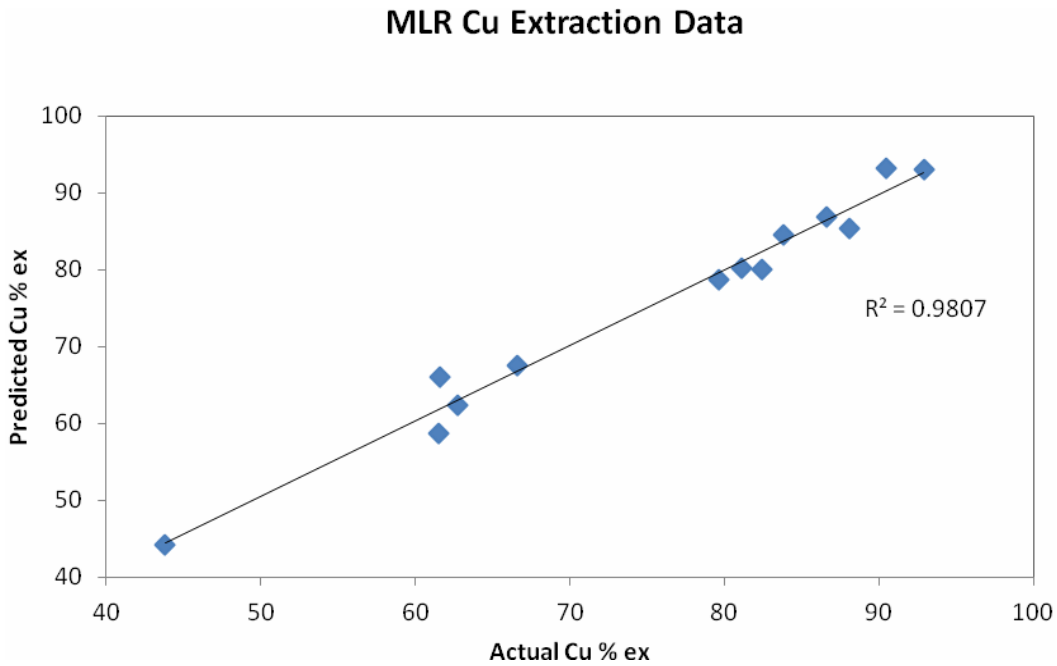
Figure 17: Verification of Multiple Linear Regression Copper Extraction Model

Metals Recovery

At the present time three metals recovery circuits are under consideration, production of hydroxide intermediates, sulphides intermediates and nickel metal by SX/EW. These processes are well established and are illustrated in Figure 18 below.
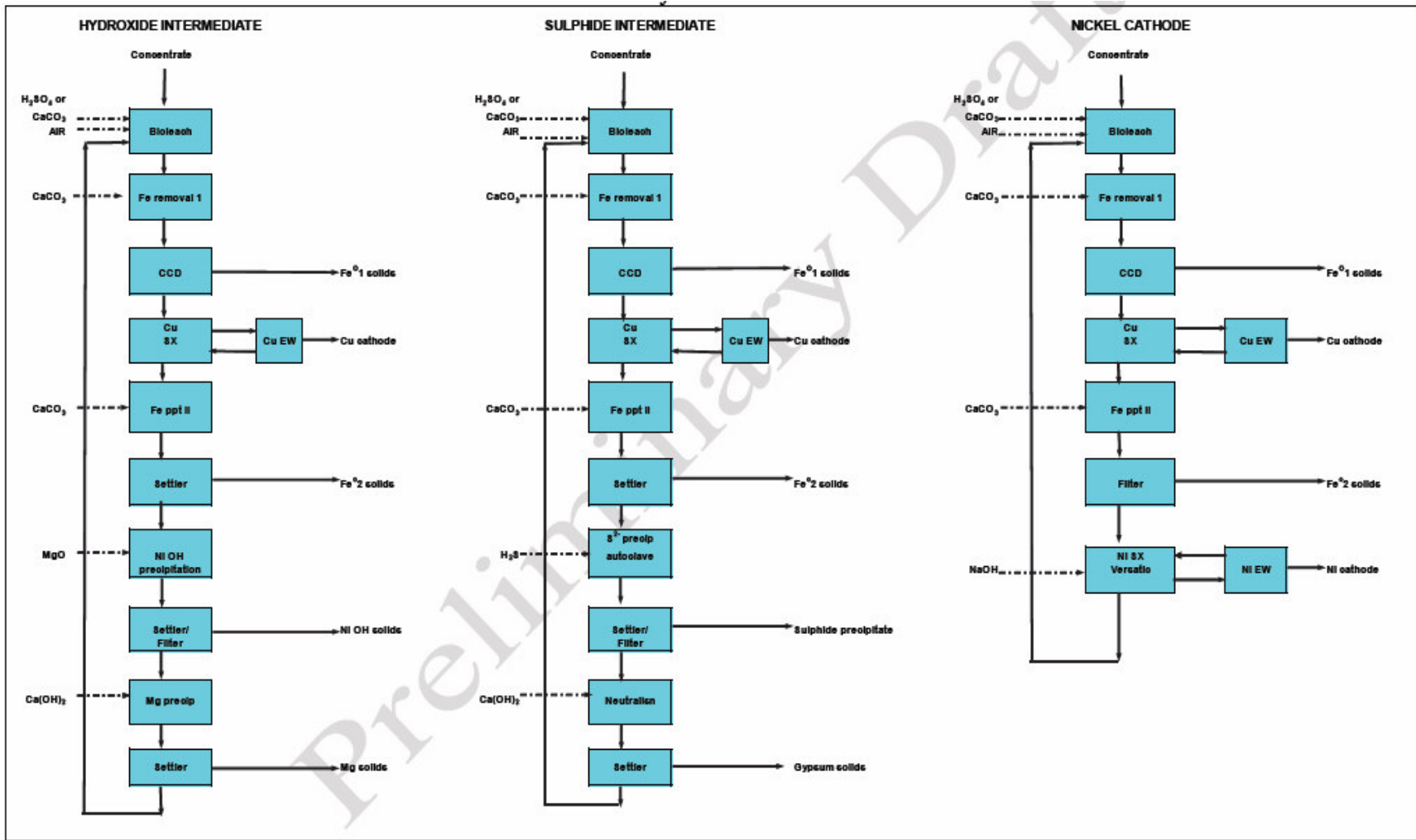
Figure 18: Metals Recovery Circuit Options

Hydroxide precipitation: This is conceptually the simplest route to follow. Nickel is precipitated as a hydroxide by the addition of magnesia. This is the least sophisticated option, it generates a lower-quality product, which is difficult to dewater and more expensive to transport. However, it is environmentally more benign than the other routes, provided inexpensive supplies of lime and magnesia can be obtained. The production of an intermediate metal salt does not preclude the option of producing metal by SX-EW. The metal salt could be re-dissolved and the solution used as a feed to a refinery including nickel SXEW. Such a refinery could be added at a later stage; this would reduce the technical risk associated with the project.

Sulphide precipitation: This process involves a higher degree of complexity, requiring pressurised reactors and a low cost source of hydrocarbon or H_2S. This route also has environmental concerns, owing to the use of pressurised reactors and the production of toxic and flammable gases, and it requires a more sophisticated workforce. However, the product has a lower moisture content than the hydroxide product, and is therefore less expensive to transport.

Solvent extraction and electro winning: Nickel SX-EW is not as well-established as copper SX, and the process circuits are complex, difficult to operate, with high capital and operating costs, and requiring a skilled workforce. A reliable power supply is required. This route is suitable if refining charges are high and the additional capital expenditure can be justified.

PRELIMINARY COST ESTIMATES

Cost estimates for each of the recovery options under consideration have been developed by Mintek and these are illustrated in Figures 18 through 20.
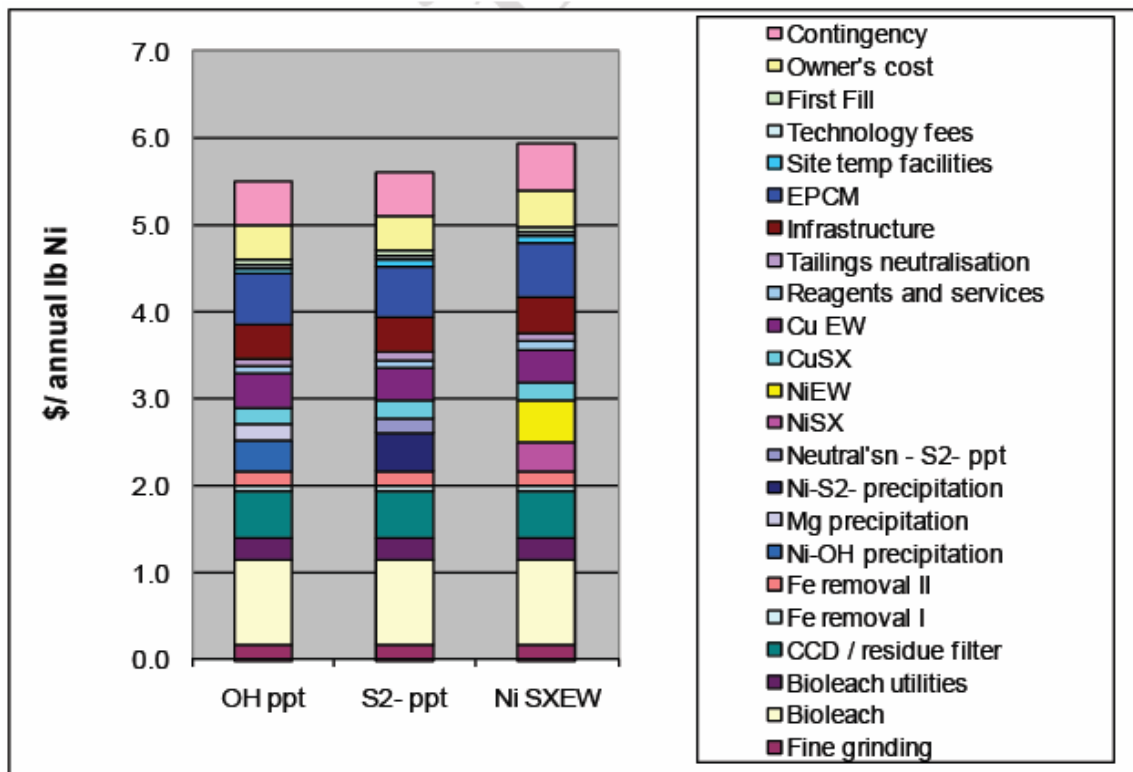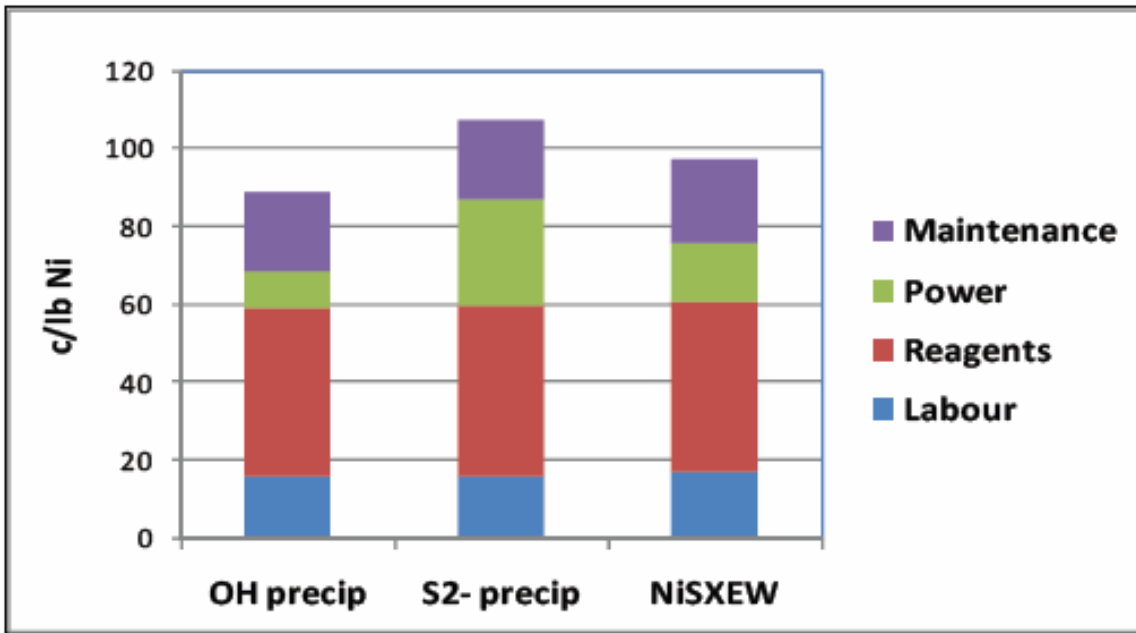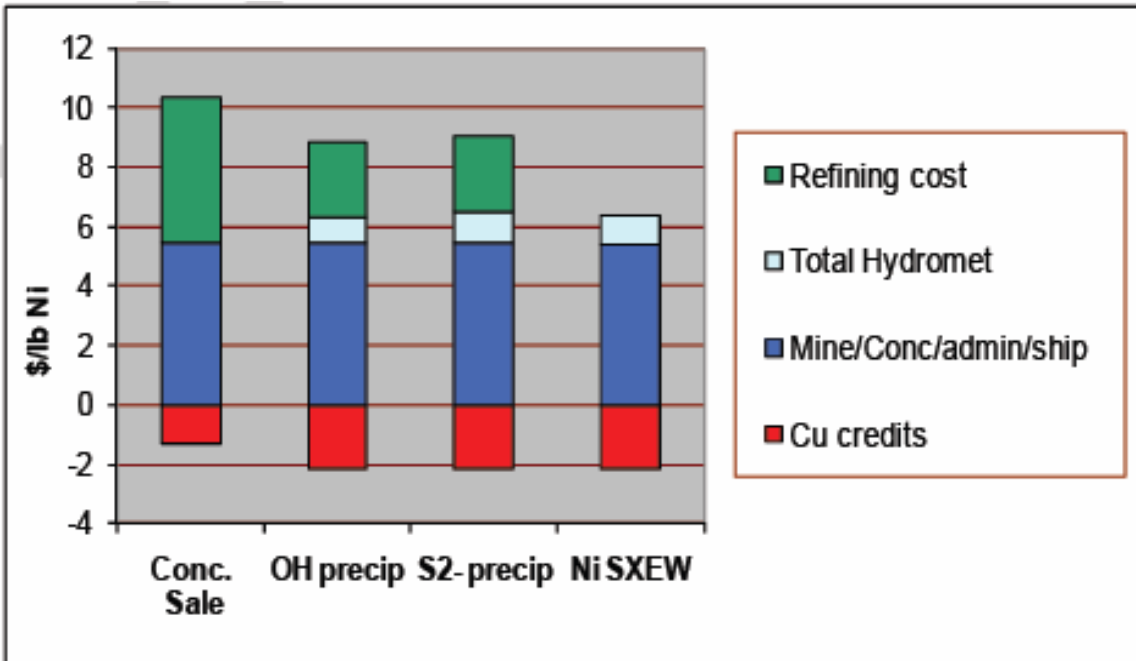

Figure 18: Metals Recovery Options Capital Cost Capacity Factors by Area

Figure 18. shows that there is little difference in capital requirements between hydroxides but that predictably on site production of nickel is the more expensive option. The capital cost will range between $5.50/lb and $6.00/lb of installed annual capacity depending on the recovery option selected.

Figure 19: Metals Recovery Options Direct Operating Costs Distributions

Figure 19. above shows that production of sulphide precipitates has the higher direct operating costs but that there is little difference between any of the options in terms of operating costs. Direct operating costs for metals recovery will range between $0.90/lb and $1.10/lb depending on the option selected.

Figure 20: Metals Recovery Options Overall Costs Distributions

Figure 20 confirms the findings of the pre-feasibility study that onsite production of either intermediates or finished metal will be cheaper than the production of separate concentrates and that in terms of overall cost. All in costs are anticipated to be between $6.00/lb and $9.00/lb depending on the recovery option selected.

CURRENT WORK

Current work is focussed on cobalt recovery and early indications are (Table 10) that excellent cobalt recoveries may also be anticipated. Cobalt extraction sensitivity to grind is intermediate between that of Nickel and Copper.

	Co extractions (%)			
	R1	R2	R3	R4
Accumulative residence time (d)	3	4	5	6
(d_{90}) =10 µm	88.7	90.4	89.4	89.9

	Co extractions (%)		
	R1	R2	R3
Accumulative residence time (d)	3	4.5	6
(d_{90}) =20 µm	87.0	89.3	92.0
(d_{90}) =40 µm	80.3	84.9	84.8

Table 10: Thermophile Cobalt Extraction Data

	R1	R2	R3	R4
10% solids:				
Ni extraction (%)	97.8	99.2	99.0	99.2
Cu extraction (%)	79.6	86.6	90.5	92.9
S^{2-} extraction (%)	96.2	97.9	98.5	98.9
12% solids:				
Ni extraction (%)	97.0	99.0	98.9	99.0
Cu extraction (%)	78.7	87.4	91.9	93.7
S^{2-} extraction (%)	94.5	97.5	98.3	98.9
15% solids:				
Ni extraction (%)	94.1	97.1	96.9	97.2
Cu extraction (%)	78.9	87.7	88.7	90.9
S^{2-} extraction (%)	94.4	97.7	97.8	98.7

Table 11: Thermophile Metals Extraction Data vs. Feed Solids Concentration

Although in general the performance, in terms of extraction, of thermophiles is superior to moderate thermophiles, a major drawback of using thermopiles is the low solids concentration at which they are able to operate, typically 10% solids. This compares to 20% for moderate thermophiles. Feed density has a significant impact on both capital and operating costs. Hence there is an incentive to increase solids concentrations for thermophile operation. Preliminary indications are that it is possible to increase solids concentration to as high as 15% with a slight penalty in terms of metals extraction but that thermophiles are currently unable to operate above 17% solids concentration. This implies that the use of moderate thermophiles can't be ruled out at this stage and that a carefully considered trade-off study will be required in order to properly assess the relative merits of both systems.
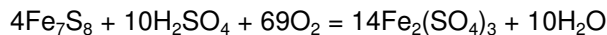
OPPORTUNITIES

There remain a number of opportunities to be evaluated in regard to both bioleaching and metals recovery.

Bioleaching

The bulk concentrate is extremely high in Pyrrhotite content at nearly 53%. Biooxidation of pyrrhotite has a very high oxygen demand,

$$4Fe_7S_8 + 10H_2SO_4 + 69O_2 = 14Fe_2(SO_4)_3 + 10H_2O$$

Most of the costs in bioleaching/biooxidation are associated with getting oxygen into the process, so biooxidation of Pyrrhotite is expensive. The oxygen demand can be greatly reduced by recycling ferric solution produced during the leach to a Pyrrhotite pre-leach in order to remove as much Pyrrhotite in the feed as possible.

$$Fe_7S_8 + 7Fe_2(SO_4)_3 = 21FeSO_4 + 8S$$
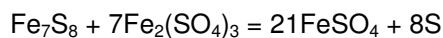
The oxygen requirement to re-oxidize ferrous sulphate and elemental sulphur is much less on a molal basis,

$$4FeSO_4 + 2H_2SO_4 + O_2 = 2Fe_2(SO_4)_3 + 2H_2O$$

$$2S + 3O_2 + 2H_2O = 2H_2SO_4$$
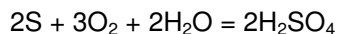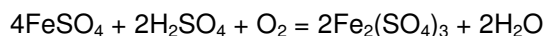
Another advantage is that Pentlandite and Chalcopyrite are also oxidized via direct ferric attack,

$$Ni_3Fe_6S_8 + 9Fe_2(SO_4)_3 = 24FeSO_4 + 3NiSO_4 + 8S$$

$$CuFeS_2 + 2Fe_2(SO_4)_3 = CuSO_4 + 5FeSO_4 + 2S$$
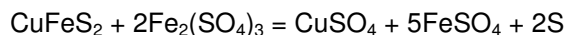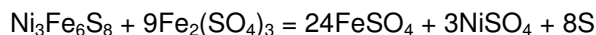
So recycling ferric can lead to significant savings in both capital and operating costs by reducing the oxidative load on the process.

Metals Recovery

The question naturally arises, are there any alternatives to electro winning for the production of finished metal on site. Hydrogen reduction is an obvious choice. A process often overlooked but possibly worthy of revisiting is the direct hydrogen reduction of the metal hydroxide, as developed by Derry and Whitmore. This offers the possibility of producing Nickel metal directly from a hydroxide intermediate.

Derry Process – Hydrogen Reduction of Hydroxide.

$$Ni(OH)_2 + H_2 = Ni + 2H_2O$$
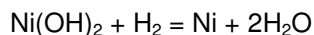
Alternatively oxalates or basic carbonates can be produced from nickel sulphate solutions. The oxalates and carbonates may be readily converted to the oxide.

Oxalate and Hydrogen Reduction Route.

$$NiC_2O_4.2H_2O + heat = NiC_2O_4 + H_2O$$

Under continued heating the oxalate undergoes thermal decomposition into the oxide.

$$NiC_2O_4 + heat = NiO + CO + CO_2$$
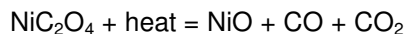
The oxide is then reduced directly to the metal with hydrogen.

$$NiO + H_2 = Ni + H_2O$$
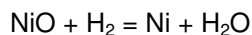
Carbonate and hydrogen reduction route.

Basic Nickel Carbonate can be produced by reacting nickel sulphate with sodium carbonate

$$Na_2CO_3 + NiSO_4 = NiCO_3 + Na_2SO_4$$

More specifically,

$$4 Ni^{2+} + Na_2CO_3 + 6 OH^- + 4 H_2O \rightarrow Ni_4CO_3(OH)_6(H_2O)_4 + 2 Na^+$$
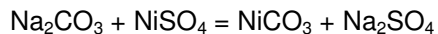
Nickel Carbonate is hydrolysed in acidic aqueous solutions producing water and CO_2.

Calcination of these carbonates gives NiO

$$NiCO_3 \rightarrow NiO + CO_2$$

The oxide is then reduced as before.

The efficacy of these alternative routes to nickel metal remains to be demonstrated by further study.

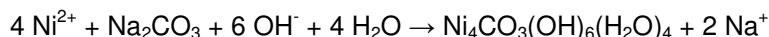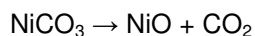## SUMMARY

The current test work and development program has demonstrated that bioleaching may be used to successfully extract Nickel, Copper and Cobalt from low grade Lynn Lake concentrates. Also that the costs of recovery are comparable to existent processes. Further that there are a number of options that can be further developed in order to optimise the process and significantly reduce costs.

RECOMMENDATIONS

Going forward it will be important to,

- Update process costs based on incorporation of a Ferric recycle.
- Conduct the necessary trade-offs between moderate thermophile and thermophile based processes.
- Evaluate further alternatives for Nickel metal production.
- Update the Pre-feasibility Economics.
- Establish the basis for progressing the project to feasibility study level.

REFERENCES

Other than the Wardrop pre-feasibility study and resource update, which are in the public domain and may be found on SEDAR, the other cited references remain private or confidential communications.

1. Lynn Lake Nickel Project Pre-Feasibility Study, Wardrop, December 5th 2007, SEDAR.

2. Technical Report on the Lynn Lake Nickel Project Northern Manitoba, Canada, Wardrop January 28th 2010, SEDAR.

3. Interim Report #1, Bioleaching of Lynn Lake Concentrate, M. Gerike, Mintek, Feb 11th 2011.

4. Interim Report #2, FLOTATION AND BIOLEACH AMENABILITY TESTWORK ON THE LYNN LAKE CONCENTRATE, M Gericke, E Mabaso, SW Robertson, March 28th 2011.

TALVIVAARA SOTKAMO MINE – BIOHEAPLEACHING OF A POLYMETALLIC NICKEL ORE IN SUBARCTIC CONDITIONS

By

Marja Riekkola-Vanhanen

Talvivaara Mining Company Ltd., Finland

Presenter and Corresponding Author

Marja Riekkola-Vanhanen
marja.riekkola-vanhanen@talvivaara.com

ABSTRACT

Talvivaara deposits, Kuusilampi and Kolmisoppi, comprise one of the largest sulfide nickel resources in the world with 1121 Mt in measured and indicated resource categories, sufficient to support an anticipated production for 46 years. Production at the mine started in October 2008 with the precipitation of the first metal sulfides. The planned annual nickel production of 50,000 tonnes is anticipated to be reached in 2012. As by-products the mine will also produce approximately 90,000 tonnes of zinc, 15,000 tonnes of copper and 1,800 tonnes of cobalt.

The process consists of mining, crushing, bioheapleaching and metals recovery. Crushing is done in four stages. The crushed material is agglomerated with sulfuric acid in order to consolidate the fines with coarser ore particles. The agglomerated material is conveyed and stacked eight meters high on the primary pad for bioheapleaching. After one and a half years leaching on the primary pad, the leached ore is reclaimed and restacked onto the secondary pad, where it is leached further in order to raise the metal recovery. In metals recovery copper, zinc, nickel and cobalt are precipitated as sulfides from the pregnant leaching solution. These metal intermediates are supplied to companies with metal refining operations.

The Talvivaara deposits are well-suited for open pit mining due to the thin overburden, favorable resource geometry and low waste to ore ratio. The ore is relatively low grade, but well suited to bioheapleaching due to its high sulfide content.

INTRODUCTION

The Talvivaara Deposits are located approximately 350 km south of the Arctic Circle about 35 km south-west of Sotkamo. The climate is characterized by extreme seasonal changes in temperature and light. Average daylight hours in summer (June to August) are 20 hours whereas in winter (November to March) this is reduced to seven hours. Winter temperatures range from 0 to minus 20°C with exceptional short-lived cold spells of below 30°C. The average annual snowfall is 0.7 m.

Talvivaara deposits, Kuusilampi and Kolmisoppi, comprise one of the largest sulfide nickel resources in the world with 1121 Mt in measured and indicated resource categories (Table 1). Talvivaara's preferred extraction technology is bioheapleaching, which is widely used for other metals, notably copper and gold. The company has demonstrated the viability of bioheapleaching technology for the extraction of nickel on site using Talvivaara ore (1, 2). The leaching process generates heat and is therefore suitable for the subarctic conditions. The planned annual nickel production of 50,000 tonnes is anticipated to be reached in 2012. As by-products the mine will also produce approximately 90,000 tonnes of zinc, 15,000 tonnes of copper and 1,800 tonnes of cobalt.

Table 1: Total mineral resources at 0.07 % nickel cut-off

Category	Year	Mt	Nickel (%)	Zinc (%)	Cobalt (%)	Copper (%)
Measured	**2010**	**432**	**0.23**	**0.50**	**0.02**	**0.13**
	2008	*364*	*0.23*	*0.51*	*0.02*	*0.13*
Indicated	**2010**	**689**	**0.23**	**0.50**	**0.02**	**0.13**
	2008	*278*	*0.22*	*0.49*	*0.02*	*0.13*
Subtotal	**2010**	**1,121**	**0.23**	**0.50**	**0.02**	**0.13**
	2008	*642*	*0.23*	*0.50*	*0.02*	*0.13*
Inferred	**2010**	**429**	**0.20**	**0.47**	**0.02**	**0.12**
	2008	*363*	*0.20*	*0.49*	*0.02*	*0.12*
Total	**2010**	**1,550**	**0.22**	**0.49**	**0.02**	**0.13**
	2008	*1,004*	*0.22*	*0.50*	*0.02*	*0.13*

PROJECT HISTORY

Geological work in the Talvivaara area commenced in the early 1900's when geological mapping of bedrock was conducted by the Geological Survey of Finland (GSF) and continued through 1951. Between 1951 and 1962, various Finnish companies carried out exploration activities in the area. The result of this phase led GSF to commence detailed exploration in the area in 1977. As a result of the work done by GSF, two polymetallic deposits, Kuusilampi and Kolmisoppi, were established. Outokumpu acquired the deposits from the Finnish State in 1985 and the mining license covering the Talvivaara Deposits was granted to Outokumpu in 1986. Between 1989 and 1992, Outokumpu focused on further geological work on the Talvivaara Deposits.

Despite extensive exploration in the Talvivaara area that established the presence of large deposits, it was concluded at the time that exploitation of the relatively low-grade deposits would not be economically viable using conventional techniques. Therefore, the Talvivaara Deposits remained unexploited until the Talvivaara Project acquired the rights to the deposits in February 2004 and continued the geological work by focusing on sampling for metallurgical purposes and investigating sample areas for the pilot trial.

With the deposits Talvivaara was assigned the right to use all exploration data and research documentation relating to various process options studied. Bioheapleaching seemed to be the most economical option. Construction of a 17 000 tonnes on-site pilot heap was started in May 2005 and initial bioheapleaching was started in August of that year. A metals recovery pilot using the PLS from the process was run in 2006 in the OMG plant in Kokkola. The environmental permit was granted in March 2007 followed by the commencement of the construction phase of the project. In April 2008 ore mining started at Kuusilampi open pit and in July 2008 bioheapleaching was initiated. The first metal sulfides were produced at the plant in October 2008.

DEPOSIT GEOLOGY

Talvivaara is situated in the southern part of the Early Proterozoic Kainuu Schist belt. The Ni-Cu-Co-Zn mineralisations are hosted almost entirely by high-grade metamorphosed and intensively folded black schist. About 90 % of the ore is hosted by black schist and the rest by metacarbonate rocks, mica schists, quartzites, graywackes and quartz wackes. The main mineral assemblage in the black schist is quartz, micas, graphite and sulfides. The valuable metal containing sulfides are pyrrhotite, pyrite, sphalerite, pentlandite, violarite and chalcopyrite. The average content of the ore using the cut-off of 0.07 % of nickel is 0.23 % Ni, 0.50 % Zn, 0.13 % Cu, 0.02 % Co, 10.3 % Fe and 8.4 % S. The distribution of nickel in different sulfides is pentlandite 66 %, pyrrhotite 33 % and pyrite 1 %. The distribution of cobalt is pentlandite 11 %, pyrrhotite 26 % and pyrite 63 %. All copper is in chalcopyrite and zinc in sphalerite.

The Talvivaara deposit consists of two orebodies, Kuusilampi and Kolmisoppi, about 3 km apart. Known dimensions for the Kuusilampi deposit are length 2600 m, width 40 – 1000 m and depth 600 m, and for Kolmisoppi 1500 m, 30 – 350 m and 300 m respectively. The metal distribution in the deposits is homogeneous and grade control procedures are fairly simple. Ore boundary definitions are based on diamond drilling in 50 m x 50 m grid. In places the boundary is further defined by assaying blast hole cuttings with portable XRF analyzer. Geotechnical logging and mapping are very important duties for mine geologists because of the graphite bearing host rocks.

PRODUCTION PROCESS

Overview

The mining method selected for use at Talvivaara is large scale open pit mining. Materials handling covers all the physical ore processing steps from the primary crusher to the heaps. After 13-14 months of bioleaching on the primary pad, the leached ore is reclaimed, conveyed and re-stacked onto the secondary heap pad. After secondary leaching, the barren ore will remain permanently in the secondary heaps. In the metals recovery process, the metals are precipitated from the pregnant leaching solution (PLS) using gaseous hydrogen sulfide (Figure 1). The resulting products are intermediates to be transported for further processing in refineries operated by the Group's customers.
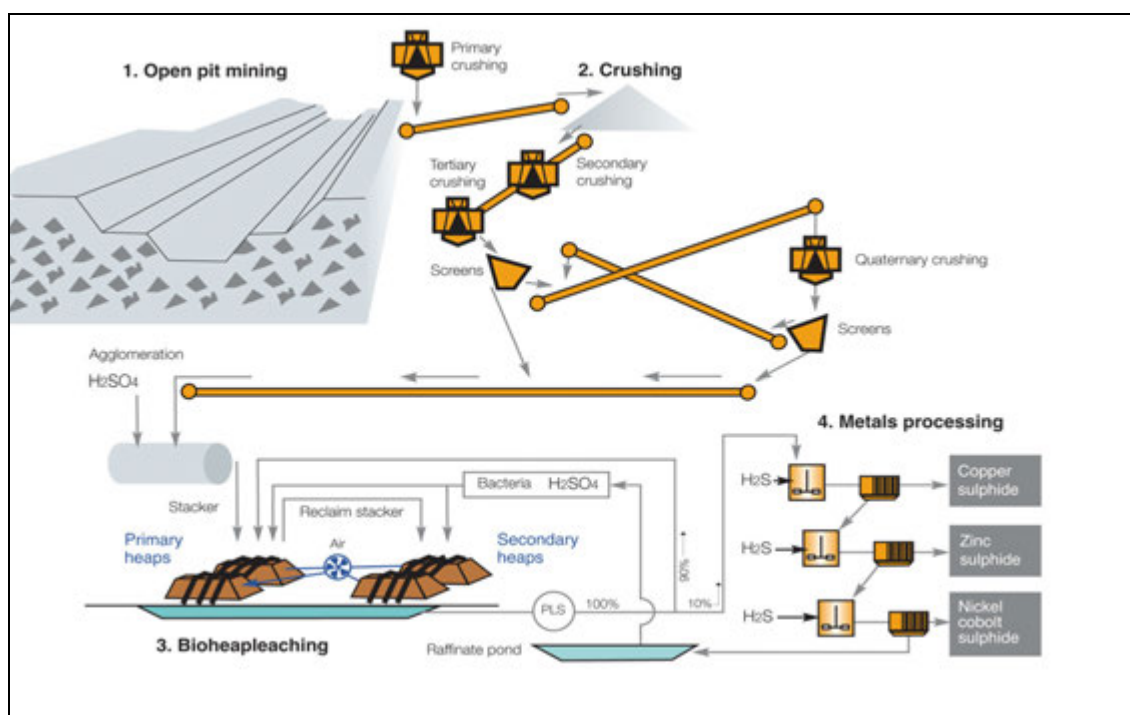

Figure 1: Process flow sheet

Open Pit Mining

Planned annual ore production is approximately 25 million tonnes. Sufficient areas to extend the pit will be prepared in subsequent years, normally a year prior to when mining is scheduled to commence. Any overburden or moraine not required for road, perimeter wall or other construction, is stockpiled for later use in rehabilitation.

Ore and waste are extracted using conventional large scale open pit drill and blast methods. A fleet of self-propelled diesel hydraulic track drill rigs are used. Fragmentation by blasting is preferred to crushing because of lower costs. It is also beneficial to create more fracturing at blasting stage which increases the surface area and therefore improves leaching solution entry and consequently leaching efficiency. As a result, the drilling pattern and hole sizes are on average smaller than in mines with similar production rates. The material movement to primary crushing is done by truck and shovel.

Materials Handling

Materials handling in Talvivaara covers all the physical ore processing steps from the primary crusher to the final locations on the secondary heaps. Bioheapleaching takes ownership of the ore when it is discharged from the primary heap stacker onto the primary leach pad. Materials handling is responsible for reclaiming the ore at the end of primary leaching period and restacking it into the secondary leaching pad. Secondary leaching is the responsibility of bioheapleaching.

During the process, the ore is crushed and screened in four stages into p80< 8mm. After primary crushing, the ore is conveyed to the fine crushing station where it is crushed and screened in three phases. All material <10 mm continues to agglomeration and is agglomerated for bioheapleaching. Agglomeration takes place in a rotating drum, where sulfuric acid is added to the ore in order to consolidate the fine ore particles with coarser ore particles. This preconditioning step makes the ore permeable to air and water for bioheapleaching.

After agglomeration, the ore is conveyed and stacked eight meters high on the primary heap pad for one and one-half years of bioheapleaching. The heap pad is equipped with piping, laid on the bottom of the pad, through which low-pressure fans supply air to the stacked ore. From the top, the heap is irrigated with leaching solution, which is collected from the bottom of the heap. A ten percent side flow is taken for metals recovery and the rest of the solution is diluted with water in order to keep the amount of solution constant. The pH value of the solution is also adjusted at this stage.

After one and one-half years of leaching on the primary pad, the leached ore is reclaimed, conveyed and re-stacked onto the secondary heap pad, where it is leached further in order to recover metals from those parts of the primary heaps where leaching solution has had poor contact. Such areas include, for example, the slopes of the heaps and areas between channels formed by the circulating leaching solution. After secondary leaching, the barren ore is expected to remain permanently on the secondary heaps.

Bioleaching

Bioleaching is the process of extracting metals from their ores by using bacteria. This process occurs spontaneously in nature under favorable conditions. The bacteria used in the Talvivaara process grow naturally in the ore and the process of bioleaching is technically viable by creating optimal conditions for growth of the bacteria.

The design criteria applied in the heap leaching design were as following:
- ore production   25 Mtpa
- ore bulk density   1.8 t/m^3
- ore particle size   p80 – 8 mm
- heap temperature range   20 – 80°C
- leaching time
  - primary heap   13-14 months
  - secondary heap   3.5 years
- irrigation rate
  - primary heap   5 l/m^2xh
  - secondary heap   2 l/m^2xh

- aeration   forced 0.08 m^3/txh
- sulfuric acid consumption
  - primary heap   15 kg/t
  - secondary heap   2 kg/t
- primary leach pad
  - operation principle   dynamic pad
  - height   8 m
  - surface area   2 x 400 x 2400 m
- secondary leach pads
  - operation principle   permanent pad
  - height   4 x 15 m lifts

The designed parameters above were based on laboratory test work, experience from other mine sites and pilot heap operation. The main reason to install a secondary leaching phase is to get better recoveries of copper and cobalt. Copper is in chalcopyrite and the main part of cobalt in pyrite. As sulfide minerals have semiconductor properties, galvanic interactions appear when there is an electrical contact among mineralogical phases. During dissolution of a mineral assembly of different sulfides, those minerals that have the highest rest potentials behave as cathodes which means that they are galvanically protected and their leaching is hindered until the minerals with lower rest potentials have been leached. The electrochemical potentials of chalcopyrite and pyrite are higher than the ones of pyrrhotite, pentlandite and sphalerite. The leached material also remains on the secondary pad. The formed about 60 meter high heap will be covered air- and water-tight and re-vegetated.

The primary heap comprises of two heap pads, a lower section and an upper section and a 40 m wide corridor between them reserved for a service area, pipelines and two fixed conveyor lines. (Figure 2). The heap pads are 2400 m long and 400 m wide, the entire surface area is 210 hectares. The heap pad sections are further divided in four sectors. The heap pads are designed so that in the longitudinal direction they are horizontal and in the cross direction they slope toward the PLS ponds. The cross slopes vary from 2% to 3.5 %.
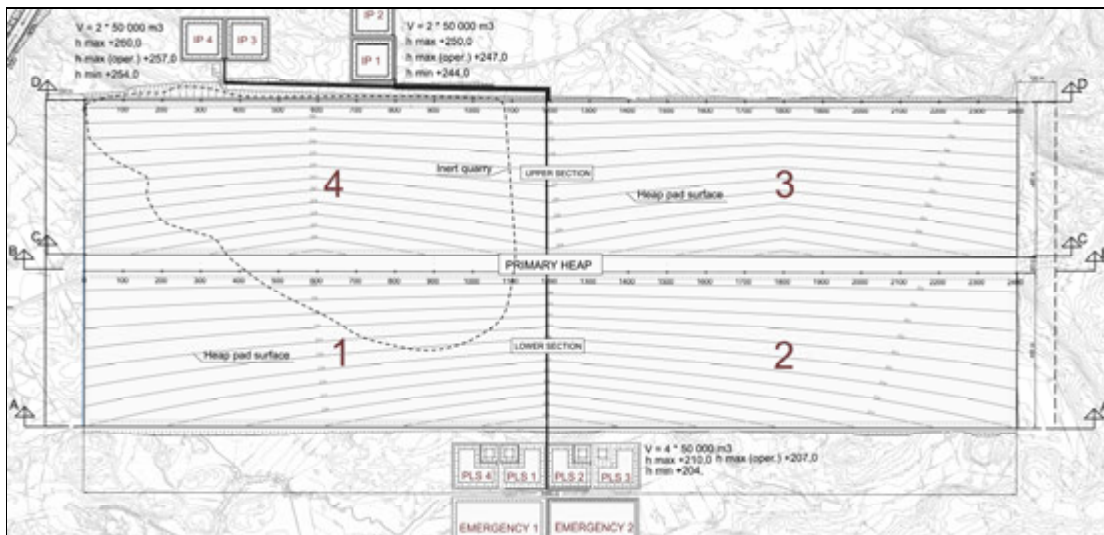
Figure 2: Primary heap layout

The secondary leaching pads are constructed on top of waste rock dumps. The benefit of the arrangement is multiple lining systems and reduced earthwork quantities. It also reduces the final footprint of the operation and final rehabilitation costs.

Primary heap is irrigated at a rate of 5 l/m^2xh. The pH value of the irrigation solution is adjusted to 1.8 and the solution is circulated evenly on the heap surface. The solution flows through the heap allowing metals to dissolve into the solution. PLS is collected with a drainage system and discharged to the PLS collection ponds. About 10 – 20 % of the solution is pumped to the metals recovery plant and the rest of the solution is circulated back to the heap. The amount of solution is kept constant by adding process water.

The bioleaching bacteria require oxygen, which is the electron acceptor in the leaching process. Carbon dioxide is also important, because the bacteria need it as carbon source for their growth. Carbon dioxide is usually not limiting bioleaching because it is a constituent of the air used for aeration and it is produced by dissolution of the carbonate minerals from the ore. However, oxygen can become limiting. The amount of air needed has been calculated based on the amount of ore to be leached, the amount of sulfide to be oxidized and the bioleaching time used. An efficiency factor is included in the calculation formula.

The aeration system for the primary heap consists of 32 low pressure fans which have been installed in 16 movable containers. The pipelines have been dimensioned with a flow speed between 5 – 10 m/s in order to reduce pressure losses in pipelines. The yield of each fan is 11.5 m^3/s totaling 1.3 Mm^3/h.

The PLS from the heaps is analyzed for pH, redox potential, acidity, total iron concentration, ferrous iron levels and metal concentrations. Acidity and pH measurements indicate the extent of acid conditioning of the heap and provide insight into the oxidation of pyrite. Redox potential, iron concentrations, ferrous to ferric ratios provide information on pyrite and other iron-bearing mineral dissolution and the performance of iron oxidizing bacteria. Solid samples are collected at different depths and locations throughout the heap leach period and are assayed for metal concentrations and mineralogy.   This provides inventory measurements as well as performance indication. Temperature measurements at various depths and locations throughout the heap provide information of pyrrhotite and pyrite oxidation.

The validity of these monitoring techniques is predicated on obtaining a sufficient number of representative samples and having accurate baseline parameters. Moreover, the most valuable information is gained by correlating the chemical and physical conditions of the heap and the specific samples with microbial assays and molecular biology data.

Metals Recovery

In the metals recovery process, the metals are precipitated from the PLS using hydrogen sulfide. The resulting products are intermediates, such as copper and zinc sulfides and a mixed nickel cobalt sulfide. These intermediates are transported for further processing in refineries operated by Talvivaara's customers.

The metal recovery includes the following process parts (Figure 3):
- precipitation of copper sulfide
- precipitation of zinc sulfide
- neutralization/aluminum removal
- precipitation of mixed nickel/cobalt sulfide
- iron removal
- final precipitation

Some of the reagents used must be produced on site. Hence also the following production units have been built:
- two hydrogen plants
- two hydrogen sulfide plants
- a grinding and elutriation plant for lime and slaked lime
- an oxygen plant

The sulfide precipitation lines for different metals are very similar. The process flow is divided into two parallel working trains of equal size.

Copper Precipitation

The incoming flow to the metal plant comes from the PLS pond. The temperature of the solution is about 40^oC. Copper is precipitated with gaseous hydrogen sulfide. The reaction is controlled with flow measurements regulating the equivalent ratio between Cu and H_2S. The metal levels in the flows are analyzed with on-line analyzers. When the feed of H_2S is 1.0 – 1.2 times the equivalent amount of copper the precipitation of copper is quite complete with minimal co-precipitation of zinc or other metals. With a higher ratio the amount of zinc remains higher. Sulfuric acid is formed in the reaction. The reaction time is 30 minutes. In the reactors a slight under pressure is preserved and the stirrers are equipped with water seals. All hydrogen sulfide reactors are situated in the same

EX-protected space. No other equipment is placed in this space.

The off gases from the sulfide reactors are absorbed in two stirred reactors filled with NaOH-solution. The gases from one reactor train (CuS+ZnS+NiCoS) go to one absorption reactor and the gases from the other train to the other one. The unreacted H_2S in the off gas reacts with NaOH generating NaHS slurry. This slurry is recycled back to the NiCoS precipitation reactors as a reagent.

The precipitated copper sulfide is separated in thickeners. The overflow from the thickeners goes to the feeding tank of the zinc sulfide precipitation. If needed a part of the underflow can be recycled back to the precipitation as seed particles for the precipitation. The main part of the underflow from the thickener is filtered with belt filters. The copper cake is thoroughly washed to enhance the purity of the product. At the end of the belt filters it goes through a squeezing device to remove as much moisture as possible. The wash water from the belt filters is circulated back to the bioheapleaching circuit.
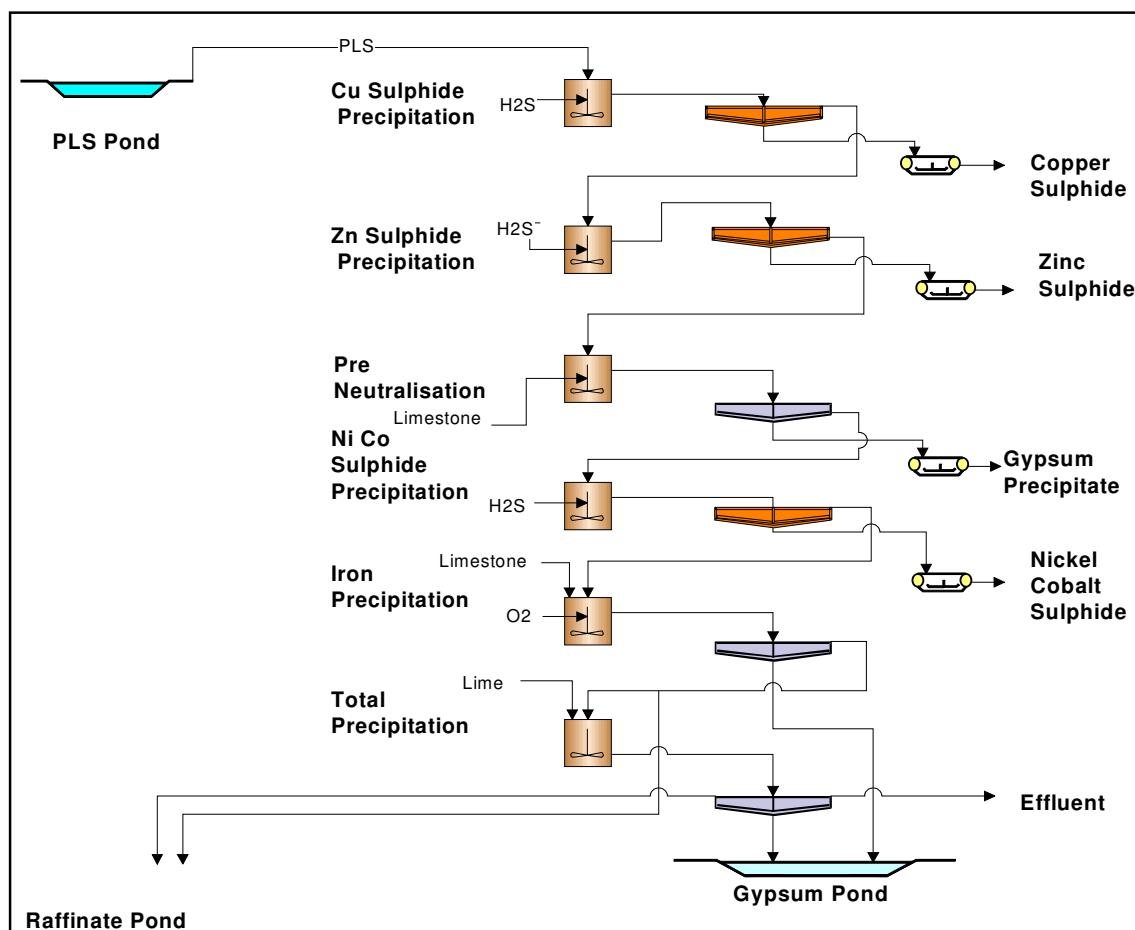

Figure 3: Flow sheet of the metal recovery process

Zinc Precipitation

After copper precipitation zinc is also recovered by sulfide precipitation. The precipitation is nearly similar to the copper precipitation. When the feed of H_2S is 1.2 – 1.5 times the equivalent amount of zinc the precipitation of zinc is almost complete with minimal co-precipitation of nickel and cobalt. The reaction time in zinc precipitation is one hour because of the low pH-value. The precipitated zinc sulfide is separated in the same way as copper sulfide.

Preneutralisation

The precipitation of nickel and cobalt mixed sulfide must be made at a higher pH value than for copper and zinc. In preneutralisation the acidity in the feed and the acid formed in copper and zinc sulfide precipitation are neutralized. At the same time a considerable part of the aluminum in the

solution is precipitated. It is not favorable to aim at a too high aluminum removal in this stage because it can generate considerable nickel/cobalt losses. Careful pH control is needed in order to minimize the amount of impurities in the Ni/Co precipitate and at the same time avoid nickel/cobalt losses to the neutralization precipitate. The pH value is adjusted to 3.7 – 4.0 with a slurry of water/limestone. The reaction time is one hour. The aluminum containing precipitate is separated in thickeners. The overflow from the thickeners goes to the feeding tank of Ni/Co precipitation. The amount of precipitate formed is large. The underflow from the thickeners is filtered on belt filters. The cake is thoroughly washed to avoid losses of nickel and cobalt. The precipitate is transported to the waste rock area as a filter dry product.

Nickel and Cobalt Mixed Sulfide Precipitation

Nickel and cobalt are precipitated with hydrogen sulfide using sodium hydroxide as a neutralizing agent. The neutralization is partly made with the recycled NaHS-solution from the absorption reactors. The precipitation is otherwise similar to copper and zinc precipitations. The pH value is kept at about 3.6 – 3.8 and hydrogen sulfide is fed at an equivalent amount. Without pH control the precipitation ceases. The resident time is one hour. The precipitated nickel/cobalt sulfide is separated in thickeners and treated like the copper and zinc sulfides.

Iron Removal

After nickel and cobalt precipitation the process solution contains considerably amounts of iron, manganese and magnesium. Iron is removed from the solution as goethite and/or hydroxide with the following process:
- Fe^{2+} is oxidized to Fe^{3+} in a series of reactors. Oxygen is used as oxidant.
- Oxidized iron is precipitated as goethite ($FeOOH$) or hydroxide ($Fe(OH)_3$) in the same reactor system.
- Iron slurry goes to a thickener.
- The underflow from the thickener is pumped to the gypsum pond. Clarified water from the pond is recycled back to the heap leaching circuit.
- The overflow from the thickener can be divided into two streams. One stream is recycled to the heap leaching circuit'; the other one goes to the final precipitation.

Final Precipitation

The final precipitation is the outlet for manganese and magnesium in the Talvivaara process. Remaining iron and gypsum also precipitate in this step. After iron removal the solution goes to the final precipitation where the pH value is raised to a value of 9 – 10 with a slurry of slaked lime. The remaining metals precipitate as hydroxides. The precipitate also contains gypsum. The residence time is one hour. This step is made in a single reactor system where the solution is pumped from both trains. The slurry from the reactors goes to a thickener. The underflow is pumped as slurry to the gypsum pond. The slurry has to be carefully analyzed to ensure its suitability for the gypsum pond. The overflow from the thickener is recycled to the heap circuit.

Hydrogen and Hydrogen Sulfide Production

The products of Talvivaara are precipitated as sulfides. Gaseous hydrogen sulfide is used as reagent. Hydrogen sulfide is produced by reacting hydrogen gas and molten elemental sulfur. Hydrogen is produced from propane which is reformed with steam at high temperature using a nickel catalyst. The hydrogen rich gas is purified in an absorption process.

The hydrogen sulfide plant consists of the following parts:
- H_2S generator where hydrogen gas and molten sulfur react forming hydrogen sulfide.
- Resistance space where the temperature of sulfur is raised using electrical resistances.
- H_2S tower where the generated hydrogen sulfide is cooled with circulating sulfur.
- Cooler for the H_2S gas.

From the cooler the gas flows to a pressure balancing tank where a pressure of 3.5 – 4.5 bar is preserved. From this tank the hydrogen sulfide is taken to the precipitation reactors.

Major Items of Equipment

Table 2 lists the major units of process equipment in the metals processing area.

Table 2: Major items of equipment

	Precipitation	Thickening	Filtration
Copper recovery	4 reactors 350 m^3 each	2 thickeners Ø 30 m	2 belt filters Area 32 m^2
Zinc recovery	6 reactors 350 m^3 each	2 thickeners Ø 30 m	2 belt filters Area 32 m^2
Neutralization and aluminum removal	6 reactors 350 m^3 each	6 thickeners Ø 30 m	6 belt filters Area 60 m^2
Nickel Cobalt recovery	6 reactors 450 m^3 each	2 thickeners Ø 30 m	2 belt filters Area 44 m^2
Iron removal	6 reactors 625 m^3 each	4 thickeners Ø 30 m	
Final precipitation	4 reactors 450 m^3 each	6 thickener Ø 30 m	

The materials used in the equipment have been chosen very carefully. The solution coming to the metal plant contains iron oxidizing bacteria; there are oxidizing and reducing conditions in various reactors. The reactors are built from fiberglass; reinforced plastic is also used a lot. Suitable steels are AISI 254 SMO or AISI 904L. Stirrers have been coated with butyl rubber and the valves lined with PTFE and PVA.

Water Management

The water management in Talvivaara includes all relevant pipelines, ponds and pump stations related to the processes outside the metals recovery plant area. It also includes surface water management, effluent treatment and other surface water construction projects.

Water management plays an important role at the operation. The most important component is the recycling of the leaching solution from the irrigation pond to the heap and thereafter to the PLS pond. From the PLS pond, approximately 90 per cent of the solution is recycled back to irrigation to increase the metal grade, while about 10 per cent is lead to metals recovery. After metals precipitation, the remaining solution goes into the raffinate pond for pH adjustment and is reused to irrigate the heaps.

LAND AND INFRASTRUCTURE

General

Prior to construction of the pilot operation in 2005, the Talvivaara Deposits had no existing mining facilities. Development of the infrastructure and services included:

- Access roads, internal roads and railway.
- Power supply.
- Fuel services.
- Drinking water supply/water management.
- Sewage and waste management.
- Buildings and plants needed for production.

The first construction phase commenced in February 2007 with construction of roads to allow good access to the site and between the construction areas. The majority of all earthworks were completed by the end of 2008.

The Talvivaara operational area totals 61 km^2 and requires construction of buildings with total space of approximately 63,000 square meters (Figure 4).
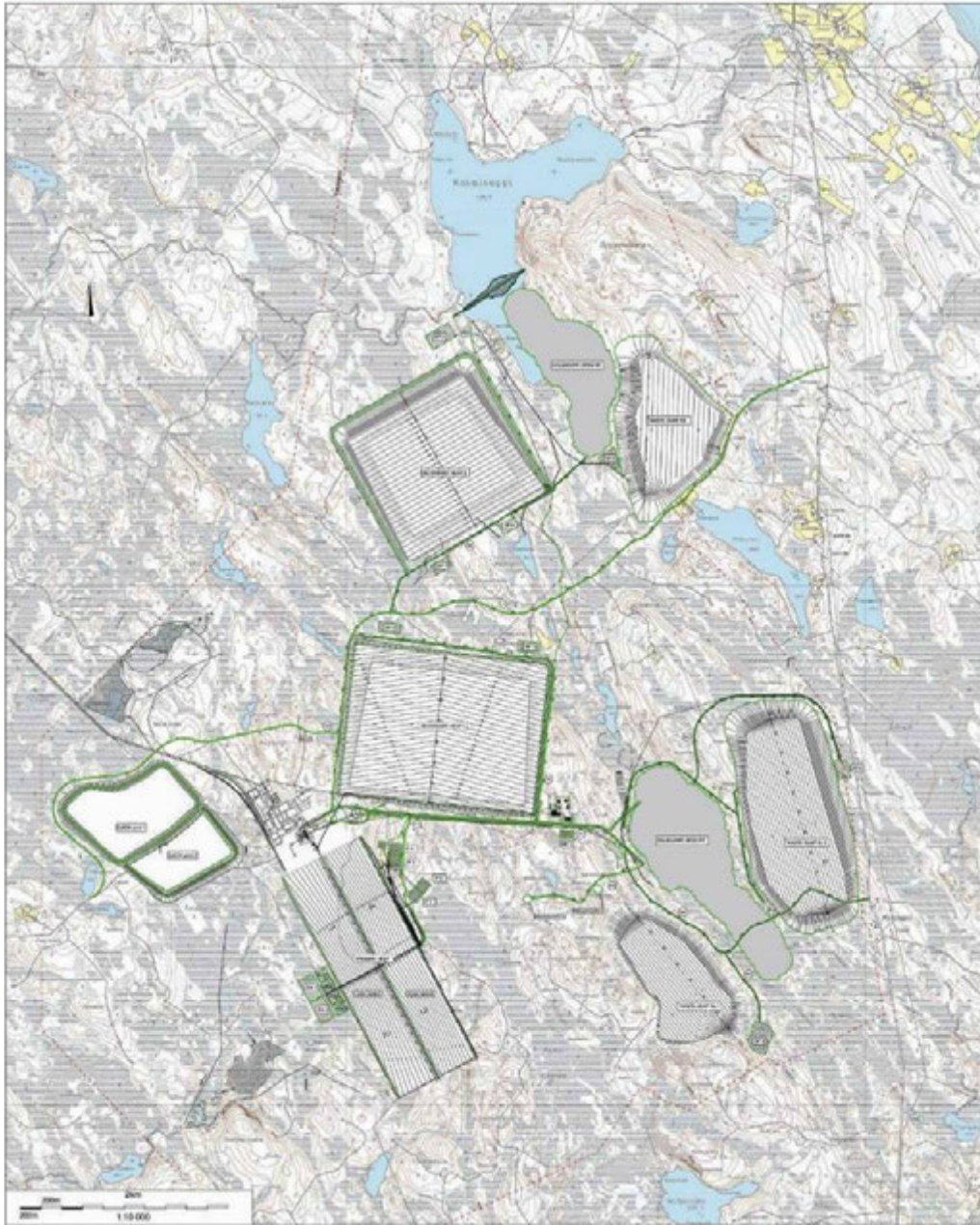
Figure 4: Location of the Talvivaara mine

Access Roads and Railway

Access roads, internal roads and railway transport are needed for the incoming transport of materials used in the production process, the outgoing transport of products and maintenance transport. The main access to Talvivaara is a regional highway. The site is well connected to the highway network via the local roads in all directions and benefits from being close to the main railway network. Transportation to or from ports in Kokkola, Raahe and Oulu can be arranged either via road or rail. A 26 km rail connection was completed in summer 2009.

Power and Fuel Supply

The main power source is electricity. The 110 kV power line constructed from the Vuolijoki substation to Talvivaara mine was connected to the Finnish main national grid in Mid January 2008. The 43 km power line was constructed and connected ahead of schedule. A main power station was constructed at the plant. The length of the internal power line network is about 19 kilometers. The majority of fuel consumption is utilized in the mining process. Fuel is supplied to the site by road.

Sewage and Waste Treatment

Sewage is treated on-site and is partly discharged with the process effluent and partly returned to the process. The quality requirement for any discharged water is set out in the environmental permit. All construction, industrial and house waste produced by the operation is transported to an authorized waste disposal site by contractors.

PRODUCTION RAMP-UP

Year 2008 marked the transformation of Talvivaara from a project to an operating mine. During the year, the construction project went through its most intensive periods, providing work for some 2,000 contractor employees during the peak installation months in late summer and early autumn. As a result of this sizeable and multidimensional effort, the project reached all its operational milestones on time enabling start-up of production processes in stages beginning with the first blast of ore in April. Some final construction and installation work remained to be completed in 2009 and 2010. In total the amount of work required to bring the mine into full operation was approximately 3,500 man-years.

Talvivaara's focus has remained firmly on production ramp-up throughout the years 2009 - 2010. Optimization of the already operating equipment and processes continued, and pre-requisites for full-scale production were fulfilled through the commissioning of the second production line at the metals recovery plant, completion of initial sections of the secondary leaching areas, installation of the secondary heap stacking and primary heap reclaiming systems, and finally the commissioning of the second hydrogen and hydrogen sulfide plants.

The scalability of the production processes and progress in ramp-up were confirmed by the production volumes achieved in 2010: 10,382 t of nickel (2009: 735 t) and 25,462 t of zinc (2009: 3,133 t). Although the production fell short of the originally budgeted figures, the ramp-up trend seen from the secondary quarter in 2010 onwards was encouraging with a relatively steady, close to 20 % quarterly increase in nickel production.

The operations have faced a series of technical challenges, ranging from a hydrogen plant failure to insufficient hydrogen sulfide capacity caused by installation faults in the hydrogen sulfide generator. Also, hydrogen sulfide emissions forced production levels to be restricted for several months because of the odor discharges. A break-through in controlling the odours was made through the use of hydrogen peroxide as the odour controlling chemical. The necessary plant modifications to enable the permanent use of hydrogen peroxide in the process were planned during the end of last year and are now under construction.

Mining has performed well throughout the year 2010, blasting 13.3 Mt (2009: 10.8 Mt) of ore and 17.7 Mt (2009: 4.3 Mt) of waste, increasing the total mining output by 99 % from the previous year. Waste mining increased significantly as waste rock has been used for the leveling of the secondary heap foundations.

The crushing processes in materials handling have caused the biggest problems in the process. The primary crusher had to be fitted with a new mantle. The fine crushing circuit had to be redesigned and more crushers had to be added. The volume of crushed and stacked ore in 2010 amounted to 13.3 Mt (2009: 8.5 Mt). Although the increase in output has been substantial and the peak production levels have improved, the overall availability of the crushing circuit still remains below target.

The installation and commissioning of the primary heap reclaiming and secondary heap stacking systems have represented a major challenge. Both systems were started up in the autumn 2010 and the secondary stacker has since then been in production with good results. Commissioning of the primary heap reclaiming equipment has however been slower, resulting in reduced overall crushing and stacking output.

In bioheapleaching the building of the first heap sector proceeded much too slowly due to difficulties in crushing. Irrigation and aeration could only be started when about 25 m of heap had been built. The agglomerates started to break apart during that time. The particle size was also smaller than planned. When irrigation and aeration were started, there were difficulties in getting an even airflow through the heap. With improved crushing systems the bioheapleaching started to progress

according to expectations. The primary heap was fully stacked for the first time in November 2010, and secondary leaching started with good results. In process development, particular attention has been paid to improve aeration. As a result, nickel grades in leach solution have increased especially in the newer heap sections, reaching levels well above 3 g/l.

The first commissioning runs at the metal plant produced saleable quality of nickel and zinc sulfides, with the first commercial deliveries in February 2009. The process were run in campaigns until mid September 2009, when the amount of leach solution available for metals precipitation was determined to be sufficient for continuous production. The goal of uninterrupted production was not yet achieved due to technical problems.

The successful and timely commissioning of the second production line in the summer 2010 and the start-up of the second hydrogen plant and hydrogen sulfide generator in the autumn provided means for the metals recovery plant to increase production. However, in its first year of continuous operation the metals recovery plant also suffered from various technical start-up problems and related down-time. Furthermore, process optimization and de-bottlenecking were ongoing through the year and will continue this year. At year-end 2010 plant availability and throughput had already improved especially on the first production line.

The quality of both zinc and nickel/cobalt sulfides has been good. Nickel/cobalt sulfide contains about 48 % nickel and 1.5 % cobalt; the moisture content is under 20 %. Zinc sulfide contains about 64 % zinc and its moisture content is about 20 %. The impurity levels in both sulfides are very low. Copper concentrations have just started to rise in the PLS and Talvivaara has not yet produced any saleable amounts of copper sulfide.

PERSONNEL

The total number of employees at Talvivaara is about 400. The personnel are mostly recruited locally from the Kainuu region, where Talvivaara is the largest provider of new job opportunities.

The average age of the personnel is 38.5 years, and the age distribution of employees is comparable to the industry average in Finland. In its recruitment process, Talvivaara has sought to maintain a representative staff age structure, in spite of the exceptionally vigorous rate of recruitment. Although the mining industry has conventionally been male dominated, Talvivaara seeks to hire employees representing both genders. This has however proven difficult due to the limited number of female applicants.

SUSTAINABLE DEVELOPMENT

Talvivaara has developed its operations according to its sustainable development policy which emphasizes continuous improvement and operational excellence. With respect to safety issues Talvivaara's goal is a safe and healthy working environment. The company has continued to develop its safety culture based on zero accident philosophy. The company is also committed to continuous improvement in environmental efficiency, operational risk management and reduction of environmental impact.

A major milestone in the Company's environmental management was reached in December 2010, when Talvivaara was awarded certification for the environmental management system ISO 14001 covering all operations of the Company. In line with the guidelines set by the ISO 14001 system, the goals in Talvivaara's operations in the future include continuous improvement, sustainable and economic use of natural resources, and development of all processes to minimize the environmental impact of the mine.

BUSINESS DEVELOPMENT

Extraction of Uranium as a By-Product

Talvivaara ore contains about 15 – 20 ppm of uranium which is leached in the bioleaching process. In the process a small part of uranium is precipitated with nickel and cobalt in the nickel/cobalt sulfide product and the main part in the gypsum residue. The company has done a lot of research to

find a method to recover uranium from the bioleaching solution. A new solvent extraction method has been shown to work efficiently (Figure 5). The work has been focused on industrial scale development and the basic and detailed engineering of the planned production unit.

Talvivaara announced in February 2010 that it is planning to initiate the recovery of uranium in the form of uranium intermediate, yellow cake. The planned investment in the solvent extraction plant is estimated at approximately EUR 40 – 50 million and the annual production costs at approximately EUR 2 million. The annual production volume is estimated at 350 tonnes of uranium.

The planned uranium production is subject to necessary permits, including an approval by the Government of Finland. Talvivaara applied in April 2010 to the Ministry of Employment and Economy for a permit to extract uranium as a by-product, in accordance with the Nuclear Energy Act. The Environmental Impact Assessment Process as well as the preparations for submitting the application for the Environmental Permit relating to the uranium extraction process is ongoing.

Talvivaara signed a uranium off-take agreement with Cameco in February 2011. The agreement is subject to ratification by the Euratom Supply Agency and the approval of European Commission pursuant to Euratom Treaty.
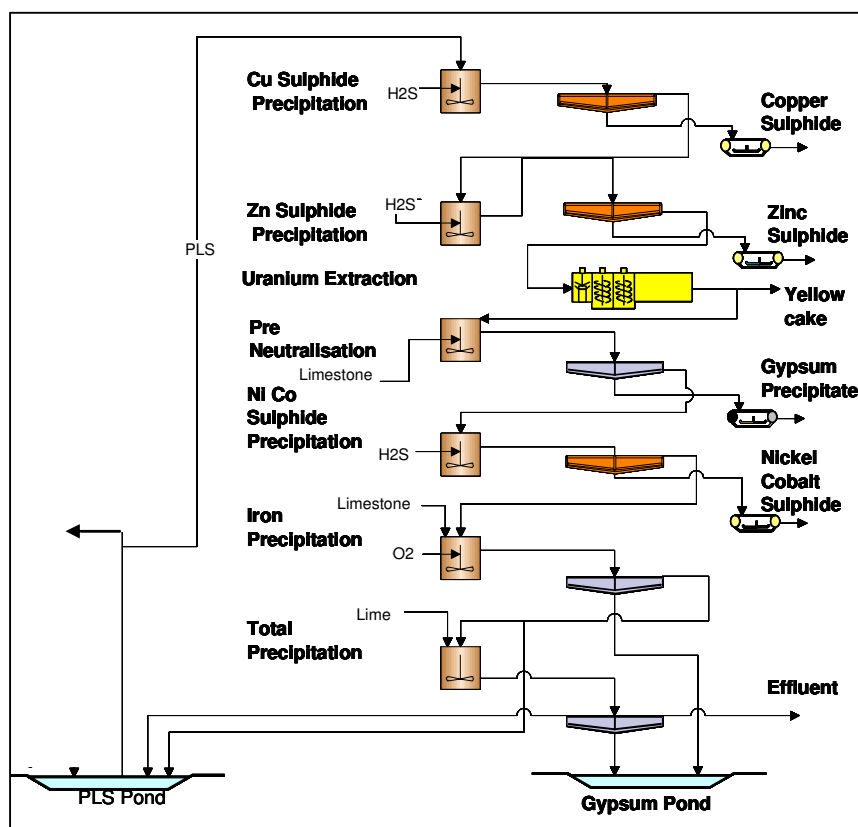

Figure 5: Yellow cake production unit in Talvívaara flow sheet

Expansion beyond 50,000 tpa nickel

Following the announcement in October 2010 of a 54 % upgrade in total mineral resources at Talvivaara, the Company established a project to evaluate the options for further expansion of production capacity at the Sotkamo mine. The key areas of evaluation include product and capacity options, raw materials and supplies availability and logistics, financial feasibility and permitting. Scoping studies and permitting work will be in focus in 2011, while it is estimated that the initial stages of the expanded production could commence in 2015 at the earliest.

REFERENCES

1. Riekkola-Vanhanen M. Talvivaara black schist bioheapleaching demonstration plant. Advanced Materials Research Vols. 20-21 (2007) pp 30-33.

2. Riekkola-Vanhanen M. Talvivaara Sotkamo Mine – bioleaching of a polymetallic nickel ore in subarctic conditions. Nova Biotechnologica 10-1 (2010) pp 7-14.

A STUDY INTO THE POSSIBLE APPLICATION OF BIOHEAP TECHNOLOGY TO FORRESTANIA

By

Jason Fewings

Western Areas NL, Australia

Presenter and Corresponding Author

Jason Fewings
jfewings@westernareas.com.au

ABSTRACT

Western Areas NL is an Australian based nickel miner, with core high grade nickel assets in the Forrestania region of Western Australia. Aside from the high grade Flying Fox and Spotted Quoll deposits, Western Areas has interests in a number of deposits in the area, and overseas, and are currently investigating methods for extracting maximum value from those deposits.

The most advanced of those deposits are the Digger Rocks/Diggers South mine and the New Morning deposit. One of the alternatives being investigated is a potential bacterial leach utilizing the BioHeap™ technology that the company acquired in 2009.

This paper outlines the main nickel assets owned by Western Areas and reports on a scoping study investigating the bacterial leaching of Forrestania ores, with an emphasis on the New Morning case study.

BACKGROUND

Western Areas NL is an Australian based nickel miner listed on the ASX and TSX. The main asset is the 100% owned Forrestania Nickel Project, 400 km east of Perth, which is currently sourcing ore from the Flying Fox and Spotted Quoll deposits, and producing a high grade concentrate for sale within Australia and overseas. In addition, Western Areas has interests in a number of nearby deposits and highly prospective areas in the Forrestania region, that forms the focus of ongoing exploration and drilling.

Western Areas owns 19.9% of the Canadian nickel company, Mustang Minerals Corp, 75% of Finnish nickel company, FinnAust Mining Plc and 100% of the BioHeap sulphide leaching process.

Western Areas is targeting total mine production from Flying Fox and Spotted Quoll, of 25,000t Ni in the the 2011 calender year, making it Australia's third largest nickel miner. Flying Fox is one of the highest grade nickel mines in Australia and has been in production since 2006. Spotted Quoll commenced high grade production in mid 2010.

Western Areas has the lowest cash costs in Australia at less than $2.50 US/lb Nickel, before smelting and refining charges. Western Areas are in a strong position to take advantage of the current nickel prices, with recently completed concentrator upgrades, and completed surface infrastructure to support the operation.

Western Areas is an independent producer with offtake contracts in Australia and China, with a proven logistics chain for delivering high quality concentrate to it's customers.

Western Areas acquired BioHeap in 2009, including the technology and key personnel. The BioHeap technology utilizes microbes for leaching of base metal sulphides, including primary copper, nickel and zinc sulphides. The BioHeap cultures have been developed through an extensive research and development program lasting more than a decade. Cultures are available that target primary copper (chalcopyrite), base metals, with or without salt tolerance (up to 200,000 ppm TDS) and/or arsenic resistance over a wide range of pH and temperatures.

An extensive patent suite protects the technology and the development methods for the extremely versatile and hardy cultures that BioHeap has available.

Operations

Western Areas is active in the nickel provinces as shown in figures 1 and 2 below. The main operation is located at Forrestania, with the Cosmic Boy Concentrator, Flying Fox and Spotted Quoll mines. Joint Ventures and other nickel interests are illustrated in Figure 2.

Concentrate is trucked to Kambalda and Esperance port as illustrated in Figure 2. Concentrate delivered to the Esperance port is then shipped to Jinchuan in China.
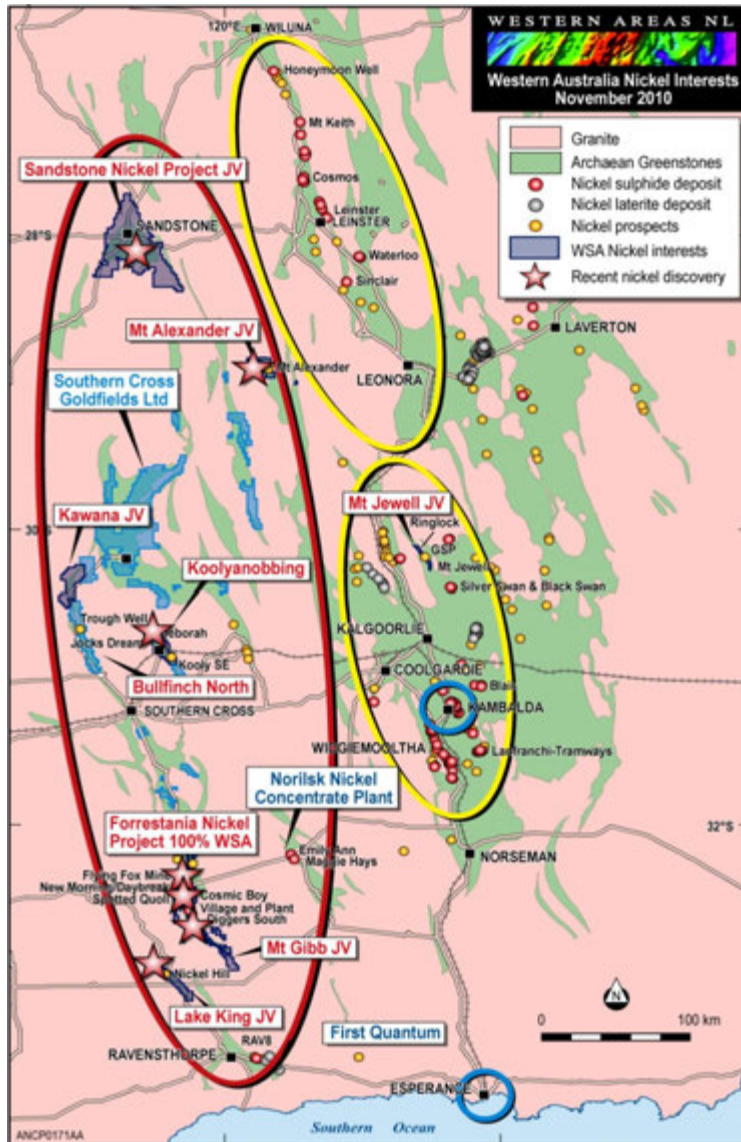

Figure 1: Main nickel provinces in Western Australia

Figure 2: Western Areas operations and interests[1]

Flying Fox Mine

The Flying Fox mine has been the main source of ore for the concentrator since 2006, and has the main decline developed to a depth of over 1000m, as mining in the T5 ore body commences. Flying Fox has continuous high grade nickel to a depth of 1300m and the orebody is open at depth.

The probable ore reserve is 1,062,000t at 5.7% nickel, for a total of 58,370t of Nickel. Ore grades increase at depth from 3.9% to 5.9% nickel.

Current production is mainly from the T4 deposit, Lounge Lizard and the T5 deposit. The T4 deposit is fully developed with an ore reserve of 7,860t nickel at 4.0%. Lounge Lizard is subject to an agreement with Kagara to mine and process 50,000 tpa ore. The T5 deposit has recently commenced production and has reserves of 50,560t nickel @ 5.9% with the best intersection being 78m @ 9.3% nickel.

There is potential to extend the resource both to the north and below T5. Drilling is in progress to test T6, T7 and T8. The best intersection to date is 9.3m @ 5.1% nickel in T7.
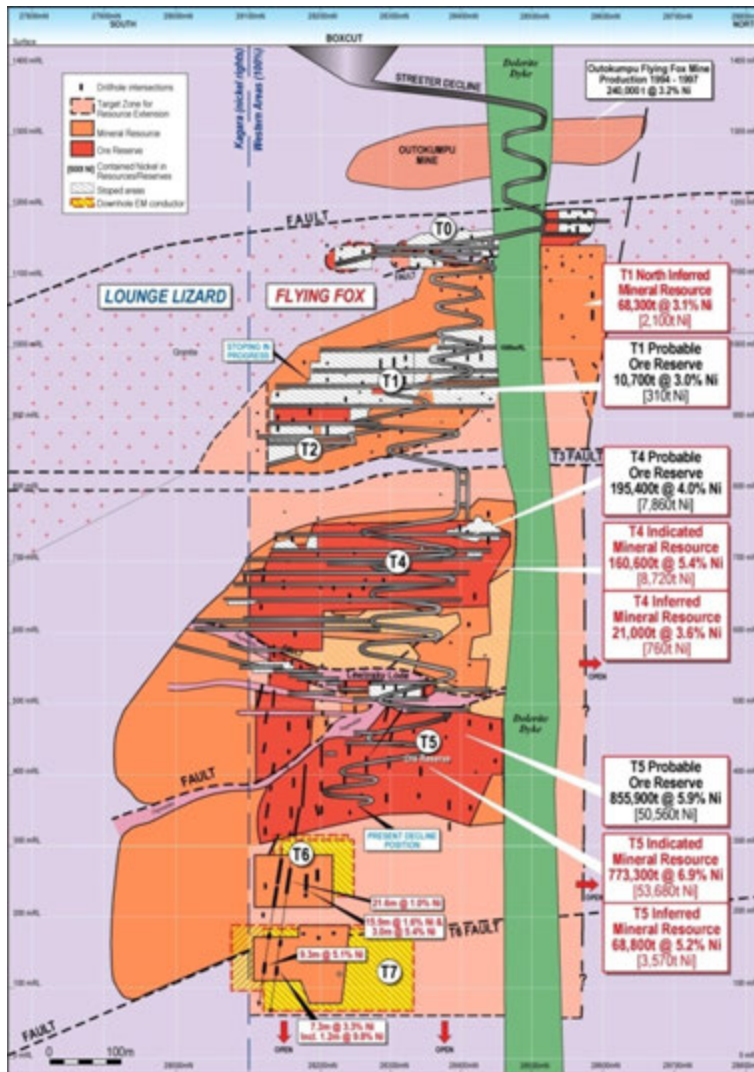
Figure 3: Flying Fox [1]

Spotted Quoll Mine

Spotted Quoll is the second mine supplying ore to the Cosmic Boy Concentrator, and started delivering ore in 2010. The open pit contains a probably ore reserve of 254,700t of ore at 4.9% nickel, for 12, 490t of nickel. Development of the decline has begun to access the underground mine, which has a probable ore reserve of 1,725,000t at 4.1% nickel, containing 70,200t of nickel.

Figure 4: Spotted Quoll Mine

Some key figures for the Spotted Quoll mine are summarised below.

Table 1: Spotted Quoll Key Figures

Ni Price US$/lb	$6.00	$8.00	$10.00	$12.00
Exchange Rate US:AUD	0.80	0.90	0.95	1.00
NPV(BT)	A$90M	A$184M	A$297M	A$385
IRR(BT)	41%	67%	96%	116%
C1 Cost (US$/lb Ni in Conc.)	$2.29	$2.57	$2.71	$2.86
TOTAL NET CASH A$ M	$162M	$320M	$500M	$640M

The Spotted Quoll orebody is open at depth with continuous mineralisation to 1700m down plunge (~1200m depth). The best intersections to date for extensions 400m below the mineral resource are 3.7m at 8.2% nickel and 3.5m at 6.5% nickel. Western Areas is targeting a significant resource upgrade by 30 June 2011.

Cosmic Boy Concentrator

The Cosmic Boy Concentrator begun concentrate production in early 2009, and was upgraded in 2010 it's current throughput of 550,000 tpa.

The plant features primary, secondary and tertiary crushing feeding a closed circuit ball mill. The Cyclone underflow reports to a flash float, with the overflow feeding roughers and scavs. A cleaning circuit is incorporated to improve nickel grades, and concentrate of 14% nickel at 90% recovery is the average product of the plant at the current time. Total concentrate capacity is in excess of 25,000 tpa.

Concentrate is sent to BHPB at Kambalda as well as to Jinchuan in China, utilizing over 1000 sealed shipping containers.

The following figure summarizes Western Areas nickel offtake arrangements.
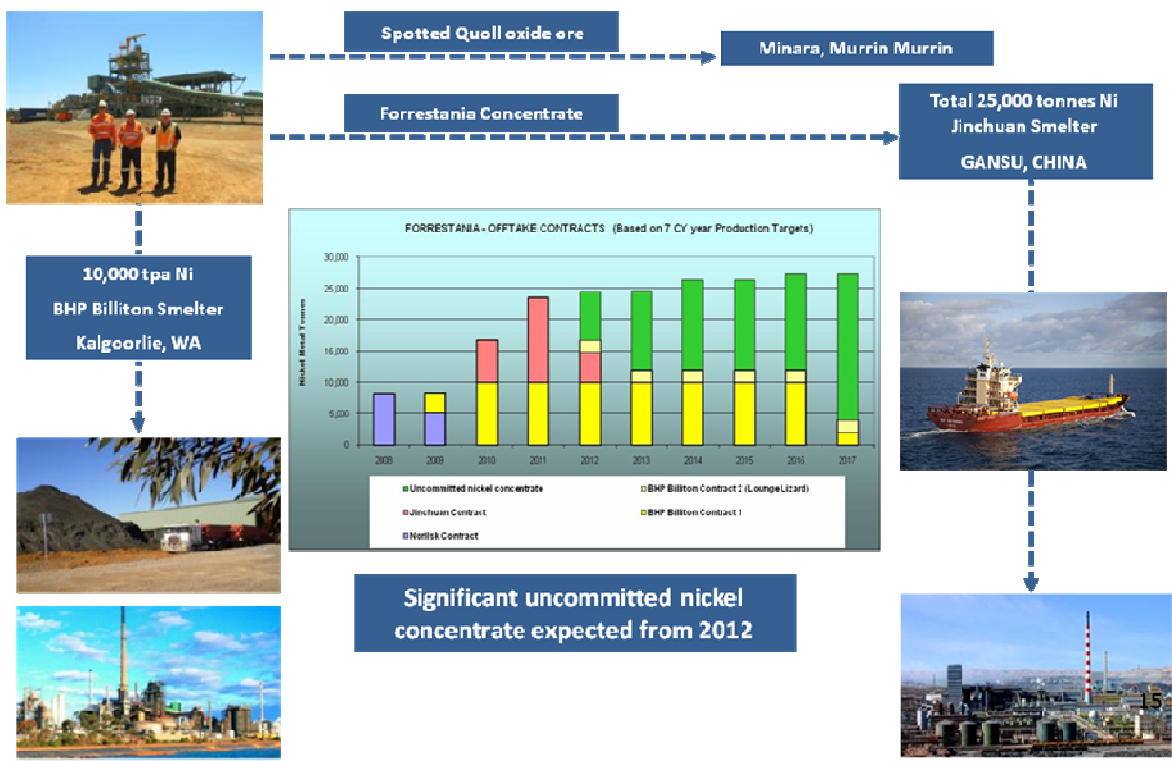

Figure 5: Western Areas Offtake Arrangements (May 2011)

Exploration and Growth

Western Areas has had an outstanding track record for discoveries using sophisticated geophysical and drilling techniques. The exploration budget for 2011 has been increased by 30% to $20M AUD, with the majority to be sent on drilling. The drilling priority will be within an 8km zone (below) within the 100km strike length of prospective ground of the Forrestania Nickel Project. Any new discoveries would be able to access existing mine and processing infrastructure.
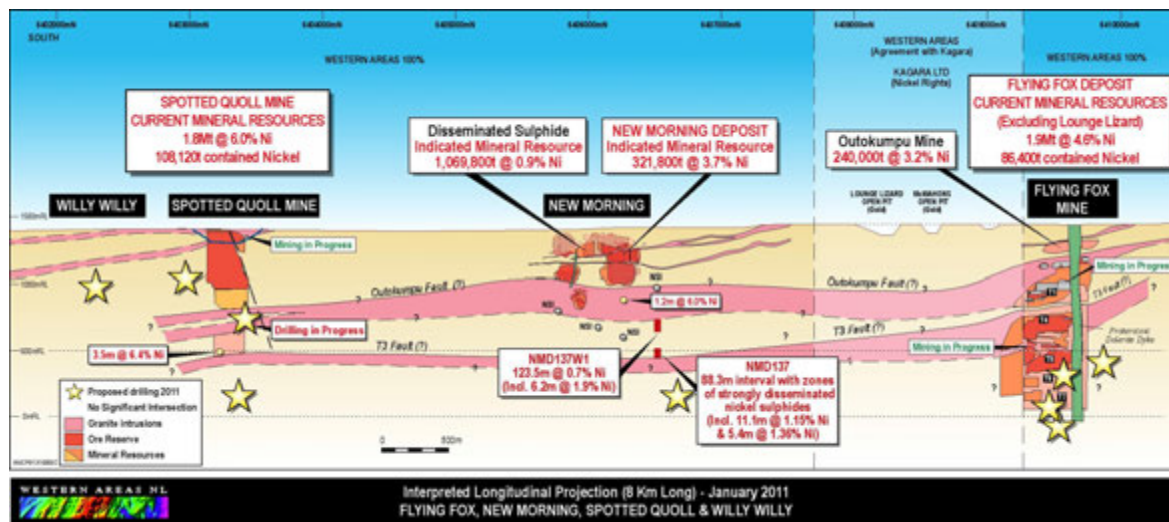

Figure 6: Western Areas Drilling Priority

Diggers South

Diggers South is one of the more advanced targets, with plans in place for an underground mine. Diggers South has an indicated mineral resource of 3.0 Mt at 1.48% Ni for 44,00t of contained nickel, as well as a mineralized halo of 4.8Mt at 0.74% Ni for 35,600t contained nickel. Digger Rocks has an indicated resource of 54,900t at 3.7% Ni.. The Stage 1 feasibility study and surface works are complete. Major dewatering infrastructure is in place. The existing mine can be used to access the higher grade Core Zone, and to give access to the extensive disseminated ore.

To date $25 million AUD has been spent on exploration and infrastructure, with approximately $100 million in capex required to fully develop the mine and the 1 Mtpa plant expansion. As part of the bioleaching study, an examination of treating the Diggers ore using a bacterial heap leach was done to assess the potential of this alternative.
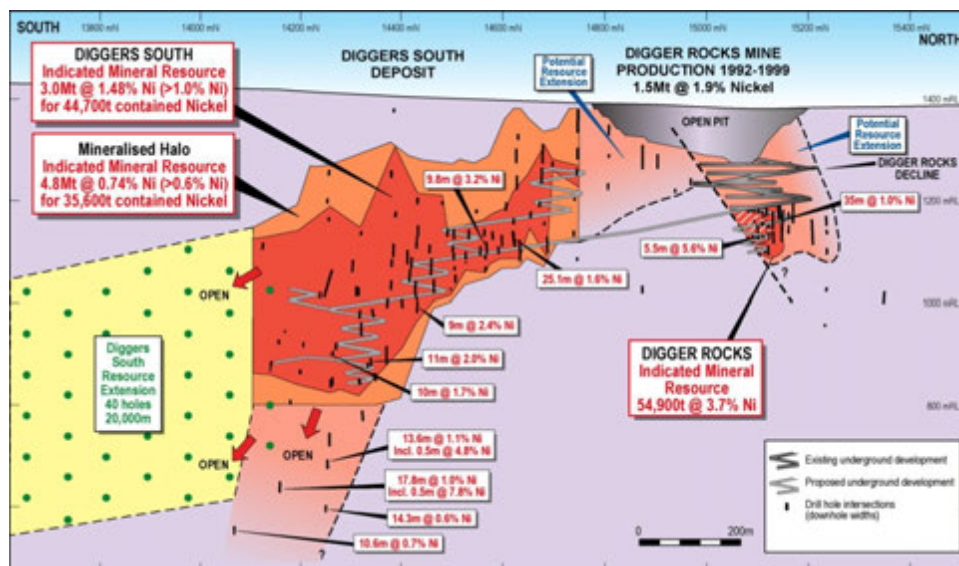

Figure 7: Digger Rocks and Diggers South Orebodies

A drilling program is planned for Diggers in 2011 with the aim of increasing ore reserves to greater than 60,000t of Nickel with sustainable production of 6,000 tpa Nickel. Western Areas are looking for a strategic partner to help fund this project.

New Morning

New morning is a small high grade deposit with an indicated mineral resource of 321,800t at 3.7% nickel and a indicated disseminated sulphide mineral resource of 1,069,800t at 0.9% nickel located between Flying Fox and Spotted Quoll, as shown in Figure 6, above.

An evaluation was made on the potential of heap leaching ore from this deposit during the Bioleaching study.

FinnAust Mining PLC

FinnAust Mining PLC is a 78% WSA owned company with significant tenement holdings in highly prospective areas of Finland. FinnAust Mining covers six exploration projects in the Kainuu Schist Belt and three exploration projects in the adjacent Outocumpu – Savonranta Belt. Western Areas has already earned 75% interest in the Kainuu Schist Belt and can earn 75% interest in the Outocumpu – Savonranta belt subject to meeting certain conditions.

Current production in the Kainuu Schist Belt is dominated by the large Talvivaara open pit mine (owned by Talvivaara Mining Plc), which is using a bacterial leaching technology to extract nickel, zinc, copper and cobalt from low grade sulphide mineralisation in a black schist ore host.
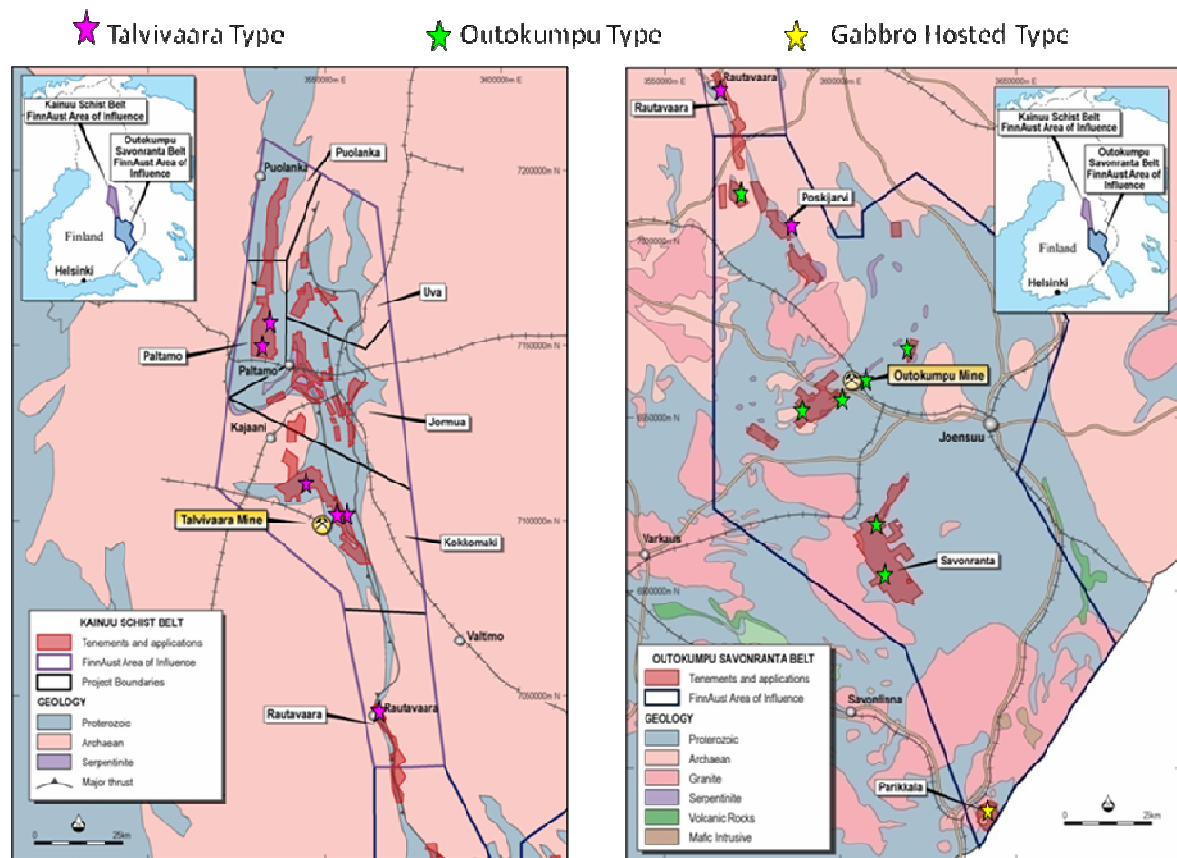
Figure 8: FinnAust Mining PLC Area of Influence[1]

Metal production in the past has been dominated by the underground mines at Outokumpu, which produced approximately 42 million tonnes of ore between 1913 and 1988. FinnAust Mining has large holdings in the immediate area of the Outokumpu mine and 20km south in the Savonranta area.

FinnAust Mining is currently aiming to raise Pre-IPO funding of €5-7 million to fund a drilling program to test high priority targets including:

- Hakonen – 3km east of Talvivaara
- Ala-Siikajarvi – 60km north of Outokumpu
- Kuusijarvi – 10km west of Outokumpu
- Paltamo – 60km north of Talvivaara
- Rautavaara – 55km south of Talvivaara (extension of the R1 resource)
- Parikkala intrusion – 130km south of Outokumpu

Funding will also be used to conduct metallurgical testwork and to conduct a scoping study on Rautavaara and other deposits.

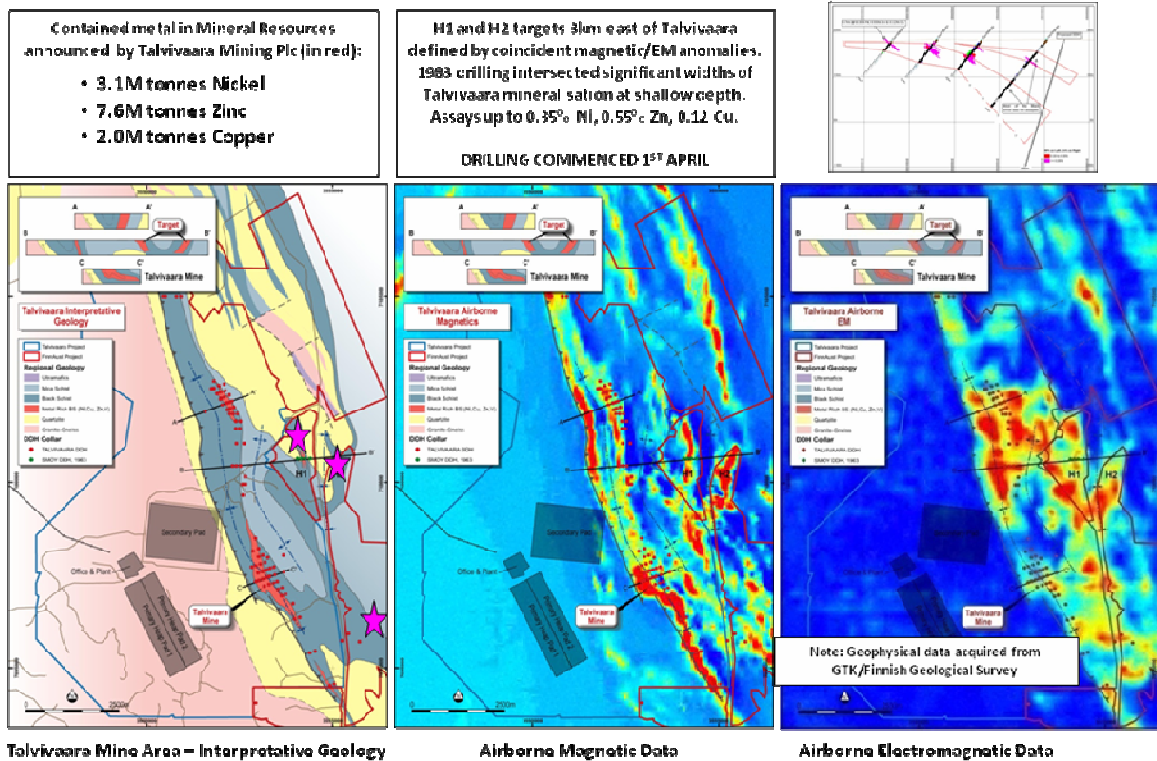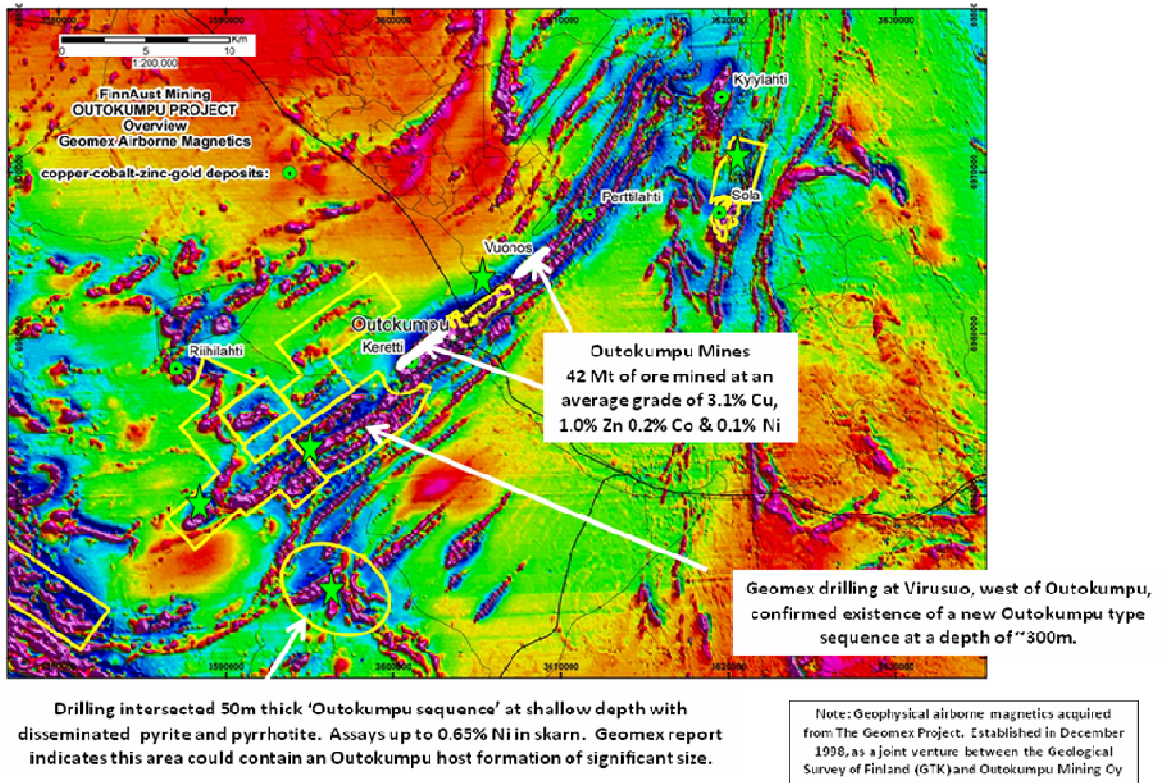Plans are to seek a London AIM listing in late 2011 or early 2012.

**Figure 9: FinnAust Mining Hakonen Project**

Figure 10: FinnAust Mining Outokumpu Project

Mustang Minerals

Western Areas own 19.9% of Mustang Minerals, which is a Canadian listed nickel and PGM company. Mustang has an interest in two deposits in Manitoba, being Makwa and Mayville. Mustang recently raised $6.5 million CDN for purchase of a flotation plant, and to complete the feasibility study for a mine and production facility treating 5000 tpa of nickel.

In March 2011, Mustang announced a potentially significant palladium and platinum discovery in Manitoba including 41.2m of 2.9 g/t platinum and palladium from 34.1m depth, including 9.1m of 9.5 g.t platinum and palladium from 55.5m depth. The highest grade is 1.5m at 8.9 g.t platinum, 22.6 g/t palladium and 0.7 g/t rhodium.
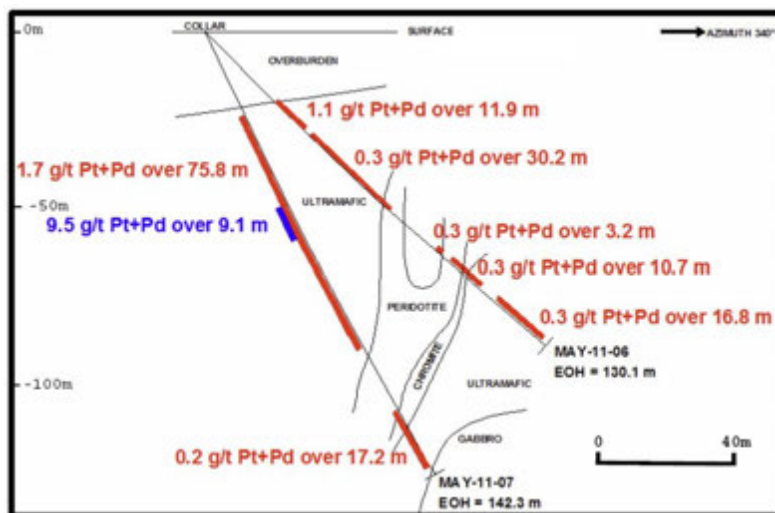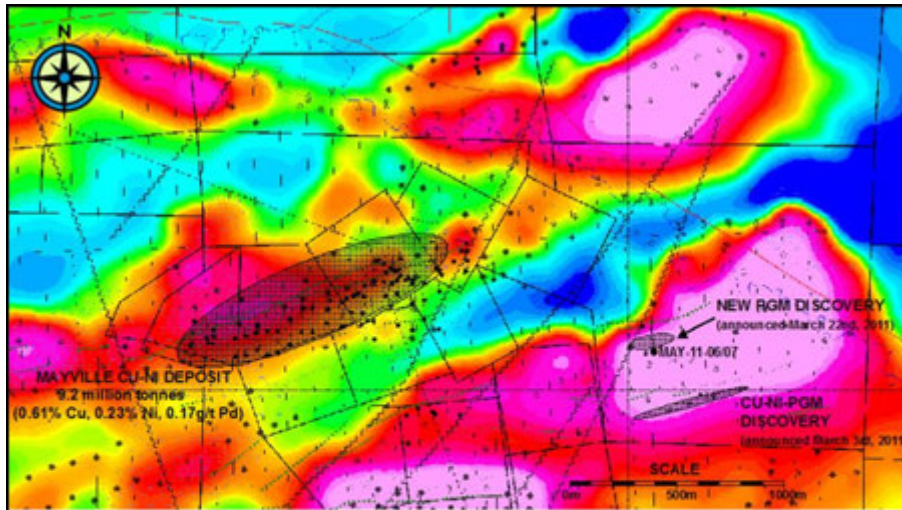

Figure 11: Mayville Platinum and Palladium[3]

Figure 12: Mayville Deposit[(3)]

Growth Targets

The main focus of growth for the company during the next 12 months is focused on longevity of the core business, being concentrate production. To this end, Western Areas has a number of specific goals.

- Increase ore reserves of Flying Fox and Spotted Quoll to 10+ years of production
- Commence development of the Diggers South mine
- Discover a new high grade nickel deposit at Forrestania

Outside of the Forrestania area the company is also striving to:

- Confirm the potential of Sandstone JV project as a new nickel camp
- List FinnAust Mining Plc (75% WSA) for the Finnish assets.

Aside from the core business of concentrate production, Western Areas has a wide resource base that may be amenable to alternative extraction methods. Western Areas are aiming to maximize the production from it's resources and are investigating alternative extraction methods for these deposits that can work in parallel, or enhance the existing operation. Bioleaching is one of the alternatives being investigated, and is the subject of this paper.

FORRESTANIA BIOLEACHING SCOPING STUDY

Western Areas have a range of deposits within the Forrestania region that may be candidates for treatment with the BioHeap process, and are in the process of evaluating a number of deposits as feed sources for a concentrator expansion.

As part of the ongoing process of trying to extract maximum value from it's assets, Western Areas commissioned a scoping study to investigate bacterial leach options as an expansion option at Forrestania. This study was to examine capital and operating costs of a bioleaching operation at Forrestania, identify key infrastructure requirements, to make recommendations as to the future direction of the project and identify additional works required.

The depostis examined during this study were limited to Digger Rocks/Diggers South, New Morning and Cosmic Boy, however this is by no means an exhaustive list of deposits in the area that may be suited to the BioHeap process.

The study included:

- Open pit and underground mining studies
- Ore preparation, leaching and metal recovery circuits
- Tank and heap leach options
- Hydroxide and sulphide precipitation circuits for metals recovery

- Infrastructure requirements

As investigation and evaluation of the scoping study is ongoing, it is not possible to publish the final results of the study at this stage, however some comments will be provided on the New Morning Heap Leaching case study.

New Morning Case Study[2]

An initial testwork program of amenability testing and Nitric Acid Digests (for crush size optimization) was undertaken for the scoping study. Amenability testing demonstrated that the ore was highly amenable to testing with 94% of the nickel leaching in a short period of time. Low acid consumptions were noted for this testwork program.

The nitric acid digest testwork evaluated the liberation of the sulphides at a range of crush sizes from 6mm to 25mm. The optimum crush size for this ore was determined to be 9.5mm, at which 97% of the nickel was liberated and is expected to leach.

Proteus Engineers were engaged to develop the flowsheet and process models for the scoping study, and to prepare capital and operating cost estimates of the processing plant. The New Morning BioHeap Plant was designed to extract nickel and cobalt from New Morning crushed ore, to produce a nickel sulphide product. The processing plant is nominally divided into 12 areas as follows:

- Area 01 Bacterial Farm
- Area 02 Ore Preparation
- Area 03 CCD Wash Circuit
- Area 04 Heap Leach
- Area 05 Iron Removal
- Area 06 Nickel / Cobalt Precipitation
- Area 07 Tailings Storage
- Area 08 Blowers
- Area 09 Limestone Milling
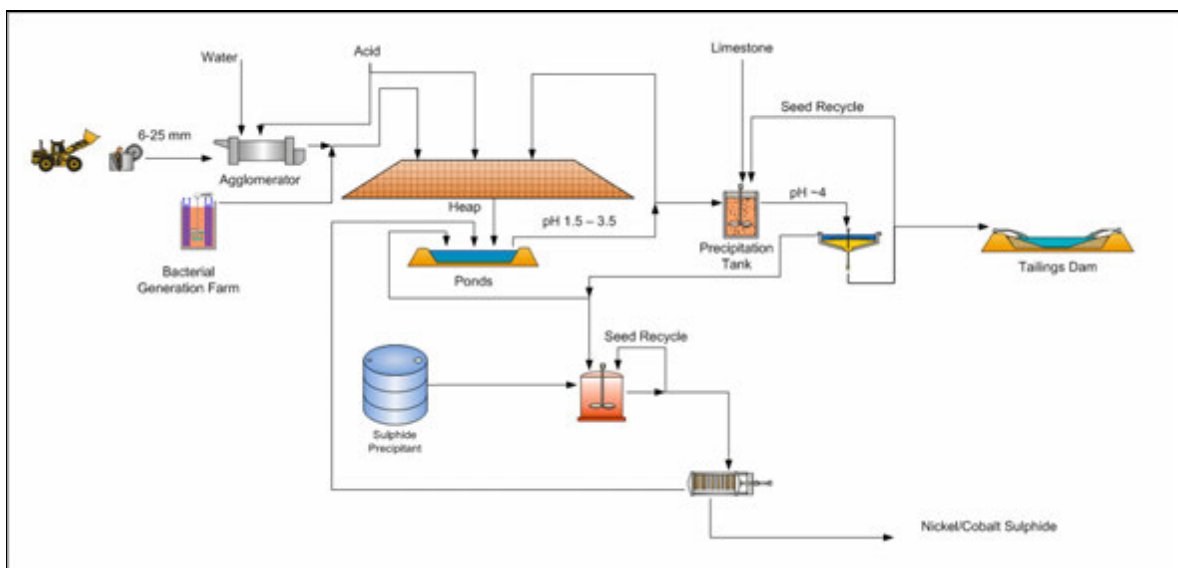- Area 10 Reagents
- Area 11 Services
- Area 12 Infrastructure

Figure 12: Simplified Flowsheet for the New Morning Case Study[2]

Area 01 – Bacterial Farm

A containerized bacterial farm will be used for continuous breeding of bacteria for inoculation of the ore prior to stacking, and for continual supply to the leaching process should it be required. Raw water, power, sulphuric acid will be supplied from the main systems, and periodic manual addition of concentrate to the feed hopper will occur as required.

Slurry from the final tank will be added to the agglomerated ore prior to stacking to maximize bacterial distribution throughout the heap.

Area 02 – Ore Preparation

An open circuit primary and secondary crusher will feed a closed circuit tertiary crusher and screen to produce ore passing 9.5mm. Crushed ore from the fine ore bin will be fed into a drum agglomerator where sulphuric acid and water will be used to agglomerate fine particles.

Agglomerated ore will be stockpiled prior to stacking using grass hopper conveyors.

Area 03 - CCD Circuit

The CCD circuit consists of seven thickeners in series. Wash water is added to the seventh thickener and gravitates down the thickeners sequentially, washing the solids, whilst solids are pumped via thickener underflows counter current back up the train.

Solids from the final thickener report to the tailings storage facility, while solution from the first thickener reports to a surge tank from where it is split to downstream treatment or to the heap leach for solution nickel content upgrade. Flocculant is added to each thickener.

Area 04 - Heap Leach

Overflow solution exiting the first of the CCD thickeners reports to a surge tank. A stream from this is pumped to the CCD circuit for density control, and the excess solution flow is pumped to the heap leach barren / recirculation pond.

Reagent additions (Sulphuric acid, nutrients, bacteria) and water makeup are added to the barren / recirculation pond. Barren solution is then pumped up to the heap leach at a rate of nominally $5L/m_2/hr$.

Pregnant solution gravitates to the pregnant pond from where a stream is pumped back to the Cosmic boy solution treatment plant iron removal stage. Excess pregnant solution overflows to the barren / recirculation pond and is recirculated back onto the heap. A higher overflow point from the pregnant pond flows to an emergency storage pond which is sized to handle heap outflow for a period of 48 hours to allow for line, pump or power failure correction.

Area 05 - Iron Removal

The iron removal circuit receives pregnant solution flow either from the CCD wash circuit direct or via the heap leach, and uses limestone to neutralise free acid and precipitate iron from the solution ahead of the nickel / cobalt sulphide precipitation circuit.

One stage of iron removal is proposed via a series of six precipitation tanks where the pH is gradually raised to 3.5. Air is sparged into the slurries to promote and maintain a high ferric to ferrous ratio to optimise the precipitation process. Steam is sparged into the tanks to maintain a precipitation temperature of $60^{o}C$.

The discharge slurry is thickened in a clarifier, with the clear overflow solution reporting to nickel / cobalt precipitation circuit. The underflow stream containing solution still high in base metals, reports back to the common de-aeration box ahead of the CCD wash circuit. An internal seed recycle is achieved by recirculating a 50% split from the thickener underflow back to the front of the iron removal circuit.

Area 06 Nickel / Cobalt Precipitation

The precipitation circuit receives pregnant solution discharge from the iron removal thickener overflow. Nickel and cobalt are precipitated in a series of six precipitation tanks where staged NaSH addition occurs in the first and third tanks. Steam is sparged into the tanks to maintain a precipitation temperature of 60^oC.

An internal seed recycle is achieved by recirculating a 50% split from the thickener underflow back to the front of the precipitation circuit. The precipitation circuit discharge slurry reports to a thickener for initial dewatering with the underflow fed to a filter to produce a filter cake product.
Solution overflow from the thickener and discharged from the filter are predominantly sent to an evaporation pond.

Area 07 Tailings Storage

TSF

Washed solids from the CCD underflow report to a new tailings storage facility. The new dam will butt up against one side of the existing ground level square dam, predominantly to minimise earthwork costs for the new dam but also in an attempt to utilise some of the existing tailings dam ground water monitoring bores.

Dam construction will be adjusted to suit the ground contours, but will nominally be a standard square shape with centre decant tower to maximise the surface area to volume ratio to enhance natural evaporation. It is anticipated that decant water will be reused in the existing concentrator, however an allowance will be made for a portion of the decant water to report to the evaporation facility should the Cosmic Boy water balance require it.

Evaporation Pond

A large area shallow HDPE lined pond will be required close to the Bioleach plant for the purposes of evaporating high Mg / high SO_4 solution that cannot be reused in the processing plant.
An evaporation pond sized to handle flow from the Sulphide precipitation thickener and from the tailings dam decant water return already exists within the Cosmic Boy infrastructure so no new evaporation pond is required.

Area 08 Blowers

High volume low pressure air required for the Bioleach processing plant, including the the iron removal circuit, will be supplied by dedicated blowers. To ensure parts and operating commonality, an identical blower will be installed at the heap leach area for heap aeration.

Area 09 Limestone Milling

Limestone will be used predominantly for the iron removal circuit. Limestone will be supplied in bulk tankers and pneumatically transferred into the limestone silo. Limestone will be fed onto a belt via screw feeder and into a small ball mill to ensure a finely ground slurry to enhance reaction rates. The limestone mill discharge will report to two cyclones, with the overflow reporting to a storage tank and the underflow returning to the mill for further grinding. Limestone slurry from the storage tank will be circulated via a ring-main with dosing streams taken from the ring main flow as required.

Area 10 Reagents

Sulphuric Acid
Sulphuric acid will be brought to site in bulk tankers. Bulk site storage will be supplied at the heap leach site.
The bulk storage facility will have direct dosing systems without ring main facilities.

NaSH
NaSH will initially be brought to site premixed at 35% w/w. Iron sulphite / iron sulphides contaminants normally in the reagent will have been removed during the offsite mixing process.

Flocculant
Both anionic and cationic flocculants will be brought to site as dry powder and mixed on site in the respective batching systems.
Flocculant will be distributed via dedicated variable speed dosing pump for each thickener with one swing standby pump per system.

Nutrients
Premixed NPK nutrients will be supplied to site as a dry powder and batch mixed on site.
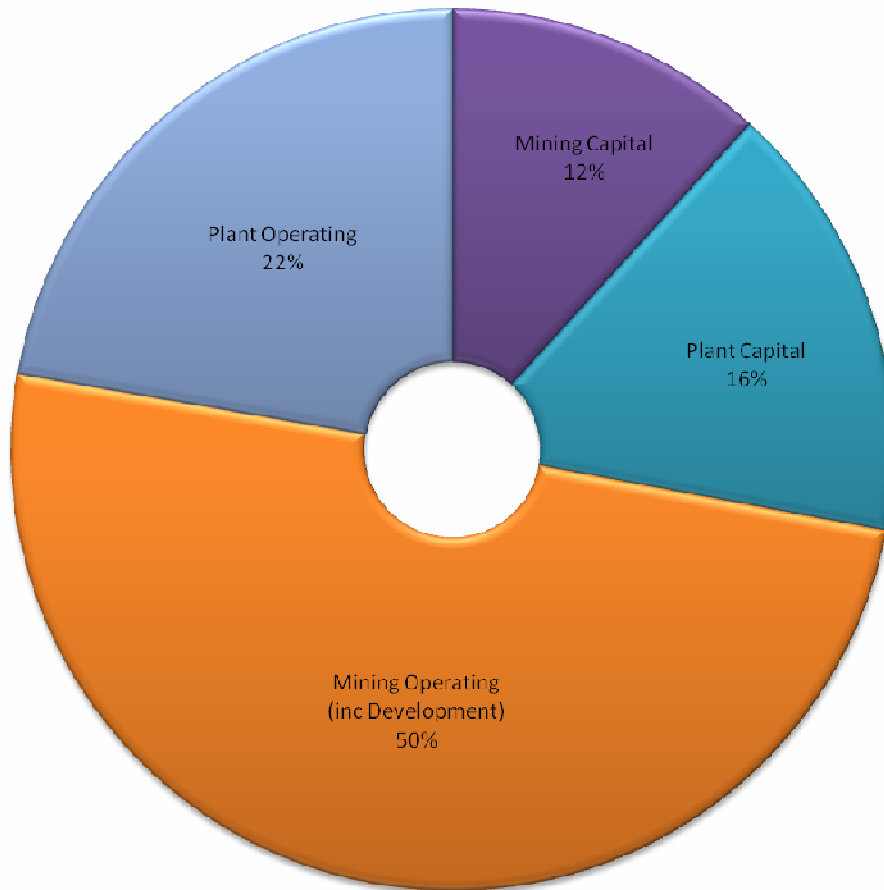
Cost Breakdown

Below are two figures that compare the cost breakdown of the New Morning Case Study. Costs are broadly assigned to 4 categories, and no provision has been included for interest, depreciation, amortization or tax, however the costs do include contingency provisions.
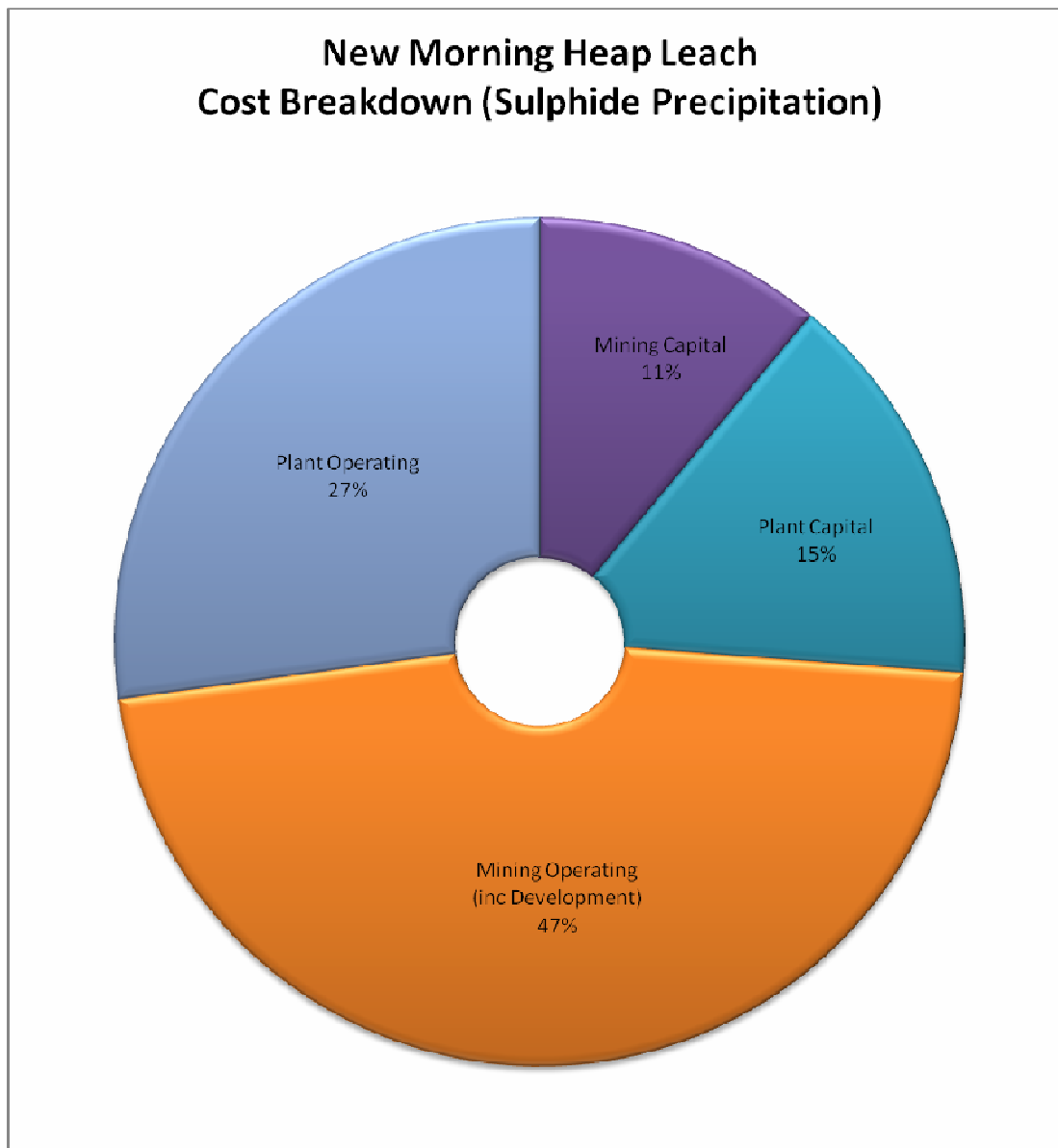
Figure 13: New Morning Sulphide Precipitation Option Cost Breakdown

Figure 14: New Morning Hydroxide Precipitation Cost Breakdown

What is apparent is that the hydroxide option has lower plant capital and operating costs than the sulphide precipitation option, however these cost savings do not offset the reduced payability for the hydroxide product. Out of the two options, sulphide precipitation is the preferred option for this project.

CONCLUSIONS

A number of conclusions can be drawn from these cost breakdowns. The mining component of this project is significant, and generally the mining cost should not be underestimated when making estimates at the scoping level. Also it is not possible to apply mining costs from one project to another project for the purposes of doing quick estimates.

What is not apparent from these diagrams, but became apparent during the study is that the metals recovery section of the plant should not be underestimated. For copper SX/EW costs are quite well understood, but for nickel the recovery costs are not so cut and dry. Operating and capital associated with the metals recovery and reagents make up a significant portion of the plant capital and plant operating sections, much more than was first expected.

Acid consumption is often touted as the single largest item concerning bacterial leaching, and while sulphuric acid costs are significant and made up a large portion of the leaching section, in the overall project costs, they are less important than costs associated with metals recovery. This is also true of ores that were considered medium acid consumers. It is important to have an understanding of the acid consumption of the ore, but even more important is to have a good understanding of the overall acid balance.

Acid consumption alone is not sufficient to make first pass estimates of the operating cost of a bacterial leaching project (as is often done).

Infrastructure is critically important to implementing a bacterial leach project, and in regional WA it is expensive. It is better to over-estimate infrastructure requirements than to underestimate them.

Good quality water is required for leaching projects. This is true, even if you have salt tolerant bacteria, as we do. While hyper-saline water can be used in the leaching process, significant amounts of good quality water are required for cooling and product wash. Good quality water is expensive to produce from saline and hyper-saline sources. Provision should be included for a significant RO plant or for sourcing good quality water for use in these areas.

Power requirements can also be significant, especially for tank leaching. Aside from the crushing circuit, large amounts of power are required for agitation and for the air blowers. Erection of power transmission lines, or even upgrades to the power supply can be very expensive. Unit power costs within WA remain high and contribute significantly to the project operating costs.

REFERENCES

1. Western Areas NL "2010 Annual Report", Perth, Australia, 2010.

2. Fewings J, Knapton P, Peters T, Cullinan P, Haywood J, Seet S "Forrestania BioLeach Desktop Study – DRAFT", Unpublished, Australia, 2011.

3. Mustang Minerals Corp "http://www.mustangminerals.com/pages/plat_properties.html", Canada, 2011.

ALTA 2011
NICKEL/COBALT/COPPER

SOLID-LIQUID SEPARATION

NOVEL AUTOMATIC PRESSURE FILTER FOR HYDROMETALLURGICAL AND FLOTATION CONCENTRATE DEWATERING APPLICATIONS

By

D. Pepper and P Jay,

FLSmidth, Australia/USA

Presenter and Corresponding Author

Patrick Jay
Patrick.Jay@flsmidth.com

ABSTRACT

Pneumapress Automatic Pressure Filters have unique features for use in minerals applications, such as dewatering of flotation concentrate and washing and dewatering in a plethora of applications in hydrometallurgy. The Pneumapress operation cycle which follows classical cake dewatering phases, without the use of membranes, is discussed and various features and benefits are highlighted and compared to traditional tower press filters which utilize membranes.

Two new applications in hydrometallurgical circuits are described, followed by a case study on Pneumapress filters dewatering hot, corrosive, abrasive slurry at a hydro thermal power plant, which is similar to many hydrometallurgical flow sheets. Two Copper flotation concentrates concentrate dewatering applications are discussed, one at an existing operation, that has a relatively course particle size distribution, and one at an undisclosed source with a relatively fine PSD. The effect of variable and versatile cake formation conditions on the subsequent cake drying stage is demonstrated.

BACKGROUND

Although several designs for pressure filters exist in the minerals industry, there are similarities between the different designs and their operation. Most pressure filters are designed with actuated filter plates and, whether the filter plates are arranged vertically or horizontally, the filter plates are mechanically linked to open and close in sequence usually by a hydraulic cylinder(s). Once closed, chambers are formed between the filter plates. Slurry is pumped into the chambers and solids are retained on the filter cloth inside the chamber to form a filter cake. The solids are consolidated either under pump pressure and/or by a rubber/plastic membrane, which is inflated with compressed air or pressurized water. After consolidation, the solids can be further dried by forcing compressed air to flow through the filter cakes.
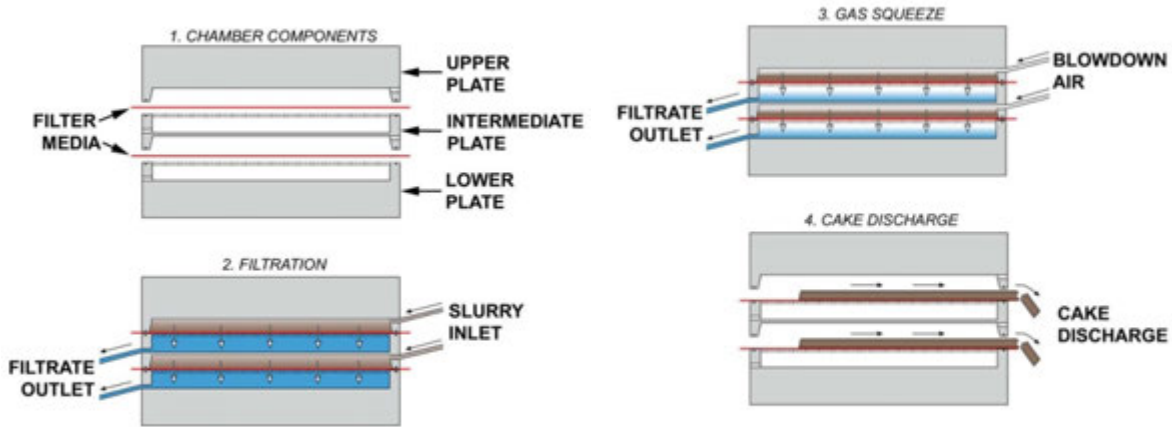
PNEUMAPRESS® PRESSURE FILTERS

Figure 1 is an illustration of a Pneumapress filter with main components and connections identified.
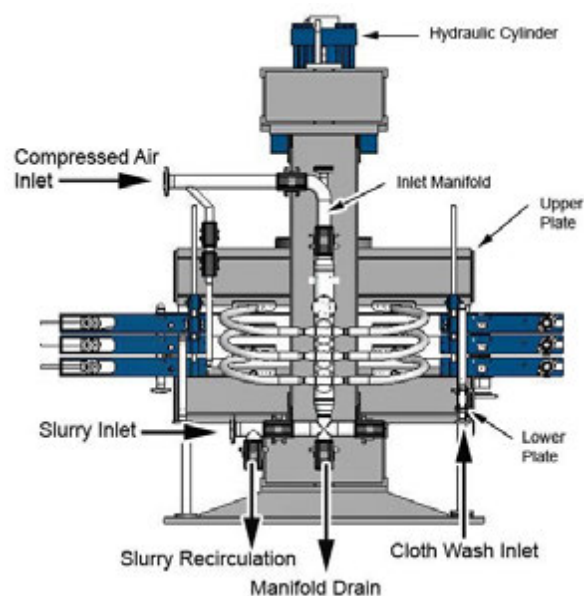

Figure 1: Pneumapress Filter and piping layout

The Pneumapress® filter plates are oriented horizontally in a vertical assembly, as shown in figure 1, with as few as one and as many as twenty filter plates installed in one filter.

Figure 2: Dewatering process diagram

The process of dewatering slurry using a Pneumapress® filter is shown in figure 2. After the plates are closed, thickened slurry is pumped into the chambers. The typical feed pressure is in the range of 3-6 bars, and is not necessarily always used to consolidate a cake; instead it can be used for just filling the manifold, feed pipes, and all chambers with thickened slurry. Time and Pressure of slurry feeding can be varied to alter cake thickness and cake porosity. Unlike other recessed chamber filter presses, cake thickness is variable and only restrained by the maximum chamber height. Any cake thickness between the maximum and 1 mm can be formed inside the chamber. The ability to vary the cake thickness allows one to optimize the cake formation time and cake resistance for variable process conditions.
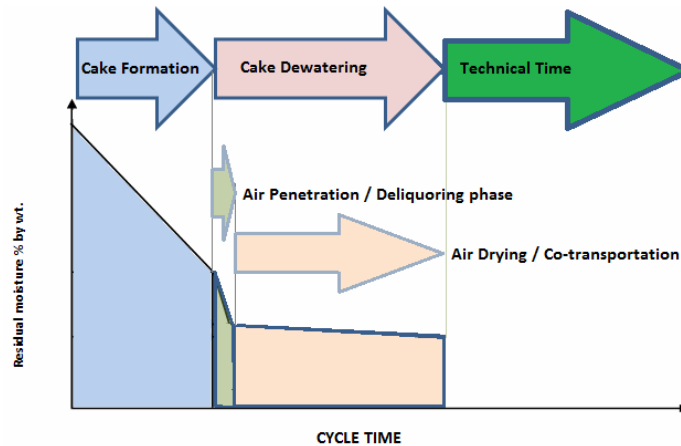
Figure 3: Phases in a Dewatering cycle – Cake Filtration showing deliquoring by Gas pressure.

Compressed air or wash water then enters the manifold forcing slurry from the manifold and feed pipes, into the chambers, forming the cake on top of the filter cloth.

The cake thus formed can have its permeability and average cake resistance adjusted, depending on the forming pressure applied by the compressed air or wash liquor.

184
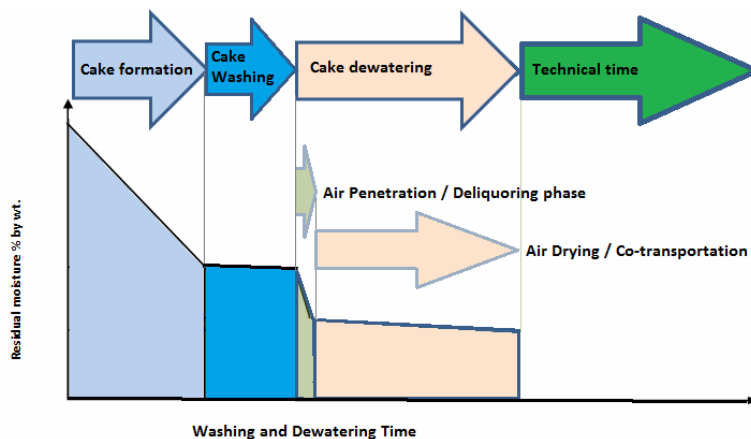
Figure 4: Phases in a Washing and Dewatering cycle – Cake Filtration with displacement washing and subsequent deliquoring by Gas pressure

If a washing stage is applied, the wash liquor enters the chambers and is forced through the cake by pressure applied by a centrifugal pump. The degree of washing can be adjusted to achieve a desired wash result, and the pressure can be adjusted to slightly above the forming pressure to ensure penetration of finer pores within the filter cake. Washing takes place by means of various mechanisms, including a) Idealized piston, or plug-flow or displacement, b) Axial dispersion in major pores, c) Diffusion from dead end pores, d) mother liquor extracted from the solids within the cake. (W. Bender 1983)

The minimum wash liquid consumption being equivalent to the volume of the manifold and chambers less the cake solids volume. This minimum quantity can be adjusted by the initial selection of chamber depth, relative to the optimum cake thickness, whilst the optimum amount is adjusted in practice by varying the wash liquor pumping time and pressure. As the Pneumapress has no elastomeric membranes in the chamber, a greater selection of more aggressive wash liquors is can be used with greater economy. Hot slurries and wash liquors can be used to exploit the advantageous effects of a lowered liquor viscosity on the filtration speed. Steam and hot air can also be applied. Limitations exist on the selection of the filter media, and the cost benefit played off against the increased consumption of filter media at higher temperatures. Ongoing research in collaboration with media manufacturers are yielding some promising results which can be covered under separate heading in future.

After the cake formation, the dewatering stage occurs in two distinct phases namely Air Penetration / deliquoring phase, and the Air Drying or Co-transportation phase. During the Air penetration phase, the air overcomes the capillary pressure of the pores in the surface of the filter cakes and pushes the mother liquor out of the cake forming channels within the cake. The initial deliquoring speed depends on the cake thickness and applied pressure, and is selected for optimum economy depending on the application.

Air penetration is the most economical, energy efficient phase of dewatering as the air consumption is equivalent to the manifold and chamber volume, less the solids volume of the cake, and the flow rate is very small. See examples of Dewatering of a finely ground Copper Concentrate below. (Landero Andres 2011)

The quantity of air consumed in this penetration phase can be likened to that used to inflate membranes in conventional tower press units, with the distinct advantage that this air is not expelled to atmosphere and "wasted", through a muffler as in traditional tower press utilizing air for membrane compression, but rather is used to dry the filter cake by being expelled through the cakes as drying air during the subsequent deliquoring phase [see Figure 3]. The higher pressure deliquoring air is allowed to dissipate through the cake until it reaches the more economical pressure for air blow drying. It is important to measure and to scale-up the gas flow from realistic experiments, since in most cases the capacity of the compressor and minimizing the flow rate of air is the limiting factor, not the pressure. (Solid – Liquid Separation).

185

The subsequent Air Drying phase is characterized by co transportation of filtrate with the air that flows through the cake, and is less effective as depicted by the shallower slope of the air drying and co transportation phase in the figures 3 & 4 above. Longer air blowing time is required at substantially higher flow rates than for the preceding, deliquoring phase. The thermal drying by hot air flow can further reduce the cake moisture, however the effects are still relatively small compared to the mechanical effects of deliquoring phase because of the comparably small mass of air flowing through the cake. (H. Anlauf, 1986). FLSmidth have used both hot air and steam as deliquoring and drying gas in Pneumapress filters with some advantageous outcomes. The results of pilot tests and initial installations can be covered in a separate paper.

Technical, or dead time refers to time during the cycle used for opening and closing the plate pack, driving the cloth to discharge cakes, miscellaneous time for example valve actuation interlocks. During the technical portion of a pressure filter cycle, the filter cannot perform the work it is installed to do; it is not separating any solids from the feed slurry. It is instead performing steps to ready its self for that function again. Minimizing the dead time is critical for optimizing the filter cycle. Typical Pneumapress® technical times are in the range of 45 to 120 seconds. The filter cakes are discharged on one side of the filter by advancing the cloths around the cloth roller; any remaining cake is scraped off by a scraper bar before the cloth is spray washed with high pressure water. Each filter plate has one filter cloth installed, and the filter area is cleaned by overlapping wash nozzles on a spray bar, at the end of each filter cycle. The degree of cloth washing is adjusted to optimum by adjusting the washing time, and pressure. The cloth can also be reversed relative to filtrate flow in consecutive cycles by adjusting the number of plate lengths that it is allowed to travel.

There are two significant advantages of the Pneumapress® filter plate design:

1) No membranes, and

2) Isolatable filter plates.

By eliminating the need for squeezing membranes, the Pneumapress® filter plate design is less complex i.e. without a membrane or the retaining brackets the number of parts per filter plate is reduced. The technical time of the filtration cycle is also reduced as the manifold does not have to be emptied and flushed between the stages of operation preceding or following the membrane compression, as is required by tower presses fitted with membranes in order to avoid bending the filter plates by blocked feed ports. This is an unnecessary precaution for isolatable filter plates with larger and more numerous feed ports, consequently the Pneumapress has a shorter overall cycle time by comparison, which results in higher unit filtration rates. In Membrane tower presses the size of the feed ports is restricted to prevent the membranes being squeezed into them and damaged. A Pneumapress can practically have a large slot as a feed port within the plate; however large directed ports are employed to optimize slurry distribution.

Membrane filter plates of traditional tower press units are more costly to maintain than Pneumapress plates because there are far more components to replace. Purveyors of this equipment can count their profits in the quantity of membranes, plate seal, grids, and filtrate vats that customers replace each year, and a significant sales effort is put into securing supply contracts for these items as early as possible in the lifetime of these filter installations. Furthermore a membrane failure in a single plate would require the entire filter to be taken off line to prevent slurry entering the system behind other membranes and further damaging the entire filter with solids propelled by high velocity pressing air.

Pneumapress® filter chambers are constructed of 50-mm thick steel and are strong enough to operate at a pressure differential of 14 bars depending on plate size. Isolatable plates for higher differential pressures can also be prepared by replacing the solid steel web with two thinner steel webs spaced to achieve specific bending resistance and stiffness if an application requires this.

When one filter plate requires maintenance, such as a cloth replacement, the operator can shut-off the filter plate and continue to operate the filter with the rest of the filter plates until a convenient time for maintenance. By comparison, tower presses, with non-isolatable plates need to be taken off line completely for this routine maintenance requirement, and would thus have lower availability. If a single bearing fails on one plate of a traditional tower press, the entire filter cloth, which can >100 meters long in larger models, can be folded and destroyed at substantial cost to the operation. By contrast, a similar bearing failure would potentially damage only one short piece of cloth in one plate, and result in minimal down time and loss of production, on a Pneumapress filter.

Each filter plate is equipped with independent filter cloth and cloth drive system, and Pneumapress filters are typically far heavier and more robust than other tower press filters as a consequence, which does add to the capital cost of the units. The cloths are however shorter, more numerous and cheaper to change than cloths on traditional tower presses.

Pneumapress Applications in Hydrometallurgy.

- Impurities removal residue in all flow sheets where a tower press, automated filter presses or horizontal belt filters are deployed.
- Most applications where the mother liquor is washed from the solids, whether it is to remove a soluble impurity or recover valuable liquor from the filter cake.
- Nickel intermediate products and precipitates such as $Ni(OH)_2$ or NiS .
- Precipitated impurities in copper processes such as Fe, Al, Mn
- Autoclaves used to oxidize refractory gold ore, dissolve Ni and Co in lateritic ores, dissolve copper with Fe+3 and H_2SO_4 from concentrates, dissolve Mo from concentrates.
- Autoclave leach discharge is potentially filtered in smaller production facilities.
- Uranium recovery as yellow cake.
- Precipitated solids in waste water treatment plants at hydrometallurgical plants.

Hydrometallurgical Application

Pneumapress filters have recently been selected for two applications in a hydrometallurgical flow sheet: autoclave discharge and alkaline-leach residue filtration. Successful laboratory testing was completed and based on these results; the full-scale equipment was ordered and is currently being manufactured in USA.
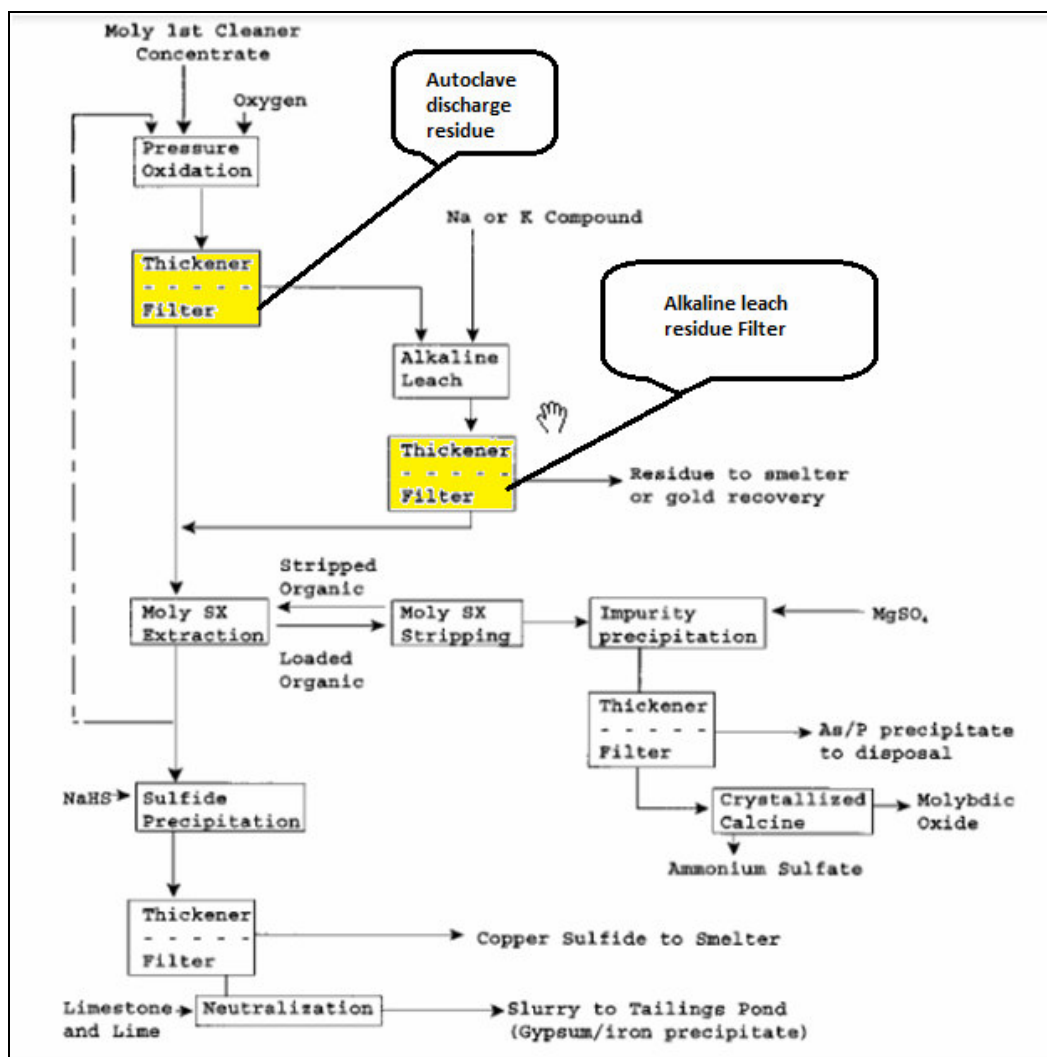
Figure 4: Undisclosed Hydrometallurgical flow sheet for which two Pneumapress filters have been purchased

The residue filter is the basic Pneumapress Automatic Pressure Filter, which has a few unique features: single-sided discharge, isolatable filter plates, and elimination of membranes and rubber seals. These features provide simple plant layout, high equipment availability, and low maintenance costs.

It has been shown that pressure filters can produce filter cake with low moisture content without membranes in this application by means laboratory test work on controlled representative samples. In general, the Pneumapress technology is applicable to both incompressible and compressible cakes, although in some rare applications in the mining industry; excessive cake cracking of highly compressible cakes would make Pneumapress unsuitable. This phenomenon is always thoroughly checked during test filtration and pilot operations to eliminate the improper application of Pneumapress.

The Pneumapress, Leach residue filter configuration, is designed to filter thickened slurry received from the residue thickener. The filter cake is washed to recover soluble solids and then discharged into a tank where it is repulped. The filtrate and highly concentrated wash filtrate reports to the

residue thickener overflow tank causing minimal dilution. The target filter cake moisture content is less than 30%w/w. This application can reduce the size and quantity of thickeners in a CCD train, and improve the economics of the operation overall.

The autoclave discharge filter is more interesting because it utilizes the first isolatable filter plate with polypropylene chambers. Thermoplastics have been used as materials of construction for filter plates for a long time; however standard filter plates cannot be isolated from the plate pack because of potential damage due to the forces exerted on the isolated plate from the pressure applied inside the adjacent chambers. Pneumapress filter plates, commonly constructed of steel; have the strength and stiffness to withstand these forces.

The new Pneumapress composite filter plate also has the strength and stiffness required to be isolatable. The benefit of using composite material is corrosion resistance. In this particular case, either 2205 duplex steel or C276 "Hastelloy" would have been required to withstand the low pH application.

The Pneumapress autoclave discharge filter is designed to filter slurry received from the Autoclave Discharge thickener, wash acid from the filter cakes, and then deliver the filter cake to a repulping tank.

The filtrate reports to the autoclave discharge thickener feed tank. The key process performance metrics are wash efficiency / liquor recovery and moisture content of the cake. The Pneumapress is able to meet and exceed specification in this regard.
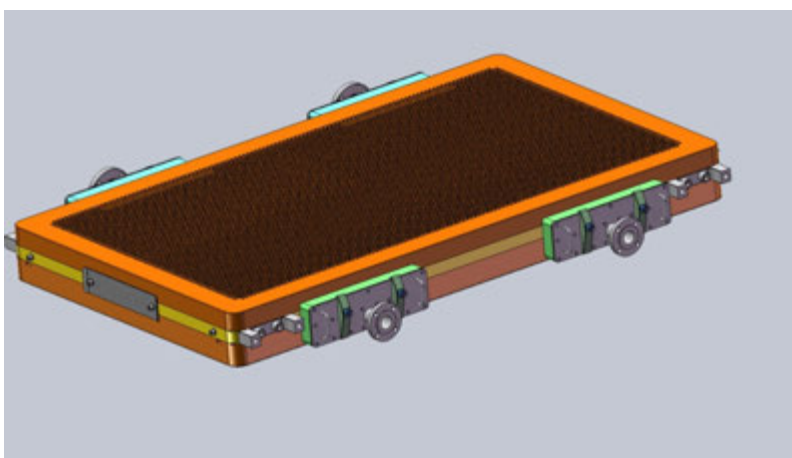

Figure 5: Solid Model of Isolatable, Composite filter plate

189

Figure 6: Samples of Autoclave Discharge Cakes, and filtrate and feed slurry.

It is fairly common with leach residues to observe a layer of fine material on top of the cake, as can be seen on the sample at left in Figure 6. This fine material can have smaller pore diameters, and thus higher capillary entry pressures, which can also have an advantageous effect of expressing liquid from the cake below the layer by mechanical compression comparable to a mechanical diaphragm, before the air pressure overcomes the threshold pressure, and penetrates the layer. (M. Shirato, Filtration + Separation (1987) no. 2).

The filter feed slurry contains 50-g/l H_2SO_4, and hence is quite corrosive to steel and stainless steel. Therefore, the wetted components of the pressure filter need to be constructed of either exotic steel alloys or inert thermoplastics, such as polypropylene. FLSmidth designed and constructed the Pneumapress composite filter plate in order to reduce the cost of the equipment without sacrificing the isolatable filter plate feature. The composite plate is so named because of the polypropylene chambers attached to a steel skeleton – it is a composite of corrosion resistant material and steel.
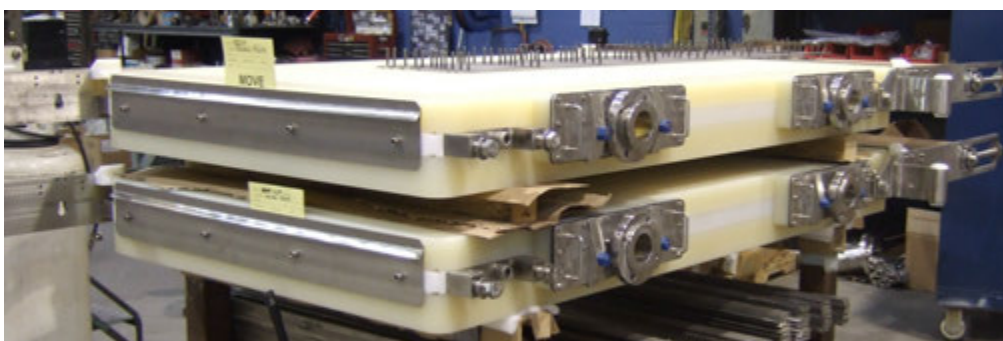
Figure 7: Composite filter plate in manufacturing

Geothermal Fluid Filtration Application

In the Imperial Valley of California, a geothermal power generation facility uses a dual flash, crystallizer-clarifier process to control solids precipitated as the geothermal stream cools. Precipitated silica solids must be continuously removed from the system to maintain effective

190

operation. The solids are removed at the clarifier underflows from a 106°C stream containing approximately 33%w/w solids and approximately 30%-w/w dissolved chloride salts.

Among equipment previously utilized to de-water underflow sludge were plate & frame filter presses, cavity filter presses, centrifuges, sludge drying beds, vacuum trucks, horizontal plate filters and high-pressure mechanical expression filters.

In the past, horizontal filter presses and membrane squeeze filters have been the most attractive equipment to dewater geothermal sludge. Benefits of utilizing horizontal plate filtration include uniform distribution of filtered solids and a large filter area. However, the hot corrosive geothermal slurry limits the choice of materials utilized in the filters. Elastomeric products, such as gaskets, diaphragms, and chamber seals became consumables requiring a significant amount of manpower to replace on regular intervals. Problems such as joint leakage, separation of components, and crushing of horizontal divider plates occurred with the filter presses. Elastomeric diaphragms used to squeeze the hot brine slurry through woven filter media failed at regular intervals and therefore required frequent replacement.

One factor limiting production with the expression membrane squeeze filters is the operating cycle time. The inflation and deflation of the membranes requires additional technical cycle time. Due to the reduced porosity of the filter cake after squeezing, effective cake washing to remove soluble solids required several minutes, increasing the operating cycle time further. A typical membrane squeeze filter produced a filter cake every 8 to 12 minutes when the filter was in good working order. The Pneumapress® filter, which used shorter cycle times (2 to 4 minutes), substantially outperformed the expression filter with much less filter area – see figure 5.0.

The limitations in production described above were overcome with the Pneumapress® filter by eliminating diaphragms and expression mechanical equipment, inflatable chamber seals, and diaphragm fill and retract equipment. The problem of crushing filter plate components was overcome by using more suitable filter components and incorporating design parameters better adapted to service the filtering application. To accommodate the severe operating environment of the hot corrosive geothermal slurry and maintain structural integrity, wetted filter components were fabricated from a corrosion resistant alloy using fabrication techniques that remove internal residual stresses from the structure, eliminate deformation while in service and prevent sensitization of the filter components. Furthermore, the filter structure is designed to provide effective distribution of the internal pressure and resulting forces, thus enabling the filter to withstand high operating pressures. Another benefit of the Pneumapress® Filter is the introduction of technology to eliminate leakage of slurry and filtrate during filter operation without the use of consumables such as gaskets, o-rings or inflatable seals.

Eliminating specialized equipment, eliminating consumable components and adapting appropriate fabrication techniques using corrosion resistant alloys have enhanced the reliability of the Pneumapress® Filter and reduced the cost of operating the Geothermal Plant.
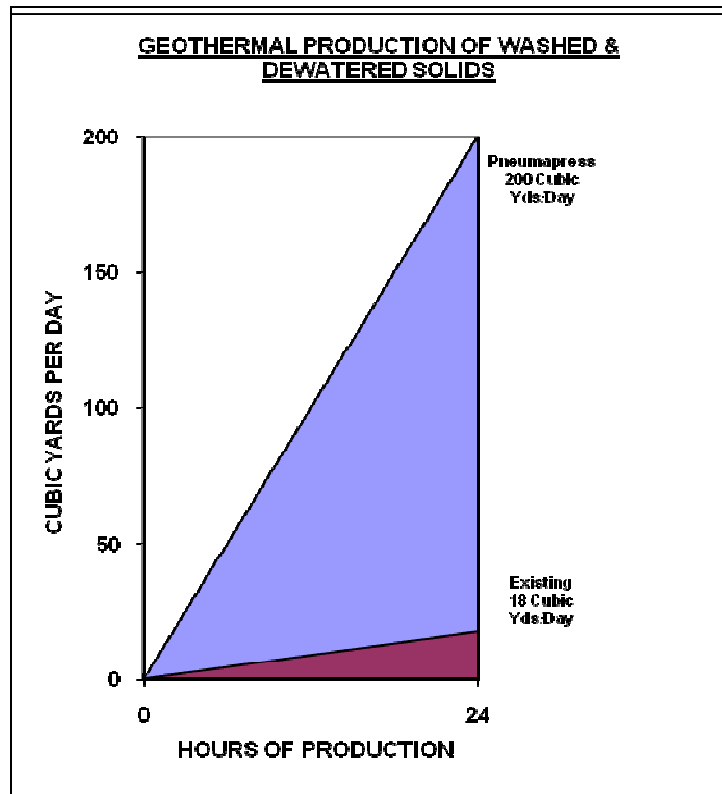
191

Figure 8: Pneumapress production rate at geothermal mine

Concentrate Dewatering

Teck Highland valley Copper, Canada

Figure 9: Pneumapress discharging filter cake at HVC.

Copper concentrate with particle size distribution P80n of 63um is dewatered to final Transportable moisture Limit (TML), of 7.5% on Pneumapress filters.

Filtration rates in excess of 1000 kg/m^2 hr can be achieved in a cycle time as short as 4 minutes.
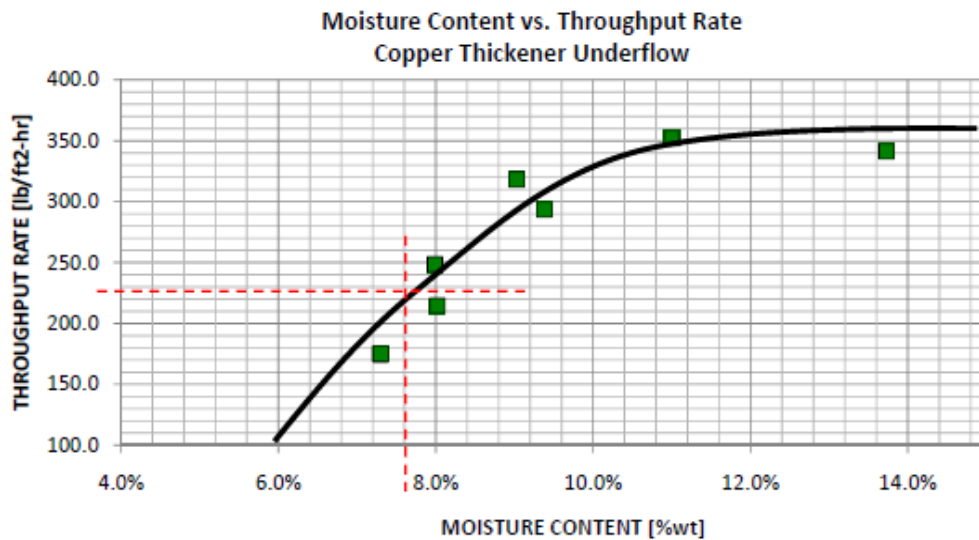
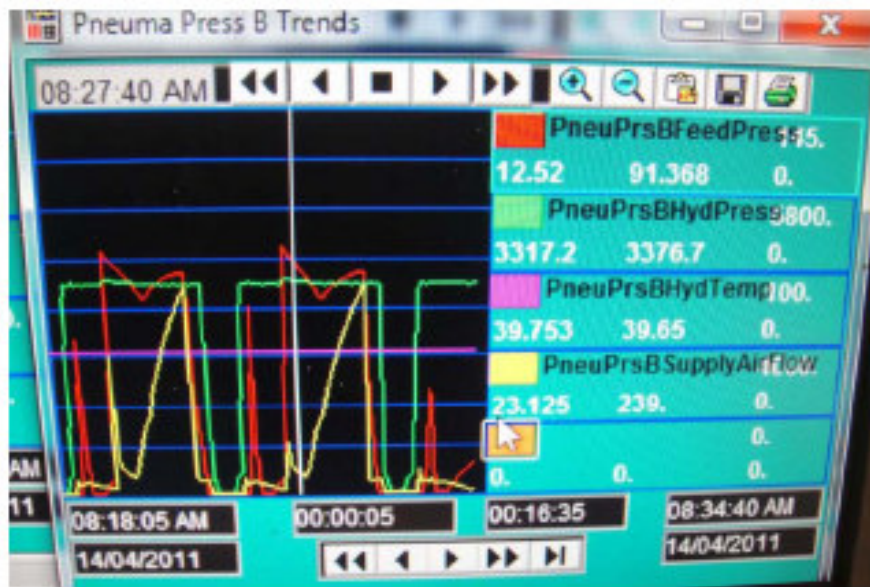**Figure 10: HVC Moisture vs. capacity curve.**

Figure 11: Photo of Human Machine Interface at HVC showing pressure trends during consecutive cycles of operation.
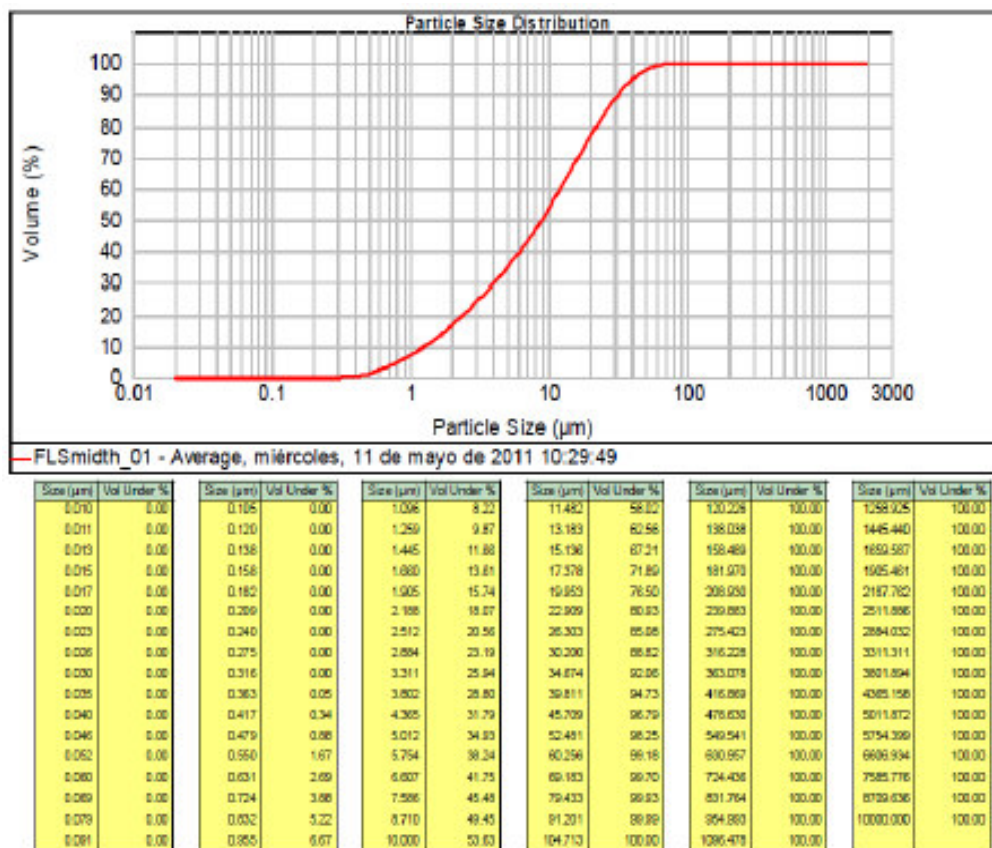
Numerous new developments in the plate pack have been tested and proven during the commissioning and start up period to enhance cloth life and further improve the Pneumapress for minerals concentrate applications.

The isolatable filter plates and individual drive mechanism per chamber have enabled FLSmidth to concurrently test and prove several different permutations of new component such as plate seal, cloth, and washing regimen in the same filter. This ability has vastly reduced the development time of new product enhancement features and led to further improvement in design which greatly improves the life of the filter media. Peak cloth life of over 9000 cycles has been observed to date. Close collaboration with the owners and after sales support has led to many optimizations some of which are now standard on future Pneumapress filters for mineral concentrates and can be provided as optimizers for other existing installations.

Example of Pneumapress Capabilities with Very Fine Milled Copper Concentrates.

194

The exceedingly good market price of copper, which is driven by the continued growing demand for commodities such as electrical appliances and motor vehicles in China, has led to the exploitation of highly disseminated ores that were previously deemed uneconomical to exploit. Typically the beneficiation of these ores requires finer grinding. Finer grinding produces flotation concentrates which are harder to dewater, creating new opportunities for Pneumapress filters.

In this example, a filtration test was conducted on a laboratory scale with sulphide Cu concentrates which had a PSD with D80<22um, D50<10um, D20 <2.5um, as shown in the distribution curve below.

FLSmidth_01 - Average, miércoles, 11 de mayo de 2011 10:29:49

| Size (µm)	Vol Under %	Size (µm)	Vol Under %	Size (µm)	Vol Under %	Size (µm)	Vol Under %	Size (µm)	Vol Under %	Size (µm)	Vol Under %
0.010	0.00	0.105	0.00	1.096	8.22	11.482	58.02	120.226	100.00	1258.925	100.00
0.011	0.00	0.120	0.00	1.259	9.87	13.183	62.56	138.038	100.00	1445.440	100.00
0.013	0.00	0.138	0.00	1.445	11.88	15.136	67.21	158.489	100.00	1659.587	100.00
0.015	0.00	0.158	0.00	1.660	13.61	17.378	71.89	181.970	100.00	1905.461	100.00
0.017	0.00	0.182	0.00	1.905	15.74	19.953	76.50	208.930	100.00	2187.762	100.00
0.020	0.00	0.209	0.00	2.188	18.07	22.909	80.93	239.883	100.00	2511.886	100.00
0.023	0.00	0.240	0.00	2.512	20.56	26.303	85.08	275.423	100.00	2884.032	100.00
0.026	0.00	0.275	0.00	2.884	23.19	30.200	88.82	316.228	100.00	3311.311	100.00
0.030	0.00	0.316	0.00	3.311	25.94	34.674	92.06	363.078	100.00	3801.894	100.00
0.035	0.00	0.363	0.05	3.802	28.80	39.811	94.73	416.869	100.00	4365.158	100.00
0.040	0.00	0.417	0.34	4.365	31.79	45.709	96.79	478.630	100.00	5011.872	100.00
0.046	0.00	0.479	0.88	5.012	34.93	52.481	98.25	549.541	100.00	5754.399	100.00
0.052	0.00	0.550	1.67	5.754	38.24	60.256	99.18	630.957	100.00	6606.934	100.00
0.060	0.00	0.631	2.69	6.607	41.75	69.183	99.70	724.436	100.00	7585.776	100.00
0.069	0.00	0.724	3.88	7.586	45.46	79.433	99.93	831.764	100.00	8709.636	100.00
0.079	0.00	0.832	5.22	8.710	49.45	91.201	99.99	954.890	100.00	10000.000	100.00
0.091	0.00	0.955	6.67	10.000	53.63	104.713	100.00	1096.478	100.00		

Figure 12: Particle Size distribution curve of a Finely ground sulphide Copper flotation concentrate.

This very fine material exhibits much lower filtration rates and yet it is still filterable, and feasible, as an application of Pneumapress filters. The filtration rates are closer to those measured for Platinum (Cu/Ni sulphide flotation concentrates in South Africa. [(D Pepper, C Rule, M Mulligan 2010)

In the course of extensive laboratory trials on representative samples, various cake forming pressures were used to determine the optimum pressure to achieve the highest possible filtration rate at a TML of 9% cake moisture. It was demonstrated that an increase in the initial cake forming pressure from 8.6 bars to 15 bars increased the filtration rate by 66% from 150 to 250 kg/m^{2}hr.
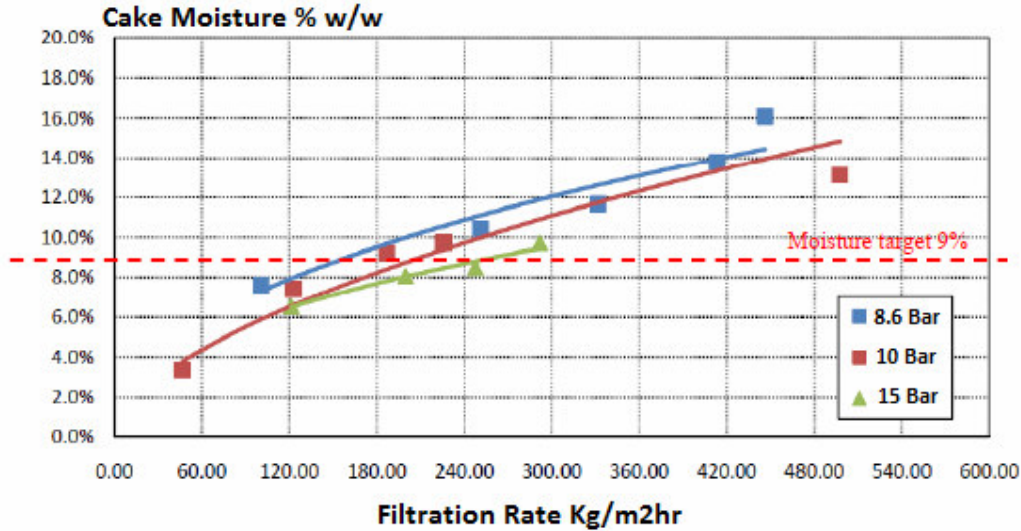
Figure 13: Moisture vs. capacity curve of a finely ground Copper Concentrate.

The total requirement for drying air was also significantly reduced, as can be seen by the plot of Drying Correlation factor [Minutes of air blow drying time, required per kg/m^2]. This factor is derived by dividing the cake mass per Square meter of filtration area by the drying time, for different cake thicknesses, and different drying pressures (Perry's Chemical Engineering Handbook).
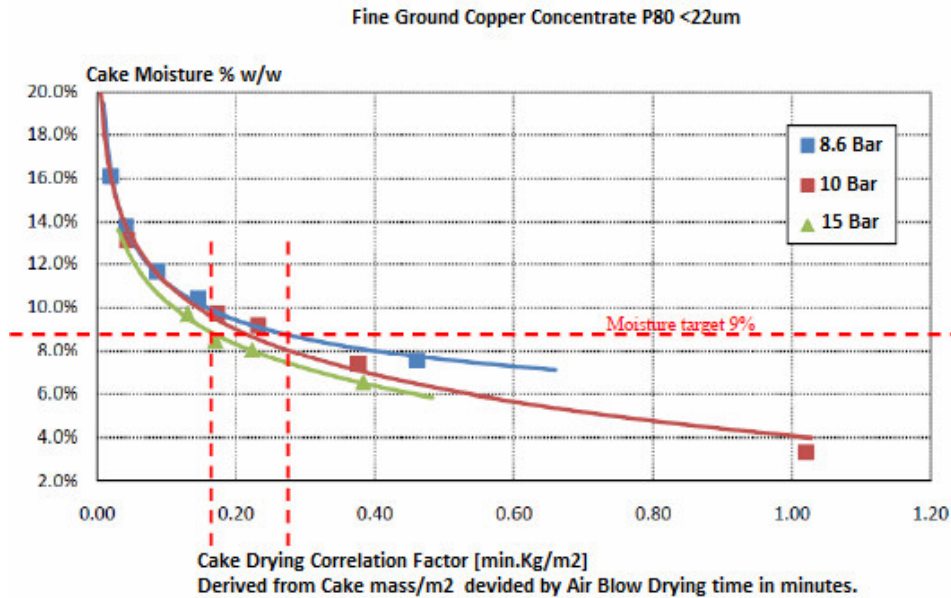
Figure 14: Drying Curve of a finely ground Copper concentrate.

The chart shows that in this particular case, the total air drying requirement during the high consumption, co-transportation drying phase of dewatering is reduced by roughly 30%, by increasing the pressure of the air in the low consumption, air deliquoring phase. Subsequently, the total energy requirement of cake dewatering is significantly reduced. The phenomenon has been previously investigated and modeled by (Wakeman n.d.). Scale up of laboratory and pilot testing has proved accurate for current installations with the possible exception of an isolated case where it was found after start up, that more rigorous cloth washing was needed than was originally expected. Effects of filtration on filter media life and blinding of the filter media are always difficult to determine based on short laboratory and pilot scale tests. This challenge is being overcome by installing additional plates into the existing frame, and upgrading the cloth washing pump.

REFERENCES AND CITATIONS

1. ALMELA, N., OJA, M. The effect of compressibility of different starches on starch washing and dewatering. Lappeenranta University.

2. PEPPER, D. RULE, C.M., MULLIGAN, M. Cost-effective pressure filtration for platinum concentrates. Fourth Annual International Platinum Conference. 2010.

3. Compressed Air Eases Dewatering Woes. Chemical Engineering, June 1996.

4. H. Anlauf, F. (1986). VDI, Reihe 3, 114.

5. Landero Andres, G. G. (2011). Confidential test report - Undisclosed material source.

6. M. Shirato, T. M. ((1987) no. 2). Filtr. Sep. 24 , 115 – 119.

7. Solid – Liquid Separation, Introduction

    a. Walter Gosele, Heidelberg, Federal Republic of Germany (Chaps. 1 – 7)
    b. Christian Alt, Munchen, Federal Republic of Germany (Chaps. 8 – 11) W. Bender, C. I. (1983). Chem. Ing. Tech.

8. Wakeman, J.W., "Pressure Filtration", in Solid-Liquid Separation, ed. L. Svarovsky, Butterworths, Amsterdam (1972).

9. Wakeman, J.W. and Tarleton, E.S., Filtration: Equipment Selection Modeling and Process Simulation, Elsevier Advanced Technologies, Oxford (1999).

10. Chi Tien, Introduction to Cake Filtration Analyses, Experiments and Applications, Department of Biomedical and Chemical Engineering, Syracuse University, New York, USA.

11. Metso handbook, and Cake Filtration Paper (Anon).

12. Perry's Chemical Engineers Handbook.

13. Ian Townsend, Automatic Pressure Filtration in mining and Metallurgy, EMI Solid liquids separation Conference proceedings 2002.

ALTA 2011
NICKEL/COBALT/COPPER

SX/IX/EW

OXIDATION IN COPPER SX PROCESSES

By

Troy Bednarski, Matthew Soderstrom and Shane Wiggett
Cytec Industries Inc.

Presenter and Corresponding Author

Shane Wiggett
shane.wiggett@cytec.com

ABSTRACT

Manganese present in the electrolyte solution of the copper SX-EW process can be oxidized in the tankhouse during electrowinning. This can cause formation of permanganate or other high oxidation states of manganese in the electrolyte and oxidize the organic during the strip stage of the SX process. Once the permanganate ion is contacted with the organic phase during the SX operation the organic components are oxidized and the permanganate is reduced resulting in lower electrolyte ORP values. Oxidation of the organic phase may result in oxime degradation and often forms products that are interfacially active. The oxidation products can affect the metallurgical and physical properties of the organic, resulting in lower copper transfer, decreased reagent kinetics, and extended phase disengagement time.

Cytec Industries Inc. latest reagent development is the ACORGA™ OR series of extractants. The ACORGA™ OR reagents (ACORGA™ OR15 and ACORGA™ OR25) are specifically formulated to provide an extra level of oxidative degradation protection for use at operations where the likelihood of solutions having a high oxidation-reduction potential exists.

INTRODUCTION

Historically, severe oxidation in copper SX plants appears to be a relatively rare occurrence, with few commercial plants reporting issues. More recently, a growing number of existing operations and new projects have had exposure to manganese issues[1]. The primary concern is manganese in the feed solution, which can transfer to the electrolyte via physical entrainment, crud runs, and plant upsets.

Manganese present in the +2 state has no detrimental effects in electrowinning but at higher oxidation states pose problems in the tankhouse and to the organic in the SX circuit. Manganese can have valence states of +2, +3, +4 and +7[2]. The manganese oxidation state will be dependent on cell dynamics[3,4] and solution chemistries[5]. Manganese can be present at high oxidation states if measures are not taken to control it. The most widely used reaction for controlling manganese valence is iron reduction.

This paper will review the impact of the permanganate ion on the solvent extraction process, primarily focusing on the physical and metallurgical properties of the organic phase.

ORGANIC OXIDATION

The rate of organic oxidation by the permanganate ion (MnO_4^- or Mn^{7+}) is shown in Figure 1 below. The organic phase (a standard copper SX reagent) was diluted to 10 Vol % in an aliphatic diluent and mixed at a 1:1 organic to aqueous (O/A) ratio at 600 rpm, with synthetic electrolyte containing 30 gpl copper, 200 ppm Mn^{7+}, and 180 gpl acid. Samples were taken over time and the oxidation-reduction potential (ORP) of the aqueous phase was measured using an Ag/AgCl reference electrode with 4M KCl filling solution.
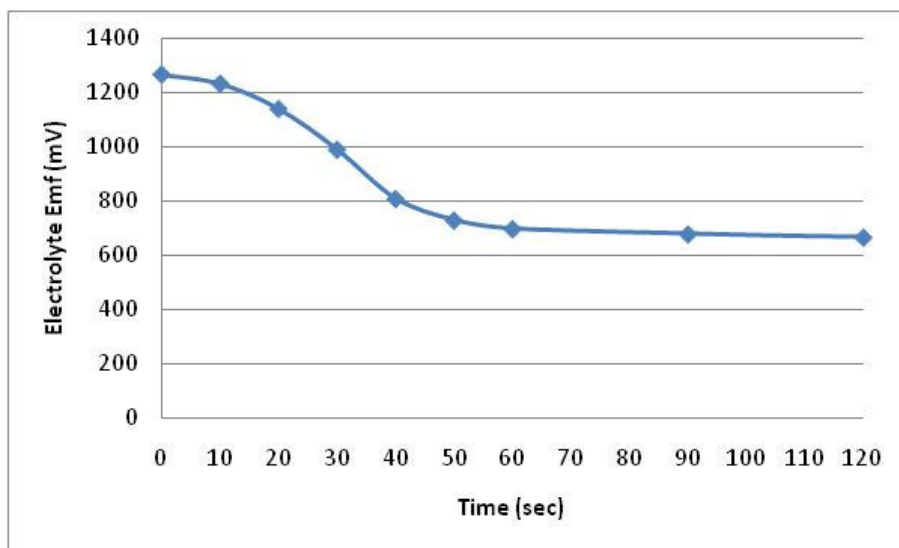
Figure 1: Oxidation-Reduction Potential vs. Time

The figure shows the permanganate ion was reduced over time as the organic phase is oxidized. The electrolyte ORP dropped from 1270 mV and approached an equilibrium value at approximately 600 mV. The purple coloration of the electrolyte (permanganate ion) diminished at approximately 40 seconds where the solution returned to blue, indicating a lower oxidation state. Even at a lower ORP of 800 mV, oxidation continued to occur until approximately 600 mV. The oxidation of the organic phase approached completion at approximately 120 seconds, under the specified mixing conditions.

Two metallurgical grade diluents (one aliphatic and one containing approximately 20 % aromatics) and a standard copper SX reagent (10 Vol % diluted with an aliphatic diluent) were contacted with a synthetic electrolyte containing 30 gpl copper, 500 ppm Mn^{7+}, and 180 gpl acid (ORP 1288 mV). The organic phases were contacted multiple times with fresh electrolyte at a 1:1 O/A ratio, mixing at 600 rpm for 10 minutes. The ORP of the aqueous phase was measured after each contact. The results are shown in Table 1.

Table 1: Aqueous ORP (mV) after Organic Contact

	Contact 1	Contact 2	Contact 3
Standard Copper SX Reagent	550	564	585
Aromatic Diluent	1278	1290	1291
after solids settled	678	776	783
Aliphatic Diluent	1287	1286	1287

The ORP of the aqueous solution after contact with the standard copper SX reagent dropped from 1288 mV to a range of 550-585 mV, indicating oxidation of the organic occurred during each contact. During the contact with the aromatic diluent a brownish-black precipitate formed on the glass wall of the vessel and in the aqueous phase (believed to be MnO_2), indicating some oxidation of the organic also occurred. The ORP values were essentially unchanged from the starting condition until the solids settled at which time a lower ORP value (680-780 mV) was measured. Following multiple contacts with the aliphatic diluent, no change in the electrolyte ORP measurement was observed and the purple coloration remained, indicating very little or no oxidation of the aliphatic diluent occurred.

The organic solutions following the third contact with electrolyte were collected and the dynamic interfacial tension (IFT) of the diluents and reagent were measured. A Kruss model DVT50, dynamic drop volume tensiometer, was used for the IFT measurements. Each organic solution was measured against distilled water at a constant flow rate. The results are shown in Table 2.

Table 2: Interfacial Tension Measurements

	IFT (dyne/cm)
Standard Copper SX Reagent	37.11
Oxidized Standard Reagent	23.44
Clay Treated Oxidized Standard Reagent	30.91
Aromatic Diluent	47.80
Oxidized Aromatic Diluent	38.06
Clay Treated Oxidized Aromatic Diluent	47.48
Aliphatic Diluent	40.35
Oxidized Aliphatic Diluent	38.78

In each case, permanganate oxidation of the diluent and/or reagent resulted in lower IFT values. This indicates that some interfacially active oxidation degradation products are formed. Clay treatment (50 gpl) did remove the interfacially active components, resulting in higher IFT values. The 50 gpl clay treatment restored the quality of the aromatic diluent to its original state. A higher dosage of clay or a second clay treatment may be necessary to restore the quality of the degraded reagent (depending on severity of oxidation).

Two reagents (1 standard and 1 with oxidative degradation resistance ACORGA™ OR25) diluted to 10 Vol % in an aromatic diluent, were contacted with a synthetic electrolyte (30 gpl copper and 180 gpl acid) containing permanganate at a 1:1 O/A ratio. They were mixed for 10 minutes at 600 rpm and allowed to separate. The phase disengagement times associated with the degree of oxidation are shown in Table 3.

Table 3: Strip Phase Disengagement Time

	Concentration Mn^{7+} (ppm)	Oxidation - Strip Phase Disengagement Time					
		Baseline	Contact 1	Contact 2	Contact 3	Contact 4	Contact 5
Standard Copper SX Reagent	200	33"	5' 55"	6' 13"	6' 30"	6' 30"	6' 38"
ACORGA™ OR25	200	23"	5' 15"	5' 35"	5' 38"	6' 13"	6' 25"
Standard Copper SX Reagent	2	33"	34"	36"	35"	37"	38"

The phase disengagement times increased dramatically once the organic was contacted with permanganate. Similar strip phase disengagement times were obtained with the ACORGA™ OR25 and the standard copper SX reagent. The subsequent contacts had a reduced effect on increasing phase disengagement times once oxidation had occurred. The degree of oxidation (permanganate concentration) played an important role on the physical properties. With 2 ppm Mn^{7+} present in the

electrolyte, (although oxidation had clearly taken place via the reduction in EMF value) no significant effect on phase disengagement time was apparent.

The degree of organic degradation for the above samples is shown in Table 4. Samples of the organics were taken after each contact and max loaded with copper (the organic was mixed at 1/8 O/A ratio with a 10 gpl copper solution buffered to pH 5). The organic solutions were measured for copper by Atomic Absorption.

Table 4: Organic Oxidation – Mn^{7+} Concentration

	Concentration Mn^{7+} (ppm)	Contact with electrolyte, Max load analysis (Org Cu gpl)						Oxidation Rate gpl Cu/Contact
		0	1	2	3	4	5	
Standard Copper SX Reagent	200	5.31	5.16	5.08	4.94	4.84	4.80	-0.103
ACORGA™ OR25	200	5.61	5.59	5.54	5.51	5.45	5.39	-0.044
Standard Copper SX Reagent	2	5.31	5.29	5.30	5.31	5.32	5.30	0.001
Standard Copper SX Reagent	500	5.42	-	-	4.71	-	-	-0.237

The reduction in maximum copper load was due to the oxime being oxidized by the permanganate ion and no longer able to extract copper. The initial reagent concentrations were approximately 10 Vol %. The resulting oxime concentrations after 5 contacts with 200 ppm Mn^{7+} were 9 Vol % for the standard reagent and 9.6 Vol % for the ACORGA™ OR25. The rate of oxidation is dependent on the permanganate concentration and reagent formulation. The ACORGA™ OR25 formulation showed less oxime oxidation compared to the standard copper SX reagent under the same conditions (200 ppm Mn^{7+}). The rate of oxidation increased with increasing permanganate concentration and was proportional to the drop in maximum copper loading. At 200 ppm permanganate, the reduction in maximum copper loading was approximately 0.1 gpl copper per contact, at 2.5 times the permanganate concentration (500 ppm) the maximum copper loading reduction was 0.24 gpl per contact.

The effect of O/A ratio on organic oxidation was also investigated as shown in Table 5. The organic phase was contacted multiple times with synthetic electrolyte containing 30 gpl copper, 200 ppm Mn^{7+}, and 180 gpl acid at an O/A ratio of 5/1. Samples were taken after each 5 contacts, max loaded and analyzed for copper concentration.

Table 5: Organic Oxidation – O/A Ratio

	Contact with electrolyte, Max load analysis (Org Cu gpl)						Oxidation Rate gpl Cu/Contact
	0	5	10	15	20	25	
Standard Copper SX Reagent (O/A=5)	5.31	5.22	5.13	5.06	4.94	4.85	-0.018

The drop in maximum copper load per contact was reduced to 0.018 gpl due to the organic being present at 5 times the volume of the aqueous. On an equal volume basis, O/A of 1:1 the oxidation rate would be expected to be 5 times greater. This would correspond to a maximum load drop of 0.09 gpl per contact compared to the experimental value of 0.103 recorded in table 4.

IMPACT ON SX PLANT PERFORMANCE

The presence of permanganate in the electrolyte will ultimately have adverse effects on the SX performance due to oxidation of the organic phase. Organic oxidation will lead to physical issues including extended phase disengagement times, and increased aqueous in organic and organic in aqueous entrainments. These higher entrainments can lead to increased reagent losses and impurity transfer to the electrolyte. Metallurgical issues include: lower stage efficiency, loss of copper/iron selectivity, and reduced copper transfer due to loss of oxime. If the aqueous solution does achieve a high EMF value, oxidation of the organic is likely to occur, the effects of which can be minimized by the use of the ACORGA™ OR Series of reagents. Table 6 shows a comparison between a standard copper SX reagent and the ACORGA™ OR reagent before and after oxidation and clay treatment. The stage efficiency values were based on kinetics curves generated at a mixer speed of 600 rpm (PLS containing 6 gpl copper, 3 gpl iron at pH 2) using standard batch stage efficiency calculations[6]. The stage efficiency estimates were based on an operation utilizing a primary and secondary mixer with 90 second retention time in each.

Table 6: Physical and Metallurgical Performance

Reagent Conditions	Stage Efficiency	Cu/Fe Selectivity	Extract Org Cont	Extract Aq Cont	Strip Org Cont
Standard Copper SX Reagent (Fresh)	94%	10480	29"	1' 15"	33"
Standard Copper SX Reagent (Oxidized)	72%	163	>15'	1' 28"	6' 40"
Standard Copper SX Reagent (Clay Treated 50 gpl)	87%	743	2' 34"	1' 18"	2' 44"
ACORGA™ OR25 (Fresh)	94%	4514	27"	53"	23"
ACORGA™ OR25 (Oxidized)	75%	1042	8' 50"	1' 19"	5' 00"
ACORGA™ OR25 (Clay Treated 50 gpl)	92%	2104	2' 08"	1' 34"	2' 15"

The stage efficiency of the oxidized organic was significantly reduced for both reagents. ACORGA™ OR25 did show slightly higher stage efficiency, possibly as a result of reduced oxime oxidation. Organic oxidation also reduced the copper/iron selectivity of both reagents, however with ACORGA™ OR25 showing better performance in this area. In addition to increased strip phase disengagement times, the organic continuous extract phase disengagement times were severely affected. The aqueous continuous phase breaks, showed reasonable phase disengagement times and were not influenced by the lower interfacial tension. Clay treatment of the organic phase improved both the physical and metallurgical performance of the organic phase, increasing the stage efficiency, selectivity, and reducing organic continuous phase disengagement times.

CIRCUIT PREDICTIONS

Circuit predictions were compared using the stage efficiencies located in Table 6 for the fresh, oxidized, and clay treated organic. The circuit conditions considered were:

- PLS copper grade 1.55 gpl at pH 2
- Electrolyte 30 gpl copper, 200 ppm manganese, and 180 gpl sulfuric acid
- Electrolyte Advance 45 gpl copper
- O/A ratio 1:1 with flow rates of 4000 gpm
- 125,000 gal of organic inventory
- Series-Parallel circuit
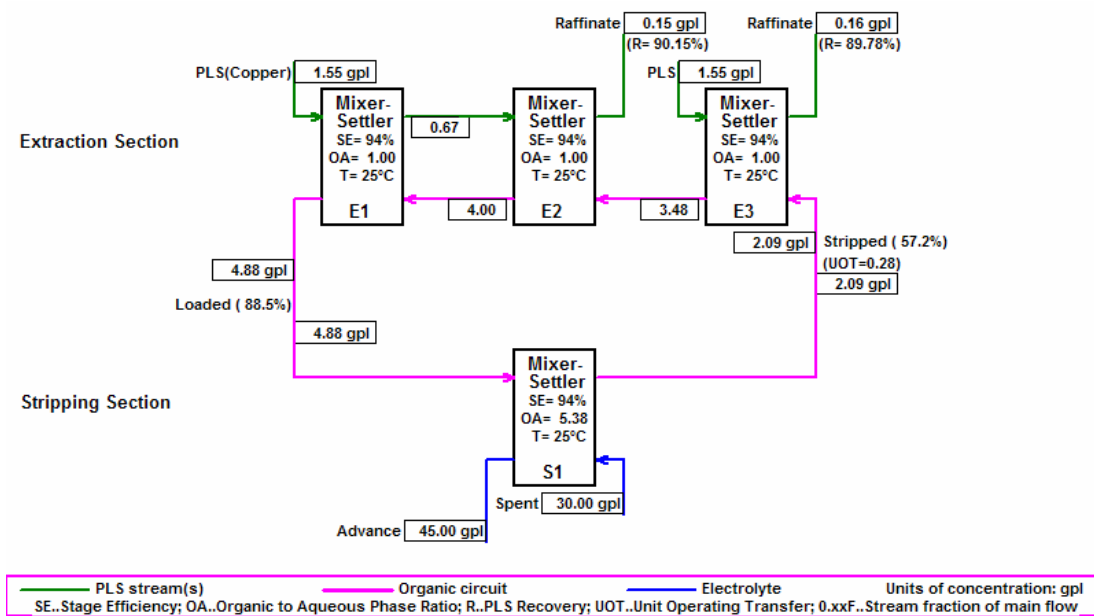
Figure 2: 10 Vol % Standard Copper SX Reagent - Normal Operation

The Figure above represents a normal operation using a 10 Vol % solution of a standard copper SX reagent formulation, with 94 % stage efficiency achieving a copper recovery of 90 % and producing 22,200 MT/yr of copper.

A plant operating under these conditions (experiencing high ORP values in the electrolyte) would complete one contact of oxidation (one turnover of the organic inventory) in approximately 30 minutes. Running the strip stage at an O/A ratio of 5/1 would require 2.5 hours for a one contact equivalent. Therefore in approximately 12.5 hours, the organic would be oxidized to the 5 contact equivalent from Table 4 or 1 Vol % reduction in reagent concentration. This was used as a worst case scenario to show the potential impact of oxidation. The copper recovery and stage efficiency would gradually decrease over the 12.5 hour period, under the assumed oxidizing conditions. The circuit model for the oxidized organic is shown in Figure 3.
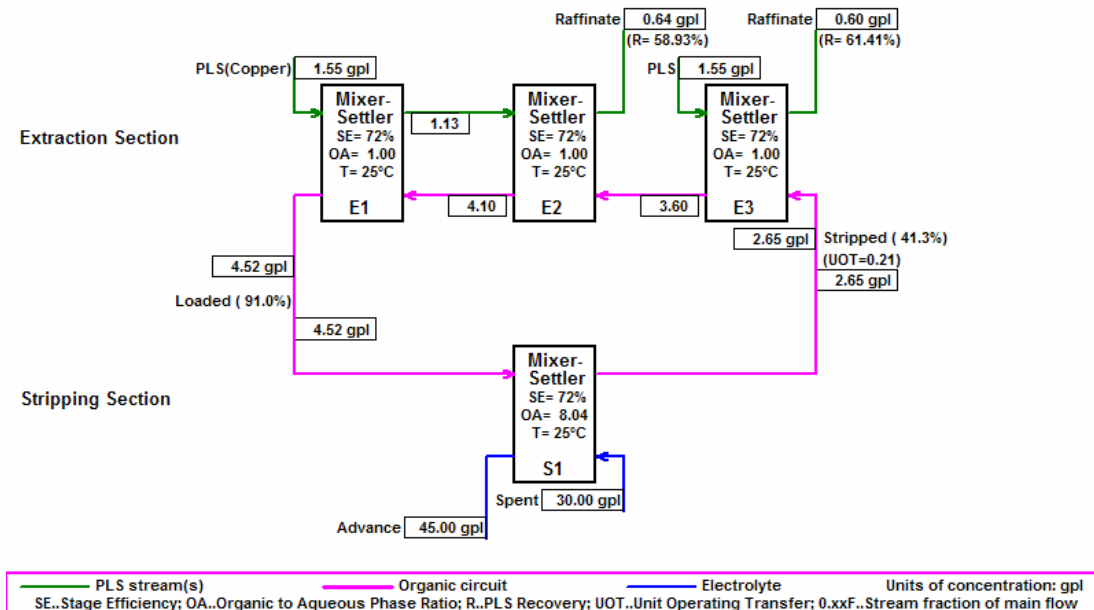
Figure 3: 9 Vol % Oxidized Standard Copper SX Reagent

The circuit in Figure 3 shows the impact of stage efficiency and lower reagent concentration on copper recovery. The stage efficiency would be expected to drop to 72 % and overall copper recovery would be expected to drop to 60 %, resulting in copper production of 14,800 MT/yr.

In order to increase the stage efficiency, the total organic inventory would need to be clay treated. The circuit below shows the increase in stage efficiency when the organic is clay treated using a 50 gpl dosage. To further increase the stage efficiency and remove the remaining oxidation products from the organic phase an additional clay treatment would be necessary.
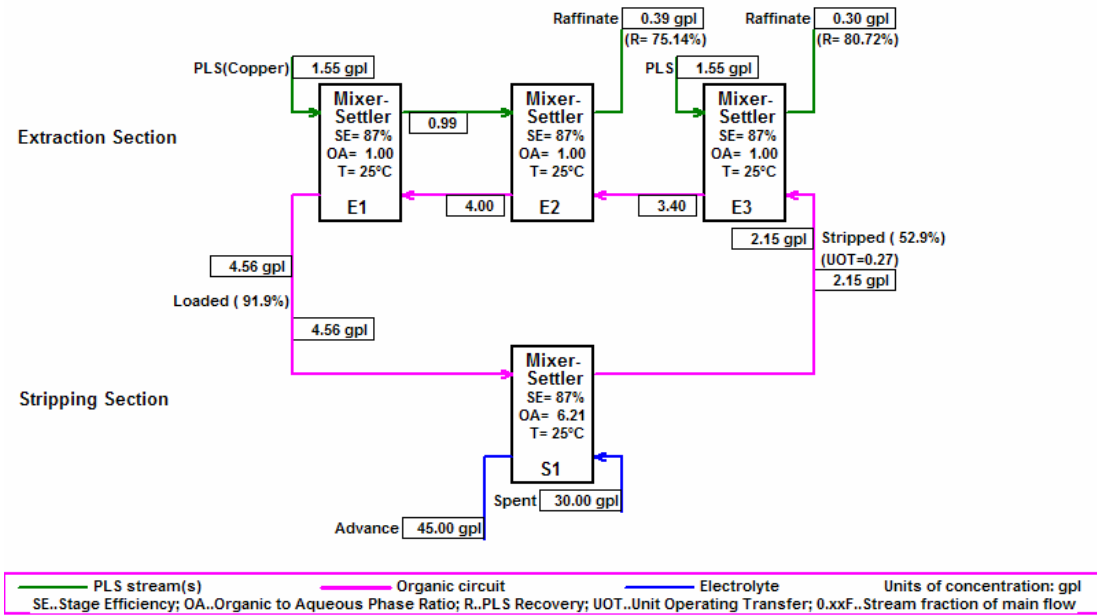
Figure 4: 9 Vol % Oxidized and Clay Treated Standard Copper SX Reagent

Figure 4 shows by clay treating the organic the stage efficiency would increase to 87 %, bringing the overall copper recovery to 78 %, resulting in copper production of 19,200 MT/yr.

Additional clay treatment would be necessary to further increase the stage efficiency or additional reagent could be added to increase the copper recovery to 90 %.

The circuit models below show the comparison of ACORGA™ OR25 under oxidized and clay treated conditions.
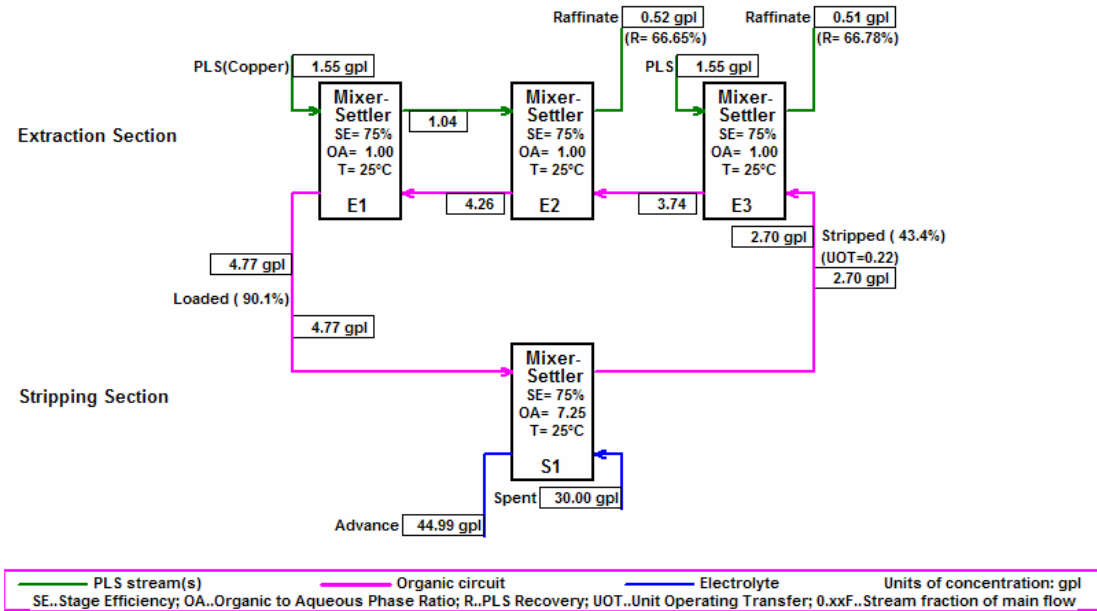
Figure 5: 9.6 Vol % Oxidized ACORGA™ OR25

Under the oxidized organic conditions the ACORGA™ OR25 concentration would decrease by 0.4 Vol % and achieve a stage efficiency of 75 %, a copper recovery of 67 %, resulting in copper production of 18,800 MT/yr.
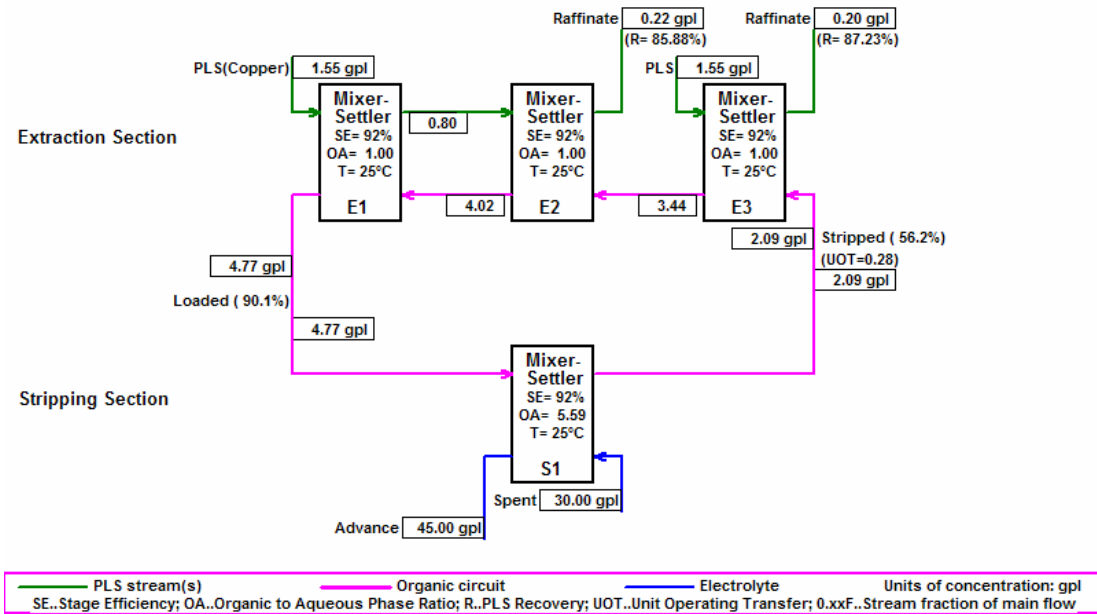
Figure 6: Oxidized and Clay Treated ACORGA™ OR25

The clay treated ACORGA™ OR25 would increase the stage efficiency to 92 %, increasing copper recovery to 86.5 %, resulting in copper production of 21,300 MT/yr. The table below shows the costs associated with organic oxidation such as reagent loss and reduced copper production due to lower stage efficiency. The calculations are based on a copper price of $ 4.20 USD/lb and reagent cost of $ 40 USD/gal.

Table 7: Cost of Reagent Oxidation

	Standard Copper SX Reagent	ACORGA™ OR25
Organic inventory (gal)	125,000	125,000
Reagent inventory 10 vol% (gal)	12500	12500
Reagent inventory after Oxidation (gal)	11250	12000
Reagent Loss Due to Oxidation (gal)	1250	500
Reagent addition to maintain production (gal)	11250	1375
Cost Due to Organic Oxidation	$50,000	$20,000
Copper Production/Year at Normal Stage Efficiency (94%)	$205,143,000	
Copper Production/Year Due to 1% Drop in Stage Efficiency (93%)	$202,202,000	
Copper Production/Year Due to 2% Drop in Stage Efficiency (92%)	$200,732,000	
Copper Production/Year Due to 4% Drop in Stage Efficiency (90%)	$195,585,000	

The major cost associated with organic oxidation would be the reduction in copper transfer due to oxime loss and reduction in stage efficiency. Under oxidizing conditions the oxime concentration and stage efficiency will continuously decrease. This rate is dependent on the severity of the oxidizing conditions (Mn^{7+} concentration, O/A ratio, and contact time) and can happen rather quickly under severe conditions. Hopefully any oxidation conditions would have been noticed by routine ORP measurements or by the increased phase disengagement times (notable under organic continuity), and corrected before impacting copper production.

The severity of the oxidation could be limited through the use of an oxidative resistant formulation.

CONCLUSIONS

- Minimizing manganese transfer to the copper electrolyte should be the first step in preventing the possibility of higher manganese oxidation states in the electrolyte.
  - This can be done by reducing aqueous in organic entrainments by maintaining organic quality, proper organic depths in the settlers, using coalescing media in settlers (picket fences), minimizing crud, etc.

- Solution chemistries can influence the formation of the permanganate ion and maintaining the 5/1 ferrous to manganese ratio in the electrolyte will help to maintain manganese in the +2 state.

- Contact time, concentration, O/A ratio and reagent formulation influences the oxidation of the organic when the permanganate ion is present in the electrolyte.

- ORP values above 600 mV can cause oxidation of the organic; equilibrium ORP values of approximately 600 mV (using a standard Ag/AgCl electrode) have been obtained when permanganate was reduced in synthetic solutions.
  - ORP measurements of the electrolyte should be monitored.
  - The differences in the ORP values of the spent and rich electrolyte can be used as an indication of oxidation.

- Both the reagent and diluent can be affected due to oxidation.

- The oxidative degradation products are interfacially active resulting in reduced physical and metallurgical performance of the SX reagent.

- The physical effects of organic oxidation are slow phase disengagement times which can lead to increased entrainments (organic losses and impurity transfer). Likely only to be seen under organic continuity.
- The metallurgical effects are reduced oxime concentration, lower copper transfer, and lower stage efficiency. All resulting in lower copper production.

- If oxidation occurs in the SX plant, clay treatment or the organic is necessary to improve the quality of the organic.

- The reagent choice is also important in limiting oxidation of the organic and the ACORGA™ OR series of extractant allows for improved performance under oxidizing conditions.

REFERENCES

1. G. Miller, "Methods of Managing Manganese Effects on Copper SX-EW Operations", Miller Metallurgical services, Australia.

2. C.Y. Cheng, C.A. Hughes, K.R. Barnard, K. Larcombe, "Manganese in copper solvent extraction and electrowinning", Hydrometallurgy 58 (2000) 135-150.

3. K.C. Sole, K. Viljoen, and B.K. Ferreira, *Anglo Research,* M.D. Soderstrom, O. Tinkler, and L.Hoffmann, *Cytec Industries Inc.* "Customizing Copper-Iron Selectivity Using Modified Aldoxime Extractants: Pilot Plant Evaluation".

4. T. Bednarski, "Behavior of Iron and Manganese in Electrowinning Solutions – A Hull Cell Study", Tucson SME December 2008, Cytec Industries Inc.

5. G. Zarate, "Manganese in SX/EW Plants", Cytec Seminar, Antofagasta, October 2010, Anglo American.

6. M. Soderstrom, T. Bednarski, E. Villegas, Cytec Industries Inc. "Stage Efficiency in Copper Solvent Extraction Plants".

MANGANESE IN SX-EW PLANTS

Gabriel Zárate

Anglo American, Chile

Presenter and Corresponding Author

Gabriel Zárate
gzarate@anglochile.cl

ABSTRACT

The published information about manganese behavior in SX/EW plants has been reviewed and its application to a number of Chilean plants has been analyzed. It is usually recommended to keep the manganese concentration in the electrolyte below 0.05 g/l, because under certain conditions, manganese can cause a number of problems, among them: reduction in the extractant loading capacity and extraction kinetics, chlorine generation in electrolytic cells, stainless steel cathode pitting corrosion, accelerated anode corrosion and precipitation of amorphous MnO_2.

The measures usually proposed to keep the manganese concentration in the electrolyte under control are mainly focused on reducing PLS entrainment and keeping it as Mn+2 by maintaining a minimum iron concentration of 1 g/l and/or a Fe/Mn ratio of 10:1 or 8:1 in the electrolyte.

The operating data of several electrowinning tankhouses has been collected and analyzed in relation to the recommendations mentioned above. This data includes the redox potential and the concentrations of manganese, total iron, ferrous iron and chloride in the electrolyte.

The data analysis carried out, as well as the conclusions and recommendations obtained, are discussed in this paper.

INTRODUCTION

In Chile there are several heap leaching-SX-EW plants processing copper oxide ores, copper sulfide ores or copper mixed ores. Most of the ores contain manganese as copper wad in variable proportions, depending on the ore being treated. Accordingly, the manganese content in the ore can be quite variable, ranging from less than 0.01% up to 1%, and as a result the manganese concentration in the pregnant leach solution (PLS) can vary from 0.1 up to 15 g/l.

Therefore, the occurrence of significant concentrations of manganese as manganous ion, Mn^{+2}, in copper leach solutions feeding SX plants is becoming increasingly common. However, the literature about manganese effects on an industrial scale is sparse. Only Codelco-Chuquicamata in Chile[1] and Girilambone in Australia[2] have published some information about manganese problems in their SX-EW plants, although the presence of manganese in electrolyte solutions in EW operations around the world is well known [3,] as shown in Table 1.

At Chilean operations, the manganese concentration in the PLS is quite variable as mentioned above. As a consequence, the manganese concentration in the electrolyte is also highly variable, ranging from less than 0.01 up to 0.5 g/l.

Table 1: Manganese Concentration in Electrolyte Solutions[3]

| Plant	Mn (ppm)
El Abra	38
Mantoverde	40
Andacollo	60-100
Cananea	26
Nacozari	300
Toquepala	100
Cerro Verde	70
Tyrone	<100
Chino	150-350
Morenci	40
Nifty	90
Mt. Cuthbert	80

REVIEW OF MANGANESE EFFECTS IN COPPER SX-EW

An analysis of the manganese problems in copper SX-EW by Miller[2] lists some of the main problems as reduction in the extractant loading capacity and extraction kinetics, chlorine generation in electrolytic cells, stainless steel cathode pitting corrosion, accelerated anode corrosion, and precipitation of amorphous MnO_2. These problems are caused by the high oxidation potential of Mn^{+7}, which could be generated by the highly oxidative environment of EW cells particularly during the early weeks of plant operation, when no electrolyte bleed is being utilized due to low iron concentrations in both PLS and electrolyte. As a result, the electrolyte redox potential increases from a normal level of 400 mV to as high as 900mV (the reference electrode is not mentioned).

According to Soderstrom[4], from Cytec, at a high enough redox potential the oxime is degraded. As a recommendation, it is stated to be highly concerned at 800 mV and no question of oxime degradation if the potential ever approaches 1,000 mV (reference silver/silver chloride).

In a recent publication by Tjandrawan et al[5], it was concluded that permanganate is unstable in the presence of Mn^{+2} ions and thus it will only be observed in the electrolyte at low concentrations of manganese ions under which conditions it is metastable. On the other hand, Mn^{+3} ions are unstable except in very concentrated acid solutions and disproportionate in MnO_2 and Mn^{+2}.

The effect of manganese on lead anodes has been summarized in a presentation made by Ellis[6], of RSR Technologies, as follows:

- Manganese can react with the stable PbO_2 corrosion layer on the anode surface making it unstable, less dense, less adherent, susceptible to shedding. It causes MnO_2 to build up in the layer according to

$$MnSO_4 + PbO_2 = PbSO_4 + MnO_2 \qquad (1)$$
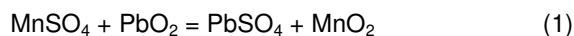
- The PbSO4 is converted back to PbO2, but it is now deposited in loose layers which are easily spalled off causing contamination of the copper cathode.

Tjandrawan et al[5] concluded that this is the likely mechanism according to their results.

The measures conventionally used to keep manganese under control focus on reducing PLS entrainment in the loaded organic and maintaining manganese as Mn^{+2}. In the first case, PLS entrainment can be reduced by using coalescers and/or washing stages and by reducing crud generation.

In the second case, two techniques are applied to maintain manganese as Mn^{+2}, the most common being the use of Fe^{+2} oxidized by permanganate, according to reaction:

$$Mn^{+7} + 5\,Fe^{+2} = Mn^{+2} + 5\,Fe^{+3} \qquad (2)$$
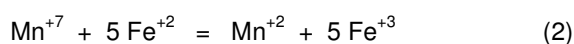
High levels of Fe^{+2} (or total iron) need to be maintained to obtain low levels of Mn^{+7}. The published recommendations in this respect are, however, not clear cut:

- A minimum ratio of 8:1 or 10:1 (assumed to be Fe:Mn) is necessary to keep manganese effects under control[2].

- A minimum of 1 g/l of total iron is necessary to prevent high redox potential levels in the electrolyte[2].

- For an operation with 2 g/L iron, the maximum safe level of manganese is 200 mg/L, which means a Fe:Mn ratio of 10:1[2].

- A Fe^{+2}:Mn ratio of 6:1 is necessary to keep redox potential under control[7].

The second technique to keep manganese under control is limited to the use of either sulphur dioxide or hydrogen peroxide. Since peroxide can strongly attack the extractant it is unsuitable. SO_2 at low dosages is suitable. Girilambone has reported its use in a copper system to obtain rapid reduction of permanganate ions in the electrolyte inventory [2].

## APPLICATION TO CHILEAN SX-EW PLANTS

Information on electrolyte composition from several Chilean SX-EW plants was collected. Monthly averages were calculated for concentrations of total iron (Fe), ferrous iron (Fe^{+2}), manganese (Mn) and chloride (Cl⁻) and for redox potential (all values have the standard hydrogen electrode (SHE) as reference). From these data, monthly averages were estimated for Fe/Mn and Fe^{+2}/Mn ratios. The effect of all these variables on the redox potential is next discussed.

Effect of Fe/Mn and Fe^{+2}/Mn Ratio

The effect of Fe/Mn and Fe^{+2}/Mn ratios on redox potential is shown in Figures 1 and 2. It can be seen that redox potential does not change significantly for a wide range of Fe/Mn ratios, going from 6 to 250. Moreover, the highest potential of 800 mV corresponds to a Fe/Mn ratio of 140. The same is observed for the Fe^{+2}/Mn ratio. In this latter case, this ratio goes from as low as 0.7 to as high as 25 without a significant effect on the redox potential.

Both results are in disagreement with all the recommendations, except the second one, which is also partially met as it is next discussed.
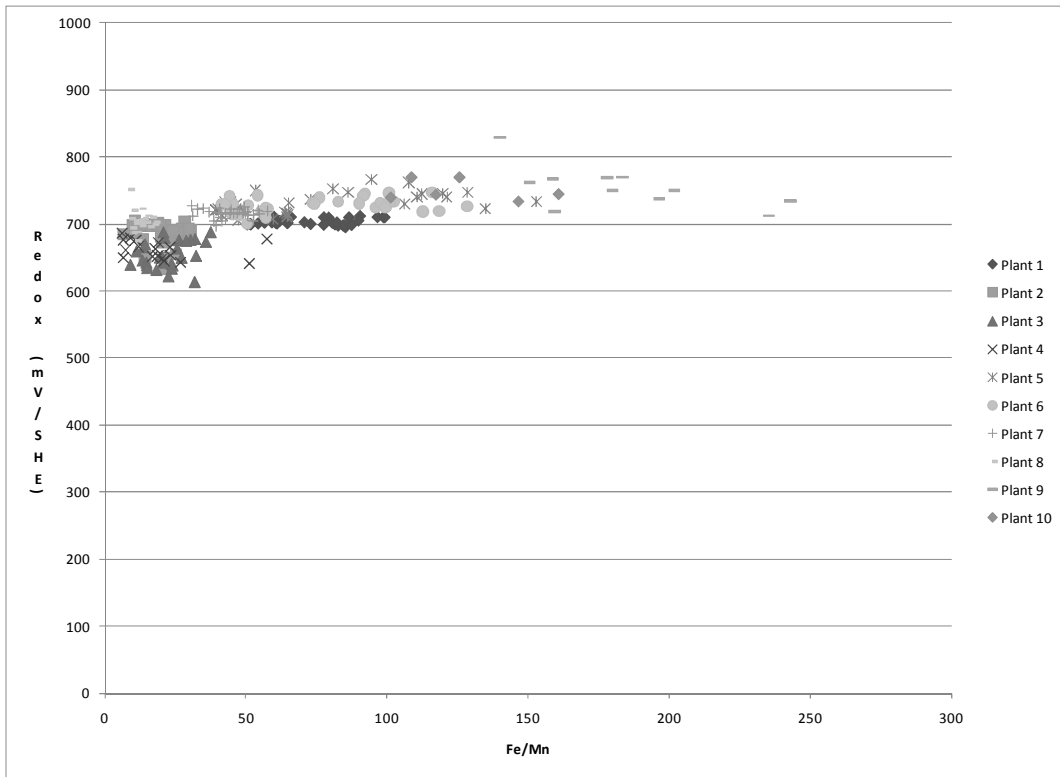
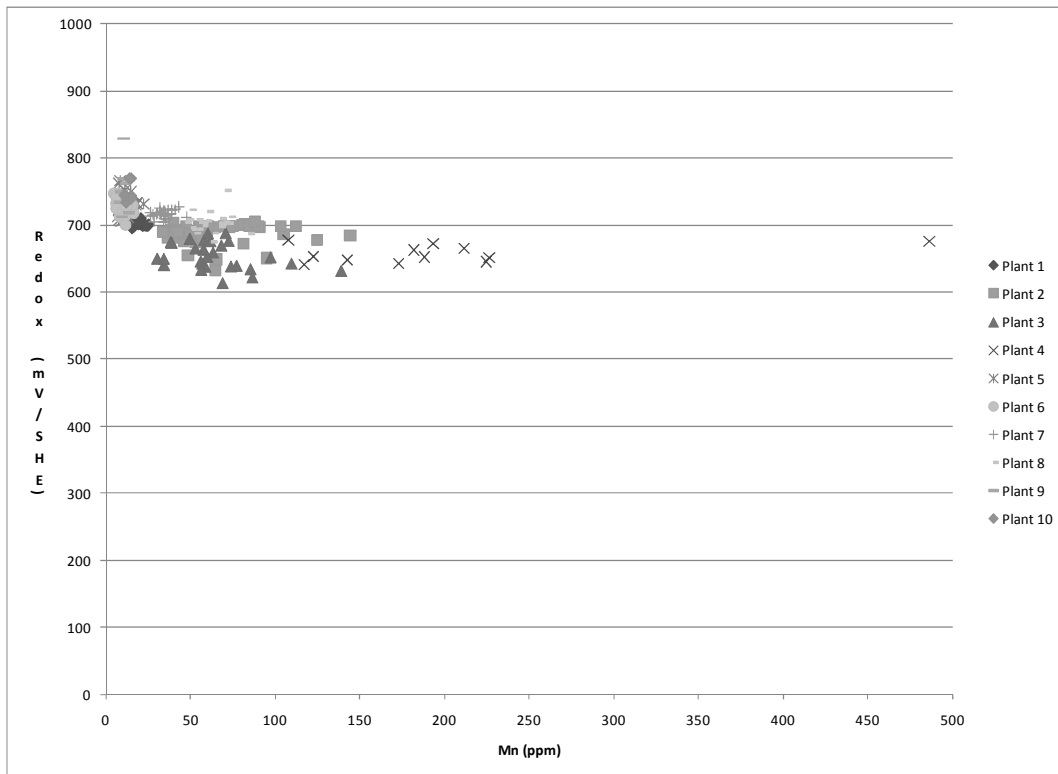**Figure 1: Redox Potential and Fe/Mn Ratio**
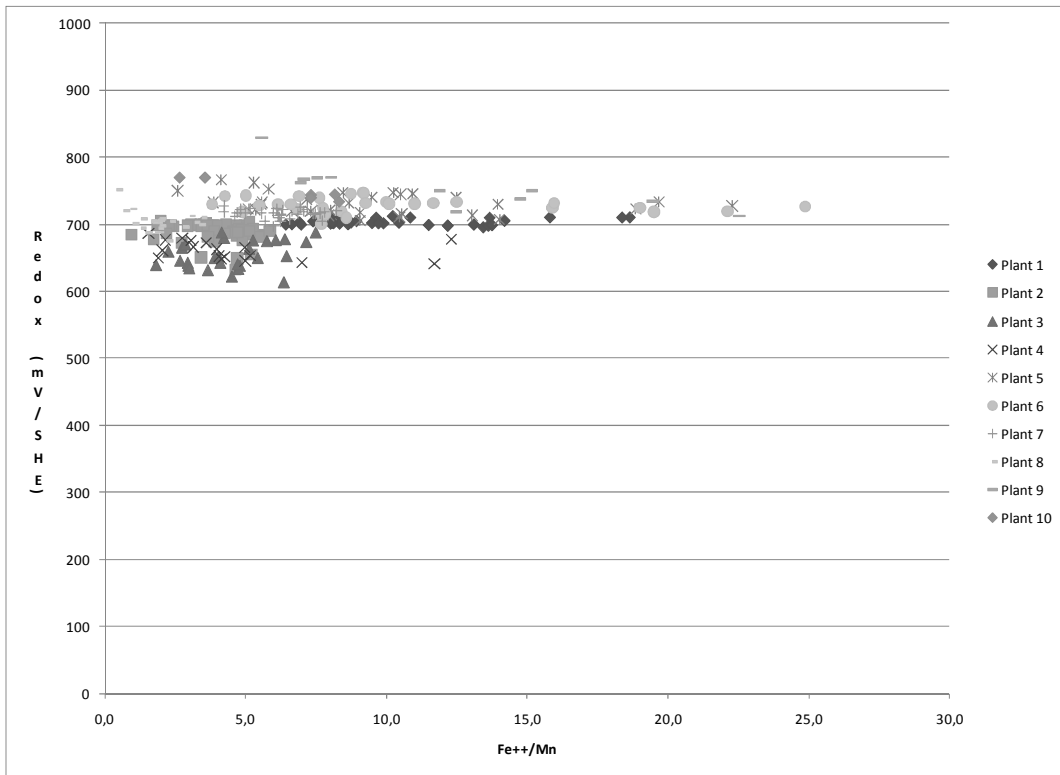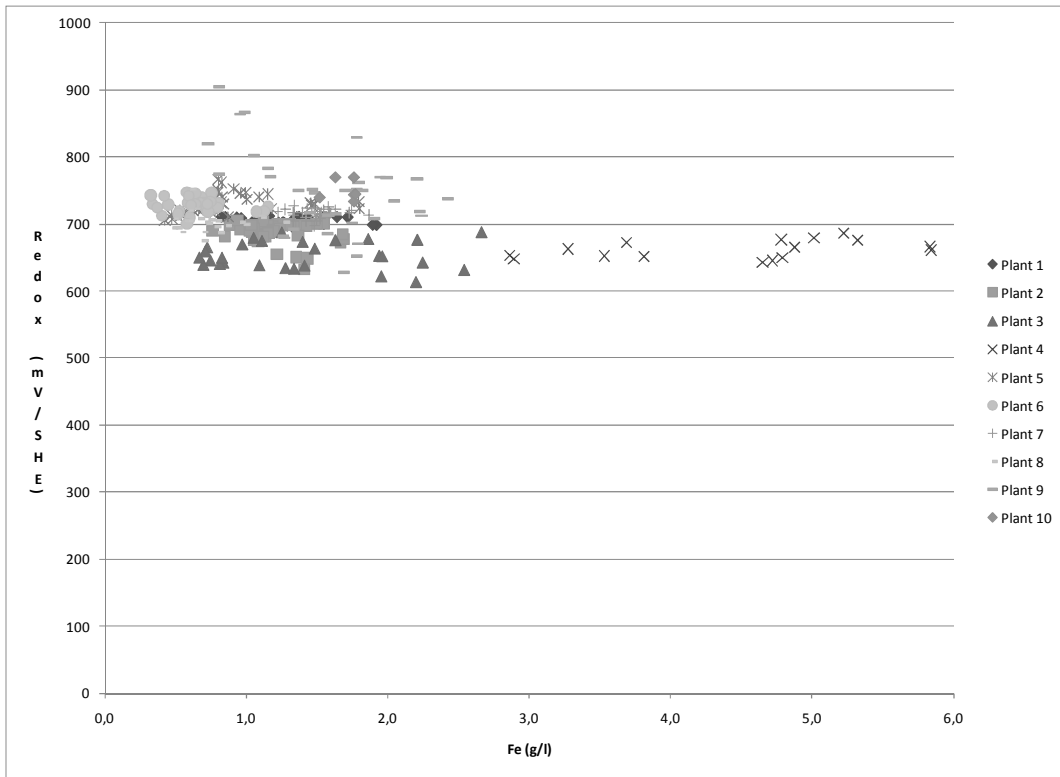

Figure 2: Redox Potential and Fe^{+2}/Mn Ratio

Effect of Iron, Manganese and Chloride Concentration

The effect of iron, manganese and chloride concentration in electrolyte on redox potential is shown in Figures 3, 4 and 5. The following observations can be made:

- In all the plants, except Plant 9 under specific conditions, the redox potential is far below 800 mV.

- There is no a significant effect of the manganese concentration in the redox potential, except at very low concentrations (<10 ppm). Even though, the redox potential at this concentration is below 800 mV. Unfortunately there is no information during the early weeks of operation of each plant to confirm if the redox potential reaches more than 900 mV at very low iron concentrations[2]. However, this problem can be easily solved by including an iron sulfate addition system, as it was done in Plants 1, 2 and 9.

- A more significant effect on the redox potential is shown at a high chloride concentration combined with a low iron concentration. For instance, at 40 ppm of chloride and 1 g/l of iron, the redox potential was at its highest average value with 905 mV in Plant 9. In this plant, the manganese concentration is <20 ppm and it has not been measured on a routine basis until very recently.

Figure 3: Redox Potential and Manganese Concentration

Figure 4: Redox Potential and Iron Concentration
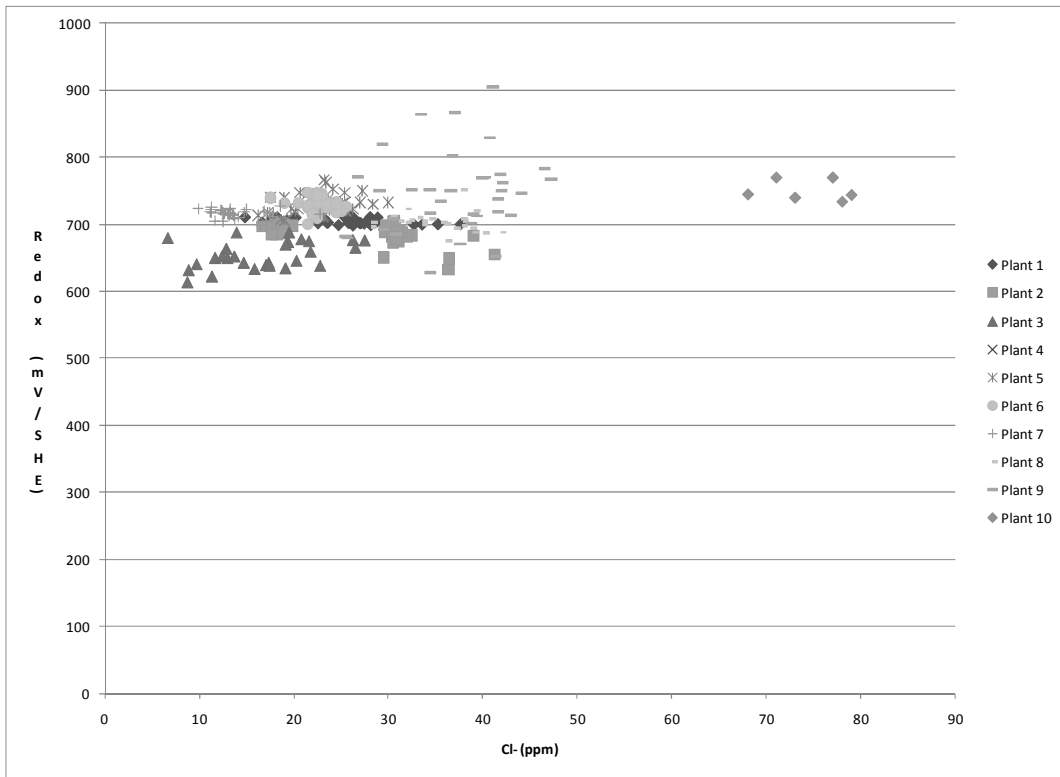
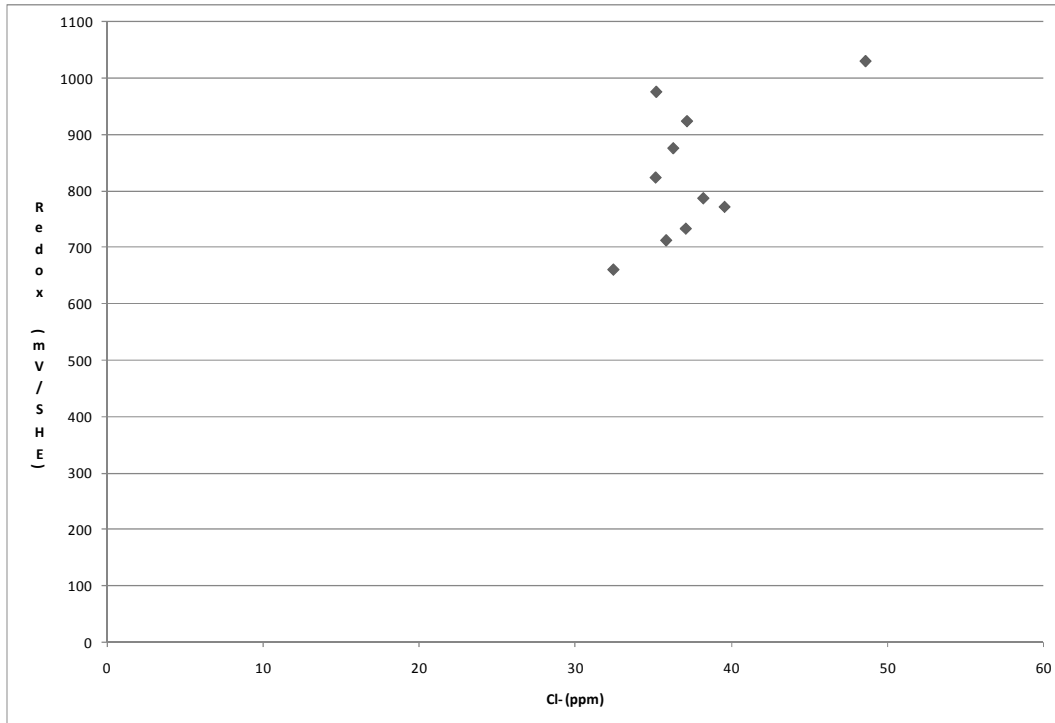**Figure 5: Redox Potential and Chloride Concentration**

The combined effect of iron and chloride concentration was evaluated in more detail by using daily information from the same operation, Plant 9. For this purpose, average chloride concentrations were estimated for 50 mV ranges of redox potential going from 600 up to 1100 mV. Results show that the highest redox potentials, above 900 mV, are obtained at chloride concentrations between

35 and 50 ppm when iron concentration is below 1 g/l (see Figures 6 and 7). In order to maintain redox potentials below 800 mV, at these chloride concentrations, the iron concentration should be above 1.5 g/l.

For this plant, the following equation correlates redox potential and chloride and iron concentrations in the electrolyte. Figure 8 compares the measured and the predicted values.

$$\text{Redox (mV/SHE)} = 838 + 8.7 * (\text{ppm Cl}^-) - 262.4 * (\text{gpl Fe}) \qquad (3)$$

All these previous results are confirmed by Plant 10 data. At this plant, the chloride concentration in electrolyte is the highest, from 46 up to 85 ppm, but the iron concentration in electrolyte has been consistently above 1.2 g/l with a grand average of 1.7 g/l. The few redox potential data provided ranges only from 733 to 769 mV (SHE).

Figure 6: Redox Potential and Chloride Concentration for Plant 9
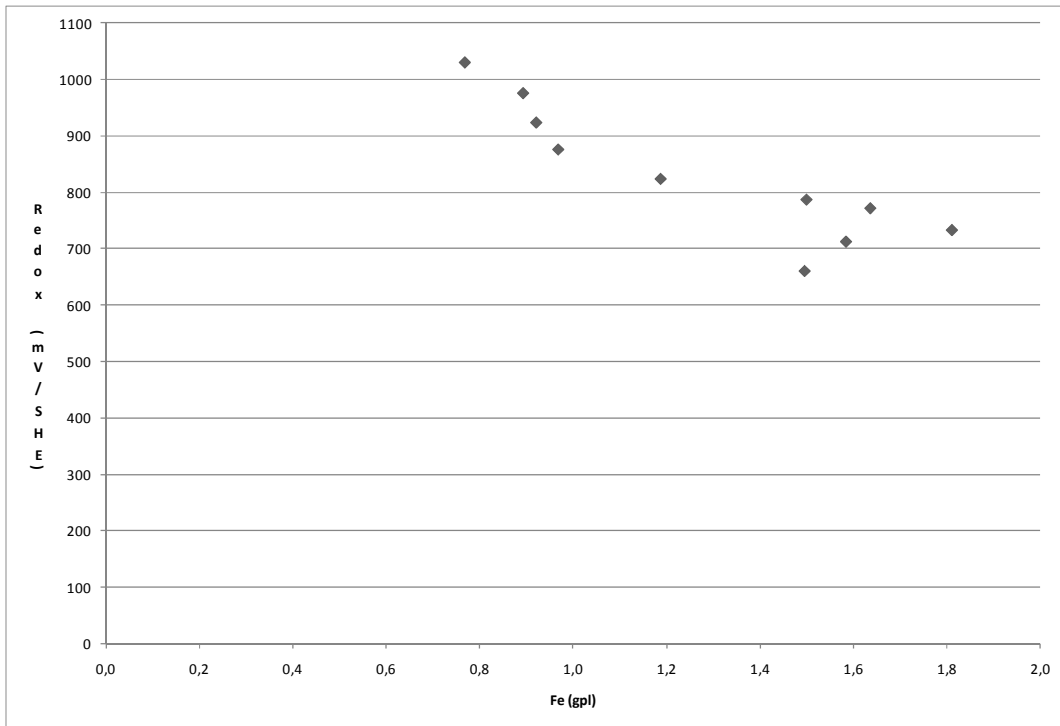
Figure 7: Redox Potential and Iron Concentration for Plant 9
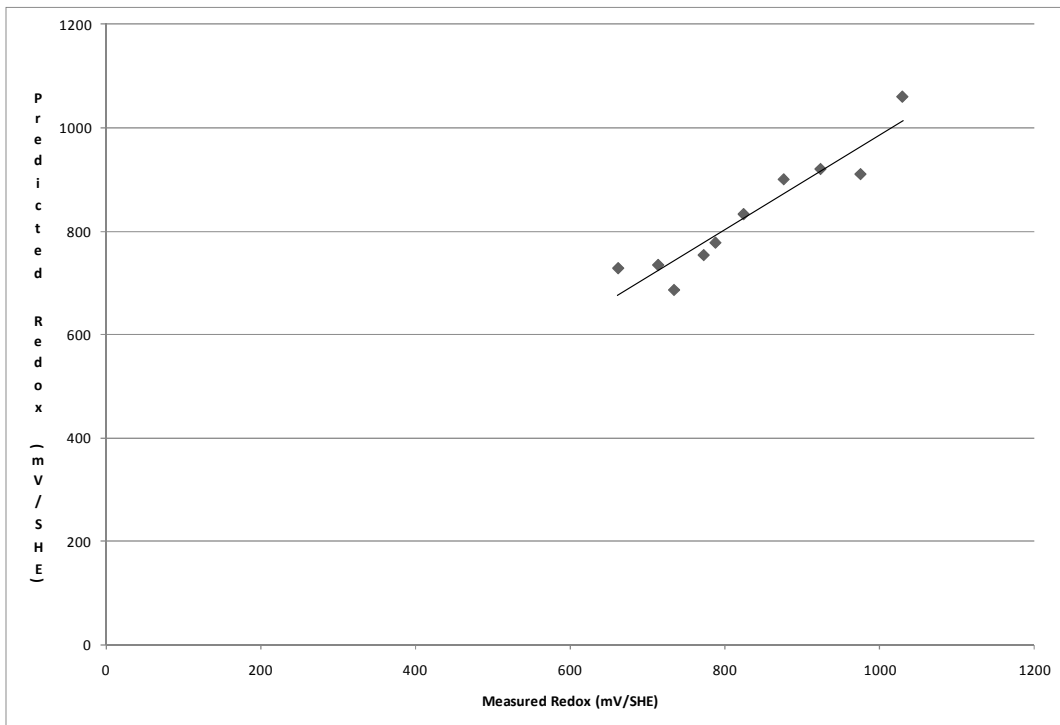
Figure 8: Measured and Predicted Redox Potential for Plant 9

CONCLUSIONS

The information of redox potential and its relationship with manganese, iron and chloride concentrations in the electrolyte has been reviewed for several Chilean SX-EW plants, in order to verify if the published recommendations to maintain redox potential under control are met, namely:

- A minimum Fe:Mn ratio of 8:1 or 10:1.
- A minimum 1 g/l of total iron.
- A Fe^{+2}:Mn ratio of 6:1.

It has been found that, in general, only one of these recommendations is partially met and that the redox potential is highly dependent on the combined effect of chloride and iron concentration in the electrolyte. The highest redox potentials, above 900 mV, are obtained at chloride concentrations between 35 and 50 ppm when iron concentration is below 1 g/l. In order to maintain redox potentials below 800 mV, at these chloride concentrations, the iron concentration should be above 1.5 g/l.

It has also been found that there is no significant effect of the manganese concentration in the redox potential, except at very low concentrations (<10 ppm). Even though, the redox potential at this concentration is below 800 mV.

As there was no information during the early weeks of operation of each plant, it was not possible to confirm if the redox potential reaches more than 900 mV at very low iron and manganese concentrations, as it is mentioned in one of the references. However, this problem can be easily solved by including an iron sulfate addition system, as it has been done in Plants 1, 2 and 9.

ACKNOWLEDGEMENTS

REFERENCES

1. L. Farías and G. Alvarez, "Experiencia de Operación en las Plantas de SX-EW, Subgerencia de Oxidos, Chuquicamata", Workshop Electro-Obtención de Cobre, Viña del Mar, Mayo 1993.

2. G. Miller, "The Problem of Manganese and its Effects on Copper SX-EW Operations", Copper 95-Cobre 95, Eds. W.C.Cooper et al., CIM, 1995, pp.649-663.

3. T. Robinson, J. Jenkins, S. Rasmussen, M. King, and W. G. Davenport, "Copper electrowinning-2003 World Tankhouse Operating Data," Copper 2003-Cobre 2003, Eds. J.E.Dutrizac et al, CIM, 2003, pp. 421-469.

4. M. Soderstrom, Personal Communication, November 2010.

5. V. Tjandrawan and M.J. Nicol, "The Oxidation of Manganese Ions on Lead Alloys During the Electrowinning of Copper", Copper 2010, Vol. 4, GDMB, pp. 1699-1712.

6. J. Gagnon, T. Ellis, A. Mirza, P.Ugarte, "RSR Anodes for Copper Electrowinning", Anglo American-RSR Anodes Seminar for Copper Electrowinning. Santiago, August 9th, 2010.

7. C. Hecker, Consultant Report N° 6. December 2005 and January 2006. Oxide Plant. Compañía Minera Doña Inés de Collahuasi.

CONTAMINATION MANAGEMENT IN SOLVENT EXTRACTION PLANTS

By

Graeme Miller

Miller Metallurgical Services, Australia

Presenter and Corresponding Author

Graeme Miller
gmiller@millermet.com

ABSTRACT

Most solvent extraction plants are used to remove contaminants and to concentrate the ion species of interest for further processing. This activity can be significantly impaired by the cross contamination of the process streams with other species that can be transferred across the phases. These species can have significant impacts on the operation of the SX plant itself, operation and chemical contamination of the concentrated stream and further impacts on the process applied to the raffinate stream.

The minimisation of this cross contamination is a major driver for: PLS treatment, SX circuit design, reagent selection, internal SX plant unit operations for contamination minimisation, reagent regeneration systems, and subsequent treatment of the concentrated stream and raffinate. A wide variety of these systems is available to the plant designer and operator. The selection and use of them is not straight forward or obvious until (generally) after an upset event has occurred.

The paper describes many of the methods of contamination control as well as criteria for their selection. Management of one level of contamination often introduces a further upset condition that also has to be addressed for a successful implementation to be achieved. A hierarchy of such issues has been developed to allow practitioners to understand these interactions and to successfully implement programmes of contamination management.

INTRODUCTION

The solvent extraction (SX) process is used to purify and concentrate an ion of interest so that it can be subsequently recovered. SX operation and the purity of the product can be severely affected by contaminants transferred from the PLS, and contaminants carried over from the SX operation itself. Contamination of the raffinate and concentrate stream from the SX plant can also generate significant problems in the downstream process activities.

One of the issues with identifying that a contamination problem exists is that the symptoms often occur in a process that is remote from the contamination. This has been identified[1] " …the perceived problems (in SX) were soon discovered to be symptoms of a problem occurring elsewhere in the circuit…". It has also been shown[2] that the effect of contamination was "…complex with many symptom and parameter interactions…". It is generally a difficult process to untangle the obvious symptoms in an operation; and to follow the thread of contamination upstream to the primary source of the problem.

The other significant issue is that many plant designers are not aware of, or do not take sufficient cognisance of the effects that contamination can have on the SX and other process sections. There are a number of references covering a range of internal SX contamination caused by the PLS constituents[2-10]. The recognition that contamination can and will occur is a prime driver for the selection of the overall flow sheet and appropriate processes, unit operations and controls that are included; to minimise or prevent the subsequent effects. This paper includes *only some* of the available references to illustrate the range of contamination and the potential effects that ensue.

Table 1 summarises the overall structure of the contamination issues with:

- The contaminant and its source
- The direct effect on the process
- Effects on subsequent process stages
- Direct treatment / prevention
- Treatment of indirect or subsequent symptoms that develop

SOURCES OF CONTAMINATION

The major sources of contamination are: the PLS constituents, the transfer of PLS constituent(s) to the SX concentrate stream and the transfer of the SX reagent to the raffinate and the concentrate streams.

PLS Contamination

The PLS constituents are impacted by the upstream process and operations. The actual SX operation itself determines if a PLS characteristic is a contaminant or not. Amphoteric ions such as Mo, Bi, Zr can have dramatic effects on U SX[1)(5)(6)(9] but have none on Cu SX. Whereas silica can affect all SX plants when it is in a polymerisable form[1)(6)(8)(9]. Many contaminants cause issues in SX plants independent of the SX process used. The most significant of these are:

- Suspended solids including biomass
- Scale forming ions especially calcium
- Surfactants
    - Emulsifiers
    - Flocculant
    - Biomass[11]
    - Oils from gear box failures and mining equipment maintenance
- High TDS and /or solution viscosity can be the cause of poor SX performance that leads to downstream contamination issues
- Humates that can transfer deleterious ions[6] (acting much like carboxylic acids, e.g. V10, to transfer via the organic phase)
- Highly oxidizing conditions from nitrates or high Eh in the leach
- Organic and extractant from upstream SX operations
- PLS ions when present in sufficient concentration
    - Amphoteric ions
    - Fe with D2EPHA, C272 and other phosphorous based extractants

- Cu in circuits using C272, C301, Carboxylic acids
- Chloride in tertiary amine USX circuits that co-extract with the uranium.

The PLS ions themselves can be contaminants not only to the SX plant, but to downstream processes in the concentrated stream. The wide range of 'contaminants' is so broad that their potential effects are not always properly considered. The identification of the main ones is obvious (solids, surfactants, known poisons for each extractant); but the more subtle ones are often overlooked until such time as adverse operation is evident; when remedial measures are more urgent and costly. The prime example of this is the presence of cruds[1] in the early uranium SX plants that had not been evident in the laboratory or pilot plants.

Contamination from the SX operation

SX Internal Contamination

Internal contamination from the SX operation is related to additional issues that arise within the plant, that contribute to the contamination seen within the exit streams or as upset conditions in the SX – poor phase disengagement, poor transfer capacity or poor transfer kinetics being typical outcomes. The main causes of internal contamination are associated with chemical changes in either the aqueous or organic phases; or internal generated addition of other components.

Chemical changes in the aqueous stream
- Scale formation from increases in calcium content (especially in V10 nickel SX extraction)
- Chemical changes during SX that can create precipitates[13,14] that in turn can:
    - Cause blockage of the plant and poor utilisation
    - Form crud with the precipitate
    - Create stable emulsions
    - Create a stable 'third phase' that interferes with the phase separation activity
- Polymerisation of silica (and other amphoteric ions) creating voluminous floating crud.

Chemical changes in the organic stream
- Degradation of alcohol modifier to carboxylic acids
- Oxidation of organic to surface active species, an inactive components (nitration reactions)
- High loading leading to third phase formation
- Poisoning by extracted ions that can lead to major reductions in transfer capacity and kinetics:
    - Cu on Cyanex 301
    - Fe on D2EPHA
    - Cl on tertiary amines
    - Rare Earths on D2EPHA for Zn extraction
    - Mo & Cr for tertiary amines
    - Cr for Cyanex 272.

Addition of other components is in interesting area that can have some unusual input vectors
- Air entrainment during mixing leading to:
    - Stable emulsions
    - Low density emulsions that float rather than sit at the interface
    - Air disengagement that can upset the settler flow patterns and increase entrainments
    - Increased entrainment of aqueous attached to the air bubbles
- Oil contamination from gear box seal failures
- Glycerine contamination from failure of peristaltic pumps
- Massive insect infestation with addition of proteins, humic acids and other organic species that can interfere with all aspects of organic health. This particular aspect has been a feature of arid areas in Australia after significant rain events; with Bogong moths at GCC and grasshopper at Whim Creek as examples.

SX Output Contamination

The contamination from the output of SX plant (raffinate, wash/scrub effluent and concentrate streams) is related to the transfer of a deleterious species from the PLS or the organic itself to the exit stream(s). This contamination then affects the SX operation directly or has downstream effects on the exiting streams. It is the internal contamination events that can be difficult to diagnose due to the complex interactions that can occur.

The more common (and simpler) contaminations involve:

- The entrainment of PLS species into the concentrate stream
- The chemical transfer of non-target ions to the concentrate stream
- The entrainment of the SX organic into the raffinate and concentrate stream(s)
- Transfer of any one phase into another part of the SX circuit via crud formation and movement (a "crud run")[12]
- Other physical methods of passing one phase to another part of the plant where it is a liability (such as leaking baffles and partitions, valves that do not close properly etc). These can be very difficult to diagnose and then find.

More complex transfer mechanisms can involve closed loops[8] and chemical positive feedback. The most well known is the manganese degradation of copper SX organic, in the absence of Eh control in the electrowinning (EW) plant.

- Manganese in the PLS is transferred by entrainment (or more often silica based floating crud) into the copper electrolyte.
- It is oxidized to Mn^{7+} in the EW operation
- The Mn^{7+} returns in the spent electrolyte sent to the SX and oxidizes the organic
- The oxidized organic has slower phase separation times leading to more entrainment of the PLS to the electrolyte
- The higher concentration of oxidized manganese in the electrolyte gives a faster degradation of the SX organic finally leading to a catastrophic collapse of the SX operation.

Another involving a closed loop is that experienced at the Olympic Dam Operation which has a sequential Cu SX and U SX circuit. The problem experienced was chloride transfer into the EW with the stainless steel cathodes being corroded with the copper sticking and not being stripped[4]. The eventual culprit was found to be the USX reagent that was entrained in the raffinate.

- The tertiary ammine can transfer chloride
- It was being lost to the raffinate in such quantities that it was returning to the copper PLS via the leach and CCD circuit.
- In the Cu SX it was transferring the chloride to the EW electrolyte with disastrous results for the stainless steel cathodes.
- The cause of the high losses was not purely entrainment but physical transfer during start and stop transients; especially the extraction system that released much of the contactor organic contents to the raffinate tank on shut down.

EFFECTS OF CONTAMINATION

All of the sources of contamination have some level of effect within the SX plant, or on downstream operations. Generally the effects are obvious with formation of crud, transfer of unwanted species to the concentrate stream, poor internal operation of the SX (slow phase disengagement, reduced chemical transfer capacity and formation of stable emulsion) and adverse operation of the downstream process. Large scale examples of these effects are experienced in the copper industry, with organic contamination of the advance electrolyte. The organic causes changes in the copper growth morphology which entrains the organic in the copper ("organic burn"). This is a major economic loss to the operation that must be controlled. Similarly the transfer of iron to the electrolyte lowers the current efficiency and the productivity of the EW plant.

Most contamination transfer events have economic and plant utility effects, that need to be minimised. Organic in the SX raffinate is a direct loss while it can also have major consequences on the downstream process plant[4][9][13]. The Bulong plant had a sequential cobalt and Nickel SX with Cyanex 272 and Versatic 10 as the extractants. Only 0.5% of C272 in the nickel circuit gave massive calcium transfer in extraction and uncontrolled gypsum precipitation in E1, E2 and the scrub stages. They replaced their entire nickel SX organic inventory due to the contamination.

Silica and solids based crud make the C272 in the cobalt raffinate partially hydrophilic and the air flotation column efficiency was badly affected. This passed C272 to the V10 nickel circuit. However one of the main causes of the transfer were the shared facilities between the two plants – crud treatment and extraction clean up sumps and pumps. Cross contamination was readily achieved

through these avenues. Subsequent similar plant designs had totally separate crud and spillage handling for all SX plants[10].

If the raffinate is recycled in the plant then any elastomers need to be resistant to the organic constituents[4] or premature failure will result. The direct second stage SX treatment of SX raffinate can have severe consequences from organic entrainment.

The downstream operation in turn can have an effect on the SX plant when these are in closed loops with each other. A well documented case is that of Olympic Dam[4]. The Cu SX reagent in the U SX feed (Cu SX raffinate) causes poor phase separation and significant transfer of deleterious species to the ADU product.

The poisoning of the SX reagent by extraction, interference or adsorption has many manifestations that can be seen as secondary affects:

- Reduced transfer capacity from sites occupied by ions that do not strip
  - Fe in D2EHPA
  - Cu in C301
  - Cr, Mo, etc in USX
  - Cr in C272
  - Rare Earths in D2EPHA in Zn SX
- Reduced transfer kinetics from reduced affective interfacial area – generally involving some sort of surfactant
- Reduced phase separation time due to interference with the surface tension and contact mechanisms – again surfactants or amphoteric ions
- Production of stable emulsions and third phases that do not separate in the time available from reagent degradation, amphoteric ions, silica etc
- Poor selectivity as other ions are transferred by the contaminants particularly humic and other organic acids from plant and animal sources.

Oxidation of the organic can occur in a number of mechanisms:

- Permanganate oxidation of Cu SX via EW electrolyte
- Nitrate oxidation / nitration of Cu SX reagents in Chile
- Air / oxygen oxidation of Cyanex 301.

The oxidation products themselves are the vector for the reduction in SX performance as many are either polar or surfactants or both.

The most widely experienced contamination is that of suspended solids or precipitates within the SX plant. This is the seed for crud formation and all the ills that are associated with this stable three phase emulsion.

Figure 1: Severe Crud Infestation in a Settler

It is the effects of internal SX contamination that can generate primary, secondary and sometime tertiary symptoms that can be very difficult to unravel symptoms from underlying causes[1][9]. The listing in Table1 provides some of the more usual effects but is not sufficiently detailed to try to unravel all the potential outcomes, interactions and symptoms seen. Once a significant event has occurred it is a site specific activity to understand the sequence of events, the closed loops and the interactions of the plant sections in the development of the site of symptoms that are being experienced.

METHODS OF CONTAMINATION CONTROL

The methods of contamination control are based on a hierarchal approach. This approach has shown its strength in the ability to differentiate between the observed symptoms and the real underlying cause of a plant upset condition. It starts with the plant process and mechanical design with the recognition that contamination will occur often. The subsequent steps in the control hierarchy are:

- Eliminate the contamination route
- Prevent the contamination from occurring, which itself may create further effects or subsequent process upsets
- Minimise or control the contamination effects by other methods and hardware. This is the most commonly used method and has generated the widest range of methods and approaches as shown in Table 1
- Treat the resultant symptoms and outcomes to minimise their economic and process impacts. This approach has also generated a myriad of methods and techniques to address the symptoms.

Table 1 contains a short list of the more usual methods of control, minimisation and treatment that have been used in the SX industry. Many others exist that are less well known or have a narrower range of application. Many of the methods are graded on how much of the contamination that they actually remove. For instance dual media filters can remove down to < 5 ppm of entrained organic in the stream. This is acceptable for Cu EW but is not enough for Ni EW. In this case < 1 ppm total (entrained and dissolved) is required and a second stage of organic removal using activated carbon is required.

Elimination

Elimination is not often an option or is costly in hardware or reagents. It is unusual to change leach conditions, but relatively easy to control flocculant addition. More usual is the treatment of PLS before SX to prevent contaminants such as: solids, polymerisable silica, surfactants and other organic contaminating materials. Some strategies in the category include:

• Oil control by containment
• Elimination of treated sewage water from the process water supply (humic and adipic acids)
• Alternate reagent selection that is not affected by the contaminant[12]. This is particularly important for systems containing nitrate in the PLS where organic nitration can be an issue
• Diluent wash of the PLS to remove organic contaminants
• Use of an anti-scalant to either prevent precipitation or to make the precipitate less likely to form crud and to pass out of the SX in the raffinate
• Precipitation of deleterious species esp – Fe, Cr, Mn. Many of these ions that can be precipitated at modest pH can be eliminated in the iron removal step. A two stage process, with recycle of the second stage solids to leach, as used at Bulong and Tati[10][13], was found be to allow higher pH operation with acceptable losses of Ni and Co
• A diluent scrub of the Ni PLS from a C272 cobalt SX was effective in elimination of the entrained C272 at Bulong[13]. A unique saponification method of recovery of the C272 from the scrub diluent meant that it could be returned to the circuit without upsetting the diluent balance.

Figure 2: Diluent Scrub at Bulong- including Saponification section.

By eliminating the contaminant from entering the SX the risks of upsets can be minimised.

Prevention

The prevention strategies are seldom totally effective and minimisation is rather the goal. Physical removal methods fall into this category as does chemical modification of the PLS.

• The major PLS treatment is for removal of suspended solids to ppm levels as a means of crud control
• The other major element to be prevented from entering the SX is silica in a polymerisable form. This can be precipitated when an iron removal stage is used; or sequestered with long chain poly-ethylene-glycols (PEG)[6]. This is a significant issue in uranium SX where the aggressive leach conditions often result in high silica levels in the PLS.
• Filtration, coalescing of organics, activated clay treatment (for organic and Eh control) and PLS diluent and peroxide wash[9] are all methods of managing the PLS constituents

- Adjustments to upstream PLS preparation can also be made to minimise the chemical risk: iron removal by precipitation can minimise the amount of D2EHPA that needs ferric removal by scrubbing. Similarly the removal by precipitation can minimise the presence of other amphoteric ions.

One of the most difficult things is to continue the prevention strategy throughout the life of the operation. As plant management changes so much of the history can be lost and plant operation revert back to less difficult methods. In some cases this has led to a recurrence of the problems that had been sorted out by the elimination strategy.

Minimisation and Control

This strategy is aimed at minimising the effects inside the SX plant and trying to control the level of contamination effects that result. It uses very similar strategies to the symptom treatment protocols. As a result it is often difficult to separate the control aspect from the symptom treatment aspect. Some of the more obvious minimisation methods are:

- Ensuring maximum loading of the desired species on the organic to crowd off unwanted ions. This is an especially effected method in Cu SX where iron crowding can be achieved
- Use of synergistic reagent mixture that can all but eliminate the transfer of an unwanted ion[13]. Recent developments in Ni SX have shown that the calcium transfer in extraction can be managed to eliminate gypsum precipitation in the circuit
- Use of higher aromatic diluent (20%) can minimise crud production while enhancing transfer kinetics[18]
- Selection of unmodified reagents in Cu SX can minimise crud production[12]. Alternatively a different modifier can be used that has less of an effect on crud production
- In U SX the organic can ne pre-protonated to minimise the co-extraction of other ions[4]. This in turn minimises the organic poisoning by the other ions
- Provision of an inert gas atmosphere in some operations is required to minimise the organic oxidation by atmospheric air. The Ga SX in WA and Goro Nickel are two recent examples of this technique

Figure 3: Gallium SX Plant with Nitrogen Atmosphere.

- Use of VSD's on pump mixers can:
  - Minimise crud production
  - Reduce air entrainment
  - Improved phase break times
  - Minimise entrainment
- Planning tools for manganese control in Cu EW can provide good guidance on the strategy to be adopted in minimisation of this ion transfer[2]. By understanding the transfer mechanisms and the methods of management a coherent plan can be developed.

Symptom Treatment

Symptom treatment has received a lot of attention especially for control of PLS transferred to the concentrated strip solutions. Physical methods of entrainment control include:

- Settler enhancements and improved internal designs to improve phase separation[15]
- Coalescing of PLS from the loaded organic[16]
- Washing the loaded organic to dilute the entrainment[10]
- Coalescing, filtration, diluent scrubbing, of organic from the raffinate and concentrate streams
- Change of the organic mix to enhance phase separation such as an alternate reagent or addition of the third phase modifier [6][9][12][15]
- Regular removal and separation of crud to lower the risk of a crud run[16].

Figure 4: Settler Coalescing Media in use

Figure 5: Loaded Organic Coalescer ready for cleaning

Chemical control relates to both the transfer of ions to the concentrate stream as well as removal of poisons from the organic phase. Transfer controls include scrubbing of the ion from the organic as

well as reductive stripping for multivalent ions. Organic rehabilitation methods are quite SX system specific but are widely practiced.

- Activated bentonite clay treatment of copper oxime/ketoxime extractants[18]
- Caustic scrubbing of U SX reagents to remove amphoteric ions and humic acid[1][9]
- Ethanol regeneration of U SX organic to remove Cu SX organic entrained in the PLS[4].

Many of these activities have led to the development of specific hardware and methods to undertake the symptom treatment.

- Dual media filters with and without internal coalescing systems
- Loaded organic coalescing tanks
- After settlers and coalescing systems
- Organic recovery from ponds with rope mops and floating skimmers

Figure 6: Organic Recovery from Raffinate Pond with a Rope Mop

- Operator friendly crud removal systems that eliminate much of drudgery associated with this activity
- Easier crud treatment with three phase centrifuges of robust construction and relatively high capacity

Figure 7: Permanent Crud Removal Piping in a Settler

- Clay treatment of Cu SX reagents using pressure filters and more recently three phase centrifuges
- On line bypassing (and a spare mixer-settler) in systems with high scaling and gypsum precipitation risks
- Provision of both organic and aqueous recycles to allow operation of all stages in either continuity as required by the presence of silica, crud, precipitates etc.
- Use of pre-saponification of C272 and D2EPHA reagents to eliminate the risk of precipitation when using NaOH for pH adjustment.

Subsequent symptoms treatment follows the same path of physical and chemical controls. The best known of these is the combination of primary controls and secondary symptom treatment for controlling manganese oxidation in Cu EW transferred as a result of silica based floating crud[8][16].

- All stages of SX are run in organic continuity to form interfacial compacting crud
- The high (and even extreme) entrainment of PLS in the loaded organic is managed by improved settler performance and stream specific coalescing of the loaded organic
- A wash stage is included to wash the entrained PLS Fe and Mn but to retain the Fe chemically transferred on the organic
- Regular removal of interfacial crud to limit the risk of a "crud run" transferring high volumes of PLS
- Regular clay treatment of the organic to remove the degradation products of the residual levels of manganese oxidation
- Maintenance of a high Fe:Mn ratio in electrolyte by either increasing Fe SX transfer (less selective reagent, more reagent, altering the wash conditions) or addition of ferrous sulphate to the electrolyte
- Potential use of Eh management in electrolyte with options such as: copper metal reduction tower, SO_2 gas reduction, iron addition via ferrous sulphate or iron shavings and high concentration of cobalt in electrolyte.

This particularly complex solution set is not untypical of the lengths to which process and equipment need to be added, to change the operating conditions; and to address the contamination management and the secondary after effects of the primary programme adopted.

CONCLUSION

Contamination management is specific to the SX system; as to what contaminants are important and what techniques to use - U SX is very different to Cu SX.

Some PLS contaminants are universal – surfactants, silica, humic acids etc and their management is also reasonably straight forward. Others are not as widely encountered and their management is very site specific.

Often the management of a specific contaminant will entail the management of secondary and tertiary effects of the primary activity. These can become complex and interactive.

Many tools are available, from which to select an appropriate set, to address each specific contaminant.

ACKNOWLEDGEMENTS

REFERENCES

1. Ritcey, G. "Enhancement of Plant Performance by Control of Organic Surfactants and Poisons", ISEC 2005, pp 1205-1210.

2. Miller, G. & Readett, D. "Solvent Extraction Entrainment Control – Needs and Strategies", ALTA 2003 SX/IX World Summit, Perth.

3. Barnard, K. R. "Aqueous in Organic Entrainment Analysis" ISEC 2008 Vol II, pp 909-914.

4. Dudley, D., Lawson, B. & Wilson D. "Hydrometallurgical Operations at Olympic Dam", ALTA Copper Conference 2003, ALTA Metallurgical Services, Perth.

5. Laitala H., Ekman E. & Karcas G. "Some Practical Aspects for Impurity and Crud Control in Solvent-Extraction Processes", ISEC 2008, Vol I, pp 473-478.

6. McKenzie, M. "Emulsions in solvent Extraction some Interfacial Chemistry Concepts" LIX Users Conference 2008, Pilanesberg, August, Cogis Corporation.

7. Menacho, J. M., Gutierrez, L. E. & Zivkovic, Y. I."A Dynamic Model for Chloride control in SX Plants", Copper 2003 – Cobre 2003, Vol VI Hydrometallurgy of Copper (Book 2), P. A. Riveros, D. Dixon, D. B.Dreisinger & J. Menacho (eds), pp 517 – 529.

8. Miller, G. M., Readett, D. J. & Hutchinson, P. "Experience in Operating the Girilambone Copper Circuit in changing Chemical Environments", Minerals Engineering, Vol 10, No5, pp 467-481, 1997.

9. Ritcey, G. "Some Design and Operating Problems Encountered in Solvent Extraction Plants", ISEC 2002, K. C. Sole, P. M. Cole, J. S. Preston & D. J. Robinson (eds) pp 871 – 878.

10. Robles, E., Cronje, I. & Nel, G. "Solvent Extraction Design Considerations for the Tati Activox(R) plant. Hydrometallurgy Conference 2009, the SAIMM, pp 257-271.

11. Collao I, N., Jenneman, G. E., Sublette, K., Bishop, M. D., Young, S. K. & Morrison A. G. "Biological Degradation of Solvent Extraction Circuit Plant Organic", Hydrometallurgy 2003 – Fifth International Conference in Honour of Professor Ian Ritchie, Vol I: Leaching and Solution Purification, C. A. Young, A. M. Alfantasi, C. G. Anderson, D. B. Dreisinger, B. Harris & A. James (eds) TMS, pp 1003- 1022.

12. Kordosky, G. & Virnig, M. "Equilibrium Modifiers in Copper Solvent Extraction Reagents – Friend or Foe?" Hydrometallurgy 2003 – Fifth International Conference in Honour of Professor Ian Ritchie, Vol I: Leaching and Solution Purification, C. A. Young, A. M. Alfantasi, C. G. Anderson, D. B. Dreisinger, B. Harris & A. James (eds) TMS, pp 905-916.

13. Nofal, P., Allen, S., Hosking, P. & Showell, T. "Gypsum control at Bulong the final hurdle? ", ALTA Ni-Co Conference 2001, ALTA Metallurgical Services, Perth.

14. du Preez, R., Kotze, M., Nel, G., Donegan, S., & Masiiwa, H., "Solvent Extraction Test Work to Evaluate a Versatic 10 and Versatic 10/NicksynTM Synergistic System for Nickel-Calcium Separation", SAIMM, Fourth Southern African Conference on Base Metals, pp 193-210, 2010.

15. Polski, I. "Extreme Situations of Emulsions Separation in the Copper Solvent Extraction Plants", Hydroprocess 2006, E. M. Domic & J. M. Casas de Prada (eds), pp 169-178.

16. Miller, G., Readett, D. & Hutchinson, P. "Entrainment Coalescing in Copper SX Circuits" ISEC '96, Vol II, pp 795-800.

17. Feather, A., Virnig, M., Bender, J. & Crane, P. "Degradation Problems with Uranium Solvent Extraction Organic", ALTA Uranium Conference 2009, ALTA Metallurgical Services, Perth.

18. Haig, P. "Diluent Chemistry & SX Safety", LIX Users Conference 2008, Pilanesberg, South Africa, August, Cognis Corporation.

Table 1: Contamination Sources, Effects and Treatments

Source	Contamination	Direct effect on process	Indirect effect on process	Treatment - direct	Treatment - indirect / symptom	References
Further Upstream	Leached ions - Zr, Cr, Mn, Fe, Mo, RE, Si	Solvent poisoning,	Reduced extraction, impurity transfer,	Modify leach conditions, add steps to eliminate ion - precipitate, IX , Si coagulant.	Organic NaOH/Na2CO3 scrub, HCl scrub, wash	4,9
Feed to SX (PLS)	Solids, scale	Crud, poor phase separation	Impurity transfer	Thicken, clarify, filtration	Settler water spray => Compact crud	5,9
					Alternate organic to minimise crud (extractant, diluent, modifier); alternate process - RIP ??	5, 9, 12, 17
	Saturated calcium	Co-extraction & scale formation	Crud, vessel blockage,	Max load organic, change pH profile, Ca scrubbing, anti-scalant, synergistic reagent	Increase pipe sizes, bypass & on line cleaning	10, 13, 14
	Extreme TDS & viscosity	Poor phase separation, stable emulsions	Downstream contamination, organic losses	Improved settler coalescing medium		15, 16
	Nitrate from U IX eluate	High Eh & organic degradation	Low transfer capacity		Iron wire Eh reduction, bleed	17
	Chloride in U SX	Co-extract with U	Chloride contamination of product	Pre-protonate reagent to minimise co-extraction	Loaded solvent scrubbing & washing	4,9
	Emulsifiers (detergents, humates, S dispersant, wetting agents, flocculant)	Stable emulsions & slow phase separation, crud, biomass growth in SX,	Impurity transfer, equipment blockage	PLS treatment - diluent wash, H2O2, activated carbon, biocide addition, Si coagulant	Clay treat Cu SX organic, NaOH / Na2CO3 solvent scrub	1, 4, 6, 9, 10, 18
	Amphoteric metals (Bi, Zr, Si)	Crud generation	Stable emulsions, slow phase separation impurity transfer	Si with coagulants in PLS treatment	Change operating pH, change mixer continuity, in-settler coalescing, use non-modified reagent	1, 8, 9, 12, 16
	Flocculant,	Foaming, floating crud ('cheese', 'snot' etc)	Slow phase separation, impurity transfer	Diluent wash of PLS, H2O2 PLS treatment	NaOH/Na$_2$CO$_3$ solvent wash	1, 9, 18
	Extractant from upstream SX	Poor ionic separation, poor phase disengagement	Impurity transfer, contaminated product	Crud removal, after settler, diluent wash, organic flotation, dual media filtration, activated carbon removal	Oxime scrub with methanol in USX, replace organic inventory	1, 4, 10, 13
	Biomass	Biomass growth in SX, crud, organic degradation, third phase formation	Crud, high organic & diluent consumption, poor phase separation, poor recovery	Regular cleaning to remove biomass, add biocide	Organic clay treatment, continual crud removal to reduce biomass	8, 9, 11
	High Eh / oxidant / temperature	Organic oxidation / degradation	Poor selectivity, poor phase disengagement, crud	Reduce leach oxidant add, Eh reduction- Cu scrap, SO2, Fe:Mn ratio control, Fe add to Cu EW	Caustic wash, clay treatment, reduce contact time, change reagent	3, 8, 9, 12, 16
SX Internal	Scale formation	Crud, poor phase separation	Solvent loss	Antiscalant, PLS dilution	Change upstream process	5, 13
	Degradation of alcohol phase modifier to carboxylic acid	Extract non target metals with carboxylic acid	Contamination of 'purified' stream	NaOH organic wash,		1, 9 , 18
	Air entrainment in mixers	Organic oxidation / degradation	Poor selectivity, poor phase disengagement, crud	Inert gas blanket (Goro, Ga SX)	Caustic wash	9
		Stable emulsion formation, aerosol formation	Slow phase separation, impurity transfer, fire risk	VSD on pump mixer, advance valve for high launder operation		8, 9
	Oil from mixer gear boxes	Stable emulsion, organic contamination	Slow phase separation, impurity transfer, poor extraction	Oil catch trays	Clay treat organic	9, 12
	Insects - organic acids & proteins	Stable emulsions, organic contamination	Slow phase separation, impurity transfer, reduced selectivity, crud	Enclosed mixer-settlers	Clay treat organic, increase aromatic content of diluent,	9, 18
	High organic loading,	Third phase formation	Poor phase separation, high organic consumption	Add modifier, increase diluent aromatic content		4, 9
	PLS in loaded organic	Contamination of strip solution	Impurity transfer, poor product quality	Improve settler performance - picket fences, coalescing; loaded organic coalescer, change operating continuity, change extractant to minimise entrainment	Washing / scrubbing stage(s)	3, 4, 5, 8, 12, 16
				Improve mixer phase stability O:A control	Change reagent, add third phase modifier	1, 4 9, 10 ,12
SX Output	PLS entrained to EW	Chloride pitting SS EW cathodes	Chlorine gas evolution	Improve settler performance - picket fences, coalescing systems, feed distribution, organic depth,	Coalescer on organic, wash stage	7, 8, 16
	Organic entrained to EW	Organic burn (Cu), cathode pitting (Ni, Zn & Co)	Hydrogen gas evolution	Organic removal- MM filter, flotation, activated carbon	In-settler coalescing	8,16
	Organic entrained to raffinate	Reagent loss, contaminate down stream SX plant	Elastomer degradation,	Change pH	In-settler enhancements, after settler, stream coalescing, flotation, MM filter, diluent scrub, activated carbon, change pH	8, 10, 12, 13, 14, 16

231

CYANEX™ 272 EXTRACTANT PROCESS MODELLING UPDATE

By

Matthew Soderstrom, Cyril Bourget, Boban Jakovljevic

Cytec Industries Inc., USA

Presenter and Corresponding Author

Cyril Bourget
cyril.bourget@Cytec.com

ABSTRACT

The Minchem program for predicting the expected metallurgical performance of CYANEX 272 circuits is continually being enhanced. To overcome the challenges of non-convergence, a methodology has been developed for quicker assessment of circuit conditions.

The optimum configuration of a plant will vary depending on the specific feed conditions and targeted separations. The program allows a quick assessment of these variables and provides data to enable capex / opex calculations to be made. The program supports quick assess when the addition of staging has reached the point of diminishing returns and also allows an operator to focus on the optimum pH to achieve high reagent utilization while maximizing metal separations.

Much time has been spent to develop base data, a simulation approach and program the logic. This automation requires expert management and some manual work to provide the output. The system will be further developed over the next year to improve ease of use although it is fully effective in its current form.

INTRODUCTION

The simulation software program for Ni/Co applications, CYANEX™ Minchem, has been developed to assist operators and engineering companies to optimize and design solvent extraction circuits utilizing CYANEX™ 272 extractant. This modelling software has succeeded in assessing multiple circuit configurations and better defines the trade-off between capital and operating expense.

This paper will review some challenges that were encountered with the program and the enhancement steps taken. It also describes the methodology currently being used to assess various metal separations along with the learning from the simulations completed to-date.

CURRENT STATUS / CHALLENGES

The program calculates the outlet composition of a mixer given the inlet composition, equilibrium pH, and O/A ratio. The calculation involves the simultaneous solution of multiple equilibrium calculations based on pre-generated equilibrium data. It takes into account metal / metal organic phase interactions as well as alterations in the metal ligand complex. The calculated outlet compositions can then be used to obtain an iterative solution to a multi stage plant.

The program completes a number of iterations until all mass balance conditions have been met to a given sensitivity. It will then provide a summary of the expected metal compositions for each stage dependent on the specified operating conditions (stage pH, O/A, stage efficiency).

An example of the program output is shown in Figure 1 where a feed containing Co, Mn, and Mg is treated in a 3 extract stage configuration utilizing 10 vol% CYANEX 272 at 50 deg C.
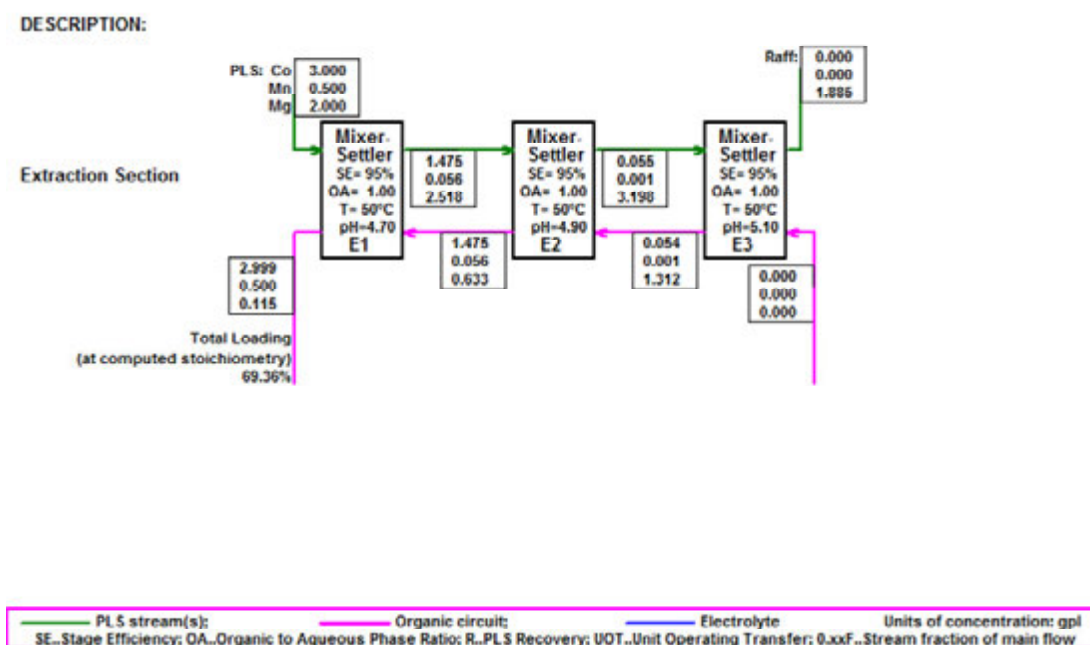

Figure 1: Simulation of 3 stages of extraction

As shown, the calculated circuit indicates the loaded organic would contain all of the cobalt and manganese, while co-extracting 115 ppm of the Mg. The interstage metal compositions show what would be expected to occur in each stage. As indicated, by stage E2 essentially all of the Mn would be expected to have loaded and by E3 all of the Co.

Unfortunately, at present, with 4 stages of extraction (and a high E4 pH) the program is not able to converge on a solution. The iterative calculations fail due to the inlet/outlet composition of stage E4 being too low (the near zero value is used within the subsequent equilibrium calculations resulting in the error). Figure 2 shows the NON CONVERGED output, while Figure 3 shows the program will

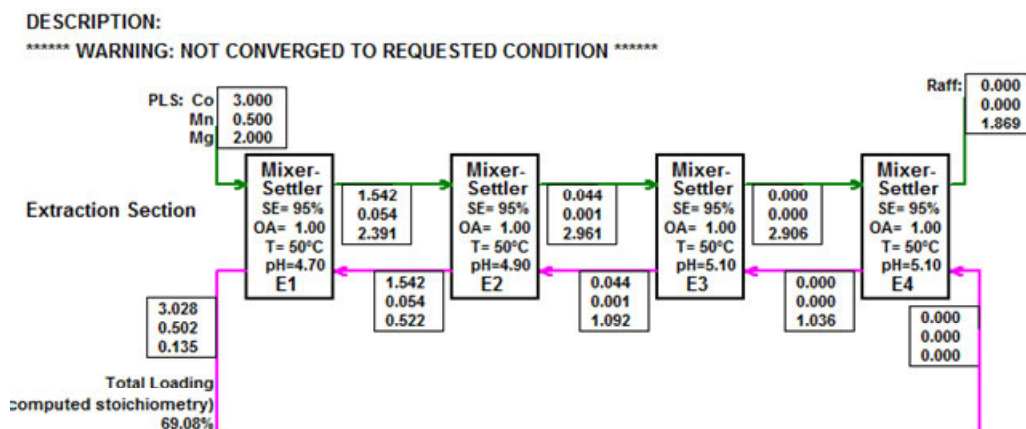converge if the conditions are altered slightly to avoid the calculated zero value (avoided with a lower E4 pH).

Figure 2: Non-converged circuit due to excessive staging relative to the aqueous metal composition
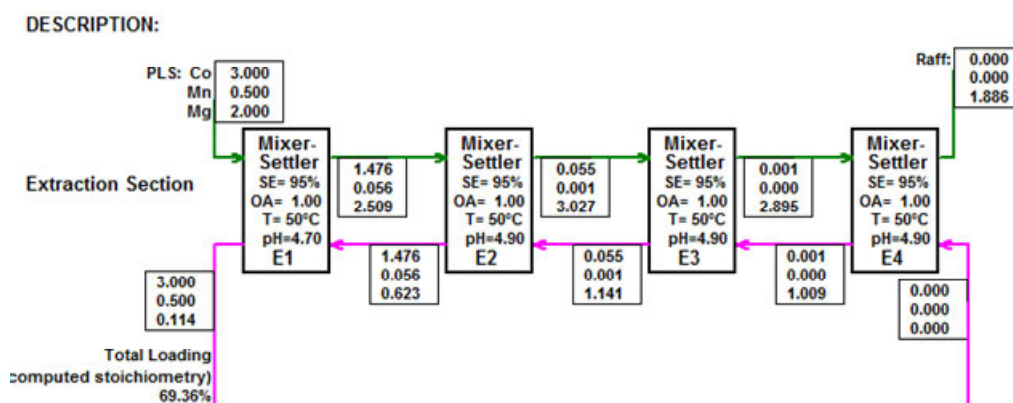

Figure 3: Converged 4 stage extraction circuit

Work is underway to exclude metals from the iterative calculations when their equilibrium concentrations approach zero. In the meantime, in order to simulate a complex circuit, the program is being used to provide the equilibrium output from a single stage and then this output is being used to complete the iteration by hand.

ITERATIVE SOLUTION

For a four stage circuit, the calculations are completed for stage E1 assuming an input of the full PLS composition and metal free barren organic. The program solves all the simultaneous equations based on the pre-generated equilibrium data, The outlet aqueous composition is then used as the feed to stage E2 again with a metal free barren organic as a first stage approximation. The calculated outlet composition is recorded (both aqueous and organic metal concentrations) and the aqueous is used as the inlet composition for stage E3. Similarly, the iterative process is carried out for E3 and E4. For the second series of iterations again the PLS composition will be entered as the feed to E1 but the estimated E2 organic composition from the first series of calculations will be used as the organic metal input. The stepwise iteration will be continued until there is a full mass balance across the entire extraction circuit; where the (PLS – Raffinate) / O/A ratio = Loaded organic – Barren organic for each metal of concern. With the step wise iteration, it is possible to eliminate any

metals from the single stage calculation if the iterative process indicates the metal should not be present for a given stage.

Table 1 shows a few iterative steps for a plant treating a Co, Mg, Ni feed. A suitable answer for this feed was obtained after 88 stage wise calculations.

Table1: Step wise iteration process for a three component feed

Metal	E1 PLS input	E1 Org input	E1 Aq output (Raff to E2)	E1 Org Output (Final Loaded Org)	E2 Aq input	E2 ORG input	E2 Aq output (Raff to E3)	E2 Org output (Org to E1)	E3 Aq input	E3 ORG input	E3 Aq output (Raff to E4)	E3 Org output (Org to E2)	E4 Aq input	E4 ORG input	E4 Aq output (Raff)	E4 Org output (Org to E3)
Co	1.800	0.000	0.024	1.776	0.024	0.000	0.000	0.024	0.000	0.000	0.000	0.000	0.000	0.000	0.000	0.000
Mg	1.000	0.000	0.645	0.355	0.645	0.000	0.250	0.395	0.250	0.000	0.077	0.173	0.077	0.000	0.022	0.055
Ni	120.000	0.000	119.706	0.294	119.706	0.000	119.037	0.669	119.037	0.000	118.211	0.826	118.211	0.000	117.297	0.914
Co	1.800	0.024	0.026	1.798	0.026	0.000	0.000	0.026	0.000	0.000	0.000	0.000	0.000	0.000	0.000	0.000
Mg	1.000	0.395	0.957	0.438	0.957	0.173	0.495	0.635	0.495	0.055	0.205	0.345	0.205	0.000	0.060	0.145
Ni	120.000	0.669	120.409	0.260	120.409	0.826	120.717	0.519	120.717	0.914	120.915	0.716	120.915	0.000	120.061	0.854
Co	1.800	0.026	0.027	1.799	0.027	0.000	0.000	0.027	0.000	0.000	0.000	0.000	0.000	0.000	0.000	0.000
Mg	1.000	0.635	1.159	0.476	1.159	0.345	0.710	0.794	0.710	0.145	0.358	0.497	0.358	0.000	0.125	0.233
Ni	120.000	0.519	120.277	0.242	120.277	0.716	120.571	0.422	120.571	0.854	120.811	0.614	120.811	0.000	120.020	0.791
Co	1.800	0.027	0.028	1.799	0.028	0.000	0.000	0.028	0.000	0.000	0.000	0.000	0.000	0.000	0.000	0.000
Mg	1.000	0.794	1.299	0.495	1.299	0.497	0.896	0.900	0.896	0.233	0.492	0.637	0.492	0.000	0.181	0.311
Ni	120.000	0.422	120.188	0.234	120.188	0.614	120.433	0.369	120.433	0.791	120.700	0.524	120.700	0.000	119.964	0.736
Co	1.800	0.028	0.028	1.799	0.028	0.000	0.000	0.028	0.000	0.000	0.000	0.000	0.000	0.000	0.000	0.000
Mg	1.000	1.101	1.574	0.526	1.574	0.999	1.471	1.102	1.471	0.620	1.092	0.999	1.092	0.000	0.472	0.620
Ni	120.000	0.269	120.049	0.220	120.049	0.323	120.103	0.269	120.103	0.532	120.312	0.323	120.312	0.000	119.780	0.532
Co	1.800	0.028	**0.028**	**1.799**	0.028	0.000	**0.000**	0.028	0.000	0.000	**0.000**	**0.000**	0.000	0.000	**0.000**	**0.000**
Mg	1.000	1.102	**1.575**	**0.527**	1.575	0.999	**1.472**	1.102	1.472	0.620	**1.093**	**0.999**	1.093	0.000	**0.473**	**0.620**
Ni	120.000	0.269	**120.049**	**0.220**	120.049	0.323	**120.103**	0.269	120.103	0.532	**120.312**	**0.323**	120.312	0.000	**119.780**	**0.532**

As shown, a number of calculations and iterations need to be completed to fully assess a circuit if the program does not converge on its own. In order to minimize the number of 'manual' calculations, a methodology has been developed to help narrow the range of circuit configurations/conditions requiring evaluation.

SIMPLIFICATION OF EXTRACT MODEL CRITERIA

Given a specific feed, an extract O/A ratio is chosen along with the appropriate reagent concentration to achieve a reasonable reagent utilization (based on best guess loading estimates). The reagent concentrations that can be assessed at present are 10, 20 and 30 vol% CYANEX 272 at 50 degrees C. The program is then used to assess the selectivity and recovery achievable as a function of pH and staging for the specified O/A. In cases where the metals present in the feed are clearly going to be fully extracted (resulting in a zero inlet composition and non convergence), the investigative simulations are completed on the critical elements (those with the most similar extraction properties). Once these simulations have narrowed in on the stage and pH requirements – the full step wise circuit analysis may be completed by hand.

Determination of O/A and Reagent Concentration

Given a feed containing Co, Mg, Ni, Mn, and Zn, as depicted in Table 2, with the goal of achieving 100% Co recovery and minimal Mg or Ni extraction, an estimate is made (from experience and S curve data) on what metals are expected to load in an ideal extraction circuit.

Table 2: PLS feed composition

Metal	Co	Mg	Ni	Mn	Zn
Concentration (ppm)	2000	5000	80,000	350	20

S-curves for CYANEX 272 shown in Figure 4, give a relative indication of the metal ligand complex strength. Although the S-curves are only indicative, they do allow one to estimate the relative order of metal loading. From the data, it would be expected that all Zn would load first (being at a lower pH than Co), the Co and Mn would co-load (due to the similarity in the metal complex strength for similar conditions), and there would be some Mg co-extraction (as an estimate say 400 ppm – due to its S curve position relative to Co). Based on this assessment, the moles of ligand which would be involved in the extraction reactions can be estimated for a 1:1 O/A ratio as shown in Table 3.
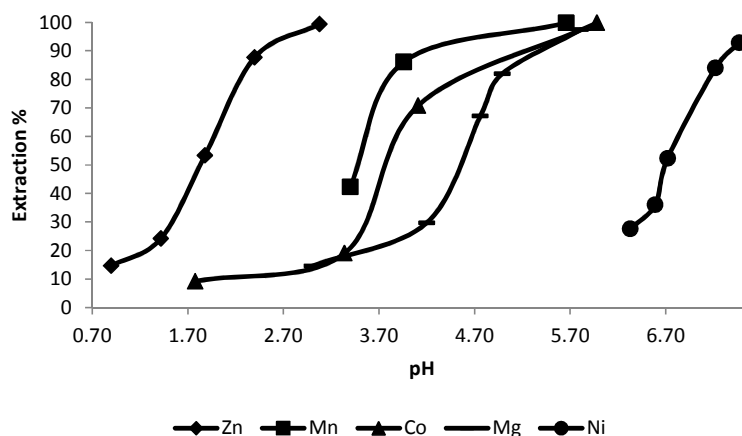
Figure 4: Standard S-curve data for CYANEX 272

Solution conditions: 0.001 M Metal (as sulfates), 0.1 M CYANEX 272, O/A=1, Temp=50°C

Table 3: Estimate of organic metal composition

Metal	Co	Mg	Ni	Mn	Zn
Assumed Organic Metal Composition (ppm)	2000	400	0	350	20
Organic Metal (moles)	0.034	0.016	0	0.0064	0.0003
Ligand required (moles)	0.068	0.032	0	0.0128	0.0006
Total Stoichiometric Moles Ligand involved	0.114				

To achieve high reagent utilization while minimizing risk of phase disengagement issues due to excessive loading, a target load of ~55% of the stoichiometric load is recommended. For the above case, the total stoichiometric moles of ligand required would be 0.114. 10 vol% CYANEX 272 contains ~0.27 Moles of phosphinic acid, which would give a percent loading of 0.114/0.27 or ~42%. In order to achieve 55% loading, the O/A ratio in extract could be lower making more metal available to the reagent in the extract stage. In this case, an O/A ratio of 0.77 (0.42/0.55) or a lower reagent concentration (7.7 vol% corresponding to 0.21 moles ligand) could be utilized to achieve high organic loading. At this time (since the calculations are currently limited to a fixed initial reagent concentration), the O/A ratio is estimated to achieve high loading for one of the fixed reagent concentrations (10, 20, or 30 vol%).

Optimization of Ph and Staging on Specific Metal Separation

Once the target reagent concentration and O/A ratio are known, the program is then used to estimate the pH and staging requirements needed to achieve the targeted goal. Since the Co/Mg separation would be expected to be the most difficult for the specified feed, the program would be used to quickly focus on the conditions that would best achieve that separation.

As shown in Table 4, high cobalt recovery (>99%) would be achievable in 2 extract stages operating at a pH of ~4.8 while achieving a Co/Mg ratio in the loaded organic of ~7.0. The use of additional extract stages, would allow the use of lower pH's (improving the Co/Mg separation) while still achieving high cobalt recovery. The exact number of extract stages chosen would be dependent on the specific Co/Mg ratio targeted in the loaded organic.

Table 4: Simulated program output for Co/Mg at varying pH and extract stages

Extract Staging	pH	LO Co (g/L)	LO Mg (g/L)	Raff Co (g/L)	Raff Mg (g/L)	LO Co/Mg Ratio
2	4.70	2.558	0.316	0.030	4.756	8.1
2	4.80	2.579	0.382	0.014	4.706	6.8
2	4.90	2.586	0.424	0.009	4.674	6.1
3	4.50	2.558	0.197	0.031	4.848	13.0
3	4.70	2.595	0.309	0.002	4.762	8.4
4	4.50	2.582	0.192	0.004	4.852	13.4
4	4.40	2.542	0.144	0.043	4.889	17.7
5	4.50	2.597	0.192	0.000	4.852	13.5
5	4.40	2.582	0.140	0.012	4.892	18.4

Once the program has been used to narrow in on what should be near optimum pH conditions and the extract staging has been chosen, the entire circuit may then be simulated in a step wise manner, if necessary, (including the additional metals) to provide the expected performance.

Based on the results from Table 4, a circuit was modelled for a 3 stage extraction circuit with a pH profile of 4.5 to 4.7 across E1-E3 (lowest E1 pH to achieve high selectivity while highest E3 pH to ensure high cobalt recovery). The converged process flow diagram is shown below in Figure 5. Had the circuit not converged, the manual simulation would produce the same results (just requiring significantly more time to complete all the iterations).
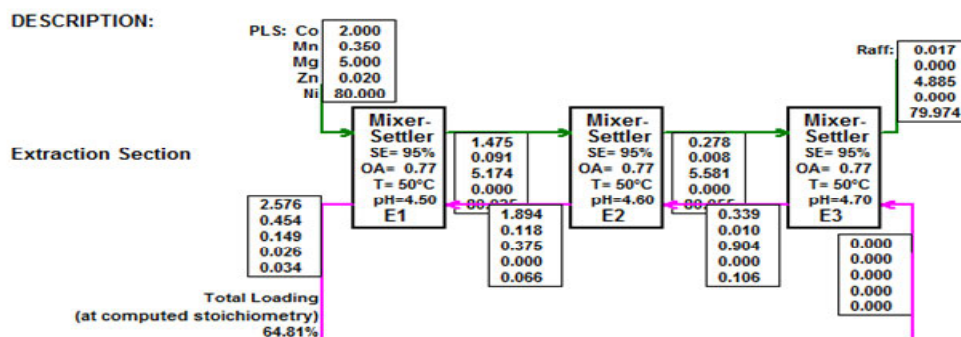
Figure 5: Simulated process flow diagram with a pH Profile of 4.5 (E1), 4.6 (E2) and 4.7 (E3)

SCRUB STAGE MODELLING

Similar calculations/methodology as used in extract may be used to simulate the scrub stage configuration/pH. Again, to simplify and reduce the number of iterations, the initial modelling may be focused on the most difficult separation.

For this series of simulations, a loaded organic feed composition of 2.55 gpl Co and 0.20 gpl Mg was used (estimated LO composition from Table 4 (excluding the additional metals)). The scrub liquor utilized in the simulations was acidified water. Table 5 shows the results for varying pH and scrub staging utilizing the cobalt free scrub liquor. The amount of cobalt which would need to be recycled from the spent scrub liquor was calculated based on a 50 m^3/hr organic flow, 10:1 scrub O/A ratio, and 0.77 extract O/A ratio. The cobalt recycle (spent scrub liquor Co content) was estimated as a percentage of the cobalt in the feed to extract.

Table 5: Simulation output for scrub

Stage	Co Scrub (g/L)	pH	LO Co (g/L)	LO Mg (g/L)	Spent Scrub Co (g/L)	Spent Scrub Mg (g/L)	LO Co/Mg	% recycle
1	0	4.00	2.067	0.022	4.809	1.785	94.0	18.5
1	0	4.20	2.286	0.039	2.642	1.610	58.6	10.2
2	0	4.20	2.215	0.010	3.353	1.900	221.5	12.9
2	0	4.30	2.321	0.017	2.289	1.828	136.5	8.8
3	0	4.20	2.188	0.003	3.616	1.974	729.3	13.9
3	0	4.30	2.310	0.006	2.404	1.945	385.0	9.3
4	0	4.30	2.306	0.002	2.440	1.980	1153.0	9.4
4	0	4.40	2.392	0.007	1.577	1.935	341.7	6.1

As shown, the ratio of Co to Mg in the scrubbed loaded organic can be increased from ~10:1 in extract up to 1000:1 dependent on the number of stages utilized. The pH of the scrub staging has a direct impact on the amount of Co recycled in the spent scrub liquor back to the feed solution. There is a direct trade-off between the separation achieved and the amount of cobalt which would need to be reprocessed.

Based on these evaluations, a full scrub stage circuit was modelled utilizing 2 scrub stages. The intention was to achieve as high a Co/Mg selectivity as possible while not exceeding a Co recycle of 10-12%. The pH targeted for the two scrub stages was 4.2 in Sc2 and 4.4 in Sc1 (as indicated by Table 5 simulations).

The loaded organic was taken from the converged extract model including the Co, Mn, Mg, Zn and Ni (E1 organic composition from Figure 5). In a two stage scrub circuit the program would not converge and required a stepwise iteration. Following ~14 iterations a reasonable mass balance was obtained and the results are shown in Figure 6.
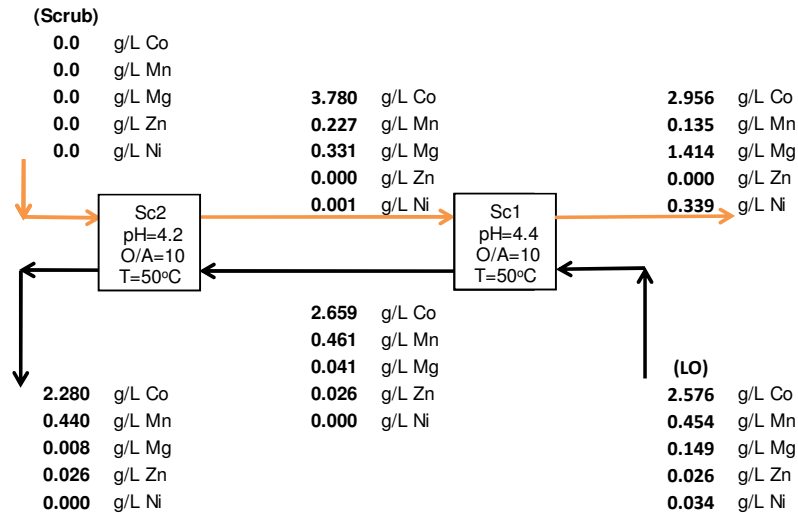
Figure 6: Simulated scrub process flow diagram with a pH Profile of 4.4 (Sc1) and 4.2 (Sc2)

Utilizing two scrub stages, the Co/Mg selectivity was increased from ~17.3 to 285, while generating a Co recirculating load of 11.4% (similar to what would be expected based on the simplified modelling).

CONCLUSIONS

The Minchem program for predicting the expected metallurgical performance of CYANEX 272 circuits is continually being enhanced. To overcome the challenges of non-convergence, a methodology has been developed for quicker assessment of circuit conditions.

The optimum configuration of a plant will vary depending on the specific feed conditions and targeted separations. The program allows a quick assessment of these variables and provides data to enable capex / opex calculations to be made. The program supports quick assess when the addition of staging has reached the point of diminishing returns and also allows an operator to focus on the optimum pH to achieve high reagent utilization while maximizing metal separations.

Much time has been spent to develop base data, a simulation approach and program the logic. This automation requires expert management and some manual work to provide the output. The system will be further developed over the next year to improve ease of use although it is fully effective in it's current form.

THE DEVELOPMENT OF A NEW DSX PROCESS FOR THE SEPARATION OF NICKEL AND COBALT FROM IRON AND ALUMINIUM AND OTHER IMPURITIES

By

C.Y. Cheng, Z. Zhu and Y. Pranolo

The Parker Centre / CSIRO Process Science and Engineering /
CSIRO Minerals Down Under National Research Flagship, Australia,

Presenter and Corresponding Author

Chu Yong Cheng
chu.cheng@csiro.au

ABSTRACT

A new synergistic solvent extraction (SSX) system has been developed in CSIRO recently to separate nickel and cobalt from iron and aluminium and other impurities. A new CSIRO DSX process has been created using the new SSX technology to directly recover nickel and cobalt from laterite leach solutions without intermediate precipitation and re-leach steps. This is a significant development for the recovery of nickel and cobalt from laterite leach solutions, especially from heap leaching (HL) and atmospheric leaching (AL) solutions. The new CSIRO DSX process has the following advantages:

- Making the direct recovery of nickel and cobalt from HL, AL and HPAL solutions possible without the removal of iron and aluminium,

- Separation of nickel and cobalt from iron, aluminium and other impurities in low pH to avoid nickel and cobalt losses in neutralisation or precipitation steps,

- Possible savings in capital and operating costs if applied to HPAL processes since the CCD system for neutralisation, precipitation and solid/liquid separation can be simplified,

- All organic reagents are commercially available and in reasonable prices,

- The process flowsheet is much simplified to save capital and operating costs.

- The new CSIRO DSX process can be readily coupled with nickel hydrolysis, electrowinning and hydrogen reduction to obtain different nickel products.

INTRODUCTION

The world mineral industry is experiencing an unprecedented interest in nickel-cobalt extraction from laterite ores through high pressure acid leach (HPAL) and subsequent recovery processes. In WA, the Murrin Murrin (Motteram et al., 1996) nickel plant is in operation and the Ravensthorpe nickel plant is being reactivated. In New Caledonia, the Goro nickel plant (Mihaylov et al. 2000) is in the process of commissioning. The HPAL process for these projects is very similar with very high capital investments and high operation costs.

Heap leaching (HL) needs much less capital and operating costs than those for HPAL. However, the separation of nickel and cobalt from iron and aluminium is much more difficult in the HL leach solution than that in the HPAL leach solution. In the later, the concentration of iron and aluminium concentration is in the range of 1-2 g/L (Motteram *et al.* 1996). When the iron and aluminium are precipitated in the pH range of 4-5, only a small acceptable amount of Ni and Co would be lost due to adsorption because the amount of precipitated solids is small. A typical atmospheric leach (AL) solutions contains about 6 g/L Fe and Al (Liu *et al.* 2004) and a typical HL solution contains about 25 g/L Fe^{3+} and Fe^{2+} and 3 g/L Al (Diniz 2006). If all iron and aluminium are precipitated, most nickel and cobalt would be lost in the precipitates.

To separate nickel and cobalt from iron and aluminium has been a long-standing problem. Investigations started from early 1980s using SSX systems consisting of di-nonylnaphthelene sulphonic acid (DNNSA) and N-alkylated bis-picolylamines were tested with very good results (Grinstead 1980, Ginstead and Tsang 1983, Inoue *et al.* 1997a and 1997b). The metal extraction order was found to be Ni > Co > Fe(III)/Mn/Al/Mg. Nickel was preferably extracted and could be separated from cobalt and iron at pH < 2.0. The separation of cobalt from iron required pH around 2.6. However, no commercialisation of this system has taken place due to poor phase disengagement (Flett 2004).

The solvent extraction of Ni and Co by a synergistic system, containing DNNSA and 2,6-bis-[5-n-nonylpyrazol-3-yl]pyridine (BNPP) was studied (Zhou and Pesic 1997). In terms of pH_{50}, the system extracted Cu, Ni and Co (<1.0) selectively over Fe, Mn (1.62), Ca (2.47) and Al (3.22) from acidic sulphate solutions as low as pH 0.5. The separation of Ni and Co could be achieved either during loading or stripping because of the difference in extraction and stripping kinetics of the two metals. The system was found to be poisoned by copper and also suffered from slow kinetics of nickel. Preston and du Preez (1998) studied the synergistic solvent extraction of base metals with DNNSA and pyridinecarboxylates. The metal extraction order was found to be Cu > Ni > Al > Co > Ca > Zn > Al > Fe(III) > Mg with 3-pyridinecarboxylates and Cu > Ni > Co > Zn > Al > Fe(III) > Ca > Mg with 2 and 4-pyridinecarboxylates. In four-stage batch counter-current extraction tests, up to 95% Ni was extracted with a co-extraction of up to 19% Ca and 9% Fe. The relative high Ca and Fe co-extraction after 4-stage extraction could be a concern.

A resin-in-pulp process using Ion exchange (IX) with Dowex M4195 resin was reported by Duyvesteyn and Omofoma (1997) for the separation of Ni from Co and Fe in laterite leach solutions. The disadvantages of this process are that nickel cannot be completely separated from Fe(III) especially if the concentration of Fe(III) is high, and Co cannot be recovered. This process was improved by reducing all iron from ferric to ferrous state followed by recovering both Ni and Co (Duyvesteyn et al. 2002) at pH 3.0. The resin-in-pulp obviously suffers from resin loss, resulting in high operating costs.

Liu et al. (2002) proposed a two-stage IX strategy with Dowex M4195 resin to recover Ni and Co from laterite leach solutions. In the first stage, Ni and Fe(III) are separated from Co and Fe(II) at pH 1.0-2.5. The eluate is then neutralised to make a mixed hydroxide product (MHP) containing Ni and Fe(III), which is roasted to obtain ferronickel product. In the second stage, after partial iron precipitation, the Co is separated from Fe(II) using the same resin at pH 2.0-3.0. The disadvantages of this process are that Ni and Co are separated from iron and recovered in different stages, which makes the process complicated, and the difficulty of adjusting the pH in IX columns presents a practical problem. The low efficiency of ion exchange process is its biggest disadvantage, especially when the absorbed metal's concentration is high such nickel in the range of a few g/L.

The brief literature review above shows that the nickel industry needs SX or SSX systems with commercially available reagents to separate nickel and cobalt from iron, aluminium and other impurities in HL, AL and HPAL solutions. The CSIRO SX group developed SSX systems used for its DSX processes to meet this needs. The development of SSX systems and DSX processes for the purification of nickel and cobalt in laterite leach solutions has passed five phases including:

Phase 1: SSX system consisting of Versatic 10 and CLX50 for the Bulong DSX process to separate Ni from Ca and to solve its gypsum formation problem in 2000-2001 (Cheng 2000).

Phase 2: SSX system consisting of Versatic 10 and 4PC for the BHP Billiton DSX process for the separation of Ni and Co from manganese, magnesium and calcium in 2001-2002 (Cheng 2003, Cheng et al. 2003 and 2004, Cheng and Urbani 2005a).

Phase 3: SSX system consisting of Cyanex 272 and LIX84 for Minera Resources for the separation of copper and zinc from nickel and cobalt in 2004-2006 (Cheng and Rodriguez 2006, Cheng et al. 2007 and 2008).

Phase 4: SSX system consisting of Versatic 10 and LIX63 for the Baja Mining Corp. DSX process for the separation of cobalt and zinc from manganese, magnesium and calcium in the period of 2004-2006 (Cheng and Urbani 2005b, Cheng 2006, Cheng et al. 2010, Dreisinger et al. 2010).

Phase 5: SSX system consisting of Versatic 10, LIX63 and TBP for the Rio Tinto DSX process for the separation of nickel and cobalt from manganese, magnesium and calcium in 2008-2009 (Cheng and Urbani 2005c, Cheng 2006, Cheng et al. 2009a and 2009b, Cheng et al. 2010a, 2010b and 2010c).

The above SSX systems solved the problem for the nickel laterite industry to directly recover nickel and cobalt from leach solutions without intermediate precipitation and re-leach steps from HPAL solutions after iron and aluminium removal. However, they cannot be used for HPAL and HL solutions without iron and aluminium removal. In the other hand, there is no SX system with a single extractant to separate nickel and cobalt from iron and aluminium and the development of such reagents would be very difficult and very expensive. Therefore, the only alternative is to develop SSX systems using commercially available reagents to achieve this goal and to meet the very important and urgent need of the nickel industry.

Recently, the CSIRO SX group has developed new SSX systems and DSX processes, which marked the development of CSIRO DSX processes entering **Phase 6**: new SSX system to separate nickel and cobalt from iron and aluminium and other impurities. This is a significant technology development and will be reported in this paper.

THE CSIRO DSX PROCESSES FOR HL AND AL SOLUTIONS

As shown above, both heap leach (HL) solution and atmospheric leach (AL) solution contain high concentrations of Fe and Al. In this study, a synthetic solution containing high concentrations of Fe and Al was tested.

The New SSX System to Separate Ni/Co from Fe/Al

The new SSX system consists of two reagents in a diluent, and all these reagents are commercially available. The chemical composition of the synthetic leach solution is shown in Table 1. The aqueous solution contained 9 g/L Fe(III) and 3 g/L Al.

Table 1: The chemical composition of the synthetic leach solution.

Concentration (g/L)									
Ni	Co	Cu	Zn	Fe(III)	Al	Mn	Mg	Ca	Cr
2.5	0.2	0.5	0.2	9.0	3.0	0.4	8.2	0.2	0.04

Metal Extraction pH Isotherms

Batch tests were conducted to determine the metal extraction pH isotherms with the SSX system and the synthetic laterite leach solution (Fig. 1). It is clear that the metal extraction order in terms of pH_{50} values is (Table 2):

Cu > Ni >Co > Zn > Mn > Al ~ Mg ~ Fe(III) ~ Ca

Table 2: Metal pH$_{50}$ values and separation factors over Fe(III) and Al.

Metals	Ni	Co	Cu	Zn	Fe(III)	Al	Mn	Mg	Ca	Cr
pH$_{50}$	1.3	2.1	<1.0	~2.6	>>2.6	>>2.6	>2.6	>>2.6	>>2.6	>>2.6
$\beta_{M/Fe}$*	1067	65	6878	66	1	---	---	---	---	---
$\beta_{M/Al}$**	896	55	5776	55	---	1	---	---	---	---

$\beta_{M/Fe}$* = separation factor of metals over Fe(III) at pH 2.0
$\beta_{M/Al}$** = separation factor of metals over Al at pH 2.0

The separation factors of Cu and Ni over Fe(III) and Al are over 5000 and 1000, respectively, indicating that the separation of these two metals from Fe(III) and Al and other impurities are easy and complete. The separation factors of Co over Fe(III) and Al are in the range of 55 – 65, indicating that the separation of Co from Fe and Al is possible, although a number of extraction and scrubbing stages could be needed.

The metal pH isotherms also suggest that the stripping of Ni and Co can be achieved at pH 0.5 or with a free acid concentration of 15 g/L H$_2$SO$_4$. The complete stripping of Cu needs a strip solution with a much higher acidity, probably at pH 0 or with a free acid concentration of 50 g/L H$_2$SO$_4$.

Metal Extraction Kinetics

The metal extraction kinetics with the new SSX system and the synthetic heap leach solution at pH 2.0 are shown in Fig. 2. Within 30 seconds, all copper, 97% nickel, 70% cobalt and 42% zinc were extracted, suggesting very fast extraction kinetics of these metals. The extractions of zinc and other impurities, such as manganese, iron, calcium, magnesium and aluminium were decreased after one minute of mixing, probably caused by the crowding effect of nickel. The metal extraction almost reached equilibrium in 1 minute, again, suggesting very fast extraction kinetics.

Metal Stripping Kinetics

The stripping kinetics of nickel, cobalt, zinc and copper with a strip solution containing 25 g/L sulphuric acid are shown in Fig. 3. It can be seen that the stripping kinetics of nickel, cobalt and zinc are very fast: within 30 seconds, almost all of these metals were stripped. The stripping of copper was slow: 46% was stripping within 30 seconds and this increased to 47% in 10 minutes, suggesting the acidity was not high enough for its complete stripping. A further test with 100 g/L H$_2$SO$_4$ showed that all copper was completely stripped, indicating that an organic bleeding with a strong acidic solution can be used to keep the copper in a low level.

The DSX Process Coupled with Ni Hydrolysis

A conceptual flowsheet consisting of HL – DSX – Ni hydrolysis is shown in Fig. 4.

- The pH of the HL solution is adjusted to 1.8-2.0 using laterite ores. After S/L separation, the aqueous solution is subjected to extraction with the DSX process to obtain (a) an aqueous raffinate containing almost all the iron, aluminium, arsenic, chromium, manganese, magnesium, calcium and chloride and some zinc (b) a loaded organic solution containing almost all the copper, nickel, cobalt and some zinc and residual iron.

- The organic solution from the extraction step is subjected to scrubbing, resulting in (a) a scrubbed organic solution containing nickel, copper, cobalt and zinc and (b) a loaded scrub liquor containing mainly iron and small amount of cobalt, zinc nickel and copper, which is recycled to the extraction step.

- The scrubbed organic solution is subjected to stripping using a hydrochloride acid from the nickel hydrolysis step, resulting in (a) a loaded strip liquor containing nickel, cobalt, copper and zinc and (b) a stripped organic solution containing almost no metals and is recycled to the extraction step.

- The loaded strip liquor from the DSX circuit enters another SX circuit using tri-octyl- and decyl-amine (Alamine 336) for extraction and water for stripping, resulting in (a) a loaded strip liquor containing all cobalt, copper and zinc, and (b) a raffinate with high concentration of nickel, which is subjected to hydrolysis to obtain NiO product and HCl solution recycled for stripping.

- The loaded strip liquor containing cobalt, copper and zinc is subjected to ion exchange with Purolite S-950 resin using acid for stripping, resulting in (a) a cobalt solution for recovery of pure cobalt product, and (b) a mixed copper and zinc solution for recovery as a bulk product or further separation for individual products.

The DSX Process Coupled with Ni Electrowinning

A conceptual flowsheet consisting of HL – DSX – Ni electrowinning (EW) is shown in Fig. 5. Until stripping, all process steps are the same as shown in the above HL-DSX-Hydrolysis flowsheet.

- The scrubbed organic solution is subjected to stripping using a mixture of concentrated sulphuric acid and part of Ni spent electrolyte from the nickel EW step, resulting in (a) a loaded strip liquor containing nickel, cobalt, copper and zinc and (b) a stripped organic solution containing some copper and is recycled to the extraction step.

- An organic bleed is required using relative strong sulphuric acid to keep the copper concentration in the organic solution at a low level. The loaded strip liquor joins the strip solution.

- The loaded strip liquor from the DSX circuit is subjected to another SX circuit using Cyanex 272 for extraction and sulphuric acid for stripping, resulting in (a) a loaded strip liquor containing all cobalt, copper and zinc, and (b) a raffinate with high concentration of nickel, which is subjected to EW to obtain Ni cathodes. Part of the Ni spent electrolyte is recycled to EW after combining with the raffinate from the Cyanex 272 circuit.

- The loaded strip liquor from the Cyanex 272 circuit containing cobalt, copper and zinc is subjected to the same treatment as in the above HL-DSX- Hydrolysis flowsheet.

The DSX Process Coupled with Ni Hydrogen Reduction

A conceptual flowsheet consisting of HL – DSX – Ni hydrogen reduction (HR) is shown in Fig. 6. Until the treatment of the raffinate from the second SX circuit with Cyanex 272, all process steps are the same as shown in the HL-SX-EW flowsheet.

- The raffinate with high concentration of nickel from the Cyanex 272 circuit is subjected to solution making with ammonium sulphate and hydrogen reduction to obtain Ni product.

- The raffinate from the HR enters a small SX circuit using the same SSX system as in the DSX circuit to recover the residual Ni, which is recycled to the HR circuit. The Ni-depleted $(NH_4)_2SO_4$ solution is used for solution making for the HR circuit or for making $(NH_4)_2SO_4$ product for sale.

- The loaded strip liquor from the Cyanex 272 circuit containing cobalt, copper and zinc is subjected to the same treatment as in the HL-DSX- Hydrolysis flowsheet.

THE CSIRO DSX PROCESS FOR HPAL SOLUTIONS

If the new SSX system is used for HPAL solutions, the CCD system for neutralisation, precipitation and solid/liquid separation can be simplified, suggesting capital and operating savings. The same as for the HL and AL solutions, the DSX process can be coupled with either hydrolysis or electrowinning or hydrogen reduction to obtain different Ni products.

THE STABILITY OF THE NEW SSX SYSTEM

The commercial reagents used in the new SSX system are chemically stable individually and confirmed by researchers and industrial users. The combination of the reagents or the SSX system has been stable during the developing period through numerous tests. Although no apparent organic degradation has been noticed, a long turn stability study should be carried out in the future research.

CONCLUSIONS

The new CSIRO DSX process using the new SSX system has the following advantages:

- Making the direct recovery of nickel and cobalt from HL, AL and HPAL solutions possible,

- Separation of nickel and cobalt from iron, aluminium and other impurities in low pH to avoid nickel and cobalt losses in neutralisation or precipitation steps,

- Possible saving capital and operating costs if applied to HPAL processes since the CCD system for neutralisation, precipitation and solid/liquid separation can be simplified,

- All organic reagents are commercially available and in reasonable price,

- The process flowsheet is much simplified to save capital costs.

- The new CSIRO DSX process can be readily coupled with nickel hydrolysis, electrowinning and hydrogen reduction to obtain different nickel products.

This new CSIRO DSX process is a significant technology development to separate Ni/Co from Fe/Al and other impurities. It will largely simplify the process flowsheet and to significantly save capital and operating costs.

ACKNOWLEDGEMENT

REFERENCES

Cheng, C. Y., 2000. Separation of nickel from calcium by synergistic solvent extraction. ALTA SX/IX – 1, Adelaide, 2000, ALTA Metallurgical Services.

Cheng, C. Y., 2003. SX application for nickel and cobalt: pros and cons of existing processes and possible future development, Proceedings of ALTA SX/IX World Summit, ALTA Metallurgical Services, Perth, Australia, May, 2003, ALTA Metallurgical Service.

Cheng, C. Y., Urbani, M. D. and Houchin, M., 2003. Synergistic solvent extraction and its potential application to nickel and cobalt recovery. Hydrometallurgy 2003 - Fifth International Conference in Honour of Professor Ian Ritchie, Vol. 1: Leaching and Solution Purification, Vancouver, Canada, August, 2003, 787-798.

Cheng, C. Y., Urbani, M. D. and Houchin, M., 2004. Manganese separation by solvent extraction in nickel laterite processing. International laterite Nickel Symposium - 2004 - TMS 2004 Annual Meeting, Charlotte, North Carolina, USA, March 2004, 429-447.

Cheng, C. Y. and Urbani, M. D. 2005a. The recovery of nickel and cobalt from leach solutions by solvent extraction: process overview, recent research and development, Proceeding of ISEC 2005, Beijing, China, September 2005, 503-526.

Cheng, C. Y. and Urbani, M. D., 2005b. Solvent extraction process for separation cobalt and/or manganese from impurities in leach solutions. Patent Application No PCT/AU2005/000088 and Patent Publication No. WO 2005/073415 A1.

Cheng, C. Y. and Urbani, M. D., 2005c. Solvent extraction process for separation cobalt and/or nickel from impurities in leach solutions. Patent Application No PCT/AU2005/000099 and Patent Publication No. WO 2005/073416 A1.

Cheng, C. Y., 2006. Solvent extraction of nickel and cobalt with synergistic systems consisting of carboxylic acid and aliphatic hydroxyoxime. Hydrometallurgy, 84: 109-107.

Cheng, C. Y. and Rodriguez, M., 2006. Upgrading cobalt product using synergistic solvent extraction technology at Murrin Murrin Operation of Minara Resources. ALTA Ni/Co, Perth, Australia, May, 2006, ALTA Metallurgical Services.

Cheng, C. Y., Zhang, W. and M. Rodriguez, M., 2007. Separation of copper, iron and zinc from cobalt and nickel in Minara process liquor by synergistic solvent extraction: pilot plant operation. ALTA Ni/Co, Perth, May, 2007, ALTA Metallurgical Services.

Cheng, C. Y., Zhang, W. and Pranolo, Y., 2007. Recovery of cobalt and zinc from Boleo leach solutions using the CSIRO DSX process. ALTA Ni/Co, Perth, May, 2007, ALTA Metallurgical Services.

Cheng, C. Y., Zhang, W. and Pranolo, Y., 2008. Recovery of cobalt and zinc from Boleo leach solutions using the CSIRO DSX process. Proceedings of ISEC '2008, Solvent Extraction: Fundamentals to Industrial Applications, Tucson, USA, September, 2008, 163-168.

Zhang, W., Cheng, C. Y., Rodriguez, M. and Pranolo, Y., 2008. Separation of copper, iron and zinc from cobalt and nickel with mixed Cyanex 272 and LIX84 extractants. Proceedings of ISEC '2008, Solvent Extraction: Fundamentals to Industrial Applications, Tucson, USA, September, 2008, 177-182. Published.

Cheng, C. Y., Boddy, G., Zhang, W., Godfrey, M., Robinson, D., Pranolo, Y., Zhu, Z, Wang, W and Zeng, L., 2009a. A DSX process for Ni and Co recovery from Rio Tinto laterite leach solutions using SSX technology - from batch tests to pilot plant operation. ALTA Nickel/Cobalt, Perth Australia, May 2009, ALTA Metallurgical Services.

Cheng, C. Y., Boddy, G., Zhang, W., Godfrey, M., Robinson, D. J., Pranolo, Y., Zhu, Z., Zeng L. and Wang, W., 2009b. Direct solvent extraction for recovery of nickel and cobalt from Rio Tinto laterite leach solutions. Proceedings of International Symposium, Hydrometallurgy of Nickel and Cobalt 2009, 243-254.

Cheng, C. Y., Boddy, G., Zhang, W., Godfrey, G., Barnard, K. R., Robinson, D. J., Pranolo, Y., Zhu, Z., Wang, W., Zeng, L., Turner, N. L. and Hill, T. N., 2010a. Separation of nickel and cobalt from manganese, magnesium and calcium by synergistic solvent extraction - from batch tests to pilot plant operation. Proceedings of the International Mineral Processing Conference, Brisbane Australia, September 2010, 285-297.

Cheng, C.Y., Boddy, G., Zhang, W., Godfrey, M., Robinson, D.J., Pranolo, Y., Zhu, Z. and Wang, W., 2010b. Recovery of nickel and cobalt from laterite leach solutions using direct solvent extraction: Part 1 – selection of a synergistic SX system. Hydrometallurgy , 104: 45-52.

Cheng, C.Y., Boddy, G., Zhang, W., Godfrey, M., Robinson, D.J., Pranolo, Y., Zhu, Z., Zeng, L. and Wang, W., 2010c. Recovery of nickel and cobalt from laterite leach solutions using direct solvent extraction: Part 2 – semi - and fully - continuous tests. Hydrometallurgy, 104: 53-60.

Cheng, C.Y., Zhang, W. and Pranolo, Y., 2010. Separation of cobalt and zincfrom manganese, magnesium and calcium using synergistic solvent extraction system consisting of Versatic 10 and LIX63. Solvent Extraction and Ion Exchange, 28: 604-624.

Diniz, C.V., 2006. Private communication.

Dreisinger, D., Cheng, C. Y., Zhang, W. and Pranolo, Y. 2010. Development of Boleo process flowsheet and its direct solvent extraction (DSX) circuit. Proceedings of the International Mineral Processing Conference, Brisbane Australia, September 2010, 309-317.

Duyvesteyn, W.P.C. and Omofoma, M., 1997. Recovery of nickel from bioleach solution. US Patent No. 5626648-A.

Duyvesteyn, W. P C, Weenink, E. M and Neudorf, D. A, 2002. Resin-in-pulp method for recovery of nickel and cobalt. US Patent No. 6350420-B1.

Flett, D. S., 2004. Cobalt-nickel separation in hydrometallurgy – a review. Chemistry for Sustainable Development, 12: 81-91.

Grinstead, R. R., 1980. Extractant systems for nickel and cobalt based on organic sulfonates. International Solvent Extraction Conferences, Paper 80-170.

Grinstead, R. R., and Tsang, A. L., 1983. A selective metallurgical extractant system to recover nickel and cobalt from acid solutions. International Solvent Extraction Conferences: ISEC '83, S. N., Denver, Colorado, USA, 230-231.

Inoue, K., Zhang, P., Koga, Y., and Eguchi, H., 1997a. Development of synergistic solvent extraction system for the recovery of nickel and cobalt from spent hydrodesulfurization catalysts. Hydrometallurgy and Refining of Nickel and Cobalt, Annual Hydrometallurgy Meeting of CIM, 27th, Sudbury, Ont., Aug. 17-20, 1997, 221-233

Inoue, K., Koga, Y., Yoshizuka, K., Owatari, K. and Tsuyama, H., 1997b. Recovery of nickel and/or cobalt from aluminium-containing aqueous solution. JP Patent No. 09194965.

Liu, H., Duarte, A. Melhack, W. and Ratchev, I. P., 2006. Production of ferro-nickel or nickel matte by a combined hydrometallurgical and pyrometallurgical process. WO Patent No. 029443 A1.

Manson, P. G., Groutsch, J. V., Mayze, R. S. and White, D., 1997. Process development and plant design for the Cawse nickel project, Nickel and Cobalt Pressure Leaching and Hydrometallurgy Forum, Perth, Western Australia, May, 1997. ALTA Metallurgical Services.

Mihaylov, I., Krause, E., Colton, D. F., Okita, Y., Duterque, J. –P and Perraud, J. –J, 2000. The development of a novel hydrometallurgical process for nickel and cobalt recovery from Goro laterite ore. CIM Bulletin, Vol. 93, No 1041, p124.

Motteram, G., Ryan, M., Berezowsky, R. and Raudsepp, R., 1996. Murrin Murrin nickel and cobalt project: Project development overview, Nickel and Cobalt Pressure Leaching and Hydrometallurgy Forum, Perth, Western Australia, May, 1996. ALTA Metallurgical Services.

Preston, J.S.; du Preez, A.C. Solvent extraction of nickel from acidic solutions using synergistic mixtures containing pyridinecarboxylate esters. Part 3. Systems based on arylsulphonic acids. *J. Chem. Tech. Biotechnol.* 1998, 71: 43–50.
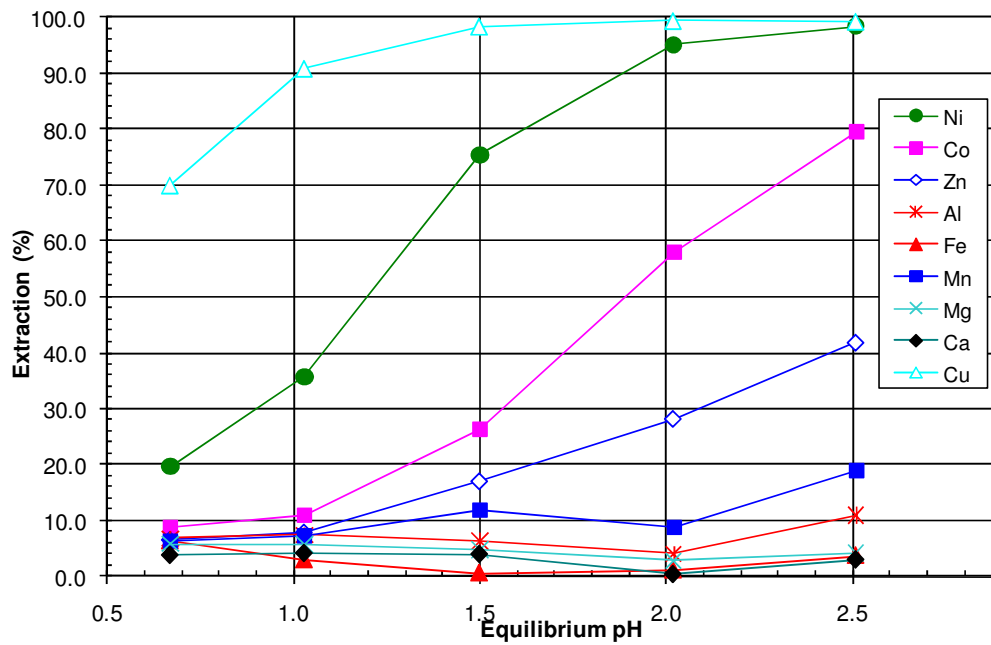
**Fig. 1: Extraction pH isotherms of metals with the novel SSX system
and the synthetic laterite heap leach solution.**
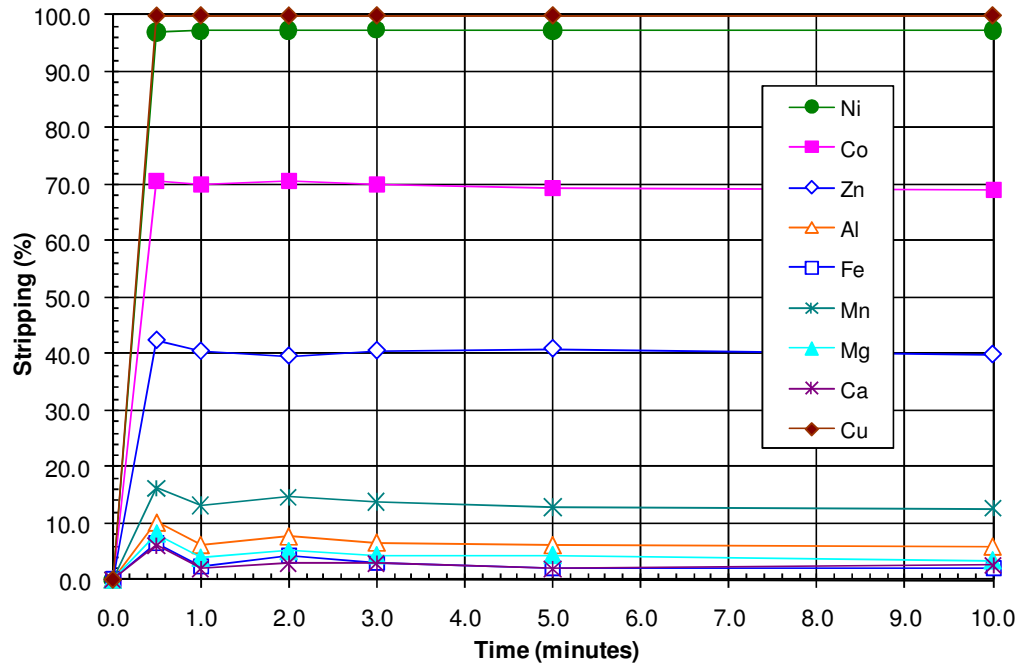
**Fig. 2: Metal extraction kinetics with the novel SSX system
and the synthetic laterite heap leach solution.**
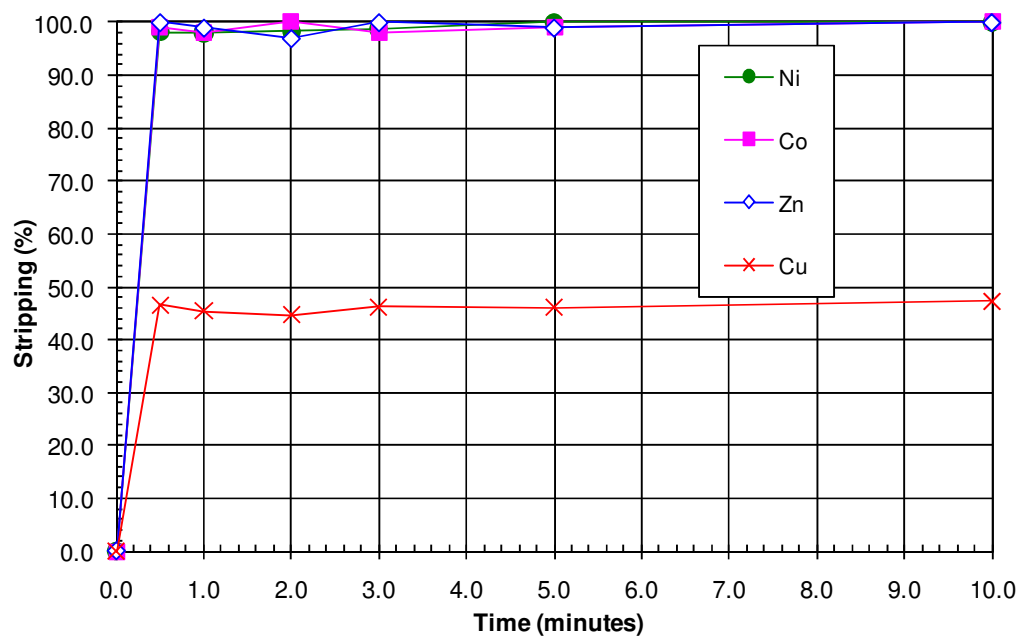
**Fig. 3: Metal stripping kinetics from the loaded SSX system
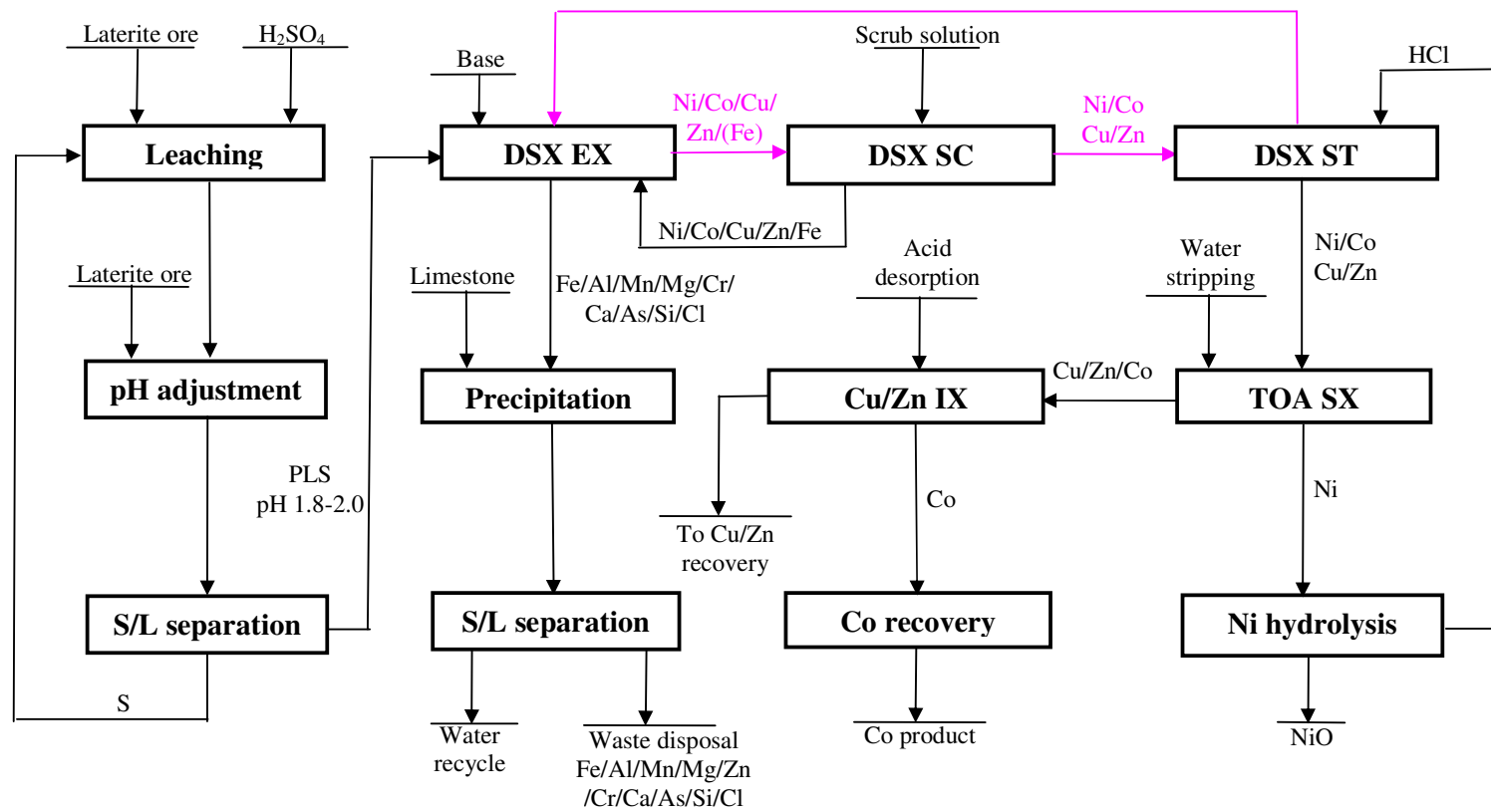with 25 g/L sulphuric acid solution.**

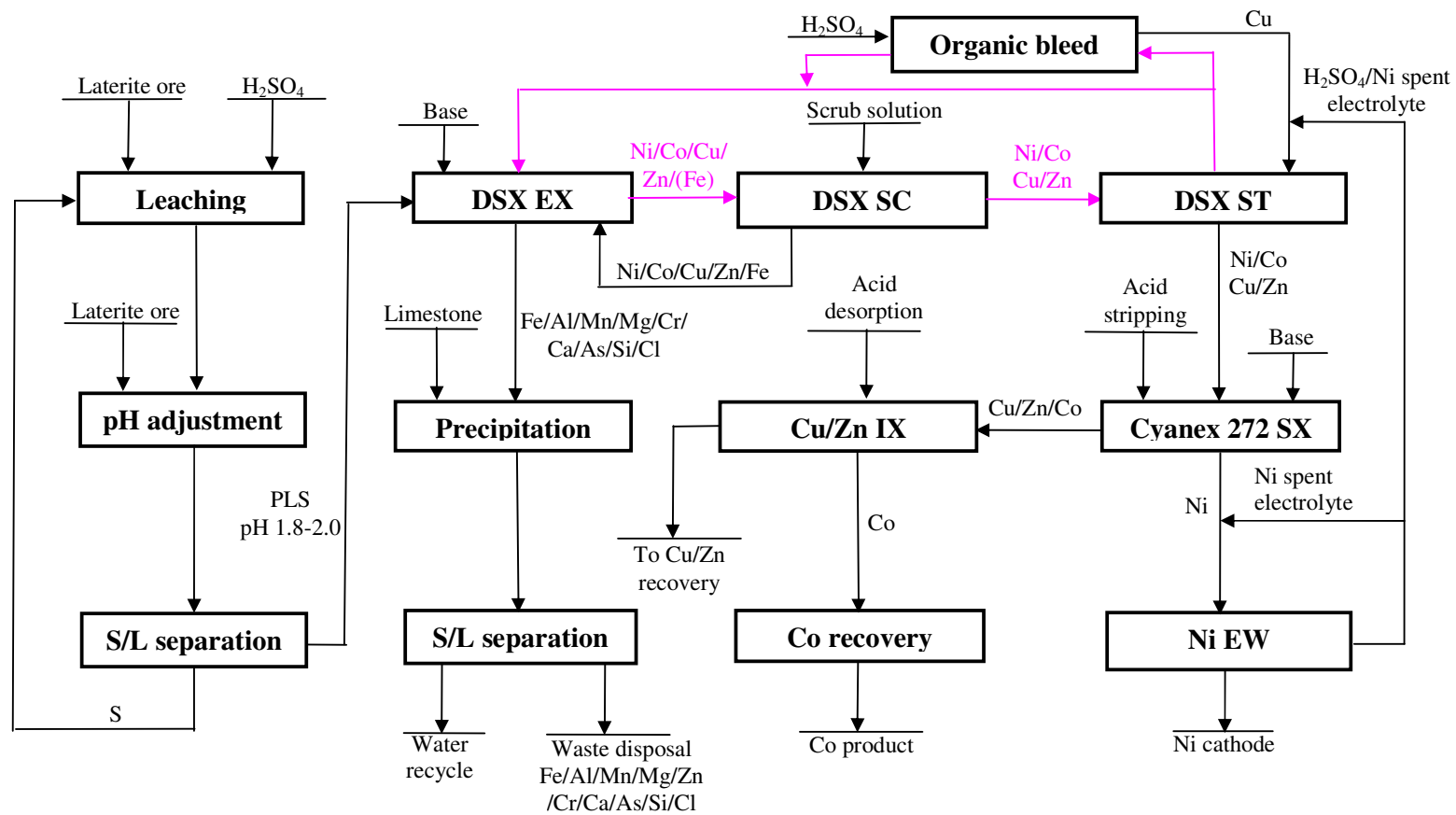**Fig. 4: A conceptual process flowsheet with HL – DSX – Ni hydrolysis.**

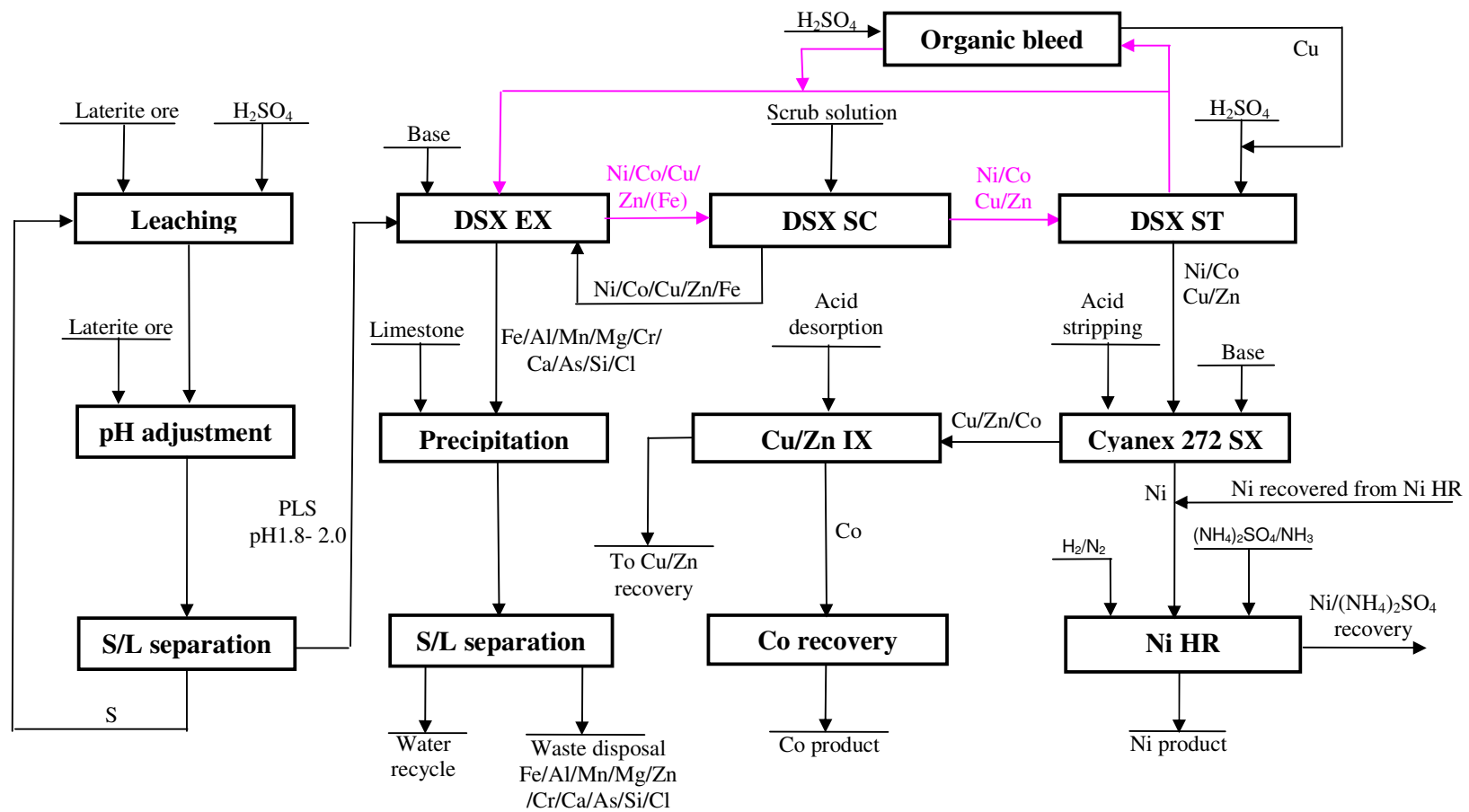**Fig. 5: A conceptual process flowsheet with HL – DSX – Ni electrowinning.**

Fig. 6: A conceptual process flowsheet with HL – DSX – Ni hydrogen reduction.

SELECTIVE SEPARATIONS IN THE COBALT, URANIUM AND SULFURIC ACID INDUSTRIES

By

Steven R. Izatt, Neil E. Izatt, and Ronald L. Bruening

IBC Advanced Technologies, Inc., USA

Presenter and Corresponding Author

Neil E. Izatt
nizatt@ibcmrt.com

ABSTRACT

IBC Advanced Technologies' Molecular Recognition Technology (MRT) SuperLig® products selectively and rapidly bind with target metal ions to remove them from solution. The MRT process can produce a high purity separation product of maximum added value at low cost. This paper discusses applications for MRT in the cobalt industry, including removal of Cd, Cu, Pb, and Ni. Additional separations of interest to the Australian mining industry will also be discussed, including Hg removal from sulfuric acid and uranium separations.

INTRODUCTION

This paper deals with the following topics of interest to the Australian mining industry: (1) production of pure Co by removal of Fe, Ni, Cu, Cd, Pb, and other metals from actual and synthetic Co streams, (2) U separation from two synthetic solutions containing complex matrices, and (3) removal of Hg impurity from H_2SO_4. A common thread in these separations is the need to produce primary products of high purity and to recover impurities removed in the process in pure and concentrated form suitable either for sale or for disposal in an environmentally safe manner.

The process used to effect these separations is IBC's Molecular Recognition Technology (MRT) process[1][2]. Use of MRT permits the selective binding of metals at the mg/L to µg/L levels. At these low levels, traditional separation techniques such as ion exchange (IX), solvent extractions (SX), and precipitation become increasingly ineffective. This observation has also been made by Gedgagov[3] who states that the purity requirements for metals by modern technology require improved separation procedures.

Increasingly stringent environmental requirements worldwide provide an incentive to separate, recover, and purify metals present in low-grade streams. The MRT process is ideal for this task due to its ability to selectively recover and concentrate these metal impurities at the mg/L to µg/L level. The effluent from the MRT system is normally suitable for discharge into culinary water streams or can be used for agricultural purposes.

The MRT process is now described followed by examples of the use of MRT in separations of interest to the Co and U industries. Technical and economic advantages of the MRT process in these separations will be presented.

DESCRIPTION OF MOLECULAR RECOGTION TECHNOLOGY

MRT is a highly selective, non-ion exchange system, using specially designed organic chelators or ligands that are chemically bonded to solid supports such as silica gel or polymer substrates. The MRT process[1][2] utilizes "lock and key," or "host guest" chemistry as a basis for its high selectivity. The solid-phase system consists of small particles to which the selective ligand is attached (SuperLig®). The SuperLig® product is packed into fixed bed columns that, in commercial operation, can be built in skid-mounted modular form, and can be fully automated for continuous operation. The feed solution is passed through the column and the target ion is removed from the solution.

SuperLig® products are designed to bind selectively with ions based on multiple parameters such as size, coordination chemistry, and geometry. In contrast, conventional separation methods such as precipitation, IX, and SX generally recognize differences between ions based only on a single parameter (i.e., charge, solubility, size). SuperLig® products can bind ions even when they are present in highly acidic or highly basic solutions and/or in solutions containing high concentrations of competing ions. The MRT process exhibits high selectivity, high binding factors, and rapid reaction kinetics, resulting in a very efficient separation. The simple elution chemistry uses small volumes of eluate. Thus, dilute solutions, such as those expected from the dissolution of low-grade resources are concentrated and can be treated to produce, with minimal environmental impact, either marketable products of high-added value or pure products that can be disposed of in an environmentally safe manner. Due to high selectivity, high loading capacities, and rapid loading and release kinetics of the SuperLig® materials, application of the IBC MRT procedure to commercial scale operations results in substantially lower capital and operating costs than are found for other technologies like IX, SX, and chemical precipitation. Because relatively small quantities of the appropriate SuperLig® product are required, the scale of the installation can be smaller; solution wash and elution chemical requirements and volumes are substantially less; and high feed solution flow rates are possible. Higher efficiencies are attained due to single-pass high percentage removal of the target species. SuperLig® products have a long life expectancy and do not introduce contaminants into the separation process.

MRT can be used to accomplish metal separations at low mg/L to µg/L levels that are not possible using traditional technologies[1][2]. The effectiveness of traditional technologies decreases sharply as the metal content in the feed stock decreases toward the mg/L level. The commercially pure products produced from such feed stocks using MRT can be sold or recycled. This is an important factor from the standpoints of cost, the environment, and waste disposal. A wide choice of eluent formulations is usually available to ensure compatibility with particular plant requirements. Highly

concentrated eluent solutions can be produced from which the simple recovery of a high purity, high value-added product is possible. The use of MRT has wide applicability to the removal of metals directly from low-grade feed stocks producing, within detectable limits, a metal-free eluent.

EXAMPLES OF THE USE OF MOLECULAR RECOGNITION TECHNOLOGY IN THE COBALT INDUSTRY

Specifications for Co in high-tech applications such as rechargeable batteries and catalysts are constantly increasing. For example, in the case of the use of Co for rechargeable battery manufacture, specifications are particularly tight for certain elemental impurities[4-7]. The impurities exert a deleterious effect on current efficiency, as well as on the nature and purity of the cobalt deposit. Major elements of concern are Fe, Cu, Ni, Zn, Mg, Cd, Pb, and Se. SuperLig® products are available for extraction of a number of these critical impurities from Co process and waste streams[4][5][8][9].

A summary of MRT separations for purification of Co and for removal of selected base metals from Co streams is given together with the SuperLig® products that effect the separations in Table I[10].

_____

Table 1: Summary of MRT Separations for Purification of Cobalt and Cobalt Separations

Application	SuperLig® Number	Reference
Extraction and polishing of iron from a cobalt stream in a sulfuric acid matrix	SuperLig® 48	4
Cadmium removal from cobalt electrolyte	SuperLig® 177	11
Extraction and purification of copper from a cobalt process stream	SuperLig® 77	8
Extraction and polishing of nickel from a cobalt stream in a sulfuric acid matrix	SuperLig® 241	9
Extraction and polishing of nickel from a cobalt stream in a nitric acid matrix	SuperLig® 199	9
Co-extraction of copper, iron, and nickel from a cobalt stream in a sulfuric acid matrix	SuperLig® 176	12
Co-extraction of cobalt and nickel from a nickel laterite ore process stream with separate elutions for nickel and cobalt	SuperLig® 138	9

Table 1: Summary of MRT Separations for Purification of Cobalt and Cobalt Separations (Continued)

Application	SuperLig® Number	Reference
Separate extractions of nickel, copper, and iron from concentrated acidic cobalt/base metal solution with separate elutions producing pure salt products	Solution pH 1 Cu: SuperLig® 86 Fe: SuperLig®14 Ni: SuperLig® 199 Co: SuperLig® 86	
Separate extractions of copper/iron, nickel and cobalt from concentrated acidic cobalt/base metal solution with separate elutions producing pure salt products	Solution pH 2 Cu/Fe: SuperLig® 145 Ni: SuperLig® 199 Co: SuperLig® 138	

The last two entries in Table 1 demonstrate the way that the MRT process can be fine-tuned to separate metals at particular pH values. A variety of SuperLig® products is available for use. Which product is used depends on solution conditions such as pH. For example, in the last two cases, the SuperLig® product used, in several cases, varies from pH 1 to pH 2.

In all cases in Table 1, the impurity metal is removed to the <0.1 mg/L level. The impurity metal is then eluted from the column in concentrated, pure form which can be marketed or disposed of in an environmentally safe manner.

REMOVAL OF CADMIUM AND LEAD FROM A COBALT ELECTROLYTE SOLUTION CONTAINING A COMPLEX MATRIX

Cobalt metal specifications are stringent. One of the important impurities in Co electrolyte solutions is Cd. SuperLig®177 is capable of removing Cd and, thus, meeting the required specifications for Grade A Co[11]. SuperLig®177 was tested for its ability to remove Cd (~6 mg/L) from a Co electrolyte solution containing 60 g/L Co. The Co electrolyte solution also contained Mg, Al, Si, Ca, Mn, Fe, Ni, Cu, and Zn. High Cd loadings were obtained with the SuperLig® product, i.e., 2.9 g/L Cd from a feed solution containing ~6 mg/L Cd (upgrading ratio of 480). The Cd was eluted and recovered as a pure product. The amounts of Co and the matrix elements in the eluent were nearly non-detectable making the selectivity factors for Cd over these elements very large. For example, selectivity factors at pH 2 for Cd over Co, Mg, and Mn were 3.03×10^4, 2.6×10^5, and 3.55×10^3, respectively. Similar selectivity factors were found at pH 4.

The ability of SuperLig® 177 to selectively remove Cd was found[11] to be much greater than that of either the solvent extraction agent di-2-ethylhexyl phosphoric acid (D_2EHPA) or the adsorption agent amino-methyl phosphoric acid resin (Purolite S950). For example, the selectivity factors for these reagents at pH 4 for Cd over Co, Mg, and Mn were 16, 213, and 5, respectively, for Purolite S950 and 33, 7, and 0.5, respectively, for D_2 EHPA at pH 2.5. These selectivity factors were much lower than those shown earlier for SuperLig® 177, which is clearly the superior reagent for Cd removal from Co electrolyte. The Cd removed by SuperLig® 177 is recovered directly as a pure product which can be sold to help defray the costs of the separation.

Lead often accompanies Cd in Co electrolyte solutions. SuperLig®177 is also effective in removing Pb, if present, from these solutions. Lead can subsequently be separated from Cd using other SuperLig® products depending on the experimental conditions. In one instance, Cd and Pb present at sub-mg/L levels were removed from a Co (multiple g/L) feed stream by SuperLig®177 to levels <0.5 µg/L (a reduction of 60-fold) in the treated feed stream. The µg/L results were obtained by passing a portion of the feed stream through a column loaded with SuperLig®177, washing the column, and

then eluting the column with a small volume of eluent creating a solution concentrated twenty times in Cd and Pb and containing, within detectable limits, no other metal impurities. The raffinate solution was analyzed after pre-concentration for the very low levels of Cd and Pb present using ICP and the measured concentrations were then divided by the pre-concentration factor to get the actual values in the original raffinate samples. These experiments demonstrate the ability of the MRT procedure to remove Cd and Pb impurities to low µg/L levels and to concentrate the purified Cd and Pb to a degree sufficient to allow ICP analysis. The procedure is rapid and can be automated. Other impurities and the Co are separated from the Cd and Pb allowing the ICP analysis to proceed without interference.

REMOVAL OF URANIUM FROM SELECTED SOLUTIONS

The use of SX and IX resins is the present technology of choice for extraction of U from clarified mine leach solutions, leached pulp, and slurries[13]. The application of MRT to U extraction from these feed streams, as well as to evaporation ponds, waste streams, and environmental streams, offers a viable, highly competitive alternative to SX and IX resins. Due to the extremely high selectivity of SuperLig® products, MRT offers the potential to dramatically simplify the flow sheet for U recovery from these solution matrices. The MRT process can selectively separate U directly from the feed solution and produce a concentrated, high purity U product.

One example of the MRT procedure is given below and consists of successful laboratory test work to separate U from two solutions. This test work was commissioned and paid for by UraniumSA Limited (Norwood, South Australia). Extraction of U by the SuperLig® products and elution of U from the column in concentrated form was accomplished for both solutions. Solution 1 was prepared by adding metal salts to prepare a mimic of seawater. Uranyl nitrate was added to Solution 1 to make the UO_2^{2+} concentration 30 mg/L. Passage of Solution 1 through a packed SuperLig® 268 column resulted in selected retention of the U All other metals present in Solution 1 passed through the column without binding to SuperLig® 268. The U was bound as uranyl tricarbonate ion, $UO_2(CO_3)_3^{4-}$. Elution of the U from the column was accomplished using 1 M HCl. Concentrations of the impurity metals were <1 mg/L in the eluent. The U was concentrated to ~2g/L.

The salt composition of Solution 2 was identical to that of Solution 1, except that 2 g/L Fe was added as $FeSO_4$ together with sufficient H_2SO_4 to make the solution 0.1 M in H_2SO_4. Uranyl nitrate was added to make the solution ~100 mg/L in UO_2^{2+}. Solution 2 was then passed through a column packed with SuperLig® 171, which is selective for the anionic $U(SO_4)_4^{2-}$ species. The anionic uranyl sulfate species was retained on the column while all remaining metals passed through it. Following washing of the column with a dilute H_2SO_4 solution and/or water, the bound U was eluted using 1 M HCl. The concentrations of the metals originally present in the feed solution were <1 mg/L in the eluent and the U was concentrated to ~4g/L.

These laboratory scale results show the versatility of the MRT process. Depending on species present and experimental conditions, different SuperLig® products can be used. Also, certain of the SuperLig® products have affinity for anions which increases the usefulness of the MRT approach. The U is obtained rapidly and in a pure form. The remaining metals can be retrieved, using other SuperLig® products, as pure metals suitable for resale or environmentally safe disposal.

REMOVAL OF MERCURY FROM SULFURIC ACID STREAMS

Mercury is found in Zn, Pb, Cu, Au, Mn, and pyrite ores. When these sulfide ores are treated in thermal processes, such as smelting and roasting, the Hg volatilizes and will appear in downstream products such as H_2SO_4, which is generated at most of these operations. Consequently, the Hg eventually finds its way into the environment and commercial products, such as fertilizer, where the potential damage to the ecosystem is severe. Thus, a real need exists to eliminate, or minimize, the Hg output from these massive worldwide metallurgical operations.

IBC has developed and commercialized a Hg-selective product (SuperLig® 88) that can be used to remove Hg from concentrated H_2SO_4, which is produced as a byproduct of various metallurgical roasting and smelting operations[14]. The MRT process can be used alone as the primary Hg removal technology for bulk removal of the Hg, or as a "polisher." In bulk-removal mode, the system is capable of treating feed concentrations of up to 150 mg/L Hg, and in polishing mode, would generally treat feed solutions with Hg concentrations <10 mg/L. The system is capable of consistently producing a Hg concentration of <0.1 mg/L in the output stream for most inputs which contain ≤25 mg/L Hg. SuperLig® 88 selectively binds Hg^{2+} and to a lesser extent Hg_2^{2+} out of

concentrated H_2SO_4. The MRT Hg removal process has been successfully piloted at a number of locations for both bulk removal and polishing applications.

CONCLUSIONS

Molecular Recognition Technology provides an effective means to make selective separations of metals over wide concentration ranges including at the mg/L to µg/L level where conventional separation technologies are not effective. The Co and U industries have needs where MRT can be helpful in selective separations and in the recovery and purification of impurity metals. The use of SuperLig® products for the selective removal from Co streams of Fe, Ni, Cu, and Cd under a variety of experimental conditions is described. The maintenance using SuperLig® 177 of Cd and Pb at low mg/L to µg/L levels in Co streams is presented as an example of the use of MRT in on-line control of impurity levels in commercial Co streams. A description is presented of two ways in which MRT has the potential to dramatically simplify the flow sheets for selective U recovery from salt solutions (mimic of seawater) and from similar salt solutions which are 0.1M in H_2SO_4. The U separations illustrate the versatility of the MRT approach in using separate SuperLig® products that have affinity for U in two different complex anion forms. Mercury is a common impurity in many sulfide ores. The use of SuperLig® 88 to remove Hg from H_2SO_4 streams to low mg/L to µg/L levels is given. The examples presented in this paper illustrate the environmental advantages MRT has over conventional technologies in making chemical separations. These advantages include the ability to recover impurities in pure, separated form even at mg/L to µg/L levels; on-line incorporation of MRT into flow sheets making process separations faster, cleaner, and more effective; produce a pure primary product as needed in current technology; and leave waste streams, devoid of impurity metals, that can be discharged into culinary water sources or used for agricultural purposes.

REFERENCES

1. N.E. Izatt, R.L. Bruening, K.E. Krakowiak, and S.R.Izatt, "Contributions of Professor Reed M. Izatt to Molecular Recognition Technology: From Laboratory to Commercial Application," Industrial &. Engineering Chemistry Research, Vol. 39, 2000, 3405-3411.

2. R.M. Izatt, J.S. Bradshaw, and R.L. Bruening, R.L., "Ion Separations in Membrane and Solid Phase Extraction Systems," Supramolecular Materials and Technologies (Series: Perspectives in Supramolecular Chemistry, Vol. 4), D.N. Reinhoudt, Ed., John Wiley & Sons: New York, NY, USA, 1999, 225-243.

3. I. Gedgagov, "Improvement of Techniques for Purification and Separation of Metals Using Modified and Nano-Structured Sorbent Agents and Their Application in Industry," First International Congress Non-Ferrous Metals of Siberia – 2009 Part III .Non-Ferrous and Rare Metals Production. Retrieved 10 May 2010 from website: www.nfmsib.com/pdf/sbornik/360.pdf.

4. S. R, Izatt, R. L. Bruening, N. E. Izatt, and J. B. Dale, "The Application of Molecular Recognition Technology (MRT) for Removal of Impurities from Cobalt Feed Streams in the Production of High Purity Cobalt and Cobalt Chemicals," ALTA 2008 Nickel/Cobalt Conference, Perth, Australia, June 16-21, 2008.

5. S.R. Izatt, N.E. Izatt, R.L. Bruening, and J.B. Dale, "The Application of Molecular Recognition Technology (MRT) in the Purification of Cobalt Process and Electrowinning Streams," ALTA 2009 Nickel-Cobalt, Copper & Uranium Conference, Perth, Australia, May 25-30, 2009.

6. A.E. Elsherief, "Effects of Cobalt, Temperature and Certain Impurities upon Cobalt Electrowinning from Sulfate Solutions," Journal of Applied Electrochemistry, Vol.33, 2003, 43-49.

7. S. Wang, "Cobalt—Its Recovery, Recycling, and Application," Journal of Metals, October 2006, 47-50.

8. P. Kiggala, A. Silungwe, S. Saungweme, M. Mugabi S. R. Izatt, J.B. Dale, N.E. Izatt, and R.L. Bruening, "Environmentally Friendly Processing and Purification of Cobalt at Kasese Cobalt Company Limited Using Molecular Recognition Technology," ALTA Nickel/Cobalt Conference, Perth, Australia, May 21-26, 2007.

9. S.R. Izatt, J.B. Dale, N.E. Izatt and R.L. Bruening, "Recent Advances in the Application of MRT to Nickel and Cobalt Separations from Primary and Secondary Process Streams," ALTA Nickel/Cobalt Conference, Perth, Australia, May 15-17, 2006.

10. S.R. Izatt, R.L. Bruening, N.E. Izatt, and J.B. Dale, "An Update On the Application of Molecular Recognition Technology (MRT) for Ni/Cu/Co Hydrometallurgical Process Separations and for the Purification of Cobalt Streams," Fifth Southern African Base Metals Conference, Kasane, Botswana, July 27-31, 2009. Base Metals Conference, Symposium Series S56, Southern African Institute of Mining and Metallurgy: Johannesburg, Republic of South Africa, 2009, pp. 323-340.

11. J. van Deventer, R. du Preez, S. Scott, and S.R. Izatt, "Cadmium Removal from Cobalt Electrolyte," The Southern African Institute of Mining and Metallurgy, The Fourth Southern African Conference on Base Metals, Symposium Series S47, Swakopmund, Namibia, July 23-27, 2007, 377-392.

12. S.R. Izatt, N.E. Izatt, R.L. Bruening, and J.B. Dale, "Separation, Extraction, and Refining of Cobalt and Nickel from Base Metal Feed Streams Using Molecular Recognition Technology (MRT)," ALTA Nickel/Cobalt Conference, Perth, Australia, May 19-20, 2003.

13. World Nuclear Association, "Some Chemistry of Uranium." Retrieved 29 April 2011 from www.world-nuclear.org/education/chem.htm.

14. S.R .Izatt, R.L. Bruening, N.E. Izatt, and J.B. Dale, "Extraction and Recovery of Mercury from Concentrated Sulfuric Acid Streams Using Molecular Recognition Technology," 132nd Annual Meeting, TMS (The Minerals, Metals & Materials Society), San Diego, CA, U.S.A., March 2-6, 2003 In: EPD Congress 2003, Schlesinger, M.E., Ed., TMS, Warrendale, PA, U.S.A. 135-145.

DEVELOPMENT OF A NOVEL SMART ANODE FOR ENVIRONMENTALLY FRIENDLY ELECTROWINNING PROCESS

By

Masatsugu Morimitsu

Department of Environmental Systems Science, Doshisha University, Japan

Presenter and Corresponding Author

Masatsugu Morimitsu
mmorimit@mail.doshisha.ac.jp

ABSTRACT

This paper presents performance data of a novel smart anode, MSA[TM(1)], for electrowinning of non-ferrous metals such as copper, zinc, nickel, and cobalt. The smart anode consists of a titanium substrate coated with a catalytic oxide layer prepared by thermal decomposition of a precursor solution at 400 ^{o}C or less. Such a low temperature decomposition produces amorphous or less crystalline oxide coatings comprising iridium oxide-based mixture or ruthenium oxide-based mixture. The application of the smart anode in electrowinning with constant current results in a remarkable reduction in cell voltage compared to other anodes, *e.g.*, commercially available coated titanium electrodes and lead alloy electrodes. The test data has demonstrated that a maximum voltage reduction by *ca.* 30% is possible compared to lead alloy anodes for copper electrowinning. The smart anode also gives some additional merits in suppressing unwanted deposits on the anode; *i.e.*, deposition of MnOOH, PbO_2, or CoOOH. The electrowinning with the smart anode is possible to be an environmentally friendly process with less energy consumption and less anode deposits.

A BRIEF HISTORY OF DEVELOPMENT OF SMART ANODE

A titanium electrode coated with iridium oxide-based or ruthenium oxide-based catalytic layers is well known as an insoluble anode for oxygen or chlorine evolution in industrial electrolysis and is usually called "Dimensionally Stable Anode" with the registered trademark, DSA^R. The application covers chloro-alkali electrolysis, electrogalvanizing or electrotinning of a steel, a thin film production by electrodeposition such as copper foil production (CFP), water electrolysis, and electrowinning of nonferrous metals. The anode is commercially produced by thermal decomposition of a precursor solution painted on a titanium substrate, and the decomposition is usually performed at 450 ^{o}C or more. This process is repeated to obtain a desired thickness of the catalytic oxide coating for each application, but the catalytic coating formed on the substrate contains crystalline oxide as an active component to oxygen or chlorine evolution. The author of this paper had met a problem of such a crystalline oxide coating in the application of copper foil production; the anode was unable to be used for a long period because of a large amount of lead oxide (PbO_2) being deposited on the anode, and the cell voltage was seen to continuously increase and drastically rise by the accumulated PbO_2. In the case, the voltage reduction by replacing a lead alloy anode with the dimensionally stable anode was initially observed, but was gradually lost and disappeared. Therefore, the author of this paper aimed and investigated to suppress the unwanted side reaction on the anode, and finally invented a new class of coating based on an amorphous iridium oxide mixture in 2003[2]. The invented coating was obtained at a low temperature thermal decomposition, *e.g.*, 360 ^{o}C, and resulted in the coating consisting of amorphous iridium oxide and amorphous tantalum oxide. This invention achieved that oxygen evolution potential shifted more negative so that the cell voltage was reduced, and no PbO_2 was deposited in the electrolyte of CFP[3-4]. Then, such amorphous oxide coatings were further applied in electrowinning processes to reduce the electric energy consumption and to suppress other unwanted side reactions occurring in electrowinning solutions[5-11]. As a result, it has been found that the cell voltage can be significantly decreased, and the anodic deposition of MnOOH or CoOOH known as the unwanted side reaction of copper, nickel, cobalt, or zinc electrowinning can be also suppressed on the amorphous IrO_2-based or RuO_2-based coating[12-16]. Recently, a commercial application of the amorphous oxide anode has been successfully carried out in FCX's Chino copper electrowinning plant[17].

PREPARATION AND CHARACTERIZATION OF ANODE

The anode, MSA^{TM}, is prepared by thermal decomposition of a precursor solution painted on a titanium substrate such as titanium plate or mesh (see Figure 1). Two typical coatings are available with different type of precursor solutions; the solution containing Ir(IV) and Ta(V) is used for the mixed oxide coating of IrO_2 and Ta_2O_5. The solution containing Ru(III) and Ti(IV) is used to produce the composite oxide coating of $Ru_xTi_{1-x}O_2$. Such precursor solutions can be obtained using some kinds of solvents such as n-butanol, water, and others. The mole ratio of metal components is possible to be changed; one example of Ir-Ta system is 80 mol% Ir and 20 mol% Ta, while the typical composition of Ru-Ti system is 30 mol% Ru and 70 mol% Ti. Titanium substrates are pre-treated for degreasing and etching before painting and then are calcined at a temperature below 400 ^{o}C.
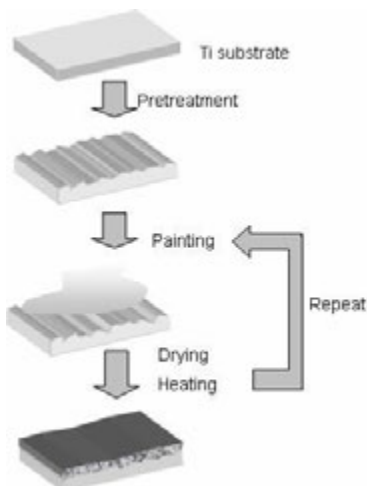

Figure 1: Preparation Procedure of Oxide Coated Titanium Electrodes

The crystallographic structure of the obtained coating is characterized by X-ray diffraction (XRD), and the surface morphology is observed using SEM. Figure 2 shows typical XRD patterns of IrO_2-Ta_2O_5 coated Ti electrodes prepared at different temperatures. The electrodes calcined at high temperatures such as 530 ^oC and 470 ^oC present clear diffraction peaks corresponding to (110) and (101) of crystalline IrO_2 along with sharp peaks of the titanium substrate. No diffraction peaks of crystalline Ta_2O_5 are seen in this figure, suggesting that Ta_2O_5 is amorphous in the coatings. This is reasonable, because thermal decomposition of a precursor solution containing $TaCl_5$ produces amorphous Ta_2O_5 when the decomposition temperature is lower than 600 ^oC. Thermal decomposition at 380 ^oC or less results in no diffraction peaks of crystalline IrO_2, indicating that the coatings prepared at such low temperatures comprise amorphous IrO_2. From these results, two types of IrO_2-Ta_2O_5 coatings are shown in Fig. 2; one is a mixture of crystalline IrO_2 and amorphous Ta_2O_5, and the other is a mixture of amorphous IrO_2 and amorphous Ta_2O_5. The former is similar to that of commercially available coated titanium anodes, and the latter is typical to that developed as MSA[TM]. It is noted that the phase transition temperature of IrO_2 in an IrO_2-Ta_2O_5 system prepared by a thermal decomposition depends on the nature of the precursor solution such as the solvent, the Ir:Ta mole ratio, and some components other than metals added into the solution. As for $Ru_xTi_{1-x}O_2$ coatings, the peak intensity of the composite oxide is also reduced with decreasing thermal decomposition temperature[13], suggesting that the crystallinity of the composite oxide becomes low or amorphous.
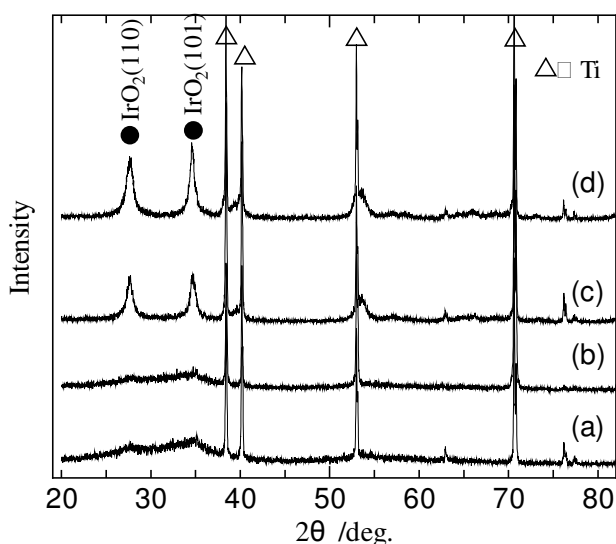
Figure 2: XRD Patterns of IrO_2-Ta_2O_5/Ti Electrodes Prepared at 360 ^oC (a), 380 ^oC (b), 470 ^oC (c), and 530 ^oC (d).

A clear difference between amorphous and crystalline coatings can be found in those surface morphologies (Figure 3). The coating with crystalline IrO_2 shows a well-known feature of IrO_2-Ta_2O_5 coatings; there are aggregated IrO_2 particles, flat areas, and cracks. Cracks are at least a few micro meters in length, and the morphology is heterogeneous and a so-called "mud-cracked" surface. However, the MSA[TM] coating with amorphous IrO_2 presents a smooth surface with no IrO_2 particle, although cracks are still seen.
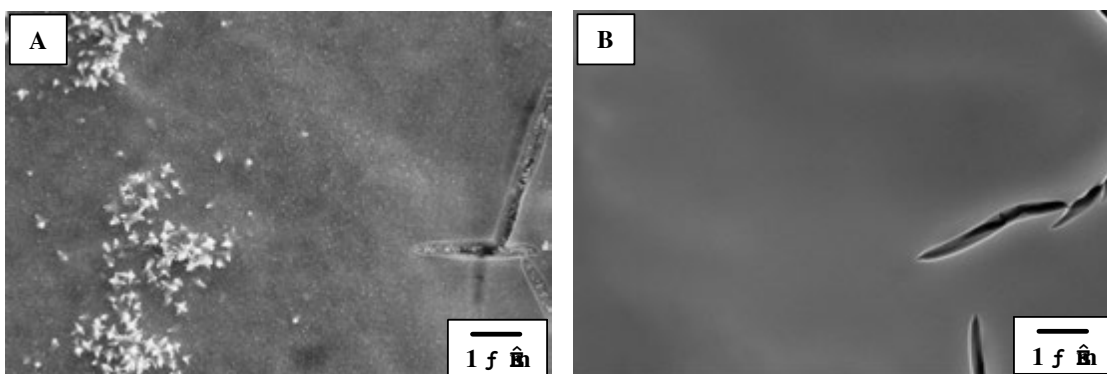
Figure 3: Surface Morphologies of Crystalline (left) and Amorphous IrO_2-Ta_2O_5 Coatings.

ANODE'S PERFORMANCE

Cell Voltage

Cell voltage measurements were performed using three kinds of anodes; amorphous IrO_2-Ta_2O_5/Ti, crystalline IrO_2-Ta_2O_5/Ti, and Pb-Sb alloy (5% Sb). Each electrode was mounted in a PTFE holder so that the surface area of the electrode was 1 x 1 cm^2. The electrolyte compositions used in the measurements are shown in Table 1. All electrolytes comprised sulfates, and sulfuric acid was used to adjust pH. Two kinds of electrolytes were used for zinc electrowinning; one contains zinc ions, and the other contains manganese ions in addition to zinc ions to investigate the effect of MnOOH deposition on the anode. Copper, zinc, or cobalt plates (2 x 2 cm^2) were used as the cathode. The current density was 50 mA/cm^2 based on the exposed surface area of the anode.

Table 1: Composition, pH, and Temperature of Electrolytes for Cell Voltage Measurements of Copper, Zinc, and Cobalt Electrowinning

Abbreviation	Composition	pH	Temp.
Cu	H_2SO_4 (9.0×10^{-1} mol/L)	0.11	40 ^{o}C
	$CuSO_4$ (6.0×10^{-1} mol/L)		
Zn	H_2SO_4 (2.0 mol/L)	-0.57	
	$ZnSO_4$ (8.0×10^{-1} mol/L)		
Zn(Mn)	H_2SO_4 (2.0 mol/L)	-0.39	
	$ZnSO_4$ (8.0×10^{-1} mol/L)		
	$MnSO_4$ (9.0×10^{-3} mol/L)		
Co	H_2SO_4 (2.0×10^{-3} mol/L)	2.87	
	$CoSO_4$ (3.0×10^{-1} mol/L)		

The cell voltage data are summarized in Table 2. In the case of copper electrowinning, the cell voltage with the amorphous IrO_2-Ta_2O_5/Ti anode was 0.55 V lower than that with the Pb alloy anode and was 0.18 V lower than that with the crystalline IrO_2-Ta_2O_5/Ti anode. The voltage reduction in zinc electrowinning was 0.55 V by replacing the Pb alloy anode and 0.16 V by replacing the crystalline IrO_2-Ta_2O_5/Ti anode with the amorphous IrO_2-Ta_2O_5/Ti anode. A similar trend was also observed for zinc electrowinning using the electrolyte containing manganese ions. The amorphous IrO_2-Ta_2O_5/Ti anode also showed 0.25 V lower voltage than the Pb alloy anode and 0.1 V lower voltage than the crystalline IrO_2-Ta_2O_5/Ti anode for cobalt electrowinning.

Table 2: Cell Voltages of Constant Current Electrolysis at 50 mA/cm^2 for Copper, Zinc, and Cobalt Electrowinning

Anode		Amorphous IrO_2-Ta_2O_5	Crystalline IrO_2-Ta_2O_5	Pb-5%Sb
Cell voltage	Cu	1.37 V	1.55 V	1.92 V
	Zn	2.46 V	2.62 V	3.01 V
	Zn(Mn)	2.52 V	2.65 V	3.10 V
	Co	2.1 V	2.2 V	2.35 V

The cell voltage during nickel electrowinning was also measured with $Ru_xTi_{1-x}O_2$/Ti electrodes prepared at different temperatures. The electrolyte contained 60 g/L Ni^{2+}, and pH was 1.5 by HCl. The electrolyte temperature was 60 ^{o}C. From the results shown in Table 3, amorphous $Ru_xTi_{1-x}O_2$/Ti can reduce the cell voltage for nickel electrowinning, which is more than 0.1 V.

Table 3: Cell Voltages of Constant Current Electrolysis for Nickel Electrowinning

Anode		Amorphous $Ru_xTi_{1-x}O_2$	Crystalline $Ru_xTi_{1-x}O_2$
Cell Voltage	50 mA/cm^2	1.71 V	1.81 V
	100 mA/cm^2	1.76 V	1.98 V

COMMERCIALIZATION

The patents of the electrowinning anodes and methods owned by Doshisha University have been licensed to Republic Alternative Technologies, Inc. (Strongsville, Ohio, USA) to commercialize MSA^{TM}. The anodes are produced with their sophisticated technology, RGT^{TM} (Republic Green Technology).

CONCLUSIONS

Amorphous oxide anodes, MSA^{TM}, comprising amorphous iridium oxide or ruthenium oxide have a low oxygen or chlorine evolution potential so that the cell voltage of electrowinning using acidic sulfate or chloride solutions can be significantly reduced compared to Pb alloy anodes or other dimensionally stable anodes. This amorphous oxide anode is effective to energy-efficient and environmentally friendly electrowinning processes of copper, zinc, cobalt, nickel, and other metals.

ACKNOWLEDGEMENTS

REFERENCES

1. MSA^{TM} represents "Morimitsu Smart Anode".

2. M. Morimitsu, M. Matsunaga, R. Otogawa, "Oxygen evolution electrode", JP patent No. 3914162.

3. M. Morimitsu, K. Matsumoto, R. Otogawa, M. Matsunaga, "Anodic deposition of PbO_2 on IrO_2-Ta_2O_5 coated Ti electrodes, Effects of thermal decomposition temperature", Proceedings of 27th Symposium on Electrolysis Technology, pp. 76-69, Yokohama, Japan, November 25-26, 2003.

4. M. Morimitsu, K. Matsumoto, M. Takao, R. Otogawa, M. Matsunaga, "Optimization of structure and composition of IrO_2-Ta_2O_5/Ti anodes for copper foil production", Paper No. 721, 54th Meeting of The International Society of Electrochemistry, Sao Pedro, Brazil, August 31-September 5, 2003.

5. M. Morimitsu, "Anodes and method for zinc electrowinning", JP patent No. 4516617.

6. M. Morimitsu, "Anodes and method for cobalt electrowinning", JP patent No. 4516618.

7. M. Morimitsu, "Anodes for electrolytic winning of zinc and cobalt and method for electrolytic winning", WIPO international patent application No. PCT/JP2009/060504.

8. M. Morimitsu, "Metal electrowinning system and method", JP patent application No. 2009-278607.

9. M. Morimitsu, "Metal electrowinning system and method", WIPO international patent application No. PCT/JP2009/70809.

10. S. Sandoval, M. Waite, M. Morimitsu, C. Clayton, "Multi-coated electrode and method of making", U.S. Patent Application Ser. No. 12/432454.

11. S. Sandoval, M. Waite, M. Morimitsu, C. Clayton, "Multi-coated electrode and method of making", WIPO international patent application No. PCT/US2009/044341.

12. M. Morimitsu, N. Oshiumi, "Accelerated oxygen evolution and suppressed MnOOH deposition on amorphous IrO_2-Ta_2O_5 coatings", Chemistry Letters, Vol. 38, pp. 822-823, 2008.

13. M. Morimitsu, K. Kawaguchi, "A novel bifunctionality of RuO_2-TiO_2 electrocatalyst prepared by low temperature thermal decomposition", Journal of Surface Finishing Society of Japan, Vol. 60, pp. 817-819, 2009.

14. M. Morimitsu, K. Uno, "A novel electrode for cobalt electrowinning to suppress CoOOH deposition", Proceedings of Hydrometallurgy of Nickel and Cobalt 2009, pp. 571-580, Sudbury, Canada, August 23-27, 2009.

15. M. Morimitsu, N. Oshiumi, N. Wada, "Smart anodes for electrochemical processing of copper production", Proceedings of Copper 2010, Volume 4, Electrowinning and Refining, pp. 1511-1520, Hamburg, Germany, June 6-9, 2010.

16. M. Morimitsu, N. Oshiumi, T. Yamaguchi, "Amorphous oxide coated anode for energy saving of zinc electrowinning", Proceedings of Lead-Zinc 2010, pp. 813-818, Vancouver, Canada, October 3-7, 2010.

17. S. Sandoval, C. Clyaton, S. Dominguez, C. Unger, T. Robinson, "Development and commercialization of alternative anodes for copper electrowinning", Proceedings of Copper 2010, Volume 4, Electrowinning and Refining, pp. 1635-1647, Hamburg, Germany, June 6-9, 2010.

DEVELOPMENT OF ANODE BAG TECHNOLOGY IN NICKEL ELECTROWINNING

By

[1]Ville Nieminen, [2]Noora Kaakkolammi, [1]Henri Virtanen, [1]Eero Tuuppa, [2]Rauno Luoma

[1]Outotec, Finland
[2]Norilsk Nickel Harjavalta Oy, Finland

Presenter and Corresponding Author

Ville Nieminen
ville.nieminen@outotec.com

ABSTRACT

In 2008 Outotec and Norilsk Nickel Harjavalta started a joint effort to develop anode bag technology to be used in sulfate based nickel electrowinning (Ni EW). Using anode bags instead of cathode bags is an efficient way to suppress acid mist and nickel emissions in the tankhouse environment. Furthermore, anode bags enable other process possibilities, such as recirculation of the electrolyte and recovery of anodically evolved oxygen. The aim of the development work was to obtain a high anolyte sulfuric acid concentration of 80 g/l, in other words, a high ΔNi, the difference in nickel concentration between rich electrolyte and anolyte, without a negative impact on cathode quality. The high acid and low nickel concentrations in anolyte are economic when it is recirculated in the leaching stage. A further aim was to find good and efficient tankhouse practices with anode bag technology.

Electrolyte flow control through the diaphragm inside the anode bags was first studied in laboratory scale Ni EW experiments. At a current density of 200 Am^{-2} a high anolyte sulfuric acid concentration, up to 120 g/l, was obtained. A commercial scale pilot cell containing anodes in specially designed bags was operated for over two years. Easily operated bag frames were developed in the course of the campaign. The new bag system enabled good control of the electrolyte flow. A small amount of sodium lauryl sulfate was used as an additive to obtain smooth cathode surfaces. Catholyte overflow from the cell was circulated and pH was controlled by neutralization with caustic. Anolyte and anode gas were withdrawn from the bags by suction using dip tubes located below the catholyte level. The anolyte acid concentration and ΔNi were maximized by carefully controlling the catholyte flow through the diaphragm inside the anode bags; a sulfuric acid concentration of 80 g/l in anolyte and a ΔNi of 50 g/l were obtained. The current efficiency was very high, typically 98%. The gas contents inside the bags were measured indicating that the gas mixture contained high amounts of oxygen, around 98% by volume, which is highly suitable for the oxygen recovery to be used in the leaching stage. CellSense™, an automatic cell monitoring system, was used to detect changes in cell voltage and temperature. The monitoring system made it possible to detect short circuits as a drop and fluctuation in the cell voltage as much as a day before removing the shorts was actually needed. A higher current efficiency and a lower number of torn bags were obtained as a result. The stable operation of the anode bag cell was achieved.

266

INTRODUCTION

Norilsk Nickel Harjavalta and Outotec started a joint project to develop anode bag technology in nickel electrowinning (Ni EW) at the beginning of 2008. In the anode bagging process, the catholyte is fed directly to the bottom of the cell via a manifold pipe and recirculated in the cell via the overflow. The anolyte is directly removed from the anode bags, along with the acid mist and Ni-emissions due to oxygen evolution. Anode bagging electrowinning technology is commonly employed in chloride processes and is known to have been in use with sulfate process solutions in Cawse, Australia in 1999-2002. The sulfate-based anode bag technique has been tested by the Anglo Platinum Base Metal Refinery, in South Africa[1]. It was stated that the process criteria regarding anolyte acid concentration were the main stumbling blocks in the implementation. The anode bags functioned under low pressure, which was necessary to remove both aerosols and anolyte from the anode bag, resulting in pulling a low acid concentration through the anode bags, which further caused a significant addition in the amount of nickel electrolyte that was circulated. The aim of the development work was to obtain a high anolyte sulfuric acid concentration (or a high ΔNi, the difference between rich electrolyte and anolyte nickel concentrations) of 80 g/l with no negative impact on cathode quality. High acid and low nickel concentrations are economic when anolyte is recirculated in the leaching stage. A further aim was to find good and efficient tank house practices with the anode bags. The work consisted of a pilot cell testing that has been running since summer 2008. The essential findings of the pilot campaign are reported here.

Terminology

In order to avoid confusion, the terms for different type of solutions used in this paper are defined below.

- **Rich electrolyte** = Electrolyte fed to the tankhouse (or electrolysis process)

- **Catholyte** = Electrolyte fed to the cell. It is a mixture of recirculated catholyte (or lean catholyte, see below) and rich electrolyte

- **Anolyte** = Electrolyte suctioned from the anode bags and removed from the tankhouse (or electrolysis process). Can also be regarded as *lean electrolyte*.

- **Lean catholyte** = Electrolyte overflow from the electrolysis cell. This solution is recirculated in the electrolysis process, neutralized, mixed with rich electrolyte, and fed to the cell as catholyte.


LABORATORY EXPERIMENTS

Electrolyte flow control through the diaphragm inside anode bags was first studied by means of electrolyte permeability tests through different fabrics and laboratory-scale Ni EW experiments.

Electrolyte Permeability Tests

A set of different fabrics were first characterized based on their electrolyte permeability in order to select the most suitable fabric for use as a diaphragm material. A specially designed device was used, in which it was possible to adjust the height of the electrolyte column and measure the electrolyte permeability per square meter and hour. Different electrolytes with varying viscosities were synthesized and the electrolyte permeabilities were determined as a function of viscosities at different electrolyte column heights. The fitted electrolyte permeability plots for two fabrics are given in Fig. 1. As can be seen, the electrolyte permeability through the diaphragm depends not only on the fabric used but also on the electrolyte viscosity and hydrostatic pressure. Based on this information, the optimal diaphragm fabric can be chosen for given electrolysis conditions.

267
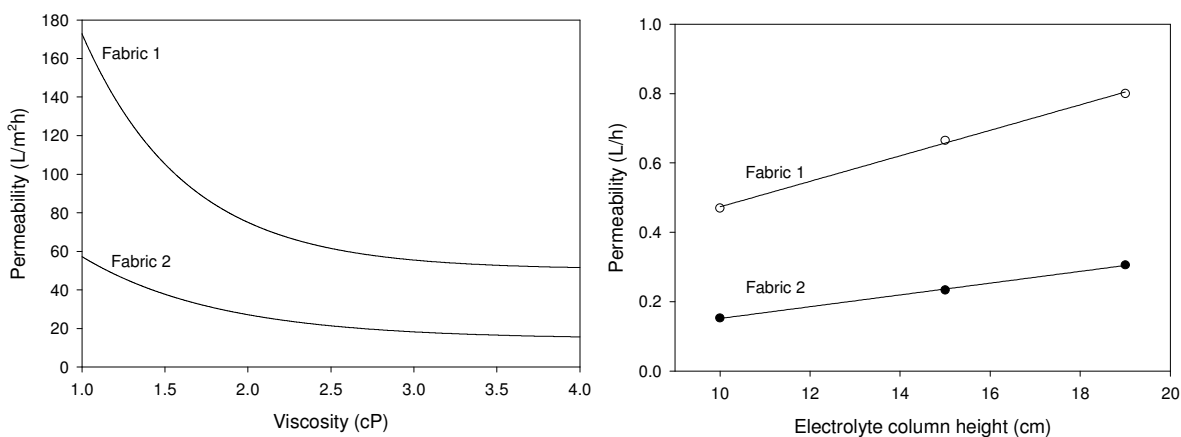
Figure 1: The electrolyte permeability tests for two diaphragm fabrics. Left: permeability per area as a function of electrolyte viscosity. Right: Total permeability with a viscosity of 2.73 cP (Ni 87 g/l) as a function of electrolyte column height.

Electrowinning Tests with Different Diaphragms

The electrowinning tests were carried out in a 27 L cell with three anode bag frames and two cathodes. Catholyte was pumped to the cell and lean catholyte was removed as overflow and collected in a circulation tank, to which rich electrolyte was added. Anolyte was removed from the anode bags as overflow. Thus the anolyte flow was defined by the electrolyte flux through the diaphragms and rich electrolyte feed was adjusted to be equal to the anolyte removal rate. Nickel starter sheets (17.5 cm x 9.5 cm) were used as cathodes and three Pb alloys were used as anodes (18 x 10 cm) inside the anode bags. The electrolysis was run for 24 h at 57 °C and approx. 200 Am^{-2}, the catholyte feed Ni concentration was 106 g/l and the pumping rate 6 l/h. Here we report the results of two fabrics, designated "tight" and "loose", which were tested with the following electrolyte permeabilities: 280 ml/h for "tight" and 2070 ml/h for "loose" per anode bag (tested with an electrolyte Ni concentration of about 70 g/l at room temperature). Hydrostatic heads (i.e. difference between anolyte and catholyte surfaces, the latter being higher) of 30 and 20 mm were used for "tight" and "loose", respectively. The main parameters are given in Table 1

Table: 1. Parameters and results of laboratory-scale Ni EW experiments with anode bags.

Parameter	Unit	Diaphragm	
		Tight	Loose
Catholyte feed temperature	°C	57	57
Voltage	V	4.4 - 3.9	4.1
Anolyte Ni concentration	g/l	93	102
Catholyte Ni concentration	g/l	106	106
Hydrostatic head	mm	30	20
Anolyte acid concentration	g/l	124	28
Anolyte flow removed from bags	l/h	0.34	3.4
Current density (cathodic)	A/m^{-2}	197	190
Electrolysis time	h	24	24
Catholyte pH in the cell		3.1 $\rightarrow$ 1.5	3.7 $\rightarrow$ 3.1
Catholyte feed to the cell	l/h	6	6
Current efficiency	%	94	~100

Results

The main results are given in Table 1. The anolyte overflow for the "tight" fabric was only 0.34 l/h, while it was ten-fold higher for the "loose" fabric, 3.4 l/h. Since the same amount of electric current was used, the anolyte acid concentrations were different, 124 and 28 g/l for "tight" and "loose",

268

respectively, and the anolyte Ni concentrations were 93 and 102 g/l for "tight" and "loose", respectively, indicating a larger ΔNi for the tighter diaphragm. The catholyte pH decreased for the "tight" diaphragm from 3.1 to 1.5. It appears that the hydrostatic head and slow electrolyte flux through the diaphragm could not prevent hydrogen ion migration from the anolyte to catholyte compartment. Consequently the current efficiency was 94% and the Ni cathode surface contained pitting. No pH measurement was taken during the experiment and therefore it is reasonable to assume that the pH drop below 2 in the catholyte took place at the very end of the experiment. The cell voltage dropped from 4.4 to 3.9 during the electrolysis experiment. For the "loose" diaphragm the catholyte pH dropped only from 3.7 to 3.1 while the cell voltage remained at 4.1 V. The current efficiency was virtually 100%, but even so some pitting was present in the Ni cathodes. It is to be noted that no surface agents were used, e.g. sodium lauryl sulfate, which is known to prevent pitting by aiding the continuous discharging of hydrogen bubbles due to the lowering of the surface tension[2][3].

As demonstrated above, a high acid concentration in anolyte can be obtained in Ni EW anode bag technology by carefully controlling the catholyte flow through the diaphragm into the anolyte compartment.

PILOT CELL CAMPAIGN

A simplified flowsheet of the pilot cell setup is given in Fig. 2. The catholyte was fed to the cell via a manifold, the overflow was collected in the circulation tank, and the pH of the recirculated lean catholyte was controlled by the addition of caustic. Embedded anolyte collection pipes were located on the inner sides of the cell, connected individually to each anode bag via a suction pipe. The cell could fit 40 or 47 cathodes and an additional external resistance unit was designed and built for it. The temperature of the cell was controlled by measurement of the overflowing catholyte with the CellSense™ system. Anolyte, along with acid mist and oxygen, was removed from the anode bags by individual pipes from each anode frame connected to the anolyte collection piping embedded in the cell walls. The suctioned acid mist was washed with a scrubber. A small amount of sodium lauryl sulfate was added to the catholyte to avoid pitting of the nickel cathodes[2].
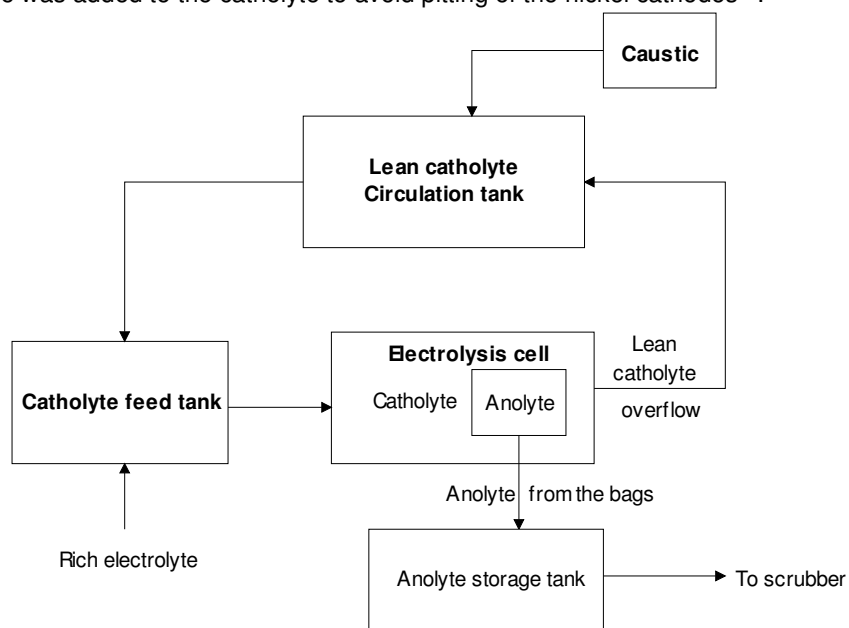
Figure 2: A simplified flowsheet of the Ni EW anode bag pilot cell campaign.

Cell

The cell was made of UNICELL® material, a vinyl ester-based composite. This material is very resistant to corrosion but has some weakness with heat shocks. Unicell allows embedded features, like the anolyte collection piping. The anolyte piping has two rows of holes to the cell, enabling Ni EW experiments with varying spacing distances. The catholyte exits the cell via an adjustable V-notch over-flow. The inner cell dimensions are length 6680 mm, depth 1600 mm and width 1242 mm. The total inner volume of the cell is then approx. 11.9 m^3. The cell weighs approx. 8 metric

269

tons. The cell accommodated 40 cathode and 41 anodes with an electrode spacing of 160 mm and 47 cathodes and 48 anodes with an electrode spacing of 135 mm.

Anodes and Cathodes

The Pb-Ca-Sn anodes made by Royston (UK) were prepared by hot rolling, with dimensions of 8 mm (thickness) x 971 mm (length) x 810 mm (width), with smooth edges and corners to ease placement in the anode frames. The U-shaped bar and the anode are connected with a hanger bar covering made of a lead alloy containing 5-6% of antimony. Nickel starter sheets were used as cathodes.

Electric Contacts

The cell is provided with double contact busbars, which are normally designed for a cell pair, but in this pilot it was used only for one cell. The busbar itself is made of a single metallic bar, but the electrical input to the busbar is made via four copper risers on each side in order to give more even current distribution along the busbar. The double contact busbar worked well and one clear benefit using them was an increase of slightly over 1% in current efficiency; overall, the current efficiency was very high, approx. 98% in most of the harvest cycles. The increase in current efficiency was also confirmed in the tests carried out in the tankhouse production cells with cathode bags.

Anode Bag Frame and Diaphragm

After over two years of testing and development work, an easily operated and fully functional anode bag frame was developed and several diaphragm fabrics were tested in the course of the pilot campaign. The optimal diaphragm fabric was found and used in the pilot campaign.

Cell Voltage and CellSense

The catholyte temperature and voltage were tracked by a wireless Outotec CellSense™ electrolytic cell performance monitoring system. Previously the system had been used in the copper electrorefining and copper and zinc electrowinning tankhouses, but here calibration was carried out for nickel electrowinning, in the anode bag pilot cell and also in the production cells with cathode bags. Essential information of the electrolysis process can be obtained by monitoring the cell voltage. The voltage of the pilot cell as a function of time during one cathode harvest (7 days) is presented in Fig. 3. The intensive drops in the cell voltage for a short period of time are due to temporary current drops/peaks in the production cells, caused by separating a cell or group of cells from the circuit for cell maintenance activities. In general, the voltage drops constantly as nickel is deposited on the starter sheet. The cathode harvests are clearly seen as voltage peaks.
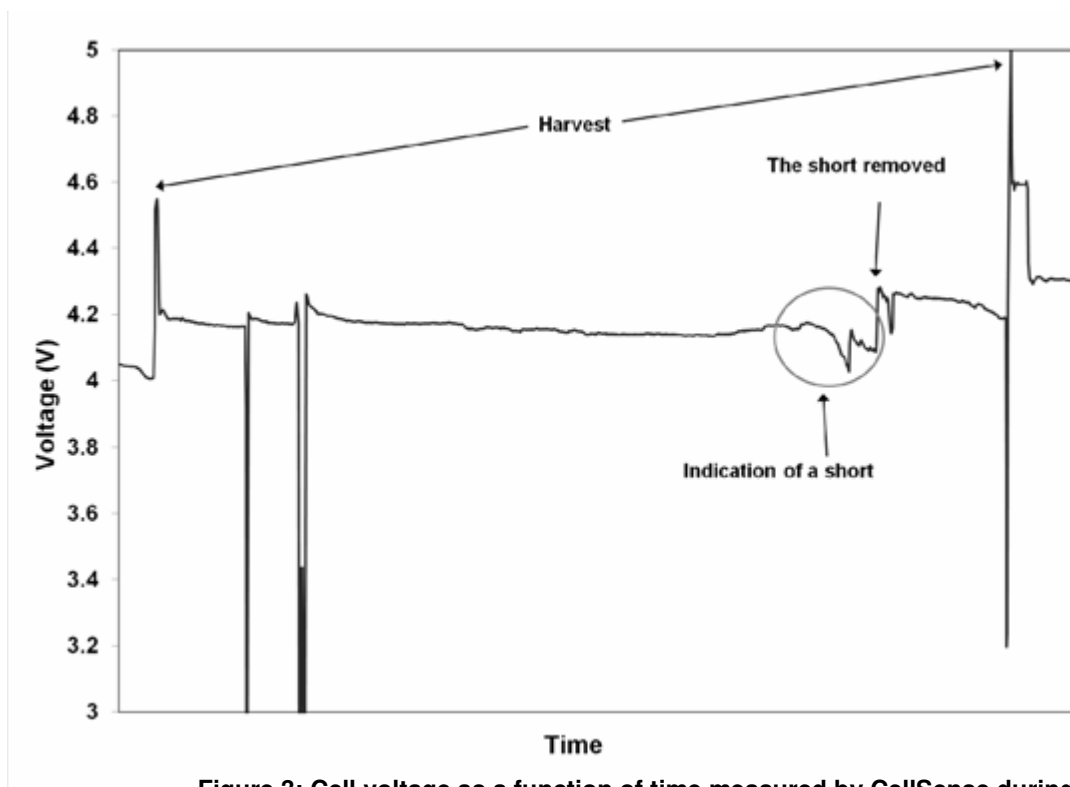
Figure 3: Cell voltage as a function of time measured by CellSense during one harvest cycle, 7 days.

The main benefit of automatic voltage measurement is the prediction of short circuits. Before a short circuit is formed the voltage starts to fluctuate and drop (See Fig. 3) and the CellSense alerts the tankhouse staff to remove the short in the cell. Early identification and correction of short circuits is beneficial to protect the process equipment and to minimize the loss of electricity and production: the current efficiency is improved and the number of torn anode bags is reduced. This is also a safety issue. If several anode bags are torn by shorts, the acid can migrate to the catholyte compartment and consequently the decrease in pH leads to hydrogen evolution at the cathode. Bad contacts between the cathode and bus bar increase the cell voltage, and the current density in the next cathode leading to a higher risk of shorts. The limiting values of the cell voltage for alerting were calibrated in the course of the pilot campaign and new values were needed when the parameters were changed, e.g. when the spacing was decreased from 160 mm to 135 mm.

Naturally, the decrease in spacing decreased the cell voltage and the cell voltage increased when the current density was increased. During electrolysis, the voltage also decreased due to cathode growth. At 200 A/m^2 with 160 mm spacing, the cell voltage was 4.8 ± 0.2 V and decreased to 4.6 ± 0.2 V. The need for short removal typically occurred at a cell voltage of 4.5 V. At 220 A/m^2 and 135 mm spacing the cell voltage was approx. 0.4 V lower.

General Discussion

Typical parameters and results are given in Table 2. The overflow catholyte temperature was typically approx. 60-65 °C while the catholyte feed temperature was around 55 °C. Nickel concentration in the rich electrolyte varied mainly between 100-120 g/l. A typical hydrostatic head was 20 mm. The harvesting cycle was seven days but at a high current density it was necessary to use a six-day harvest cycle to obtain a good quality deposit. The pilot started at a current density of 200 Am^{-2} and an electrode spacing of 160 mm. These parameters were changed to optimize the production per cell and finally at a current density of 217 Am^{-2} and 135 mm spacing, the nickel deposit quality was adequate without dendritic growth and only a few nodules. When decreasing the spacing, it is very important to have straight starting sheets. Otherwise bent sheets increase the risk of short circuits and consequently result in torn anode bags. The recycling rate of the catholyte was tested by varying it between 1.5 and 5 m^{3}h^{-1}. The catholyte pH is easier to control with a higher circulation rate and therefore a good quality nickel deposit can be obtained. Recirculation of the catholyte also helps to obtain a higher ΔNi value with higher catholyte flow rates. When the

271

cathodes are located inside the bags, very high ΔNi values are problematic, since the residence time of the catholyte in the bag increases considerably.

The ΔNi and anolyte acid concentration were rather modest for the first 10 harvests and the anolyte sulfuric acid concentration was below 40 g/l. By using a more suitable anode bag diaphragm and decreasing the catholyte flow through the diaphragm inside the anode bags, the sulfuric acid concentration increased to almost 60 g/ during the next 20 harvest cycles. Further development enabled better control of the catholyte flow through the diaphragm and stable operation of the pilot cell. By the end of the campaign, stable harvest operation was achieved and the anolyte sulfuric acid concentration of 80 g/l was obtained. In Fig. 4, average values are given for the anolyte acid concentration and the anolyte flow from the individual harvest cycles under stable operation, with a spacing of 160 mm and an average maximum current density of 220 Am^{-2}. The acid concentration is lower at higher anolyte flow rates and *vice versa*. The behavior is close to that observed in the laboratory-scale experiments.

A stable operation practice for running the anode bag cell was achieved. The bag consumption or the number of torn bags was very low and in several consecutive runs there were no torn bags. The average number of torn bags under stable operation was 0.16 bags per metric ton of produced nickel. The typical reason for a torn bag was a bent starter sheet.

Under stable operation the current efficiency was 98%. The catholyte overflow pH was typically 2.5-2.6. The measured catholyte pH and the current efficiency are given in Fig. 5. In general at the lower pH the current efficiency was lower, but some fluctuation was present. Under stable operation with a spacing of 160 mm the averages for feed catholyte pH and overflow catholyte pH were and 2.6, respectively, and with a 135 mm spacing, the feed catholyte pH was 3.3 and overflow catholyte pH was 2.5. A photograph of the cathode harvest is shown in Fig. 6.

Table 2: Main parameters and results of the Ni EW anode bag pilot cell campaign.

| Parameter	Value	Unit	Remark
Catholyte overflow temperature	mainly 60-65	ºC	Monitored by CellSense™
Voltage	4.0-4.8	V	Depends on the spacing, see text
Anolyte acid concentration	26-84	g/l	>70 g/l under stable operation
Anolyte flow	0.36-1.1	m^3/h	
Current density (cathodic)	up to 235	A/m^{-2}	
Electrolysis time / harvest cycle	6-7	days	6 days at higher current density
Catholyte pH, adjusted	4.0		
Catholyte feed to the cell	1.5-5.0	m^3/h	
Electrode spacing	160 and 135	mm	
Current efficiency	98	%	Under stable operation
Cathodes	40/47		Spacing 160 mm / 135 mm
Anodes	41/48		Spacing 160 mm / 135 mm
Applied current	11-17	kA	
Cathodes	Nickel starter sheets		
Rich electrolyte Ni concentration	82-125	g/l	
Catholyte Ni concentration	51-115	g/l	
Anodes	Pb-Ca-Sn alloy		Rolled
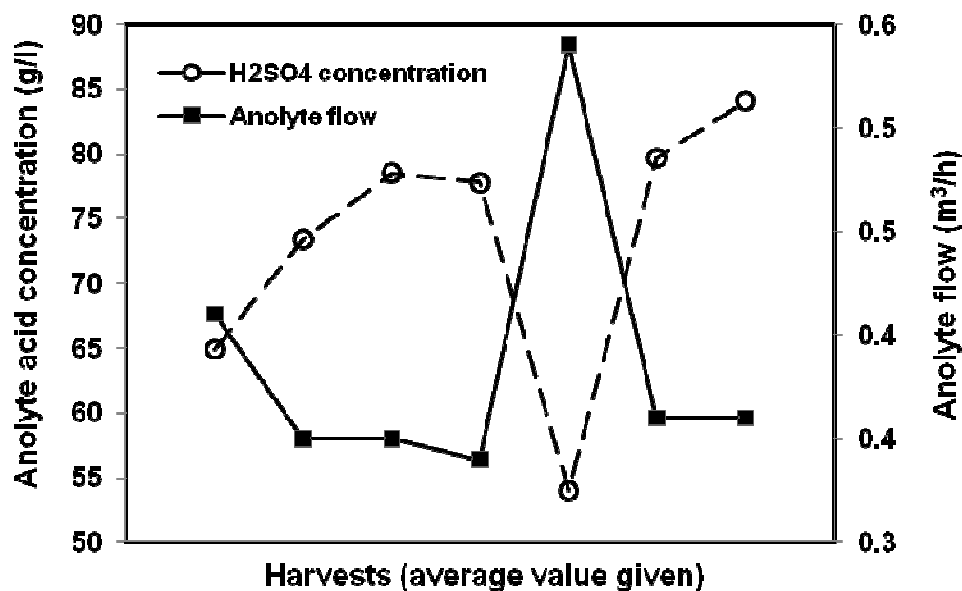
Figure 4: Average values of anolyte sulfuric acid concentrations and anolyte flows of individual harvesting cycles under stable operation of the pilot cell. The average maximum current density was 220 A/m^{-2} and electrode spacing 160 mm.
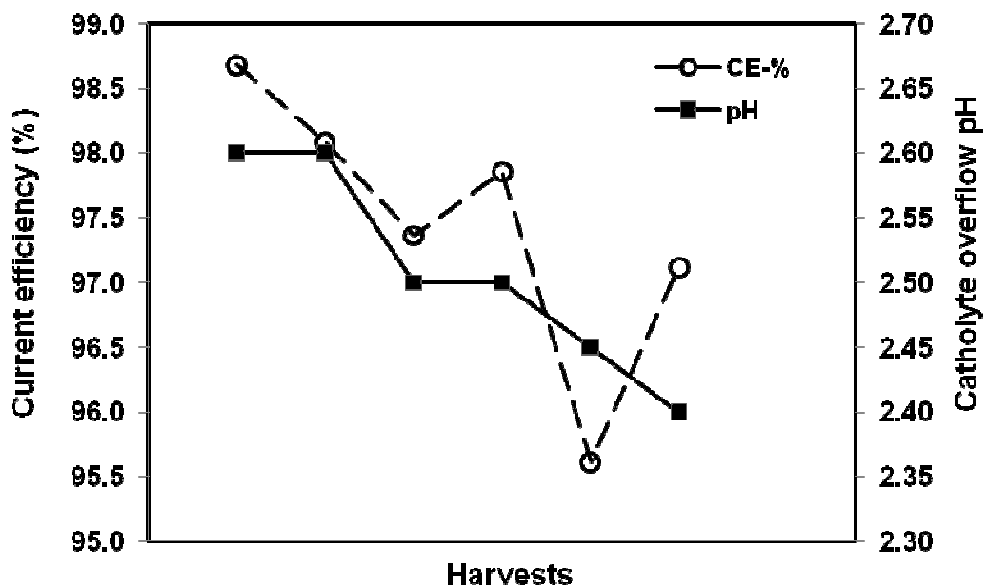

Figure 5: Current efficiency and pH of catholyte overflow measured during the different harvest cycles. The average maximum current density was 220 A/m^{-2} and electrode spacing 135 mm.

Figure 6: A photo of the cathode harvest.

Gas Measurements

In addition to re-circulating the catholyte, anode bag technology also allows the collection of anodically evolved oxygen to be used in the leaching step. Gas-impermeable bag covers above the electrolyte level prevent acid mist and nickel emissions in the tankhouse environment. Since the pilot cell was located in the same hall as the production cells, it was not possible to evaluate the effect of anode bags on the tankhouse environment; instead the oxygen levels inside the bags were measured. The gas samples were taken from the valves located on the bags opposite the suction point; the oxygen, CO_2 and H_2 contents were analyzed on-line. Samples were taken from four bags; from the middle and both ends of the cell. The oxygen content was very high at 98% by volume with one exception of 95% by volume, see Table 3. This indicates that the bags are gas-impermeable and the gas content is rather pure with respect to anodically generated oxygen. Therefore, it is possible to recirculate oxygen to the leaching step of the process. In addition, due to the high oxygen content, it can be concluded that there is no leaking from the bags and it is assumed that acid mist and nickel emissions can be collected without any emissions entering the tankhouse environment. There was also some hydrogen present in the anode bag gas environment.

Table 3: Gas content in % by volume
measured from the anode bags.

Anode bag #	O_2	H_2	CO_2
5	95	1.2	0.1
10*	98	1.3	0.2
20	98	1.2	0.2
36	98	1.3	0.2

* Gas sample taken from the anolyte suction
valve, no anolyte removal during the measurement

274

Summary of the Anode Bag Pilot Cell Campaign

Compared to cathode bag technology, many advantages can be gained by using bagged anodes as discussed in[4][5]. The main observations from the pilot cell campaign are given below:

- Good and efficient tankhouse practices were learned using anode bag technology. Stable operation was possible with good current efficiency.
- By careful control of the catholyte flow through the diaphragm to the anode bags, a higher anolyte acid concentration and consequently a higher ΔNi can be obtained. At lower anolyte flow rates higher acid concentrations were obtained. The aim - a sulfuric acid concentration of 80 g/l in anolyte - was achieved in the pilot campaign.
- Catholyte can be circulated and higher catholyte flow rates obtained. This improved the cathode surface finish, since the nickel concentration, pH, and temperature were easier to control.
- Very high oxygen content was measured inside the anode bag and thus it is possible to recover anodically evolved oxygen, which in turn can be re-circulated to the leaching step.
- Due to gas-impermeable anode bags above electrolyte level, acid mist control can be improved and virtually all Ni emissions can be recovered, resulting in a cleaner tankhouse environment.
- The number of torn bags can be reduced. This is due to several reasons
  - Access to the cathodes is easier, since they are not located inside the bags, and consequently there are fewer damaged bags during the harvest.
  - By monitoring the cell voltage with CellSense™, prediction of short circuits was possible. Removing the shorts early enough decreased the number of torn bags and increased the current efficiency.
- Bent starter sheets increased the number of shorts and torn bags. At the same time, the current efficiency was decreased. Therefore it is important to ensure that the starter sheets are straight.
- Double contact bus bars increased the current efficiency by approx. 1%.
- Lead precipitates from the deterioration of the anodes could be minimized since they were collected in the anode bags.

ACKNOWLEDGEMENTS

REFERENCES

1. L.J. Bryson, N.J. Graham, E.P. Bogosi, D.L. Erasmus, "Nickel Electrowinning Tankhouse Developments at Anglo Platinum Base Metal Refinery", proceedings of ALTA 2008 - Nickel/Cobalt, Copper & Uranium Conference, June 16-18, 2008.

2. E.A. Orlova, N.N. Tsamakalova, Yu.L. Saravaiskaya, "Effect of surface-active substances on cathode nickel quality", Soviet J. Non-Ferrous Met. 29 (1988)2, pp. 41-42.

3. T. Zhilin, C. Changan, "Pits forming and preventing in the process of the nickel electrowinning", Extractive Metallurgy of Copper, Nickel and Cobalt, Vol. I: Fundamental Aspects, pp. 1003–1014, Eds. R.G. Reddy, R.N. Weizenbach.

4. D.J. Robinson, R. Fraser, C. Panaou, K. Gottliebsen, M. Van Rooyan, G. Nel, "The Tati Nickel Electrowinning Plant", METSOC Hydrometallurgy of Nickel and Cobalt 2009, Proceedings of the 48th Conference of Metallurgists of CIM, August 26, 2009, Sudbury, Canada,

5. T. Robinson, M. Weatherseed, E. Tuuppa, E. Heyting, "Developments in Nickel Electrowinning Cellhouse Design", Technical proceedings of ALTA 2002 Nickel/Cobalt, ALTA Metallurgical Services, Melbourne, 2002.

ALTA 2011
NICKEL/COBALT/COPPER

LEACHING OF SULPHIDES

RECOVERING COPPER AND GOLD IN CHLORIDE SYSTEM BY NIKKO CHLORIDE PROCESS

By

Kazuaki Takebayashi, Kazuhiro Hatano, Hiroshi Hosaka, Yoshifumi Abe

JX Nippon Mining and Metals Corporation, Japan

Presenter and Corresponding Author

Yoshifumi Abe
yoshifumi.abe@nmm.jx-group.co.jp

ABSTRACT

JX Nippon Mining & Metals Corporation (NMM) has been developing a process which makes copper and gold recovery easy and effective. The process, named Nikko Chloride Process, employs sodium chloride media and is composed of copper leaching and copper recovery, gold leaching and gold recovery and silver recovery. Leaching of copper and gold is performed under ambient pressure with only aeration. Nikko Chloride Process recovers copper by solvent extraction, then produces copper cathode from sulphate solution. Some bromide helps gold leaching from gold bearing copper concentrate. Gold is recovered on activated carbon or by solvent extraction. Silver is recovered by solvent extraction.

NMM built a pilot plant for the process in Perth. The pilot plant has operated well. More than 98% of copper is leached and high quality copper cathode is produced. More than 90% of gold is leached. Applying floatation could recover 5% more of the gold from the gold leach residue. NMM is trying to apply gold recovery by solvent extraction.

INTRODUCTION

The Nikko Chloride Process is a hydrometallurgical process to treat copper sulphide concentrate that has a low copper grade and some gold. The process can leach copper and gold into same leach solution. The process can treat high impurity concentrate and can recover minor elements like nickel and cobalt which are usually not suitable for recovery by pyrometallurgical processing. The Nikko Chloride Process treats sulphide concentrate in a chloride system, and leaching is performed under ambient pressure and at a temperature less than boiling point.

The process is composed of copper leaching, copper solvent extraction and electrowinning, gold leaching and gold recovery and silver recovery.

REVIEW OF CHEMICAL REACTIONS

Ferric chloride and cupric chloride leach copper sulphide concentrate and release copper and iron[1][2][3]. Sulphur is left in the residue as elemental sulphur. Cuprous ion is unstable in aqueous solution. The leach solution of the Nikko Chloride Process contains some sodium chloride to make the cuprous ion stable.

(1) $CuFeS_2 + 3FeCl_3 \rightarrow CuCl + 4FeCl_2 + 2S$

(2) $CuFeS_2 + 3CuCl_2 \rightarrow 4CuCl + FeCl_2 + 2S$

(3) $FeCl_2 + HCl + \frac{1}{4}O_2 \rightarrow FeCl_3 + \frac{1}{2}H_2O$
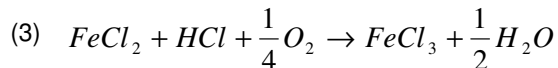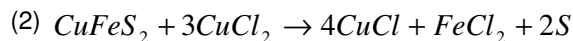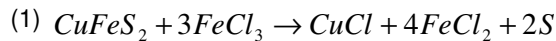
When the leach solution contains proton and the pH value of the solution is high enough, ferrous ion is oxidized to ferric ion by oxygen and ferric iron is precipitated.

(4) $FeCl_3 + 2H_2O \rightarrow FeO \cdot OH + 3HCl$
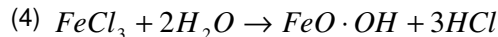
Cuprous ion is also oxidized to cupric ion.

(5) $4CuCl + 4HCl + O_2 \rightarrow 4CuCl_2 + 2H_2O$
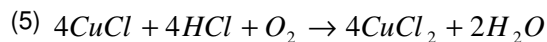
Overall reaction would be as follows.

(6) $CuFeS_2 + 2HCl + \frac{5}{4}O_2 \rightarrow CuCl_2 + FeO \cdot OH + \frac{1}{2}H_2O + 2S$
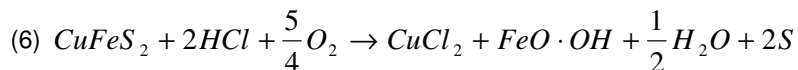
Two moles of hydrochloric acid and oxygen are needed to dissolve one mole of chalcopyrite. On the other hand, solvent extraction applied for recovering cupric copper extracts one mole of cupric ion and generates two moles of hydrochloric acid. The reaction is given below.

(7) $2RH + CuCl_2 \rightarrow R_2Cu + 2HCl$
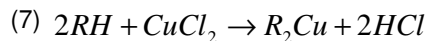
When copper extraction raffinate is returned to the copper leaching stage, hydrochloric acid generated at the copper extraction stage can oxidize cuprous copper and ferrous iron with oxygen in air. Cupric chloride and ferric chloride are good oxidants in chloride media and can progress sulphide leaching in the pH range without adding any acid.

When some impurities like arsenic exist in the copper concentrate, they are co-precipitated with iron[4].

Copper loaded organic extractant is stripped with sulphuric acid, then copper is converted to copper sulphate from copper chloride in the leach solution. Copper electrowinning from copper sulphate solution is a well known method to recover copper.

When copper sulphide is leached in halide solution, gold in concentrate begins to be soluble when cthe opper content is low enough[5]. Bromide ion forms a stable complex with gold and reduces the redox potential of gold oxidation compared with the chloride complex[6][7]. Figure 1 shows the standard redox potential of gold in the aqueous halide system. The standard redox potential of each half-cell reaction is shown in V vs SHE.

The Nernst equation for the gold halide complex is,

$$E = E^o + \frac{RT}{nF} \ln \frac{[AuX_{n+1}{}^-]}{[X]^{n+1}} \tag{8}$$

According to equation (8), low gold concentration in a solution makes the redox potential lower. When gold concentration is low enough, ferric ion or cupric ion is suitable for leaching gold in bromide containing solution.

Leach solution is returned and leaches the concentrate many times and some minor elements in the concentrate are accumulated in the leach solution. These elements can be recovered from a part of leach solution with a combination of solvent extraction and/or ion exchange resin.
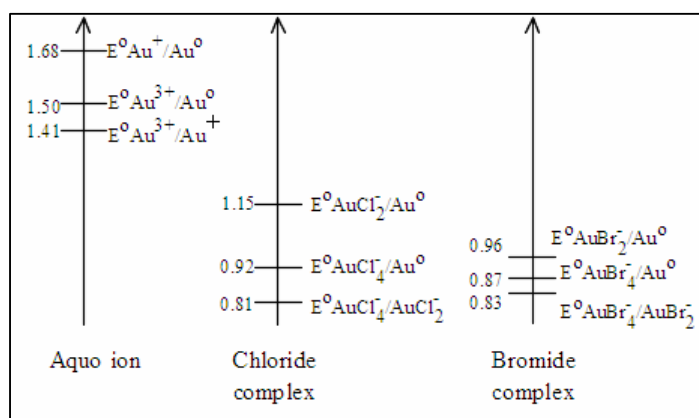
Figure 1: Standard redox potential of gold complex

PROCESS EXAMINATION

Bench scale testing was performed at the Technology Development Center in Hitachi, Japan. A concentrate sample was composed of chalcocite, chalcopyrite, silicate and pyrite. It contained   15 - 23% of copper, 21 - 24% of iron, 20 - 27% of sulphur and 54 – 84 g/t of gold. The reaction was performed in a glass beaker at 85 degree centigrade.

Copper Leaching

Figure 2 shows copper content change in leach residue. The copper concentrate was leached in chloride solution which contained 20 g/l of copper chloride and 5 g/l of iron chloride. Chloride concentration in the leach solution was 2.4, 4.0 and 5.1 mol/l. Temperature was 85 degrees centigrade. Copper content in residue was reduced to less than 0.5% in 20 hours in the solution containing over 4.0 mol/l of sodium chloride. More than 4.0 mol/l of chloride had no effect to shorten the reaction time with this sample. 2.4 mol/l of chloride had a little longer reaction time but enough to leach copper.
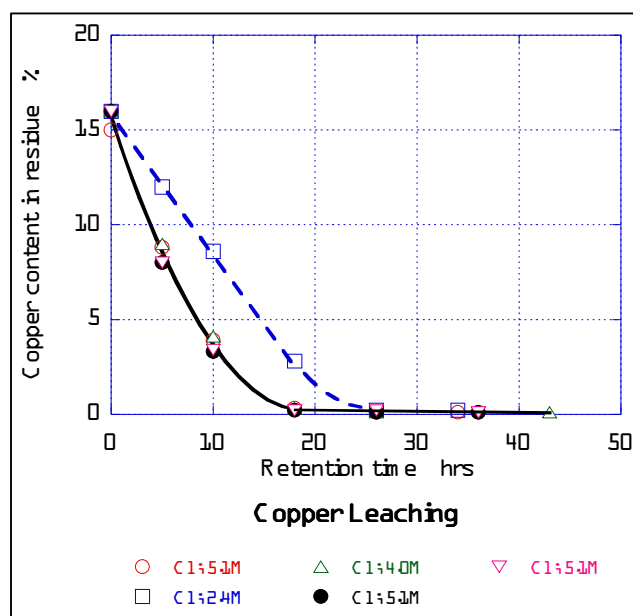
Figure 2: Copper content change in residue at copper leaching

Copper Solvent Extraction

Copper recovery by solvent extraction from chloride media has been applied in a number of processes. Hydroxyoximes, ACORGA CLX-50 and amine have been used as the copper extractant[8]. Sulphuric acid or water were used to strip copper from these extractants. NMM was familiar with copper electrowinning from sulphate media and selected the hydroxyoxime, LIX series[9].

Table 1: Cupric copper extraction with various extractants

	pH after Ex	Analysis Cu g/l		Calculated Cu g/l
		Raffinate	Strip	Organic
LIX860	0.05	3.26	4.94	2.3
LIX84–I	0.27	6.14	3.57	0.8
LIX622	0.05	4.10	4.62	1.8
LIX984	0.10	4.46	4.51	1.5

There were four candidates for the extractant. These were LIX860, LIX84-I, LIX622 and LIX984. 20% of each extractant was diluted in Isoper. The copper solution contained 3 mol/l of sodium chloride, 18 g/l of sodium bromide and 10.5 g/l of copper as cupric chloride and the pH was adjusted to pH 2. The result was on Table 1.

According to the result, LIX860 has a good isothermal curve and a good effective loading capacity. LIX84-I has a good stripping behavior. NMM selected LIX984 for the process extractant because of loading capacity and low copper concentration after stripping.

Copper Electrowinning

Lead anode and stainless cathode were employed for copper electrowinning examination. Cobalt sulphate was added to minimize generating over potential of oxygen and to achieve a suitable power consumption. The sample cathode had a good shape and enough quality for LME A grade.

Gold Leaching

Bromide addition to a chloride solution makes gold leaching more effective than with only chloride. Figure 3 shows the effect of adding bromide.

Chloride solution leached gold in this sample, and high concentration of chloride made the gold content lower. Bromide addition to the chloride solution reduced the gold content in residue. Figure 4 shows the effect of bromide concentration in chloride solution for gold leaching.
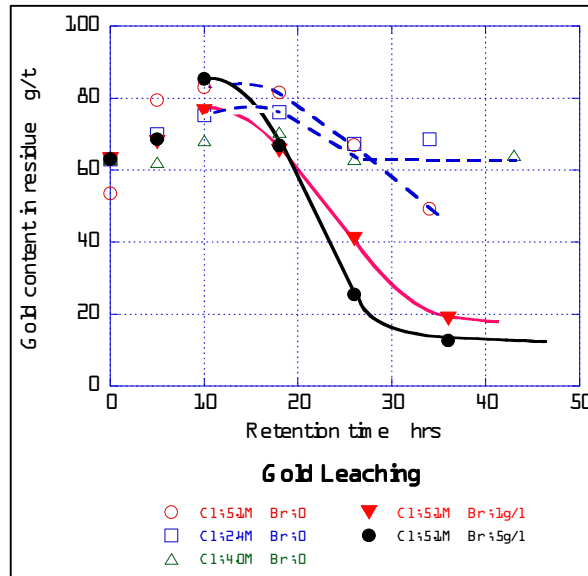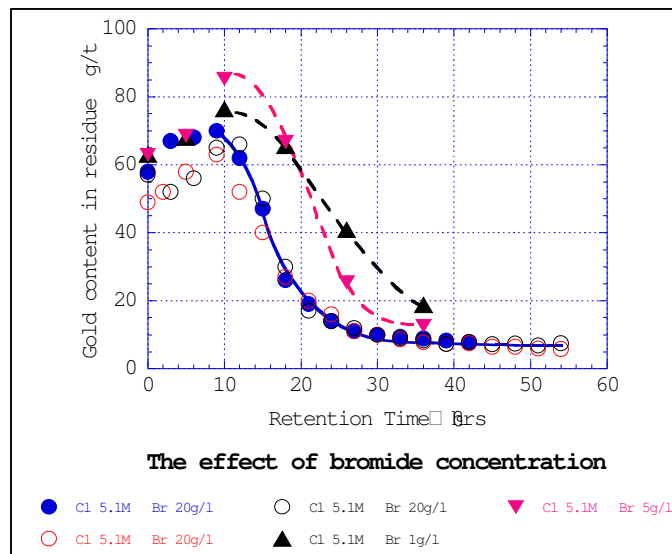

Figure 3: Gold content change in leach residue

Figure 4: Effect of bromide concentration for gold leaching

The concentration of gold in the solution should be 9 mg/l when 100 % of gold was leached in one leach solution. The bromide concentration examined in this testing was sufficient to leach and make a stable complex with gold, and there was not much difference among the bromide concentrations. It seemed that a solution that contained high concentration of bromide could leach more gold.

Silver Recovery

Silver recovery from chloride media is possible by solvent extraction. Cyanex 471X can extract silver from chloride media[10]. Cyanex 471X has a not very large distribution ratio but a certain amount of silver should be removed from leach solution. Silver is easily dissolved into the leach solution and is stable in a high chloride solution. The pregnant leach solution from the copper leach stage is sent to the copper extraction stage to recover copper and the raffinate from copper extraction is returned to the copper leach stage to contact the leach solution. Dissolved silver is accumulated in the leach solution according to its solubility. The Nikko Chloride Process oxidizes pregnant leach solution to precipitate iron before copper solvent extraction and cuprous copper is oxidized to cupric copper. Cyanex 471X has a sufficient selectivity of silver over cupric copper.

PROCESS FLOW FOR THE NIKKO CHLORIDE PROCESS

Figure 5 shows the block flow diagram for the Nikko Chloride Process.
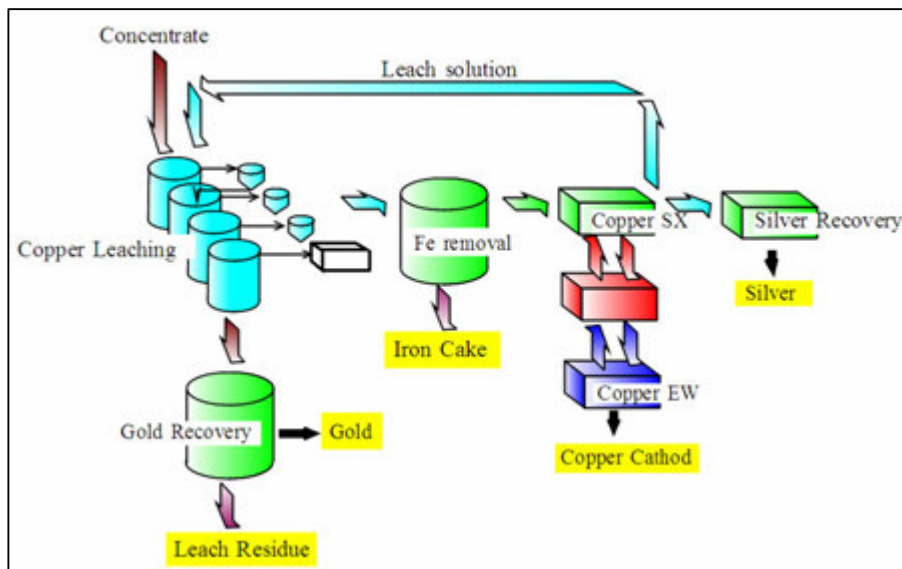
Figure 5: Flowsheet diagram of the Nikko Chloride Process

The copper leaching stage includes some steps to control copper concentration in leach solution. Copper extraction raffinate is divided in a number of parts. It is divided into four in the above case. Concentrate is added into the first copper leaching stage and agitated with one of the four portions of the leaching solution. Compressed air is sparged into the copper leaching tanks to continue oxidizing. After the first copper leaching step, the slurry flows to a thickener and is separated into overflow and spigot. The overflow solution flows to the next stage, namely the iron removal stage. The spigot is pumped to the second copper leaching step where it is mixed with another part of the leaching solution and copper leaching continues. After four stages of copper leaching, the residue is separated from the leach solution and is sent to the gold leach stage.

Dissolution of the gold in concentrate starts in the second or third copper leach step according to the copper content in residue. Gold in the pregnant leach solution is usually recovered from the overflow of the third and the fourth leach thickeners.

The thickener overflows are combined into one PLS after gold recovery and sent to the iron removal stage. Oxidation of cuprous ion and ferrous ion is performed by aeration. Copper is extracted from PLS by solvent extraction and stripped with spent electrolyte to recover copper by electrowinning. The raffinate from copper extraction is returned to the copper leaching stage as leach solution.

Copper leach residue is further processed in the gold leach stage. 80 to 85% of gold is leached in the copper leach stage. There are a number of methods for recovering the rest of gold from the copper

leach residue. One is further leaching with almost the same leach solution as the copper leach stage. CIL is employed to recover gold in this case. CIL has been applied by NMM and at the pilot plant in Perth. Another method is to recover gold with a part of the elemental sulphur as froth by flotation.

PROCESS FLOW EXAMINATION

At the Hitachi Laboratory of the Technology Development Center, NMM prepared bench scale equipment for each stage and examined the circuit work of the process. A leach solution which contains 5.1 mol/l of sodium chloride, 22 g/l of sodium bromide, 7 g/l of hydrochloric acid, 20 g/l of cupric chloride and 2 g/l of ferric chloride was prepared in a 5L glass beaker. The copper concentrate sample was added into the beaker and copper leaching started at a temperature of 85 degrees centigrade with air sparging. Copper leach slurry was filtered after defined hours of agitation. The filtrated cake was added to another 5L beaker in which copper leach solution was prepared and a second copper leach started. This procedure was repeated twice more and one copper leach residue and four filtrates were produced.

The four filtrates were combined in one solution. The solution was sent to the iron removal stage. Air was sparged into the solution to oxidize iron and precipitated iron was filtered to separate it from the copper pregnant solution.

Mixer-settlers, each of which had 1L of mixing tank and 1.6L ($0.017\ m^2$) of settler, were prepared. Two were for copper extraction, two for chloride scrubbing, one for stripping and one for sulphate scrubbing. Aqueous phase flow was at 11 ml/min and organic phase flow at 16 ml/min. Stripping solution flow was 17 ml/min. Copper was electrowon as a $0.01\ m^2$ plate from stripping solution at the current density of $300\ A/m^2$. Copper depleted raffinate was returned to leach more concentrate.

Copper Leaching and Copper Electrowinning

Figure 6 shows the copper content in copper leach residue and the copper extraction rate for this circuit examination. Copper content was reduced to about 0.5% and almost 99% of copper extracted.
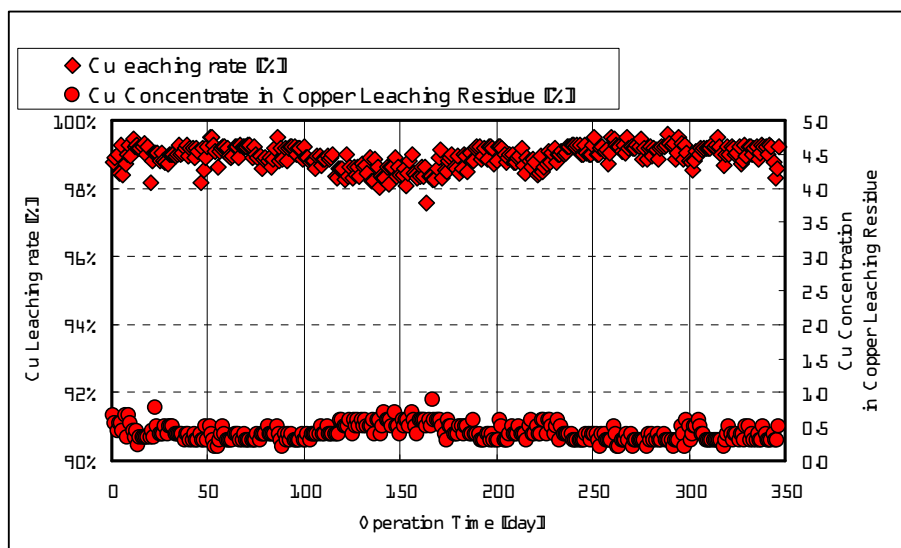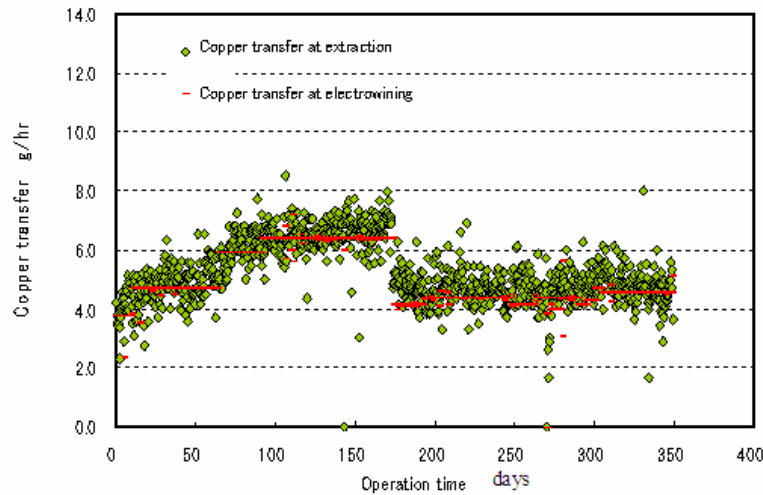

Figure 6: Copper leaching result

Figure 7 shows the amount of copper extracted at the copper solvent extraction stage and the amount electrowon at the electrowinning stage. The amount of copper extracted fluctuated somewhat but both

copper amounts changed almost in parallel, which means copper extraction and copper electrowinning were balanced.


Figure 7: Copper transfer at extraction stage and electrowinning stage

Gold Leaching

Four 3L beakers were prepared in series. Each beaker had an agitator, a heater and an air sparging pipe. They were connected together with overflow nozzles. Copper leach residue was pulped to be fed into first gold leaching beaker. The flow rate of the copper leach residue slurry was adjusted for each beaker to retain the slurry for twelve hours. The copper leach residue was continuously added into this leach equipment. Gold leach residue was also continuously eluted from the 4th beaker. Leach solution contained 180 g/l of chloride as sodium chloride, 20 g/l of bromide as sodium bromide, 5 to 20 g/l of copper and 2 g/l of iron.

Figure 8 shows the change of gold content in gold leach residue. Some adjustments to the conditions were applied in this campaign. CIL was applied from the 43rd day. Activated carbon was replaced with new carbon from the 93rd day. Retention time was changed from 48 hours to 96 hours from the 139th day. Chloride and bromide concentration were analyzed and adjusted from the 140th day. When chloride and bromide concentrations were analyzed, they were 110 g/l and 10 g/l and were adjusted to 180 g/l and 25 g/l respectively.
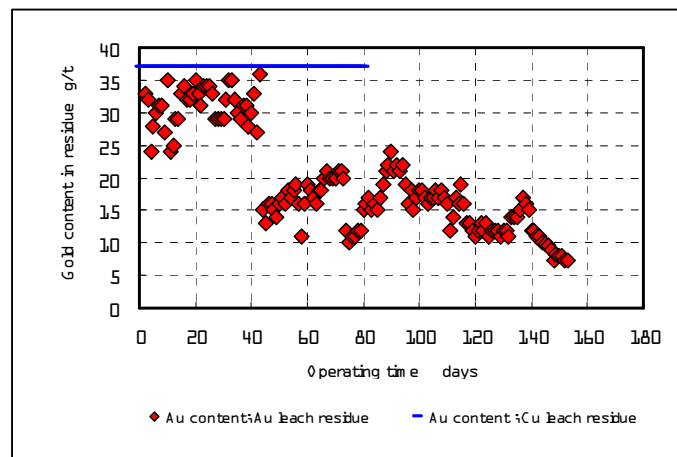
Figure 8: Gold content change in gold leach residue

The original feed concentrate had 74 g/t of gold. The copper leaching stage leached gold down to 37 g/t, which meant that 70% of gold in concentrate was extracted. The gold leach system reduced gold

content to 7 g/t. The gold extraction was over 90% because the amount of the feed was reduced to 60% of its weight.

The process flow examination was continued for one year to confirm the process performance below.

• Proton consumed in copper leaching and proton re-generated in solvent extraction were balanced.
• Copper extraction was sufficiently high.
• Quality of copper cathode was sufficiently high.
• Over 90% of the gold was leached.

PILOT PLANT IN PERTH

JX NMM built a pilot plant for the Nikko Chloride Process in Perth. The plant has the complete stages of the process. Bateman Engineering were EPCM consultant for building the pilot plant and JX NMM started the plant operation in October 2009 with Amdel.

Fig 9 shows the layout of the pilot plant. The pilot plant processed copper concentrate of which the copper content was adjusted from 20 to 12.5 %.
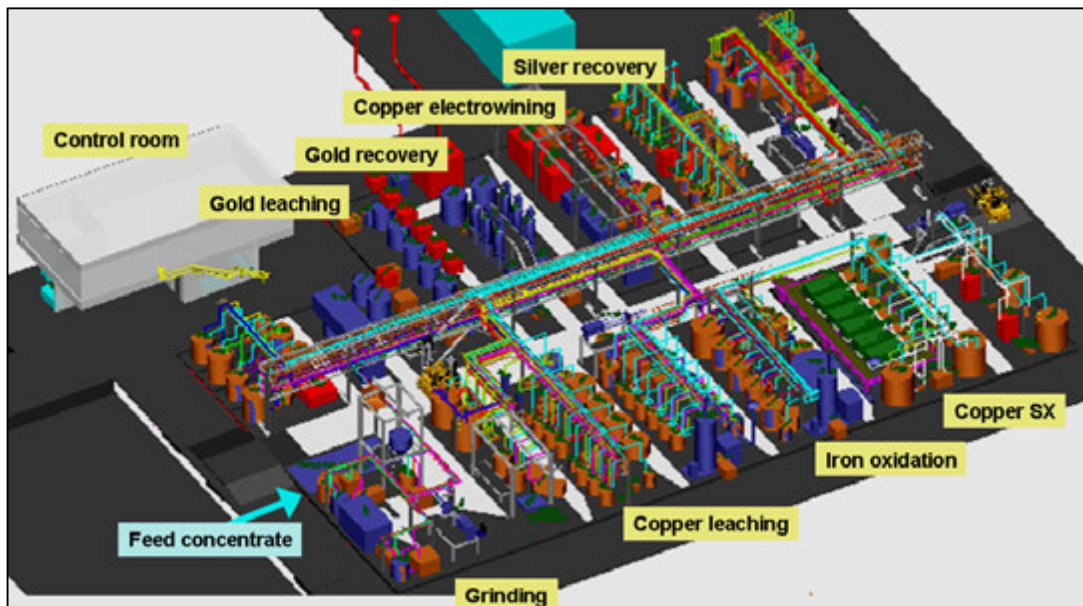
Figure 9: Layout of the pilot plant

Copper Leaching and Recovery

Fig 10 shows the copper leaching results for the pilot plant. The copper content figures for the final leach residue are shown at the bottom. They are less than 0.3%, and the copper extraction efficiency is more than 99%. The plant has four copper leaching stages. Thickeners are installed to separate copper leach solution and copper leach residue. Copper leach solution, copper extraction raffinate, was divided into four and each part of the solution contacted with feed concentrate or processing intermediate once. Thus the copper concentrate was leached four times.
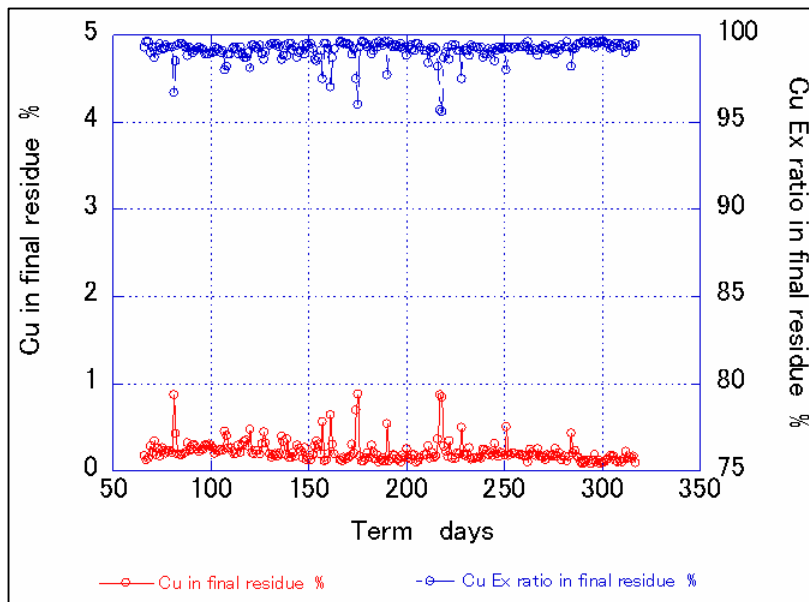
Figure 10: Results of the copper leaching stage

Four copper leach solutions were combined and oxidized by sparging air to oxidize cuprous copper and ferrous iron. The oxidized solution was sent to copper solvent extraction stage after filtration. LIX984N (LIX984 was changed to LIX984N) extracted copper from the oxidized solution and spent copper electrolyte was used to strip copper. Table 2 shows average analysis values of the copper cathode produced in the pilot plant.

Table 2: Average assay value of copper cathode

Copper Cathode	Ag	S	Fe	As	Sb	Bi	Pb
	0.2	4	1	<0.1	<0.1	<0.1	<0.1
Copper Cathode	Sn	Ni	Co	Ti	Se	Te	
	<0.1	<0.1	<0.1	<0.1	0.1	0.1	

Gold Leaching

Gold starts to be dissolved when the copper content in leach residue reduces to a certain level.   Gold is dissolved in the copper leaching stage and the gold leaching stage. A copper content less than 4% was achieved at the 3rd copper leaching step. Gold concentration of the 3rd and 4th copper leaching steps increased up to 5 mg/l as shown in Figure 11. Gold leaching in the copper leaching stage attained to 60 to 80% and around 90% of gold was extracted after the gold leaching stage.   Figure 12 shows the gold extraction changes in these two leaching stages.
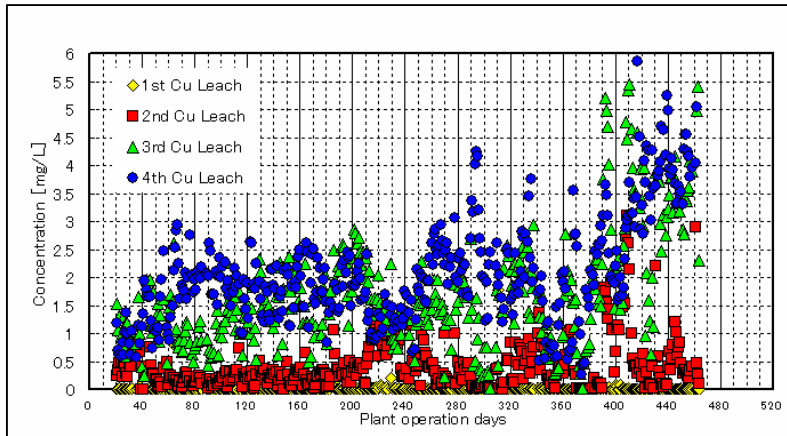
**Figure 11: Gold concentration changes in copper leaching stage**
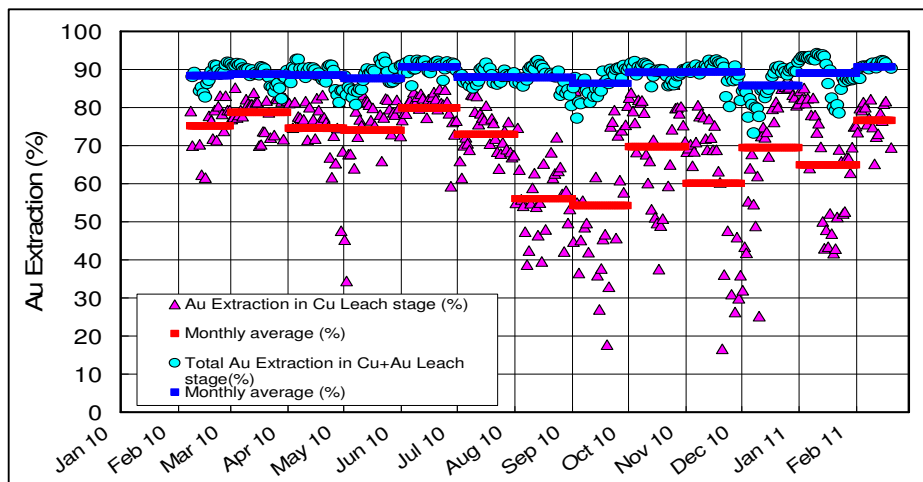
Figure 12: Gold leaching in copper leaching stage and gold leaching stage

Gold content in gold leach residue changed as Figure 13. The gold content change had a little variation. The poor leaching between 250 and 300 days was caused by the shortening of the leaching hours and mismatching between the amount of proton in leach solution and the amount of copper in feed. The gold content was reduced to about 10 g/t. An activated carbon column was installed after the 3rd and 4th copper leaching steps. The 2nd copper leach solution sometimes flowed through the activated carbon column. The activated carbon adsorbed 3,000 to 5,000 ppm of gold in this system. The capacity was too low to offset its operating cost. Therefore gold solvent extraction is being examined to replace activated carbon.
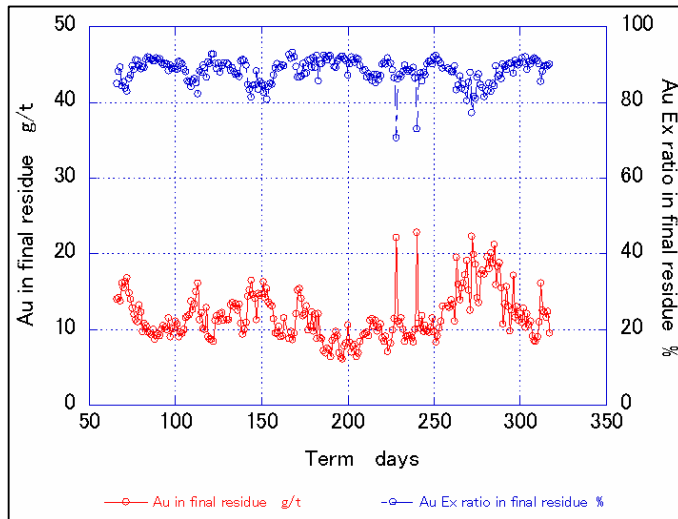
Figure 13: Gold content change in leach residue

Minor Elements

Sometimes copper concentrate contains minor elements like zinc, cobalt and nickel. With pyrometallurgical processing it is difficult to recover these elements. Nikko Chloride Process re-uses leaching solution many times; therefore these elements can accumulate in the process leach solution which makes recovery possible.

Figure 14 shows the concentration changes of the minor elements in copper leach solution. The average contents of zinc, cobalt, manganese and nickel were 906 ppm, 1,655 ppm, 472 ppm and 413 ppm, respectively. Nickel and cobalt are less soluble in this system considering the relative concentration ratio of these elements. These elements can be recovered separately by applying solvent extraction.
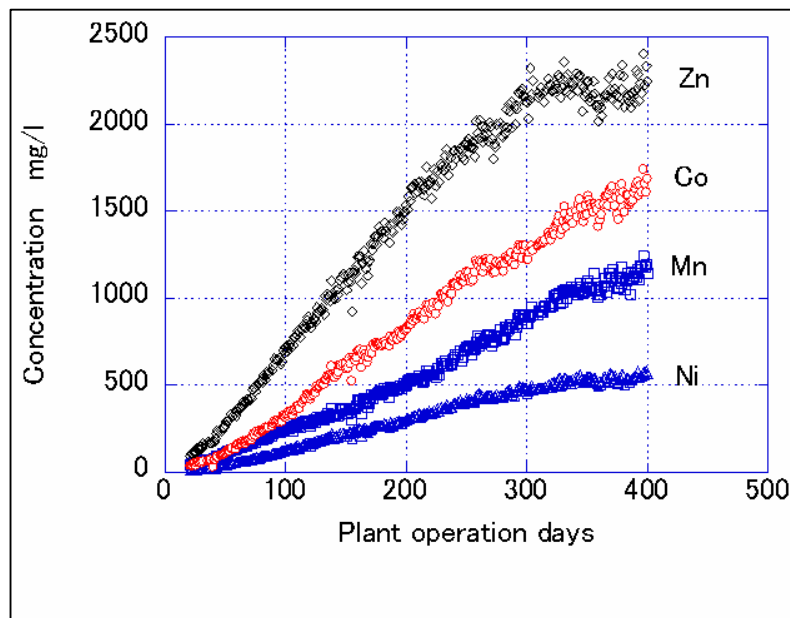
Figure 14: Minor elements build-up

288

Improvement of Process

The Nikko Chloride Process pilot plant in Perth processed copper sulphide concentrate to prove the effectiveness of the process. The process extracted more than 99% of copper in concentrate and produced high quality copper cathode with solvent extraction and electrowinning. The process leached more than 90% of gold. It is clear that the solution composed of sodium chloride and sodium bromide is suitable for treating gold bearing copper sulphide.

Gold solvent extraction has the potential to make the process effective for recovering gold. JX NMM has operated a hydrometallurgical process for copper anode slime treatment since 1997. Gold is extracted by DBC after wet chlorination and recovered by direct reduction of loaded DBC with oxalic acid in the plant. It is a simple and effective way to recover gold from chloride solution.

JX NMM examined DBC and LIX7820 for the gold extraction reagent. Gold is added as $HAuCl_4$. The oxidation reduction potential of copper leaching stage was about 550 to 630 mV vs $Ag/AgCl$. It is close to the redox potential of $AuCl_4^-/AuCl_2^-$ and according to Figure 1 $Au(I)$ extraction was also examined with a solution which was prepared by adding ferrous chloride to $HAuCl_4$ solution.

Table 3 shows the gold extraction with DBC. DBC extracted gold from the solution containing auric gold as in Run No. 1. Cuprous copper had some effect on gold extraction and ferrous iron had more effect on the extraction. The mixture of DBC and octanol extracts aurous gold[12]. Comparing Run No. 4 and 5, the mixture of DBC and octanol extracts more gold than DBC alone when solution contains ferrous iron.

Table 3: Gold solvent extraction with DBC

Run No.	Cu^{2+} g/l	Cu$^+$ g/l	Fe^{3+} g/l	Fe^{2+} g/l	Au mg/l	
					before SX	after SX
1	20	0	2	0	0.95	0.03
2	20	2	2	0	1.00	0.15
3	20	4	2	0	0.67	0.05
4	20	0	1	1	1.20	0.63
5	21	0	1.5	0.5	1.35	0.15

* Run No. 1 to 4 are extracted with DBC, Run No. 5 is with a mixture of DBC and octanol.

Table 4 shows the result of gold extraction with LIX7820. LIX7820 is a mixture of a quaternary amine and a weak acid to extract gold from cyanide solution[13]. This reagent is usually applied to alkaline solution. NMM tried gold extraction at pH 1.5 and got a result in which LIX7820 could extract gold from chloride solution with low redox potential as shown in Table 4.

Table 4: Gold solvent extraction with LIX7820

Run No.	Cu2$^+$g/l	Cu$^+$g/l	Fe3$^+$g/l	Fe2$^+$g/l	Au mg/l	
					before SX	after SX
1	20	0	2	1	0.66	< 0.01
2	20	2	2	0	1.83	0.19
3	20	2	2	1	1.34	< 0.01

When ferrous iron is added to the leach solution, its redox potential is reduced by 130 to 200 mV. Some gold would be as aurous in the solution and it becomes difficult to extract gold with DBC.

Gold extraction was performed in a mixer-settler with chloride solution and LIX7820. The chloride solution contained copper, iron and about 5 mg/l of gold. LIX7820 loaded gold to 290 mg/l. Sodium oxalate reduced gold directly from LIX7820 to produce gold powder which contained 0.45% of copper. Silver and iron were not detected in the gold powder.

CONCLUSION

Chloride processing has an ability to leach copper sulphide easily. Solvent extraction can convert chloride copper into sulphate copper and electrowinning of copper from sulphate solution can produce high quality copper plate. Various processes which combine these technologies are well known. The Nikko Chloride Process re-uses copper extraction raffinate as leach solution by dividing the raffinate in a number of parts to control copper concentration increase in the leach solution.

The Nikko Chloride Process can leach gold with only aeration by adding bromide to the leach solution ,because the gold bromide complex has a lower standard redox potential than the chloride complex and low gold concentration makes the oxidation potential lower.

The Nikko Chloride Process has been examined through bench scale tests. The process flow works well and a pilot plant has been built in Perth. The pilot plant achieved more than 99% of copper leaching and more than 90% gold leaching. Copper cathode electrowon in the plant was of very high quality.

It has become clear that the Nikko Chloride Process can be applied for copper and gold recovery from low copper grade concentrate with only air sparging under ambient pressure.

Nikko Chloride Process has many benefits mentioned below:

- Leaching copper with high extraction efficiency.
- Producing high quality copper by electrowinning in sulphate media.
- Leaching gold in concentrate by air sparging without any special oxidant (e.g. chlorine gas hydrogen peroxide).
- Accepting a wide range of copper and impurities content.
- Operating under ambient pressure and at a temperature less than boiling point

The Nikko Chloride Process can process low copper and/or high impurity concentrates that are difficult to treat by pyrometallurgical processing, and also can process gold bearing copper concentrates that cause complications in other hydrometallurgical processes.

The application of solvent extraction instead of activated carbon for improvement in gold recovery is being tried in the Perth pilot plant. The silver recovery stage is going to be verified in the pilot plant.

ACKNOWLEDGEMENT

REFERENCES

1. M. Lundstrom, J. Aromaa, O. Forsen, O. Hyvarinen and M. H. Barker, "Leaching Of Chalcopyrite In Cupric Chloride Solution", Hydrometallurgy, 77 (2005), 89-95.

2. D.S. Flett, "Chloride Hydrometallurgy For Complex Sulphides: A Review", CIM Bulletin, Vol. 95, No. 1065, October (2002).

3. M.L. O'Malley and K.C. Liddell, "Leaching Of $CuFeS_2$ By Aqueous $FeCl_3$, HCl, And NaCl: Effects Of Solution Composition and Limited Oxidant", Metallurgical Transaction B, Vol. 18B, September (1987), 505.

4. E. Krause and V.A. Ettel, "Solubility And Stability Of Scorodite, $FeAsO_4$ $2H_2O$: New Data And Further Discussion", American Mineralogist, Vol. 73, (1988), 850-854.

5. H. Hosaka, Y. Abe, "Process of Leaching Gold", AU Patent 2007205792, 28 Sep 2006.

6. T. Tran, K. Lee and K. Fernando, "Halide As Alternative Lixiviant For Gold Processing – An Update", Cyanide: Social, Industrial and Economic Aspects.

7. Dadgar, "Refractory Concentrate Gold Leaching: Cyanide vs. Bromine", JOM, December 1989.

8. J.Szymanowski, "Copper Hydrometallurgy And Extraction From Chloride Media", J. of Radioanalytical and Nuclear Chemistry Articles, Vol. 208, No. 1 (1996), 183-194.

9. Cognis Corporation, "The Chemistry of Metals Recovery Using LIX® Reagents", MCT Redbook.

10. Y. Abe, "Solvent Extraction Of Silver From Chloride Solutions By Cyanex 471X", Solvent Extraction, Part B, (1990), 1127-1132.

11. Y. Abe, H. Hiai, "Silver Recovery With Anion Exchange Resin", JP Application No. 2008-291222.

12. P. Lu, "Solvent Extraction Of Gold(I) From Alkaline Cyanide Solution By Dibutylcarbitol (DBC) With N-Octanol", J. Chem Technol Biotechnol, 83, (2008), 1428-1432.

13. Cognis Mining Chemicals Technology LIX®7820.

**IMPROVING CASH FLOW FROM LOW GRADE
NICKEL CONCENTRATES**

By

David Jones

Teck Resources Ltd/CESL, Canada

Presenter and Corresponding Author

David Jones
David.Jones@teck.com

INTRODUCTION

Teck Resources Limited

Canada's largest diversified resource company producing copper, metallurgical coal and zinc

- Mining operations in North America and South America
- World leader in zinc production
- Predecessor company, Cominco, was founded in 1896 with establishment of Trail Smelter (Pb, Zn). Smelting operations there have continued till this day
- Head office in Vancouver, Canada, with exploration office in Perth

Teck Resources Limited
Pressure Oxidation Experience

Zinc pressure leach (Trail, BC)

- A pioneering Pressure Oxidation plant built 1982, world first. $20 Million Capex
- Processes 150,000 tpy zinc concentrate to solubilize Zn at high yield
- Operating at essentially same conditions as CESL Nickel Process, i.e. similar temperature, pressure, and retention time.   Very high intensity operation.
- Has completed 29 years of operations, and now typically runs >150% design
- Produces elemental sulphur rather than sulphuric acid, hence low cost.

CESL

- Subsidiary of Teck
- Developed hydrometallurgical technology for treating Cu and Ni sulphides
  - For Cu utilizes existing technologies such as pressure oxidation, SX-EW
  - Added novel purification processes for Ni and Co.
  - Added a novel process for precious metal recovery from leach residues
  - Fifteen Patented processes, covering variety of base metal concentrates

Photos: Vale's 10K tpa copper cathode CESL refinery, Brazil

CESL Technology Solutions

CESL Process technology is a suite of processes that includes:

- Copper extraction from sulphide concentrates
- Nickel extraction from sulphide concentrates
- Recovery of both nickel and copper from bulk Cu-Ni concentrates in high yield
- Precious metal recovery from Cu process residues

Where is this Technology most useful?

Realizing value from sulphide resources that are not amenable to conventional smelting and refining technologies

- Low-grade concentrates
- Metallurgically complex concentrates, e.g.
  - Bulk concentrates, (several payable metals, Cu-Ni-Co-Zn)
  - high arsenic in copper concentrates
  - high MgO in nickel concentrates

CESL

CESL Copper Process

- Treats Cu sulphide concentrates through to refined cathodes
- Low cost, high reliability
- Successfully tested at both Pilot scale and in Demonstration plant (I tpd Cu)
- Validated at Vale's UHC plant in 2008- 2010, (design: 10,000 tpy Cu cathode)

Vale's demonstration plant in Brazil
Usina Hidrometalúrgica de Carajás
uses CESL Copper Process

Successfully Demonstrated

- 10 ,000 tpy Cu cathode design

NICKEL FORECASTS FOR SUPPLY AND DEMAND

Global Nickel Mine Supply and Demand
courtesy of Brook Hunt

Global Nickel Supply and Demand
- Base case refined output
- Consumption

2010 Mine Output
45% Sulphide
55% laterites

New refined output
required to meet demand
'unidentified'

2015 Mine Output
39% Sulphide
61% laterites

2020 Mine Output
33% Sulphide
67% laterites

2025 Mine Output
28% Sulphide
72% laterites

Figure by presenter, data sourced from Brook Hunt
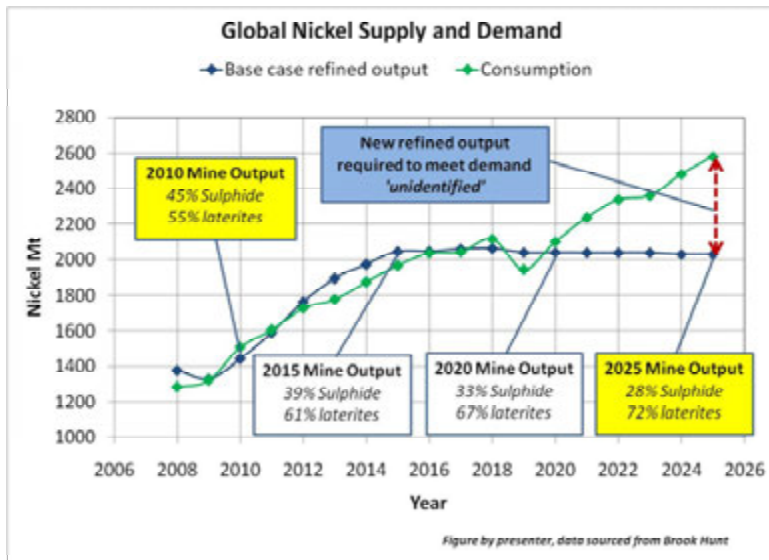
Future Projects

- By reliance on more laterites?

OR

- By exploiting Low-grade sulphides?

These can be developed by new Nickel Sulphide Hydrometallurgical Technology

Global Nickel Mine Supply and Demand

Short – Medium Term, up to 2020

- An additional 400,000 tpy Ni needed by 2020
- Supply and Demand predicted to be roughly balanced, with existing projects now starting up or under construction, e.g.
  - Koniambo, Onca Puma, Goro, Ravensthorpe, Weda Bay, etc
  - Expansion of NPI production

Longer Term, after 2020

- Another 600,000 tpy Ni needed by 2026….total of 2,600,000 tpy Ni
- Will this additional demand to be satisfied by more laterite projects or sulphides?
- Investors are wary now
- Will there be sufficient investment in laterite projects in future?

CESL NICKEL PROCESS

CESL Nickel Process

CESL has developed a hydrometallurgical technology that can unlock the value in disseminated sulphide resources

- CESL technology is capable of treating concentrates not suitable for smelting:
  - Low-grade nickel concentrates and those with high MgO content
  - Bulk nickel-copper-cobalt concentrates with no need for metal separation at the milling stage

CESL Nickel Process Features

Medium temperature pressure oxidation

- Mild conditions at low pressure and 150 °C
- Very low sulphur oxidation, results in high intensity use of autoclave
- Low capital and operating costs, compared to other autoclave processes, and high reliability

Other attributes of the CESL nickel process include:

- Well developed process, using known commercial technologies
- Low technical risk
- Treats both bulk and low-grade concentrates, even those high in MgO
- High metal recoveries for nickel, copper, and cobalt
- Effective impurity control and purification (e.g. Mn, Mg, Cu, Zn)
- Capable of operating with use of seawater
- Closed circuit, no effluent

CESL Nickel Process Flowsheet
(1 of 3)

Pressure Oxidation

Nickel Concentrate

Feed Liquor

Oxygen

Atmospheric Leach

Cu SX

Cobalt Removal

Copper Recycled Feed Liquor

CCD Wash

Leach Residue
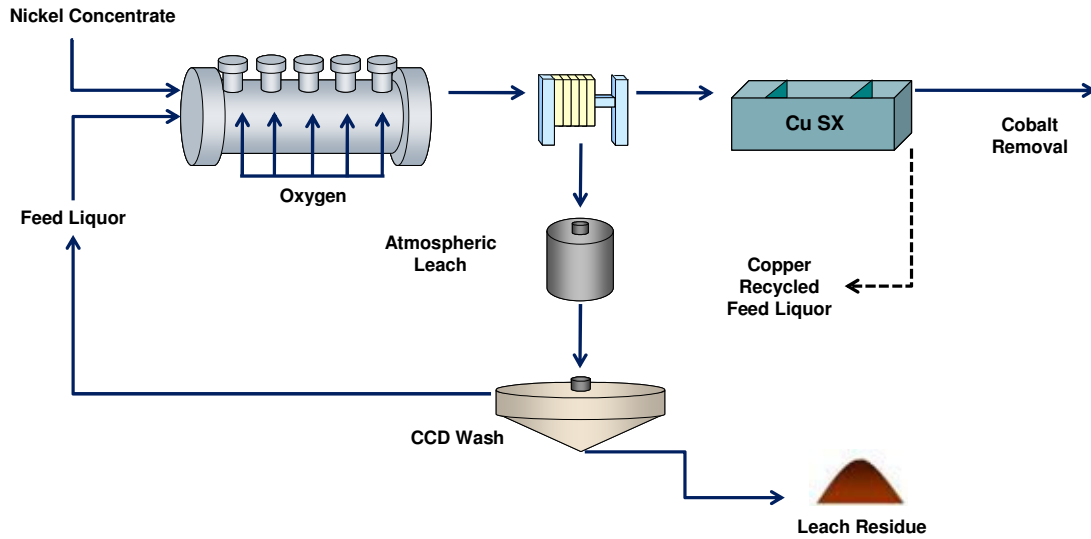
CESL Nickel Process Flowsheet
(2 of 3)

Impurity and Cobalt Removal

Co-Ni Separation

Sulphide Precipitation

Nickel Recovery

Neutralization and Fe Removal

Lime

H_2S

Co Purification

Recycle

Cu, ZnS residue

Gypsum and Fe Removal Residue

Co Product
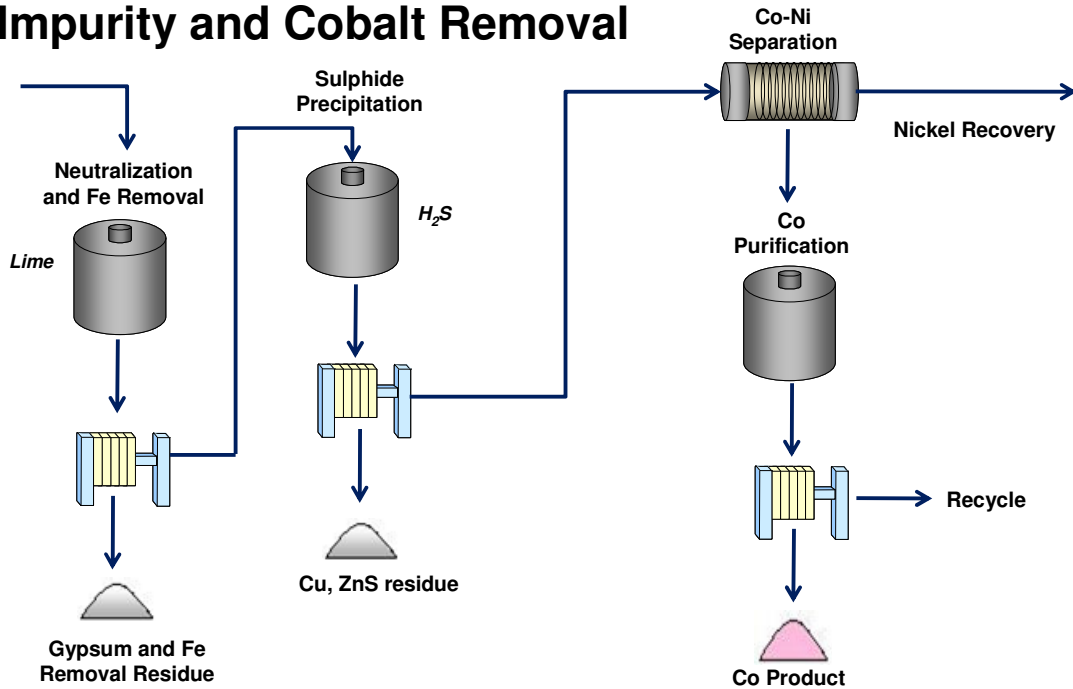
Nickel Recovery
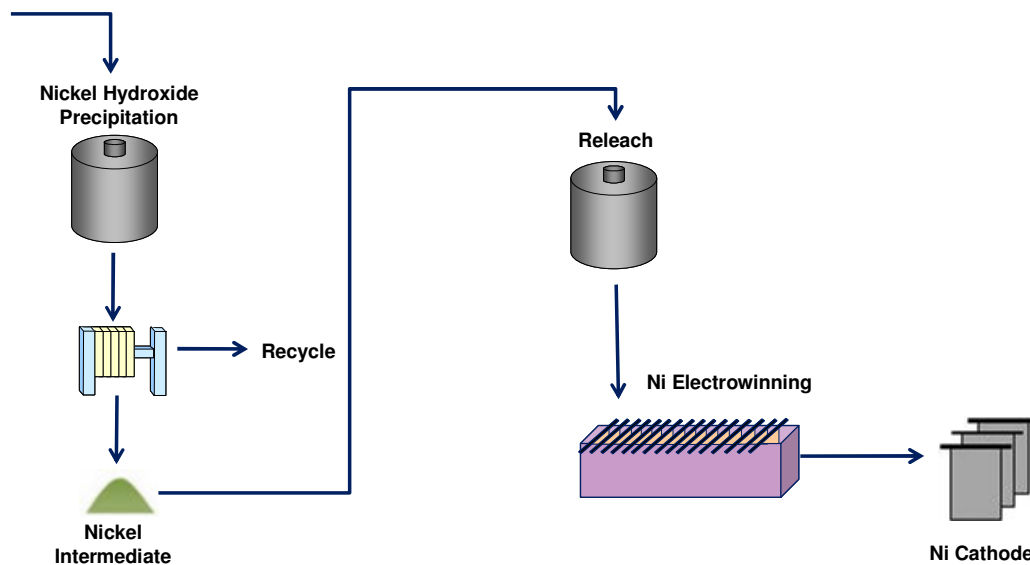
Metallurgical Results

CESL has been testing various nickel sulphide concentrates since 1994 from bench scale to continuous pilot operations

The testing on nickel sulphide concentrates under CESL Nickel Process conditions has consistently demonstrated:

- Competitive cost structure for nickel production
  – Low reagent consumption due to minimal sulphur oxidation and moderate Mg dissolution
  – Medium temperature operating conditions lead to low sustaining costs and higher availability
  – Cost effective impurity control and purification
- Metal extractions in excess of 97% for nickel, cobalt and 95% for copper
- Capable of treating low grade concentrates that smelters can't handle

Nickel Concentrates Tested

Various low-grade nickel concentrates tested at the bench scale

Concentrate	%Ni	%Cu	%Co	%Mg
A	6.3	0.3	0.3	7.2
Mesaba – 2001[1]	2.3	19.0	0.1	2.0
Mt. Keith – 2002	12.9	0.1	0.2	5.2
D	10.9	0.6	0.4	6.4
E	4.0	1.1	0.2	11.7
F	3.7	8.0	0.1	3.7
G	3.6	1.1	0.3	1.5
H	5.7	0.3	0.3	14.0

[1]*Also tested in 2007 and 2009*

Metallurgical Results

Nickel and Cobalt Extraction Results

Average Nickel Extraction - 97.6%
Average Cobalt Extraction - 98.4%

Other notables:
Average Oxygen Ratio - 0.19 t O2 / t Conc.
Average Magnesium Extraction - 32%
Average Acid Consumption - 135 kg H2SO4/t Conc.
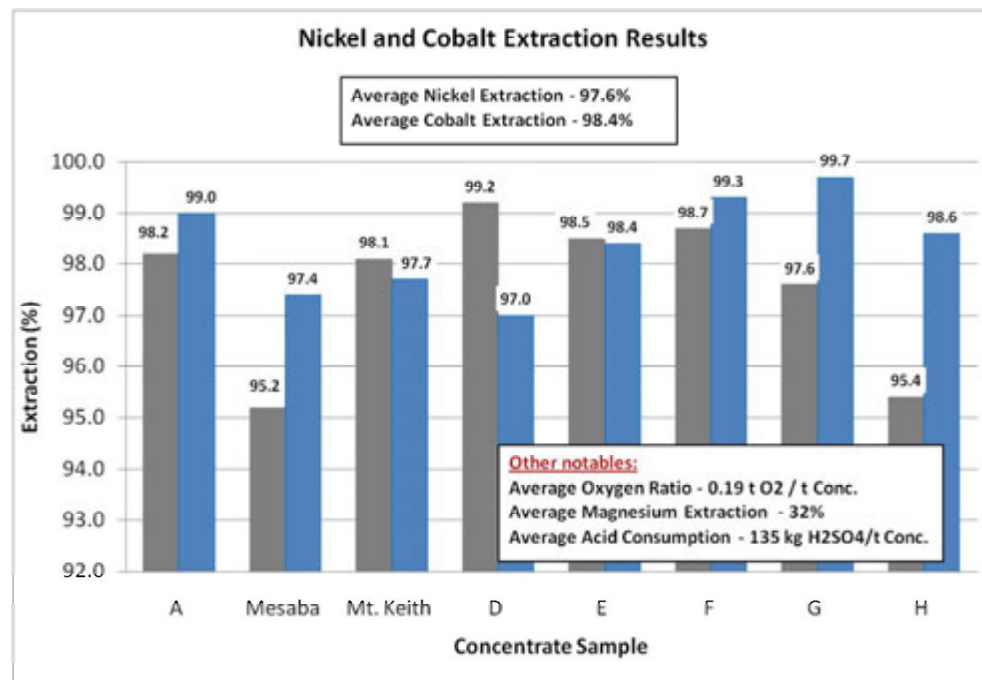
CASE STUDY

Case Study
Background

This case study illustrates the financial advantages of an on-site CESL refinery processing a low grade concentrate

- The study compares the return on selling Nickel concentrate to a smelter vs. onsite processing to Nickel metal, for a hypothetical mine.
- The study encompasses both the mine/mill producing concentrate from the ore, as well as the nickel refinery
- In the case of selling concentrate, mill recovery is assumed to be substantially lower, in order to achieve the higher grade of concentrate acceptable to the smelter
- This lower recovery with marketable concentrate reflects our own experiences and others with this type of ore
- A decision point is required to install a CESL refinery to treat a lower grade nickel concentrate or sell concentrate based on current market terms

Case Study
Two Alternatives – Key Assumptions

Concentrate Grades

▪For the 1st alternative (*selling concentrate*), a grade of 14% Ni is assumed, to guarantee max. smelter return

▪For the 2nd alternative (*processing onsite*), a grade of only 6% Ni is assumed, as this has been found satisfactory for the CESL Ni process

Metal Recoveries

▪Flotation recoveries are shown individually in each alternative, below

▪For the hydrometallurgical plant, the metallurgical results achieved on several low grade Ni concentrates under CESL Nickel Process conditions were used

Capital and Operating Costs

▪Mining and milling costs were estimated from recent projects and existing operations

▪Capital and operating costs for CESL plant were been taken from internal studies at scoping level estimates

Case Study
Concentrate Sales Option

Hypothetical Mine

▪Consider a mine which is mining low grade ore, 0.5% Ni

▪Processing it to a smeltable grade concentrate, and selling it

▪Milling rate is 35,000 tonne/day, or 12.25 Million tpy

▪Nickel recovery to concentrate is 64%, to produce 39,200 t Ni/year

▪Concentrate grades 14% Ni, 1.6% Cu, and 0.66% Co

Capital Cost

▪Total Project Cost for Mine and Mill is estimated at $35,000 per annual tonne Ni in concentrate

Operating Cost

▪Operating Cost is estimated at $4.00/lb Ni produced in concentrate, or $346 Million/year

Case Study
Mine and Resource

Assumptions

Mining Rate			Resource	
Mining Rate	12.25	Millions tpa	Nickel	0.50 %
Milling Rate	35,000	Tonnes/day	Copper	0.05 %
			Cobalt	0.02 %
			Prices ($/lb)	
			Nickel	10.80
			Copper	2.50
			Cobalt	18.00

Case Study
Concentrate Sales Option

Concentrate gross and net value

- 280,000 tonnes concentrate are produced
- Gross metal value in concentrate is $1,012 Millions per year
- Payable metal is 85% (Ni), and 45% for Co and Cu
- Net Payable value is $828 Million per year

Realization Costs for Ni Concentrate at 14% Ni

- Smelting charges include $1.75/lb Ni, $4.00/lb Co
- Total smelting charges per year amount to $165 Million/year
- Freight costs are estimated at $170/tonne or $52 Million/year

Net Cash Flow

- The cost of producing concentrate is $346 Millions per year
- After deducting all operating and realization costs, the mine realizes **$267 Millions per year cash flow** from selling concentrate (before tax)

Concentrate Sales Option
Recovery and Payables for Concentrate Sales

Concentrate	Recovery from ore to conc.		Concentrate Grade		Concentrate Production	Percent Payable	Net Revenue
Nickel	64 %	Ni	14.0 %	Ni	280,000 tpa	60 %[1]	**611 M US$/yr**
	55 %	Co	0.66 %	Co			
	75%	Cu	1.6 %	Cu			

[1] Net % payable for all metals by smelter, as % of gross metal value, less treatment / refining charges and freight

---

Value of Concentrate Sales
Compared to value in Ore as mined

Net Revenue Summary for Concentrate Sales	M US$/yr	Percent
Gross metal value in ore mined	1589	100
Gross metal value in concentrate	1012	64
Payable metal value in concentrate	828	52
Less Cost of producing concentrate	346	22
Less realization costs (smelting, refining, freight)	215	12
Net Cash Flow	**267**	**17**

- $267 Million in net revenue from sale of concentrate, out of a total of $1,589 Million in gross metal value in ore
- Due to lower metal recoveries and treatment charges **only 17 % of the contained metal value in ore is realized in net cash flow from sale of concentrate**

Case Study
CESL Ni-Co Refinery

Production and recovery

- CESL refinery treats 827,000 tpy of low-grade Ni concentrate
  - 6% Ni grade, 0.22% Co grade (high MgO)
  - This low grade allows for significant improvements to overall metal recovery

Nickel recovery to concentrate	Nickel recovery in CESL Process
81%	96%

  - Cobalt recovery to concentrate during flotation is slightly lower (75%), but in refining (96%) is same as for Nickel
  - The high % MgO to be expected in low grade Ni concentrate does not significantly affect process recoveries of Ni and Co

Case Study
Recovery and Payables for Refined Products

Products	Recovery from ore to product	Product Grade		Product (tpa)	%Payable	Net Revenue
Nickel Metal	78%	100%	Ni	47,867	100%[1]	
Cobalt Carbonate	72%	100%	Co[2]	3,675	100%[1]	1121 M US$/yr
Copper sulphide	45%	50%	Cu	2,756	30%[1]	

[1] *Percent payable by third party refiner less freight charges*

[2] *Metal content*

Value of Refined Metals
Compared to value in Ore as mined

Net Revenue Summary for Onsite Refining	Millions US $/yr	%
Gross metal value in ore mined	1,589	100
Gross metal value in concentrate	1,285	81
Value of Refined Products of CESL Process (including premiums on nickel cathodes)	1,250	79
Less: Costs of producing concentrate (Mining and Milling)	346	22
Less: Realization Costs (Operating costs for processing onsite, marketing, freight)	128	8
Net cash flow	776	49

- Due to higher metal recoveries to a low grade concentrate, **49% of the gross value in ore is realized in net revenue from refined metals**

Economic Comparison

Simple Financial Analysis	Onsite Refining	Concentrate Sales	Units
Gross Sales Revenue per year	1,249	828	M US$/yr
Less: Operating Costs	455	346	M US$/yr
Less: Realization Costs	18	215	M US$/yr
Cash flow, i.e. net of all costs	776	276	M US$/yr
Total Capex	2,042	1,372	M US$
NPV (8%) $ Million[1]	2,082	-200	M US$
IRR % (15 years)[1]	19.5	6.0	%

[1]Before Tax

CLOSING REMARKS

Summary

- Future supplies of nickel are predicated to come mostly from laterites, which are abundant

- Laterite projects however, have a history of technical difficulties and poor financial returns

- Large reserves of nickel can still be found in low grade sulphides, but have defied exploitation to date, due to metallurgical difficulties

- Up to now, all Ni concentrates have to be smelted

- Nickel Smelters require concentrates with at least a minimum grade of Ni, (>12%), and with limited MgO (< 8 % roughly)

Summary (continued)

- Poor recoveries during flotation of lower grade ores to such smelting-grade concentrates are common, due to the disseminated nature of many deposits

- Onsite processing by a low cost process can overcome these issues, by better flotation recovery combined with better payment terms for the products

- There has been no such commercial process for this, but now the CESL Nickel process offers a reliable, low cost technology to process low grade concentrates

Summary (continued)

- Our Case Study shows that a typical low grade sulphide deposit (at 0.5% Ni), is not an attractive investment, due to both low mill recovery and poor payment terms for the concentrate

- Such a deposit even if mined on a large scale to produce 40,000 tpy Ni in concentrate still has a very low IRR, unattractive to investment.

- The same deposit if processed onsite by the low cost CESL Process, should produce an outstanding return on investment

Path Forward
CESL Nickel Technology

Completed	**Completed**	**Underway**	**Goal**
▪ Intermediates	▪ Bench	▪ +/-30%	▪ 2011
▪ Metal	▪ Pilot	▪ 3rd party	▪ Ni opportunity

Flowsheet Development → Metallurgical Testing → Confirm Economics → Strategic Partner / Project
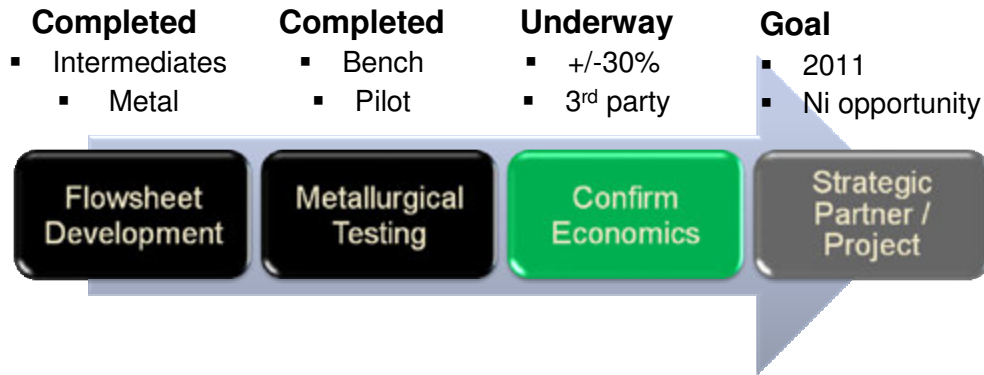
Seeking strategic partner / project to commercialize technology
- Experienced process engineering team and world class metallurgical facilities can manage, evaluate, and advance potential projects to tangible level
- Development initiative well supported by Teck Corporate Development Team

---

Acknowledgements

Teck Resources Limited

- Continued support of CESL

Nickel Process Development Team at CESL

- Jen Defreyne, Director
- Rob Mean, Business Development
- Keith Mayhew, Senior Project Metallurgist
- Tannice McCoy, Nickel Program Leader

ALTA 2011
NICKEL/COBALT/COPPER

NEW PROJECTS

ASSAREL MEDET JSC Cu SX-TF-EW PROJECT IN BULGARIA

By

Hannu Laitala, and Marko Lampi

Outotec Oyj, Finland

Presenter and Corresponding Author

Hannu Laitala
hannu.laitala@outotec.com

ABSTRACT

Assarel Medet JSC owns and operates a copper mine and concentrator in Panagyurishte, Bulgaria. The concentrator produces about 50 000 t/a copper in concentrate. Side rock and concentrator waste is dumped into a heap, where copper is leached with the aid of acidic liquid and microbiological activity. Particle size of the leached material can vary from coarse (50 – 100 mm) to very fine (< 10 µm). The material contains both oxidized and sulfidic copper compounds. From the produced solution copper was cemented with the aid of scrap iron. The copper product contained about 60 – 80 % copper, the remainder being mainly iron. Cemented copper was sold to different copper smelters.

Price for the cemented copper was low and Assarel started to investigate different process routes to produce pure copper. Process restrictions in Assarel are high solids concentration in the incoming feed (up to 1 - 2 g/L during wet season), diluted copper concentration in the feed (< 1 g/L), small capacity (2 000 t/a Cu) and harsh winter conditions. The target for the new Cu process was to produce copper in an economically viable way under these process conditions. Assarel Medet JSC's new Cu SX-TF-EW process was successfully started in December 2010. First cathode was produced 19th December, 2010.

PROJECT BACKGROUND

Assarel Medet JSC is the owner and operator of the open pit mine and copper concentrator Panagyurishte in Bulgaria. The capacity of the copper concentrator is about 50 000 t/a copper in concentrate. There are 1 000 workers at Assarel Medet JSC. Produced copper concentrate is sold to different copper smelters.

Assarel Medet is located in an area of 20 hectares, 1 000 m above sea level north-west from the town of Panagyurishte and 90 km south-east from the Bulgaria's capital city Sofia.
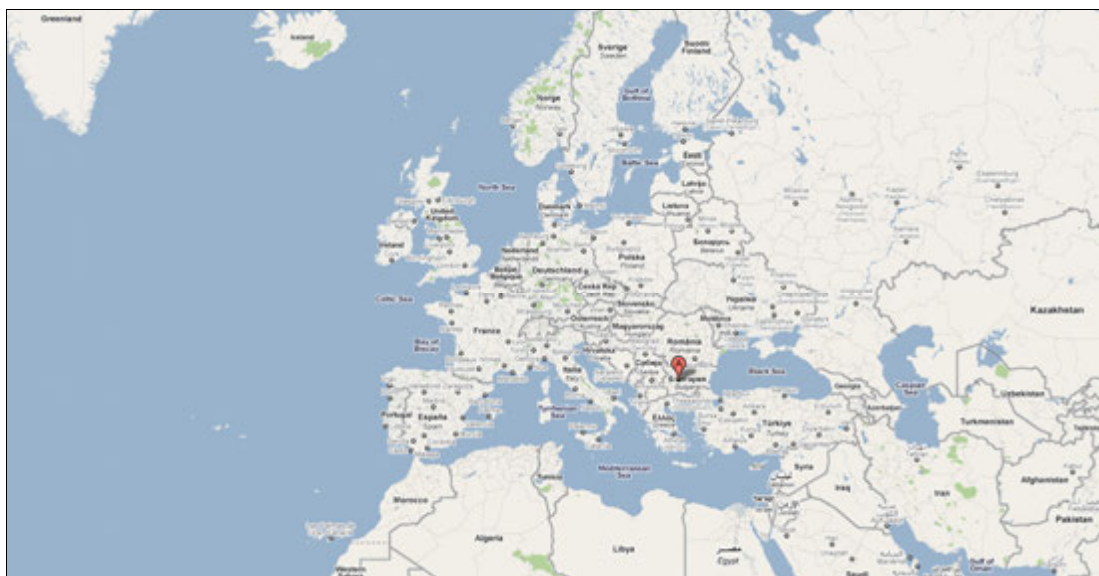
Figure 1: Location of Assarel Medet JSC.

Since 1989 Assarel Medet JSC had operated a process for dump leaching of oxidized copper ore and cementation of copper with a capacity of 5 000 m^3/d of pregnant leach solution. Copper from the PLS solution was cemented with scrap iron. Copper produced with this process is impure containing 60 - 80 % of copper, the remainder being impurities.

Figure 2: Assarel Dump Leach (left), Cementation Plant (right).

In order to increase the copper production capacity and quality, Assarel started to study the different possibilities to modernize the old copper cementation process. At the end of year 2007 Assarel decided to construct a new Cu SX-TF-EW plant. Production capacity of the new Cu SX-TF-EW plant is 2 000 t/a LME grade A copper cathode. This Cu SX-TF-EW plant was commissioned in December 2010. There was one year delay in the project schedule due to the world economic situation.

PROJECT EXECUTION

Assarel Medet JSC ordered a basic engineering and equipment package for the new Cu plant from Outotec. The package included process basic engineering of the new Cu plant, detail design of the Outotec proprietary equipment and delivery of all process equipment for the Cu SX, organic treatment, tankfarm and Cu electrowinning. The plant automation system was also delivered by Outotec. Outotec delivered also some plant auxiliary equipment like pressure air compressor, safety showers and storage tanks. The project included also a service package for training, installation supervision and commissioning and start-up services. In addition to the contracted tasks, Outotec helped Assarel to specify other parts of the process like the demiwater process, PLS purification process before the Cu SX, PLS heating and fire protection system.

The remainder of the detail engineering was carried out by a Bulgarian engineering company, with construction by a Bulgarian construction firm. Assarel Medet bought all pipelines, instruments and valves. Outotec reviewed the detail engineering during the project. The majority of Outotec delivered equipment were made in Finland and shipped to Bulgaria as fully functional units. All process tanks were shipped readymade and settler parts were shipped as prefabricated modules. Transformer-rectifiers and electrolyte filters came from USA and mixer-settler separation fences and electrowinning cells from Chile.

During the plant construction phase Outotec had supervisors at the site to supervise Outotec delivered equipment installations as well as general piping, automation and electrification installations.

Operator training was held three months before plant start-up in Spain at Cobre Las Cruces. Plant commissioning took less than one month. After commissioning support has been given to the customer with a remote connection, which is available between Outotec's Espoo office in Finland and the Assarel Cu plant automation system in Bulgaria.

PLANT LAYOUT

Assarel's new Cu SX-TF-EW plant is located indoors due to the very cold winter conditions at the site. The plant is very compact; the total floor area is 2 100 m^2. Solvent extraction and tankfarm and electrowinning areas are separated with a fire wall. Special attention is given to internal air quality to protect the process operators and equipment. All SX settlers, after settler and loaded organic tank are equipped with low roofs and all inspection and other hatches on the top of settlers are equipped with water seals. The electrowinning cells are equipped with hoods and vented to an acid mist scrubber. Stripping machine washing chamber fumes are also vented to the scrubber.
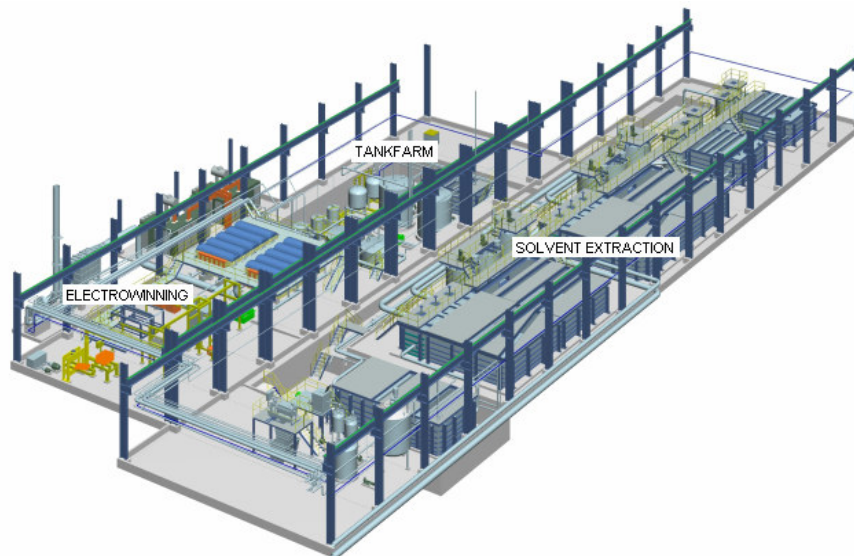
Figure 3: Assarel Cu SX-TF-EW 3D Layout.

Figure 4: Cu Solvent extraction.

Figure 5: Tankfarm and Electrowinning.

PROCESS

Solvent Extraction

The solution from the dump leaching is pumped from a PLS pond to the first extraction stage E1. In Assarel there are two extraction stages E1 and E2, connected in series. Copper is extracted from the copper containing solution with a copper selective reagent (M5640 from CYTEC). Raffinate from the last extraction stage E2 is returned to the dump leaching process. Loaded organic solution from the first extraction stage flows by gravity to the loaded organic tank. Aqueous entrainment from the

organic phase is separated in the loaded organic tank. Separated water is returned to the extraction stages.

Loaded organic solution is pumped from the loaded organic tank into a washing stage, where chemically and physically entrained impurities are washed away from the organic phase. The washed loaded organic flows by gravity from the washing stage W to the stripping stage S. In the stripping stage, copper is transferred from the organic phase to the electrolyte solution. From the stripping stage the stripped organic phase, barren organic, flows by gravity to the last extraction stage E2.

Crud is collected from the SX area into a crud tank. Acidified water is added into the crud tank and the slurry is pumped through a filter. Filtrate is returned to the crud tank. After the solution in the crud tank is free from solids, the phases are allowed to separate and returned to the SX process.

Filter cake is taken out from the filter in a dry form and it's transported to a disposal area. SX plant organic is treated by mixing bentonite into the solution and filtering the solids out. The treated organic is returned to the SX process.

Tankfarm

Rich electrolyte from the stripping stage flows by gravity into the rich electrolyte (RE) after settler. From the RE after settler rich electrolyte is pumped through electrolyte filters to the electrolyte circulation tank. Organic separated in the RE after settler is returned to the stripping stage.

The electrolyte circulation tank consists of two cylindrical vertical tanks, which are joined with interconnecting pipes. Electrolyte additives, guar and cobalt, are dosed to the EW feed electrolyte. Lean electrolyte is taken from the electrolyte circulation tank back to the solvent extraction through a heat exchanger.

Electrowinning

Electrowinning feed electrolyte, circulation electrolyte, is pumped from the electrolyte circulation tank into the EW cells where copper from the solution is reduced to metallic copper. Lean electrolyte from the EW cells flows by gravity back to the EW circulation tank.

Current from the transformer-rectifiers is passed through the electrolyte. During this process copper is deposited at the stainless steel cathode and oxygen is liberated at the anode. Copper cathodes are harvested with a crane and transferred to the stripping machine. Washed and stripped copper cathodes are stacked in bundles. The bundles are weighed, strapped and stored. The stainless steel mother blanks are returned to the EW cells.
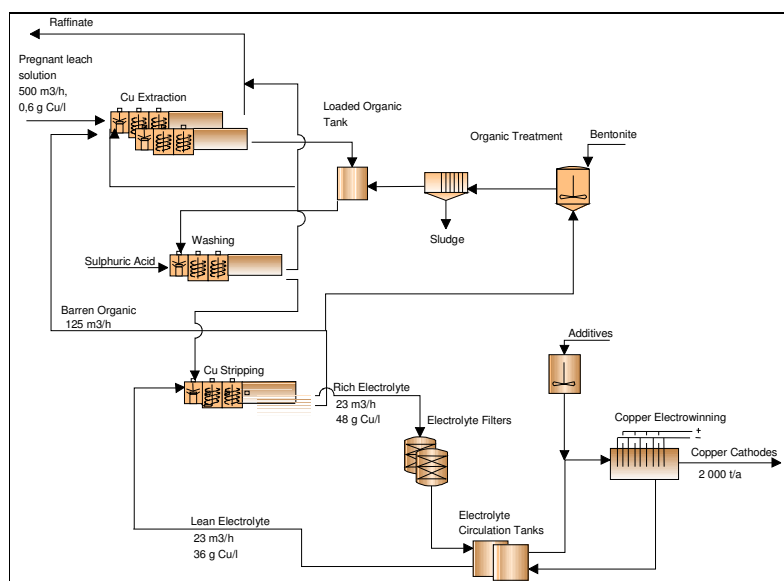
Figure 6: Assarel Cu SX-TF-EW Process Block Diagram.

SPECIAL FEATURES OF THE ASSAREL'S Cu SX-TF-EW PROCESS

Weather

Winter conditions can be very hard at Assarel. The site is located next to the open pit mine 1 000 meters above sea level in a mountainous area. Normally wind speeds can exceed 25 m/s and the temperature can drop below -20 ^{o}C. High snowfall is also very common in this area.

Figure 7: Assarel Mine During a Snow Storm.

During the wet season, the incoming solution from the dump leaching process, PLS, can contain a lot of solids. To avoid problems with the SX process, the old cementation cells were modified for use as a PLS pre-treatment process to settle out the solids from the feed solution.

Figure 8: Reconstructed Cementation Cells and PLS and Raffinate Tanks.

The temperature of the incoming solution can also drop well below 10 ^{o}C. In Assarel PLS can be heated to avoid mixing and phase separation problems in the SX process. The PLS heater is operated with steam and it is located outside. Other SX equipment, tankfarm and electrowinning are located inside.

Solvent Extraction

Process

Design feed solution flow to the Assarel Cu SX process is 500 m^3/h. PLS feed contains only 0.6 g/L of copper. Usually for this concentration range an IX process could be an option, but in the Assarel case IX was rejected due to the process conditions mentioned previously such as magnitude of the PLS flow, PLS maximum solids concentration and PLS minimum temperature. This kind of process feed can destroy IX resin quickly.

However, to make this level of Cu production and investment possible, SX required a special process design. The chosen SX configuration was 2E+LOT+1W+1S. Two extraction stages were connected in series to ensure as high as possible extraction efficiency (> 92 %). The Assarel Cu SX process uses CYTEC's M5640 reagent in Exxsol D80 diluent. Exxsol D80 diluent evaporates less than lower flashpoint diluents. Its solubility is also lower compared to the lighter diluents. Less volatile organic compounds in the process atmosphere means a cleaner and healthier environment for the operators and lower OPEX for the process.

The external O/A-ratio is very low (0.25) giving a high organic phase loading rejecting impurities, low aqueous entrainment and reducing the physical size of the washing and stripping mixer-settlers by 75 % and reducing the CAPEX accordingly. Assarel's Cu SX copper transfer capacity can be tripled without any extra process equipment investments from 2 000 t/a to 6 000 t/a.

Equipment

The Assarel mixer-settlers were designed to have stage efficiencies over 95 % and for very high settling rates. The Assarel SX settlers are designed for settling rates from 8.8 to 9.7 m3/m2/h, making them the most compact and efficient SX settlers in the world. The settling rate in Assarel is double compared to standard industrial practice reducing the equipment size by 40 % and the organic inventory 30 %. The Assarel Cu SX process is also the first Cu SX plant, where reverse flow mixer-settlers are connected with the straight flow mixer-settlers combining the advantages of the different flow profiles.

The Assarel loaded organic tank is designed to separate the bulk of the entrained aqueous solution from the organic phase thus reducing the impurity transfer to the electrolyte circuit. The Assarel loaded organic tank was designed also to act as a back-up system for process disturbances in the extraction stages.

The rich electrolyte after settler removes the bulk of the entrained organic from the electrolyte before the electrolyte filters. Separated organic can be reused in the SX process and it's returned to the stripping stage thus reducing the process OPEX.

The material used for the SX equipment was LDX2101. LDX2101 is a duplex steel grade. LDX2101's nickel content is very low, making it an economically attractive material especially when the nickel price is high. LDX2101 corrosion resistant properties are also equal or better compared to AISI316L in Cu SX-TF-EW solutions. Mechanically LDX2101 is a much harder material compared to AISI316L and investment savings can be realized in places where high mechanical material strengths are required.

Tankfarm and Electrowinning

Assarel's tankfarm and electrowinning stages are quite standard processes. The tankfarm consists of a rich electrolyte after settler, two dual media filters, RE/LE heat exchanger and electrolyte circulation tank. The RE after settler separates most of the entrained organic before the electrolyte filters. Organic separated in the RE after settler can be used in the SX process and it is returned to the stripping stage. Organic still left in the rich electrolyte is removed from the rich electrolyte in the dual media filters before the organic can contaminate the electrolyte circuit. The RE/LE heat exchanger heats up the rich electrolyte before it enters the electrolyte circulation tank and at the same time cools down the lean electrolyte before it enters the stripping stage in the SX process.

Cathodes are grown in ten electrolytic cells. One cell contains 32 pcs permanent stainless steel cathodes. The circulating electrolyte's copper concentration is 38.3 g/L and lean electrolyte is 36 g/L. Acid concentration in the electrolyte is 170 – 190 g/L. Design current density is 320 A/m^2.
Special features of Assarel's electrolytic circuit are double contact busbars and the acid mist capture system. Double contact busbars reduce the number of short-circuits in the EW system and

the acid mist capture system improves the air quality in the EW hall and reduces emissions to the environment. Also, sulphuric acid and copper sulphate washed from the EW hall air can be used as wash chemicals in the SX process washing stage and no extra acid or water is needed in the SX wash stage.

Figure 9: First Cathode Growing Cycle.

Figure 10: Assarel Medet JSC First Cathodes.

319

CONCLUSION

Challenges in the Assarel project were the very small copper production capacity, weather and low copper concentration in the incoming feed. Because of this, new kind of technical thinking was required to make sure that the Assarel project is economically viable and the investment for the project is justified. Sophisticated technological solutions like low O/A-ratio (0.25), high settling rate (9.7 m^3/m^2/h) in the SX process, double contact busbars and acid mist capture system in the EW process were applied to lower the plant's operating costs and project investment cost. Assarel Medet JSC chose Outotec as the technological supplier and project advisor to make sure that the special features of Assarel's small but important project would be taken into consideration, process design and equipment would be of a high quality and project execution, process commissioning and start-up phases would be carried out in the shortest time possible and problems, if any, would be solved without delays to the project execution. Assarel Medet JSC produced their first copper cathode on 19th December 2010 less than a month after the plant commissioning began.

ACKNOWLEDGMENTS

LADY ANNIE OPERATIONS – CST RESTART 2010

By

Anissa Horner

CST Minerals, Lady Annie, Australia

Presenter and Corresponding Author

Anissa Horner
ahorner@ladyannie.com.au

ABSTRACT

CST Minerals Lady Annie started producing copper again in November 2010 after being under care and maintenance since November 2008.

The startup was relatively trouble free thanks to a thorough overhaul of the entire processing area from crushing and stacking to SX and EW.

This paper will outline the timeline for CST Lady Annie operation so far, including mining, crushing and processing. Mining commenced in August, crushing in September and first copper metal on the 25th November 2010.

Included in the paper is stacking data, PLS grade and cathode data. There is also information on future plans for expansion and forced aeration heap leaching. All of these plans will ensure the longevity of the Lady Annie operation in NW Queensland.

INTRODUCTION

History of CST Minerals Lady Annie

The copper oxide mining and processing operation and the associated mineral tenements (collectively defined as the "Lady Annie Project") are located in the Mount Isa district of north-western Queensland, Australia.

Oxide, transition and sulphide copper Mineral Resources have been defined within the Mount Kelly, Lady Annie and Buckley River Areas at seven deposits: Lady Annie, Lady Brenda, Mount Clarke, Flying Horse, Swagman, Mount Kelly Workings and Anthill. The oxide copper ore treatment plant ("Mount Kelly process plant") is located centrally within the project tenements and is 2.5 km southwest of the Mount Kelly mining area, where copper oxide mineralisation is mined at Mount Clarke and Flying Horse. The Lady Annie mining area is located approximately 18 km to the northwest. The Anthill deposit is located 40 km south (45 km by road) of the Mount Kelly processing plant, in the Buckley River Area[1].

Mining at Mount Clarke commenced with pre-stripping in April 2007 and mining at Lady Annie commenced in October 2007. The Mount Kelly processing plant was commissioned in October 2007 with the first copper produced later that month. On 26 November 2008, CopperCo placed itself into voluntary administration, with Receivers and Managers subsequently appointed by the secured creditors. The operation was bought by Cape Lambert in July 2009 and the last copper was dispatched from site on the 8th December 2009. The mine went into care and maintenance mode after the last copper dispatch.

China Sci-Tech purchased the Lady Annie mine in March 2010 with mining restarting August 2010.

Mine Location

CST's Lady Annie copper oxide mining and processing operation and the associated tenements are located 120km northwest of Mount Isa in Northwest Queensland, Australia.
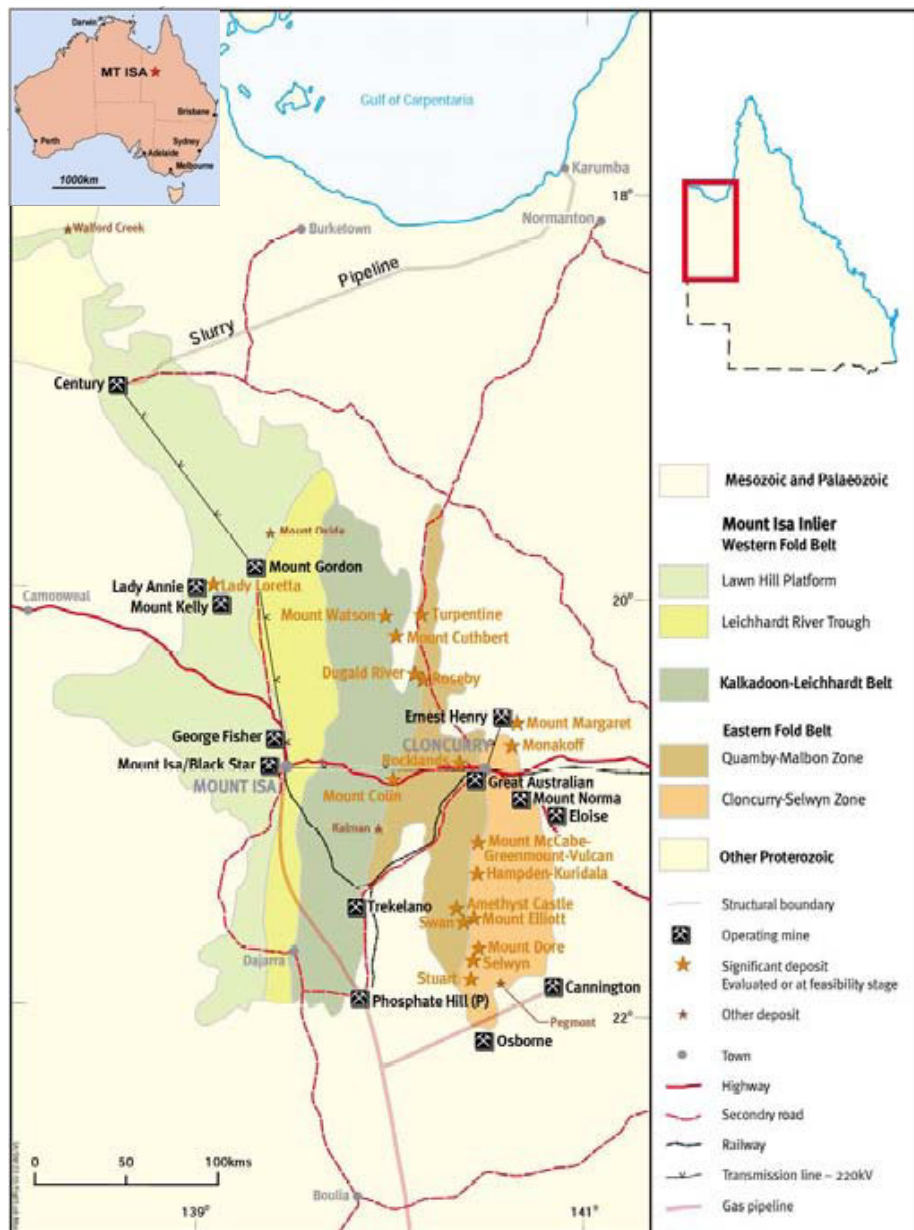
Figure 1: Location of Lady Annie Operation [1]

Geology and Mineralisation

The Lady Annie Project is located within the Mount Isa Inlier, which hosts several known copper oxide and sulphide resources and prospects. The Mount Isa Inlier consists of a north-trending belt of Early Proterozoic basement rocks (the Kalkadoon-Leichhardt Belt) flanked by two belts of Middle Proterozoic rocks, known as the Eastern and Western Fold Belts. The Lady Annie Project tenements occur within the Western Fold Belt. The Western Fold Belt is subdivided by the Mount Gordon Fault into the Lawn Hill Platform in the west and Leichardt River Trough in the east.

The geology of the area surrounding the Lady Annie Project is dominated by marine carbonate and clastic sedimentary sequences of the Proterozoic Lower McNamara Group. The Lady Annie Project overlies the north-south trending Lady Loretta High Strain Zone, which is characterised by tight, upright folding along major north-south trending faults. The project area is structurally complex, with multiple generations of folding and faulting. Major, deep-seated faults that cut or bound basement rift blocks of volcanics are considered to be important for targeting copper mineralisation. Extensive weathering has produced a base of complete oxidation at around 80 m, although there are areas with oxidation down to 300 m associated with fault zones.

The known copper mineralisation within the majority of the project area is hosted in dolomitic, carbonaceous and argillaceous sandstones and siltstones. Oxidation of these units has removed the dolomitic material leaving behind ferruginous silty sandstones or kaolinitic sandy siltstones. Mineralisation in the oxide zone is comprised predominantly of malachite, cuprite, chrysocolla, chalcocite and tenorite with relatively rare native copper. The oxide zone mineralisation appears to be controlled by the in-situ oxidation of pre-existing primary copper sulphide species. The primary copper sulphide mineralisation at depth is dominated by chalcocite and chalcopyrite, and appears to be structurally controlled[1].

Mineral Resources

The Lady Annie deposits lie within areas of multiple faulting with numerous faults showing a wide range of orientations and ages. The resource models were developed for CopperCo by reputable mining industry consultants and the resource model for the Flying Horse and Mount Kelly Workings deposits was updated by Snowden in February 2010. Geological interpretation for resource estimation incorporates fault zones, weathering horizons and mineralised domains based on lower copper cut-off grades of 0.2% Cu (Flying Horse, Mount Clarke, Mount Kelly Workings and Swagman) and 0.3% Cu (Lady Annie, Lady Brenda and Anthill).

The majority of the Mineral Resource data are based on reverse circulation drillholes. Where available, diamond core has generally been sampled as half core from HQ and NQ size core. The drilling data used to estimate the Mineral Resources have been focussed on the definition of copper mineralisation within the oxide horizon. Drillhole sections are spaced generally at 25 m along strike with a drillhole spacing of 20 m to 40 m across strike. Wider spaced drilling has been directed at identifying deeper sulphide mineralisation associated with fault zones.

A total of 1,052 diamond drill core samples from various regions of the Lady Annie, Flying Horse, Mount Clarke and Anthill deposits have been tested to evaluate the dry bulk in-situ density within oxide, transition and fresh material. Additional density data have been collected from the oxide material within the Mount Clarke and Flying Horse pits and from some surface samples at Lady Annie. This additional data has verified the density factors applied to the oxide ore at Mount Clarke and Flying Horse.

Block models were constructed using a parent block size of 10 mE by 10 mN by 5 mRL with subcelling into blocks of 2.5 mE by 2.5 mN by 2.5 mRL, for increased definition of the mineralisation at oxidation and mineralisation domain boundaries. Ordinary kriging was used for estimation of the total copper block grades.

All Mineral Resources are reported as "total copper", as there are insufficient analyses to determine acid soluble copper grades. Acid consumption and copper recovery are a function of the calcium and magnesium in the ore. A review of the current calcium and magnesium data indicates that there is a relationship between these variables and the rock type[1].

Plant Brief Description
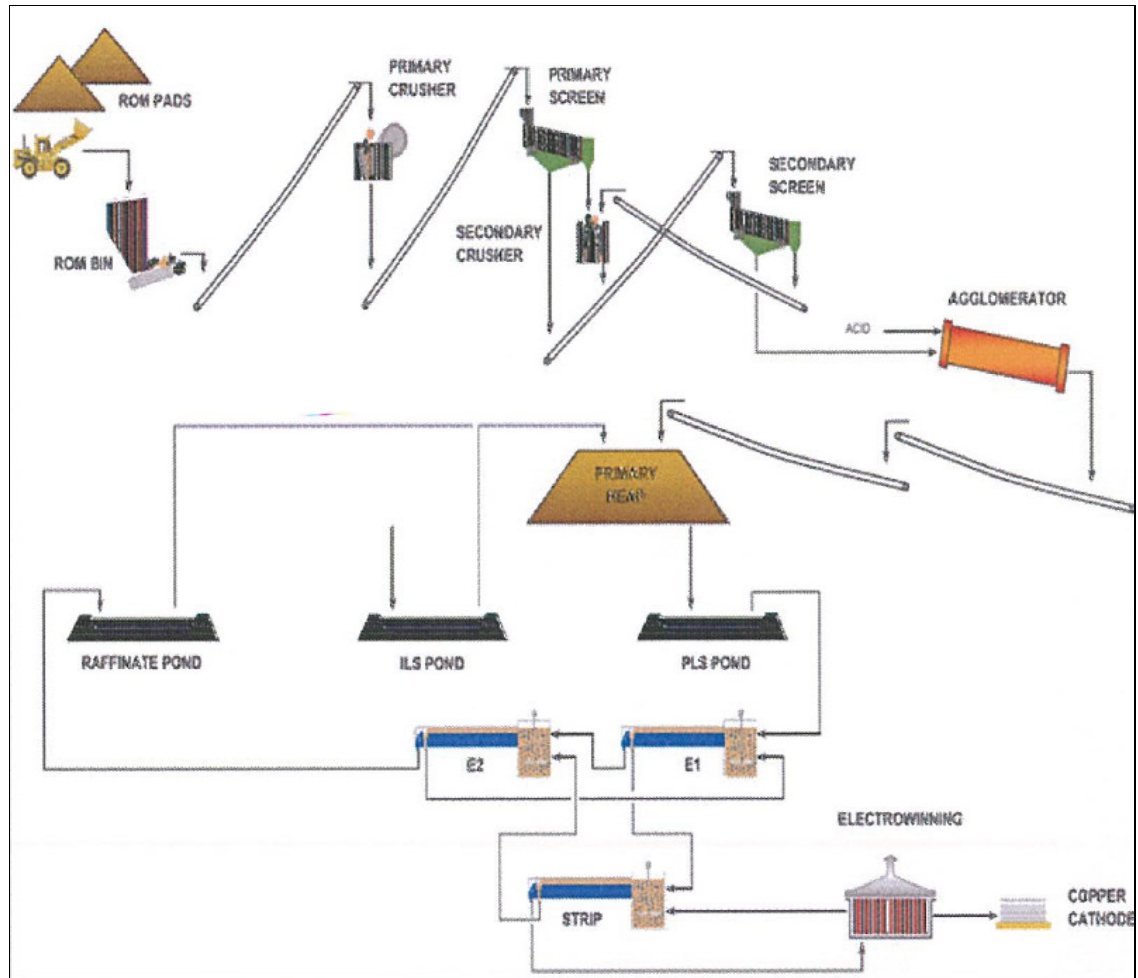
Figure 2: Overview of Lady Annie Operation

The Lady Annie operation consists of several areas; starting with the removal of copper bearing ore from the open cut pit. This ore is then crushed and transported to the heaps where it is stacked before being placed under sulfuric acid irrigation to liberate the copper. The copper sulphate solution is then put through solvent extraction to purify and concentrate before applying current in the cellhouse to produce LME A grade copper cathode.

Open Cut Pit

The Lady Annie site has several open cut pits that it draws on for its' ore. Lady Annie is the biggest pit but this material is supplemented with ore from Mt Clark, Mt Kelly and Flying Horse. At Lady Annie, ore is mined and hauled to a run of mine ("ROM") stockpile, thence loaded and hauled 18 km by road train to the crusher ROM pad. Mount Clarke and Flying Horse ore is directly carted by off-road haul trucks to the crusher ROM.

Heap Leach

The crushing and agglomerating plant is needed to get the ore into a suitable size and form so that the copper can be leached from the ore. Generally, a 70:30 ratio blend for Lady Annie : Mount Clarke ore is fed to the crusher.
Agglomeration provides improved particle size distribution which is important for solution percolation and maximises leach efficiency. It does this by binding the fine particles to the larger particles in effect making larger agglomerate that provide adequate pore spaces in the heap for solution percolation and leaching.

Once the ore has been agglomerated it is transported via a network of conveyors and stacked onto the pad to form a heap. The heap is typically 8 metres high, 350 metres long and 80 metres wide.

SX

The solvent extraction circuit at Lady Annie employs two extraction stages in series along with a parallel extraction stage. There are two strip stages. Cognis LIX 984N-C reagent is used in the circuit as the optimum extractant for compatibility with the Lady Annie heap leach SX-EW process. LIX 984N is composed of two components: LIX 860N-I Aldoxime and LIX84-I and is supplied as the separate components which are added alternately to the system.

To prevent organic from entering the cell house Spintek anthracite filters are used. Clay treatment is utilised to clean up the organic.

EW

The cellhouse has one hundred cells, with thirty-two of them being scavenger cells and the remainder being the "commercial" cells. However with the excellent results from the Spintek filters copper from all cells is LME A Grade copper.

The copper is removed from the cells and stripped off using the automated stripping machine (flexor arm type). Forty tonnes of copper is typically stripped each day (50 cells per day).

Current Capacity and Expansion Plans

A second SX circuit and cell house are available for use. This extra capacity will take the plant from a 20,000T of copper per annum processing plant to 30,000T per annum.

A robotic stripping machine is being installed this year that will make stripping the copper much less labour intensive and efficient.

CST Workforce

The recruitment process started in early July 2010 and was largely completed by November 2010. In November there were approximately 193 CST employees, with 55% of them returning from the previous incarnation of the operation.

Table 1: CST Employees

	FEBRUARY 2011
Total CST Employees	215
Additional contractors	96

The majority (35%) of Lady Annie employees fly into Townsville on the charter flight that is arranged by CST. A slightly larger percent are based in Brisbane but this accounts for employees that live interstate.

Table 2: Fly In / Fly Out Base Statistics (No. People)

	FEBRUARY 2011
Townsville	73
Brisbane(and beyond)	76
Cairns	42
Mt Isa	24

CST also keeps statistics on the percentage of employees that are from the local Kalkadoon indigenous community – the traditional owners of the area as well as indigenous workers from throughout the broader Mount Isa and Townsville region.

Table 3 : Traditional –vs- ATSI –vs- Non Indigenous (No. People)

	FEBRUARY 2011
Traditional Owner (Kalkadoon)	15
Aboriginal and Torres Strait Islander	17
Non-indigenous	183

Recent Wet Season and Yasi Associated Issues

The 2010-2011 wet season was better than other years when Lady Annie was operational. The road into Lady Annie is an un-tarred road and that is the major issue – getting vehicles in and out of site. All commodities are received into site via road-train and includes the removal of copper from the laydown area. Getting the heavily loaded trucks out of Lady Annie on boggy roads is a major problem. There were several weeks when copper did not get dispatched which led to some very busy days loading copper onto trucks while the "dry" weather held out.

Crushing and stacking have also been adversely affected by the wet season, resulting in less than half of the budget stacked ore amount. The crushing and stacking circuit is very susceptible to rain events with all of the crushers, conveyors, grasshoppers and stackers being open to the weather.

The approach of Cyclone Yasi from the eastern coast of Queensland at the start of February resulted in the site being evacuated apart from skeleton crew of core staff. Although Cyclone Yasi was downgraded from a Category 1 cyclone to a tropical depression, very high winds and heavy rains were experienced. Over the three days of the approach and passing of the rain depression approximately 185mm of rainfall occurred in the area. This resulted in the road being impassable due to high creek crossings. The incoming crew was flown in by helicopter in order to get the plant running again and bundles of copper ready to be shipped. Crushing and stacking were the victims again, with this circuit being completely shutdown for nine days in the days preceding and post Cyclone Yasi.

CRUSHING AND STACKING

ROM and Circuit Brief Description

Ore which has been mined is stockpiled on the ROM pad. The ROM pad adjacent to the crusher has a total capacity of approximately 80,000 tonnes. As mentioned previously, a 70:30 blend of Lady Annie / Mt Clark ore is maintained. The maximum design feed rate for the crushing plant is 500 dry tonnes per hour and will be operated continuously on a 2 x 12 hour shift.

It is necessary to crush the blended ore to a predetermined crush size to allow adequate solution percolation through the heap so that leaching of the ore can occur. Achieving the desired crush size is important as this ensures that the copper minerals can be leached from the ore; this is correctly referred to as liberation.

The optimum crush size is described as the p80 of the ore. For example at Lady Annie the aim is to achieve a p80 of approximately 19mm. This means that 80% of the ore will pass through a 19mm aperture screen. In this case 100% of the ore will pass through a 25mm aperture. The crush size may be changed depending on the ore type. A fine crush will result in better liberation of the copper mineralisation and quicker leaching.

However there is a tradeoff between crush size and heap permeability which has a significant effect on heap leach performance. Crush size distribution is one of the main controlling physical parameters of heap leaching. An effective size distribution will result in adequate mineral liberation while maintaining permeability.

The crush size will be set to match the ore type and characteristics based on previous test work. Changing the crush size involves changing the screen apertures and this will not occur on a regular basis.

The crushing circuit has two stages of reduction, the first or Primary stage is a Jaw Crusher (CR001; a JACQUES ST47 single toggle jaw crusher) and the Second or Secondary stage is a Cone crusher (CR002; a CEDAR RAPIDS model MVP550 roller cone crusher) in a closed circuit

with a double deck screen. Crushed rock which cannot pass through the screen is returned to the Secondary crusher while 'passing' rock (small enough) is transferred to the Agglomerator.
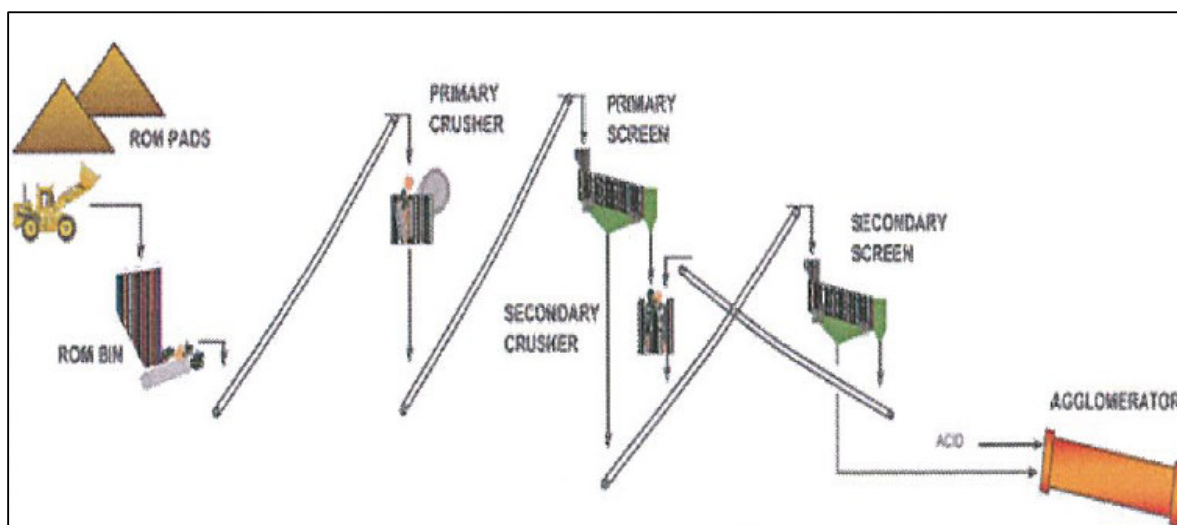
Figure 3: ROM and Crusher Circuit

Crush/Stack Actual Start Date

Crushing of ore from the ROM began on the 1st September 2010. Ore began to be stacked on Pad 6 on 2nd September 2010. Since this date, 1.29 million Tonnes of ore has been crushed and stacked.

Agglomerator Detail and Capacity

Once the ore has been crushed to the pre-determined size it is necessary to agglomerate the ore. Agglomeration provides improved particle size distribution which is important for solution percolation and maximises leach efficiency. It does this by binding the fine particles to the larger particles in effect making larger agglomerate that provide adequate pore spaces in the heap for solution percolation and leaching.

This is achieved by using a rotating agglomeration drum, where ore is fed into one end of the drum (feed end) and mixed with a pre-determined amount of acid and solution. The rolling action of the ore and solution through the drum result in the formation of 'agglomerates' or 'pellets'. The formed agglomerates travel by gravity through the rotating drum and are discharged onto a conveyor which then transfers the ore to the Heap leach for placement.

The three important variables associated with the production of high quality agglomerates are:

1. Ore feed

    One of the most important requirements for consistent production of quality pellets is constant ore feed to the agglomeration system. The drum feed bin, weightometer (belt scale); variable speed conveyor and control system are provided to ensure constant feed. The electronic equipment that controls the feed rate is a standard feedback device, which adjusts the feeder belt speed (feed rate as measured on the weightometer) to the 'Set point' value, which is set by the Operator when in automatic mode.

2. Acid addition

    Acid addition in the agglomeration drum ensures that leaching will occur in the fastest and most efficient manner. Approximately 80% of the acid requirements will be added in the agglomerator. A centrifugal, variable speed drive pump is used to add acid into the drum at a rate of up to twenty kilograms per tonne of ore. The flow rate of acid is calculated from a signal received from CV06 weightometer that is sent to the PLC at the bulk storage facility. The variable speed pump will then adjust its speed to achieve the flow rate required.

3. Make-up water addition

The additional moisture through the raffinate/water as well as acid provides the optimum moisture content to achieve the maximum benefit of agglomeration. Moisture level is critical for proper pellet formation. Raffinate or water is added to the ore via spray bar located in the drum. Moisture addition requirements are a function of ore type, ore feed moisture content, and ore feed blend. While precise characteristics of raffinate/water absorption for acceptable agglomeration cannot be predetermined with great accuracy, it is necessary to adjust the raffinate addition by monitoring the agglomeration condition. Generally, acceptable moisture levels can be determined using the 'snowball' agglomeration test. If the pellets are too wet or too dry over a prolonged period, (say 15 to 30 minutes) then the addition control setting should be changed as appropriate. Changes to raffinate/water addition should be limited to 0.2 l/s increments.

The importance of the quality of the pellets produced in the agglomeration system cannot be overemphasised. The efficiency of the heap leach function is the basis of the plant efficiency and hence viability of the entire operation. Therefore, pellet quality must be assessed on a routine basis and adjustments made if pellet quality is not adequate.

In general, it is better to make pellets that are over moist rather than too dry. This is even more critical in hot, dry climates where pellets may dry out before proper curing takes place. Unfortunately, wet pellets may cause other problems with hang-up in transfer chutes and carry-back on the belt and idlers. However, the importance of maintaining appropriate pellet quality is the first priority and the additional cleanup required is considered unfortunate but necessary.

The agglomeration drum is designed to allow the safe and efficient addition of water and acid to the crushed ore from the crusher. The water and acid help to agglomerate the finer particles in the ore, resulting in improved permeability of the stacked ore. In the drum the ore is intimately mixed with the acid, promoting rapid initial dissolution of the acid soluble copper.

Water is added via a spray bar inside the feed end of the drum. In the event of power failure, the solenoid on this system will fail closed and isolate the supply of water to the drum.

The water flow rate is measured by a magnetic flow meter with a display mounted on the platform at the discharge end of the drum. The water flow is regulated by an actuated butterfly valve controlled by a PID loop in the PLC. The control loop receives a process variable signal from the magnetic flow meter, and a water flow set point that is a specified ratio relative to the ore feed rate going into the drum. The feed rate signal comes from CV6 weightometer, and the ratio is specified by a potentiometer control located in the cabinet at the discharge end of the drum.

The acid line is fitted with an isolation valve that will fail closed in the event of a power failure. This valve is also closed when there is no feed going into the drum and when the acid delivery pump is stopped, to prevent acid draining from the spray bar. The acid line also has a pressure switch which will cut out the acid pump in the event of high pressure in the line.

The acid flow rate is measured by a magnetic flow meter with a display mounted on the platform at the discharge end of the drum. The acid flow rate is controlled by a variable frequency drive on the acid pump motor. The VF drive is controlled by a PID loop in the PLC, which receives a process variable signal from the magnetic flow meter, and an acid flow set point that is a specified ratio relative to the ore feed rate going into the drum. Acid control is operated by the control system, Citect.
The agglomerator can handle an upper throughput rate of 500T/hr, although lower rates result in better quality agglomeration. This is one of the reasons why a second agglomerator is being installed.

Stacking Method and Equipment

Stacking is the process by which the crushed and agglomerated ore is delivered and placed onto the heaps leach pad. Stacking ensures that the ore is distributed evenly over the pad to the desired heap height preventing particle segregation. The stacking method to be employed at Lady Annie Copper is by radial stacking from a conveyor system fed from the agglomeration drum. The ore is stacked in layers approximately 200mm thick, vertical layers.

Other forms of delivering the ore to the leach are by: truck or loader dumping and moonscape stacking method. The practice of radial stacking with a conveyor system has the following advantages over truck or loader dumping:

• Eliminates vehicular degradation of the heaps surface

• Reduces heap compaction

• Maximises internal void spaces

• It reduces particle segregation which can:

   o Decrease the internal void spaces which causes non-uniform solution percolation, and an increase in heap slumping and ore compaction thus reducing heap permeability.

The benefits of reduced particle segregation are the ability to maintain increased copper extraction and improved solution efficiency for prolonged periods.

Crush size distribution is one of the main controlling physical parameters of heap leaching. An effective size distribution will result in adequate mineral liberation and a balance between percolation rate and solution residence time.

The stacking system is designed to handle ore from the discharge of the Agglomerator to the leach pad. The stacking circuit comprises of a system of overland and portable conveyors.

The stacking circuit consists of several major equipment items and are as follows:

• Agglomerator Discharge Conveyor (fixed) – CV007

• Overland Conveyor (fixed) – CV008

• Mobile Tripper Conveyor (mobile) – CV009

• Ramp Portable Conveyors ('grasshoppers') (9 off, mobile) – CV010 A-I

• Horizontal Feed Conveyor (mobile) – CV012

• Horizontal Conveyor (mobile) – CV013

• Radial Stacker (mobile) – CV014

The stacking system is designed to handle ore from the discharge of the Agglomerator to the leach pad. The Agglomerator Discharge Conveyor (CV-007) transfers ore on to the Overland Conveyor (CV-008). The Mobile Tripper Cross Conveyor (CV-009) on the overland conveyor discharges on to the first of up to nine Ramp Portable Conveyors (CV-010 A-I).

The ore then moves down the string of portable conveyors to the Horizontal Feed Conveyor (CV-012) that is set up at right angles to the string of portable conveyors. This conveyor discharges ore on to the Horizontal Conveyor (CV-013) that is set up parallel to the string of portable conveyors. The horizontal conveyor delivers ore to the Radial Stacker (CV-014).
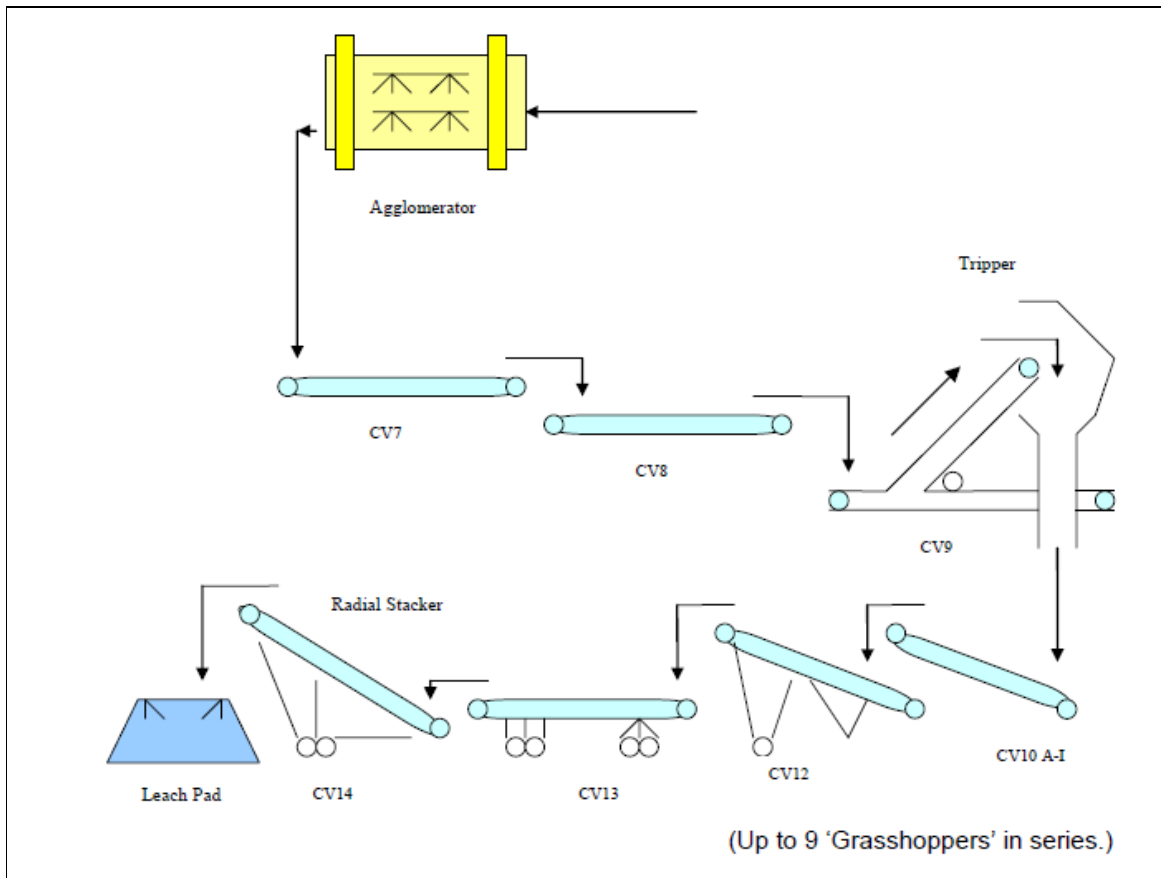
Figure 4: Stacking Flow sheet

Leach Pad Stage 1 is divided into 6 pads 350 m long x 82.5 m wide. Each of these pads is further divided into 6 cells approximately 56 m long x 82.5 m wide.

Ore will be discharged from the agglomerator onto the overland conveyor that runs 1000 m along the eastern edge of the leach pad. A mobile belt tripper will discharge ore onto a portable conveyor that will deliver ore across the conveyor corridor and onto the leach pad.

This conveyor discharges onto the first of a series of 762 mm wide 34.5 m long portable "grasshopper" conveyors. As additional lifts are added to the heap portable ramp conveyors with larger drives will be used to transport the ore up the side of the heap.

Crushed ore will be transported across the pad by a chain of portable "grasshopper" conveyors with its length varied by adding or removing individual portable conveyors. The final portable conveyor discharges onto the feed conveyor which is set up at right angles to the chain of portable conveyors. It will discharge the ore onto the radial stacker.

The radial stacker includes a 6 m retractable extension (stinger) and is designed to stack ore in cells 82.5m wide and between 6 m and 8 m high. Once the radial stacker has deposited one pass of ore onto the heap and used the effective length of the stinger the stacker will be retracted and one of the portable conveyors will be removed from the chain and the feed conveyor repositioned.

As each "pad" is completed the mobile tripper, remaining portable conveyors and radial stacker will be repositioned some 50 m to the north for placement of the next "pad". Portable conveyors will be relocated using a loader.

Once the first lift of ore has been placed conveyor ramps will be prepared on the eastern edge of the heap. Each ramp will be placed so that it facilitates ore placement in at least 5 cells.

The retreat stacking system proposed for the Lady Annie Copper Project allows freshly stacked ore to be placed under irrigation as soon as sufficient area is available.

The pad area will be constructed as a series of 82.5 m wide panels starting from the central fold line. A low earth bund will be constructed across the back and along each long side of each 82.5 x 350 m panel so formed. The whole of the leach pad surface including the bunds are lined with a 1.5 mm thick HDPE liner. An access track will run the length of the western side of the pad, parallel with and separating the pad from the W drains. The W drains are also lined with 1.5 mm HDPE.

On top of the HDPE liner an inert screened layer of earth is placed. This layer is called sub base and is 500 mm high. (The single purpose of sub-base is to protect the liner.)

A network of pipework and draincoil is installed beneath the stacked ore, on top of the sub base to collect leachate that reports to the base of the heap. Two 315 mm diameter collection pipes allow the leachate to be directed to either the PLS or ILS drain depending on the copper concentration in the solution.

Heap Height Changes

Heap heights have been increased from six metres to eight meters. This is due to the fact that the permeability of blended Mt Clark / Lady Annie stacked ore is significantly greater than 8 $L/m^2/hr$; this is the existing dripper system flux for pads 5 and 6. There is no evidence of ponding at the surface of these pads after two months of dripper irrigation.

Heap leach project data from many leach studies had been used to establish a HL amenability map. This map shows that heap leach feed of the following characteristics will be geotechnically amenable to heap leach:

- ore P_{80} (> 2.0 mm)
- ore -100μm fines fraction (≤ 60.1 %w/w)
- ore Si concentration (≥ 14.0 %w/w)

The P_{80} of Oct-Nov 2010 stacked ore was typically 15mm, the -100μm fines fraction was typically 17%, and the Si content is greater than 30%. This shows that there is no risk in increasing the stack height to 8-meters with respect to permeability (i.e. heap leach geotechnical amenability).

Several recent heap leach scoping studies evaluated the effects of stack height, lixiviant flux and acid concentration (independent variables) on metal extraction rate and extent, acid consumption, and leach duration (dependent variables). Data immediately at hand that describes these effects is from a recent nickel laterite study. The conclusions drawn from this data apply equally to most non-aerated heap leach systems, including the copper oxide leach system used at Lady Annie.

The study showed that a 50% increase in stack height resulted in a 6% to 33% increase in leach duration, with all other independent variables unchanged (agglomeration, flux, acid concentration).

At Lady Annie, we have increased stack height by 33% to 8.0 meters; therefore we should anticipate an approximately 22% increase in leach duration by increasing the stack height alone[3].

Oxide Ore, Going Into Transition Ore That Includes Chalcocite

There are two main types of ore at the Lady Annie Copper Mine:

- Carbonates (often referred to as oxide ore) and
- Sulphides

Copper carbonate minerals occur in the top part of the ore body where weather over thousands of years has oxidised the original sulphide minerals.

The main carbonate minerals present at Lady Annie Copper Mine are:

(1) Malachite - $Cu_2CO_3(OH)_2$

(2) Azurite - $Cu_3(CO_3)_2(OH)_2$

These minerals are easily leached with sulphuric acid (H_2SO_4), where the copper is basically dissolved by the acid to form copper sulphate.

Sulphide minerals occur deeper in the pit. The main sulphide minerals present at Lady Annie Copper are:

(1)   Chalcocite - Cu_2S

(2)   Chalcopyrite - $CuFeS_2$

These minerals are not leached by sulphuric acid alone as they require the presence of ferric sulphate $Fe_2(SO_4)_3$ and specific types of bacteria in the leach solution. Ferric sulphate is formed as a result of the bacterial oxidation of iron present in the irrigation solutions from its ferrous state to its ferric state. The bacterium acts as the catalyst for the sulphide leaching reactions.

For these reactions to occur oxygen is required. Air flow through the heap therefore is vital. It is very important that the heap be very permeable to enhance both solution and air flow through it. It is also important to note that airflow cannot occur if the heap is totally saturated with solution. Irrigation rate must therefore be controlled to prevent heap saturation and the formation of a phreatic head within the heap.

Selected Crushing and Stacking Charts

It can be seen from Figure 5 below that the Calcium /Magnesium levels in the stacked ore is quite high in September 2010. High calcium and magnesium levels in the ore are undesirable due to their tendency to leach preferentially to copper and use up excessive amounts of acid. This ore was stacked on Pad 6, which was initially under-acidified.

The ore size is generally within the size limits, sitting on average at a P_{80} of 15.5mm.
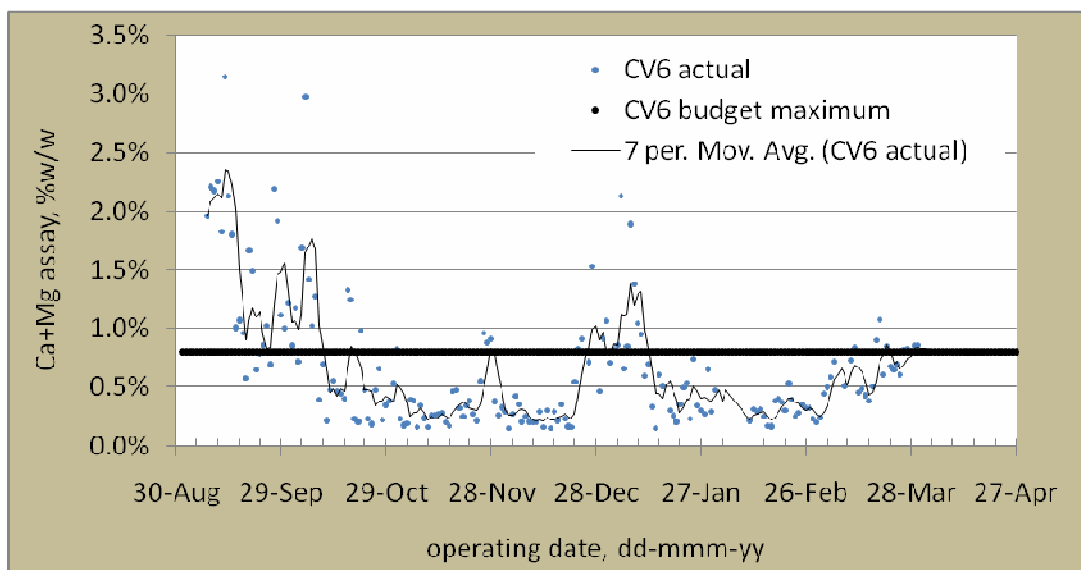
Figure 5: Ca and Mg in stacked ore
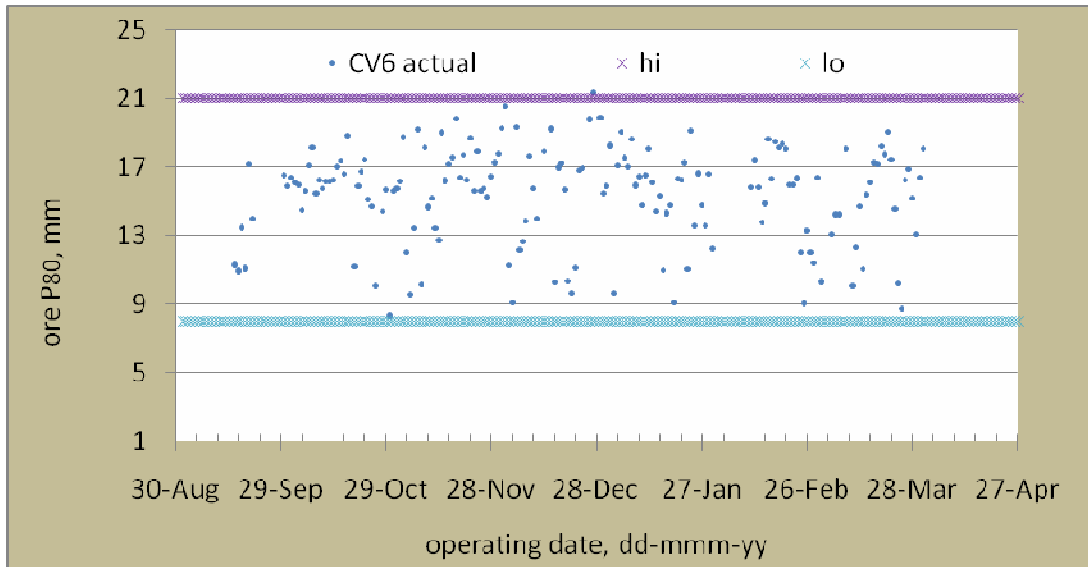
Figure 6: Stacked ore sizing
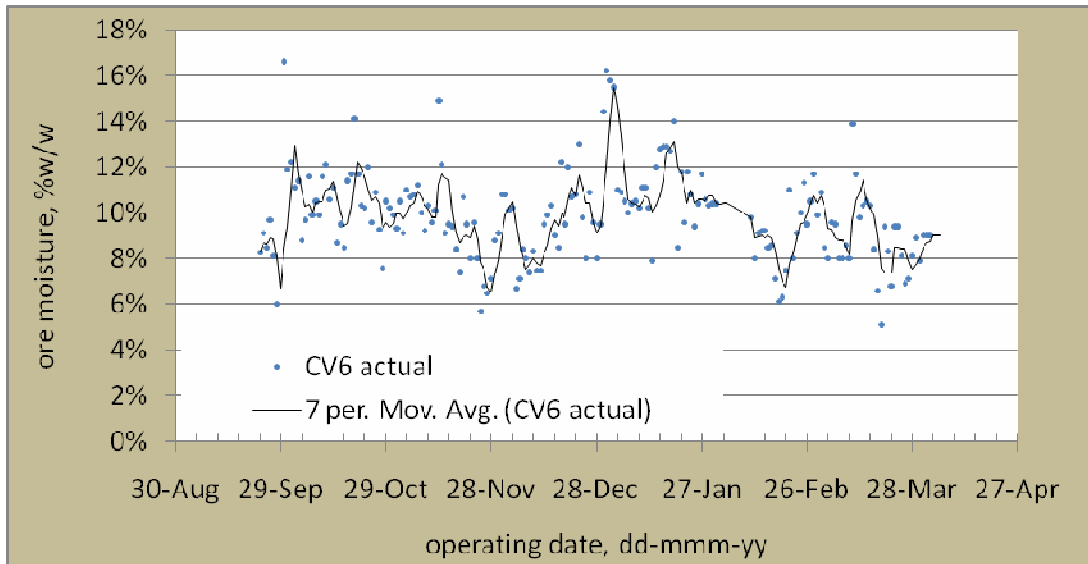
Figure 7: Stacked ore moisture
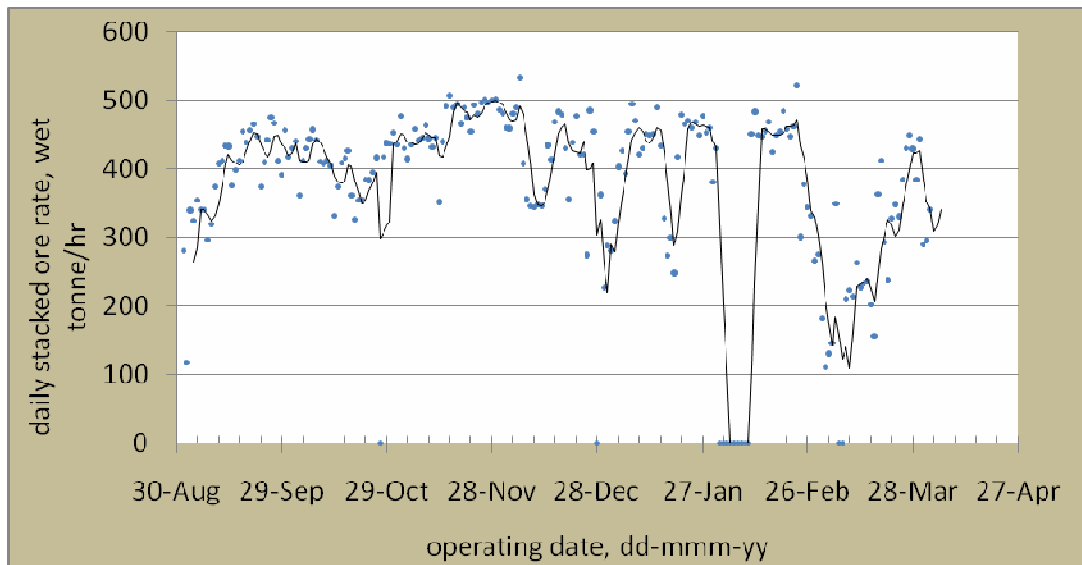
Figure 8: Ore stacking rate

The ore stacking rate decreased dramatically at the end of February and for most of March. The cyclical rainfall of the north Queensland wet season makes the ore wet and tacky. This means that bins and chutes in the crushing and stacking circuit block up easily and frequently, hence the lower stacked ore rate. The effect of Tropical Cyclone Yasi can be easily seen at the beginning of February as well. Increased ore moisture corresponds to the lower stacking rates.

HEAP LEACHING

Leach Start Date

The irrigation on the first new pad (Pad six) was started on September 23rd 2010. Since that date another six pads have been stacked and put under irrigation – five, four, three, fifteen, fourteen and thirteen.
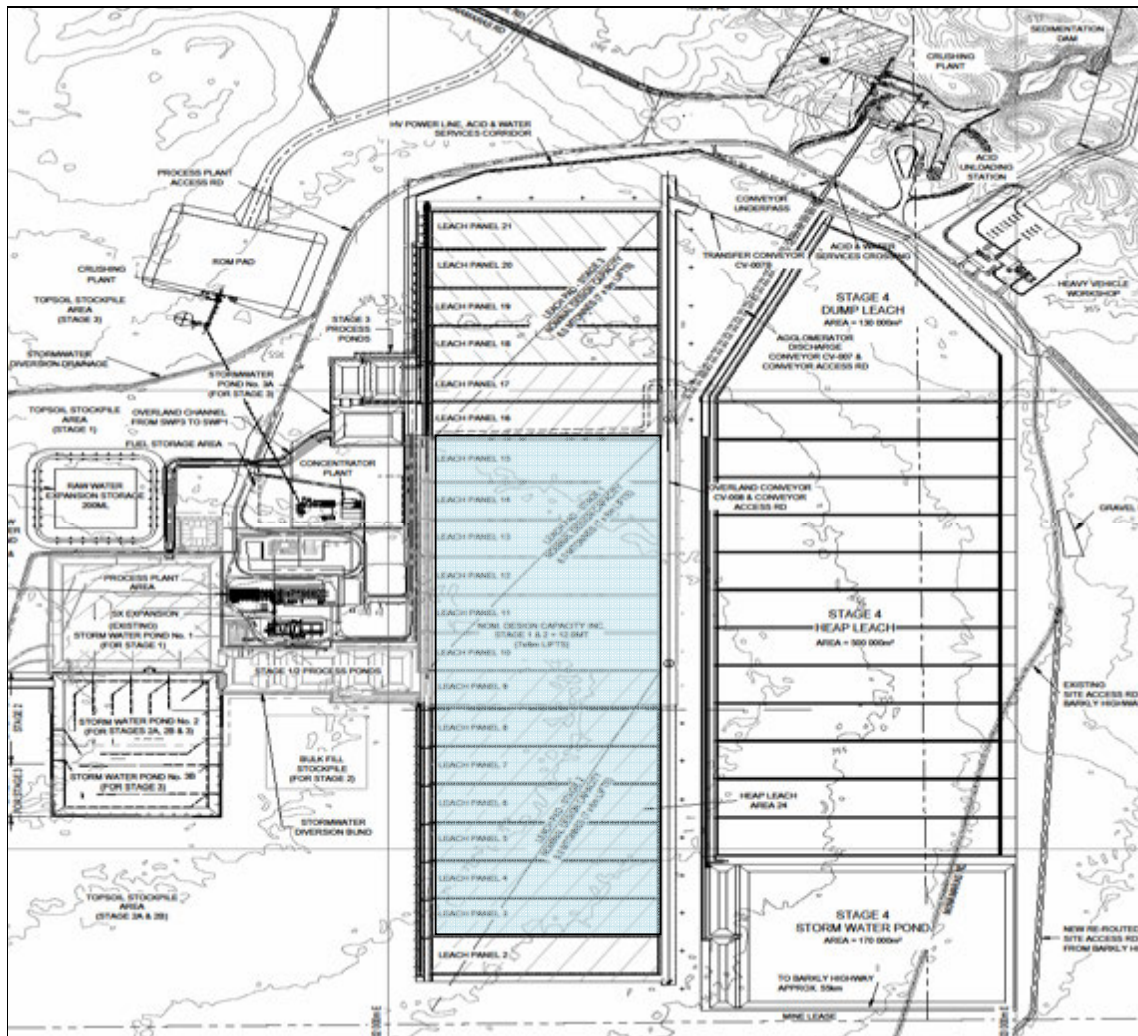
Figure 9: Leach pad layout; current and future plans

Heap Leach Brief Description

Raffinate (RAFF) or intermediate leach solution (ILS) is fed onto the heaps via an irrigation system to leach the copper from the ore. The solution flows through the heap and is collected at the base of the heap and directed into an off flow pipe. Depending on the grade of the off flow solution, the off flow pipe can be directed to either the ILS or PLS (pregnant leach solution) w-drain. The w-drains feed into the corresponding storage ponds (refer to Figure 1).

Basically the RAFF is the 'tailings' of the solvent extraction plant, it is generally higher in acid content but lower in copper content. Alternatively the ILS is higher in copper content but lower in acid content compared to the RAFF solution. Acid addition to the Heap Leach is generally via the ILS pond and in some cases the ILS solution will be made higher in acid than the Raffinate.

ILS solution is recycled back over the heaps to achieve the higher Cu grade required for feeding the solvent extraction plant. The copper grade of the heap off flow solution will determine which drain it should report to. This will depend on the total flow rates around the heap leach system and the copper requirements of the solvent extraction plant.
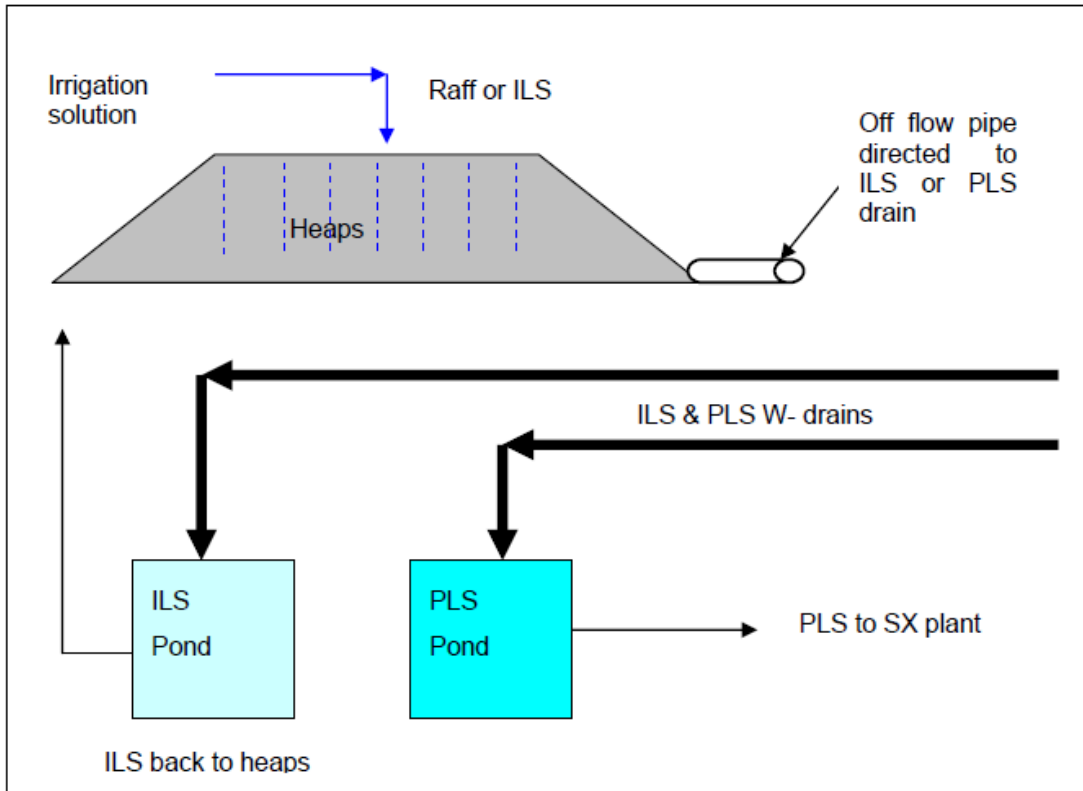
Figure 10: Basic Heap Leach layout

When a freshly stacked cell is placed under irrigation it is leached with ILS solution which contains approximately 8-10 g/l acid.

The solution recovered from a fresh panel has a higher copper grade. As a result it is directed to the Pregnant Leach Solution (PLS) pond. From the PLS pond it is pumped to the Solvent Extraction - Electrowinning (SX-EW) plant.

Panels which have been under irrigation for a longer period of time produce a lower off flow grade. This solution is called Intermediate Leach Solution (ILS), and is directed to the ILS pond. ILS solution is pumped back on to the heap to irrigate panels and upgrade the copper content of the run off to PLS grade.

Table 4: Design Criteria for Lady Annie heap leach circuit

Raffinate flow rate	m³/h	500 nominal, 560 max
ILS flow rate	m³/h	500 nominal, 700 max
PLS flow rate	m³/h	500
Irrigation rate	l/m²/h	Target 8
Pond capacity Raffinate ILS PLS	m³	 12,920 12,900 12,920
PLS copper grade	g/L	5.3
ILS copper grade	g/L	2.5
Raffinate copper grade	g/L	0.61

The amount of solution added to each heap can vary as it really depends on its percolation rate. This is linked to the heap permeability and is a result of crush size, ore type and % fines. Heap leaching is very much dependent upon physical characteristics as it is on chemistry. The physical aspects need to be correct so the chemistry can occur. Effective solution flow through the heap is required to deliver the necessary reagents to the ore so that copper leaching can occur.

Careful management of solution application rates is required to match the local acceptance rate of the heap surface. Application rates are measured and reported in litres per metre squared per hour (L/m²/h). The target solution application rate is approximately 8 L/m²/h.

The main reason for matching solution application with solution acceptance is to reduce ponding and avoid washouts, heap plugging and air ingress. While some degree of ponding is not of major concern, it contributes to the occurrence of washouts and to short-circuiting of solutions. Washouts are a significant problem as once they occur, the area around the washout cannot be leached adequately and recovery from the ore may be reduced and drains/sumps blocked.

Short-circuiting (which is slow exiting from the side of a heap) can cause continued erosion of the heap side slopes and may ultimately affect heap stability (more critical if upper lifts are involved). Short-circuiting also results in reduced copper recovery and lower heap solution off flow grades. For these reasons, short-circuiting must not be allowed to continue. Most 'short circuiting' actually occurs within the heap where channels of flow are established bypassing the ore. Once established the channels can rarely be rectified. Most surface ponding will eventually cause internal channels.

Excessive application rates can lead to a build-up of solution within the heap and this is referred to as the phreatic head. If this is allowed to build up it can mobilise the heap resulting in major heap washouts as the bottom of the heaps can slip sideways. This can significantly reduce the overall heap recovery resulting in reduced copper production, blocked W drains and sumps.

Irrigation System Brief Description

The two basic types of heap irrigation methods are drip emitters and wobblers and both have their advantages and disadvantages

The main advantages of dripper irrigation are the reduced solution evaporation rates and lower impact on the surface of the heap. The main disadvantage is their coverage area and the potential for solution channelling. Wobblers have a greater surface coverage ensuring all of the ore is wetted however they result in significant solution losses through evaporation. They are also higher impact on the surface of the heap and can mobilise fines (breaking up agglomerates) and "plug" the heap surface solution acceptance rate.

Drippers supply leach solution through plastic tubes that lie on the surface. The tubes have small openings called emitters at evenly and closely spaced intervals along distributor lines. Lady Annie uses drippers on the heaps, although one pad has been set up with wobblers.

The irrigation equipment is set up so that the greatest surface coverage of the heap is achieved, taking into account solution application rates. It also allows for easy access for heap maintenance purposes.

Each heap will be fed with a main line that can supply either RAFF or ILS from the main heap header lines. The diameter of the header line is reduced the further away from the base of the heap where it is connected to the main header line. The main header line is 225mm diameter which runs from the supply lines and will be approximately 120 metres long. The pipe is then reduced to 200mm diameter for a further 150 metres with a final reduction to 160mm (refer below to Figure 11: Heap irrigation Dripper line set-up).
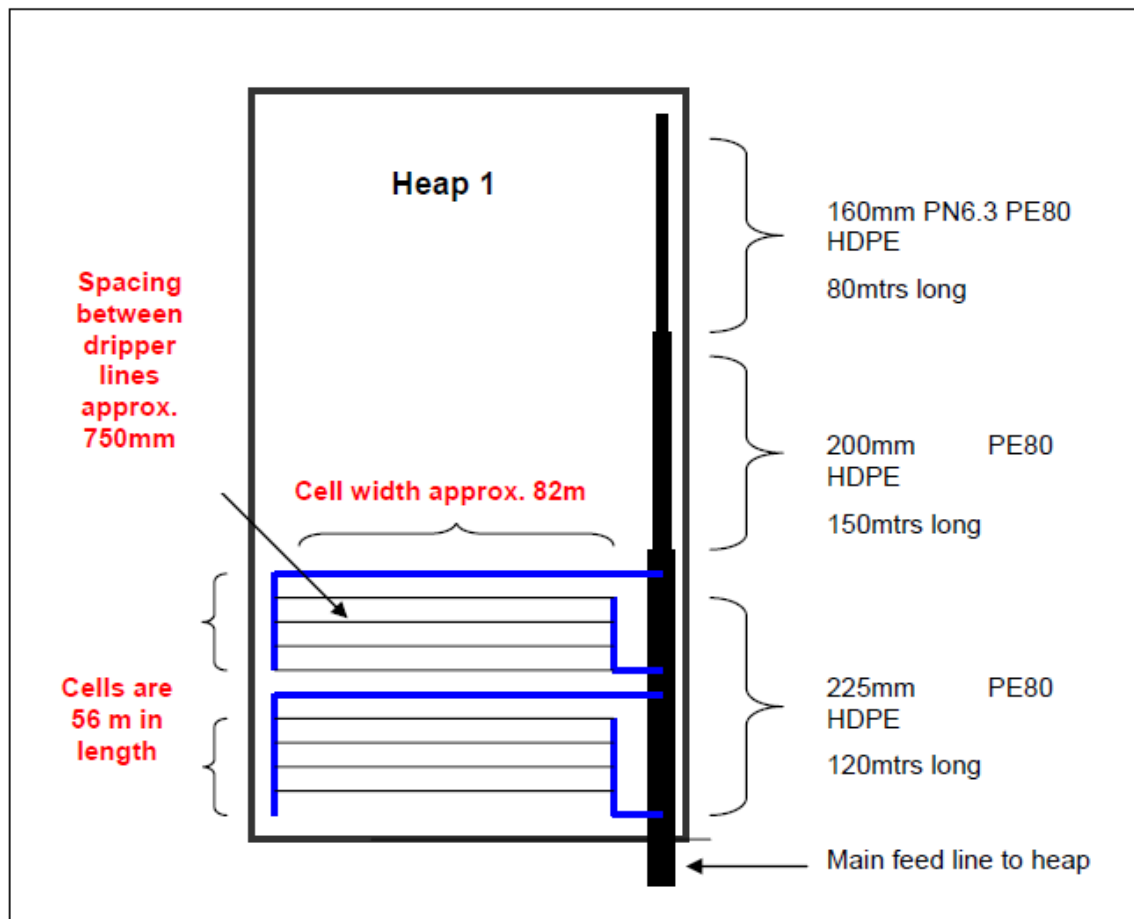
Figure 11: Heap irrigation Dripper line set-up

Heap Leach Configuration

As with most heap leach operations, ILS is used to irrigate fresh heaps, and then switched over to higher acid raffinate towards the end of the life of the heap. The higher acid level in the raffinate encourages more of the copper to leach out of the ore.

Heap Leach Variables

Due to the presence of calcium and magnesium in the ore and their tendency to leach preferentially to copper, there is a need to operate the heaps with excess acid to maintain the fastest possible copper extraction.

So far only one pad has come to the end of its' useful life, Pad 6; this pad was under irrigation for 146 days, approximately five months. Data for Pad Six can be seen in
Figure 12: Pad 6 Cu Extraction and Acid Addition.

As is normal, copper extraction occurred quickly to start with then it dropped off. The drop in copper extraction rate was due to the leaching of calcium and magnesium. Then it is clearly visible that with the increase in acid in the lixiviant the extraction rate also increased. It could be said that if a higher acid level was not employed then a lower amount of copper would have been extracted from the heap.
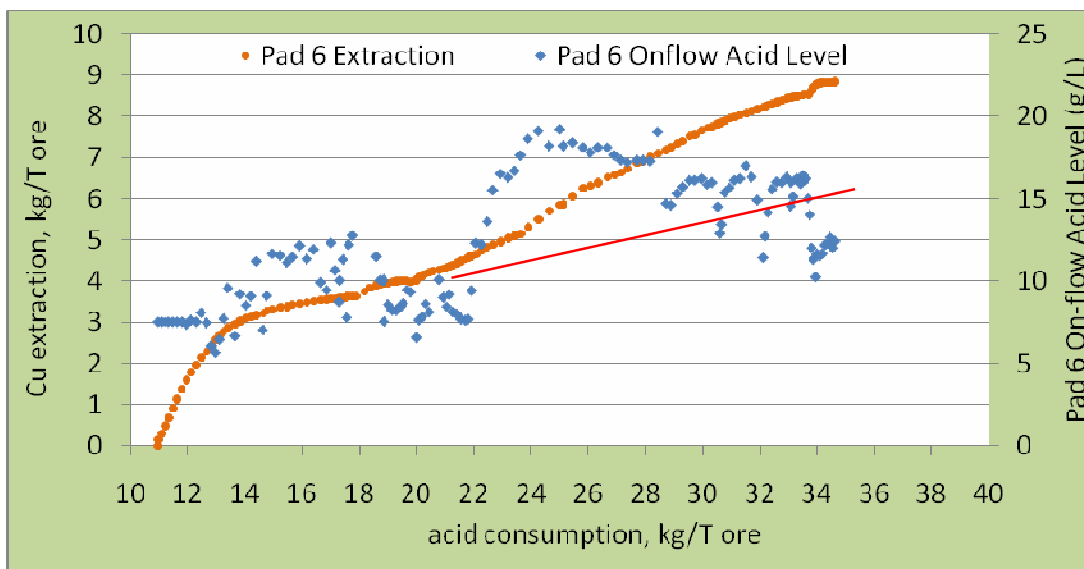
Figure 12: Pad 6 Cu Extraction and Acid Addition

ILS, Raff and PLS acid levels are shown in Figure 14: ILS Acid, Raff Acid and PLS pH levels below, as are the acid consumption curves in Figure 13: Lady Annie Heap Leach Acid Consumption curves, copper extraction curves for all six Lady Annie heap leach pads in Figure 15 and the flux across the pads in Figure 16.
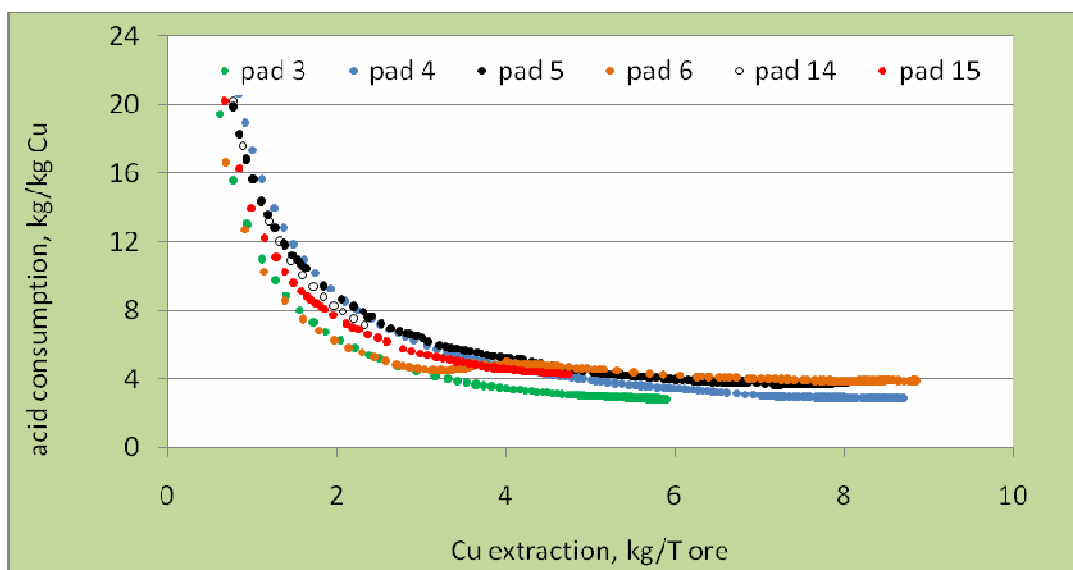
Figure 13: Lady Annie Heap Leach Acid Consumption curves
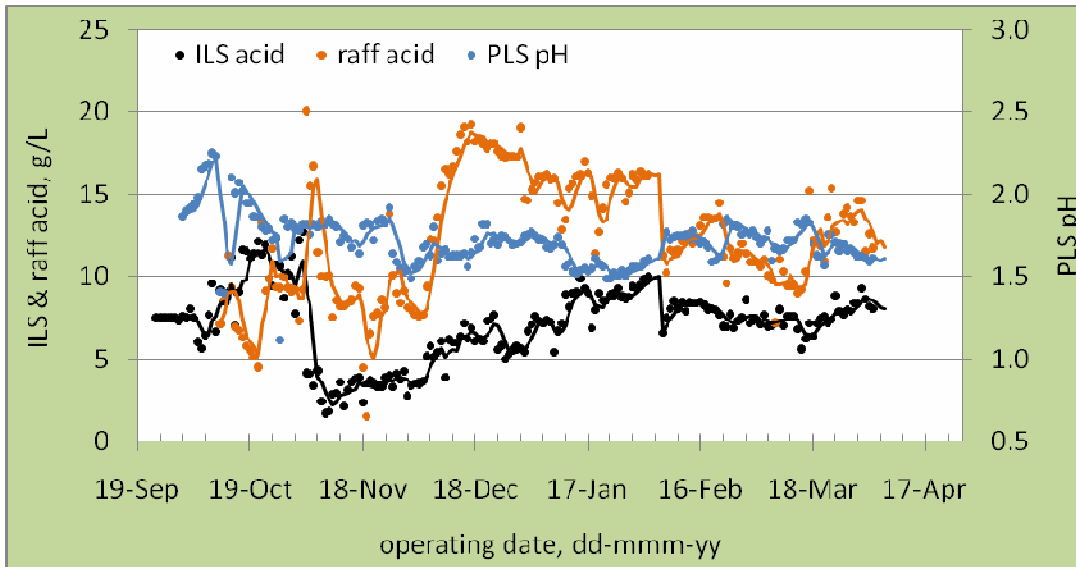
Figure 14: ILS Acid, Raff Acid and PLS pH levels
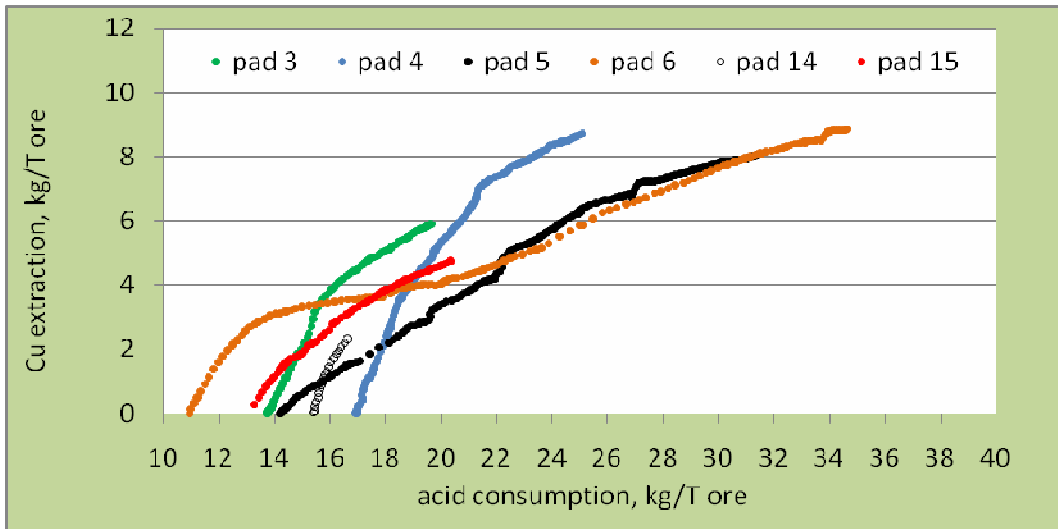
Figure 15: Lady Annie Heap Leach Copper Extraction Vs Acid Consumption
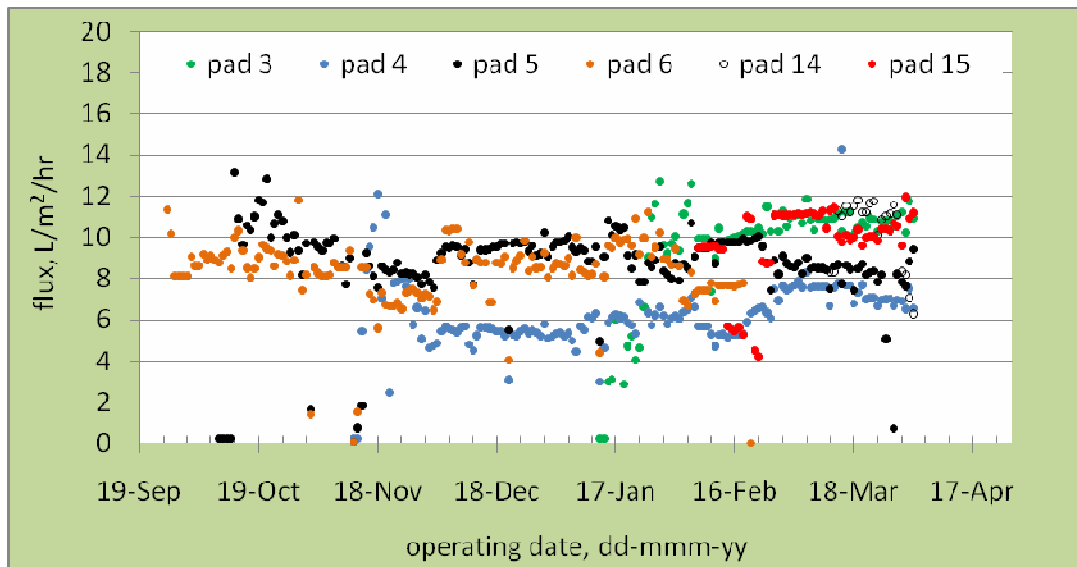
Figure 16: Lady Annie Heap Leach Pad Flux levels

PLS quality started off at a very high rate due to the fact that leaching was occurring from September until December when the SX plant was started up. The Lady Annie operation had a very high inventory of copper in the PLS, ILS and RAFF ponds. This inventory has been drawn down upon over the wet season when the stacking rate has slowed down.
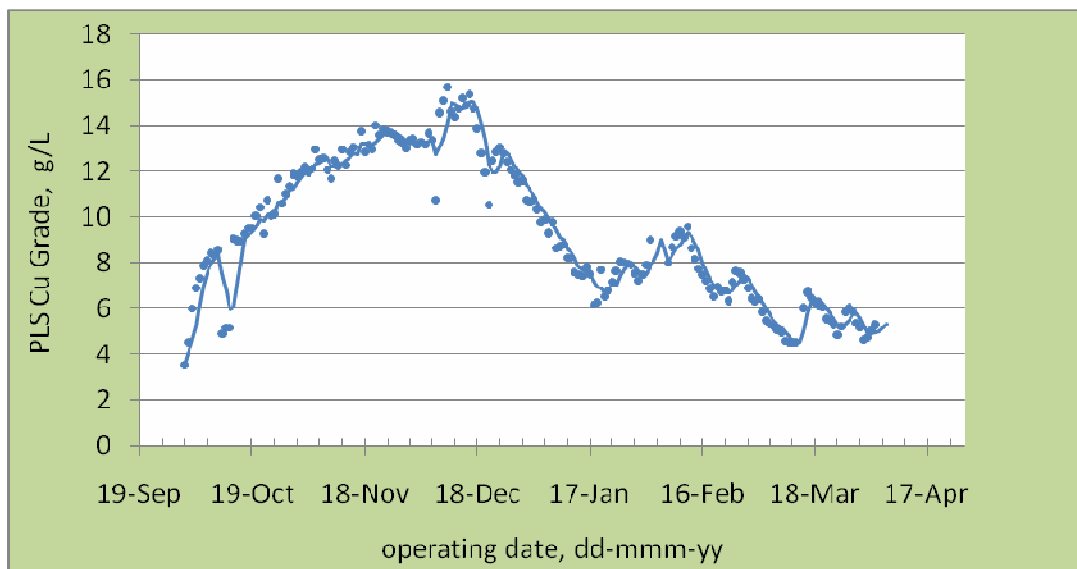
Figure 17: PLS Cu Grade (g/L)

Forced Aeration Heap Leaching

Lady Annie are expecting to mine transition ores from existing pits (Lady Annie, Mt Clark) which contains copper minerals that may be amenable to forced aeration heap leaching. Therefore LAO are undertaking a forced aeration leach column and heap leach testing program in the near future.

SOLVENT EXTRACTION

SX Start Date

The solvent extraction plant was started on 19th November 2010.

SX Brief Description

A solvent extraction stage is required to concentrate and purify the leach solution to form electrolyte suitable for electrowinning. This is achieved through a series of mixers and settlers. The leach solution is contacted with a kerosene based reagent (called organic) which selectively removes the copper from the leach solution. This is called the extraction stage where the copper is taken from the leach solution and loaded onto the organic. The final stage of the solvent extraction process is called the stripping stage where the copper is transferred from the organic into electrolyte. This is high in copper and acid concentration.

The solvent extraction plant (SX) at Lady Annie is the old plant from Mt Gordon and consists of a series of mixers, settlers and associated tanks. The circuit comprises two extraction, one extraction in parallel and two strip stages.

Each stage consists of two stages of mixing, primary and secondary and a settling phase. The mixers are where PLS (aqueous solution) and the organic are mixed together. The copper is extracted from the PLS solution into the organic. Alternatively in the stripping stage the copper is removed from the organic to form the strong electrolyte. The circuit configuration is illustrated below in Figure 18.

The extractant behaves differently depending on the acid strength of the aqueous solution it is in contact with. At low acid concentrations (PLS), copper extraction is favoured. Alternatively at high acid concentrations (spent electrolyte) stripping of copper is favoured. The PLS is very low in acid strength, typically 2-5 gpl, and therefore the organic extractant will extract copper. The electrolyte on the other hand is very strong in acid strength, typically 160-180 gpl, therefore the extractant releases the copper.

The "loaded" organic contacts spent electrolyte from the electrowinning (EW) plant in the strip stage. The acid in the spent electrolyte strips the copper from the loaded organic resulting in copper transferring to the strong electrolyte (50-55g/l copper) and stripped organic. The strong electrolyte leaves the strip stage and passes through a Spintek dual-media filter. The aim of this step is to remove entrained organic and solids before the electrolyte enters the EW circuit.

Table 5: SX Design Criteria

PLS	SX plant configuration		
Copper: 4.8 g/L (min)	Phase continuity design: Aqueous or organic		
Total iron: 0-10 g/L	Recommended: E1 – Aq or org	S1 – Org	E2 – Org
Chloride (Cl): 2.0 g/L	Primary O/A ratio: Extraction – 0.9 to 1.1: 1		Strip – 1:1
pH: 1.8 – 2.0	Secondary O/A ratio Extraction – 1:1		Strip – 3:3.1
Temperature: 14-35 ºC	Organic depth: 200 – 300mm variable (nominal 250)		Aqueous depth: 570mm
	Mixer retention times: Extraction – 100 seconds		Strip – 100 seconds
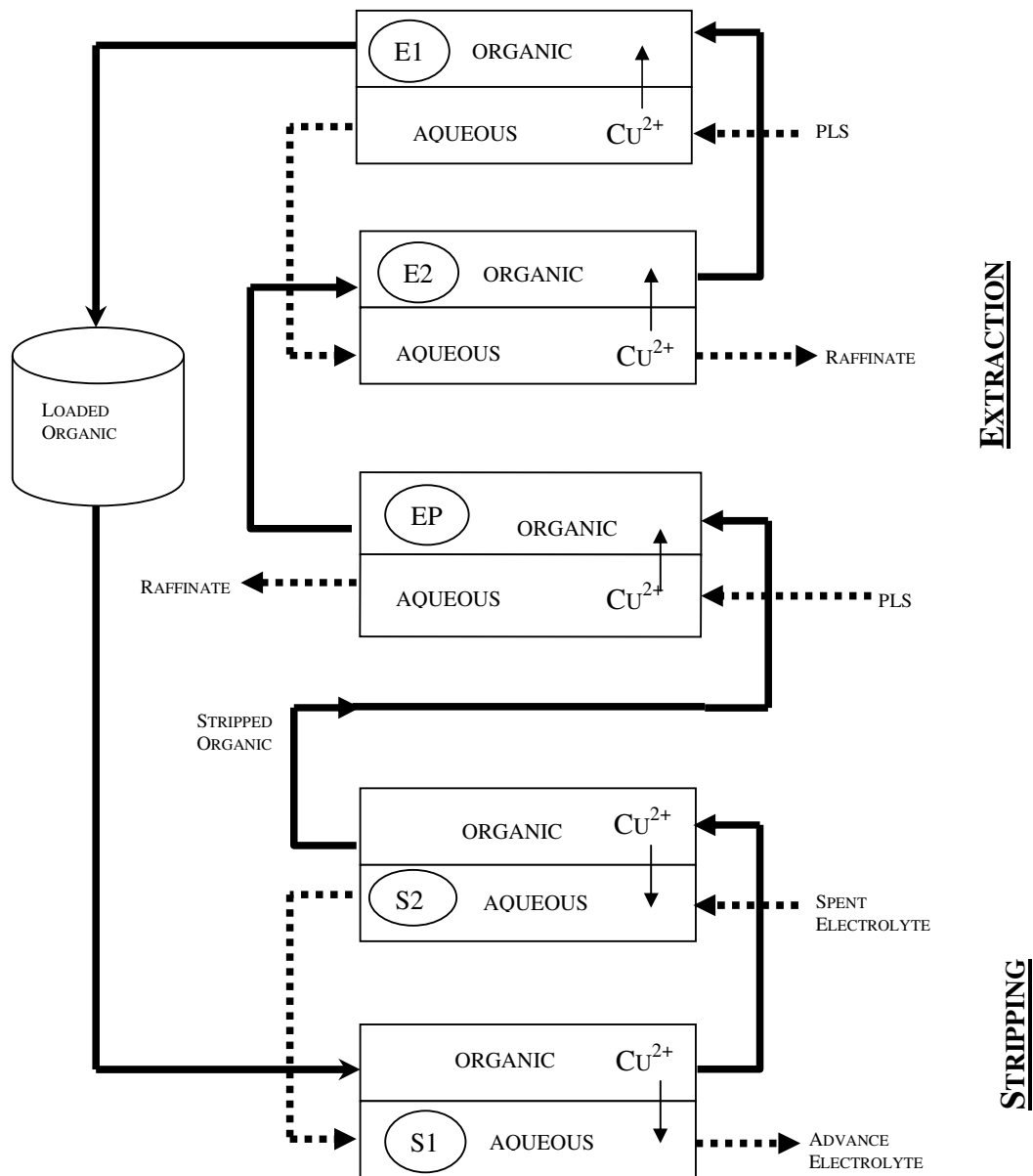
Figure 18: Lady Annie SX Circuit

Future Circuit

In the near future the "spare" E4 and S3 mixer settlers will be started up. These two additional mixer settlers will be started in conjunction with another fifty-eight electrowinning cells. The additional capacity will boost Lady Annie's production up to 30,000T of cathode copper per annum.

E3 and S3 will be run in parallel with the current circuit.

Crud

As with any solvent extraction plant, crud is an ever present issue that needs to be kept a close eye on. The Lady Annie SX settlers have provision for manual crud farming.

After recent heavy rainfall, a serious crud run occurred. It was highly possible that the settlers flipped from running OC to AC due to a large increase in solids in the PLS from the PLS pond. There was a large amount of crud in all the settlers and it deactivated coalescer media, increasing impurity transfer, increasing crud treatment activities, and increasing reagent losses; none of which are desirable.

There is no easy remedy, but it has been found that in cases where a surge of solids occurs in the PLS then organic mixer phase continuity can be maintained by dropping PLS flows and increasing organic recycle flow rates (in LAO's case in all Extract stages - E1, E2 and E3). This will increase O/A ratios and help to favour OC operation in the mixers[2].

During the Tropical Cyclone Yasi storm activity and rainfall, the plant was shutdown. Although production losses were sustained, in the long run it helped the plant due to the fact that a large amount of solids were prevented from entering the plant from the PLS ponds.

ELECTROWINNING

EW Start Date

The electrowinning plant was started up on 19th November 2010. The first copper was stripped six days later on the 25th November 2010. The first dispatch of copper occurred on 29th November 2010. There are one hundred cells in the "old" cell house and each cell holds thirty-three cathodes. At start up only twenty-two cathodes were in each cell. At the start of January 2011 enough cathodes were available to completely fill each cell with thirty-three cathodes.

EW Brief Description

The final step in copper production for Lady Annie is electrowinning where the cathode copper is produced. Here the electrolyte is fed into a series of cells containing lead anodes and stainless steel cathodes. A large current is applied and copper is extracted from the electrolyte and plated onto the stainless steel plate via an electrochemical reaction. The plates are removed from the cells every six days and the copper is stripped from the stainless steel. The stainless steel cathodes are placed back into the cells so that the next plating cycle can begin.

Reagents (salt, guar and cobalt sulphate) are added to help smooth the copper deposit and to prevent corrosion of the lead anodes.

The cellhouse has one hundred cells, with thirty-two of them being scavenger cells and the remainder being the "commercial" cells. After leaving SX the advance (strong) electrolyte is filtered through Spintek dual media filters. The excellent results from the Spintek filters mean that copper from all cells is LME A Grade copper.
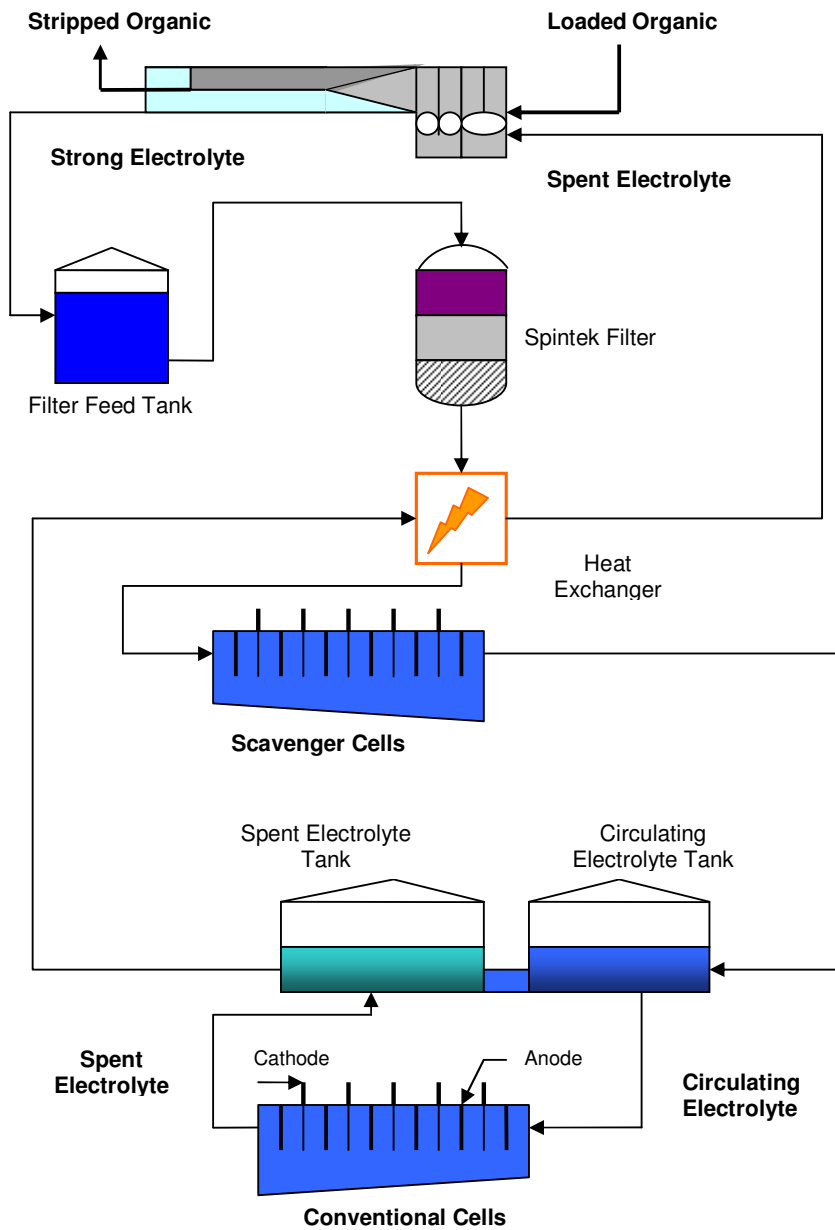
Figure 19: schematic of EW Cell house

PRODUCTION

Copper cathode has been fairly consistent over the months since the EW plant has been operational.
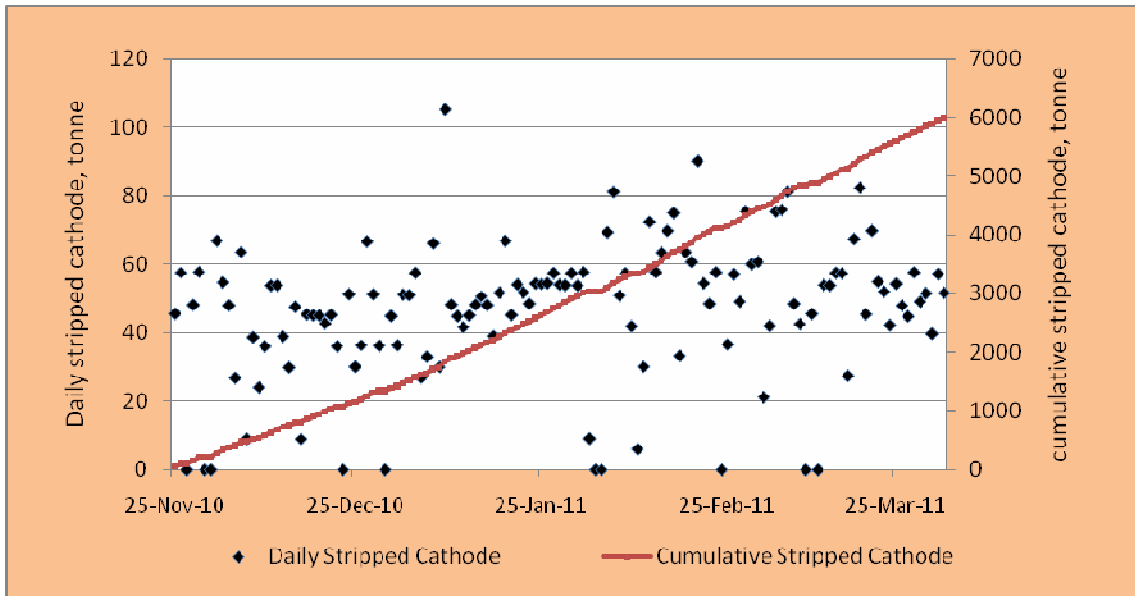
Figure 20: Daily and Cumulative Stripped Cathode

Power Levels

The power is generally at the maximum level it can be at; see Figure 21: Cell House Rectiformer Current. When only twenty-two cathodes were in each cell, maximum power of 14,500A was maintained. With thirty-three cathodes per cell the maximum power level is 21,500A.
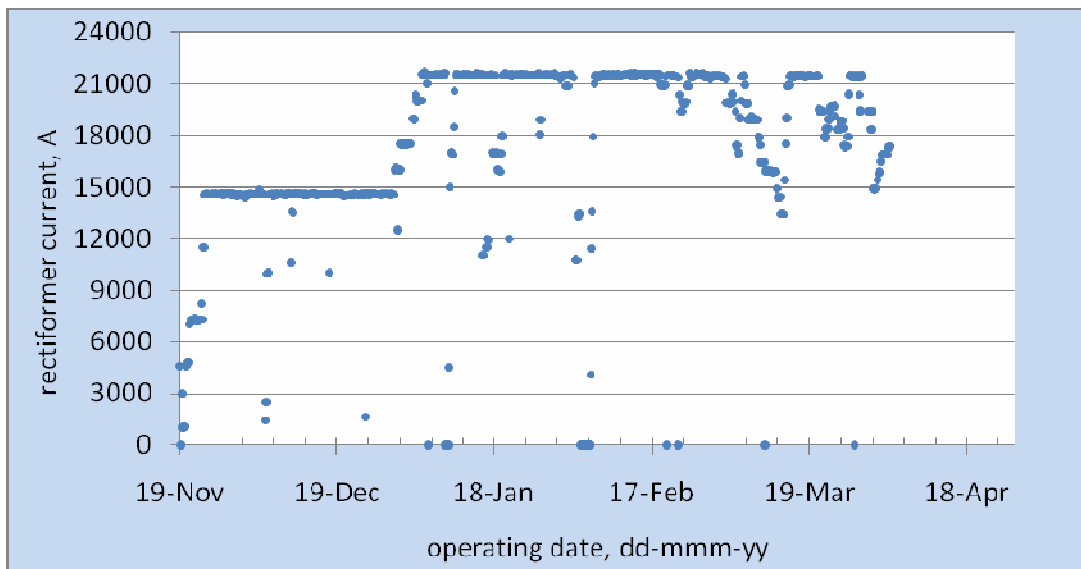
Figure 21: Cell house Rectiformer Current

Future Circuit

Once the PLS grade increases again, the "new" SX will be started and the "new" EW will be started up. There are another fifty-eight cells in the new cell house.

CATHODE QUALITY

The copper cathode produced by Lady Annie has been of LME Grade A standard since the first sheet was produced on the 25th November 2010.
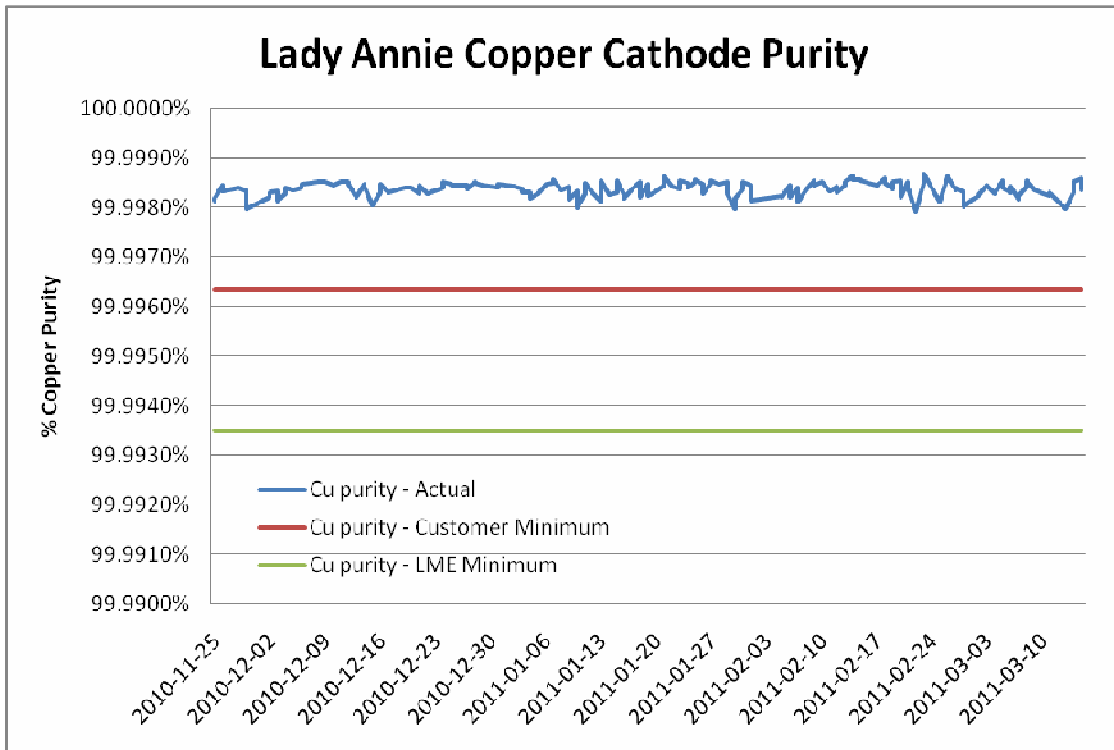
Figure 22: Copper Cathode Purity
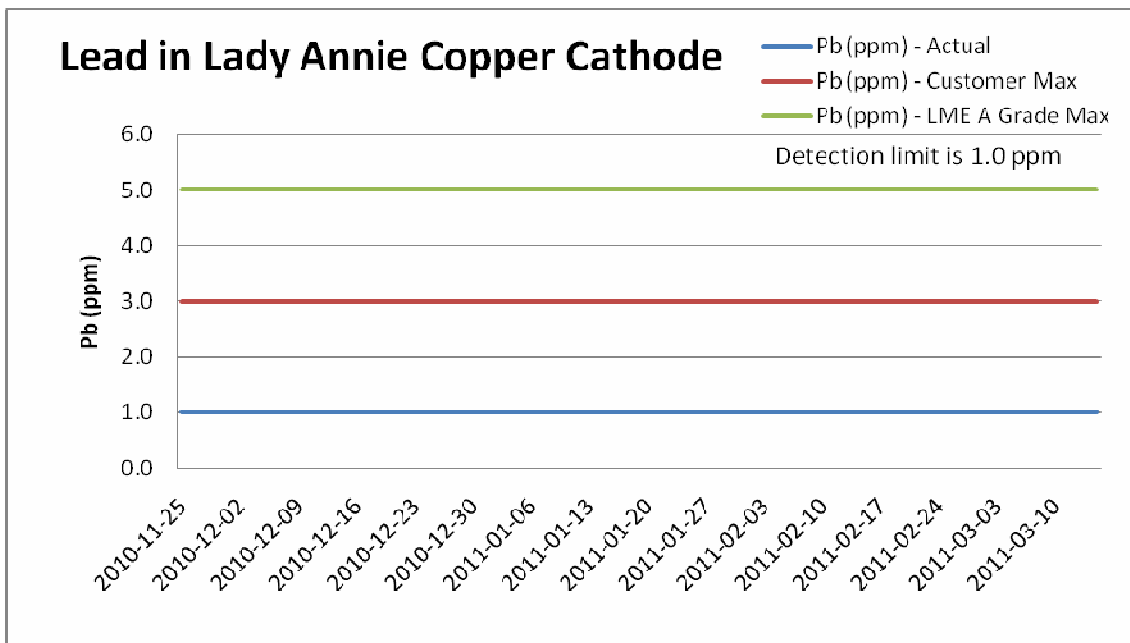
Figure 23: Lead in Cathode
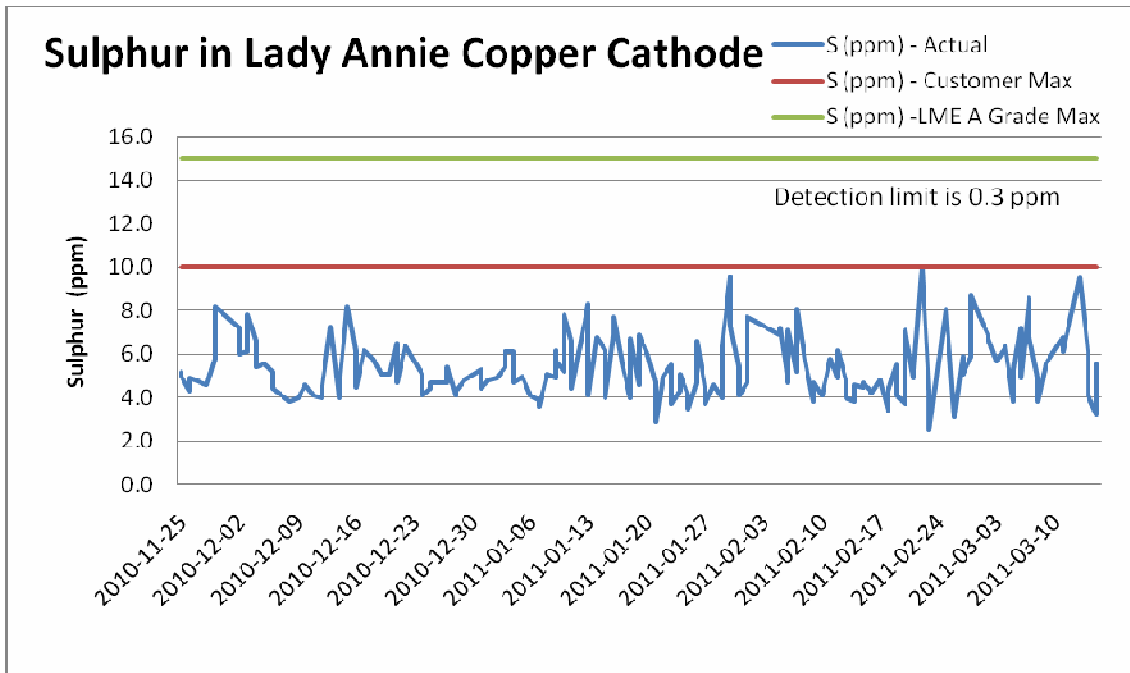
Figure 24: Sulphur in Cathode
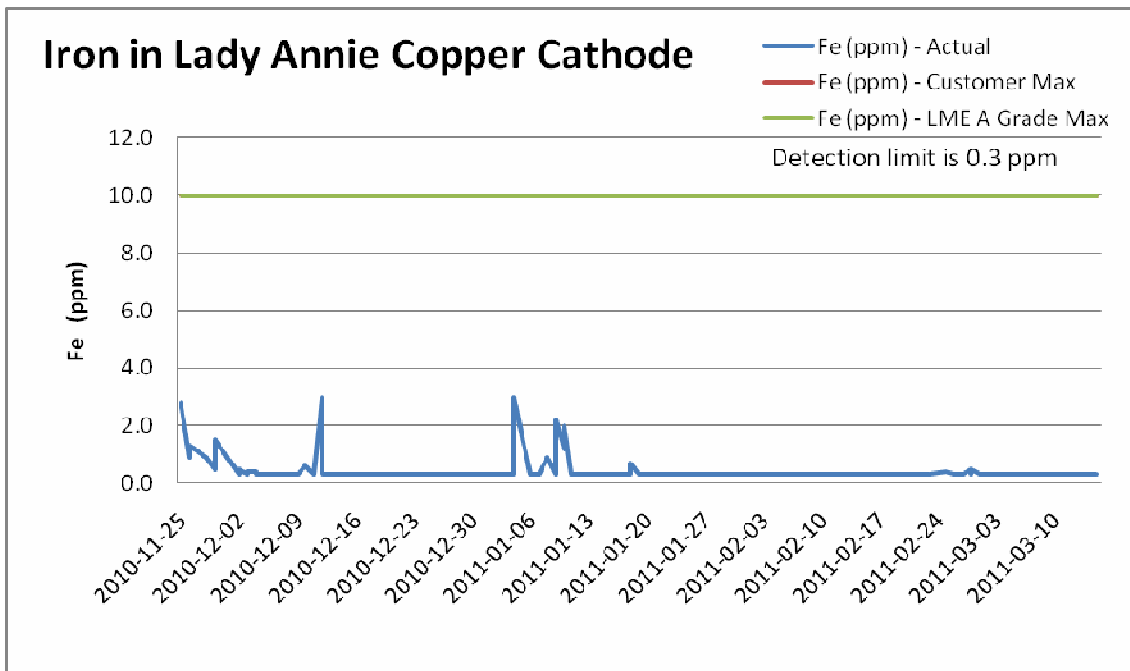
Figure 25: Iron in Cathode
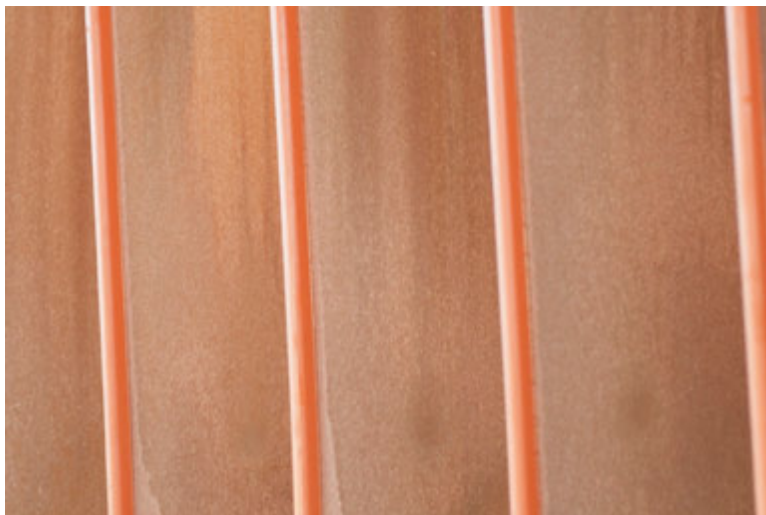
Figure 26: Copper cathode still on the mother plate

New Stripping Machine

Lady Annie is soon to install a new robotic cathode stripping machine. The machine has been developed by Xstrata Technology engineers in North Queensland. The majority of the components have been delivered on site from the manufacturing site in Japan and are awaiting installation and commissioning.

The machine is a world first and the machine to be installed at Lady Annie is the first commercial production model.

The machine is capable of stripping 150 cathode plates an hour – generally 550 cathodes are stripped per day (fifty cells a day).

The new machine will increase throughput, improve safety and enhance product quality by removing the risk of damage through manual handling. The system should require less maintenance than the current system.

CONCLUSION

The successful re-commissioning of the Lady Annie site is a testament to the commitment of the CST Lady Annie workforce and through them, the thorough overhaul of the entire processing plant, including pumping equipment, crushing and stacking infrastructure, cellhouse repairs and checks and cathode plate refurbishment. The Mt Isa business community have also been crucial to the start-up and continued success of the operation with the supply of equipment, services and additional personnel.

Copper cathode quality has been LME A Grade since the first sheet of copper was stripped.

With the new stripping machine, new sulphide deposits and test work into the treatment of these ores, as well as the oxide deposits, the future of CST Minerals looks very bright.

REFERENCES

1. F. Blanchfield, C. Standing, P. Meyers, "Technical report on the Lady Annie Project", Snowden Mining Industry Consultants Pty Ltd, May 2010.

2. P. Crane, "Cognis Technical Service Report #14", Cognis Australia Pty Ltd, March 2011.

3. A. Moroney, CST Lady Annie Memorandam, January 2011.

ATMOSPHERIC ACID LEACHING OF NKAMOUNA ASBOLINIC COBALT CONCENTRATE WITH PYRITE AS THE REDUCTANT

By

[1]Herman Schwarzer, [1]Alastair Holden, [1]Brett Crossley, [2]Roman Berezowsky and [3]Brian Briggs

[1]Lycopodium Minerals, Australia
[2]Hydrometallurgical Consultant to Geovic Cameroon, Canada
[3]Geovic Mining Corporation, USA

Presenter and Corresponding Author

Herman Schwarzer
herman.schwarzer@lycopodium.com.au

ABSTRACT

Geovic Mining Corporation's Nkamouna Cobalt-Nickel-Manganese Project is a greenfields project, located in the East Province of Cameroon in Africa. The company proposes to produce a high grade, high purity mixed cobalt nickel sulphide (MSP), as well as a manganese carbonate (MnCP) by-product for sale to third parties.

The deposit under investigation is a cobalt rich nickeliferous laterite and is unique in its mineralogy due to the high concentrations of cobalt and manganese relative to nickel. Mining will be performed using strip mining techniques. Physical upgrading of the run of mine ore will be achieved by attritioning and size separation to recover the valuable asbolinic mineral as a coarse fraction.

The resulting concentrate will contain approximately 1% cobalt, 0.85% nickel and 5.4% manganese, and about 8% aluminium and 37% iron. The concentrate will be milled in an open circuit ball mill (P_{80} of 106 μm) and leached under reducing atmospheric conditions with sulphuric acid at 95ºC in a sodium sulphate-containing solution. The leach temperature will be sustained by the exothermic leach reactions and augmented by the heat of dilution from the sulphuric acid. Ultra fine pyrite (P_{80} of 10 μm) will be utilised as the reductant in the leaching process.

The process chemistry is complex as two processes occur simultaneously in the leaching circuit:

• cobalt (95%), manganese (93%), and nickel (60%) are dissolved, as the asbolinic minerals react under the reducing acidic conditions, and
• a portion of the aluminium and a lesser amount of iron are also dissolved, but under the prevailing conditions they are largely hydrolysed and precipitated as alunite and jarosite respectively.

By judicious selection of the leaching conditions, high extractions of the value metals are able to be achieved in a single stage of atmospheric leaching, while consuming approximately 180 kg/t of sulphuric acid. The resulting pregnant leach solution contains 12 g/L Co, <1 g/L Fe, and about 6 g/L Al, and has a low terminal acidity (<5 g/L).

The Bankable Feasibility Study for the Project was concluded in April 2011 and is currently undergoing review by a number of financial institutions.

BACKGROUND

The Nkamouna Cobalt-Nickel-Manganese Project (Project) is located in the Haut Nyong Division, East Province of Cameroon in Africa, approximately 640 kilometres (km) by road from the seaport of Douala, and 400 km from the capital city of Yaoundé. The Project includes greenfields development of an open-cut mine, process plant and associated infrastructure at the Nkamouna site, and is under evaluation by Geovic Cameroon PLC (GeoCam).

Nickeliferous laterite deposits in southeast Cameroon were first discovered and investigated by the United Nations Development Programme (UNDP) during 1981 to 1986, in a cooperative venture with the Cameroon Ministry of Mines, Water and Energy. Following a regional stream sediment geochemical survey, which indicated the likely presence of laterite nickel mineralisation, eleven core holes were drilled in the Nkamouna area, which was the most accessible laterite area at that time.

In 1999 GeoCam were awarded an Exploration Permit covering 4,876 km^2 and by 2004, GeoCam had largely completed the reconnaissance sampling and had undertaken pitting and drilling programmes of varying densities at Nkamouna to define deposit parameters for a preliminary feasibility study. In 2006, GeoCam completed a programme adding five new test pits and deepening other test pits, adding over 730 m of additional sampling in preparation for the final feasibility study. During 2008 and 2009, GeoCam conducted significant infill and step out drilling and pitting in the Nkamouna, Mada and Rapodjombo areas, including an additional 975 drill holes at Nkamouna, 1,012 drill holes at Mada and 248 reverse circulation holes at Rapodjombo. These new data form the basis for the Mineral Resource estimates and subsequent Mineral Reserve estimate at Nkamouna and Mada.

The metallurgical evaluation centred on the selected process route and the objective was to establish the design parameters on which to engineer the process plant. This was achieved by first conducting a number of small scale batch experiments for each of the unit processes. The results of the batch experiments were then used to establish the operating parameters for the subsequent continuous pilot plant testwork programme. The pilot plant programme was conducted at Hazen Research, Denver, in mid 2010 over four separate campaigns and yielded comprehensive information with respect to metal recoveries, product purities, reagent consumptions, and impurity deportment. The testwork programme and associated metallurgical evaluation provided all of the required data on which to develop a detailed mass and energy balance and to subsequently design a commercial processing facility.

The Nkamouna metallurgical processing facility comprises two, essentially independent, processing circuits. Run of Mine (ROM) ore is processed in the physical upgrade (PUG) plant to produce a high grade concentrate. The concentrate is subsequently processed in the leach and recovery circuit to recover the value metal products. The objective of the PUG plant is to separate the coarse, high value material from the fine gangue material in the ROM ore. Separation of the coarse product results in a significant increase in the concentrations of the value metals (cobalt, nickel and manganese), and a significant reduction in the mass of material (concentrate) that requires subsequent processing in the leach and recovery circuit.

The primary objective of the leach and recovery circuit is to dissolve the value metals from the concentrate and then recover the liberated cobalt and nickel as a mixed sulphide product and the manganese as a manganese carbonate by-product. Secondary objectives include maximum utilisation of reagents (especially of sulphuric acid in the leach) and rejection of impurity metals, to the maximum extent possible, from the value metal products and the environmental discharge streams. A block flow diagram of the Nkamouna processing plant is shown in Figure 1.

This paper describes the hydrometallurgy behind the atmospheric sulphuric acid leaching process for the asbolinic concentrate using pyrite as the reductant. A previous flowsheet developed by Geovic had been based on a two-stage counter-current leach approach, using sulphur dioxide (or sulphurous acid) as the reductant and, in part, lixiviant, along with sulphuric acid. In late 2008, Geovic elected to pursue an alternate approach, using pyrite as the reductant, which was seen as having several advantages over the sulphur dioxide route. This included the ability to achieve the required leach results in a single stage of leaching, ease of handling the reducing reagent, the elimination of dithionate formation in the leach liquors, improve occupational health and safety conditions, etc.

Although the concept of using pyrite as a reductant in the dissolution of manganese from pyrolusite (MnO_2) ores is lesser known than the use of other, more commonly cited reductants, there has been

a limited number of studies described in the past two decades. These are provided in the list of references, and provided moderate guidance in the present studies. The application of pyrite as a reductant for asbolinic materials, with different sets and relative concentrations of impurities, especially aluminium, as well as the pursuit of more valuable metals than manganese for recovery, appears to be novel, and required a dedicated approach to define the chemistry specifically applicable to the Nkamouna concentrates.
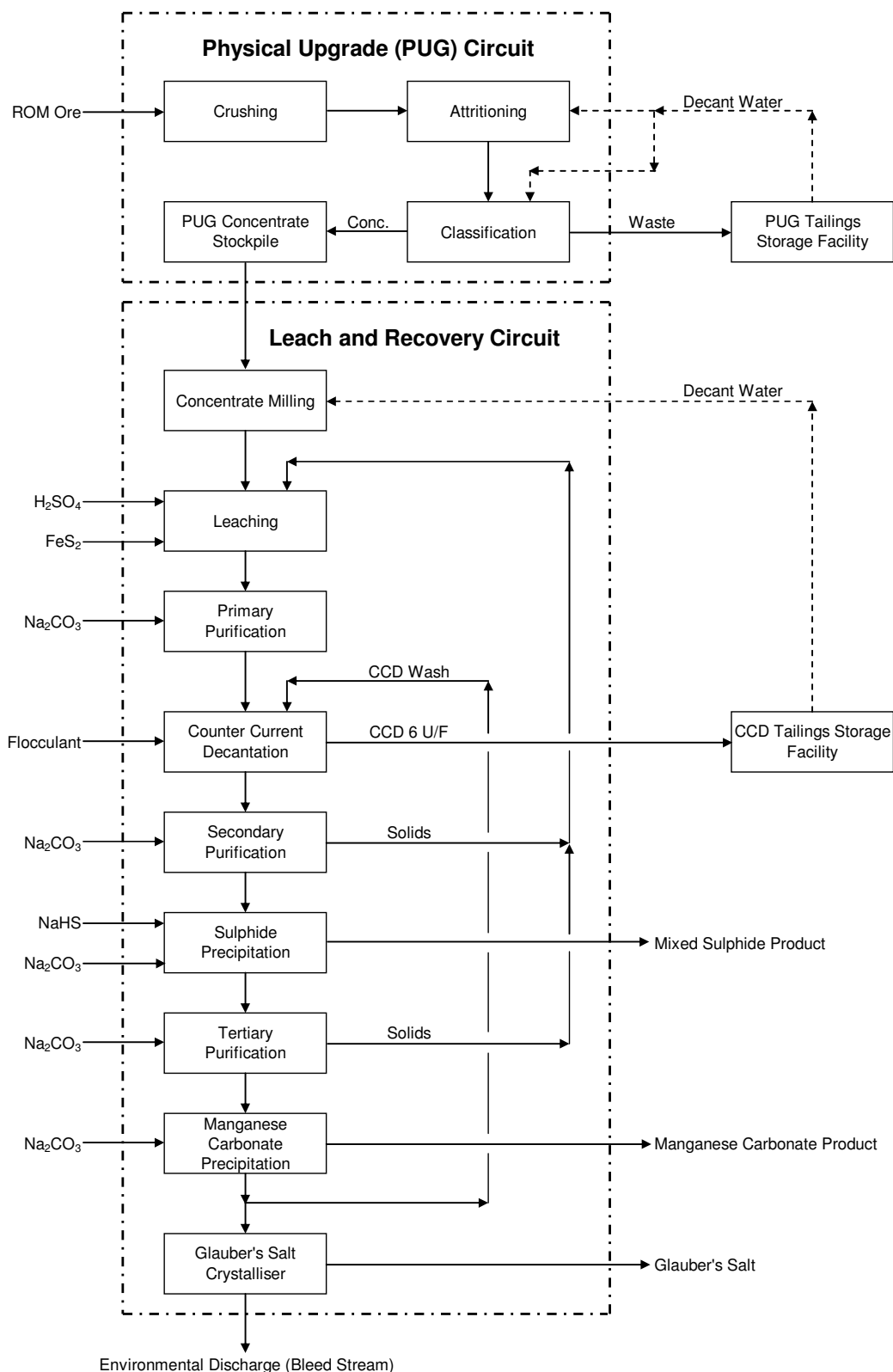
Figure 1: Simplified Block Flow Diagram of Nkamouna Flowsheet

CONCENTRATE CHARACTERISTICS

A single bulk PUG concentrate composite sample, representative of the first eight years of Project operation was prepared by Hazen Research to be used for the Technical Advisory Panel (TAP) batch leach tests and the functional component of the pilot plant continuous testwork programme. The TAP, assembled by Geovic and GeoCam, comprised John Marsden, Roman Berezowsky and Joe Ferron.

The blended composite was split into two sub-samples which were separately milled for the subsequent batch and continuous testwork. The chemical composition of these two samples is presented in Table 1. Sample 1 was used primarily in the batch testwork, and for the preliminary stages of the pilot plant studies. Sample 2 was also used in batch leach testwork, but was the primary concentrate processed in the continuous pilot plant campaigns.

Table 1: Summary Analysis of Concentrate Composite Samples

Sample	Co, %	Ni, %	Mn, %	Fe, %	Al, %	Cu, %	Zn, %
1	0.862	0.883	4.41	35.4	8.34	0.035	0.050
2	1.10	0.957	5.78	32.4	9.11	0.049	0.054

The variability of the head analyses reflects the known 'nugget' effect which can occur with the relatively coarse and high grade asbolane minerals. Appropriate particle size reduction and blending procedures are required to ensure this 'nugget' effect is eliminated.

The PUG concentrate samples were milled to a nominal size P_{80} of 106 µm in a laboratory ball mill. Bond Ball Mill Work Index testwork indicated a range of 11.2 to 13.3 kWh/t for the PUG concentrate based on a closing screen size of 106 µm.

A single composite sample of pyrite was used for the batch leaching testwork. The analysis of this sample is presented in Table 2. The pyrite sample was obtained from Inmet Mining Corporation, a potential supplier of pyrite to the commercial plant, and is produced by flotation.

Table 2: Average Analysis of Composite Pyrite Sample

Fe %	S %	Al %	Cu %	Zn %	Cr %
45.5	52.0	0.457	0.018	0.008	0.045

The mineralogical analysis conducted on the PUG concentrate is summarised in Table 3.

Table 3: PUG Concentrate Mineralogy

Specie	% w/w
Quartz	1.3
Kaolinite (clay)	0.4
Clay-FeOx/Hydrox	11.3
Fe-Hydroxide	34.9
Hematite	6.2
Magnetite (Cr)	18.4
Gibbsite	3.3
Mn(Ni/Co/Fe/K)	0.9
Mn-Al(NiCoFe)	22.5
Others	0.8

Essentially all of the cobalt, most of the manganese, and up to half of the nickel were found to be contained in the asbolane-like mineral. The occurrence of cobalt, nickel and manganese are distributed in three major mineral hosts namely, Asbolane, Cr-Magnetite, and Goethite as indicated in Table 4. Oxidation states of the cobalt and manganese in the concentrate are assumed to be +3 and +4 respectively, while nickel is in the +2 oxidation state.
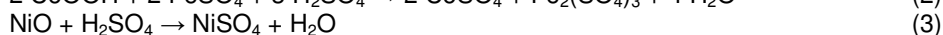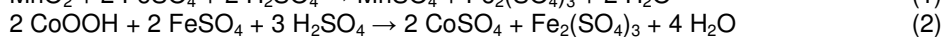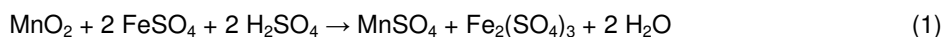
Table 4: Distribution of Co, Ni and Mn

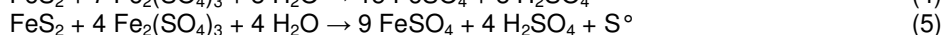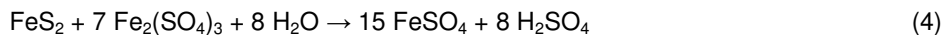| Mineral	Co (% w/w)	Ni (% w/w)	Mn (% w/w)
Asbolane	100.0	42.3	81.8
Cr-Magnetite	0.0	1.3	2.0
Goethite	0.0	56.4	16.2

CONCENTRATE LEACHING – BASIC CHEMISTRY

The objective of the concentrate leach is to dissolve cobalt, nickel and manganese from the PUG concentrate. PUG concentrate leaching was carried out at 95ºC under atmospheric pressure with sulphuric acid. Ferrous iron was the reductant, and the source of the ferrous iron, as will be described below, was pyrite.

The reductive dissolution of cobalt and manganese, and the dissolution of nickel from the asbolane mineral with ferrous iron in sulphuric acid can be represented by the following individual reaction equations:

$$MnO_2 + 2\ FeSO_4 + 2\ H_2SO_4 \rightarrow MnSO_4 + Fe_2(SO_4)_3 + 2\ H_2O \quad\quad (1)$$
$$2\ CoOOH + 2\ FeSO_4 + 3\ H_2SO_4 \rightarrow 2\ CoSO_4 + Fe_2(SO_4)_3 + 4\ H_2O \quad\quad (2)$$
$$NiO + H_2SO_4 \rightarrow NiSO_4 + H_2O \quad\quad (3)$$

The ferric iron produced in the reactions (1) and (2) above subsequently reacts with pyrite to generate additional ferrous iron, as shown by equations (4) to (6), below:

$$FeS_2 + 7\ Fe_2(SO_4)_3 + 8\ H_2O \rightarrow 15\ FeSO_4 + 8\ H_2SO_4 \quad\quad (4)$$
$$FeS_2 + 4\ Fe_2(SO_4)_3 + 4\ H_2O \rightarrow 9\ FeSO_4 + 4\ H_2SO_4 + S° \quad\quad (5)$$
$$FeS_2 + 2\ Fe_2(SO_4)_3 \rightarrow 3\ FeSO_4 + 2\ S° \quad\quad (6)$$

The preferred reaction of the pyrite with ferric iron, from the standpoint of generating the most reductant, is obviously the one depicted by equation (4), showing complete oxidation of all of the sulphur to sulphate. The reaction of pyrite within the leaching process is complex, however, with the production of elemental sulphur (Reactions (5) and (6)) also a possibility. In fact, most of the technical literature dealing with the oxidative leaching of pyrite by ferric iron in a sulphate medium indicates significant yields of elemental sulphur, up to ~ 40%, under some conditions.

Mineralogical and chemical analyses of the products in the current studies, however, have indicated that although minor quantities of elemental sulphur had been observed, these were only in isolated cases, under atypical conditions. The major oxidation product of the pyrite, under the design conditions of low steady-state ferric iron and low acid concentrations and a high oxidation potential, was sulphate sulphur, indicating the overall reaction as depicted by equation (4) to be the predominant one. This does not preclude the possibility that some elemental sulphur may have been initially formed, and had subsequently been further oxidized, but the net result was still the same.

The ferrous iron is then re-oxidised to ferric iron by the action of the Mn^{4+} and Co^{3+} (as oxidants) in the asbolane mineral as depicted in reactions 1 and 2.

The overall reaction of the MnO_2 and the CoOOH with the pyrite, through the ferrous iron intermediary, can thus be shown as follows:

$$15\ MnO_2 + 2\ FeS_2 + 14\ H_2SO_4 \rightarrow 15\ MnSO_4 + Fe_2(SO_4)_3 + 14\ H_2O \quad\quad (7)$$
$$30\ CoOOH + 2\ FeS_2 + 29\ H_2SO_4 \rightarrow 3\ CoSO_4 + Fe_2(SO_4)_3 + 44\ H_2O \quad\quad (8)$$
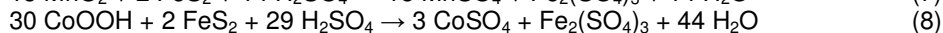
It can be seen that the complete oxidation of the sulphidic sulphur from each mole of pyrite generates sufficient sulphate for its Fe content as ferric sulphate, plus an additional one-half mole of H_2SO_4, hence contributing acid to the overall leach reactions. Additional acid is also produced from the subsequent hydrolysis of the ferric sulphate and precipitation of iron during the leach.

One interesting and important feature of the Nkamouna concentrates is that although they contain appreciable amounts of aluminium as gibbsite, only a small portion of that aluminium does, in fact,
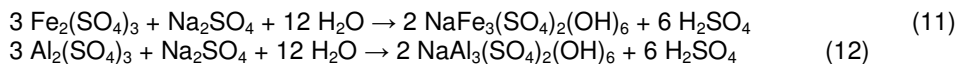
react under the design conditions. Some of the aluminium present in other forms does, however, dissolve, consuming appreciable acid, as shown in equation (9) below.

$$Al_2O_3 + 3\ H_2SO_4 \rightarrow Al_2(SO_4)_3 + 3\ H_2O \tag{9}$$

Unlike almost all typical nickeliferous laterites, only a very minor portion of the iron in the concentrate dissolves under the acidic atmospheric conditions. Its dissolution may be represented by equation (10)

$$Fe_2O_3 + 3\ H_2SO_4 \rightarrow Fe_2(SO_4)_3 + 3\ H_2O \tag{10}$$
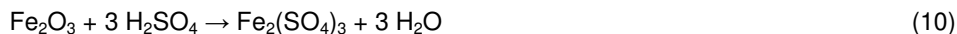
As the leach proceeds and the free acid is consumed, the iron and aluminium concentrations in solution begin to decrease as these ions are precipitated from solution, as a combination of hydronium and sodium jarosite ($NaFe_3(SO_4)_2(OH)_6$) and alunite ($NaAl_3(SO_4)_2(OH)_6$) respectively.

$$3\ Fe_2(SO_4)_3 + Na_2SO_4 + 12\ H_2O \rightarrow 2\ NaFe_3(SO_4)_2(OH)_6 + 6\ H_2SO_4 \tag{11}$$
$$3\ Al_2(SO_4)_3 + Na_2SO_4 + 12\ H_2O \rightarrow 2\ NaAl_3(SO_4)_2(OH)_6 + 6\ H_2SO_4 \tag{12}$$

It is noted that not only do these reactions remove the major impurities from the leach solutions, but they also release acid for the leaching of the value metals.

The major parameters in the reductive acid dissolution of the Nkamouna PUG concentrates with pyrite as the reductant can be listed as follows:

- **Leach Temperature**

  Adequate leach temperature is necessary to effect:

  - o oxidative leaching of the pyrite by the ferric iron to generate ferrous iron
  - o reductive acid leaching of the asbolane mineral by the ferrous iron and acid
  - o hydrolysis and precipitation of excess ferric iron
  - o hydrolysis and precipitation of the dissolved aluminium.

- **Sulphuric Acid**

  Sufficient sulphuric acid is required to solubilise the cobalt, nickel and manganese. As a consequence some impurity elements are also solubilised. A slight excess is required to maintain an adequate pH for effecting the leach, i.e. maintaining sufficient ferric iron in solution to promote the generation of the ferrous iron from the pyrite, but at the same time limiting the dissolution of iron and aluminium and other gangue components from the concentrate.

- **Pyrite**

  Adequate pyrite (mass and surface area) is required for the reductive leach to be successful. An excess of finely ground pyrite over the stoichiometric requirement suggested by equation (4) has been shown to be required. The amount added has generally been between 2 and 2.5 times the stoichiometric amount, and has been guided, to some extent, by a diagnostic leach procedure designed to test the reactivity of the pyrite. The concentrate leach testwork had shown that this requirement could be reduced by finer grinding of the pyrite, and/or the provision of additional acid to the leach, to provide for a higher ferric iron concentration in solution for reaction with the pyrite. This, however, would have been at the expense of additional grinding costs, and the cost of both additional acid for the leach and of soda ash for the subsequent removal of the additional iron and aluminium remaining in the leach solution.

- **Sodium Sulphate**

  As a consequence of the use of sulphuric acid in the leach circuit and of soda ash and sodium hydrosulphide as neutralising and precipitation reagents in downstream processes, extensive sodium sulphate production occurs. Sodium sulphate will build up in the process water circuit as a result of the requirement to have a closed circuit water balance. The sodium sulphate concentration in the process water will be controlled at acceptable levels by removing sodium sulphate in the Glauber's salt crystalliser.

Initial batch leach testwork had been conducted in a sodium sulphate-free medium. The use of fresh water and/or the complete removal of the sodium sulphate from the process water was deemed to be impractical and prohibitively expensive. Consequently a decision was taken to develop the leach parameters and metal recoveries in a sodium sulphate matrix. Unless otherwise stated, only the test results pertaining to leaching in sodium sulphate solutions are presented as the proposed commercial process will be carried out in sodium sulphate solutions.

CONCENTRATE LEACHING – BATCH TESTWORK

A laboratory batch testwork programme was initiated to determine the process parameters to be used in the subsequent pilot plant campaigns. During this testwork programme pyrite addition, sulphuric acid addition, concentrate particle size, leach retention time, and sodium sulphate concentration were varied.

Pyrite Addition

The effect of pyrite addition in the batch bench scale leaches is depicted in Figure 2. Under the conditions of these tests, additions of 40 and 50 kg per tonne of concentrate enabled extraction of 93% cobalt within 8 hours, whereas limiting the addition to 30 kg/t resulted in significantly lower cobalt extraction. The pyrite addition for the pilot plant was set at 40 kg pyrite per tonne of concentrate.
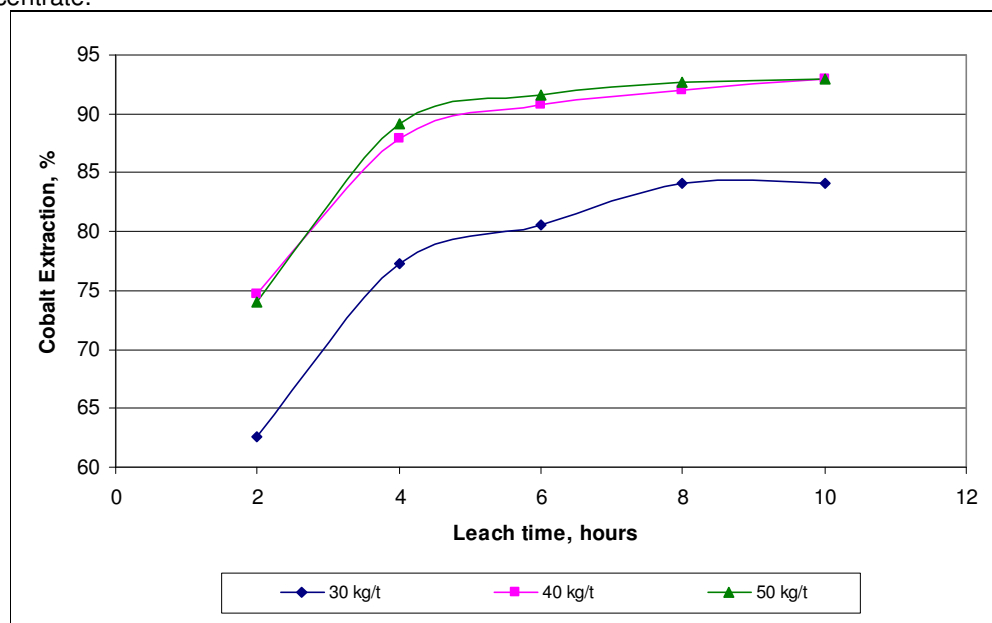
Figure 2: Effect of Pyrite Addition

Not all of the pyrite reacts in the leach reactions. Mineralogical and chemical analysis has indicated some remaining pyrite in the leach residues. In a commercial facility, this will report to the tailings storage facility (TSF) with the underflow slurry from the final counter current decantation (CCD) stage.

The effect of pyrite grind size on cobalt extraction is presented in Figure 3. The finely ground pyrite enabled extraction of about 95% of the cobalt within 6 hours. Coarse pyrite had a detrimental effect on the leach kinetics in that the extraction of cobalt was markedly slower when coarse pyrite was used. In view of the fact that the leach tests were of only 6 hours duration and, in the case of the coarse pyrite, had been terminated before the ultimate extractions had been reached, it is unclear whether the same high extractions could ultimately have been achieved with the coarse pyrite.
All of the test results presented in Figure 3 were obtained from preliminary development tests conducted without addition of sodium sulphate, at varying acid additions and temperatures between 80°C and 90°C. Consistent addition of pyrite at 50 kg/tonne was common for all tests.
Notwithstanding the variations in testwork parameters, a pyrite P_{80} of 16 µm resulted in acceptable cobalt extraction and this formed the basis of pyrite size for essentially all of the subsequent leach tests.
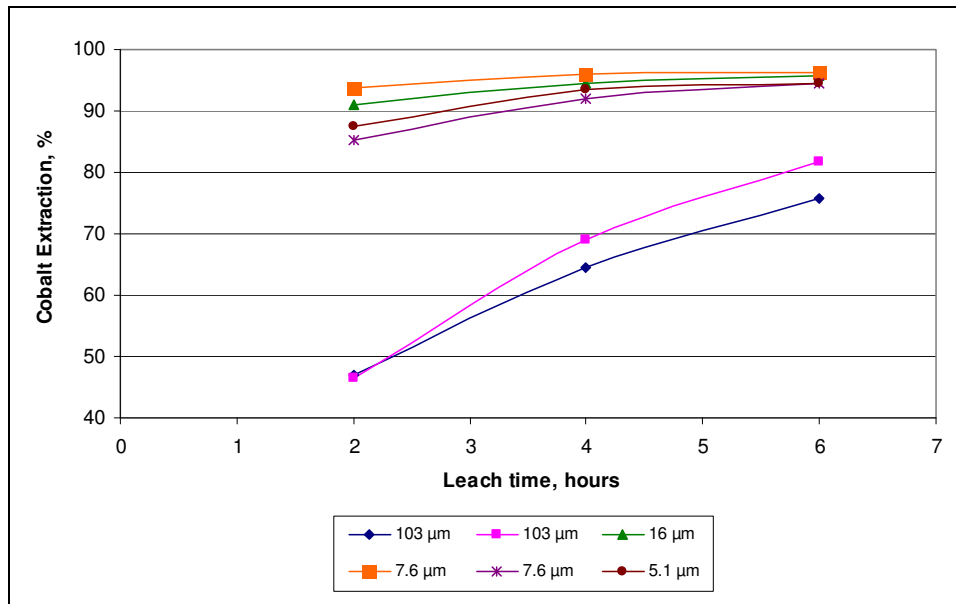
Figure 3: Effect of Pyrite Grind (P$_{80}$) Size on Cobalt Extraction
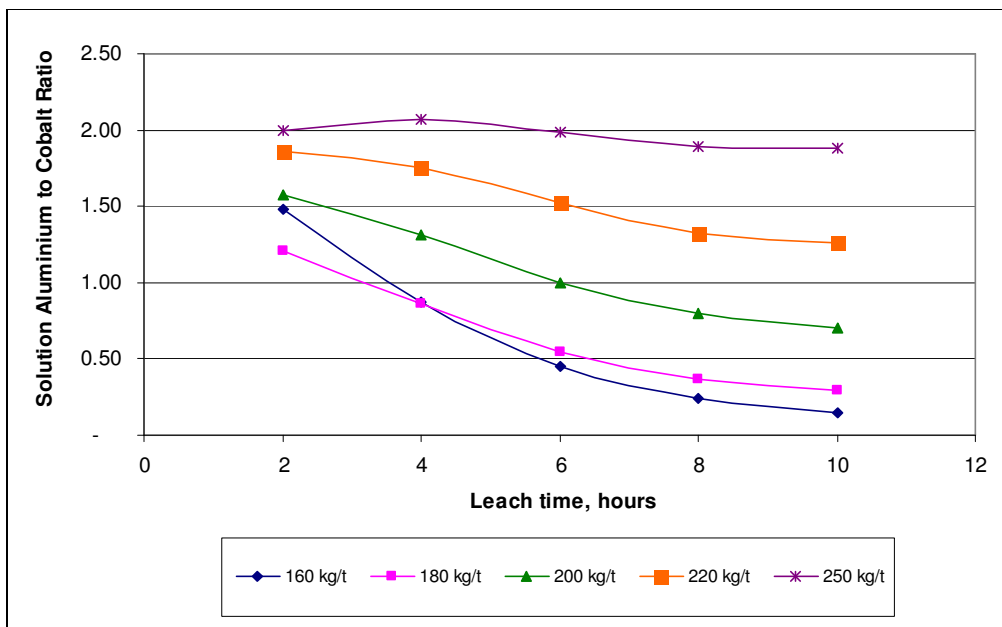
Sulphuric Acid Addition

The effect of sulphuric acid addition on the leach response is depicted in Figure 4. An increase in sulphuric acid addition resulted in increased cobalt extraction. All of the results presented in Figure 4 were obtained from tests conducted at 95°C with 50 kg/t of finely ground pyrite (P$_{80}$ = 9.2 μm) and with 175 kg/t of sodium sulphate addition, to simulate the use of recycled barren sodium sulphate-containing solutions in the process. The relatively high salt dosage used in this test series, however, was prior to the decision of incorporating a Glauber's salt plant for controlling sodium sulphate build-up.
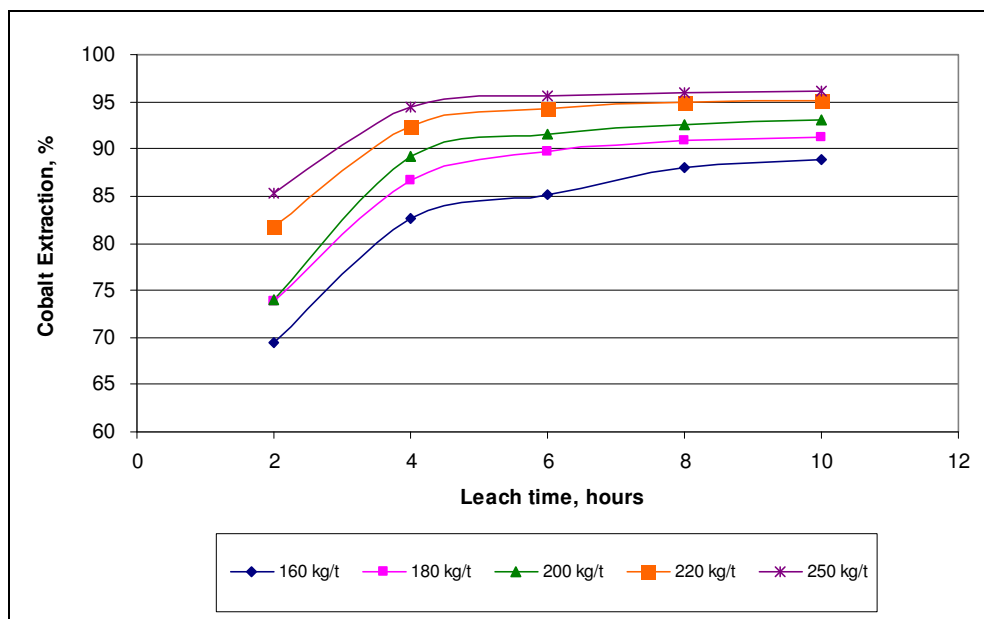
Figure 4: Effect of Sulphuric Acid Addition on Cobalt Extraction

The aluminium to cobalt concentration weight ratios in the leach solutions for representative batch bench scale tests are presented in Figure 5. The decrease in the ratio with increasing retention time, for the range of acid additions, of 160 to 250 kg/t assessed, is a consequence of increasing cobalt concentration and decreasing aluminium concentration. A decreasing aluminium concentration, however, was generally the dominant variable. This relationship is the basis for the

extended leaching time of 14 hours selected for the pilot plant testwork programme, as aluminium is an impurity that needs to be removed from solution prior to recovery of the pay metals. The aluminium concentration is minimised during leaching and its complete removal is achieved in the subsequent primary and secondary purification circuits by addition of soda ash.

Figure 5: Effect of Sulphuric Acid Addition on the Aluminium to Cobalt Ratio

Also evident from Figure 5 is the effect of sulphuric acid addition on the aluminium to cobalt concentration ratios of the leach solutions. For each of the specified retention times, the ratio generally increases with increased acid dose (detailed in the legend). The aluminium concentration in the leach solutions is essentially an equilibrium relationship with residual sulphuric acid concentration. This relationship is a contributing factor to the selection of acid dose for the pilot plant testwork programme.

Figure 6 depicts the relationship between aluminium concentration in solution and the corresponding cobalt extraction after 10 hours of leaching at 95°C and variable acid addition as indicated. Both the cobalt extraction and aluminium concentration are significantly affected by acid dose. The tests summarised in Figure 6 incorporate a pyrite addition of 50 kg/t and sodium sulphate additions of 33 and 175 kg/t. Sulphuric acid addition was varied from 160 kg/t to 250 kg/t. As the acid dose is increased, the extent of cobalt extraction and the solution aluminium concentration increased. Thus, for a leach product liquor containing about 12 g/L cobalt, the aluminium in the solution could be precipitated from the range of about 15 to 18 g/L, to as low as about 1 g/L at the lowest acid addition during the leach itself, albeit with some loss of cobalt extraction. The design conditions were, therefore, a compromise between high value metals extraction and desired degree of impurity precipitation during the leach. This relationship was further evaluated in the pilot plant testwork programme.
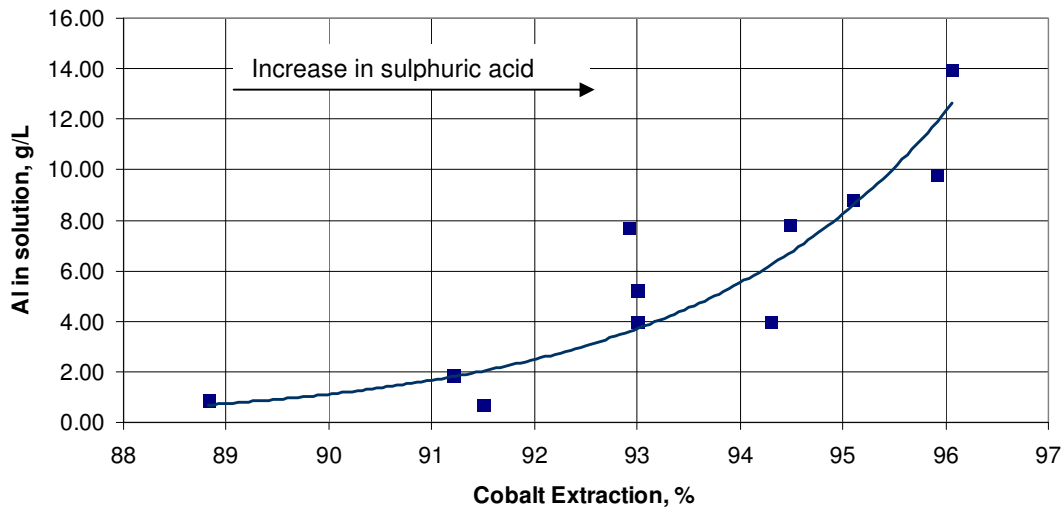
Figure 6: Aluminium in Solution vs Cobalt Extraction

Ferric iron in solution (in excess of the requirements for participating in the reaction with pyrite) behaves in a similar manner to that of aluminium. The iron to cobalt concentration ratios of the leach solutions for representative batch bench scale tests are presented in Figure 7. The decrease in the ratio with increasing retention time for the highest two acid additions assessed is a consequence of increasing cobalt concentration and decreasing iron concentration. The decreasing iron concentration is generally the dominant variable.

The iron to cobalt concentration ratios of the three lowest acid addition tests are essentially constant over the duration of the leach tests. This response is a consequence of a relatively consistent cobalt solution concentration over the duration of the leach tests and extensive precipitation of iron from solution early in the leaching period. The iron concentration remains low and consistent for the duration of the leach tests as a consequence of a sufficiently high pH (nominally greater than 2.6) to promote the near complete precipitation of ferric ion from solution. Any iron present as ferrous will require oxidation to ferric prior to precipitation from solution.

Iron is an impurity that needs to be removed from solution prior to recovery of the pay metals. The iron concentration is minimised during leaching and its complete removal is achieved in the subsequent Primary and Secondary Purification circuits by addition of soda ash.
Also evident from Figure 7 is the effect of sulphuric acid addition on the iron to cobalt concentration ratios of the leach solutions. For each of the specified retention times, the ratio generally increases with increased acid dose. The iron concentration in the leach solutions is essentially an equilibrium relationship with residual sulphuric acid concentration. This relationship is a contributing factor to the selection of acid dose for the pilot plant testwork programme, although to a lesser extent than for aluminium. It is particularly noteworthy that even such a low concentration of ferric iron was sufficient to maintain the reaction with pyrite and continue the generation of ferrous iron.
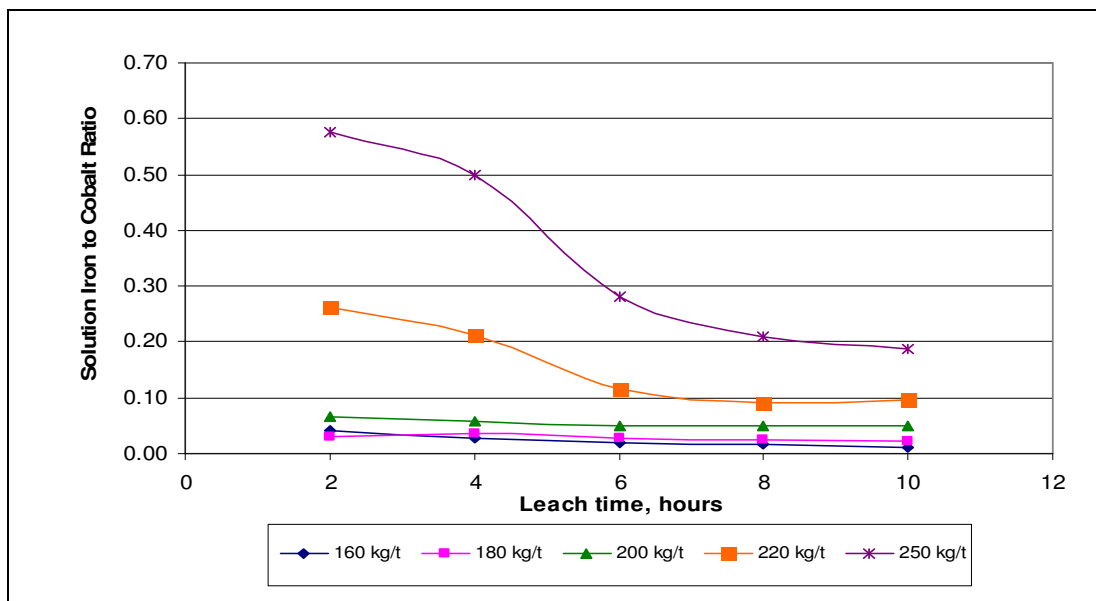
Figure 7: Effect of Sulphuric Acid Addition on the Iron to Cobalt Ratio in Leach Solution

Figure 8 depicts the relationship between iron concentration in solution and cobalt extraction after 10 hours of leaching at 95°C and variable acid addition as indicated. Both the cobalt extraction and iron concentration are significantly affected by acid dose. The tests summarised in Figure 8 incorporate a pyrite addition of 50 kg/t and sodium sulphate additions of 33 and 175 kg/t. Acid addition varied from 160 kg/t to 250 kg/t. As the acid dose is increased, the extent of cobalt extraction and the solution iron concentration increases. Additionally, as the extent of cobalt extraction increases, the ratio of ferrous to ferric iron in solution increases. But, as noted above, effective utilisation of the pyrite and extraction of 95 to 96% of the cobalt was possible, while limiting the final iron concentration to < 1 g/L. This relationship was further evaluated in the pilot plant testwork programme.
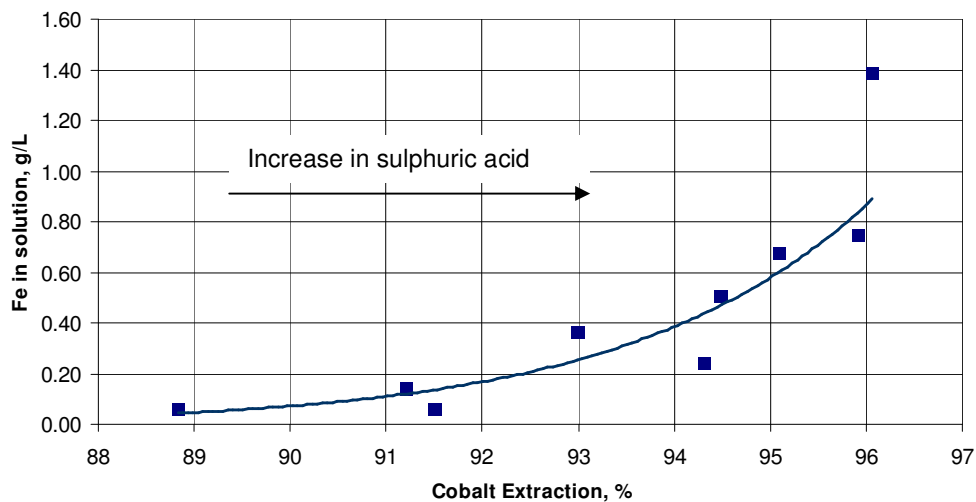
Figure 8: Iron in Solution vs Cobalt Extraction

From a review of leach test responses (value metal extractions and impurity metal concentrations) it is evident that a balance between the extent of value metal extraction and residual concentration of impurity metals in the pregnant leach solution will need to be achieved. Due to its relatively low molecular weight (27 g/mole) and its trivalent state, small increases in the residual concentration of aluminium in the pregnant leach solution result in significant increases in soda ash requirements to effect aluminium precipitation in the subsequent impurity removal process steps.

Concentrate Particle Size

The effect of concentrate grind size on the cobalt extraction is presented in Figure 9.
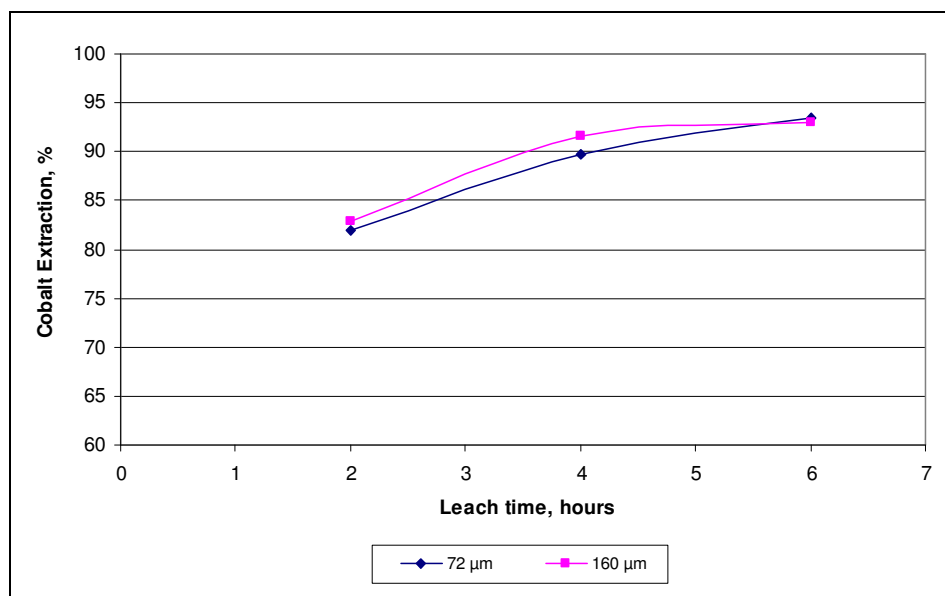
Figure 9: Effect of Concentrate Particle Size on Cobalt Extraction

Preliminary tests without sodium sulphate addition, conducted at 80 °C and with 240 kg/t H_2SO_4 and 50 kg/t pyrite addition, indicated that the extent of cobalt extraction did not appear to be affected by a concentrate P_{80} in the range of 72 to160 μm. A relatively fine concentrate P_{80} of 106 μm was used for the pilot plant operation to ensure that suspension of the high density particles could be maintained during the leaching process.

Preliminary batch tests also indicated that overgrinding (P_{80} of 48 μm) may contribute to increased gangue reactivity with a subsequent increase in sulphuric acid consumption. Overgrinding is undesirable in that it may also contribute to elevated slurry viscosities and, possibly, deteriorated solid-liquid separation characteristics.

Leaching Time

Initial batch leach tests were conducted for 6 hours, which was subsequently extended to 10 hours to promote the continued extraction of the value metals and, especially, the precipitation of aluminium and iron from the leach solutions.

The batch leach tests confirmed that, provided adequate sulphuric acid was added initially, iron and aluminium concentration in solution continued to decline after 10 hours without adversely affecting cobalt, nickel and manganese extractions. The decline in aluminium and iron concentration in solution is due to alunite and jarosite precipitation.

Retention time for the leaching circuit of the continuous pilot plant was subsequently extended to 14 hours to further increase the extent of solution iron and aluminium precipitation.

A leach temperature of 95ºC was used for the testwork to enhance the leaching kinetics of the pyrite and the reductive dissolution of the value metals, as well as to increase the extent of the aluminium and iron precipitation. Most of the energy requirement to reach the 95ºC is provided by the exothermic oxidation leach reactions.

Determination of Acid Requirements as a Function of Concentrate Composition

Based on the results of several dozen batch leach tests on the two concentrates used in the main study, a relationship was developed for defining the acid requirements for simultaneous high extraction of the cobalt, and effective rejection of iron and aluminium from solution during the leach. This relationship was further tested with five additional samples of concentrates later in the

programme, representing the initial five periods of operation, covering 24 years of operation. In total, the concentrates under study ranged in content from 0.53 to 1.05% Co, from 0.54 to 1.0% Ni, and from 2.87 to 5.47% Mn. The Mn:Co ratio varied from 5.1 to 6.6:1, whereas the aluminium content, and consequently the Al:Co ratio, varied even more widely and independently of the cobalt, from 6.2 to 11.4:1. In spite of these variations, the relationship established for estimating the acid requirements proved quite robust.

This relationship between the consumption of sulphuric acid for varying concentrate grades, representing the life of mine ore grades, is shown in Figure 10. The higher sulphuric acid consumption resulted in a cobalt extraction in the range of 95%, which is close to the maximum extractions achieved in other batch testwork (see Figure 4), while the lower sulphuric acid addition yielded reduced cobalt extraction. As the concentrate Co-Ni-Mn content increases, a linear increase in sulphuric acid addition is required to maintain a similar overall value metal extraction.
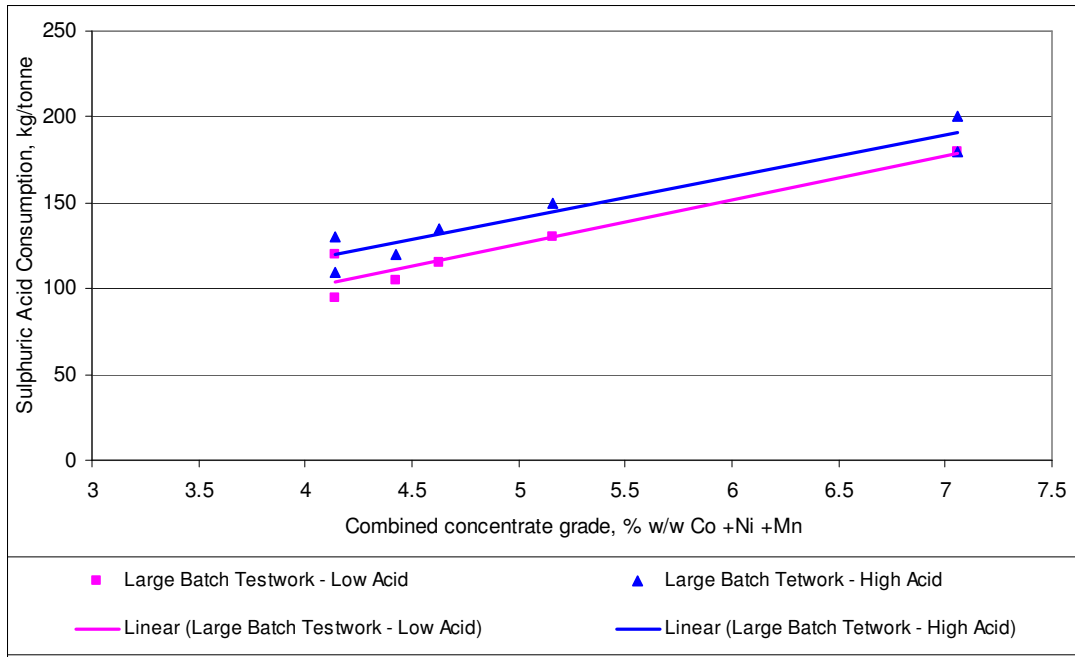
Figure 10: Sulphuric Acid Consumption vs Concentrate Grade

CONCENTRATE LEACHING – PILOT PLANT TESTWORK

The results of the laboratory batch testwork were used to define the operating parameters and conditions for the pilot plant campaigns. Table 5 summarises the pilot plant operating conditions derived from the batch testwork.

Table 5: Derived Testwork Parameters for the Pilot Plant

Parameter	Unit	Value
Sulphuric acid addition	kg/t concentrate	170
Pyrite addition	kg/t concentrate	40
Pyrite P_{80}	µm	Target = 10 to 15 Actual = 11.6
Temperature	℃	95
Concentrate P_{80}	µm	Target = 106 Actual = 101
Leach feed density	% solids w/w	55
Leach residence time	hours	14

The pilot plant leach circuit consisted of five 5 L and two 6.8 L working volume stainless steel agitated leach tanks in series which provided the nominal 14 hours leach residence time at a slurry feed rate of 2.8 L/h (2.4 kg/h solids at nominally 55% w/w solids). The leach circuit was commissioned and reached steady state in 86 hours.

Representative cobalt extraction profiles are presented in Figure 11. The profiles selected represent plant operation at H_2SO_4 addition rates of 180 to 195 kg/t and sodium concentrations in the feed slurry of 14 to 45 g/L (45 to 140 g/L sodium sulphate). Cobalt leaching was consistent with the batch leaching experiments, with close to maximum extractions being achieved after approximately 10 hours of retention time.
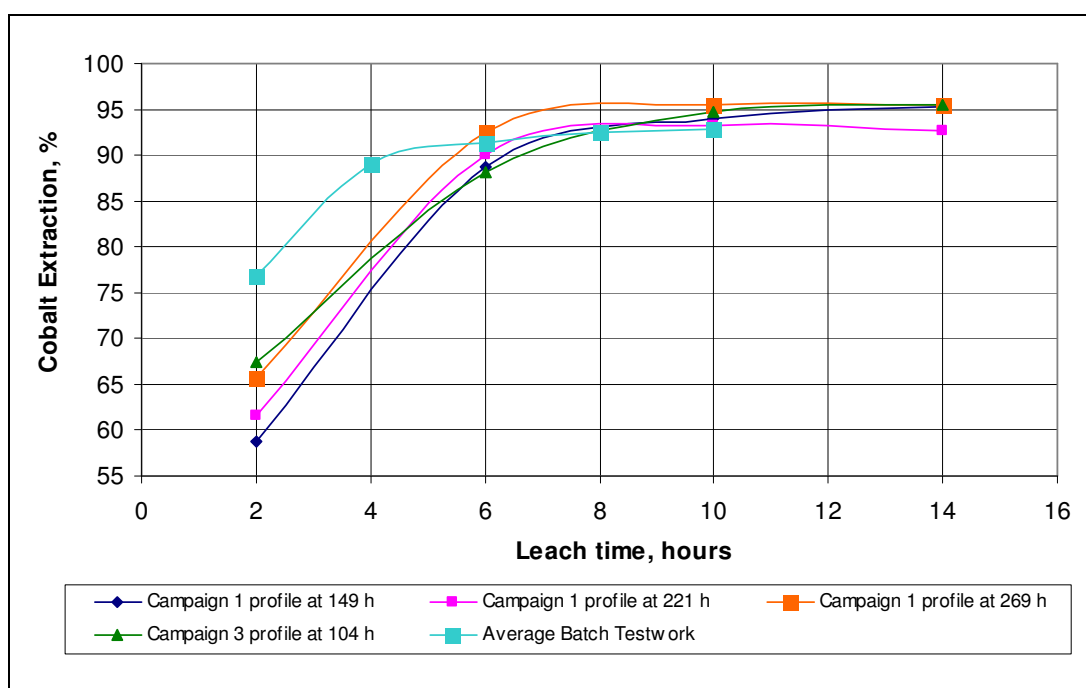
Figure 11: Cobalt Leach Profiles

Extraction of manganese followed a similar trend to that of cobalt whilst nickel extraction was lower, which was consistent with results from the batch leach tests. Typical cobalt, nickel and manganese extractions are shown in Figure 12.

364
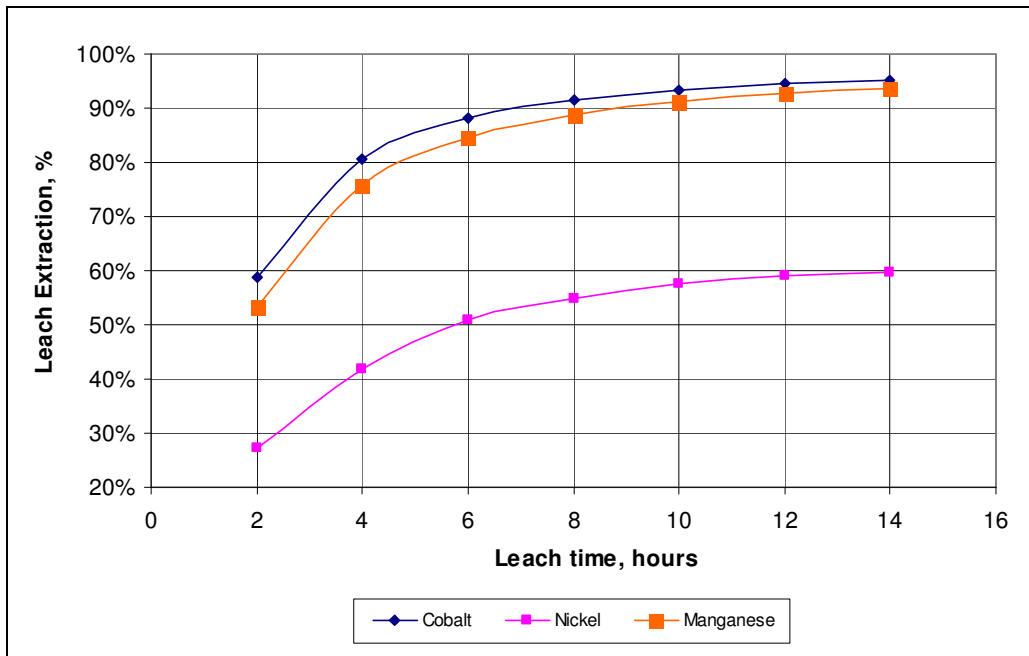
Figure 12: Typical Value Metal Leach Extractions

The effect of retention time on aluminium concentration in solution is shown in Figures 13 and 14. Aluminium concentration in solution reached a maximum after nominally 4 hours, represented by leach tank 2. After 4 hours there was a steady decline in aluminium solution concentration.

The results represent nominal H_2SO_4 addition rates between 168 and 195 kg/t. The highest aluminium concentration curve (Campaign 1 profile at 261 hours) coincides with the highest acid addition rate of 195 kg/t. The lowest aluminium concentration curves (Campaign 3 profiles at 152 and 167 hours) coincide with the lowest acid addition rate of 168 kg/t. The variation in residual aluminium concentrations provides an insight into what may be reasonably expected during commercial plant operations. The trend for iron in solution is similar to that of aluminium. Iron behaved as expected based on results from the batch bench scale experiments.
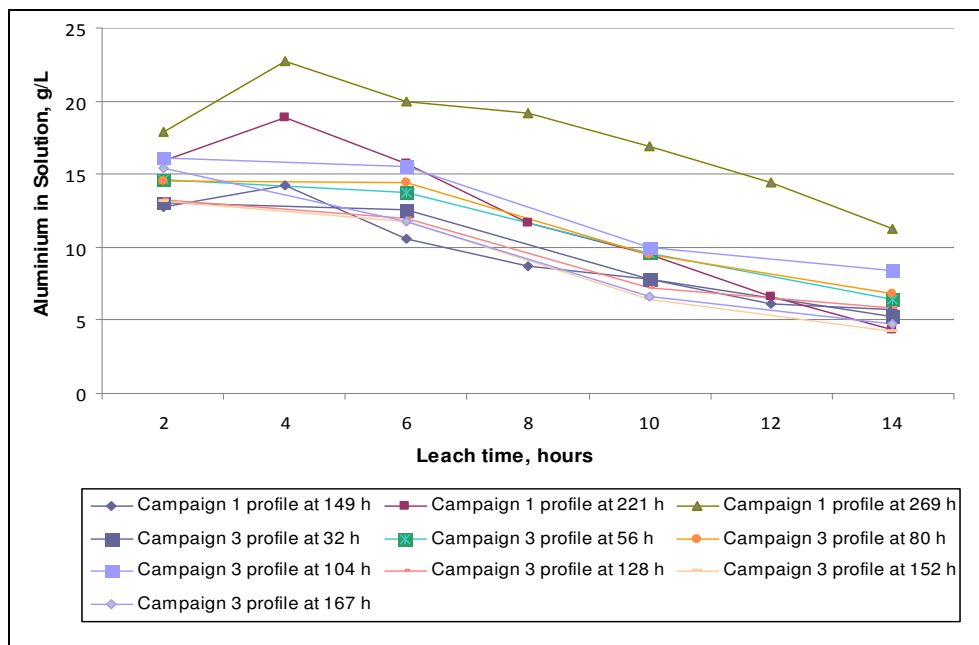
Figure 13: Aluminium in Solution as a Function of Leach Time

365

Figure 13 clearly indicates that extensive dissolution of aluminium occurs in the early phases of the leach, followed by the hydrolysis and precipitation of aluminium (as alunite) after the initial dissolution.
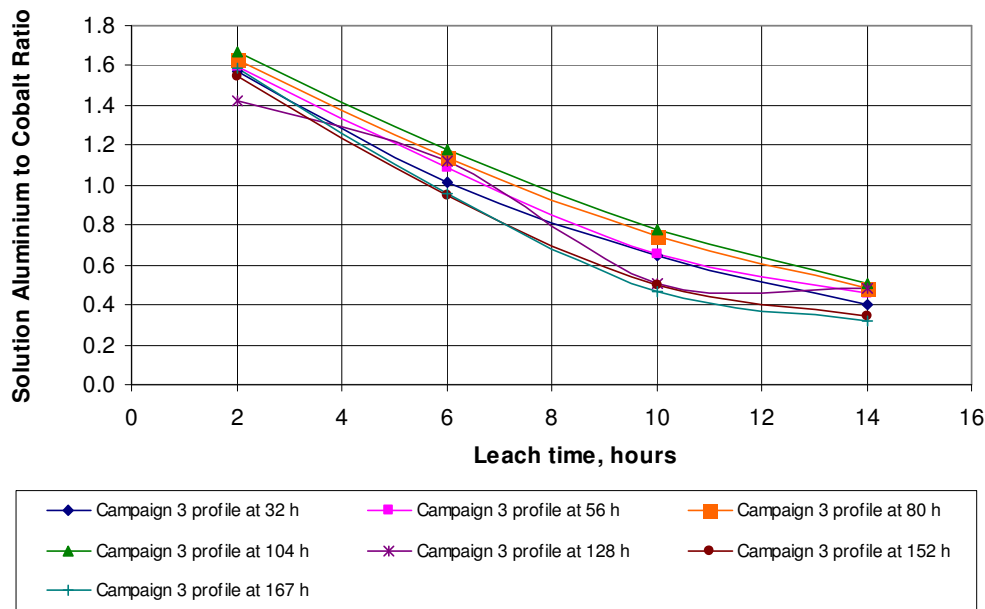
Figure 14: Soluble Aluminium to Cobalt Ratio as a Function of Leach Time

The extent of aluminium precipitation relative to cobalt concentration in solution is detailed in Figure 14 and shows that the extended leaching time is required to minimise aluminium concentration relative to cobalt concentration in the leach discharge solution. The estimated concentrate mass loss during pilot plant leaching operations was between 8 and 12%.

The neutralisation requirements for the purification processes are significantly reduced by controlling the leach conditions to achieve a relatively low terminal free acid concentration in the leach discharge and by promoting extensive precipitation of the iron and aluminium during the leach. As a result soda ash can be used as a viable preferred alternative to lime or limestone. The use of a calcium based neutralization agent would be detrimental to the manganese carbonate product quality. This is significant as the reagents are imported and transported by road from the port city of Douala for 640 km to the Nkamouna site.

Mineralogical Analysis

Mineralogical analyses were conducted on the solids obtained from leach tank 1, leach tank 7 and from the primary purification discharge stream. Averaged results are tabulated in Table 6.

Table 6: Summary of Mineralogical Analysis

	First Leach Tank	Final Leach Tank	Primary Purification Discharge
Quartz	0.9	1.4	0.9
Kaolinite (clay)	1.2	1.6	1.0
Clay-FeOx/Hydrox	11.1	2.6	2.2
Fe-oxides	49.2	36.3	38.5
Magnetite (Cr)	11.6	12.0	15.8
Cr-spinel	2.8	2.9	4.3
Gibbsite	4.0	3.4	1.8
Gibbsite-FeHydrox		0.7	0.5
Mn-oxy-hydroxide	8.8	0.2	0.1
Ti-minerals	0.2	0.2	0.1

366

	First Leach Tank	Final Leach Tank	Primary Purification Discharge
Pyrite	2.0	2.0	2.2
Clay-FeOx-pyrite intergrowth	7.4		
Jarosite and Alunite analogues		33.3	30.4
Others	1.0	3.6	6.6

The mineralogy indicates the following:

- A portion of the iron oxide reacts during leaching.
- The asbolane (Mn-Oxy-hydroxide) reacts extensively in the leach.
- A portion of the pyrite remains unreacted during leaching.
- Jarosite and alunite species form during the leaching and primary purification stages, particularly the leach.

In addition to the mineralogical analyses, multi-element chemical analyses were also conducted on a range of solution and solids samples from the pilot testwork campaigns. The chemical analysis of the leach residues showed the sodium-to-sulphate molar ratio to be in a fairly consistent range of 0.33 to 0.39 : 1, suggesting a hydronium : sodium jarosite ratio of 1 : 2.

Typical compositions of the leach, primary purification, and secondary purification discharge liquors are summarised in Table 7. The apparent reduction in concentration of the pay metals in the primary purification step is due to dilution by reagent addition. Similarly, the reduction in pay metal concentration in secondary purification is a result of both reagent addition and dilution by CCD wash solution. It is evident, therefore, that the majority of soluble iron and aluminium removal occurs in the primary purification stage, with a further reduction in secondary purification.

Table 7: Typical Liquor Analysis

Element	Leach Discharge, g/L	Primary Purification Discharge, g/L	Secondary Purification Discharge, g/L
Cobalt	12.2	10.6	5.8
Nickel	6.7	5.8	3.2
Manganese	64.4	56.9	31.1
Aluminium	5.7	0.2	0.1
Iron	0.4	0.04	0.02
Sodium Sulphate	9.5	39.9	60.8

Cobalt and nickel are ultimately recovered as a high purity mixed sulphide product using sodium hydrosulphide in a series of reactors – a typical composition is shown in Table 8.

Subsequent to the mixed sulphide precipitation circuit, manganese is precipitated as manganese carbonate in a series of agitated tanks using sodium carbonate – a typical manganese carbonate product composition is shown in Table 9.

A detailed discussion of the mixed sulphide and manganese precipitation circuits will be presented in a future publication.

Table 8: Mixed Sulphide Product Analysis

Constituent	Concentration, %w/w
Cobalt	39.6
Nickel	24.0
Sulphur	36.4
Manganese	0.12
Iron	0.35
Aluminium	0.01
Copper	0.18
Zinc	0.84

367

Table 9: Manganese Carbonate Product Analysis

Constituent	Concentration, %w/w
Manganese	48.5
Calcium	0.14
Magnesium	0.04
Sodium	1.1
Sulphur	0.36

CONCLUSIONS

The successful bench scale batch testwork, followed by extensive continuous pilot plant campaigns provided the basis for the development of the Nkamouna Cobalt-Nickel-Manganese Project leach process. The hydrometallurgy provides a unique opportunity to remove contaminants, such as aluminium and iron, during the leach by controlling the leach conditions. As a result, the consumption of reagents in the downstream processing is reduced.

The key process design parameters were derived from the testwork results and more specifically from the pilot plant campaigns. The key process design parameters are summarised in Table 10.

Table 10: Key Process Design Parameters Derived From Leaching Testwork

Parameter	Unit	Value
Sulphuric acid addition	kg/t concentrate	182
Pyrite addition	kg/t concentrate	40
Pyrite size – P_{80}	μm	<15
Temperature	ºC	95
Concentrate size – P_{80}	μm	106
Leach density	% solids	50
Leach residence time	hours	14

ACKNOWLEDGEMENTS

REFERENCES

1. Schippers, A., and B.B. Jorgensen, "Oxidation of Pyrite and Iron Sulfide by Manganese Dioxide in Marine Sediments", Geochimica and Cosmochimica Acta, Volume 65, No.6, pp. 915-922, 2001

2. Nayak, B.B., K.G.Mishra and R.K.Paramguru, "Kinetics and Mechanism of MnO_2 Dissolution in H_2SO_4 in the Presence of Pyrite", Journal of Applied Electrochemistry, Volume 29, No.2, pp. 191-200, 1999

3. Parida K.M. et al, "Kinetics and Mechanism of the Reductive Leaching of Manganese Ores by Iron Pyrites in Mild Acidic Solutions", Proceedings of EPD Congress '90, edited by D.R.Gaskell, The Minerals, Metals & Materials Society, 1990, pp 217-227

4. Nayak B.B., et al, "Reductive Leaching of Manganese Containing Material with Pyrite in a Mild Sulphuric Acid Medium", AusIMM Proceedings (Australia), Volume 300, No.1, pp. 79-84, Nov. 1995 (abstract only)

5. Qin, W.S., "Leaching of Pyrolusite-Pyrite in Sulfuric Acid Media", Mining and Metallurgical Engineering (China), Volume 13, No.4, pp. 52-56. Dec. 1993 (abstract only)

6. King, W.E. Jr. and J.A. Lewis, "Simultaneous Effects of Oxygen and Ferric Iron on Pyrite Oxidation in an Aqueous Slurry", Industrial & Engineering Chemistry Process Design and Development, 1980, 19, pp. 719-722

7. Bouffard, S.C., B.F. Rivera-Vasquez, and D.G.Dixon, "Leaching Kinetics and Stoichiometry of Pyrite Oxidation from a Pyrite-Marcasite Concentrate in Acid Ferric Sulfate Media", Hydrometallurgy, Volume 84 (2006), pp. 225-238

•   Lowson, R.T., "Aqueous Oxidation of Pyrite by Molecular Oxygen", Chemical Reviews, Volume 82, No.5, October 1982 (1982 American Society), pp. 461-497.

ALTA 2011
NICKEL/COBALT/COPPER

EQUIPMENT & MATERIALS

A – Z OF AUTOCLAVE ISOLATION

By

Pete Smith
MOGAS Industries, USA

Presenter and Corresponding Author

Pete Smith
psmith@mogas.com

ABSTRACT

This paper presents a review of practical issues along with a summary of trends encountered in autoclave isolation. This review is presented from the perspective of an equipment maintainer, equipment supplier and package engineer.

AUTOCLAVE ISOLATION

Autoclave Isolation covers the isolation of autoclaves used in pressure leaching. The main processes covered by the scope of this document include:

- Pressure Acid Leach of Ni Laterites – HPAL
    - 250 – 275 degrees Celsius
    - 40 – 50 bar
- Pressure Oxidation of Sulphide Ores – HP & MP-POx (Au, Cu, Ni, U, Zn, Mo)
    - 180 – 225 degrees Celsius
    - 20 – 30 bar

Autoclave Isolation of these processes involves isolating the following severe service conditions:

- High temperature
- High pressure
- Corrosive (Acidic, Hyper-Saline chlorides)
- Erosive (Abrasive)
- Heavy solids build-up (Precipitation of Scale)
- Viscous

BALL VALVE

Autoclave Isolation is achieved with the use of severe service, metal seated ball valves.

A ball valve can be considered simply as:

- A ball with a hole in it which floats between a pair of seats contained within a body & end connect
- The ball & seats are made of the same exotic material as the body & end
- Actuated via stem with quarter turn operation

A severe service, metal seated ball valve used for Autoclave Isolation should be considered as:

- A piece of complex machinery consisting of numerous moving parts operating in a challenging environment
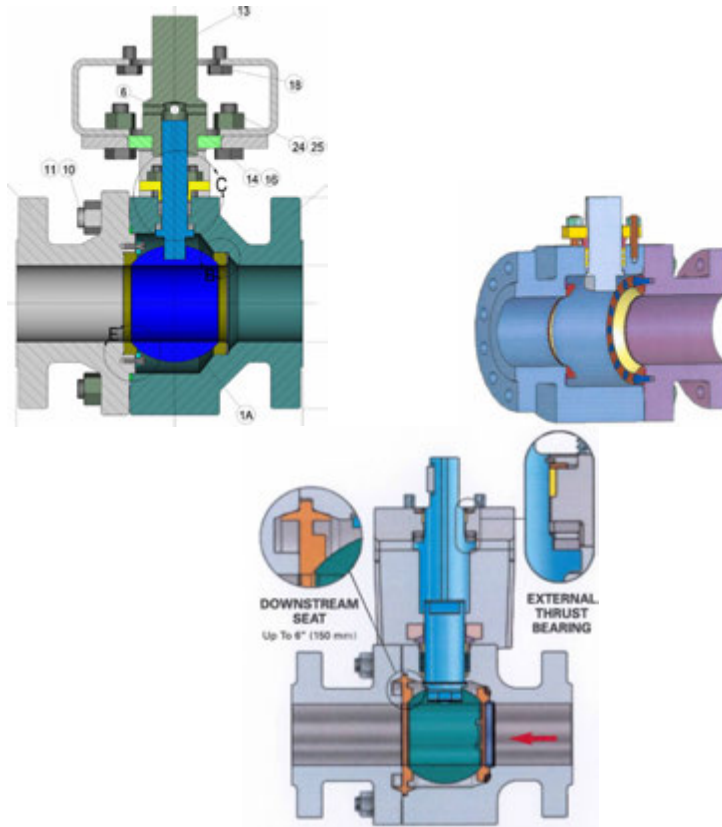
Bigger, Better

Autoclave Isolation valves are lasting longer and performing better. On the Western Australia Nickel Laterite projects built during the late nineties it wasn't uncommon for valves to last just several cycles, with valve lifetimes limited to weeks / months. Autoclave Isolation valves are no longer on the critical path for campaign life with lifetimes of 6 to 12 + months available for the most severe of services and with lifetimes of thousands of cycles for some services.

Autoclave Isolation ball valves have been tending to get bigger:

- up to 4 – 6 inches (DN100 – DN150) on the smaller claves
- up to 8 – 10 inches (DN200 – DN250)
- up to 12 – 14 inches (DN300 – DN300) on the current generation of claves in Start-up
- up to ...

Bi-directional

All Autoclave Isolation ball valves should be considered bi-directional. The primary role of autoclave isolation is to block, or box in, pressure within the autoclave, so allowing operations and maintenance personnel to pause plant operations and to attend to equipment and plant issues without shutting down and starting up from scratch. A secondary role of autoclave isolation is to

isolate the line pressure in the inlet, sparge and discharge lines. This line pressure is often higher than autoclave pressure prior to start-up.

Autoclave Isolation valves typically have a preferred pressure end which should be orientated towards the line pressure it is intended to isolate.

Cycles

Autoclave operations involve cycling or stroking the valves open and closed. A cycle is normally regarded as an open stroke and a close stroke (or vice versa). Ball valves should be cycled regularly to confirm operation, especially in order to break scale. Where cycling of a valve is not desirable due to its impact on production then partial stroking may be used where a fully open valve is stroked 10 to 15 degrees from its fully open position for a short duration (e.g., 5 to 10 seconds) at regular intervals (e.g., daily or weekly).

Cycle time (or stroke time) is typically selected using a rule of thumb of around one second per inch of bore.

For example:

- 6 seconds to stroke a 6 inch (DN150) valve open or closed
- 10 seconds to stroke a 10 inch (DN250) valve open or closed

Faster cycles times are available, with some recent client specifications including 3 seconds for 10 inch (DN250) valves, and 5 seconds for 14 inch (DN350) valves. Sometimes slower cycle times are acceptable where, for instance, electric actuators may be practical.

It is preferable to cycle smoothly throughout the stroke. The compressibility of air can lead to jerking of pneumatic actuated valves as they encounter areas of higher resistance. Use of hydraulic actuation can overcome this.

The total number of cycles accumulated on a particular valve can be used as a guide to valve performance, though high cycles can be also be a sign of plant problems leading to frequent starting and stopping of plant, especially during the earlier ramp-up stage.

Double Block & Bleed

Autoclave Isolation typically requires "Double Block & Bleed" isolation to safely isolate severe services. Double Block & Bleed consists of two valves closed with an intermediate bleed valve open to drain or vent. Valves are located as close to each other as normal piping practice allows. The bleed line is permanently directed to a safe location, with suitable procedures provided to verify that the bleed line is not plugged. A second bleed valve may be included as determined via the risk assessment process.

With the primary role of autoclave isolation to block or box in pressure within the autoclave, both double block valves should have their preferred pressure ends orientated towards the clave (Figure 1). Another school of thought is to orientate the inboard valve towards the clave, with the outboard valve orientated towards the (inlet, sparge or discharge) line (Figure 2).
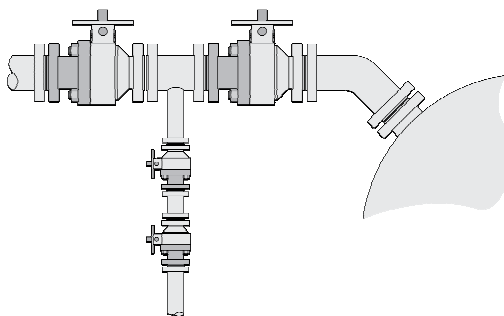

Figure 1: Double Block & Bleed
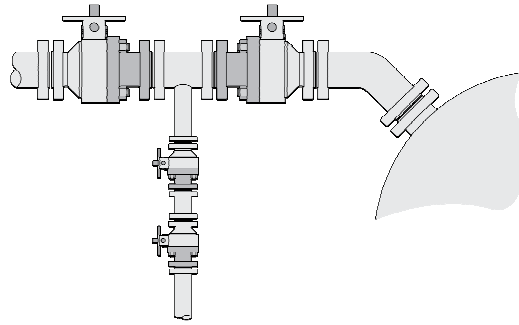
Figure 2: Double Block & Bleed (Alternative)

DISCHARGE LINE

The autoclave line that sees the most severe service is the Discharge Line which is used to discharge the hot, acidic slurry from the autoclave to the flash system. This is the stream of the clave at the highest temperature and pressure, along with abrasive, acidic slurry. The discharge line sequence needs to ensure a full line to prevent water / slurry hammer and to limit thermal stresses on downstream ceramics (e.g., Let-Down valve trim or flash tank brick work).

A variety of arrangements are available:

- Two valves mounted directly on clave (Figure 3A).
- Two valves mounted horizontally on clave deck (Figure 3B) provides maintenance access though relies on integrity of the piping elbow on the clave.
- One valve on clave, one valve at Level Control Valve (LCV) (Figure 3C) provides operational advantages in terms of filling the line during the discharge sequence.
- Dual Discharge Lines (Figure 3D) accommodate higher clave throughput while limiting discharge line size.
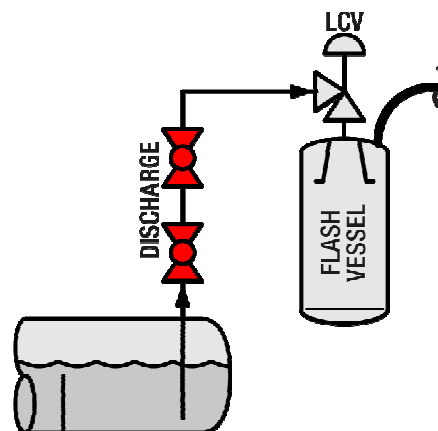
Figure 3A: Two valves on clave
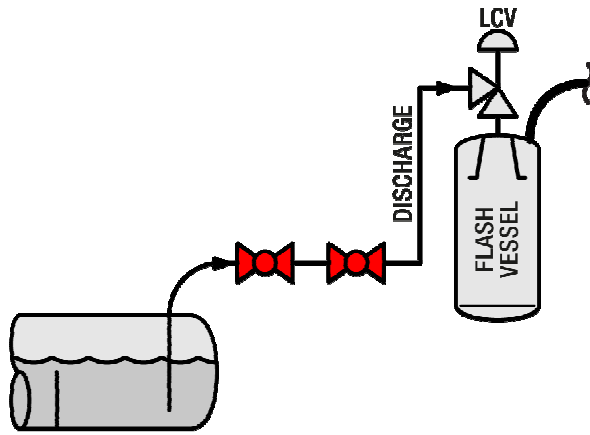
Figure 3B: Two valves on clave deck
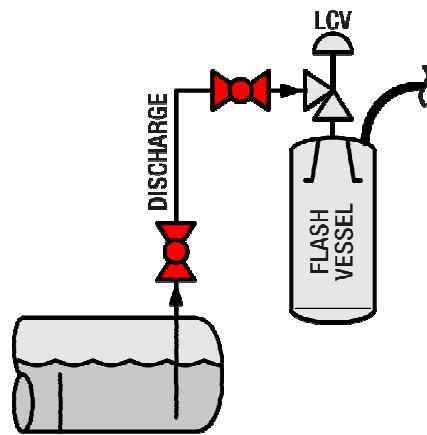
Figure 3C: One valve on clave, one at LCV
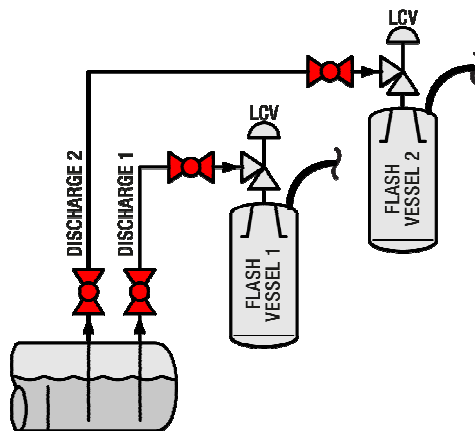
Figure 3D: Dual discharge lines

EXOTIC MATERIALS

The hot, acidic service in Pressure Leaching demands exotic materials of construction, typically super duplex stainless steel and titanium. The materials of construction of autoclave isolation valves are driven by the piping specifications, with the valve material generally following the line material.

The ignition risk of titanium in the presence of oxygen above a certain threshold pressure prevents the use of titanium in some POx services. There is application for Ti-Niobium (Ti-Nb) material in some oxygen services due to its higher threshold for handling oxygen, though super duplex is lower cost and more widely used.

Common super duplex stainless steels are listed in Table 1. Material selection may impact valve design, dependant on the tensile strength of the selected material. Ultimate Tensile Strength (UTS) of selected materials is listed in Table 2.

Table 1: Super Duplex Stainless Steel used in Pressure Leaching

Trade Name	Common Name	UNS	ASME Forging
Ferralium (Langley Alloys)	255	S32550	F61
SAF (Sandvik)	2507	S32750	F53
Zeron (Weir Materials)	100	S32760	F55

Table 2: Ultimate Tensile Strength

| Material	UTS (MPa)	UTS (psi)
A105	250	35,000
Ti Gr2	**345**	**50,000**
Ti Gr12	**480**	**70,000**
Ti-45Nb	**550**	**80,000**
316SS	580	85,000
Ti Gr28	**620**	**90,000**
F53 / F55	**750**	**110,000**
F61	**790**	**115,000**
Ti Gr5	**895**	**130,000**
17-4PH SS	1,000	145,000

Flush Ports

Flush ports can be specified on Autoclave Isolation valves to flush (or purge) solid or corrosive products from the valve and to prevent scale precipitation. Flush ports can be added to flush the valve body cavity, or to flush the seat area. Flushing typically involves piping and sequencing a flush stream to the area during stroking of the valve open or closed.
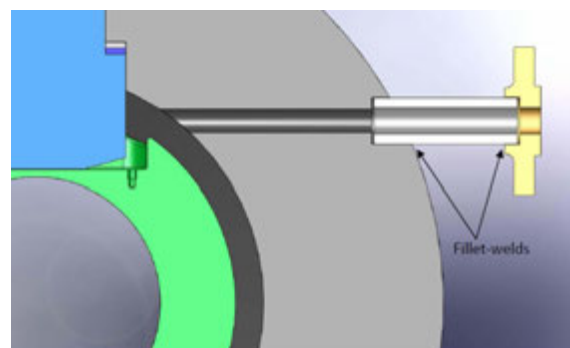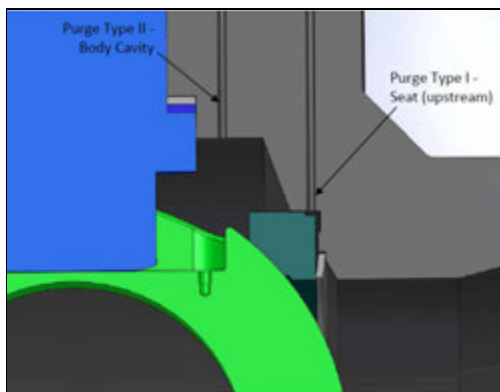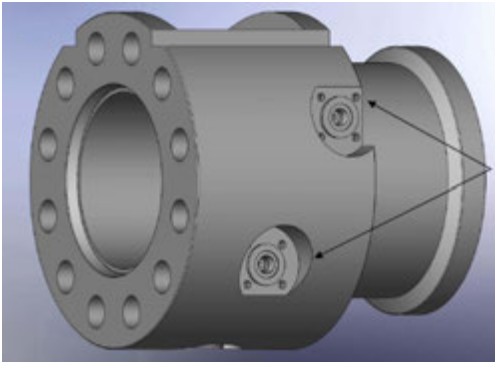
Gap

Autoclave Isolation with a metal seated ball valve relies on a seal between the ball and seat. The scraping motion of the sharp edge of the seat cleans the sealing surfaces as the ball cycles. Reverse pressure can shift the floating ball and seat away from the fixed seat, creating a gap between the ball and fixed seat. This gap can allow solids to enter, and then become trapped and compressed on the sealing surfaces once pressure returns to normal. Presence of solids can score these sealing surfaces during cycling.
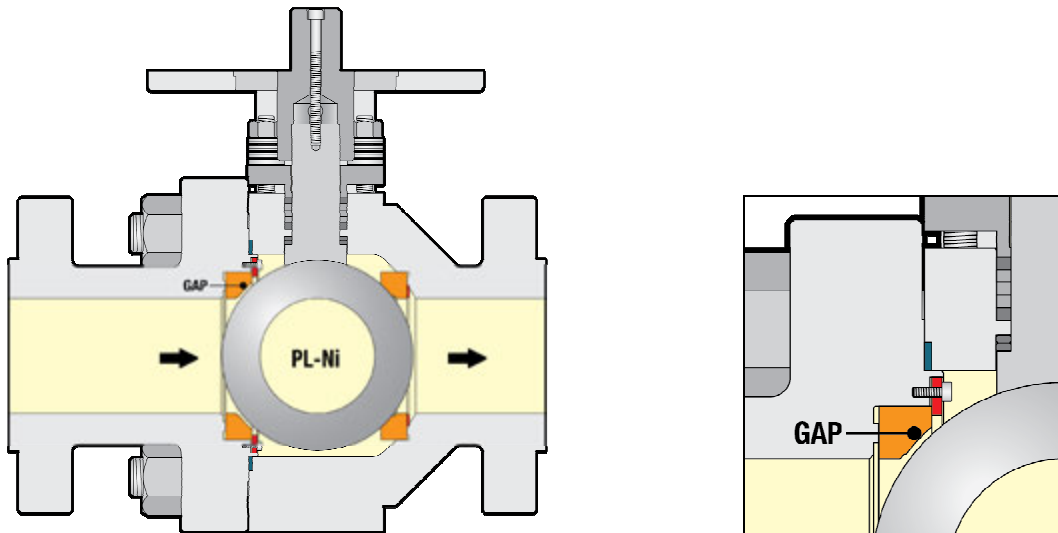
The map below shows the location of autoclave sites.

The historical development of Pressure Leaching plants is shown in the tables below.

Gold Autoclave Projects	Client	Year
McLaughlin	Homestake	1985
Sao Bento	Gold Fields	1986
Mercur	Barrick	1988
Getchell Gold	FirstMiss	1989
Goldstrike	Barrick	1990
Campbell Red Lake	Placer	1991
Porgera	Placer	1992
Nerco Con/Miramar	Nerco Minerals	1992
Lone Tree	Newmont	1994
Twin Creeks	FirstMiss	1997
Lihir	Rio Tinto	1997
Macraes	GRD	1999
Hillgrove	NEAM	1999
Kittila	Agnico-Eagle	2008
Amursk	Polymetals	2011?
Pueblo Viejo	Barrick	2011?
Lihir Expansion	Newcrest	2012?

Nickel Autoclave Projects	Client	Year
Moa Bay	Sherritt	1959
Cawse	Centaur	1999
Bulong	Barrick	1999
Murrin	Minara	1999
Coral Bay	Sumitomo	2005
Coral Bay 2	Sumitomo	2007
Ravensthorpe	BHPBilliton	2008
Goro	Vale	2010
Ambatovy	Sherritt	2011?
Ramu	MCC	2011?
Taganito	Sumitomo	2012?

Copper Autoclave Projects	Client	Year
Bagdad	Phelps Dodge	2004
Morenci	Phelps Dodge	2007
Sepon POXI	Oxiana	2005
Kansanshi	First Quantum	2007
Sossego(UHC)	Vale	2008
Sepon POXII	MMG	2009

Uranium Autoclave Projects	Client	Year
Dominion Reefs	UraniumOne	2007

HPAL

Autoclave Isolation valves in HPAL service.
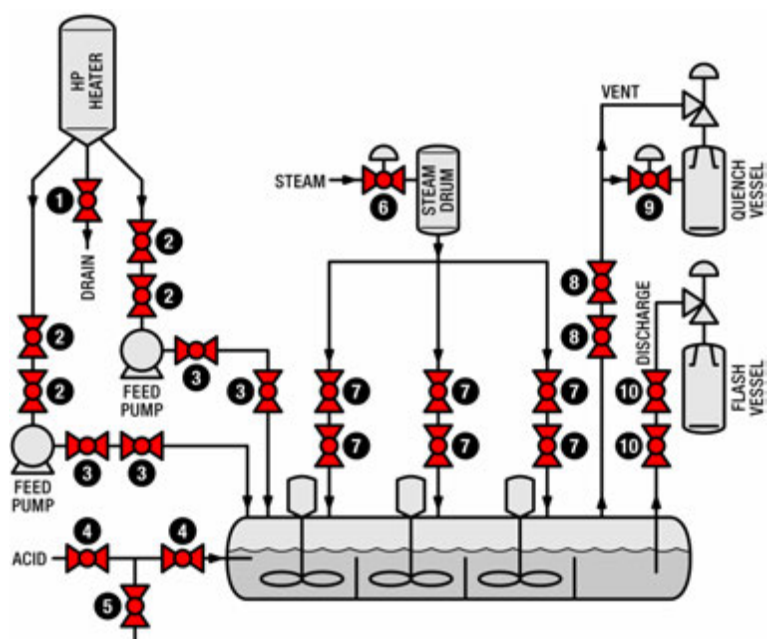
No.	Description
1	HP Heater Drain Valve
2	HP Heater Isolation Valve
3	Slurry Feed Pump Isolation Valve
4	Acid Valves
5	Acid Drain Valves
6	Steam Supply Control Valve
7	Steam Valves
8	Vent Valves
9	Rapid Decompression Valve
10	Discharge Valves

Inlet Line

The Inlet (or Feed) Autoclave Isolation valves isolate the slurry inlet line feeding from the Autoclave Feed Pumps.
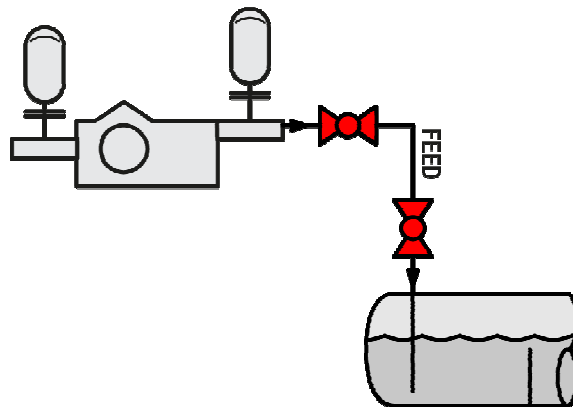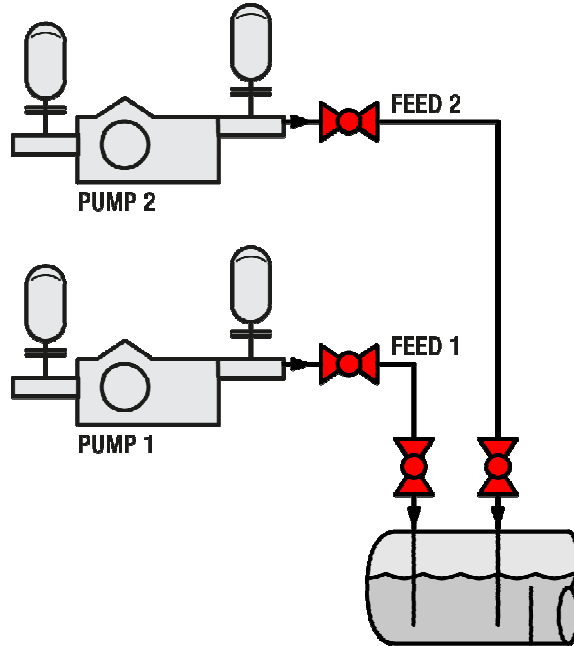

Figure 4A: Single AFP

Figure 4B: Dual AFP

Jetting

Autoclave Isolation valves will not last indefinitely. Once an Autoclave Isolation valve begins to pass following formation of a leak path then jetting will start to occur when this valve continues to be used for autoclave isolation. Jetting involves fluid under pressure shooting out in a high velocity stream. Jetting will result in erosion. Severe erosion can occur in less than a shift.

Kalrez

Kalrez is a perfluroelastomer – an elastomeric seal that performs in pressure leaching chemical environments while maintaining temperature stability up at relatively high temperatures. The supplier specifies continuous upper service temperatures of around 275 degrees Celsius. Elastomeric o-rings can be used to build valves with two tracking seats.
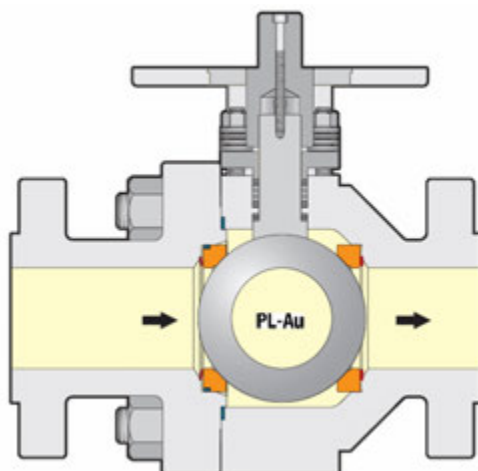
Tracking seats (with Kalrez o-ring)
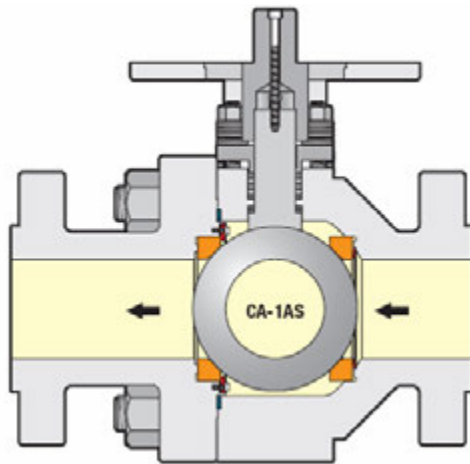
Locked-In seat

Locked In Seat

Metal Seated ball valves used for Autoclave Isolation use a floating ball, compared to trunnion mounted balls where the ball is fixed. The floating ball valve provides superior performance in slurry service. In addition the floating ball handles thermal expansion required in high temperature service.

The floating ball valve typically uses one fixed (or locked in) seat for primary sealing, and one floating seat for secondary sealing. The floating seat tracks the ball, utilizing line pressure plus a spring behind the seat.

Reverse pressure can create a gap between the ball and fixed seat allowing solids to become trapped and then crushed on the sealing surfaces once pressure returns to normal.

Elastomeric o-rings can be used to build valves with two tracking seats, replacing the fixed seat with a second floating seat, and thus, overcoming issues created by formation of this gap. Whereas metal seated floating ball valves are typically all metal construction the tracking seat design uses a Kalrez o-ring to achieve this functionality. This design is successfully used on a number of gold and copper autoclaves. It has not yet been used on the higher temperature nickel autoclaves.

Layout

Attention to layout during plant design can pay dividends in regards to providing superior access for equipment maintenance and operations. Failure of piping designers to pay due consideration to layout of "instrumentation" (including placement of 3 metre long spring return pneumatic actuators, for example) can block access ways and cause clashes with other equipment, vessels and structures.

Metal Seated, Mate Lapped

Ball Valves used for Autoclave Isolation need to be metal seated to handle the temperature, pressure, and acidity plus the corrosive and erosive nature of the slurry and other process streams used in pressure leaching.

The ball and seat surfaces are ceramically coated to prevent galling between the ball and seat and to provide a lappable surface to each. The ceramic coatings on the ball and seat are then mate lapped together to perfectly match the convex coated surface of the ball to the concave coated surface of each seat.

Nano TiO$_2$ Coating

A variety of ceramic coatings have been developed for the ball and seat coatings required for Autoclave Isolation in pressure leaching. Application of nano technology has led to significant improvements in coating performance.

POX

Oxygen Sparge

Oxygen is introduced into autoclaves for the Pressure Oxidation (POx) of Sulphide Ores via Oxygen Sparges. Other sparge streams in POx claves include steam and cooling/quench lines. Sparge streams in HPAL claves include acid and steam.

Every sparge service to the clave requires isolation with metal seated ball valves to block in clave pressure and to prevent slurry back flow into the sparge lines.

Autoclave Isolation valves in POX service.

No.	Description
1	Slurry Feed Pump Isolation Valve
2	Steam Supply Control Valve
3	Steam / Quench Valves
4	Oxygen Valves
5	Vent Valves
6	Rapid Decompression Valve
7	Discharge Valves
8	Quench Valves
9	Steam Valves
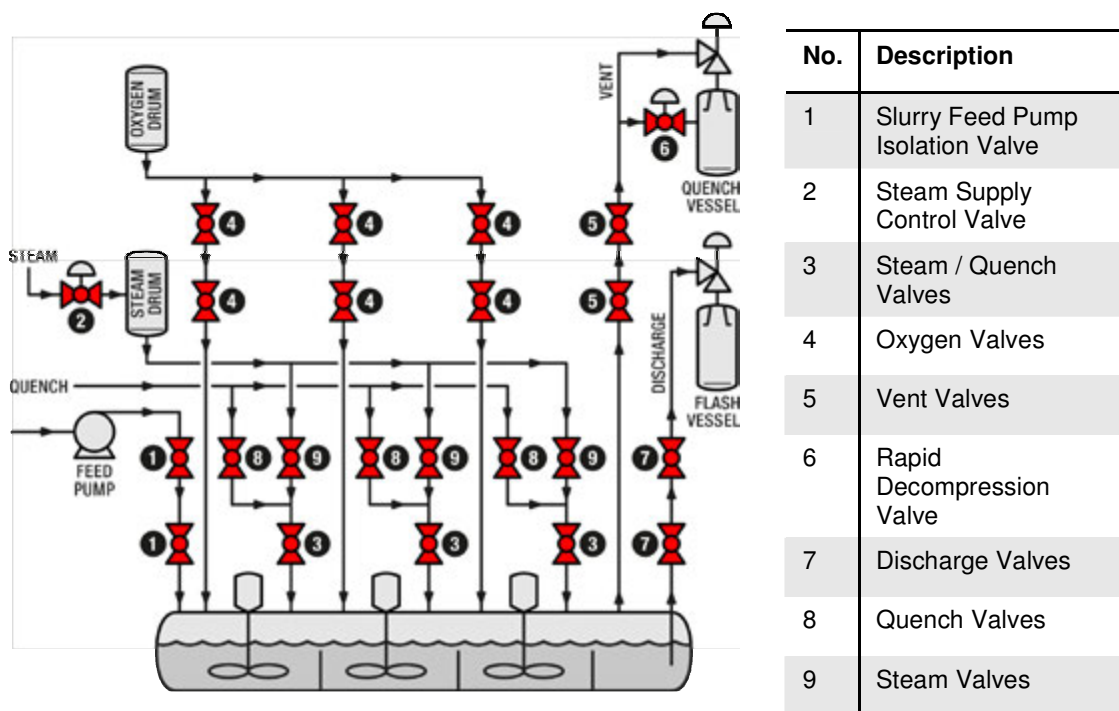
PLANNED MAINTENANCE, RATIONALIZATION AND SAFETY

The duration of autoclave campaigns, followed by planned maintenance shutdowns, are based on equipment inspection and maintenance intervals for the following equipment:

- PD Pumps
- Agitators and Seals
- Acid Injection
- Ceramic Control Valves
- Metal Seated Ball Valves
- Autoclave and pressure vessels
- Piping

Autoclave campaigns of 6, 8, 10, 12+ ... months are typical.

Quarter Turn Actuation

Ball valves turn through 90 degrees between their open and closed positions (i.e., quarter turn). Automatic actuation choices include pneumatic, electric, hydraulic and electraulic. Manual actuation choices include gear boxes with handwheels, where a mechanical advantage is required (typically above 2 inch / DN50 for metal seated ball valves), and hand levers for the smaller, lower torque valves.

The high torque requirements for Autoclave Isolation valves can lead to large pneumatic actuators, especially with fail safe, spring return actuators.
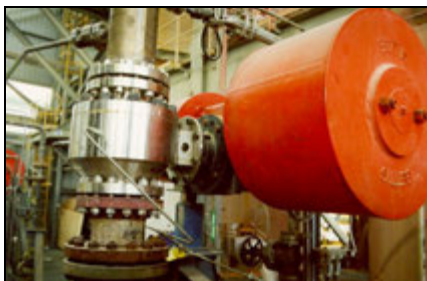
Improvements in layout can be achieved with the use of hydraulic actuation. Hydraulic actuation also provides benefits in available torque throughout the stroke, and with their inherent smoothness of operation.

Rapid Autoclave Blowdown

A Rapid Autoclave Blowdown Valve provides a controllable blowdown of the clave while limiting the rate of temperature drop to below 30 degrees Celsius per hour to protect the integrity of the brickwork.

Rationalisation

Pressure Leaching plants require a range of Autoclave Isolation valves in terms of size, pressure class and material. Economies of scale during manufacture, and reduction in spares holdings during operation, can be realised by considering opportunities to rationalise to common sizes, pressure class and / or materials.

Safety

The primary purpose of Autoclave Isolation is to block the clave in to provide a safe environment for operations and maintenance. As well as providing autoclave isolation, safe conditions of the valves relate to containment within the valve itself, including preventing leakage at the body joint and stem packing areas, and through the body.

Service Examples

Autoclave Isolation valves operating in the most severe of services will require regular servicing. Repair costs can be limited / optimised by repairing before the valves develop significant leaks. Valve repair normally involves just a clean and polish or lightly skim the machined surfaces of the valve. Sometimes leak paths will develop on the ball and seat and on the seat land. Rarely, these leak paths will lead to severe erosion. Damage caused by leak paths and erosion can be repaired by weld repair and re-machining to print.
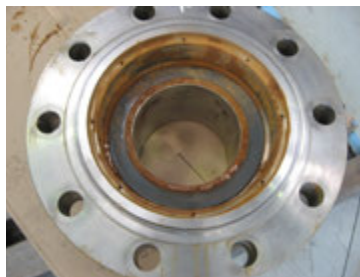
Clean & Skim only Land

Leak Path on Seat Land

Erosion on Seat Land

Trim Service Examples

In conjunction with repair of the valve body and end connect, the ball and seats will generally need attention. Sometimes trim from valves can just be "kiss-lapped" without recoating. Normally trim (balls and seats) will have some areas of coating loss, where the ball material can be re-used and recoated. Rarely, leak paths will lead to severe erosion which will require replacement with new trim.

Kiss Lap

Some coating loss

Erosion on ball

Trim Repair Cycle

Trim suitable for re-coating is cleaned of slurry and scale before the remaining coating is stripped to bare metal. The trim is recoated before lapping the seats to the ball. The stack height of the ball and seats is machined to size before flat lapping the back of the seats.

Clean & Strip

Spray

Uncontrolled Rapid Decompression

The primary purpose of Autoclave Isolation is to block the clave in to prevent needing a full and time consuming blow down and cool down of the clave to attend to maintenance and operations interruptions. Uncontrolled Rapid Decompression is at the extreme case of losing Autoclave Isolation. Though rare, this situation is typically caused by loss of pipe integrity.

Vent

The Vent line on an autoclave is used to regulate the pressure within the autoclave by venting acidic vapor from the claves vapor space into the blast spool on a quench vessel. Autoclave Isolation valves on the vent line block in the clave and isolate the pressure control valve. Emergency vent isolation valves may be used to drop pressure in the clave quicker than the pressure control valve is sized for.

Use of a Rapid Blowdown Valve using FlexStream® Technology in place of a straight Emergency Vent Isolation valve provides a controllable blowdown of the clave while limiting the rate of temperature drop to below 30 degrees Celsius per hour to protect the integrity of the brickwork. The patented FlexStream® Technology sizes the trim mounted within the bore of this ball valve to operate across the complete flow rate and ΔP range during blow down.
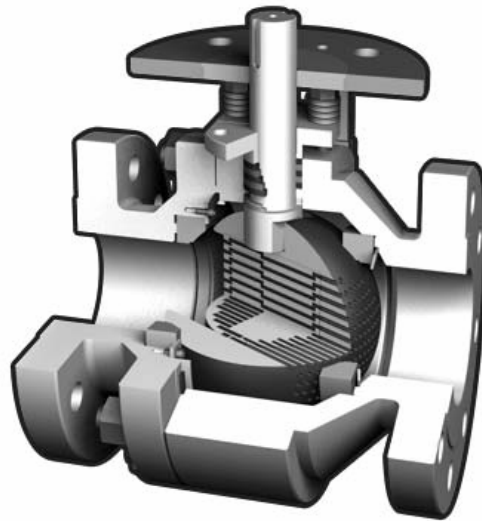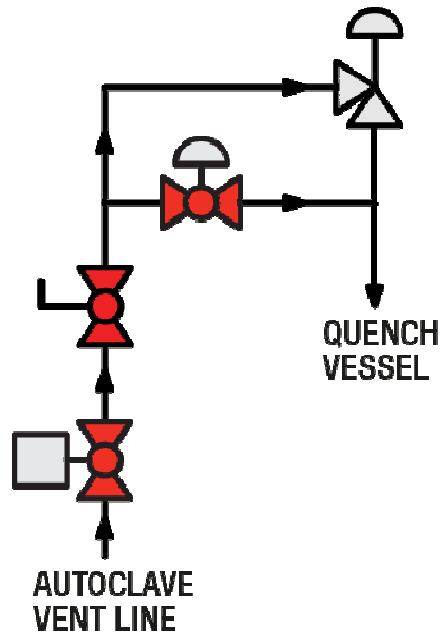
Valve Repair Cycle

The Valve Repair Cycle consists of stripping and inspecting each valve, cleaning and machining components where required, and reassembling the valve with spare trim kit before hydro testing of the valve to confirm the integrity of the valve and sealing of the seats. Spare trim kits are normally kept in stock to enable repair of valve in quick time.

Disassembly

Strip & Inspect

Machine

Weld Repair

Erosion damage can be repaired using weld repair, followed by re-machining to print.

Weld Repaired seat land

Machine

Xylan

It is not practical to use exotic materials for every item on an Autoclave Isolation valve. For example, body bolting typically uses stainless steel for its higher strength with a thermal expansion coefficient that matches the exotic valve body material. Xylan coating products are useful in providing surface protection for these non-exotic materials.

Xylan coated bolting

Zero Leakage

Metal seated ball valves used in Autoclave Isolation rely on 100 percent mate-lapping of (ball to seat) sealing areas and low sealing stresses to endure the harsh service application demands to extend valve lifecycles and provide long-term isolation. High seal stress can be created by minimising seat diameter and surface area to provide tighter initial seal in the short term, especially when tested with water / gas. The tightness of this seal does not directly translate to expected performance in severe service applications. So the urge to minimise seat sealing area to increase seat stress to meet a tight initial seal needs to be balanced against maximising seat sealing area to ensure lower sealing stresses to provide long term performance.

WHY ARE WE WAITING?

This is a not an unexpected question within the autoclave industry with the long lead time, delays and interruptions in project schedules while we wait for the next round of plant start-ups, the next Laterite and Sulphide Projects to study and select Pressure Leaching, and the next challenges to be faced in the Pressure Leaching industry.

CONCLUSION

Autoclave Isolation, from P&ID development, through equipment specification and selection, to installation, operation, and maintenance of the valves themselves can be challenging on many levels – technical, economical and practical. MOGAS provides on-going support to customers by assisting with the development of new projects, while drawing on past experience, and continually provides support to existing plants.

REFERENCES

1. A. Taylor, "The Outlook for the PAL Process", World Nickel Congress, Melbourne, Australia, 2000.
2. G.E. Kim, J. Walker, J. Williams, "Nanostructured Thermal Spray Coating for High Pressure Acid Leach Application", ISEC, 2006.
3. K. Jackson, "Controlled Rapid Autoclave Blowdown", ALTA 2009 Gold Conference, Perth, Australia, 2009.
4. J. Williams, "Field Performance Review of Autoclave Valves", ALTA 2009 Nickel Conference, Perth, Australia, 2009.
5. K. Osten, "Status and Trends in Pressure Oxidation", ALTA 2010 Gold Conference, Perth, Australia, 2010.

HIGH PRESSURE AUTOCLAVE FEEDING AT MAXIMUM SOLIDS CONCENTRATION AND EFFICIENCY

By

Heinz M. Naegel
FELUWA Pumpen GmbH, Germany

Presenter and Corresponding Author

Heinz M. Naegel, CEO
naegel@feluwa.de

ABSTRACT

Handling of mining slurries and tailings in general and high pressure autoclave feeding in Pressure Acid Leach (PAL) facilities of hydrometallurgical projects in particular can be an exceedingly challenging task for pumps. Hydraulically actuated double hose-diaphragm pumps do not only allow for high flow rates (max. 750 m³/h), working pressures (max. 320 bar) and pumping temperatures (max. 200°C), but offer decisive benefits compared to traditional diaphragm pumps that are typically applied for such duties.

With an ideal linear flow path they are especially conducive to the handling of paste and tailings at minimum wear, be they highly viscous, corrosive and/or erosive. Double hose-diaphragm pumps offer maximum efficiency and are almost exclusively of triplex upflow or downflow design, using crankshafts that are offset by 120 degrees. By this means, continuous slurry flow is ensured and sedimentation avoided. For high flow rates, single-acting quintuplex pumps provide for the further reduction of kinematic irregularities and waiving of pulsation dampeners.

392

INTRODUCTION

Reliable handling of aggressive and abrasive mining slurries and tailings is an exceptionally challenging application for pumps, even for positive displacement pumps, which are usually employed for such duties. Even the utilisation of piston diaphragm pumps has thus far been critical when it comes to solids, resistance and safety. With traditional diaphragm piston pumps, wet end and drive end are separated by a flat diaphragm. The product is both in contact with the diaphragm and the diaphragm chamber so that this chamber has to be manufactured from materials that are resistant to the product. In view of the high weight of such casings, special construction materials result in accordingly high material costs. Moreover, solids may settle around the diaphragm clamping ring and cause early failure of the sole partition between the drive end and the product. In the event of a diaphragm failure, the product (that is in many cases of an aggressive nature) breaches through and thus, contaminates the hydraulic control area, inflicts erosive and/or corrosive damage, creates considerable expense as well as unplanned and inconvenient pump downtime for cleaning and subsequent repair. Double diaphragm pumps are designed with redundant diaphragms, but basically associated with the same disadvantages as diaphragm piston pumps with a single diaphragm. Moreover, it is evident from calculations in this regard, that both diaphragms of the same diameter are subject to an identical deflection angle and hence to the same load. In the broader sense, this means that the diaphragms have identical service life expectancy.

Hydraulically actuated double hose-diaphragm pumps offer decisive advantages vs. traditional piston diaphragm pumps. They are designed without flat diaphragms, the typical character of diaphragm piston pumps. Instead, they are provided with two hose-diaphragms. These tubular diaphragms avoid all of the disadvantages of traditional diaphragm piston pumps, as described above. They ensure that the slurry will not come into contact with the pump casing, they are designed without a diaphragm clamping ring, ensure double hermetic sealing of the wet end from the drive end, and they guarantee minimum downtime. From calculations and tests it is evident that the lifespan of secondary hose-diaphragms is approx. 20 % higher than that of the primary hose-diaphragms because of differential length and deflection angles. For this reason, it is most improbable for both hose-diaphragms to fail at the same time.
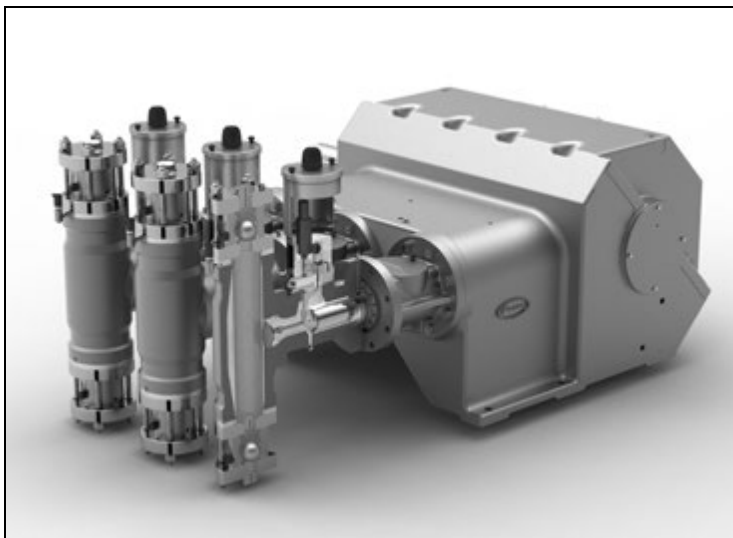
LEAK-PROOF DOUBLE HOSE-DIAPHRAGM PUMPS[1][2]

In today's world of growing environmental concerns it becomes critical to use, where feasible, leak-proof and maintenance-free pumps. Process engineering plants are subject to continuously increasing demands as to safety, availability and reliability since these are directly associated with costs for loss of production, spares, maintenance, repair, environmental protection etc.

Leakage of dangerous fluids resulting from pump malfunction is a very real and major threat for both the environment and to humans. For an increasing number of users *safety* not only means operational safety, but also the safe separation between process and environment. Double hose-diaphragm pumps provide multiple failsafe barriers between the fluid/process and the environment.

Bionics in Pump Design

A great deal of bionics is implemented into the design of double hose-diaphragm pumps that allow for pressures of up to 320 bar. At the heart of this pump are two hose-diaphragms which are arranged one inside the other and fully enclose the product so as to produce linear flow path for the pumpage. The cylindrical shape of the diaphragm favours and enhances flow characteristics and avoids the settling of solids (see Fig. 1).

393

Figure 1: Double hose-diaphragm pump

Hose-diaphragm pumps essentially mimic the natural mechanism of the human heart by the principle of contraction and release of veins via variable speed. This action provides the entire human body with blood. Venous check valves thereby prevent back-flow of conveyed blood.

The double hose-diaphragm pump is based on the same well-proven working principle. Both hose-diaphragms are actuated by the piston by means of a hydraulic fluid. In step with the piston stroke, the pair of hose-diaphragms is subject to pulsating action, comparable with that of a human vein, and provides for the displacement of the fluid throughout the pump body in a linear flow path. Check valves prevent the return of displaced product.

The resting pulse rate of a human heart varies between 50 and 80 beats per minute. Under load these figures can even be elevated to 200. When considering an average pulse of 65/min. and a lifetime of 70 years, as an example, this amounts to some 2.391.480.000 load changes for heart and veins (hose-diaphragms). Double hose-diaphragm pumps are designed for a service life of 30 years. Under continuous operation at a rate of 65 strokes per minute (spm) they would be subject to a total of 1.024.920.000 load-cycle changes. Compared to the biological concept, hose-diaphragm pumps inherently have a considerable factor of safety by virtue of their design.

Working Principle

Double hose-diaphragm pumps are provided with two hose-diaphragms, one inside the other. They fully enclose the product and create double hermetic sealing from the hydraulic drive end. Both hose-diaphragms are actuated by the piston by means of a hydraulic fluid. The cylindrical shape of the diaphragm favours and enhances flow characteristics, avoids the settling of solids and allows for a much smaller footprint than traditional systems.

Advantages of Double Hose-Diaphragm Pumps vs. Traditional Diaphragm Pump Types

With a maximised linear flow path without deviation, double hose-diaphragm pumps are especially conducive to the handling of mining slurries and tailings at minimum wear, be they highly viscous, corrosive and/or erosive. They are designed with redundant hose-diaphragms, although the pump only requires one to be fully operational. The hose-diaphragms provide for double hermetic sealing between the wet end and the drive end. Even in the event that one of the hose-diaphragms fails, the second one reliably prevents leakage of fluids, no matter whether it is the inner or the outer diaphragm that is breached, and ensures that the product neither comes into contact with the pump casing nor with the hydraulic drive area or the environment. The pump casing has no need to be manufactured from expensive special materials that are impervious to the pumpage.

The cylindrical shape of hose-diaphragms and clamping without clamping ring allows for a longer service life than traditional flat diaphragms and culminates in most favourable MTBF (mean time between failure) and MTBR (mean time between repair) figures.

394

Downflow Configuration

For extremely viscous slurries, or applications carrying solids that tend to settle and may cause breakdown of the pump resulting from blockages within the check valves, pump chamber or piping, the traditional pumping principle of double hose-diaphragm pumps can literally be turned upside down, which means that the flow is directed from top to bottom of the pump (see Fig. 2).
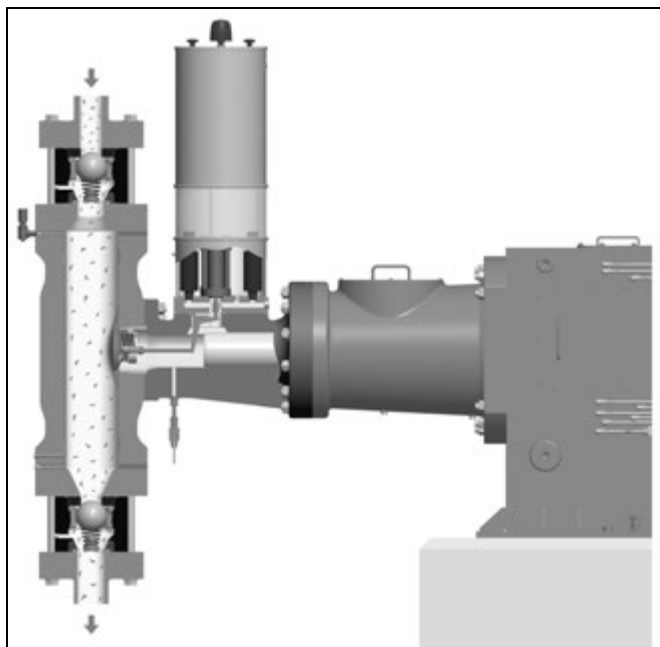

Figure 2: Downflow configuration of double hose-diaphragm pump

Check Valves

Check valves are of easily removable cassette design and virtually the sole wearing parts of this pump design. The reliability of fluid valves is particularly demonstrated when pumping abrasive suspensions. All delivery valves are individually adapted to the application, both with regard to velocity and the selection of material and flow geometry. The longest-possible lifetime is paramount when designing the valves. In addition to this, every component that is theoretically subject to wear can be removed without the prior dismantling of adjacent elements (see Fig. 3). In this context it is to be considered that valve wear not only depends on the differential pressure, but to a great extent on the degree of residual pulsations. The costs of the valve wearing parts, essentially the valve components themselves, do not increase proportionately to the size of valves, but exponentially.

395
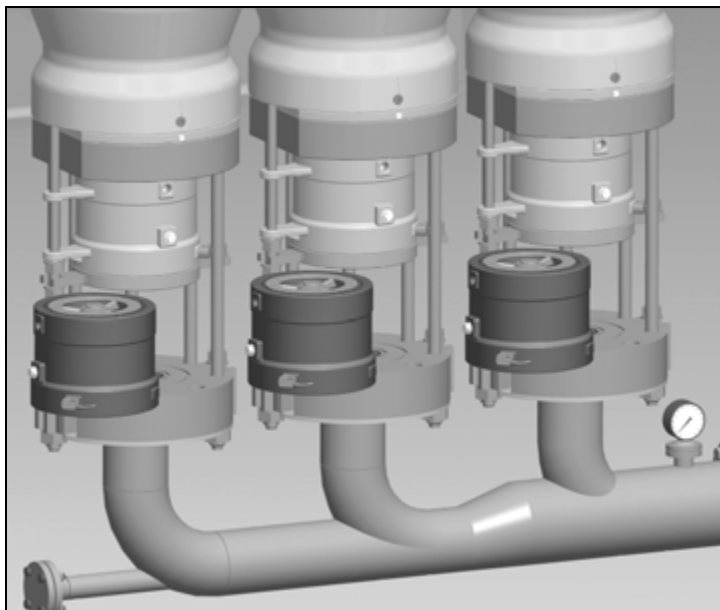
Figure 3: Easy inspection and removal of check valves

Mastering incidents of wear on pump valves has always been a problem when it comes to pumping abrasive products. Ball valves have favourable flow characteristics distinguished by almost optimum Cd values and are preferably used where media with high solids concentrations and/or viscosities are to be pumped. Valve balls have a considerably higher lifespan than valve cones, because they are continuously rotating and thus changing the sealing area on the valve seat. Users therefore prefer ball valves (instead of cone valves), provided that these are feasible from a dimensional point of view. Balls of varying materials are available with diameters up to 270 mm to provide the most suitable solution for every application and ensure the desired durability. In order to ensure sufficient lifting of the valve body from the sealing face (according to the particle size), the weight of the valve body has to be individually adapted to the respective duty.

Double valves

Use of double valves (easily removable cassette design as per Fig. 3) is recommended for media with high levels of impurities and applications which require a particularly high continuous flow. If, in the short term, a particle gets jammed between the ball or cone and the valve seat resulting in valve leakage, the second valve ensures effective sealing, thus preventing medium backflow and a resulting volume loss. Double valve configuration is moreover applied for high-pressure underground mine dewatering. In spite of the double number of check valves, wear will not double, because valve wear is dependent on the differential pressure, which is reduced by half due to the double valve arrangement.

Downflow valves

With downflow valves, it is also possible to fall back on the use of different closing body systems, depending on the technical and physical requirements involved. These may include spring loaded spherical cap valves and special floating ball valves (e.g. in the form of hollow steel balls).

Regardless of whether the traditional pump principle from bottom to top (upflow) or the reverse principle with a flow from top to bottom (downflow) is used, individually engineered delivery valves are required for pumping slurries containing large solids.

High Performance at High Pumping Temperature

The modular system of double hose-diaphragm pumps also offers a variety of options with regard to the pumping temperature:

396

Elastomer hose-diaphragms are generally employed up to 130°C. PTFE components specially developed for hose-diaphragm pumps have proven their effectiveness for higher temperatures up to 200°C. These can also be employed if the pumped medium is characterised by extremely aggressive chemical properties.

The pumps are equipped with ribbed surfaces between the wet and drive ends to master extreme temperatures ≥ 200°C. These also ensure effective heat dissipation (see Fig. 4).
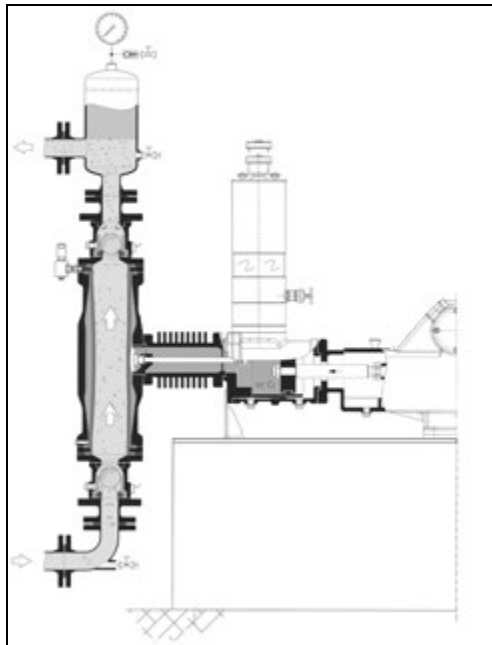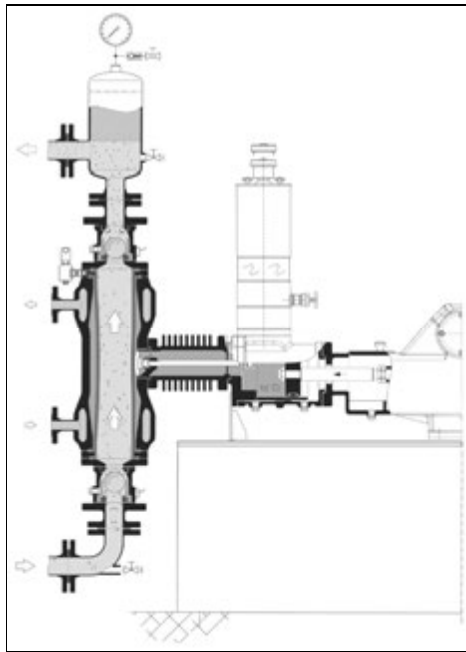

Figure 4: Double hose-diaphragm pump with ribbed casing area (convector)

Variants with double redundant diaphragms represent a further option (i.e. the combination of a double hose-diaphragm and flat diaphragm (see Fig. 5).
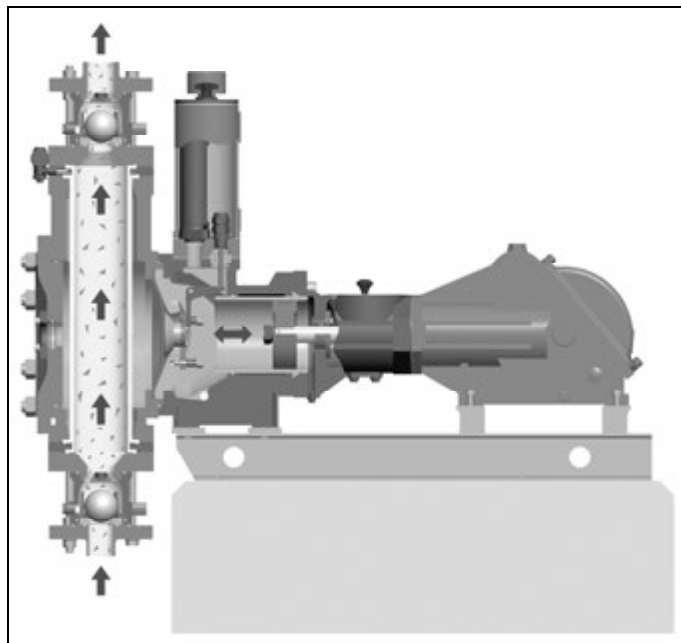
Figure 5: Double redundant pump with double hose-diaphragms and additional flat diaphragm

397

Some media require a minimum temperature if they are to retain their positive flow characteristics. In the event of a temperature drop, they will become very viscous, solidify or crystallise. The hose-diaphragm housing and, where necessary, the valve housing and connection flange are fitted with a heating jacket to ensure the pumpability of the medium (see Fig. 6).

Figure 6: Double hose-diaphragm pump with cooling or heating jacket

Quintuplex Pump Design

For high flow rates, by far the highest efficiency and lowest irregularity is achieved by means of single-acting five cylinder pumps (see Fig. 7).
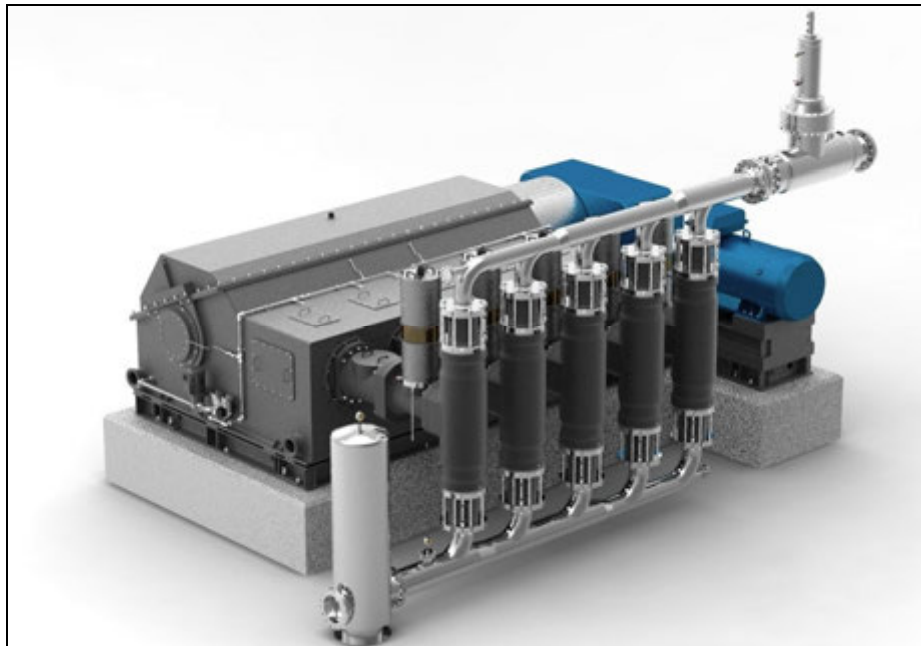

Figure 7: Double hose-diaphragm pump in quintuplex design with diagnostics
**Flow rate 525 m³/h · Power 2,200 kW**

Even without pulsation dampening, the irregularity of single-acting quintuple reciprocating pumps is reduced to 5.1% vs. 23.0% of single-acting three cylinder pumps and 32.5% of single-acting four cylinder pumps (see Fig. 8 to 10).
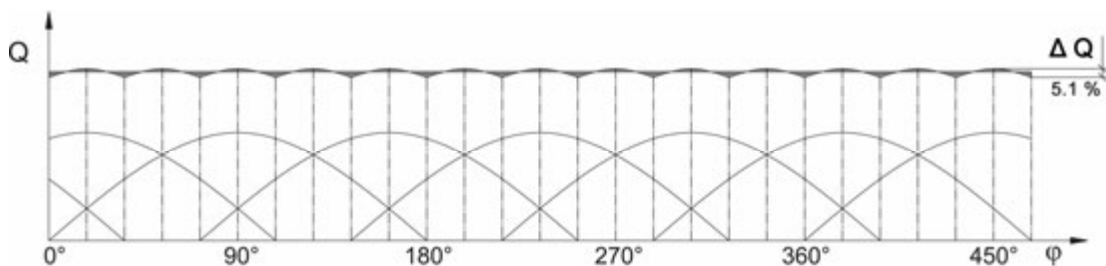
Figure 8: Irregularity of single-acting five-cylinder pumps
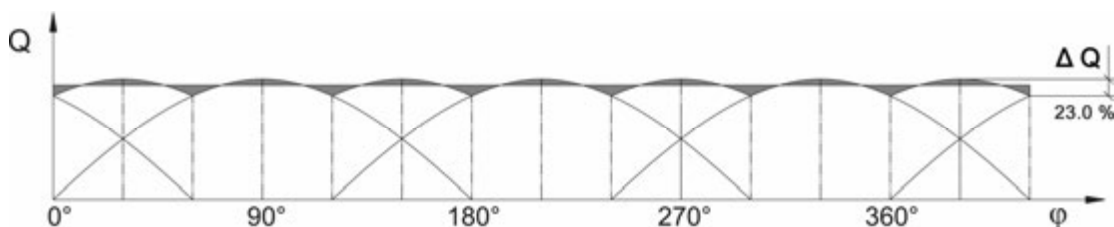
Figure 9: Irregularity of single-acting three-cylinder pumps
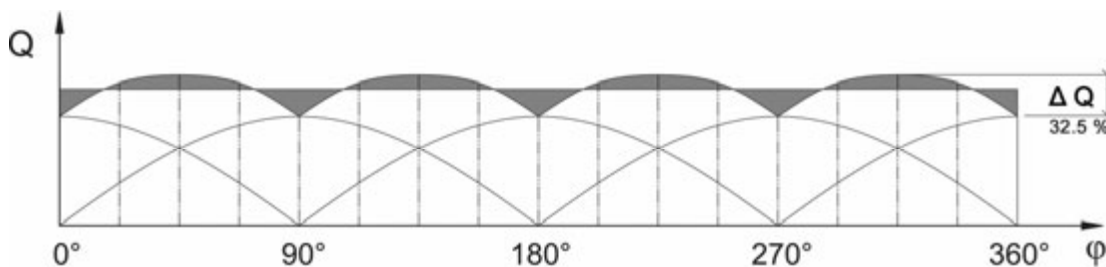
Figure 10: Irregularity of single-acting four-cylinder pumps

Quintuplex configuration not only allows for uniformities comparable with that of centrifugal pumps, but also contributes to a reduction in valve wear to an extent that has not been feasible so far.
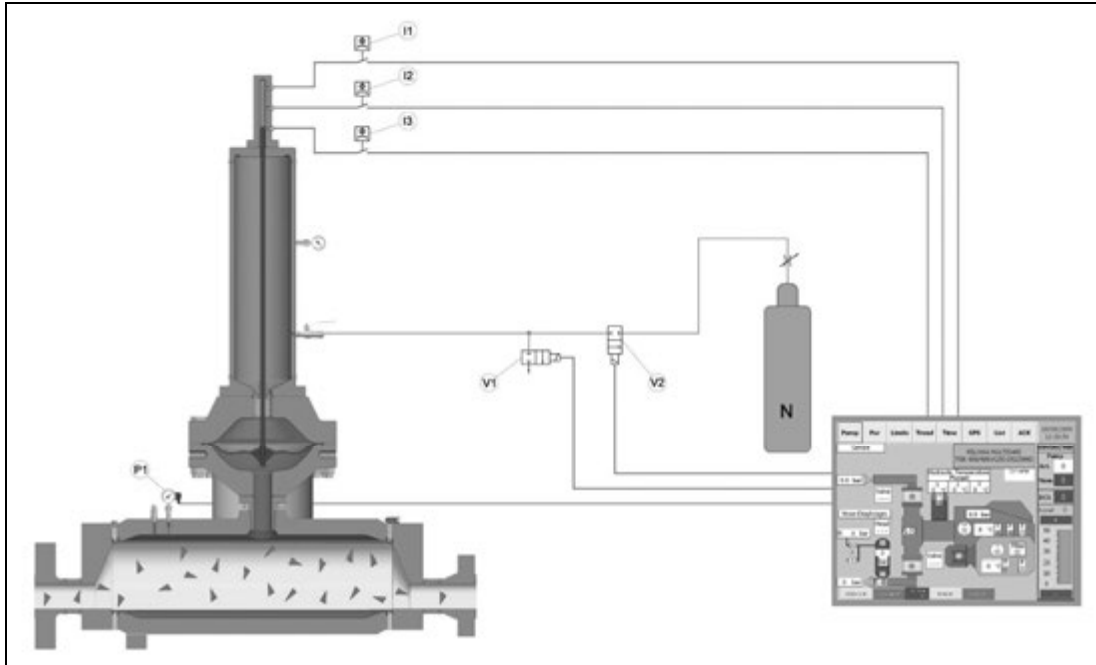
Pulsation Dampening

A typical characteristic of oscillating displacement pumps is the hydro-dynamic independency of the delivery flow from the pressure and vice versa. The reason for this feature is due to the mechanics of pressure generation by means of a displacement piston which prevents backflow and thus an escape of the displaced volume into the pipework. This principle allows for the achievement of extraordinarily high efficiencies. Conversely, the oscillating movement causes undesirable flow fluctuations and pressure pulsations. To avoid such pressure pulsations, an array of different pulsation dampeners is employed. Dependent on the actual working conditions, traditional pulsation dampeners (pressure air vessels) with air or gas cushion or hose-diaphragm pulsation dampeners with nitrogen-filled accumulators are applied.

For working pressures in the ≥ 50 bar range and for products that do not allow for contact with air or gas, extremely efficient hose-diaphragm pulsation dampeners are applied. The assembly consists of a hose-diaphragm pulsation dampener and a roller diaphragm accumulator (see Fig. 9). The system offers all the advantages of a conventional pressure air vessel. It is designed to store the pumped volume over and above the average, produced during every delivery stroke, in the hermetically sealed nitrogen accumulator. This volume is then released again during the piston suction stroke, thus compensating for unavoidable delivery fluctuations. The accumulator is pre-charged to approx. 80% of the working pressure in order to ensure maximum efficiency. When operating at different discharge pressures, pre-compression has to be adapted accordingly. In

comparison with typical bladder-type accumulators, the roller diaphragm type accumulator offers a unique advantage in that the nitrogen cushion can be individually adapted to the operating conditions by means of an automatic filling unit.

The position of the roller diaphragm is detected by utilisation of inductive transmitters. Based on this position, a co-efficient of operating pressure and pre-compression can be calculated. By means of this co-efficient, the control unit determines whether pre-compression has to be increased or decreased and nitrogen has to be added or drained, respectively. The pulsation dampener is, therefore, not sensitive to operating conditions which deviate from the design layout and allows for a reduction of the uniformity coefficient to less than 0.5% (p to p). Low pulsation results in wear reduction at the check valve and avoids significant loss of energy as a result of increased pump speed in order to compensate for loss of flow volume due to leaking check valves. In other words, proper pulsation dampening contributes to overall reduction of life cycle cost.


Figure 11: Hose-diaphragm pulsation dampener with roller diaphragm accumulator and automatic adaptation

Condition Monitoring

The Internet is gradually evolving into a comprehensive medium for the transport of all manner of data. By 2015, the number of Internet users is expected to increase to approx. five billion. Meanwhile industry is also increasingly focusing on wireless data communication and estimates that new perspectives will result from the adoption of this technology.

Double hose-diaphragm pumps are designed to avoid sudden deviation from admissible working conditions and unplanned downtime. For additional back-up of its failsafe characteristics they utilise an overall diagnostic system for permanent condition monitoring of essential components and parameters (see Fig. 12).

400
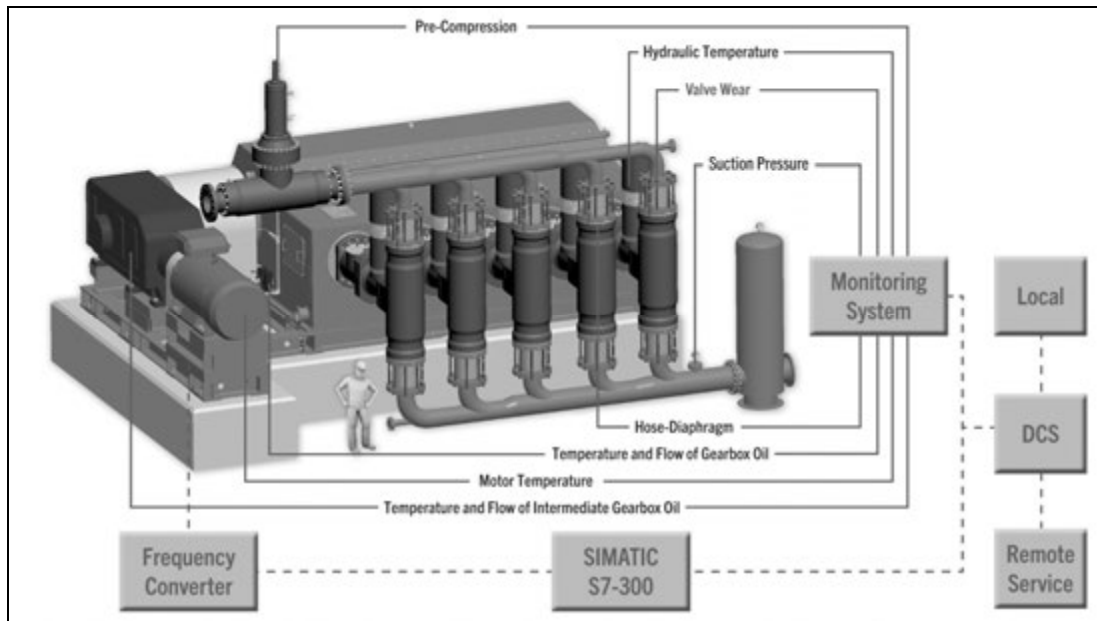
Figure 12: Double hose-diaphragm pump in quintuplex design with diagnostics

Acoustic valve diagnostics for early recognition of wear in delivery valves

By means of the Valve Performance Monitoring System (FVPMS), the operational safety and availability of pumps is significantly increased, since wear in check valves is precisely detected even if the loss of output is still less than 1.5 %, This does not only avoid loss of energy, but also allows for specific forward planning of service and repair. [3(4)]

Condition Monitoring of Hose-Diaphragms

Permanent condition monitoring of double hose-diaphragms is ensured by means of pressure sensors, pressure gauges or contact pressure gauges. In the event that one of the hose-diaphragms leaks or fails, either product or actuation fluid will penetrate into the unpressurised intermediate space. The resulting build-up of pressure is fed to the condition monitoring system, which in turn provides a signal with manifold processing options. Nevertheless, operation can be maintained with a single hose-diaphragm until the system allows for shutdown and repair.

Monitoring of suction pressure

Unrestricted inflow at an appropriate inlet pressure is essential for trouble-free operation. For reliable supervision of suction pressure, diaphragm-type pressure gauges are applied which have especially been designed for slurry handling applications.

Monitoring of temperature

Supervision of hydraulic and gearbox oil temperature is carried out by means of PT 100 temperature sensors.

Touch Panels

For early detection of faults and with the objective of ensuring maximum availability, the redundant nature of double hose-diaphragm pumps is supported by means of an overall diagnostic system. Touch panels, which are integrated into the control cabinet, give the pump a transparent character and provide the operator with information on current operating parameters and the condition of fundamental parts. Bus systems link the touch panel to local process control, whereby PROFIBUS (Process Field Bus) provides best conditions for communication and control of system frequency converters, PLC, touch panels and the valve performance monitoring system.

401

Web-based service

The system is linked to the Internet. In the event that actual values differ from the programmed nominal values, the system will email a respective notification to a service technician. In addition, a safe, bidirectional VPN conduit can be set up, which allows for remote access to the control unit of the pump. The system not only allows for higher availability and productivity, but also for a reduction of service costs. All critical parameters are displayed by means of traffic light logic. Integration of touch panels into industrial control system moreover allows for web-based service, which make site service in many cases unnecessary.

One of the decisive criteria of condition monitoring is to recognise even the merest indication of wear or any other variations from set-points at such an early state that the operator is provided the opportunity of keeping track of any further developments which may include maintenance into the process as appropriate, in order to avoid an unscheduled shutdown of the system. Since the leak-free sealing of check valves plays a decisive role, an innovative system for the early detection of wear in check valves has been developed for double hose-diaphragm pumps in cooperation with a well-known electronic manufacturer. The measuring principle of these tailor-made sensors is based on the analysis of solid-borne sound and is capable of detecting leaks between valve seat and ball or cone respectively at a time when the loss of flow is still less than 1.5 %. Multiple options are available for the transmission of the measuring results by means of a dry contact (such as Internet or Intranet) and provide the operator the opportunity of well-directed advance planning of maintenance or repair action as well as the precise determination of MTBR values. By means of the diagnostic system, the operational safety and availability of the pumps is significantly increased, whereas maintenance costs can be considerably reduced.

APPLICATION EXAMPLES

Three off double hose-diaphragm-type positive displacement pumps of triplex upflow configuration are applied in North America's largest copper mine. Two are specified for operation and the third one for standby. The duty of these units is the feeding of copper concentrate slurry into pressure leach vessels. The slurry being pumped has a most abrasive character and contains a high percentage of solids.

Three off double hose-diaphragm-type positive displacement pumps of triplex downflow configuration are applied in a well-known North American underground nickel-copper mine. Again two are specified for duty operation and one for standby. The duty of these units is single-stage high pressure mine dewatering at an underground level of 1,700 metres. Downflow configuration is applied in order to ensure high availability and both efficient intake and pumping without solids sedimentation.

CONCLUSIONS

Double hose-diaphragm pumps are especially conducive to autoclave feeding or the disposal of tailings. The redundant hose-diaphragm provides for a linear flow path without sedimentation and ensures double hermetic sealing of the wet end from the drive end. Even in the event that one of the hose-diaphragms fails, operation is maintained because the pump only requires one to be fully operational. Nevertheless, the product neither comes into contact with the pump casing nor with the hydraulic drive area with the positive benefit that the cylindrically shaped pump casings have no need to be manufactured from expensive special materials that are impervious to the pumpage. Unique pulsation dampening systems ensure reduction of pulsations to less than 0.5% (p to p) as well as energy and cost efficient pumping.

By means of comprehensive diagnostic systems and touch panels, double hose-diaphragm pumps offer an HMI (Human Machine Interface) with full integration of pump diagnostics into industrial control systems with web-based service option. The touch panels are part of the control cabinet and reveal information about prevailing operating data and readings, such as stroke rate, suction pressure, discharge pressure, pulsations, hydraulic and gearbox oil temperatures or the condition of hose-diaphragms and check valves. They not only indicate possible loss of flow and efficiency resulting thereof, but at the same time make a noticeable contribution to the reduction of energy costs.

402

REFERENCES

1. Nägel, H. M. "Hermetically Sealed Displacement Pumps", 2010, pp. 39-105.

2. Nägel, H. M. "Cost-effective handling of tailings using double hose-diaphragm pumps in up-/downflow configuration", PROCEMIN 2010, Santiago, Chile, 2010.

3. Püttmer, A. & Nägel, H. M. "Online Diagnosis of Pump Valves", atp magazine, 2003.

4. Nägel, H. M. "Predictive maintenance of process pumps by online diagnosis", Pump Engineer magazine, 2005.

AGITATOR START-UP IN SETTLED BED CONDITIONS

By

Jochen Jung and Wolfgang Keller

EKATO RMT GmbH, Germany

Presenter and Corresponding Author

Wolfgang Keller
wolfgang.keller@ekato.com

ABSTRACT

This paper discusses some aspects for the re-starting of agitators in settled bed conditions. As shown, physical correlations and design rules allow the safe design of agitators for such conditions. In any case, recommended designs or strategies can only be as good as product data available or rules of thumb applied, e.g. an assumption for the porosity of the settled solids bed.

INTRODUCTION

Operators of agitated suspension vessels often require information to develop re-start strategies after an intended or unintentional stoppage of the agitator.

A significant number of mixing applications include solids which must be brought into or kept in suspension. Typical applications are storage, leaching or precipitation vessels. If possible the geometric setup of the agitator is chosen to install impellers above settled solids levels. But often solids concentrations are high, so that impellers or the lowest impeller of a multiple impeller arrangement become embedded by sedimentation where the height is above this impeller. The pivotal question is whether the agitator has the capability to re-start and re-suspend the solids under these conditions. Another important question is the time period which is available to successfully re-start the agitator.
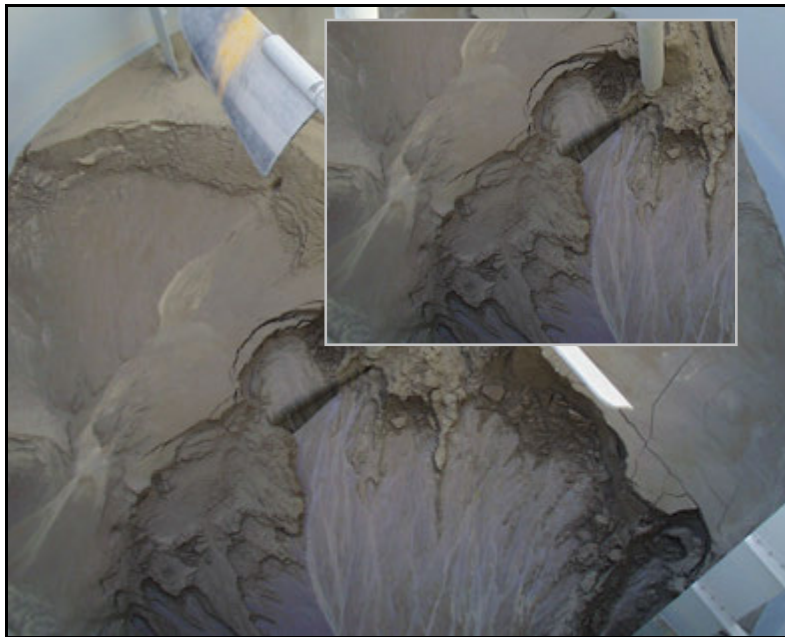
Figure 1: Settled solids in a 3200 m³ vessel

This paper describes some physics of the sedimentation of solids and discusses principle correlations of agitator start-up torques. Presented models and correlations are supported by lab testing which shows the importance of testing possibilities, ideally with original products. This finally enables the engineer to design the agitators and additional equipment, that might be required for a successful re-start, for specific applications or products.

SETTLING OF SOLID PARTICLES – THEORETICAL BACKGROUND

If agitation is stopped and all particle sizes are homogeneously distributed throughout the tank volume particles start to settle with the hindered settling velocity w_{ss} which is a function of the settling velocity of the single particles w_s and the volume concentration of solids c_v[1][2][3].

$$w_{ss} = w_s \cdot \left(1 - c_v\right)^m \quad (1)$$

At the same time the sediment at the vessel bottom starts to increase with the velocity w_{sed}. From the volume balance for the solids the velocity w_{sed} can be calculated as follows.

$$w_{sed} = \frac{w_{ss}}{\left(\dfrac{c_{v,sed}}{c_v} - 1\right)} \quad \ldots(2)$$

This leads to the simple correlation that the sediment height h_{sed} is a linear function of the time

$$h_{sed}(t) = \frac{w_{ss} \cdot t}{\left(\dfrac{c_{v,sed}}{c_v} - 1\right)} \quad \ldots(3)$$

The above described equations imply that the particles are free settling, meaning no viscosity effects such as flow limits or the like occur.

The maximum volume concentration of solids in the sediment $c_{v,sed}$ results from the porosity ε of the settled compacted product and can be derived from a measurement with the original product.

$$c_{v,sed} = 1 - \varepsilon \quad (4)$$

Porosities ε for free settling particles are typically in the range of 0.4 to 0.5.

The final sedimentation height is derived by

$$h_{sed} = h_1 \cdot \frac{c_v}{c_{v,sed}} \quad (5)$$

SETTLING OF SOLID PARTICLES – TESTING METHODS

In chapter 2 some correlations regarding the settling behavior of solids are given. Of course calculated values are only as good as the input data. Important information is the particle size used to calculate the settling velocity and the final porosity of the sediment. Both numbers can be derived by testing with original products. The particle size distribution can be obtained by several methods, e.g. a sieve analysis, whereas the porosity and the settling characteristic can be derived by testing in a measuring cylinder or a small agitated test setup.

Figure 2 shows a test with a laterite slurry in a 500 ml measuring cylinder for different time intervals.

Figure 3 shows settling curves in a 50 liter vessel. As can be seen, the sediment height increase for free settling particles is linear with time and reaches the final sediment height for the 40 wt.-% slurry after approx. 4.7 minutes. From the final sediment height a porosity of 0.425 can be derived. The symbols show the measured heights and the solid curves show the calculated settling characteristic as per equation 3. The tests carried out in the 50 liter agitated test setup were repeated for identical conditions in a 500 ml measuring cylinder. Consistent values of the calculated and measured data could be repeated. For both test scales the porosity decreased slightly with increasing solids concentration. This indicates that the porosity is a function of the absolute sediment height which has to be considered for the commercial scale.

As can be seen from the curves for the different scales the match is very good, supporting the validity of the above given equations to calculate settling heights at different time intervals. Applying these equations and test results for free settling products to production scale conditions a critical time can be predicted, before the lower impeller becomes embedded by solids.
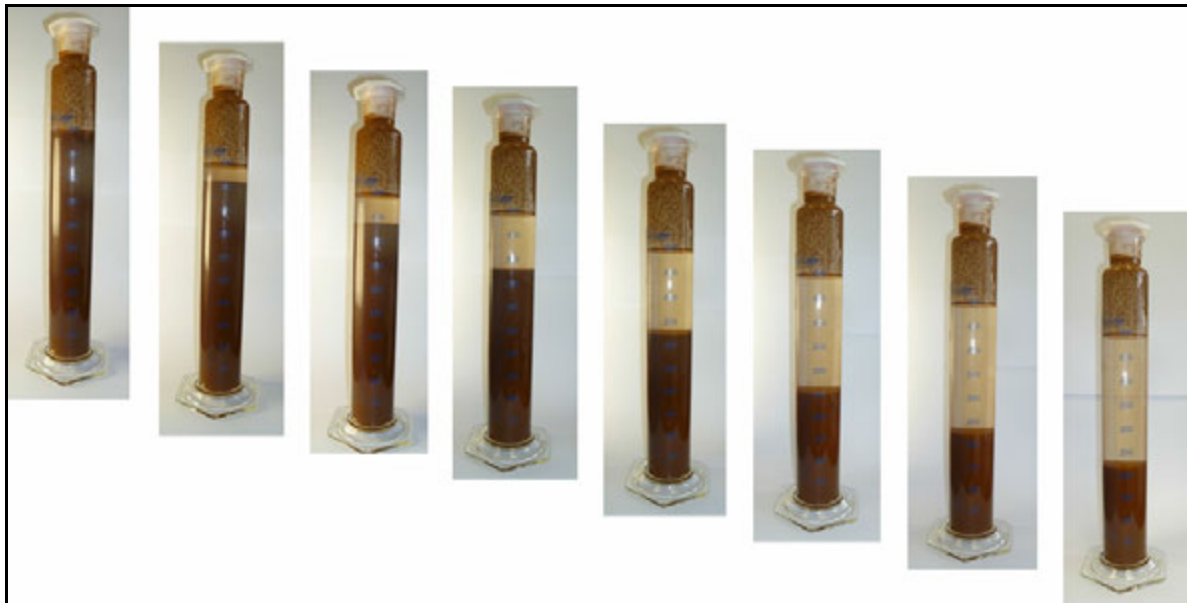
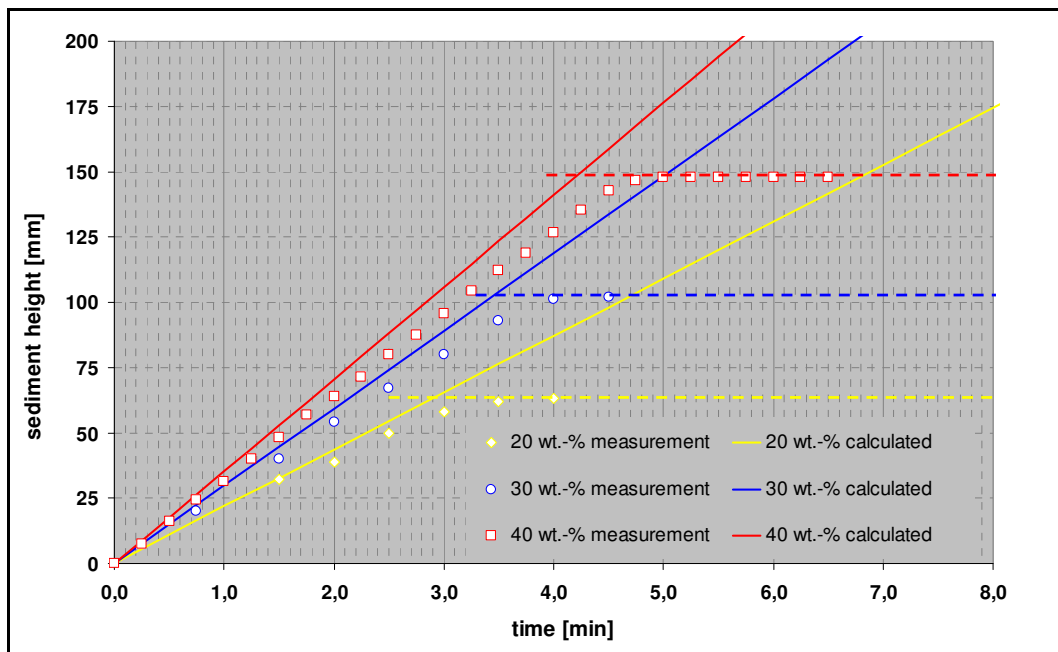**Figure 2: Settling test with a laterite slurry in a 500 ml measuring cylinder**

Figure 3: Settling curves for different solids concentrations

RESTARTING OF AGITATORS UNDER SETTLED BED CONDITIONS

If the agitator downtime is longer than the critical time resulting in the impeller becoming embedded or submerged with solids, information has to be available as whether the agitator can be re-started or not.

It is assumed that impellers being started in settled solids will follow the same physics as impellers being operated in powders or solid beds, until the solids start to be re-suspended and the settled bed is being broken up. The only difference is that the continuous phase between the solids is a liquid instead of air or a gas.

Vock in his dissertation[4])studied the behavior of different impeller types in agitated solid beds (packed bed mechanics). He shows that the results of his measurements are equivalent to fluid mechanic behavior by defining a modified Newton number Ne* and modified Reynolds number Re*.

407

$$\text{Re*} = \frac{n^2 \, d_2^2}{\left(1 - \frac{\rho_l}{\rho_{sed}}\right) y_0 \, g} \quad (6)$$

$$Ne* = \frac{P}{\rho_{sed} \, n^3 \, d_2^5} \quad (7)$$

n   shaft speed [s^{-1}]

d2   impeller diameter [m]

ρ_l density of liquid [kg/m^3]

ρ_{sed} density of sediment [kg/m^3]

y_0 submergence of impeller in settled solids bed [m]

g   gravitational constant [m/s^2]

P   power input [W]

Kipke and Weiß[5][6][7] applied this model for different types of settled suspensions and particle sizes. They showed that the same correlation as in solid beds without liquids apply, the product of the modified Newton and modified Reynolds number is constant.

$$Ne* \cdot \text{Re*} = const. \quad (8)$$

A model that can be derived from the above model allows us to calculate the start up torque $M_{t,stu}$ directly

$$M_{t,stu} = c \cdot \left[(\rho_s - \rho_l) \cdot g \cdot y_0 \right] \cdot d_2^3 \quad (9)$$

ρ_s density of solids [kg/m^3]

The constant c has to be determined in a test since it depends on the type of product and the impeller type.

Both models provide the possibility to calculate the resulting motor power and torque in production scale. In any case, the application of these models to production scale will immediately show that even at very low submergences a start-up will require several Megawatts of agitation power. This gives clear evidence that a re-start for standard agitator designs; i.e. motor powers and torques, in settled beds will not be possible or will most likely damage the equipment. Therefore, a strategy has to be at hand to allow the agitators to continue operating safely. Special measures have to be applied to restart agitators under 'settled bed' conditions.

This inevitably requires the development of re-start strategies for these critical process conditions. To support these ideas and recommendations EKATO initiated a test program in multiple test scales. The impeller torque was measured for different impeller diameters at different shaft speeds. A further variation was the submergence of the impeller with solids and the re-suspending strategy.

Figure 4 shows a measurement of the torque at different shaft speeds for different impellers at a constant submergence. As can be seen the torque is constant at low shaft speeds and then sharply drops as solids start to be re-suspended. Once particles are re-suspended, the torque increases quadratically, as expected from fluid dynamics. As a comparison, measurements were conducted in a solid bed without liquid. For these conditions the torque is also constant at low shaft speeds and then directly starts to increase without the drop as observed for the tests with liquid.
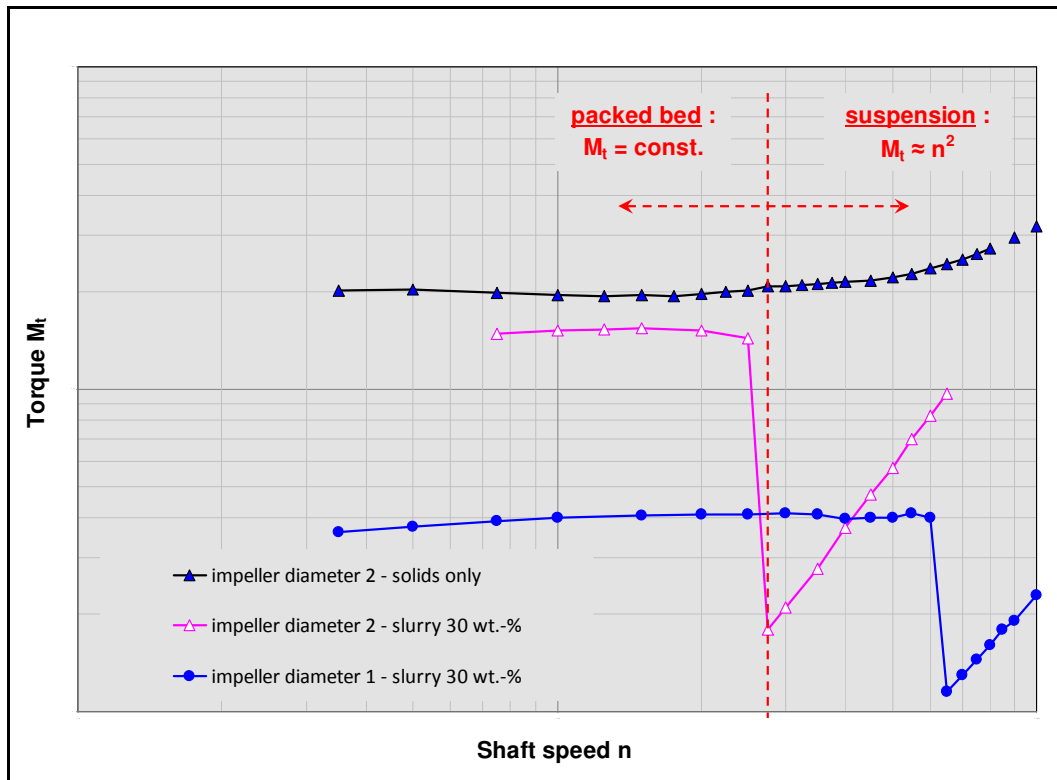

Figure 4: Torque as a function of the shaft speed for different test setups

In figure 5 test results for different submergences are related as the modified Newton number Ne* over modified Froude number Fr* which from a physical point of view seems to be a better definition than Re*.

$$Fr* = \frac{n^2\ d_2^2}{\left(1 - \rho_l\big/\rho_{sed}\right) y_0\ g} \quad (10)$$

As can be seen all test results for different submergences, solids concentrations and impeller diameters can be shown as a single curve. The change from Ne* · Fr* = constant to Ne* = constant indicates the point where the solids start to be re-suspended. These results match very well with the data derived by Kipke. Results of the tests in the solid bed without liquid do not show this distinct change but has a smooth transition.
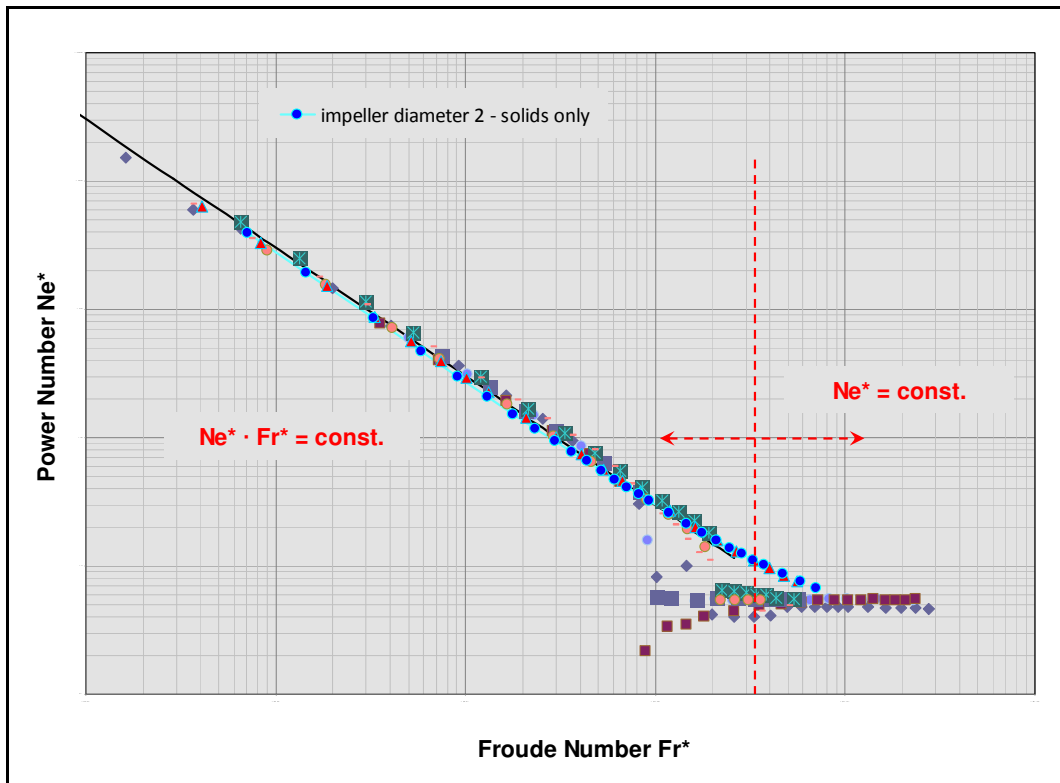
Figure 5: Test results showing modified Ne* over modified Fr*

In the next test runs different potential options to reduce the required torque and therefore power input were tested.

In the first test run the rotational direction of the agitator was reversed which is common practice in a settled condition. As can be seen from the measurements in figure 6, the start-up torque can be reduced substantially by 50 %. In the next series of tests, water was added below the impeller before the agitator was restarted. The concept is to re-suspend the solids around the impeller to facilitate the start-up. As can seen in figure 6 the start-up torque can be reduced enormously by this method. For the down-pumping operation the start-up torque can be reduced by a factor of 10, while for an up-pumping mode the reduction factor is even increased to 50 !!! In addition re-suspending of the solids will be achieved at much lower power inputs as can be concluded from the drop in torque at lower shaft speeds.
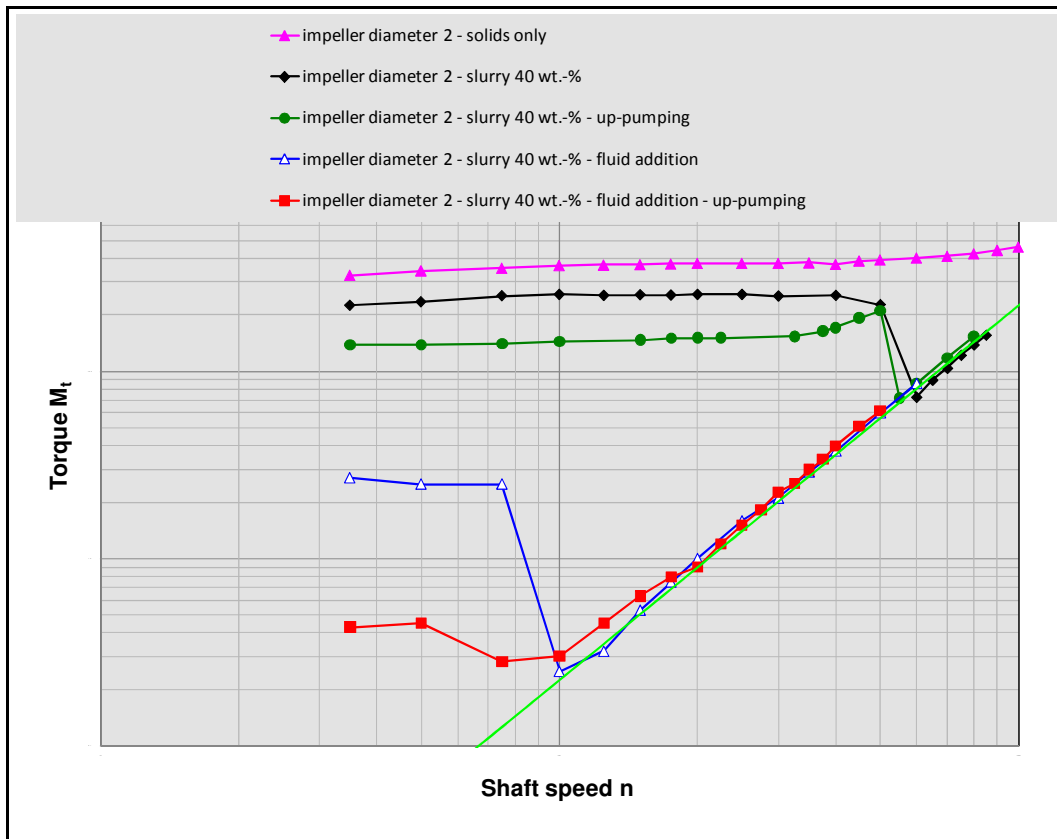
Figure 6: Reduction of the start-up torque using different techniques

RESTARTING STRATEGIES FOR SETTLED BED CONDITIONS

Following are some procedures and strategies discussed to illustrate how agitators could be re-started under settled bed conditions. Most of these strategies have to be considered in advance of the plant design as the agitator and vessel design might be influenced by the intended parameters.

	Method	Advantage	Disadvantage	Remarks
1.	adjust off bottom distance of lower impeller stage to avoid submergence	no special design considerations required	increased density at impeller for a short time after start up	
			reduced off bottom suspension of solids during normal operation	
			method limited to solids concentration of approx. 30 – 40 %	
2.	emergency power back-up for all agitators	'safe'	investment costs	
3.	emergency power back-up => alternating operation	less investment costs than 2.	control technique required	time intervals have to be known

	Method	Advantage	Disadvantage	Remarks
4.	reverse rotational direction before switch to normal operation	simple	to be considered during agitator design	applicable at low submergence
			start-up torque 'only' reduced by 50 %, restart anyhow unlikely	
5.	fluid addition to impeller	re-start possible at low torque for most conditions	additional equipment and piping required	continuous or for start-up only ; interaction of sediment / fluid to be tested before agitator design
		reduced emergency power back-up required	emergency power back-up anyhow required	
6.	air addition to impeller	re-start possible at low torque for most conditions	additional equipment and piping required	continuous or for start-up only ; interaction of sediment / fluid to be tested before agitator design
		reduced emergency power back-up required	emergency power back-up anyhow required	
			flooding of impellers might occur	

SUMMARY AND CONCLUSIONS

This paper discusses some aspects for the re-starting of agitators in settled bed conditions. As shown, physical correlations and design rules allow the safe design of agitators for such conditions. In any case, recommended designs or strategies can only be as good as product data available or rules of thumb applied, e.g. an assumption for the porosity of the settled solids bed.

Ores processed in hydrometallurgical processes vary not only in the chemical composition but in their rheological slurry behavior as well. This of course has an impact on the sedimentation characteristics and the type of solids bed formed. Depending on the type of ore and e.g. the particle size a 'normal' packed bed following solids mechanics with a constant torque at low shaft speeds occurs. Other ores, such as some laterites will not form a very dense or compact sediment and show only an increased viscosity or flow limit. In these cases the re-start will be less demanding.

The first step to assess the situation is to calculate the height of the settled bed and the settling time. As could be shown by the measurements the presented model is accurate and on the conservative side. For cases where solids are not free settling, predicted settling times will be longer which results in an increased time frame for restart, but the higher settling height has to be considered as well. In addition, it has to be considered that the porosity is a function of the absolute filling and therefore settled bed height.

In case the settled solids behave as a packed bed a strategy to re-start the agitator has to be at hand. This requirement is highlighted by the presented models and test results which show that even at quite low submergences, start-up torques and power requirements will exceed that of the installed equipment. Several options to facilitate this start-up are discussed. A customized strategy considering the 'boundary conditions' could be developed in cooperation between the end-user / owner / engineering company and equipment supplier.

Due to the existence of a wide range of product characteristics, lab testing with original products sometimes presents a good choice. Compared to the efforts, the benefits of such testing can be enormous. Design relevant data such as the particle size distribution, porosity, viscosity etc. can be derived. In addition, mixing testing in a quite small scale can reveal unknown characteristics as a reduced porosity of settled solids or a time dependent behavior of the start-up torque.

REFERENCES

1. Zwietering: 'Suspending of solid particles in liquid agitators'; Chem. Eng. Sci. 8 (1985); pp. 244-253.

2. J. F. Richardson et al: ‚Sedimentation and fluidization : Part 1'; Trans. Chem. Engrs. 32 (1954); pp. 35-53.

3. EKATO Handbook of Mixing Technology, Schopfheim (2000).

4. F. Vock: 'Zur Rührmechanik von Feststoffschüttungen'; Dissertation; Universität Karlsruhe (TH); 1975.

5. K. Kipke: 'Anfahren aus abgesetzten Suspensionen'; Chem.-Ing.-Tech. 55 (1983) No. 2; p 144-145.

6. K. Kipke: 'Anfahren aus abgesetzten Suspensionen'; Internal EKATO paper

7. G. Weiß: 'Anfahren aus abgesackten Suspensionen'; Ingenieurarbeit, Fachhochschule Nürnberg; 1980.

CHARACTERISTICS AND FABRICATION QUALITY CONTROL
OF LARGE PRESSURE LEACHING AUTOCLAVE

By

Hao Zhen-liang and Mao Lu-rong
Shanghai Morimatsu Pressure Vessel Co., Ltd, China

Presenter and Corresponding Author

Hao Zhen-liang
haozhenliang@morimatsu.cn

ABSTRACT

Hydrometallurgical pressure leaching technique, of which autoclave is the key equipment, has been increasingly applied in the extraction of zinc, gold, nickel, and uranium from ores and concentrates. Shanghai Morimatsu has been dedicating itself to the development of a series of autoclaves by continuous design improvement. Based on this, the structural characteristics of autoclaves in various processing conditions are reviewed here, and the fabrication, quality control, schedule management, hoisting and shipment of large-scale titanium clad autoclaves are summarized as well.

INTRODUCTION

Hydrometallurgical approach has been increasingly applied to various projects extracting nickel, cobalt, gold, lead, and zinc, for its high recovery efficiency, outstanding flexibility and environmental advantages. The pressure leaching process, of which autoclave is the key equipment, is the recent preference for increasing productivity in metallurgical industry.

Shanghai Morimatsu has been developing a series of autoclaves (Φ 1800, 2500, 3200, 3600, 3800, 5100, and 5230) for sulfide and laterite nickel ores, gold and other hydrometallurgical projects[1]. Autoclaves are designed based upon different operating conditions with regard to structural and material selections. Table 1 lists the major projects that Morimatsu have been supplying autoclaves for.

Table 1: Past performance of autoclaves manufactured

Project	Owner	Qty	Size mm	Material
Jinchang	JNMC	1	Φ1800×6800	16MnR+TA2
Jinchang	JNMC	3	Φ2500×8600	16MnR+TA2
Jinchang	JNMC	2	Φ3200×13000	16MnR+TA2
Jinchang	JNMC	2	Φ3800×19000	16MnR+TA2
Ramu	MCC	3	Φ5100×34000	SA-516G.70+SB-265Gr.17
Ambatovy	Sherritt	3	Φ5230×37000	SA-516G.70+SB-265Gr.17
Amursk	Polymetal	1	Φ3600×23330	SA-516G.70+Membrane+Brick

Figure 1: Shop commissioning of autoclave with agitator

DESIGN OF AUTOCLAVE

Severe operating conditions are quite common for hydrometallurgical processes due to the involvement of gas-solid-liquid mass transfer, intensive acidification, exothermic reaction and agitation impacts, which create a number of challenges for autoclave design[2]. To improve productivity, a horizontal autoclave with several chambers (1 or 2 agitators in each chamber) is preferred, which allows slurry to be processed in different chambers sequentially. At the operating temperature and pressure, acidic slurry will be mixed and react with gas and/or oxygen and so that valuable metals could be leached and/or separated.

Leaching processes for various metals like lead/zinc, nickel/cobalt, and gold have significant differences, so material and structure selection of the autoclaves varies for each process. Two typical types of structure have been recently utilized for autoclaves, namely carbon steel + (lead/rubber liner) + brick lining, and carbon steel + (Ti/other corrosion resistant metals explosive cladding).

415

In the case of gold and lead/zinc ores, autoclaves always use the structure of carbon steel + (lead/rubber liner) + brick lining. The available service temperature for lead lining does not exceed 140°C and that for the rubber liner is 110°C (as suggested by REMA Tiptop). While the carbon steel part is completed, non-destructive tests (NDTs), post weld heat treatment (PWHT), and hydrostatic test are applied (as necessary), then the inside surface treatment of autoclave is conducted after all test results are approved. After all the above procedures, lining is performed. Due to the restricted transportation weight and the possibility that brick lining could be separated from the shell, brick lining is always performed in the field. Nowadays lead lining is not preferred because of its harmful impacts on human health and environment. With the revolutionary improvement of its performance in terms of service life and temperature resistance, rubber liner is becoming widely applied in metallurgical industry.

While high grade sulfide nickel ores are being mined out, laterite nickel ores, as the alternative, are becoming the main focus for the industry and thus there is an increasing demand for titanium clad autoclaves (under more severe conditions of higher temperature and pressure but generating higher productivities). The application of large-scale titanium clad autoclaves represents the current demand for more efficient valuable metal extraction. The development of large-scale titanium clad autoclaves in Morimatsu will be reviewed as follows. Details of these units are presented in Table 2.

Table 2 PAL Autoclave parameters

Project		Ambatovy	Ramu
Dimension (mm)		Φ5230×37000(TL-TL)	Φ5100×34000(TL-TL)
Material	CS	SA-516Gr.70	SA-516Gr.70
	Cladding	SB-265Gr.17	SB-265Gr.17
Shell Thickness (mm)		118+8	118+8
Weight per Unit(tons)		783.4	766.9
Quantity		3	3

Material Selection

The pressure leaching process for extracting nickel and cobalt from laterite ores requires a severe condition of 250~270°C at 4~5MPa. Sulfuric acid is added to dissolve valuable metals such as nickel and cobalt together with iron and aluminium[3]. Iron and aluminium are removed in subsequent reactions whereas nickel and cobalt are leached selectively into the solution. Titanium is highly corrosion resistant under oxidizing and neutral condition, therefore, the parts of the autoclave that contact the acidic solution are made from titanium. However, considering the low strength of titanium at high temperature, and the cost, titanium-steel explosive clad plate is used as a substitute to meet the requirements of strength and corrosion resistance for autoclaves.

Autoclave design

Joint of Clad Plate

Titanium is not suitable for welding onto carbon steel and thus utilizing special structure is necessary to avoid direct contact between these two materials during the welding of Ti clad plates. For the butt welding of clad plates, a strip of titanium cladding at the weld locations must removed to prevent titanium fusion and weld defect. Posterior to carbon steel welding, a titanium strip (as wide as the one removed) is used to cover the areas where the cladding was removed. Then it is covered by another wider titanium strip, around which fillet weld is needed for sealing. While the carbon steel use for clad plate is always thick, narrow gap submerged arc welding is applied to avoid welding deformation and unnecessary consumption of solder.

Head Forming

For large-scale autoclaves, hemi-spherical or elliptical heads should be adopted. When it is technically difficult to form a one-piece head due to the heavy thickness or restricted module size, it is preferred to form a head with one crown and a number of segments. For the high pressure autoclave that Morimatsu has delivered, one head was formed with one crown and eight segments, see Figure 2.

416

Figure 2: Hemispherical head being welded

Nozzle Installation

Nozzles for pressure leaching autoclaves are made from integral forgings. Generally, the deviation allowance for nozzle installation is not highly restricted. However, for agitator nozzles, higher requirements must be applied. Titanium liners are fitted to nozzles. To avoid stress concentration on welds, the nozzle bottom is ground to round. The liner top is welded to sealing rings and the bottom welded to the internal sleeve. Similar to plate weld, an overlay strip is applied to the nozzle welding.

Telltale Hole

While the service conditions of autoclaves have been approaching the design limits, telltale holes are required for inspecting the integrity of materials including cladding[4]. As for circumferential welds, their cover strip is not continuous. A number of strips are welded to a weld so that they can be well protected during welding. Each weld has two telltale holes. While the strip is welded, shield gas is filled from one telltale hole and then vented from the other one. Such an approach could also be applied for final inspection and in-service inspection.

FABRICATION AND INSPECTION

The welding and assembly of equipment made of titanium clad plate should take place in a designated, clean and dry environment. At the same time, all titanium parts should be kept separate from black metal materials. The fabrication process of the main body is shown in Figure 3.
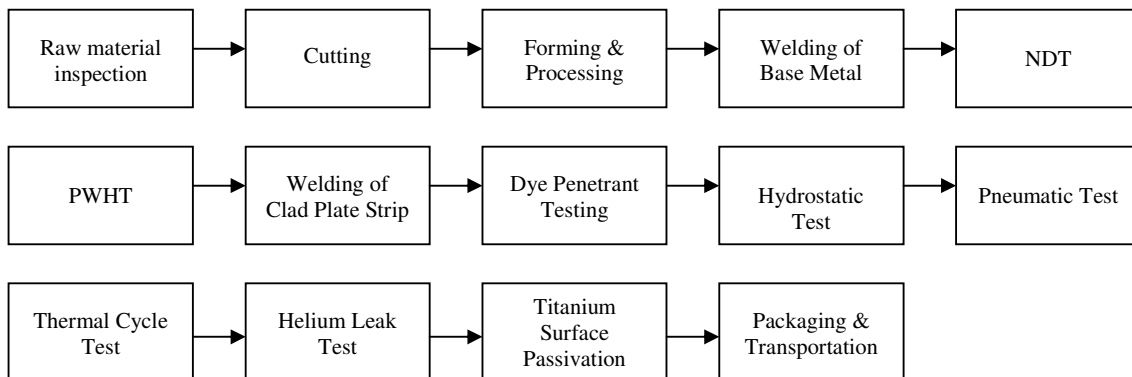
Figure 3: Autoclave fabrication process flow chart

Material Management

Materials obtained must be inspected as to whether the packaging, marking, specifications, material certificate, quality certificate, test reports and other documents are in conformity with the procurement requirements. The parameters of the mechanical properties must be re-tested. The titanium surface of clad plate is filmed in order to prevent iron contamination, see Figure 4.

417

Figure 4: Film protection for clad plate

Forming and Assembling

In order to ensure the bond between the clad and the base plate, the forming of the shell and head made of titanium clad plate should be done by cold forming process, while the effective protection of the titanium surface should be ensured during forming process. If hot forming process has to be used, the heating temperature for forming should be controlled below 600°C. The surface of the work piece should be thoroughly cleaned and coated with high temperature resistant coating to prevent surface oxidation and contamination[2].

Hemispherical Head

Hemispherical head is formed by a crown and several segments. The assembly of the segments is done on a flat, horizontal steel platform (see Figure 5); the deviation of the longitudinal sides between each of the segments must not exceed 2mm. After the 8 segments are put together, the crown is assembled on the top. The head is welded using double-sided symmetric groove welding technique on a welding positioner. Welding order is from the inside to the outside.

Figure 5: Head assembling   **Figure 6: Narrow gap submerged arc welding**

Shell Assembly Welding

The longitudinal weld groove of the shell plate needs to be processed first. Pre-bending should be done on both ends of the shell plate before rolling. Before joining the longitudinal welds, the longitudinal weld groove of the carbon steel should be polished and rust is removed. The deviation of the longitudinal welds of the clad plate in joining their counterparts should be less than 1mm. The welding of the lateral, internal side of the groove should be done using a combination of manual welding + automatic submerged arc welding technique, while the lateral, external side is done by narrow gap submerged arc welding technique (as Figure 6 indicates). After each shell section is welded and rolled into a round shape, the circumferential weld groove is processed by machine. Then, each shell section is welded together in a particular order to form a large piece. In joining the head and the first shell section by welding, a supporting shell needs to be welded to the external, lateral side of the head to facilitate the rotation of the shell on the wheel stand. After the whole autoclave shells are welded into several segments, heat treatment should be performed on each of the segments. These segments are then jointly welded to form two big segments which are then

418

combined to form a whole body. Local heat treatment is performed on the circumferential joint weld between each section.

Nozzle Installation

There are more stringent requirements for the deviation allowed for process nozzles such as agitator nozzles. In order to ensure the degree of deviation in welding the nozzles to the shell, specific tools are needed to fix the whole forging nozzle with flange support onto the shell. Welding of thick-walled nozzles to shell or head is done using the automatic saddle-groove welding technique to improve working conditions and also to ensure the welding quality[1]. However, given the large amount of welding to be performed, even if the above measures are taken, deformation is inevitable. As such, some allowance should be given to the thickness of the flange ring of the overall forging flange for processing. After the heat treatment for the shell and nozzle, nozzle flange should go through secondary processing to match the design drawing requirements.

Welding Titanium

The titanium surface should be free from ferric iron while longitudinal and circumferential welding of the strip with clad plate and in the welding of nozzle sleeves. The welding surface should be cleaned using titanium brush or other grinding methods before welding. Automatic plasma welding technique is used. Welding with high purity argon gas is used to protect and prevent the titanium from contamination when temperature rises above 370°C. Figure 7 shows the inspection qualified joints of the titanium strip.

Figure 7: Weld Joints of the titanium strip

Non-destructive Testing

The materials of the base plate and clad plate used to fabricate the titanium explosive clad plate should be UT tested in accordance with the requirements in ASME A578 and should be level B qualified. The clad plate must meet the A-level standard set out in ASME B898. The carbon base plate should be RT tested in accordance with UW-51 after completion of welding. Given the sizable thickness of the shell wall, ultrasonic testing could be done instead of RT testing under the provision of Code Case 2235. Thus, TOFD technique is used for longitudinal and circumferential weld inspection. RT testing is used to inspect the welding of nozzles to the shell and head. After hydrostatic test, internal titanium strip should be welded.

Heat Treatment

The autoclave is segmented according to the size of the heat treatment furnace. The outer surface of the carbon steel of each shell is equipped with 3 thermocouples in a top-down manner. The orientation is 0°, 90°, 180° and 270° respectively. In order to reduce the deformation of the opening of work piece during PWHT, the shell is strengthened by a stiffening ring on both ends.

Heat treatment process should be carried out in an electric furnace, and in order to prevent the oxidation of the titanium layer, the surface of the titanium clad plate is required to be coated with high temperature resistant coating for protection. Local heat treatment of the circumferential weld of each shell is done by tracking infrared electric heating. The tracking infrared electric heater is stripped to the outside of the welds. Insulation is performed on the inside and outside of the welds. The electric heater is controlled by microcomputer zoning program; the surface temperature of the

419

work piece can be displayed in real time by each thermocouple. The thermocouple has a measurement accuracy of $\pm 1^{\circ}C$.

In addition, temporary support needs to be set up on both sides of the circumferential welded shell to ensure that the center of each section is at the same horizontal level, therefore, reducing additional bending moment during the heat treatment process[5], and avoiding bending deformation of the shell caused by reduced strength of the material after heating.

Thermal Cycle Test

Due to the different properties of titanium and steel, in addition to the complex structure, even though equipment of titanium clad plate has successfully passed the hydrostatic test, there are still many occurrences of equipment failing in actual operation because of the cladding. The purpose of thermal cycle test is thus to test the reliability of the weld joints of the autoclave shell, the titanium cladding and the titanium liner of nozzles under simulated operating conditions.

Regarding the proper order between pressurization and heating, considering the impact on the strip welds imposed by temperature difference is significantly greater than that by the equipment internal pressure, the process scheme usually takes the order of heating first followed by pressurization. Equipment is heated to operating temperature before pressurized to operating pressure, then kept at the constant pressure and temperature for 1~2 hour(s), thereafter cooled down to a controlled temperature. This forms the first cycle. The equipment is then heated again to operating temperature limiting the temperature tolerance to $\pm 10^{\circ}C$, and kept at the constant temperature and pressure for 1~2 hour(s) before it is cooled down and depressurised to atmospheric pressure. This forms the second cycle. Following the thermal cycle test, a 100% PT test has to be conducted on the internal titanium welds of the equipment, and a helium leak test also needs to be performed again[6].

Helium Leak Test

For pressure vessels, the helium leak test is to detect whether the vessel has a small amount of leakage. As the key equipment in hydrometallurgical process, pressure leaching autoclave is designed to contain lots of strip structures, in view of which the safety requirements have to be more rigorous. Therefore, two telltale holes are located on each line (section) of the titanium strip welds. After the completion of titanium strip welding, the helium leak test is performed on each line (section) of the titanium strip welds using the telltale holes aforementioned. The compliance level is 1×10-5mbar•l/s.

PACKING AND SHIPPING

Each pressure leaching autoclave of these two series is more than 700t by weight; its packaging and transportation are thus a major difficulty. Shanghai Morimatsu Environment Plant is near to the Waigaoqiao Shipyard where all large autoclaves are finally assembled. After the equipment is approved by test and inspection, sand blasting and painting are done on the carbon steel surface, moreover the internal titanium cladding and the welds are pickling passivated and film protected.

All the process nozzles are equipped with gaskets and flange covers used for transportation. The inside of the equipment is filled with nitrogen for protection. 5 temporary saddles are utilized during transportation in order to improve the supporting counterforce asserted on the shell. The autoclave is transported to the Waigaoqiao Shipyard Terminal from Shanghai Morimatsu Environment plant using the hydraulic trailers.

After the precise center of gravity of the equipment is calculated, the equipment is hoisted and loaded, using two cranes that can handle a weight of 600t and 800t respectively, onto the ocean-going maritime ship for delivery. Graph 8 and Graph 9 shows the inland transportation and the hoisting of an autoclave, respectively.

420

Figure 8 Autoclave transported to the dock

Figure 9 Hoisting of the autoclave

CONCLUSION

In reference to the Ambatovy and Ramu projects, the design, fabrication, inspection and transport of large hydrometallurgical autoclaves are described in detail. Pressure leaching autoclave is the key reactor in the hydrometallurgical process. Since 2003, Shanghai Morimatsu has developed and manufactured a series of hydrometallurgical autoclaves amounting to nearly 20 units, and has therefore mastered the difference in material selection and structural characteristics of autoclaves utilized in the various hydrometallurgical processes for various ores. In actual engineering practice, an integral manufacture system, composed of design, fabrication and quality control has been formed, and a wealth of experience in the schedule management has been acquired simultaneously.

REFERENCES

1.   Lurong Mao, Honghai Xiao, "Design and Manufacture of Autoclave for Hydrometallurgy", ALTA 2008 Nickel/ Cobalt Conference, Perth, Australia, 2008,

2.   Lurong Mao, Guolun He, "Design and Manufacture of Titanium Clad Plate Pressure Reactor for Hydrometallurgy", Journal of Pressure Vessel, October 2005.

3.   Jianhua Li, Wei Cheng, Zhihai Xiao, "Processing Technology of Nickel Laterites", Journal of Hydrometallurgy of China, December 2004.

4.   Andrew Marchbank, Patrick Cheung, Brian Aird, Serge Jodoin & Robert Noble, "Managing the Fabrication & Delivery of the World's Largest Autoclaves in a New Business Environment" ALTA 2010 Nickel/Cobalt/Copper Conference, Perth, Australia, 2010.

5.   Weiming Ji, "Exploration of Coke Drum Construction Technology", the 7th National Pressure Vessel academic Conference, Wuxi, China, 2009.

6.   Jie Chen, Huaiwei Wang, "A Practice of Hot Gas Circle Test for Huge Titanium-steel Clad Pressure Vessel", the 7th National Pressure Vessel academic Conference, Wuxi, China, 2009.

7.   John G. Banker, "Titanium Clad Autoclave Performance in Nickel Laterite Hydrometallurgy", www.dynamicmaterials.com.

421

SELECTING SPECIALTY STAINLESS STEEL GRADES FOR SULPHURIC ACID LEACHING ENVIRONMENTS

By

Sophia Ekman

Outokumpu Stainless AB, Avesta Research Centre, Sweden

Presenter and Corresponding Author

Sophia Ekman
Sophia.Ekman@outokumpu.com

ABSTRACT

Treatment of metal-containing ores using sulphuric acid creates a corrosive environment and places high demands on the material used for construction of process equipment. Leaching (atmospheric or pressure) is considered the most aggressive stage, with higher acid concentrations and temperatures, as well as contamination (dissolved metal ions and chloride ions), compared to downstream processes. The combination of sulphuric acid, dissolved metal ions and chloride ions results in competing corrosion mechanisms and complicates the prediction of corrosion, making it difficult to select a suitable material. This paper contains results from laboratory corrosion tests performed on a variety of stainless steel grades at different temperatures. The tests have been performed in simulated leaching environments based on dilute sulphuric acid with addition of oxidative metal ions and different levels of chloride ions. The results have been compiled into a corrosion resistance diagram which seeks to provide a schematic guideline to the selection of specialty stainless steel grades for these environments. High alloyed austenitic stainless steel grades as well as high strength duplex grades are covered in the guideline.

INTRODUCTION

From copper wiring to the stainless steel structures of high-rise buildings, modern life is hugely dependent on the ore deposits stored in the Earth's crust. Mines are going deeper and deeper, while environmental legislation is simultaneously calling for the introduction of more sustainable extraction techniques. Hydrometallurgy has become a fast emerging process for recovery of various metal-containing ores. Treatment of these ores using sulphuric acid creates a corrosive environment and places high demands on the material used for construction of process equipment. Leaching (atmospheric or pressure) is considered the most aggressive stage within hydrometallurgy, with higher acid concentrations and temperatures, as well as contamination (dissolved metal ions and chloride ions), compared to downstream processes. To select a cost-efficient construction materials is difficult since the combination of sulphuric acid, dissolved metal ions and chloride ions result in competing corrosion mechanisms and complicates the prediction of corrosion. Stainless steels have proven to be useful materials for construction for hydrometallurgical process equipment since the corrosion resistance of the variety of stainless steel grades cover a wide range, from the low-alloyed standard austenitic grades such as 304 and 316 up to the super-austenitic grades 254 SMO®, 4565 and 654 SMO® and the super-duplex grade 2507. This paper contains results from laboratory corrosion tests performed on a variety of stainless steel grades at different temperatures. The tests have been performed in simulated leaching environments based on dilute sulphuric acid with addition of oxidative metal ions and different levels of chloride ions. The results have been compiled into a corrosion resistance diagram which seeks to provide a schematic guideline to the selection of specialty stainless steel grades for these environments. High alloyed austenitic stainless steel grades as well as high strength duplex grades are covered in the guideline.

STAINLESS STEELS

The definition of a stainless steel is an iron-base alloy with at least 10.5 % -by weight chromium. The addition of chromium creates the protective passive layer that gives the stainless steel its corrosion resistance. The passive layer mainly consists of chromium oxide that has a thickness of 2-3 nm. If the passive layer is damaged, and the steel is present in an environment that contains oxygen, the passive layer has the ability to self-heal, or re-passivate. But if the passive layer is damaged and is prevented from re-passivating by the environment, the steel may suffer from corrosion.   How corrosion resistant a stainless steel grade is depends on its alloying content. By taking into account the beneficial alloying elements that increases the corrosion resistance towards pitting corrosion in chloride containing environments, a rough estimation of the corrosion resistance of a stainless steel grade can be made. The pitting resistance equivalent value, PRE, includes the beneficial effect of chromium, molybdenum and nitrogen, and can provide a rough ranking of the different stainless steel grades, see Table 1. Another way of ranking different stainless steel grades are by performing laboratory corrosion tests. A common method used is ASTM G150 where the critical pitting temperature (CPT) is measured. The CPT value represents the lowest temperature where stable pitting corrosion occurs in a 1 M NaCl solution. A good resistance to pitting corrosion does not necessarily imply good resistance to other types of corrosion, but the alloying elements that have a beneficial influence on the PRE-values often improve the relative resistance to uniform corrosion in most acids.

There are three main families of stainless steels, Ferritic, Austenitc and Duplex grades. The names of the different families are related to their microstructure. Ferritic grades are mainly alloyed with chromium and sometimes molybdenum and are suitable for mild environments. They are therefore not further discussed here. Austenitic grades are alloyed with nickel, which gives them their austen-itic structure. The most common austenitic grades are the standard grades 304 and 316 that are general purpose grades with good resistance to atmospheric corrosion and many organic and inorganic acids. But there are others, e.g. 904L which is a higher alloyed austenitic grade that was especially developed for sulphuric acid environments and 254 SMO® (PRE = 43) which is a super-austenitic grade with high levels of chromium and molybdenum which gives it excellent resistance to localised corrosion.

654 SMO® is a super-austenitic grade that offers a level of pitting and crevice corrosion resistance beyond that of other stainless steels (PRE = 56). It is also nearly twice as strong as common austenitic stainless steels and is characterised by excellent ductility and toughness as well as good fabricability. 654 SMO® provides a combination of excellent corrosion resistance and superior mechanical properties that makes the stainless steel grade a very interesting alternative to nickel-base alloys such as Alloy C-276 and titanium.

Duplex Stainless Steels

Duplex stainless steels are characterised by a two-phase microstructure comprising interleaved austenite and ferrite with approximately a 50/50 ratio see Figure 1. The duplex microstructure combines advantages of both phases: the ferrite provides high strength and resistance to stress corrosion cracking (SCC), while the austenite contributes good ductility and general corrosion resistance. The duplex grades have lower levels of nickel and molybdenum than their austenitic counterparts. Generally, the duplex grades have approximately twice the mechanical strength as the austenitic grades, a higher surface hardness, but a lower rupture elongation.

The workhorse duplex stainless steel grade is 2205, EN 1.4462, which was developed in the 1970's. Subsequent developments have extended the range of duplex grades to both the high-performance super-duplex steels and the more economical lean duplex grades. A pioneer in the latter category is LDX 2101®, EN 1.4162, a low-alloyed, general-purpose stainless steel, where a part of the nickel content has been replaced by manganese and nitrogen, resulting in a leaner alloy[1]. The relatively low alloying content makes LDX 2101® less prone to precipitation of intermetallic phases than other duplex stainless steels and the high nitrogen content lead to good austenite reformation after welding. In 2010 a new member of the LDX® – family was introduced, LDX 2404®, which is based on the same alloying concept as LDX 2101®[2].The new member of the LDX® family fills a blank area in the established duplex steel property map and utilizes the advantages of modern production facilities. There is a distinct jump in corrosion resistance properties between 2304 and 2205. When characterizing these grades using a standard method, in this case ASTM G150, 2304 typically exhibits a CPT ≥20 °C and 2205 the significantly higher value of ≥50 °C, the new grade has been tailored to fill this gap and with the CPT value of 40 °C.
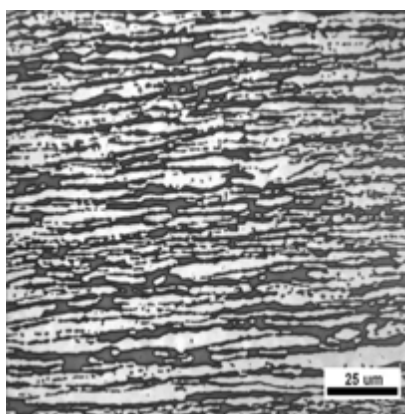
Figure 1: Example of a typical duplex microstructure, light phase austenitic, dark phase ferritic

The typical chemical composition of some duplex grades and austenitic grades with about the same levels of pitting and crevice corrosion resistance can be seen in Table 1. The Pitting Resistant Equivalent (PRE) and the Critical Pitting Temperature (CPT) values displayed in Table 1 shows that for every austenitic grade there is a corresponding duplex grade offering approximately the same corrosion resistance.

Table1: Typical Chemical Composition of Some Stainless Steel Grades

Outokumpu Grade	EN	ASTM/UNS	C	N	Cr	Ni	Mo	Others	Micro-structure	PRE	CPT [℃]
4307	1.4307	304L	0.02	-	18.1	8.1	-	-	A	18	<10
LDX 2101®	1.4162	S32101	0.03	0.22	21.5	1.5	0.3	5Mn	D	26	17±3
4404	1.4404	316L	0.02	-	17.2	10.1	2.1	-	A	24	20±2
2304	1.4362	S32304	0.02	0.1	23	4.8	0.3	-	D	26	22±3
LDX 2404®	1.4662	S82441	0.02	0.27	24	3.6	1.6	3Mn	D	33	43±2
904L	1.4539	904L	0.01	-	20	25	4.3	1.5Cu	A	34	62±3
2205	1.4462	S32205	0.02	0.17	22	5.7	3.1	-	D	35	52±3
254 SMO®	1.4547	S31254	0.01	0.2	20	18	6.1	Cu	A	43	87±3
2507	1.4410	S32750	0.02	0.27	25	7	4	-	D	43	84±2
4565	1.4565	S34656	0.02	0.45	24	17	4.5	5.5Mn	A	46	>90
654 SMO®	1.4652	S32654	0.02	0.5	24	22	7.3	3.5Mn, Cu	A	56	>90

® Registered trade names by Outokumpu, Alloying elements are given in %-by weight, A – Austenitic structure. D – Duplex (austenitic-ferritic) structure, PRE = %Cr+3.3×%Mo+16×%N, CPT – Critical pitting temperature, tested according to ASTM G150.

The typical mechanical strength values for different Outokumpu stainless steel grades are shown in Table 2. The higher mechanical strength of the duplex grades can be used to reduce the gauge of sheets and plates used in items such as tanks, where design is based on the proof strength of the material. This may result in large cost savings not only because of reduced material consumption but also because of e.g. less time required for edge preparation before welding and less consumption of filler material.

Table 2: Mechanical Properties (Typical Outokumpu Values) at 20℃ for Some Stainless Steel Grades According to[3]

Outokumpu Grade	EN	ASTM/UNS	Proof strength, $R_{p0.2}$ [Mpa]	Tensile strength, R_m [Mpa]	Elongation, A_5 [%]
4307	1.4307	304L	280	580	55
LDX 2101®	1.4162	S32101	480	700	38
4404	1.4404	316L	280	570	55
2304	1.4362	S32304	450	670	40
LDX 2404®	1.4662	S82441	480	680	33
904L	1.4539	904L	260	600	50
2205	1.4462	S32205	510	750	35
254 SMO®	1.4547	S31254	340	680	50
2507	1.4410	S32750	560	830	35
4565	1.4565	S34656	440	825	55
654 SMO®	1.4652	S32654	450	830	60

CORROSION ISSUES IN LEACHING ENVIRONMENTS

Sulphuric acid is the most commonly used acid for leaching of metal containing ores, concentrate ore matte, since it is cheap and often produced on site at facilities that treat sulphide ores. Stainless steel generally shows good corrosion resistance in oxidising acids. Sulphuric acid is an acid with dual properties. It is oxidising up to a concentration of about 40 %-by weight when it becomes reducing and very corrosive up to about 90 %-by weight, when it again becomes oxidising. If uniform or general corrosion occurs, it causes removal of material over a large surface, at a more or less constant rate. This can cause thinning of the wall thickness of a tank or pipe, until the remaining wall is unable to carry the mechanical load. But since uniform corrosion occurs at a constant rate, laboratory corrosion tests can predict the corrosion rate in different environments. In pure sulphuric acid environments the uniform corrosion rate of a stainless steel increases with acid concentration and temperature as shown in Figure 2.

Leaching process solutions rarely consist of pure sulphuric acid. There are often different types of impurities present in the process solutions. Examples of impurities are chloride ions and dissolved metal ions. Metal ions like cupric and ferrous/ferric ions are known to have a positive effect on uniform corrosion of stainless steels when added to sulphuric acid. Electrochemical investigations show that oxidising ions like Cu^{2+} and Fe^{3+} increases the open circuit potential of the sulphuric acid

solution and push the stainless steel into its passive state. The metal ions act as inhibitors for uniform corrosion on stainless steels in sulphuric acid, which makes it possible to use standard grades, like e.g. 4404 (316L), at acid concentrations and temperatures which otherwise would be far too aggressive.
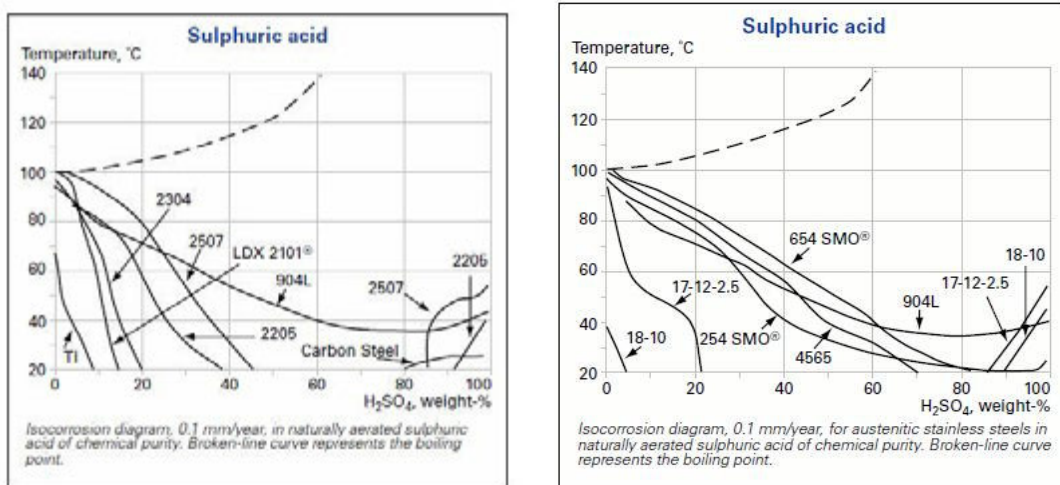
Figure 2: Iso-corrosion diagrams in pure sulphuric acid showing a corrosion rate of 0.1 mm/year for duplex stainless steels (left) and austenitic stainless steels (right), based on laboratory corrosion tests[4]. 904L is included in both diagrams for reference.

Chloride ions are often also present in leaching environments. The chloride ions may originate from the ore or concentrate its self, ground water contaminated by chlorides by the breakdown of ore or neighboring ore bodies, or even by using sea water as make-up water. Chloride ions may have three negative effects on the corrosion resistance of stainless steel, depending on content and temperature. When a sufficient amount of chlorides are added to sulphuric acid it can increase the uniform corrosion rate, above the rate in pure acid. Another affect is that chloride ions may initiate localised corrosion, such as pitting and crevice corrosion. Pitting corrosion is characterised by small holes/pits on the surface while the majority of the surface area remains unharmed. The pit acts as the anode while the rest of the surface acts as the cathode. This results in an unfavorable anode/cathode area ratio and a high corrosion rate of the anode. When the metal corrodes, dissolved metal ions generate an environment with a low pH and chloride ions migrate into the pit to balance the positive charge of the metal ions.The environment inside the pit will gradually become more and more aggressive and re-passivation of the pit becomes more unlikely.

The mechanism behind crevice corrosion is related to that for pitting corrosion. Crevice corrosion takes place in crevices or on shielded surfaces or under deposits. In narrow crevices, the influence of capillary forces is significant and it is thus almost impossible to avoid the penetration of liquid into a crevice. Oxygen and other oxidants are consumed for the maintenance of the passive layer in the crevice just as on the unshielded surface. However, in the stagnant solution inside the crevice, the supply of new oxidant is restricted. The composition of the solution within the crevice thus gradually becomes different from that of the ambient solution. This difference in composition increases the risk for corrosion as a "concentration cell" is created. The chloride ions can then easily penetrate the passive layer and crevice corrosion is initiated.

The third effect of chloride is that it can cause stress corrosion cracking. Stress corrosion cracking (SCC) is a type of brittle failure caused by the combined effect of tensile stress and a corrosive environment. Like pitting and crevice corrosion, stress corrosion of stainless steels is most frequently caused by solutions containing chloride. However, most cases of stress corrosion cracking on stainless steels occur at high temperature.

All three types of localised corrosion may cause penetration of a tank or pipe wall and subsequent risk of leakage of solution, see Figure 3. The combination of chloride ions and dissolved oxidative metal ions increases the risk for localised corrosion on stainless steels. The oxidative effect of the metal ions may push the stainless steels not only into its passive state but even over the critical potential for initiation of localised corrosion, see Figure 4. The combination of different factors like acid concentration, oxidative metal ions, chloride content and elevated temperatures, complicates the prediction of corrosion, since all the factors affect different types of corrosion.

Figure 3: Examples of chloride induce localised corrosion, pitting (left), crevice corrosion (middle) and stress corrosion cracking (right).
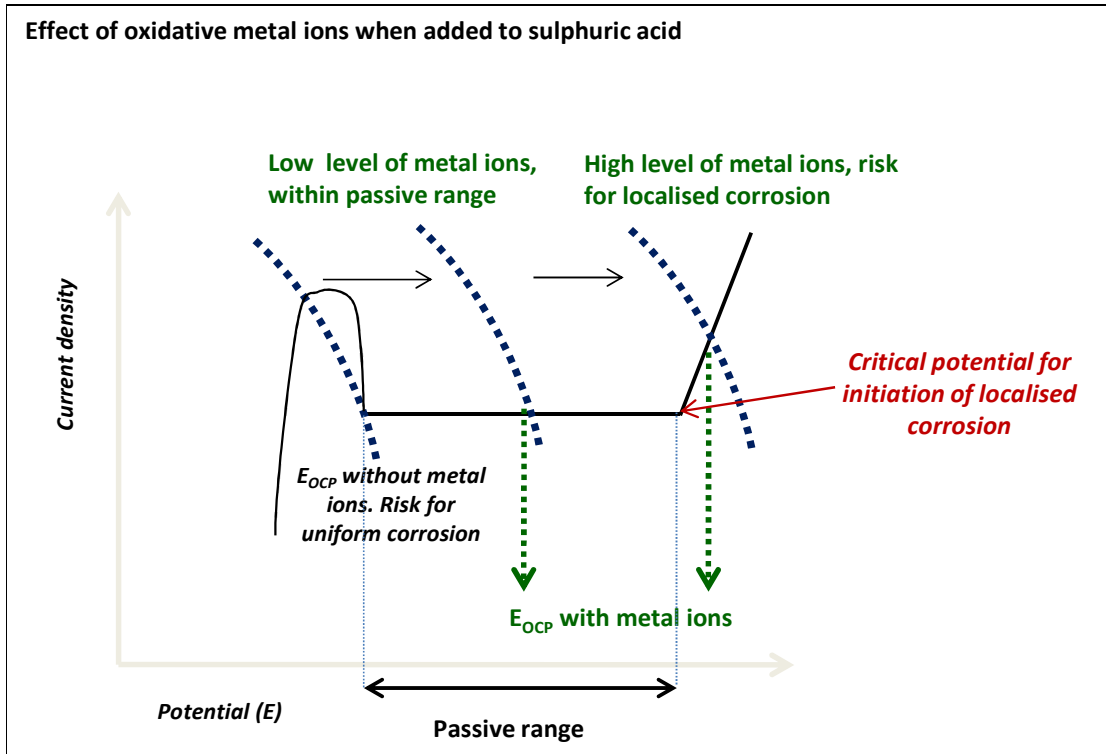

Figure 4: Schematic illustration of the oxidative effect of metal ions added to sulphuric acid

Within the hydrometallurgical industry the leaching stages (atmospheric or pressure) considered as the most demanding process step for the use of stainless steels. The acid concentrations, temperatures and chloride content are often higher during the leaching step compared to other process steps downstream. But there are possibilities to identify a suitable steel grade to use as construction material for leaching applications within the groups of superaustenitic and superduplex stainless steel grades. Tools like laboratory corrosion tests in simulated environments, field exposures in real applications and previous experience is very useful when selecting an appropriate material.

LABORATORY CORROSION TESTS

At Outokumpu Avesta Research Centre different series of laboratory corrosion tests have been performed over the years, in environments that simulate those that exist in different leaching processes. Some results have been published previously[5]. A new series of laboratory corrosion tests have been performed where the new addition to the LDX®-Family, LDX 2404®, has been tested for the first time.

Experimental Set-Up

The laboratory corrosion tests have been performed as 30-day immersion tests of stainless steel samples of different grades. Duplicate flat coupons 60 mm × 30 mm × thickness mm and welded coupons of the same size equipped with crevice washers of INCO type were used for testing. The crevice washers were tightened with a torque of 1.58 Nm to ensure a reproducible crevice for each sample. The tests were based on dilute sulphuric acid with additions of oxidative metal ions (Cu^{2+} and Fe^{3+}) and chloride ions of various contents, and at different temperatures. Most of the test were performed at atmospheric pressure but some tests were performed at higher temperatures (110-250°C) using autoclaves. The weight of the samples was noted before and after exposure so that the corrosion rate in mm/year can be calculated using the weight loss, exposure time and area of the specimens. If the corrosion rate is below 0.1 mm/year the material is considered to be corrosion resistant in that environment, provided there is no pitting or crevice corrosion attack. An example of the test specimens and the experimental set-up is shown in Figure 5.
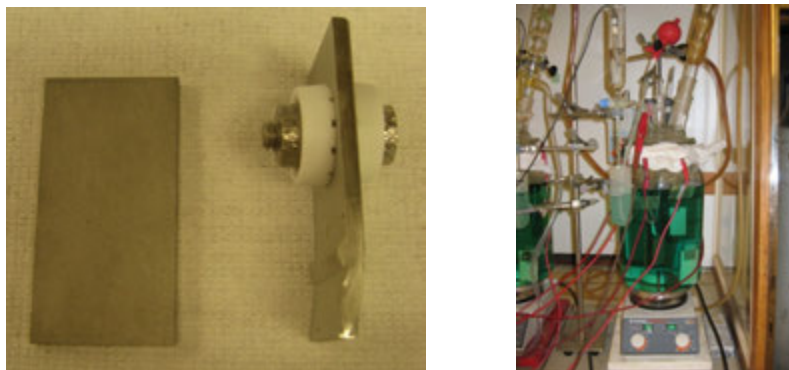
Figure 5: Examples of test coupons used in laboratory corrosion tests (left) and experi-mental set-up (right)

Laboratory Test Results

The results from the laboratory corrosion tests that previously have been published are summarised in Table 3 and Table 4. The new series were based on 18% sulphuric acid, with additions of 5 g/L Fe^{3+} and 4 g/L Cu^{2+} and 100, 500, 1000, 1500 and 2000 ppm of chlorides. The tests were per-formed at three different temperatures, 80, 60 and 40°C.The results from this new test series including LDX 2404® are shown in Table 5.

Previous tests results, shown in Table 3 and Table 4, shows that 4307 is unsuitable for these types of environments. The chloride ions initiated severe localised corrosion on the samples of this grade and the attack propagated with high corrosion rates, resulting in large weight losses. The duplex LDX 2101® and 2304 have the same PRE and rather similar pitting corrosion resistance as stated in Table 1, but behave differently in the solutions given in Table 3. LDX 2101® shows some selective corrosion of the ferritic phase where localised corrosion have been initiated. 2304 showed no pitting or crevice corrosion. Generally for all steel grades tested in these types of environments corrosion attack have mainly been of localised nature (pitting and/or crevice corrosion).

Previous test results displayed in Table 3 and Table 4 show that 4404 and LDX 2101® are useful grades if the chloride content and temperature are low. An interesting result is that the duplex grade 2205 performed just as well as the more highly alloyed and usually more expensive grade 904L. In general, higher alloyed grades are needed as the temperature and chloride content are increased. One interesting result is that in a dilute sulphuric acid solution (1%) with 5000 ppm chloride ions and at a temperature of 98°C, the superaustenitic grade 654 SMO® was the only stainless steel grade that was fully corrosion resistant. A result which is similar to that of the Ni-base alloy C-276. Test results also indicate that if the acid concentration is increased (to 10%), at 98°C, 654 SMO® could even outperform the more expensive C-276, that suffered from uniform corrosion.

Table 3: Results from laboratory corrosion tests in 10% sulphuric acid, 5 g/L Fe^{3+} and 4 g/L Cu^{2+} displayed as average corrosion rates in mm/year for duplicate coupons[4]

Temp. [°C]	[Cl] ppm	4307	LDX 2101®	4404	2304	904L	2205	254 SMO®	2507	4565
50	200	NT	NT	0	NT	0	0	0	0	NT
	500	1.961 p/c	0.001 c	0	0	0	0	0	0	0.005
	700	1.776 p/c	0 c	0	0	0	0	0	0	0.000
70	200	1.371 p/c	0.001	0.001	0.001	0	0.001	0.001	0	0.001
	500	2.516 p/c	0.001	0.765 p	0.001	0.001	0	0.002	0	0.001
	700	0.739 p/c	0	2.521 p	0	0.001	0.001	0.002	0	0
90	200	1.926 p/c	0.006	0.004	0.002	0.001	0.005	0.008	0.004	0.002
	500	2.691 p/c	0.003 p/c sel.corr	p/c	0.002	0.001	0.004 p in HAZ	0.006	0.003	0.002
	700	3.141 p/c	1.351 p/c sel.corr	Weld decay	0.002	0.001 p in HAZ	0.004	0.006	0.003	0.003
110	500	NT	NT	NT	NT	0.008 p in HAZ	0.02	0.022	0.015	NT
	700	NT	NT	NT	NT	0.009	0.03	0.025	0.019	NT
125	200	NT	NT	2.424 p/c	NT	0.127	0.056	0.125	0.046	NT
	500	NT	NT	NT	NT	0.037 p in HAZ	0.064	0.065	0.053	NT
	700	NT	NT	NT	NT	0.125	1.708 p	0.117	0.041 p	NT
150	200	NT	NT	NT	NT	0.466	0.406	0.702	0.309	NT
	500	NT	NT	NT	NT	3.82 p	3.015 p	0.751	1.318	NT
	700	NT	NT	NT	NT	4.519 p	14.337	1.278 p	3.929 p	NT

1.961 = corrosion rate of 1.961 mm/year, p = pitting corrosion, c = crevice corrosion, HAZ = Heat affected zone, sel.corr = selective corrosion, NT = Not tested

Table 4: Test results from laboratory corrosion tests in various solutions. Results are shown as average corrosion rates for duplicate coupons given in mm/year[4]

Temp [°C]	Cl⁻ [ppm]	H_2SO_4 [% by weight]	Fe^{3+} [g/L]	Cu^{2+} [g/L]	4404	904L	2205	254 SMO®	2507	654 SMO®	C-276	Ti
98	100	1	5	4	0.001	0.001	0.001	0.002	0.001	0.001	0.100	0.001
	500	1	5	4	3.140 p/c	0.904 p/c	0.615 p/c	0.001	0.001	0	0.059	0
	1000	1	5	4	4.067 p/c	2.562 p/c	1.024 p/c	0.001 p/c	0.110 p in weld	0	0.061	0
	5000	1	5	4	10.224	6.646 p/c	1.848 p/c	0.06 p/c	0.172 p/c	0	0.05	NT
	100	10	5	4	0.016	0.006	0.005	0.012	0.006	0.004	0.260	0
	100	10	25	4	0.017	0.006	0.008	0.014	0.007	0.004	0.270	0.001
	500	1	5*	4	0.155 p/c	0.621 p	0.000 p	NT	NT	NT	NT	NT
	1000	1	10*	4	0.161 p/c	0.74 p/c	0.160 p	0 p/c	0 p in weld	NT	NT	NT
150	100	0.5	5	4	NT	NT	0.015 p	0.016	0.016	0.008	1.208	0
	1000	0.5	10	4	NT	NT	2.668 p/c	0.230 p/c	0.629 p	0.034 p	0.000	0
250**	100	0.5	5	4	NT	NT	1.430 p/c	2.380	2.340	0.875	NT	0

* Additions of 3 ppm thiourea as an inhibitor. ** Test terminated after one day due to autoclave failure. 1.961 = corrosion rate of 1.961 mm/year, p = pitting corrosion, c = crevice corrosion, HAZ = Heat affected zone, NT = Not tested

Table 5: Results from laboratory corrosion tests in 18% sulphuric acid with 5 g/L Fe^{3+} and 4 g/L Cu^{2+} given as average corrosion rate in mm/year for duplicate specimens

Temp [℃]	Cl⁻ [ppm]	LDX 2101®	2304	LDX 2404®	2205	2507
80	100	0	0	0	0	0
	500	0.008 c sel.corr	0.002	0.004	0.005	0.004
	1000	1.409 p/c sel.corr	0.001 c sel.corr	0.002	0.003	0.002
	1500	3.575 p/c sel.corr	0.001	0.002	0.002	0.002
	2000	6.296 p/c sel.corr	1.005 p/c sel.corr	0.001	0.002	0.001
60	100	NT	NT	NT	NT	NT
	500	0	0	0	0	0
	1000	0	0	0	0	0
	1500	0.23 p/c	0	0	0.001	0
	2000	0.02 p	0	0	0.001	0
40	100	NT	NT	NT	NT	NT
	500	NT	NT	NT	NT	NT
	1000	NT	NT	NT	NT	NT
	1500	0	0	NT	NT	NT
	2000	0	0	NT	NT	NT

1.409 = corrosion rate of 1.409 mm/year, p = pitting corrosion, c = crevice corrosion, NT = Not tested, sel.corr = selective corrosion

The results from the new test series, shown in Table 5, show that in the environments tested the new grade LDX 2404® performed on a level with the higher alloyed grades 2205 and 2507, and showed no signs of corrosion. Both LDX 2101® and especially 2304 showed good results at low temperatures, but when the temperature and chloride content increased, both grades suffered corrosion. An interesting feature is that when LDX 2101® and 2304 suffered severe corrosion in these environments the attack propagated selectively into the ferritic phase of both grades, see Figure 6. This could be compared to the results lower chloride concentrations shown in Table 3, where 2304 did not suffer from corrosion
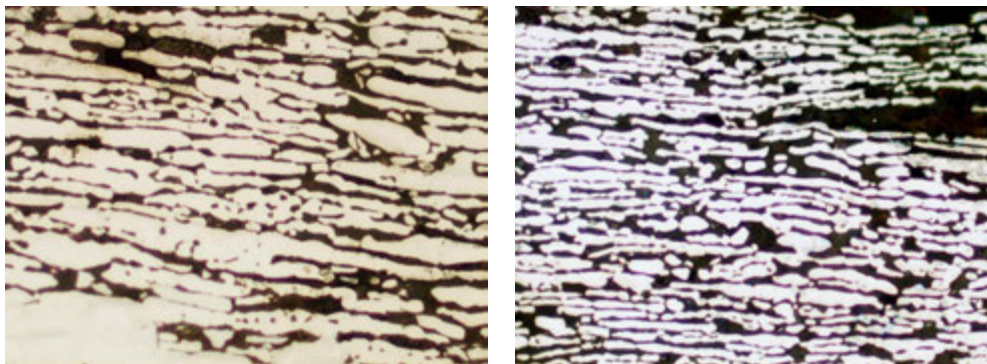
Figure 6: Cross sections at 400X magnification of LDX 2101® (left) and 2304 (right) samples exposed to a 18% sulphuric acid solution with addition of metal ions at 80℃ and 2000 ppm Cl⁻ showing selective corrosion of the ferritic phase. White phase is islands of remaining austenite

A common observation from all the environments tested is that, when a sample has suffered corrosion, localised corrosion has in most cases been the cause of failure.

CORROSION RESISTANCE DIAGRAMS

An attempt has been made to establish diagrams from the laboratory test data presented in Tables 3-5 in which it would be indicated under what environmental conditions corrosion is likely respectively unlikely to occur. How this could be done is exemplified in Figure 7. If the sample has suffered from a corrosion rate >0.1mm/year or any type of localised attack, the sample has failed and the environment is considered corrosive.

The required level of oxidizing ions like cupric and ferric ions has not been established but it is clear that the amount of oxidizing ions present in the solutions, in the range of several thousand ppm, is high enough to ensure passivity of the stainless steel surface in the majority of cases.
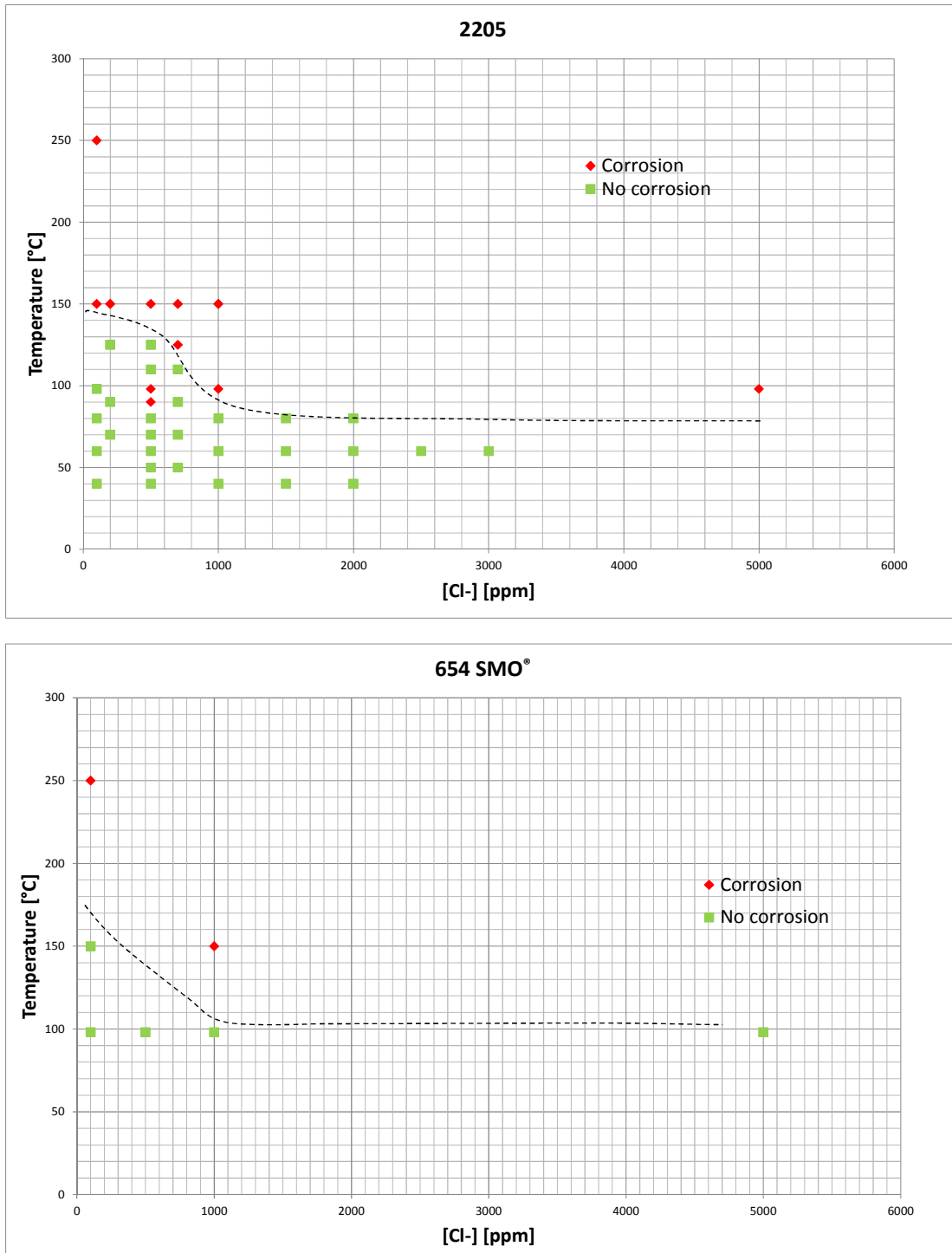
Figure 7: conditions giving a corrosion rate of 0.1 mm/year and/or localised attack on grades 2205 and 654 SMO® in sulphuric acid (0.5 – 18%) in the presence of oxidising ions

The full corrosion resistance diagram for the use of different stainless steel grades in hydrometallurgical solutions containing up to 18% sulphuric acid is shown in Figure 8 and based on the upper limits of 0.1 mm/year corrosion rate and/or the presence of localised attack. The tests have shown that the chloride content and the temperature overshadow the acid concentration (up to 18%) and thereby set the limits for the use of stainless steel grades in these types of environments. More data

is desirable, especially at chloride concentrations above 2000 ppm. There is only one set of data at 5000 ppm chlorides and the acid concentration was only 1% in that case. Thus the upper limits for 254 SMO® and 2507 are approximate. The austenitic grade 654 SMO® only showed corrosion at 250 °C, 100 ppm chlorides and 150°C and 1000 ppm chlorides where at lower temperatures the limit has not yet been established. In the tests performed at 98°C and 1000 respectively 5000 ppm chlorides all grades tested, except 654 SMO® suffered corrosion. LDX 2404® has not yet been added to the corrosion resistance diagram, since there is not enough data at the present time. But the tests performed indicate that LDX 2404® performs better than 2304 and in parity with 2205.

The corrosion resistance diagram seeks to provide a guide, not absolute design limits, for sulphuric acid solutions with high content of oxidative metal ions. Chloride content, temperature and acid concentration all play a role. If the acid concentration is increased the environment will become more corrosive and the lines in the corrosion resistance diagram will be pushed down, resulting in narrower limits for the use of stainless steels.
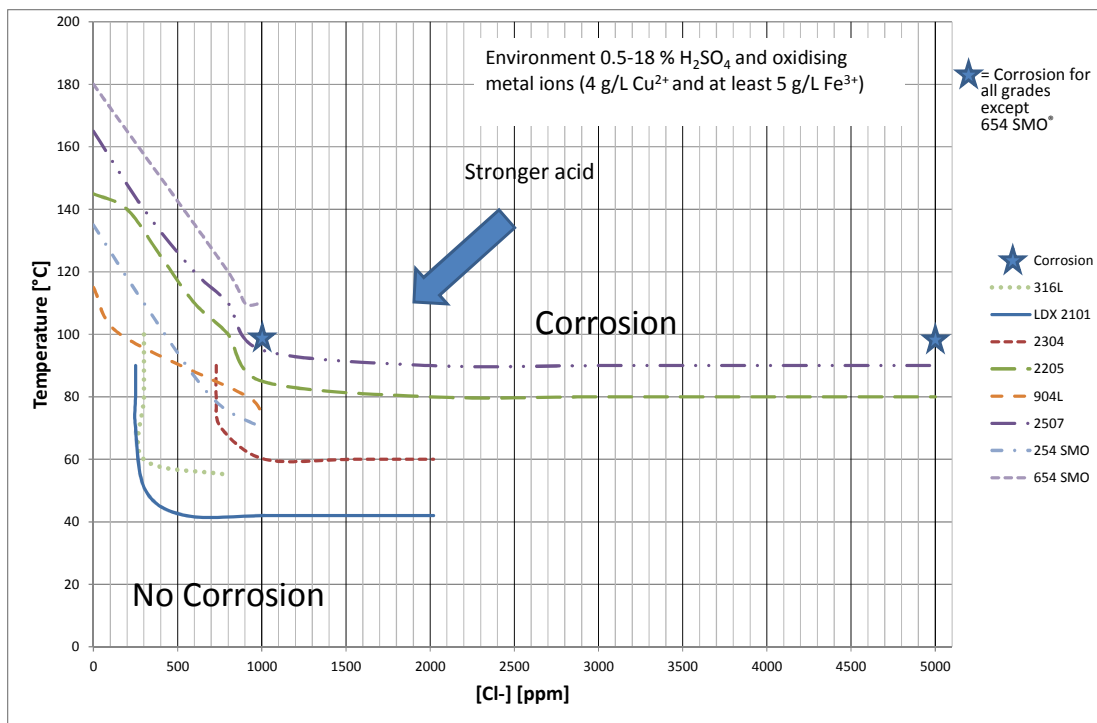
Figure 8: Corrosion resistance diagram for the use of stainless steel grades in sulphuric acid solutions (up to 18%) with additions of oxidative metal ions.

CONCLUSIONS

- The beneficial effect of dissolved oxidizing ions up to 9000 ppm on uniform corrosion is significant compared to pure sulphuric acid. The beneficial effect increases with increasing level of dissolved oxidizing ions. However, the minimum or maximum levels have yet to be established.
- Apart from addition of dissolved oxidizing ions, temperature is the most important factor influencing general corrosion on stainless steel.
- Chloride content is the second most important factor. The chloride effect overshadows the acid concentration when the latter is in the 1 – 18% range.
- The standard grade 4307 is unsuitable for exposure to 10% sulphuric acid containing 100 – 700 ppm chlorides.
- LDX 2101® and 2304 are applicable in a narrower range of acid concentrations than 2205, due to selective attack of the ferrite phase.
- Recent results for the new grade LDX 2404® indicate a great potential for usage in hydrometallurgical environments.
- 654 SMO® outperforms all other stainless steel grades in these types of environments.

REFERENCES

1. P. Johansson, M Liljas, "A new lean duplex stainless steel for construction purposes" 4th European Stainless Steel – Science and Market Congress, 10-13 June 2002, Paris, Vol. 2, 153.

2   J-O. Andersson, E. Alfonsson, C. Canderyd, H.L. Groth, "Development and Properties of New Duplex Stainless Steels", Stainless Steel World America, 5-7 October 2010, Huston, Texas, USA, Paper PSA10_040.

3   Outokumpu technical data sheet 1045EN-GB:6   "Steel Grades, Properties and Global Standards", Centrumtyryck AB, Avesta Sweden, October 2010.

4   Outokumpu Corrosion handbook, 10th edition, Sandvikens tryckeri, 2009.

5   S. Ekman and E. Torsner, "Special Stainless Steel Grades for the Hydrometallurgical Industry", Copper 2010, 6-10 June 2010, Hamburg, Germany, Vol. 5, p.p. 1857.

ALTA 2011
NICKEL/COBALT/COPPER

PAL OF LATERITES FORUM

MURRIN MURRIN OPERATIONS
PAST, PRESENT AND FUTURE

By

Matt Brown

Minara Resources, Australia

Presenter and Corresponding Author

Matt Brown

mbrown@minara.com.au

Important Notice

This presentation contains certain statements which may constitute "forward-looking statements". Such statements are only predictions and are subject to inherent risks and uncertainties which could cause actual values, results, performance or achievements to differ materially from those expressed, implied or projected in any forward-looking statements.

No representation or warranty, express or implied, is made by Minara that the material contained in this presentation will be achieved or prove to be correct.

Except for statutory liability which cannot be excluded, each of Minara, its officers, employees and advisers expressly disclaims any responsibility for the accuracy or completeness of the material contained in this presentation and excludes all liability whatsoever (including in negligence) for any loss or damage which may be suffered by any person as a consequence of any information in this presentation or any error or omission there from.

Minara accepts no responsibility to update any person regarding any inaccuracy, omission or change in information in this presentation or any other information made available to a person not any obligation to furnish the person with any further information.

Corporate Overview

- Founded in 1994 and became Minara Resources Ltd in 2003

- Murrin Murrin project is a 60/40 JV between Minara and Glencore International AG

- Glencore own approximately 70.5% of Minara

- High Pressure Acid Leach – name plate capacity 40,000 tonnes nickel and 2,500 tonnes cobalt per annum.

- Heap Leach – current plant capacity 2,000 tonnes per annum

2011 Aerial

Murrin Murrin: Location & Infrastructure

Murrin Murrin: Climate

- Arid. Some summer rain mainly from ex tropical cyclones and local thunderstorms. Little winter rains.
- Median yearly rainfall: 219 mm
- Average summer temperatures, ^oC

	Max	Min	#days >35°C
November	32.2	17.0	9
December	35.3	20.6	17
January	37.1	21.7	22
February	35.1	20.9	21
March	32.7	18.6	19
July	18.5	6.1	0

Average # days per year > 30°C = 150; >35°C =81; >40°C = 25

Murrin Murrin: Mining Areas, Tenements & Water Borefields
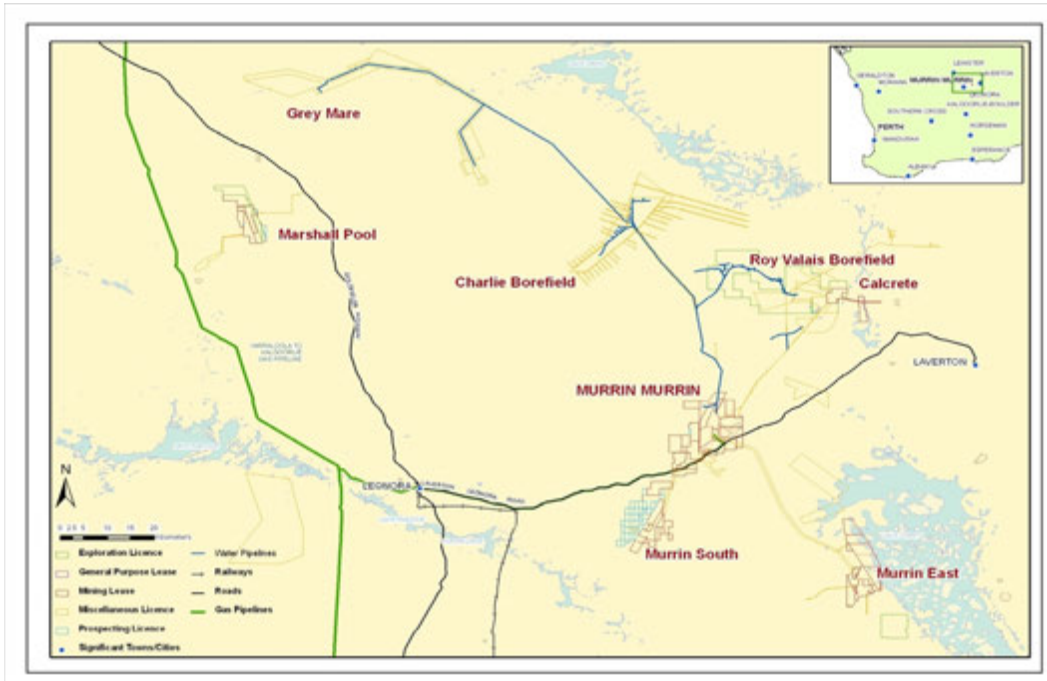
Murrin Murrin: Village (circa 2008) ~ 8km from Plant Site

Murrin Murrin - Mining

Murrin Murrin - Mining

Resources and Reserves

Murrin Murrin Resources and Reserves as at 31 December 2010: (Minara 60%)

Mineral Resources				
Resource Category	Tonnage (million tonnes)	Nickel Grade %	Cobalt Grade %	Cut-off Grade Nickel
Measured	114	1.03	0.076	0.8%
Indicated	106	0.99	0.076	0.8%
Inferred	10	0.94	0.058	0.8%
Scats	1	1.01	0.073	
Stockpiles (Measured)	37	1.02	0.068	
TOTAL	**268**	**1.01**	**0.074**	

Ore Reserves			
Reserve Category	Tonnage (million tonnes)	Nickel Grade %	Cobalt Grade %
Proven	93	1.06	0.082
Probable	65	1.04	0.079
Scats	1	1.01	0.073
Stockpiles	37	1.02	0.068
TOTAL	**196**	**1.05**	**0.078**

Murrin Murrin - Mining

- Open cut and shallow. Average depth 50-60m. No underground mining

- Multiple pits operated over a very large area approximately 200 sq km

- Over 37 Mt of ore stockpiles plus over 1 Mt of scats (feed for Heap Leach)

- Approximately 3-4 months stock on ROM pad and intermediate ROM stockpiles. ROM stocks promote "ageing" (dehydration) and some improvement of slurry feed density into the autoclaves – increasing throughput

- Mineralogy is primarily smectite clays, serpentine and iron oxides

Murrin Murrin - Mining

- Resource definition conducted on a 50m x 25m grid using vertical RC air core drilling, sampling on 1m intervals.

- Resource estimation conducted using indicator kriging.

- Grade control – vertical RC air core drilling, sampling on 1m intervals on a 12.5m x 12.5m pattern.

- Grade control modelling conducted using conditional simulation.

- Pit optimisation conducted using Whittle 4X and pit shells created from Net Value calculations including commodity prices, exchange rates, mining, milling, processing, haulage, refining and fixed costs based on multi element data (eg Ni, Co, Mg, Al, Fe).

Mining – ROM Grade, Nickel
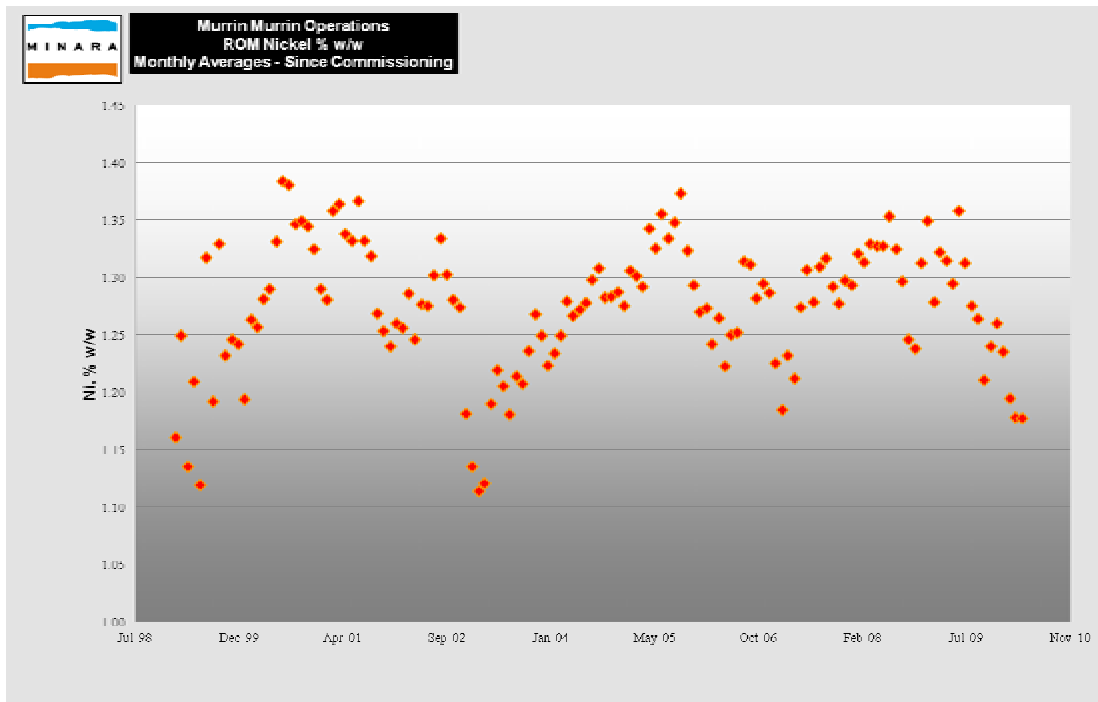
Mining – ROM Grade, Cobalt
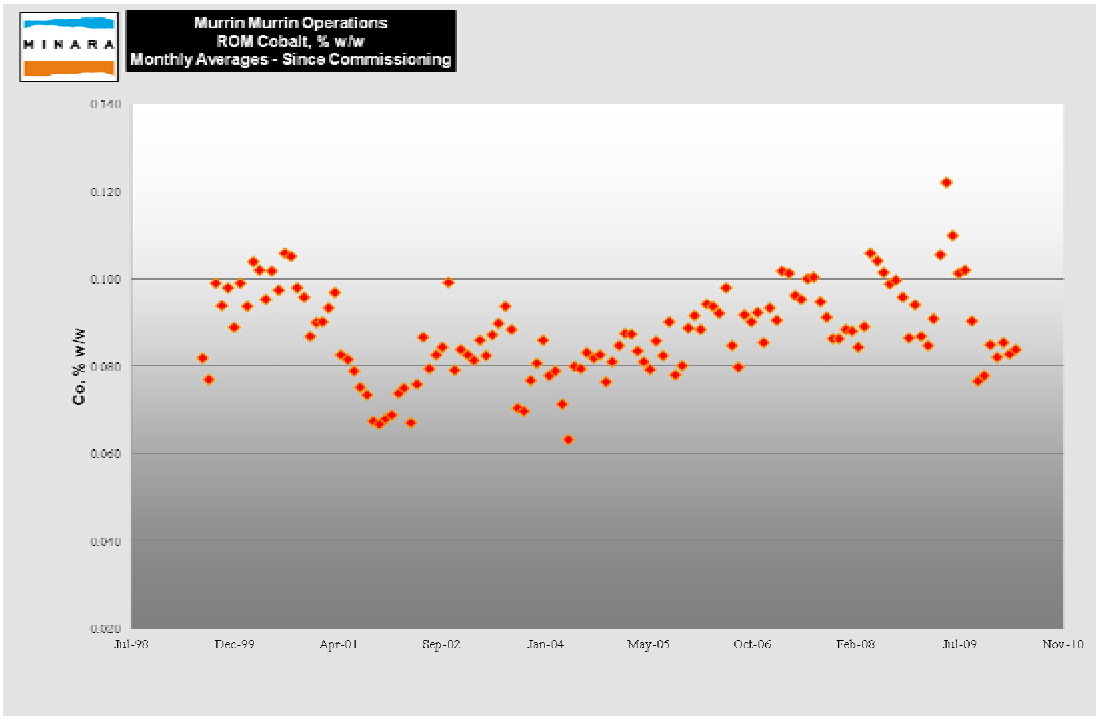
Process Plant Overview

Process Plant Overview
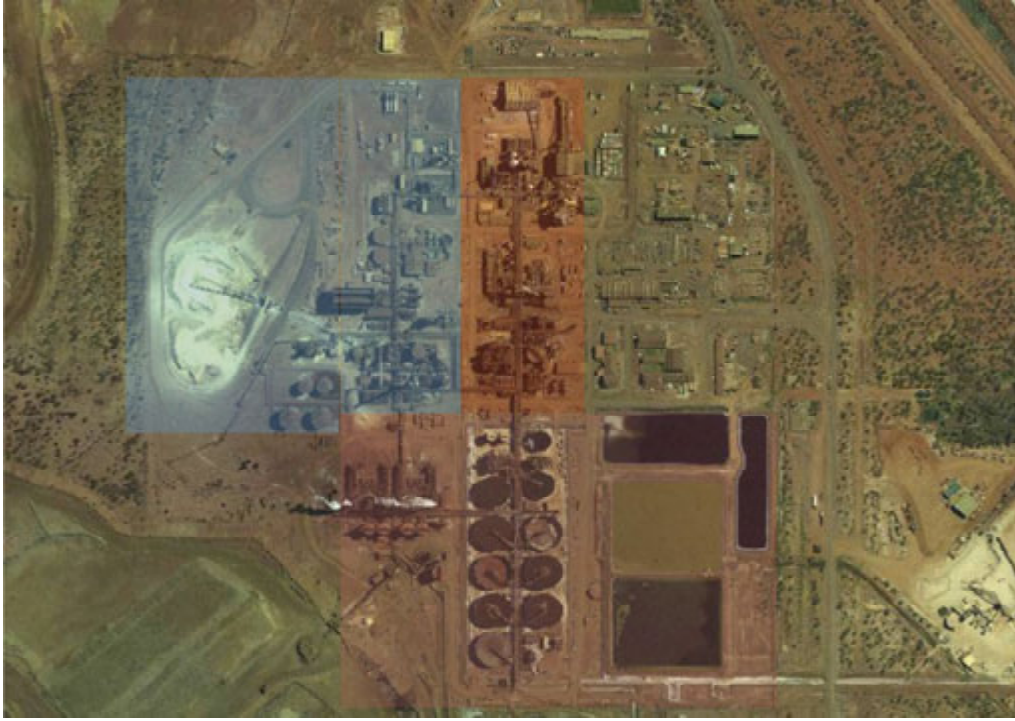
Flowsheet - Ore to Mixed Sulphides
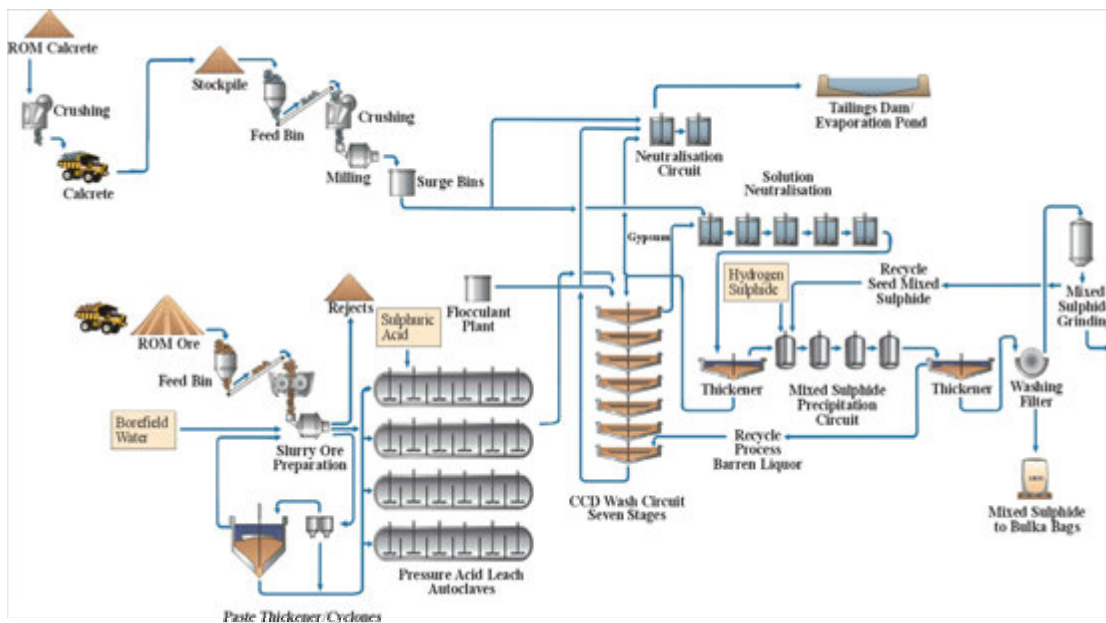
Flowsheet - Mixed Sulphides to Briquettes
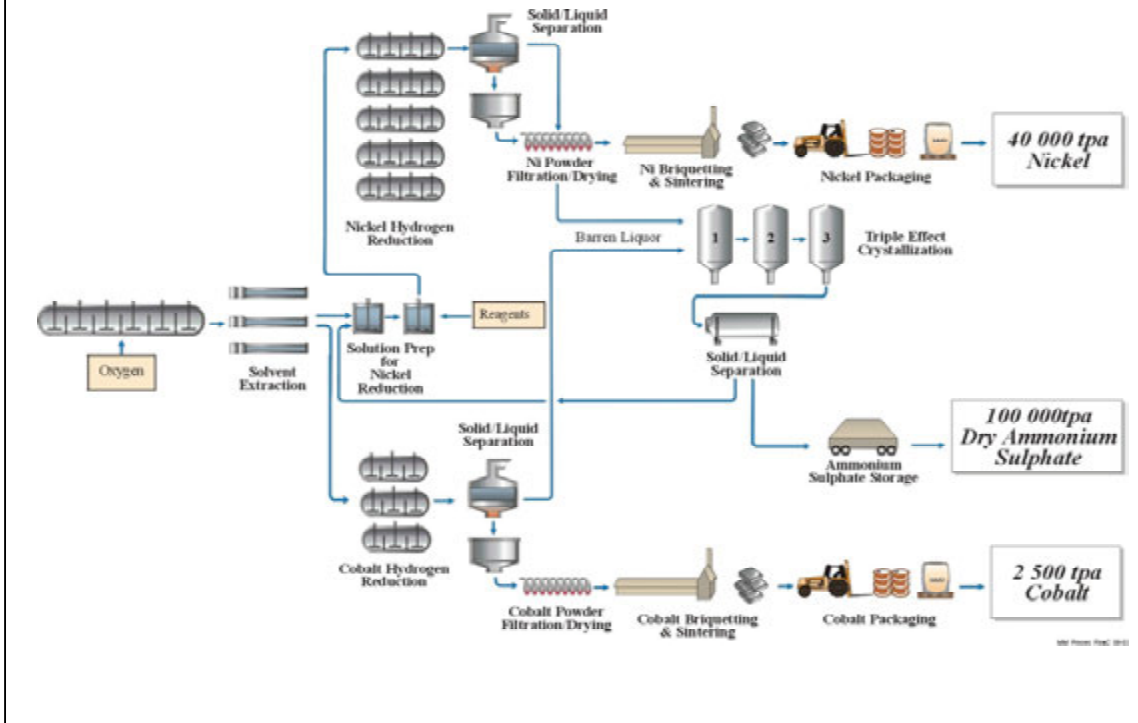
Flowsheet - Heap Leach
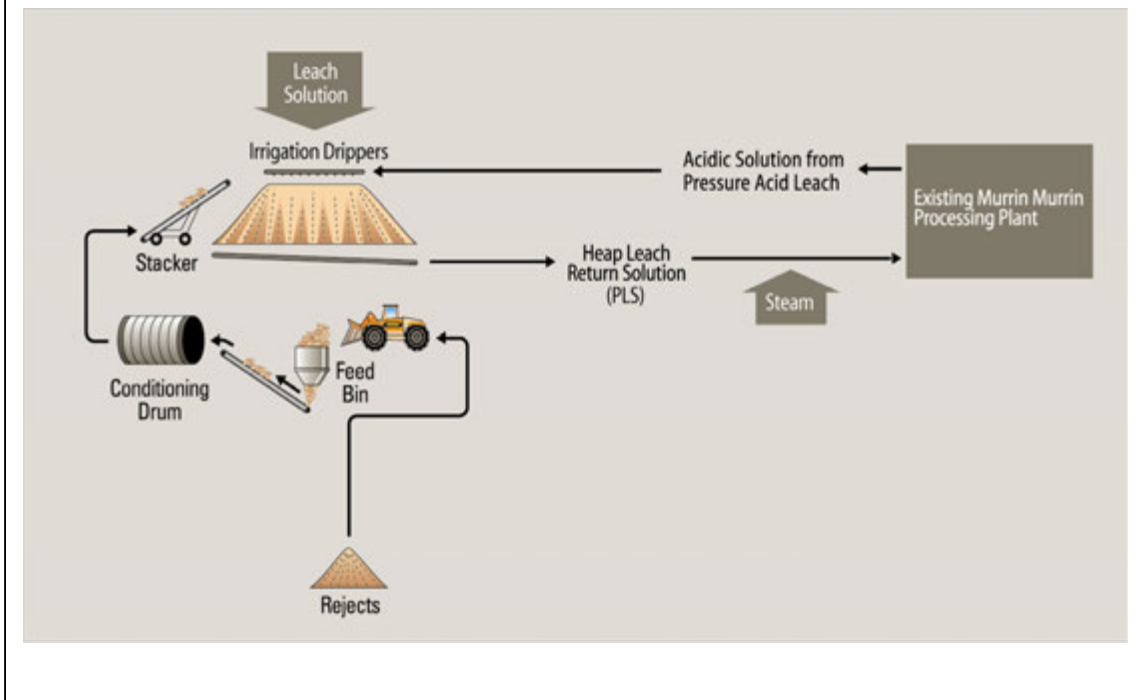
Flowsheet – Utilities
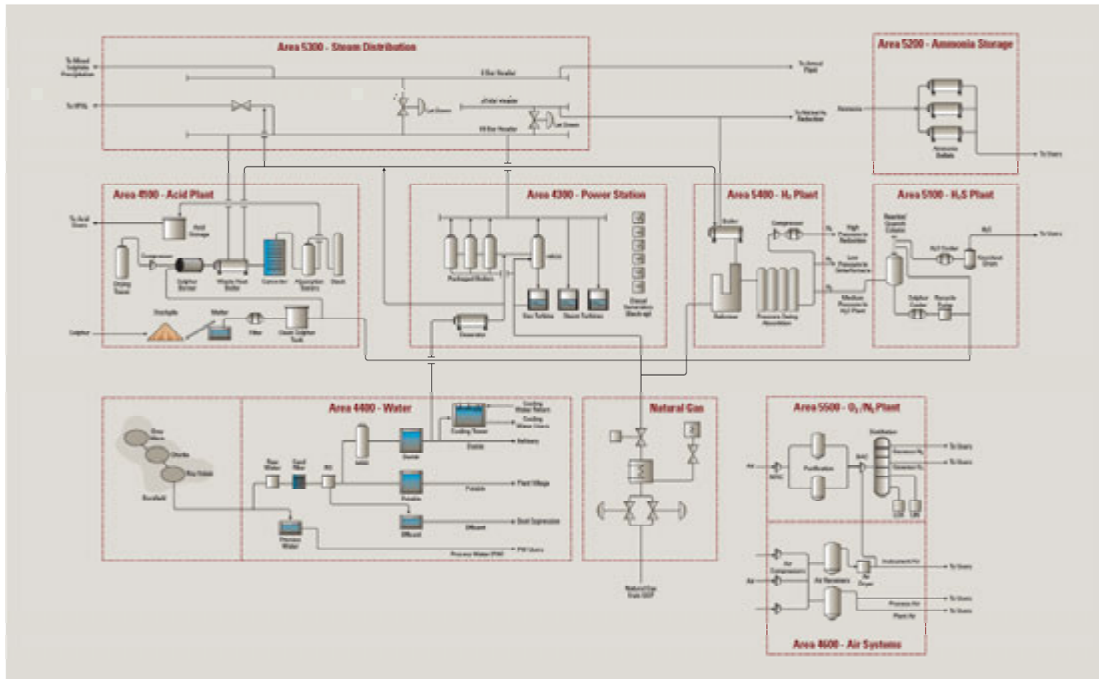
Process Operations

Ore Leach – Unit Operations and Major Facilities

- Ore Preparation
- Secondary Feed Ball Mill – oxides and sulphide ores & concentrates
- High Pressure Acid Leaching
- Heap Leaching (scats & ore)
- Counter Current Decantation
- Pre-reduction
- Neutralisation
- Tailings Disposal (Cells)
- Tailings Disposal (In-Pit)
- Seepage Recovery
- Calcrete Plant

Process Operations

Refinery – Unit Operations and Major Facilities

- Mixed Sulphide Precipitation
- Mixed Sulphide Washing and Grinding
- Mixed Sulphide Oxygen Pressure Leach
- Impurity Removal – Fe/Cu
- Zinc Solvent Extraction
- Cobalt Solvent Extraction
- Nickel Hydrogen Reduction
- Cobalt Hydrogen Reduction
- Ammonia Unloading & Storage
- Ammonium Sulphate Plant

Process Operations

Utilities – Unit Operations and Major Facilities

- Acid Plant
- Power Station
- Water Treatment Plant
- Natural Gas Supply System
- Instrument and Plant Air Systems
- Diesel Fuel Farm
- Hydrogen Sulphide Plant
- Flare System
- Steam and Condensate Systems
- Hydrogen Plant (BOC)
- Air Separation Plant (BOC)

3100 - Ore Preparation, MMD "Sizer" (Crusher)

3100 - Ore Preparation, "SAG" Mill

3100 - Ore Preparation, "SAG" Mill (with magnesite)

3100 - Ore Preparation, Paste Thickener and Cyclones

3100 - Ore Preparation – Process Objectives

- To repulp ore at high pulp density as downstream autoclaves are volumetrically restricted (positive displacement pumps used to feed autoclaves).

- Slurry density limited by slurry yield stress. At ambient conditions yield stress is typically 90 to 140 Pa (measured by vane viscometer in lab). This equates to 40-44 % w/w solids for most ores. Actual yield stress is lower in plant due to use of hot water.

- A "SAG" mill with limited ball charge is used and some grinding occurs however it is important not to over grind clays as this liberates fines and increases yield stress.

  Summary

- A simple yet sophisticated circuit - not a typical "hard-rock" milling circuit.

- Scats or rejects at > 1.7 mm are generated for Heap Leach @ 5-15% of ROM feed. Minor nickel beneficiation occurs. Some Mg beneficiation occurs minimising acid consumption.

3200 – Ore Preparation – Metallurgical Performance

Murrin Murrin Operations
Leach Feed Density - % solids w/w
Monthly Averages - Since Commissioning
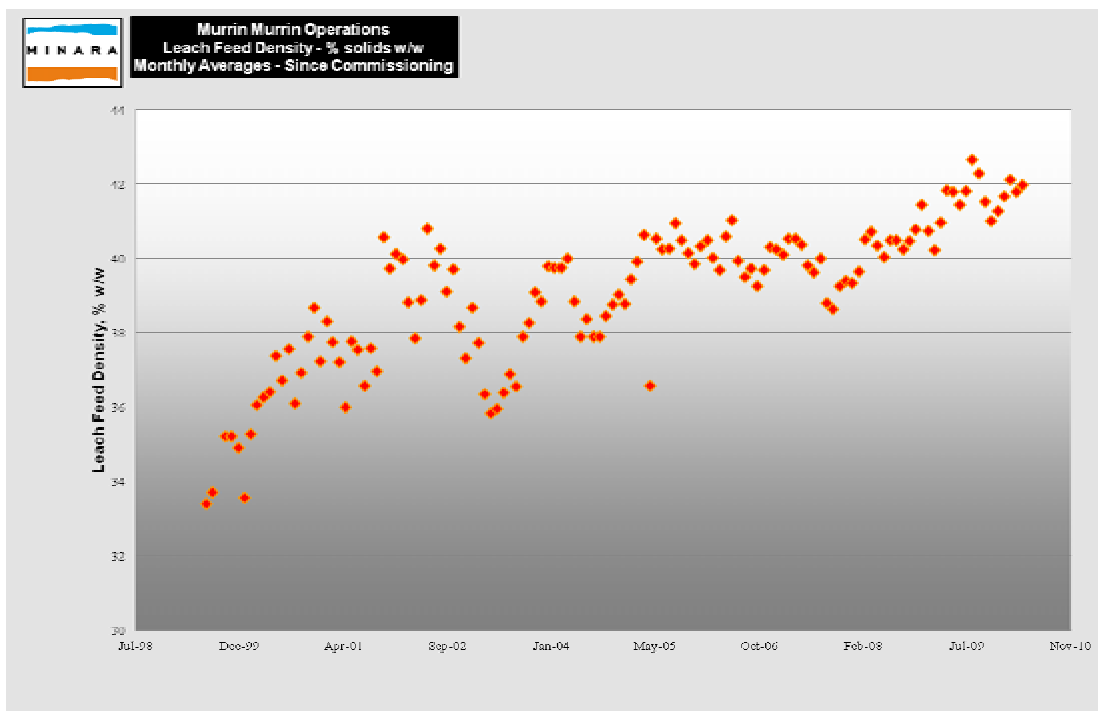
3110 – Supplementary Feed Ball Mill (SFBM)

3110 – SFBM – Process Objectives

- Allows grinding of additional "secondary" feeds eg sulphide ores and concentrates or oxides

- Open circuit mill with 1 mm screen.

- Only operates with main Ore Preparation circuit.

- Allows even distribution of secondary feed to all autoclaves for maximum metal recovery and good control of autoclave chemistry

- Western Areas oxide and supergene ore currently being treated

3120 - Concentrate Processing Opportunities at Murrin

- Murrin has treated >350,000 tonnes of supergene ore containing 2-3% sulphide sulphur.

- In 2008, 3,000 tonnes of smeltable sulphide concentrate (@ 20% nickel and 26-30% sulphide sulphur) was successfully added as a trial. Very high extractions > 98% were achieved

- In 2009 1,000 tonnes of lower grade concentrate was treated. Again with high extractions.

- Minara has a pending patent for the ferric leaching of sulphides. No additional oxidant is required.

  The primary opportunity for Minara and concentrate suppliers is to treat high MgO and/or high arsenic "dirty" concentrates thereby de-bottlenecking concentrators and smelters.

3200 - High Pressure Acid Leaching (HPAL), Overview

3200 - High Pressure Acid Leaching (HPAL), "GEHOs"

3200 - HPAL – 1st and 2nd Stage Pre-heaters
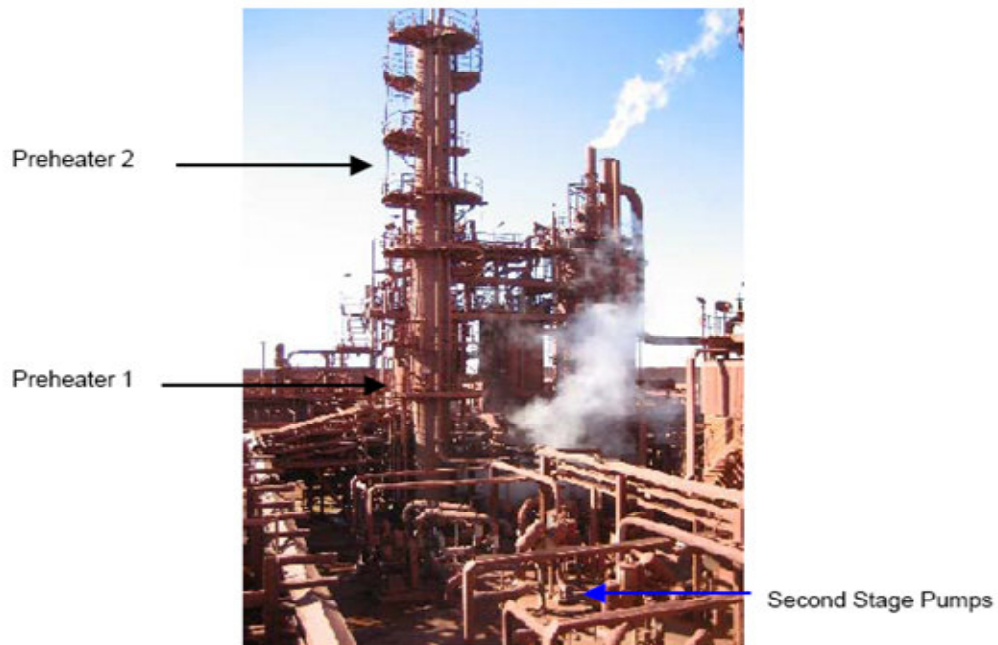
3200 - HPAL – 3rd Stage Pre-heater

3200 - High Pressure Acid Leaching (HPAL) – Flash Tank

Steam Outlet to Preheater

Steam Outlet to Vent Valve

Autoclave Slurry enters through

"Normal" slurry level

Slurry Outlet to Flash 2

Manway

Impingement Pad

Drain
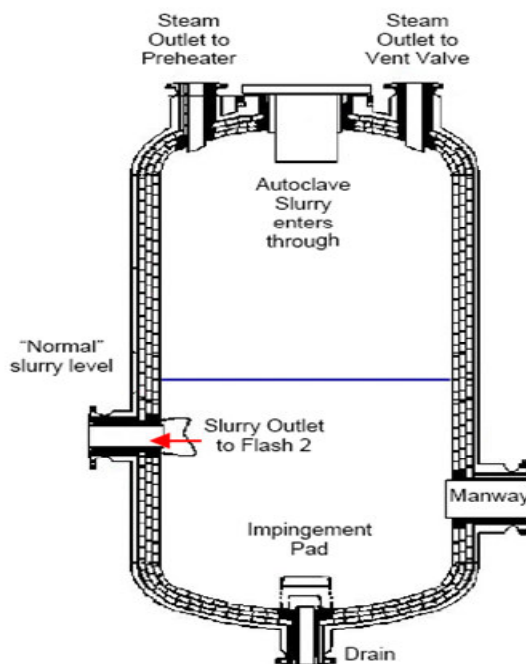
Pieces of brickwork crack when under thermal stress; this is called "Spalling"

20 Bar Steam

Vent Valve

Slurry from Clave

To Flash 3

Low Capacity Vent Steam

To 2nd Stage Preheater

Flash Vessel 1

Slurry to Flash 2
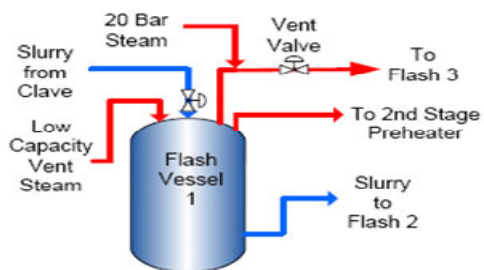
3200 - High Pressure Acid Leaching (HPAL) – Let Down Valve
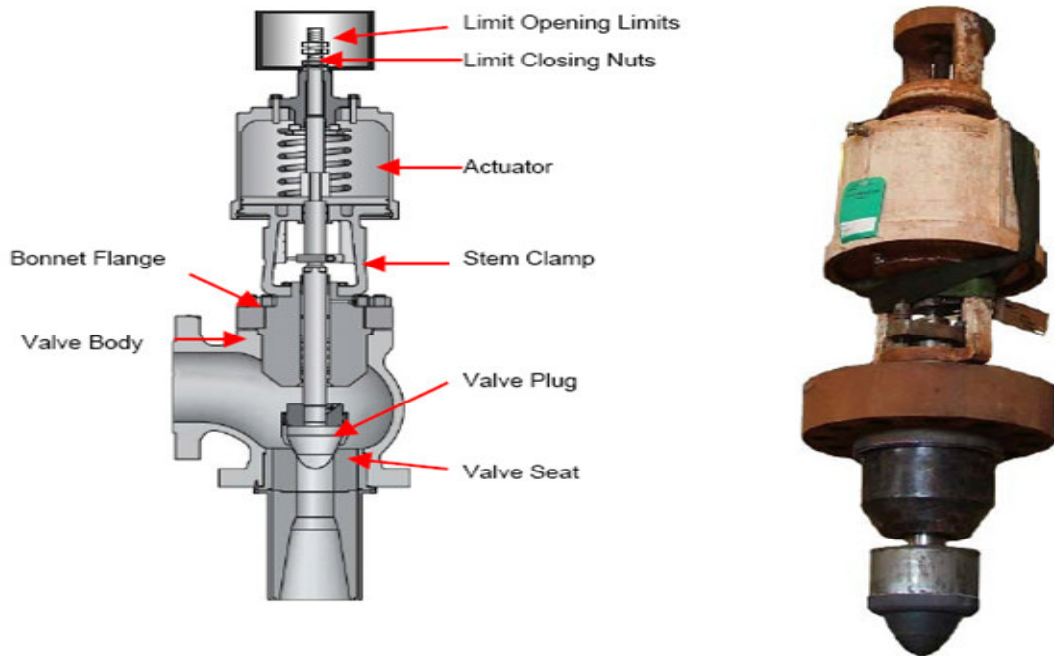
3200 - HPAL – Process Objectives

- The "heart" of the process......

- Rapid dissolution of Ni and Co @ 92-95% extraction in 70-90 minutes at 50-65 gpl free acid (cf 150-200 days for Heap Leach of scats/rejects)

- Bulk rejection of iron at 253 $^{\circ}$C as readily settled haematite. Acid recovery during ferric hydrolysis.

- Low ORP operation minimises free acid and hence overall acid addition for the same or higher Ni and Co extraction. ORP controlled by elemental sulphur addition or metal sulphide addition

- High leach feed density minimises acid and steam consumption.

- Energy recovery through a "three-stage" heater-flash circuit and heating of process water for Ore Preparation

3200 – HPAL Flowsheet - Overview
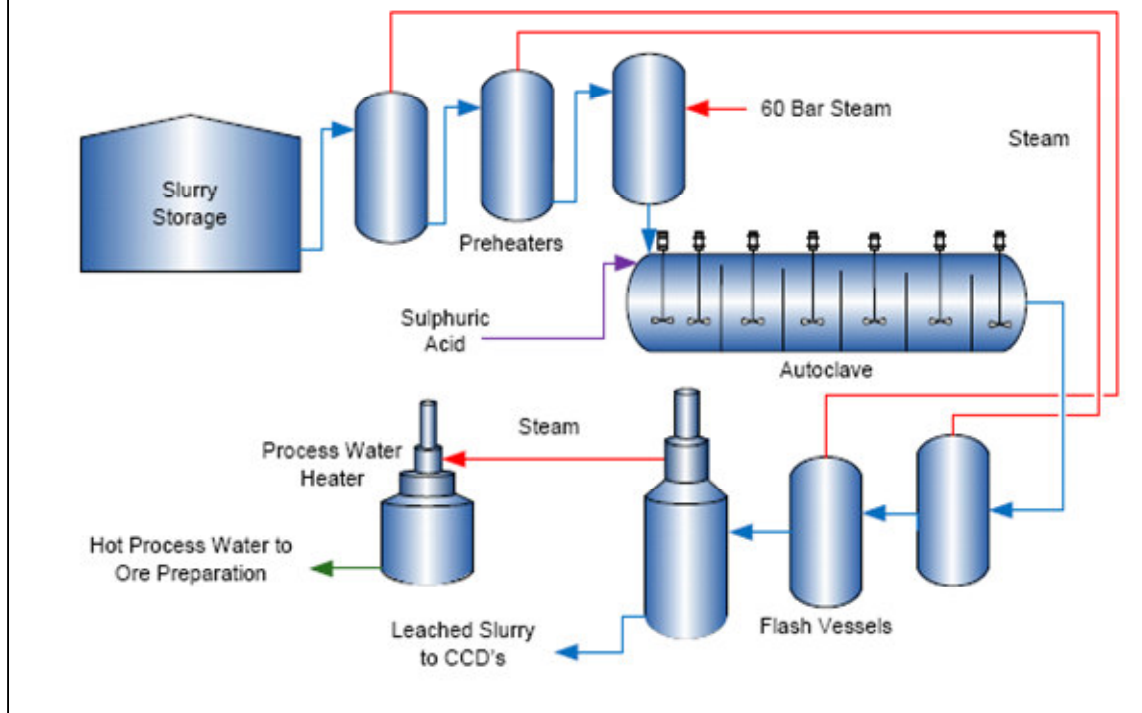
3200 - High Pressure Acid Leaching (HPAL) – Pre-heat
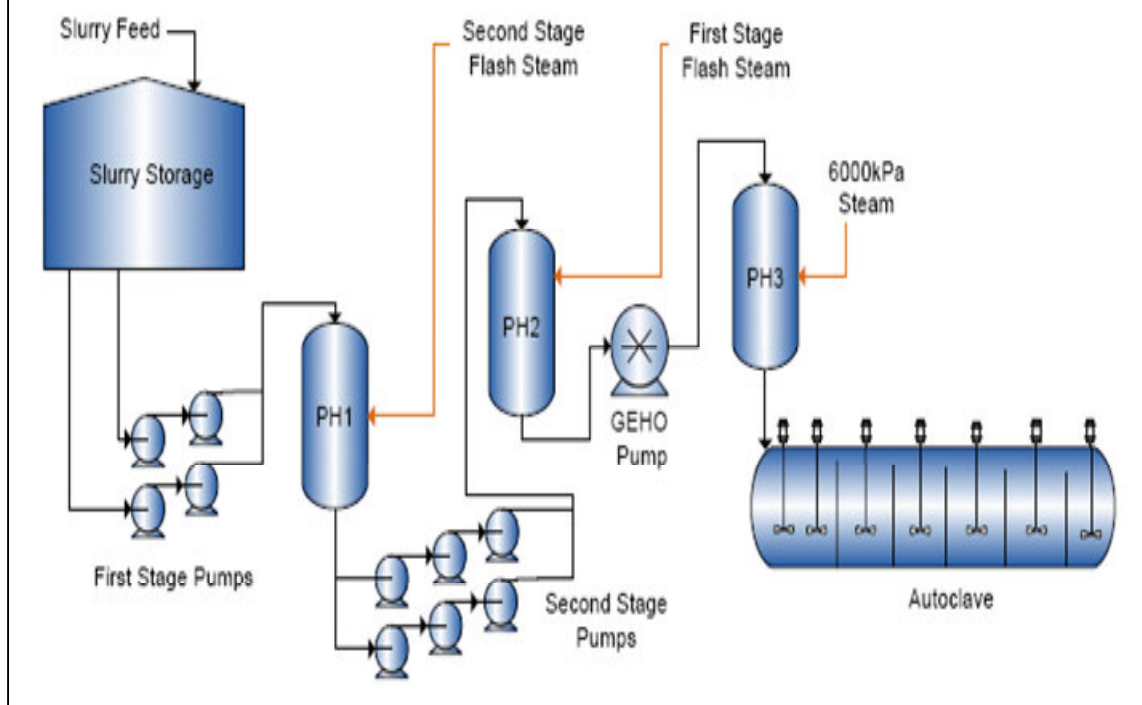
3200 - High Pressure Acid Leaching (HPAL) – Autoclave x 4
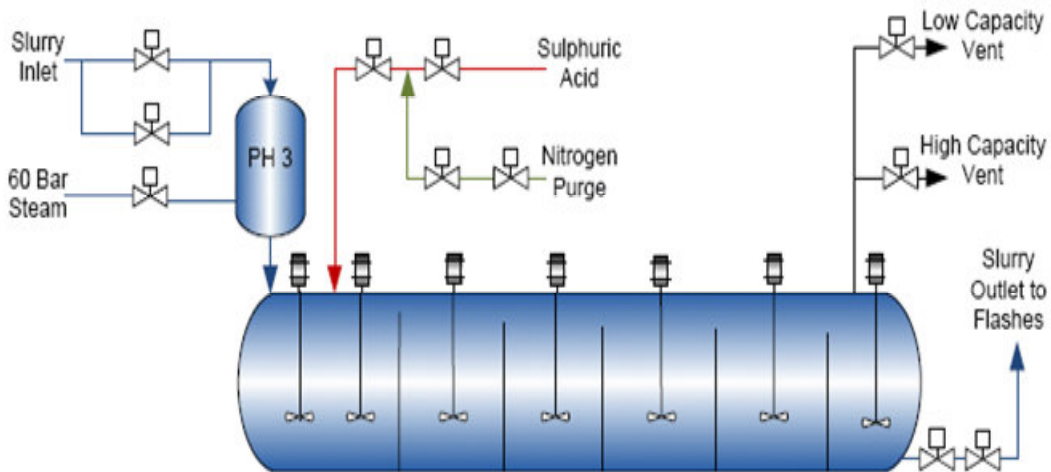
3200 - HPAL – Leach Feed Tonnes
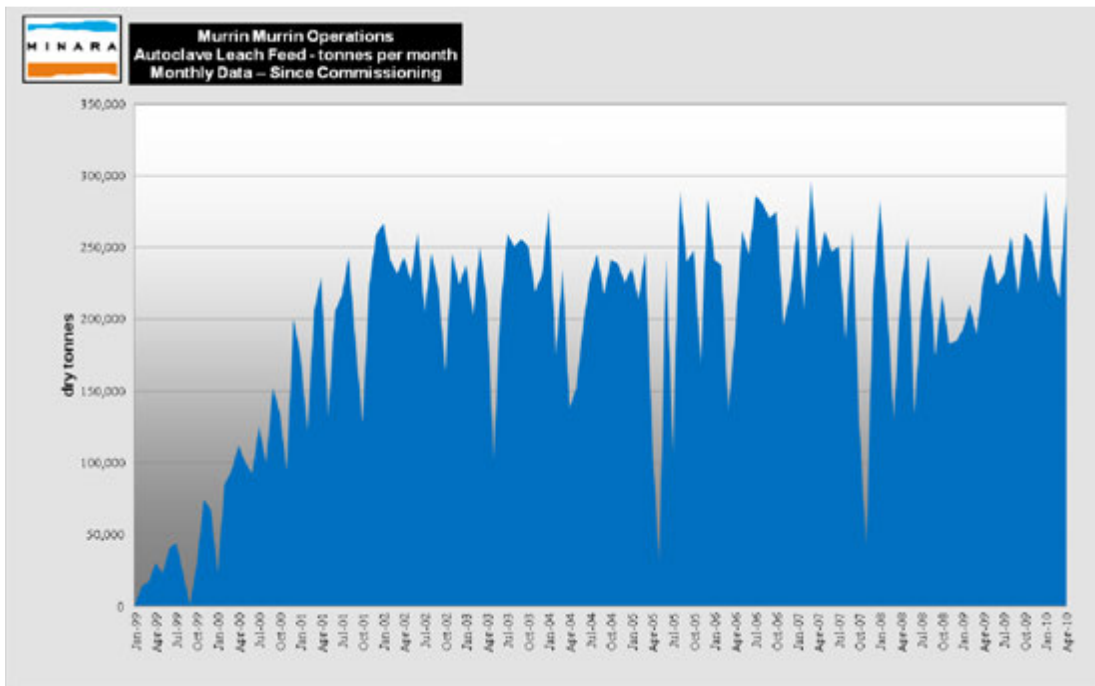
3200 - HPAL – Autoclave Availability
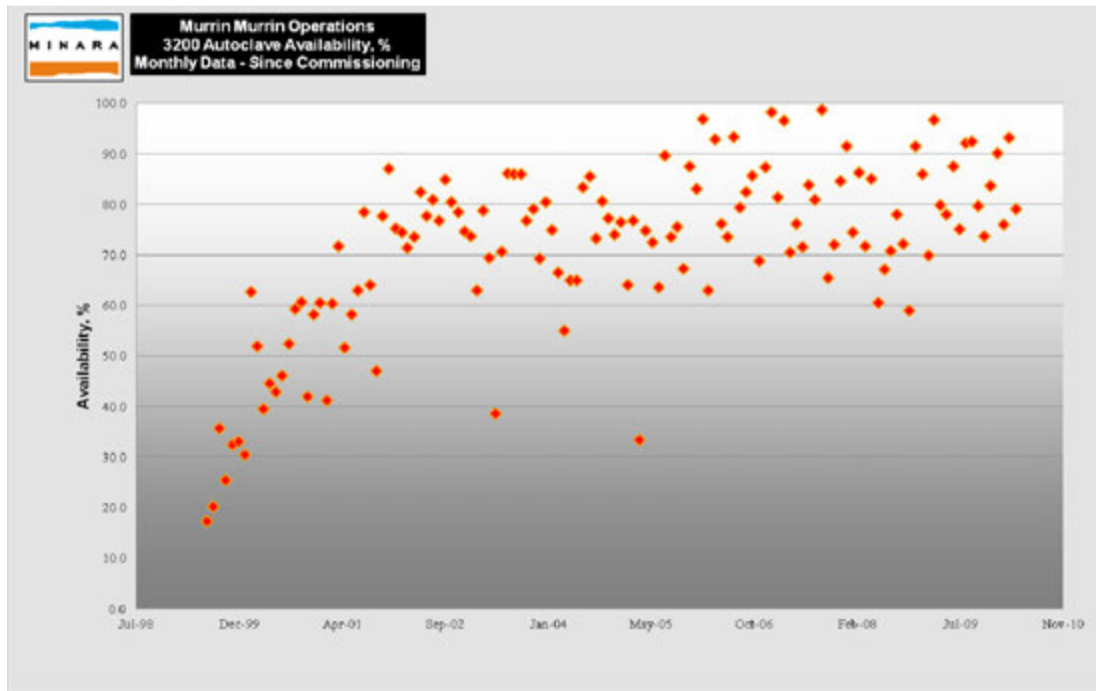
3200 - HPAL – Metallurgical Performance
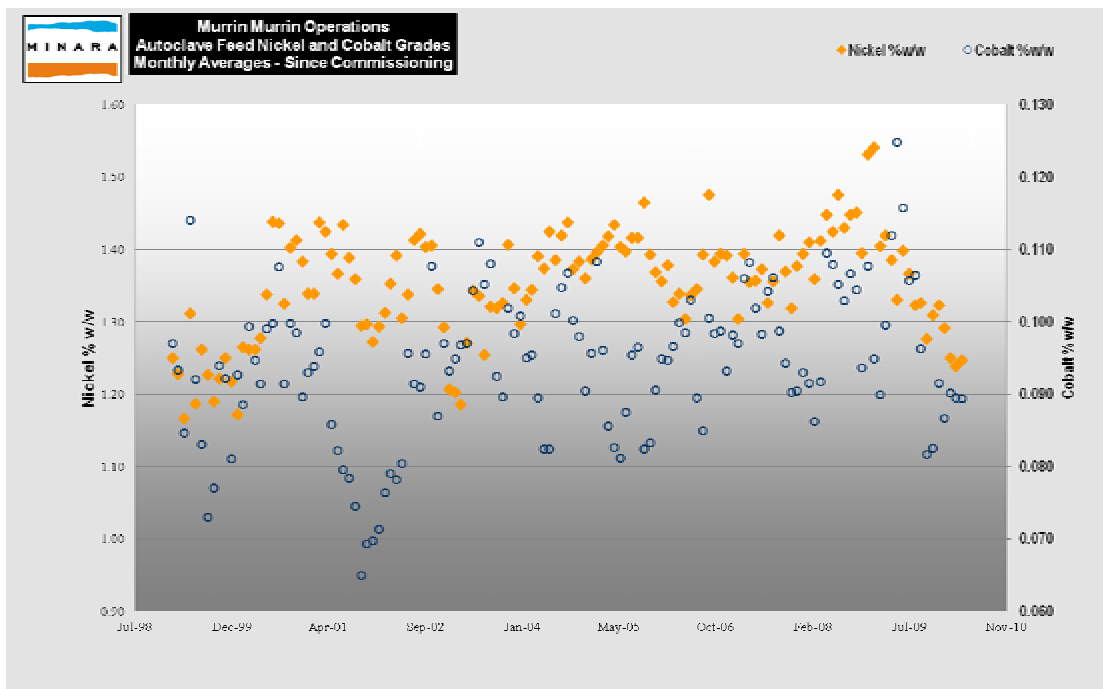
3200 - HPAL – Metallurgical Performance
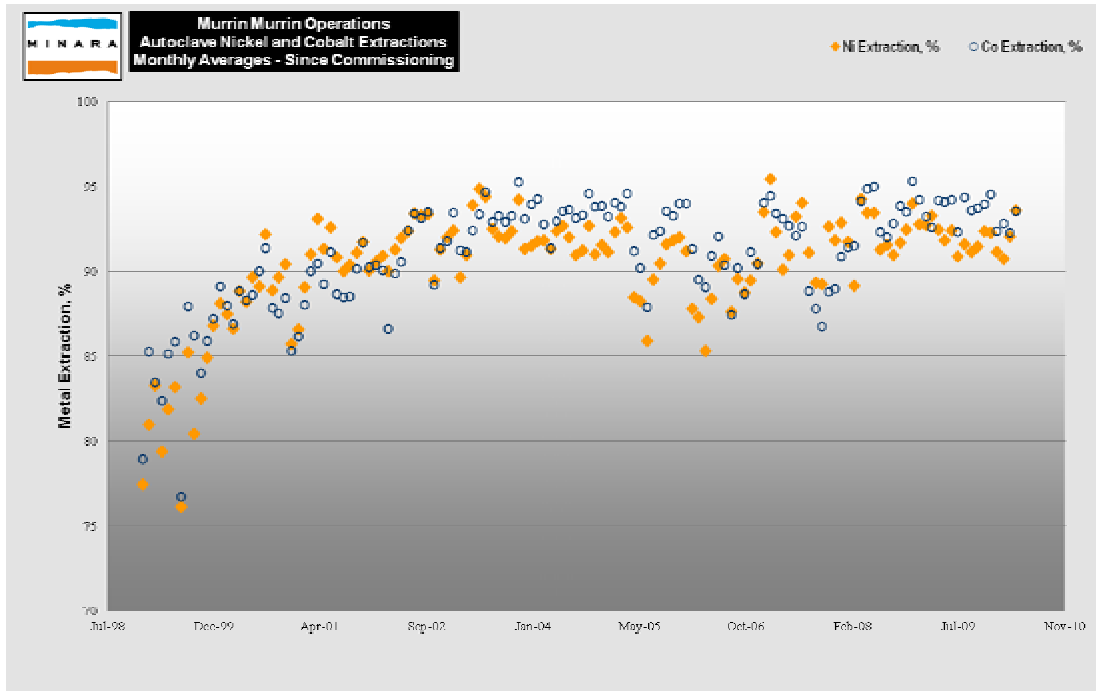
3120 – Recent Innovations – Low ORP HPAL

- Murrin Murrin (as with most laterite ores) ores are naturally oxidising in HPAL conditions (no ferrous in leach solution)

- To achieve acceptable extractions (0.10-0.15 % Ni in residue) at high ORP (>700 mV Ag-AgCl) high free acids (75-85 gpl) are required

- At low ORP (350-450 mV Ag-AgCl) low free acids (55-65 gpl) will achieve the same leach residues

- A reductant is required and elemental sulphur is added

- Sulphidic ores or concentrates can also be added to provide reductant – merely backs out sulphur.

3200 - Benefits of Low ORP/Low Free Acid (FA)

- With no loss in nickel and cobalt extraction, low ORP & low Free Acid results in the following benefits:

- Reduced acid and hence sulphur consumption and cost (albeit with less steam make)

- Reduced calcrete consumption and cost

- Reduced ferric and aluminium in HPAL discharge further lowering consumption of acid, calcrete and H2S. Also less solids to tails.

- Reduced solids loading in CCD's with higher CCD recovery

- Reduced solids to tails increasing life of tails storage facilities

- Reduced CO2 emissions (less calcrete)

Heap Leach – Current Status

- Worlds first commercial Ni Laterite Heap Leach Operating since 2007

- To date produced +5000t Ni and 350t Co

- Annualised Production Rate ~2,000tpa Ni

- Production limited by acid availability and Fe control

3120 – MMO Heap Leaching – What's so different

	Ore					Solution	
	Metal Content	Moisture Content	Fines/Clay Content	Reagent Conusmption	Mass Loss in Leach	TDS	"In Heap" Inventory
Gold	low g/t	low - mod < 10%	low - mod	low g/t	low	low (#) ppm	low < 10%
Copper	moderate 1%	low - mod < 15%	low - mod	moderate < 25 kg/t	moderate < 5%	moderate < 100 g/L	low < 10%
Nickel	moderate 1%	high > 20%	mod - high	high > 300 kg/t	high 10-30%	high > 200 g/L	high 15-30%

Au/Cu   - Downstream processing simple, well understood and compatible

Ni   - not

3120 - Heap Leach – Flowsheet - Simplified

3120 - Heap Leach – General Layout

Feed Bin and Agglomerator

ROM Pad

PLS Pond

Pad 1

Pad 2

ILS Pond

Pad 3

Storm Water Pond

Pad 4

Feed Liquor Pond

Pad 5

Pad 6

Radial Stacker

Pad 7

Pad 8

3120 - Heap Leach – General Layout

ROM Pad

PLS Pond

Pad 1

Pad 2

ILS Pond

Pad 3

Storm Water Pond

Pad 4

Feed Liquor Pond

Pad 5

Pad 6

Pad 7

Pad 8
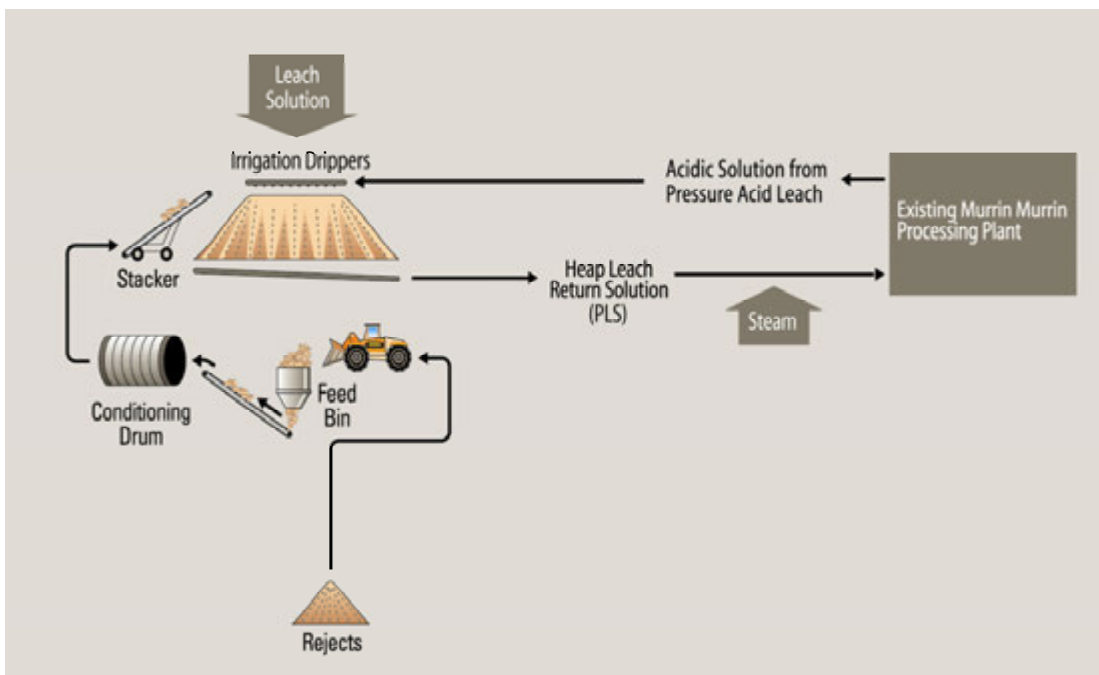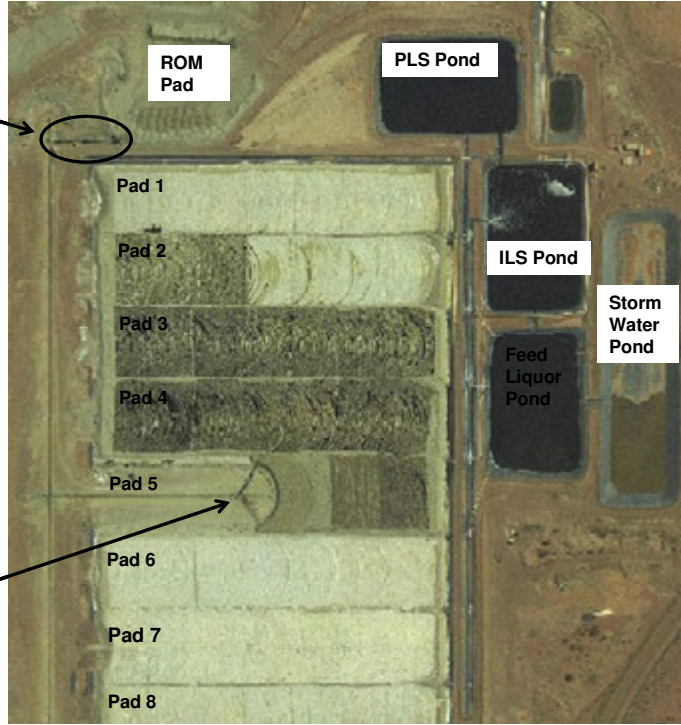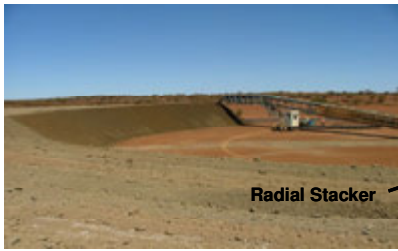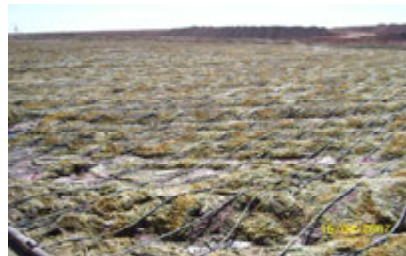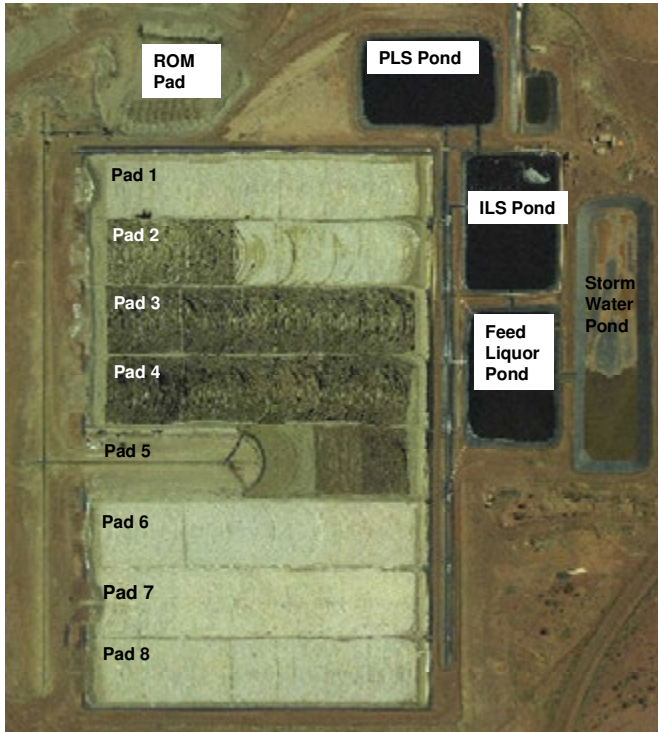
3120 - Heap Leach - On/Off Leach Pads
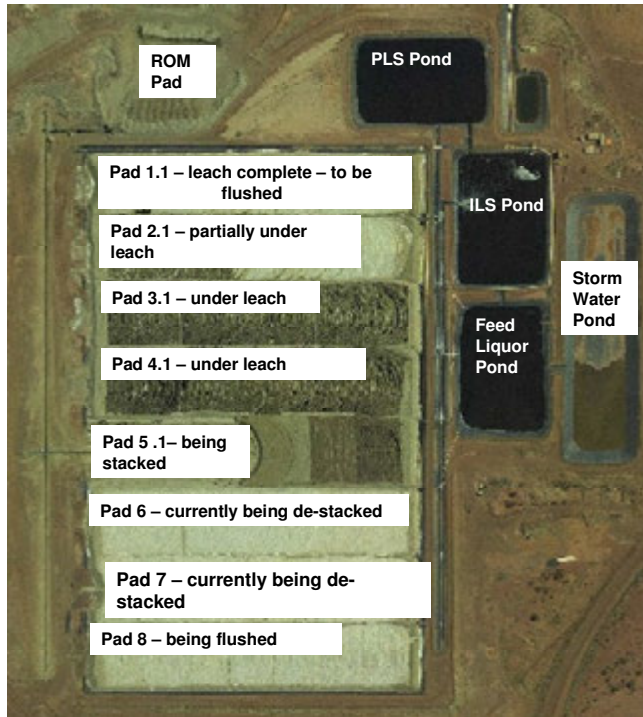
3120 - Heap Leach – Average 4m height (3m to 6m tested)

3120 – Comparative Heap Performance
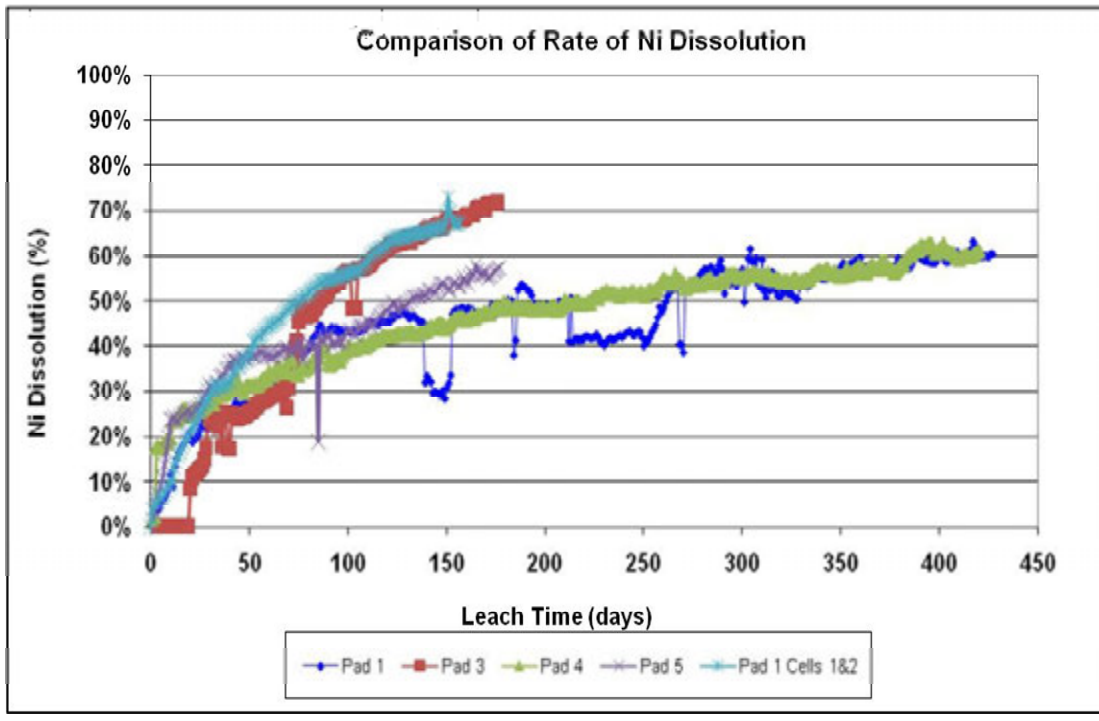
3120 – Comparative Heap Performance
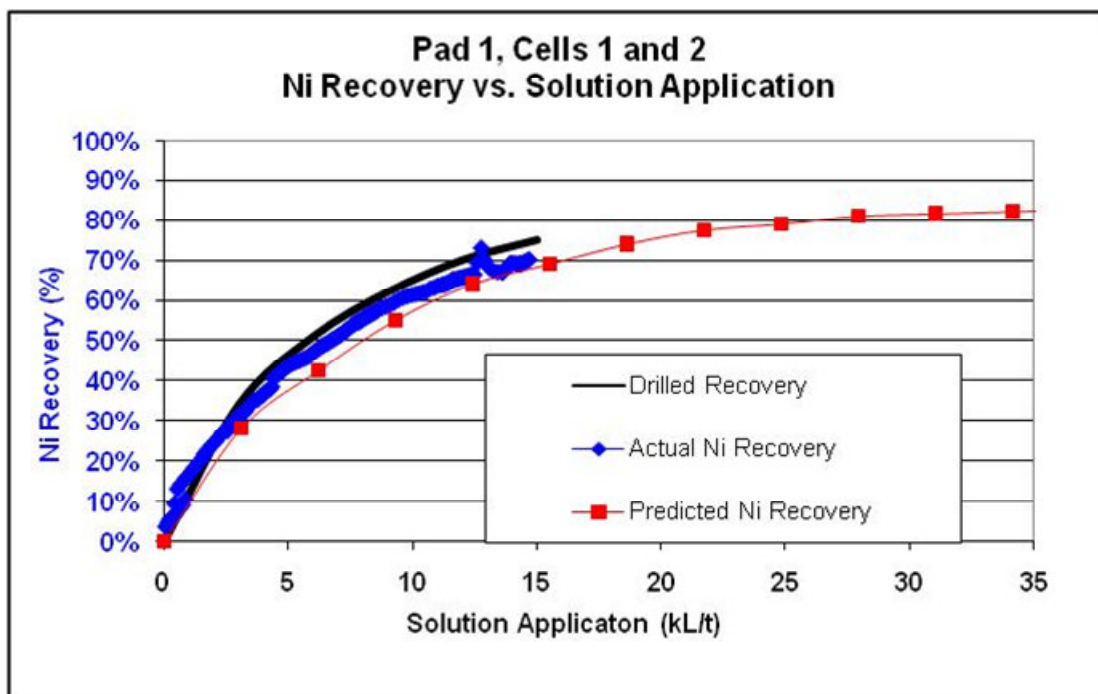
3120 – Scats, Nickel Recovery at Depth

Pad 1, 2 & 4 Ni Recovery Depth Profile

Legend: Pad 2 Cells 1-3 — Pad 2 Cells 5-7 — Pad 4 Cells 5-7 (6m) — Pad 1 Cells 1-2
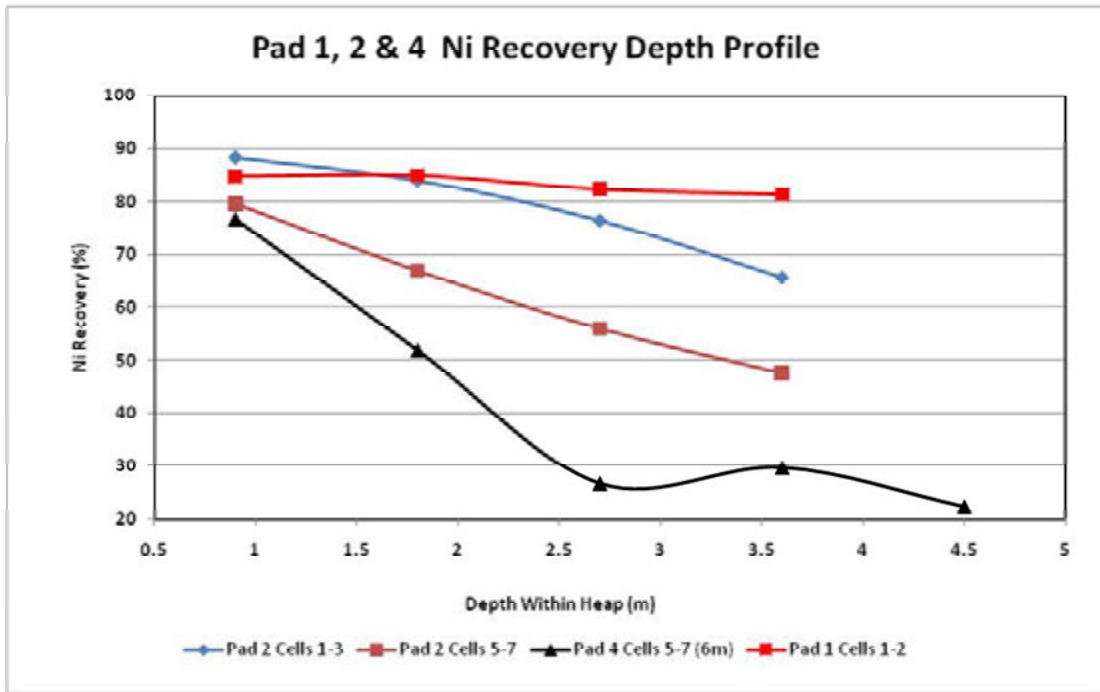
3300 - Counter Current Decantation (CCD) and Washing

3300 - Counter Current Decantation (CCD) and Washing

3300 - CCD – Process Objectives

- To recover soluble Ni and Co sulphate from leach discharge slurry and from neutralised acid slurry (gypsum)

- To present washed slurry to tailings disposal at high density.

- To achieve high Ni and Co recovery while minimising wash water to maximise PLS Ni and Co tenor in solution. High tenor improves metal recovery during later mixed sulphide precipitation.

- Aim to maximise CCD U/F pulp density (25-30 % w/w typical)

- Aim to minimise Total Suspended Solids (TSS) in CCD 1 O/F liquor – this solution is partially fed to Heap Leach

3300 - CCD – Flowsheet

To 34-TK-09

Liquor Flow

Barren Liquor from 3500
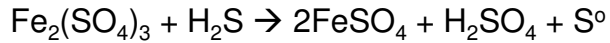
From 3200 / 34-TK-11

Slurry Flow
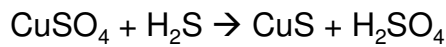
To Tails Tanks
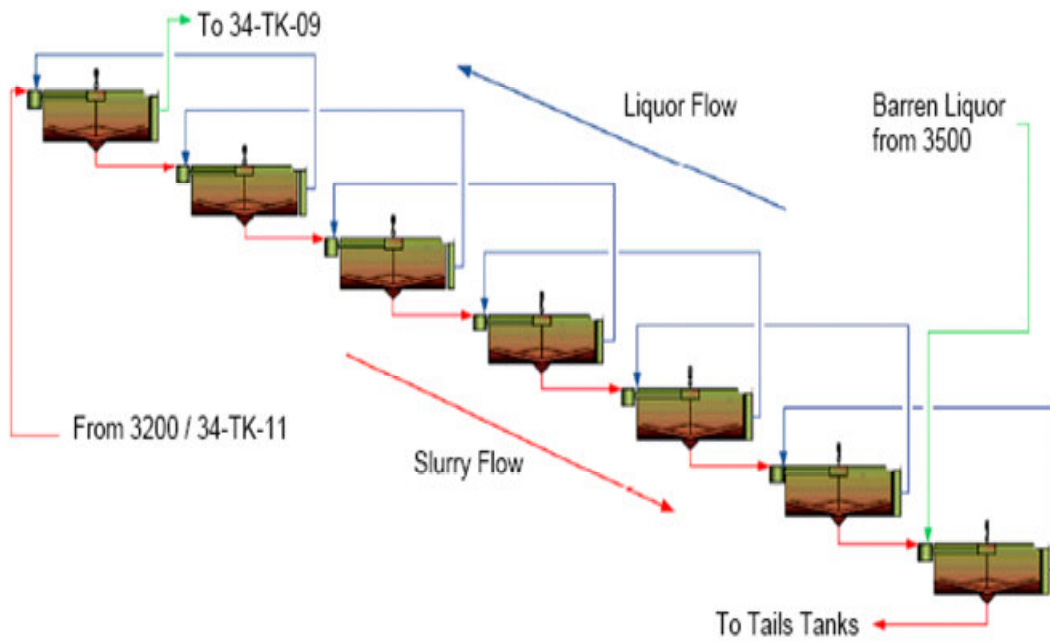
3400/3510 - Pre-reduction "Flowsheet" – TK-65

3400/3510 – Pre-reduction – Process Objectives

- To reduce ferric iron to ferrous minimising excess sulphur in mixed sulphide product

$$Fe_2(SO_4)_3 + H_2S \rightarrow 2FeSO_4 + H_2SO_4 + S^o$$

- To precipitate Cu as CuS. This is the only soluble Cu "out" in the Murrin Murrin flowsheet

$$CuSO_4 + H_2S \rightarrow CuS + H_2SO_4$$

CuS is rejected with gypsum precipitates from neutralisation to tailings via CCD's.

Note: Murrin Murrin HPAL does not normally generate Cr(VI) due to low ORP operation but if generated, Cr(VI) would also be reduced

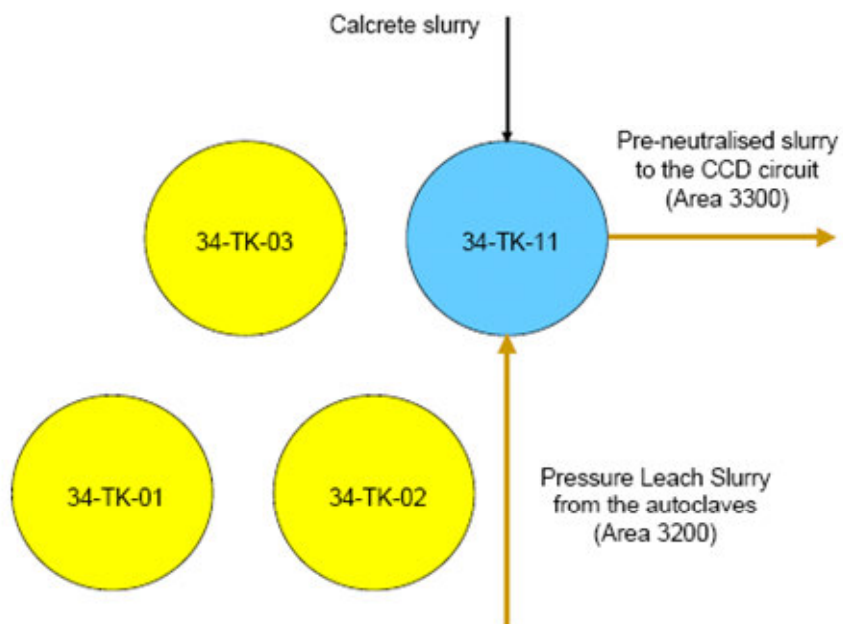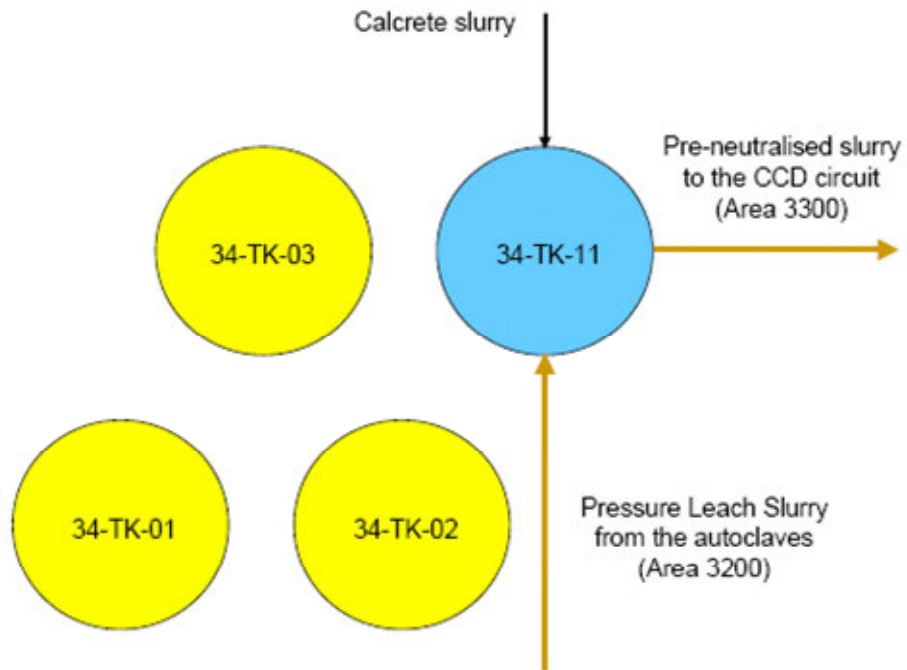## 3400/3510 – Pre-reduction – Metallurgical Performance
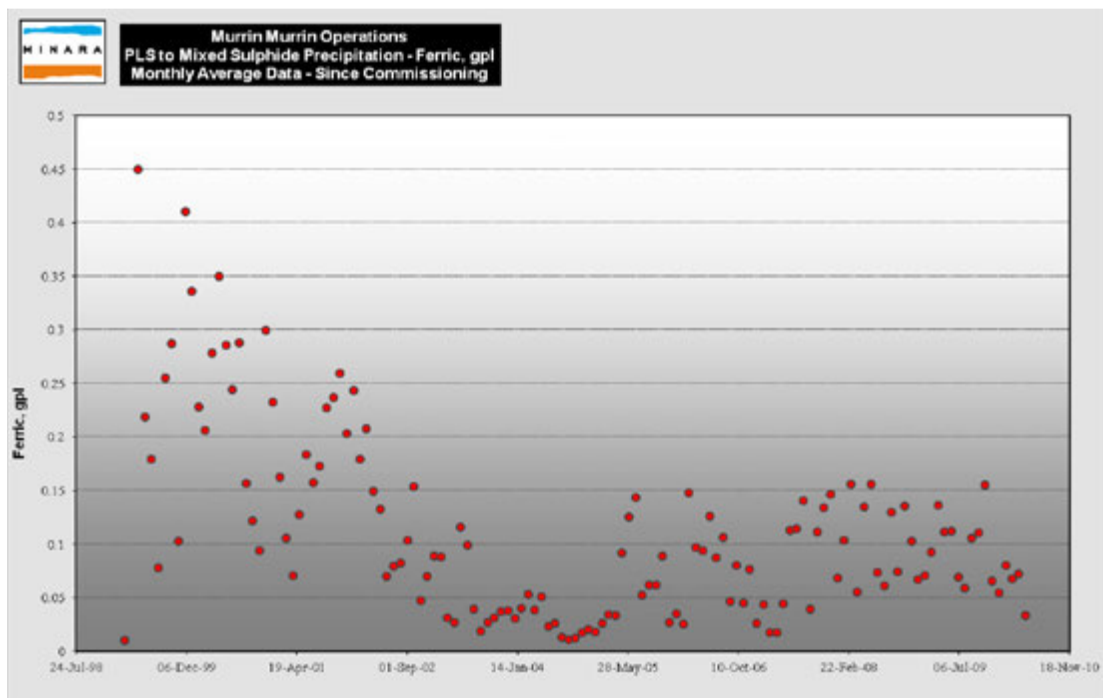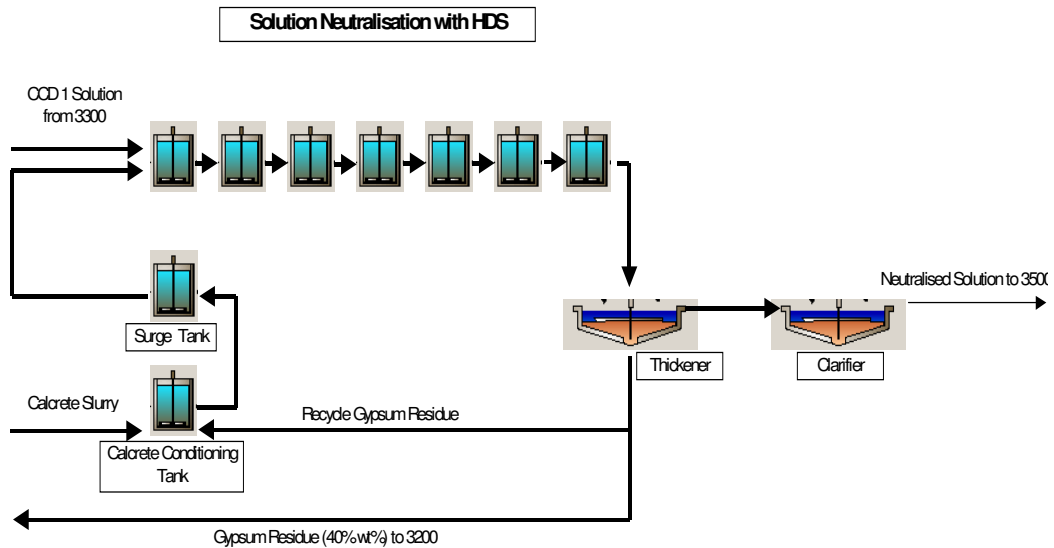
3400 Solution Neutralisation

3400 – Neutralisation Flowsheet – Original

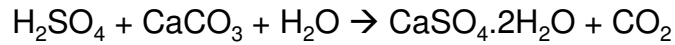**3400 – Neutralisation Flowsheet – With Slurry Neutralisation**

3400 - Neutralisation - HDS Mode circa May-June 2010

3400 – Neutralisation – Process Objectives

- To neutralise excess acid from HPAL and Heap Leach for subsequent mixed Ni/Co sulphide precipitation. pH target ~ 2.2 to 2.5

  $$H_2SO_4 + CaCO_3 + H_2O \rightarrow CaSO_4.2H_2O + CO_2$$

- To remove gypsum at high density to reduce washing load on CCD and minimise recirculation of solution thereby maximising residence time in neutralisation

- To minimise solids (TSS) in thickener O/F. There is no clarification of PLS post the thickener (soon to be changed with Pinned Bed Clarifiers)

  Excess Si in Mixed Sulphide Product (MSP) can lead to quality issues with final nickel metal.
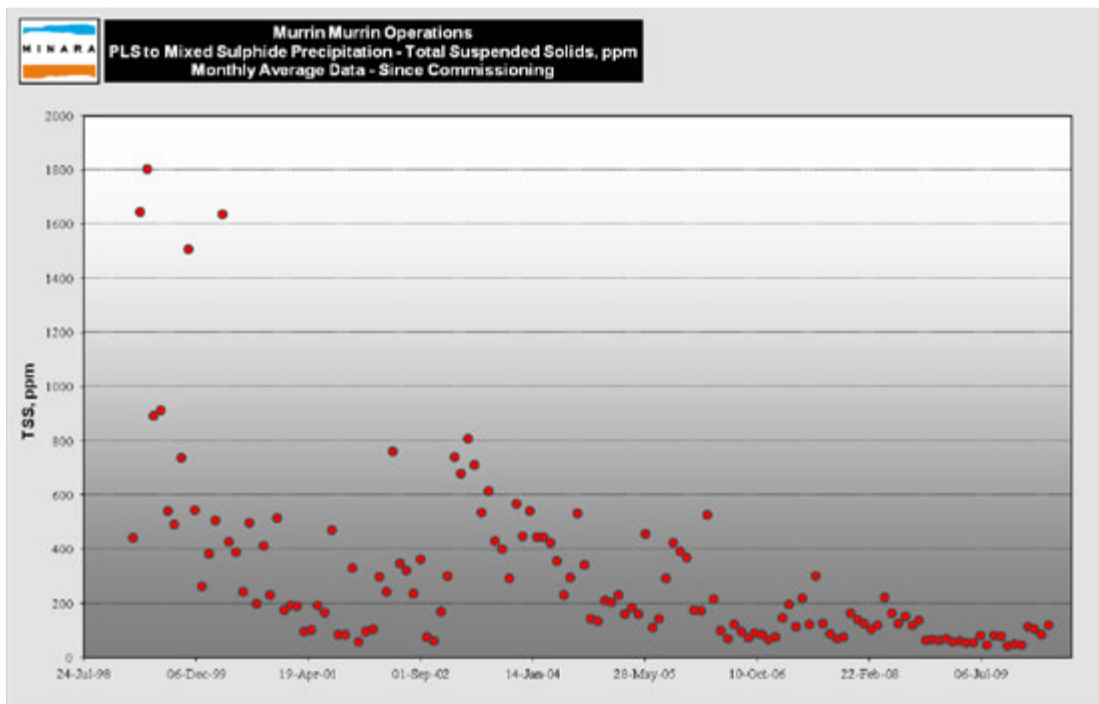
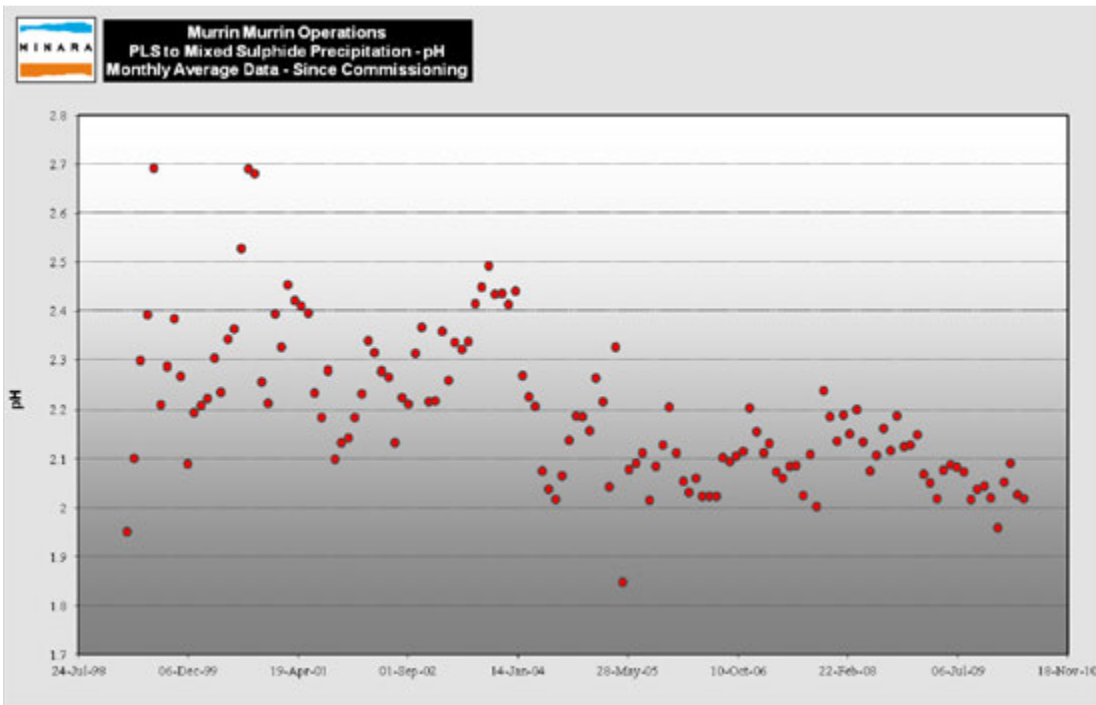
3400 – Neutralisation – Metallurgical Performance

3400 – Neutralisation – Metallurgical Performance

Murrin Murrin Operations
Neutral Thickener U/F Density, % solids w/w
Monthly Average Data - Since Commissioning

3400 – Neutralisation – Metallurgical Performance

Murrin Murrin Operations
PLS to Mixed Sulphide Precipitation - pH
Monthly Average Data - Since Commissioning

3400 – Neutralisation – Metallurgical Performance

Murrin Murrin Operations
Neutral Thickener U/F Solids - Nickel % w/w
Monthly Averages - Since Commissioning

3400 – Neutralisation – Metallurgical Performance

Murrin Murrin Operations
PLS to Mixed Sulphide Precipitation - Ni g/l (Note: Design – 3.8 gpl)
Monthly Averages - Since Commissioning

3400 – Neutralisation – Recent Changes

- Major upgrade in solution neutralisation with implementation of High Density Sludge (HDS) project. Currently being commissioned.

- Testwork showed significantly increased neutral thickener U/F density and increased CCD U/F density

- Lower calcrete addition (additional CCD 1 O/F acid to Heap Leach and increased calcrete utilisation). Also less solids in CCD's = higher metal recovery

- Lower water usage (lower calcrete usage and higher tails density)

- Increased "acid kill" capacity. Neutralisation no longer throughput bottleneck

7700 – Tails Disposal Paddock Style

~ 3.5 Mtpa of Tailings

Paddock TSF
(final design)

- 506 ha
- 15 m high
- Two cells

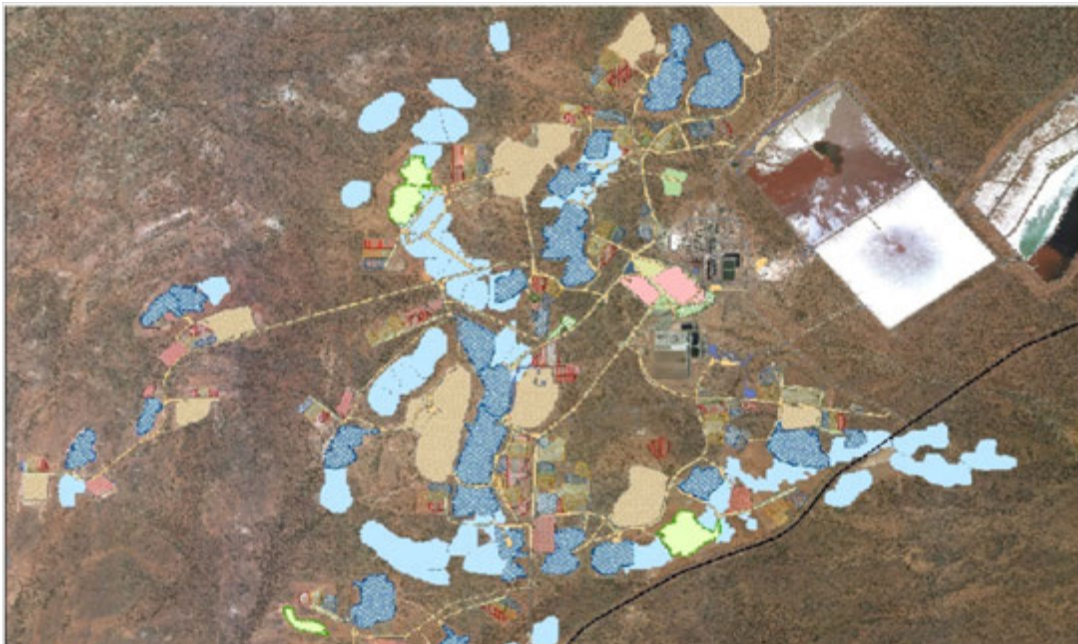## 7700 – In-Pit Tailings Disposal

Pit 2/3

Commenced deposition December 2008 and still in use

7700 – In-Pit Tails Disposal

Other mined out pits available

7700 - Tails Dam Overview, In-Pit vs Paddock Style

Significant risk reduction achieved via commissioning of "In-Pit" tailings

•Allows for improved consolidation of tails materials

•Eliminates process loss risk associated with potential tails dam wall failure. Seen as a substantial risk reduction.

•Delivers a much more cost effective method for tails disposal (~ 1/10 th on-going capital)

•Current / planned pits in close proximity to plant should cater for up to 10 years of process plant tailings

3500 - Mixed Sulphide Precipitation

3500 - Mixed Sulphide Precipitation
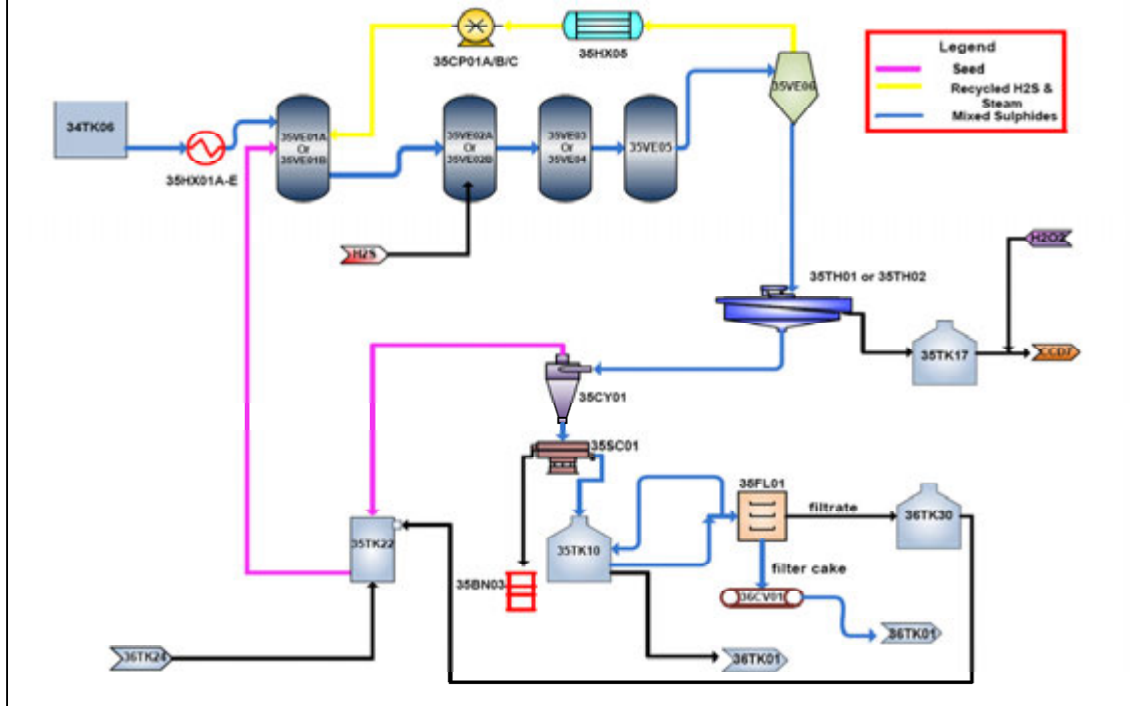
3500 – Mixed Sulphide Precipitation – Process Objectives

- To maximise precipitation of Ni and Co and recover solids formed
- To maximise flowrate as barren liquor is used as CCD wash water. High flowrates = high CCD recovery.
- Maximise seed recycle. Seed recycle is crucial to minimise scale formation.
- Minimise S/Me ratio in Mixed Sulphide Product (MSP). Excess sulphur = acid in Fe/Cu removal circuit complicating downstream solvent extraction and reducing throughput.
- Operates at ~ 95 °C to maximise recovery. Indirect HX with 6 bar steam
- Wash MSP to remove BL. Uses Larox. Must remove soluble impurities
- Grind MSP to provide P_{80} 25-30 micron in oxidation feed and maximise surface area for seed recycle

3500 - Mixed Sulphide Precipitation
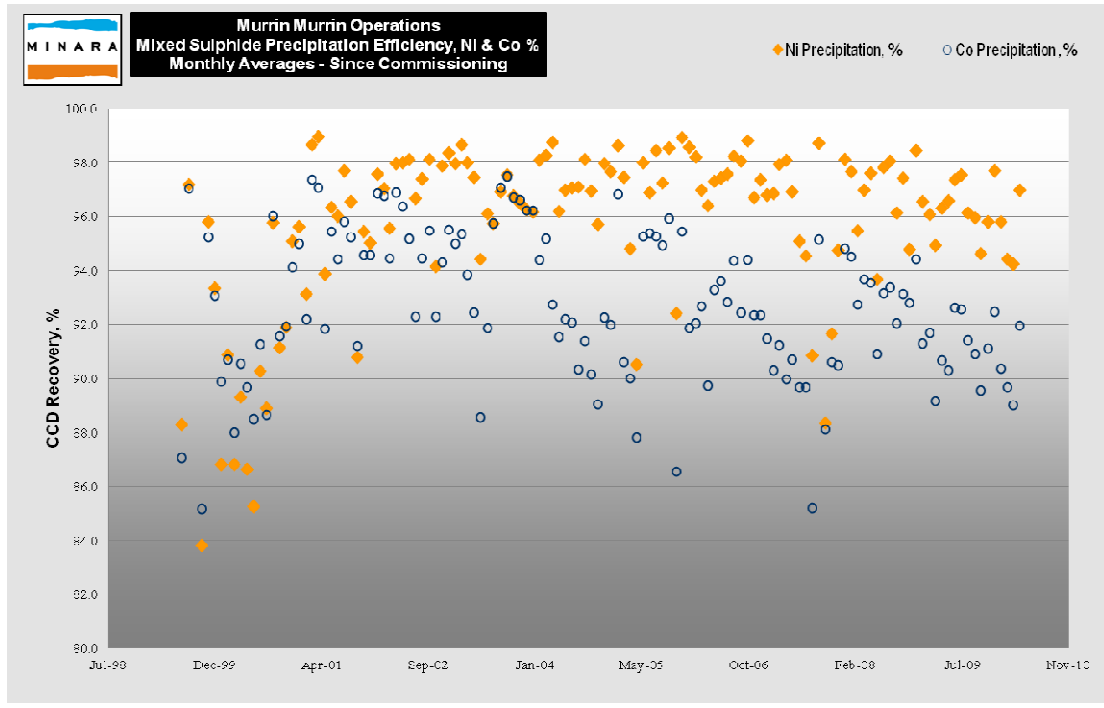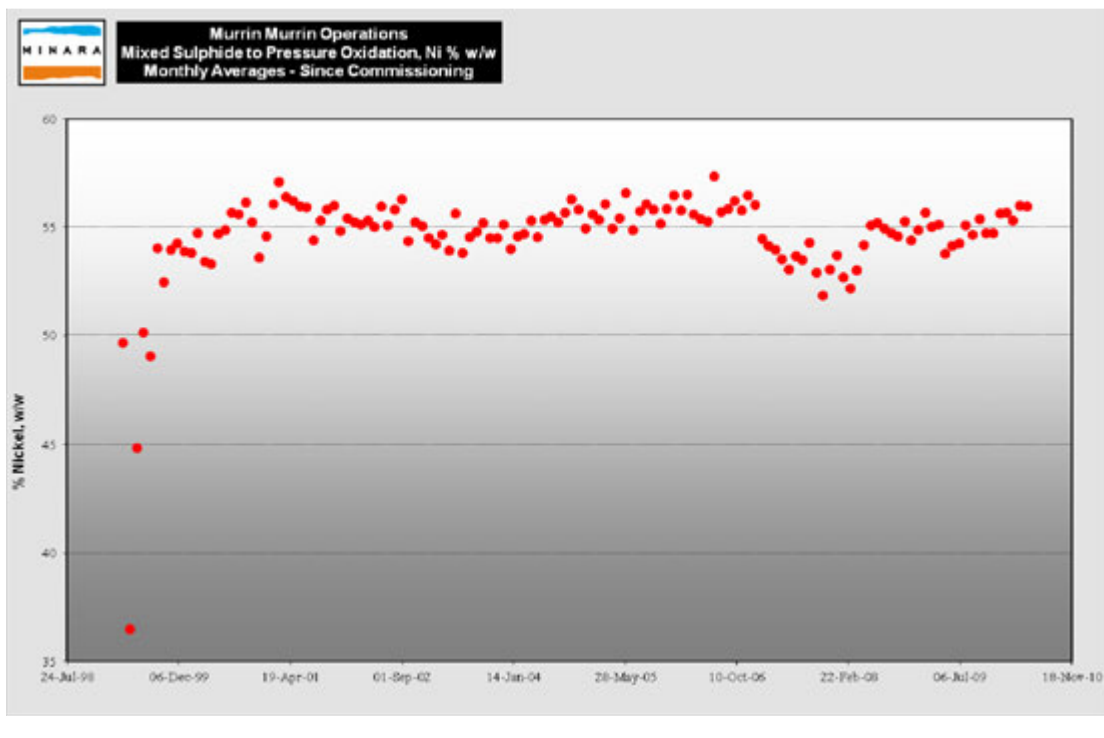
3500 - Mixed Sulphide Precipitation

3500 - Mixed Sulphide Precipitation

Murrin Murrin Operations
Mixed Sulphide to Pressure Oxidation, Sulphur % w/w
Monthly Averages - Since Commissioning

3500 - Mixed Sulphide Precipitation

Murrin Murrin Operations
Mixed Sulphide to Pressure Oxidation, Fe % w/w
Monthly Averages - Since Commissioning
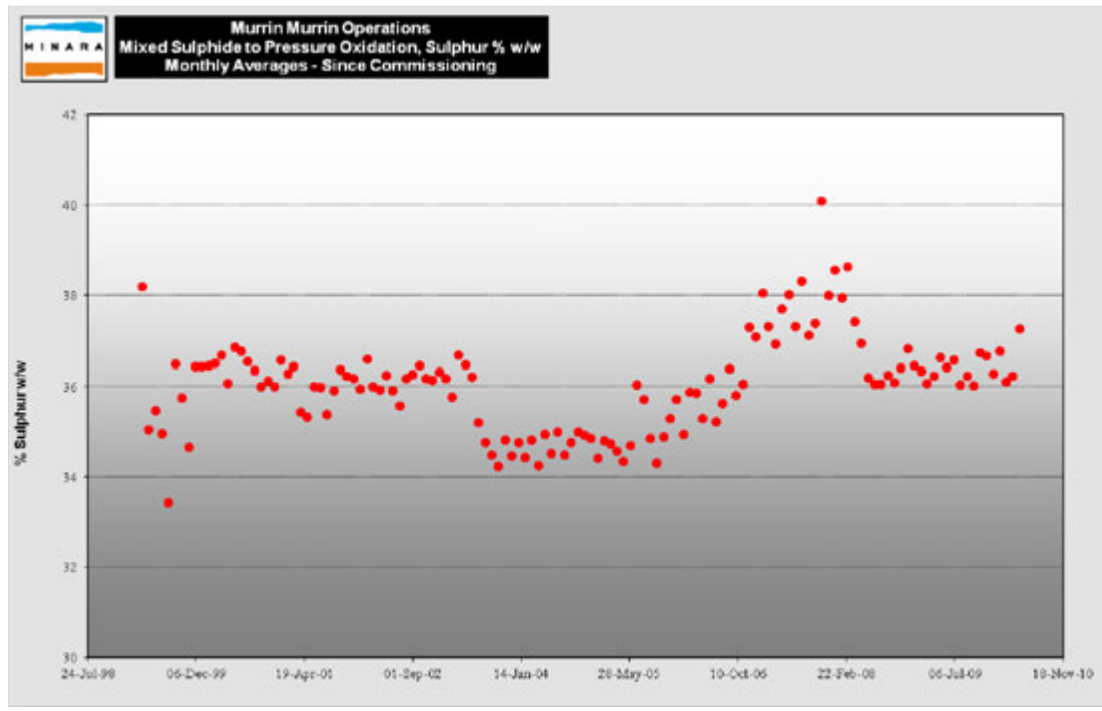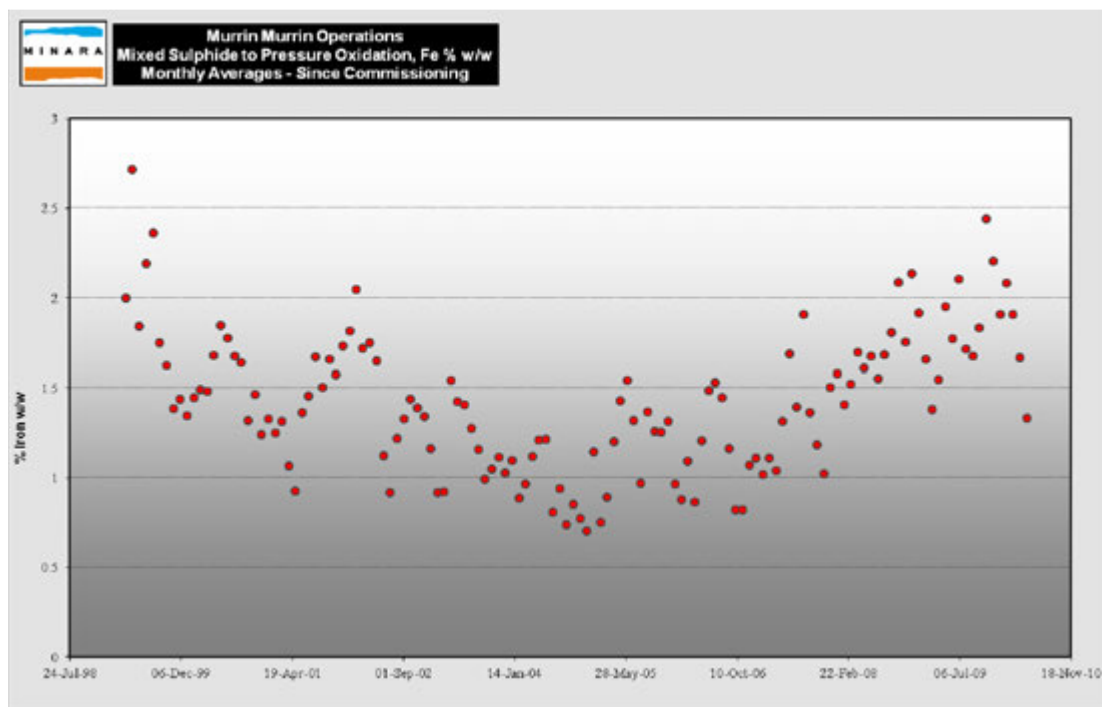
3500 - Mixed Sulphide Precipitation
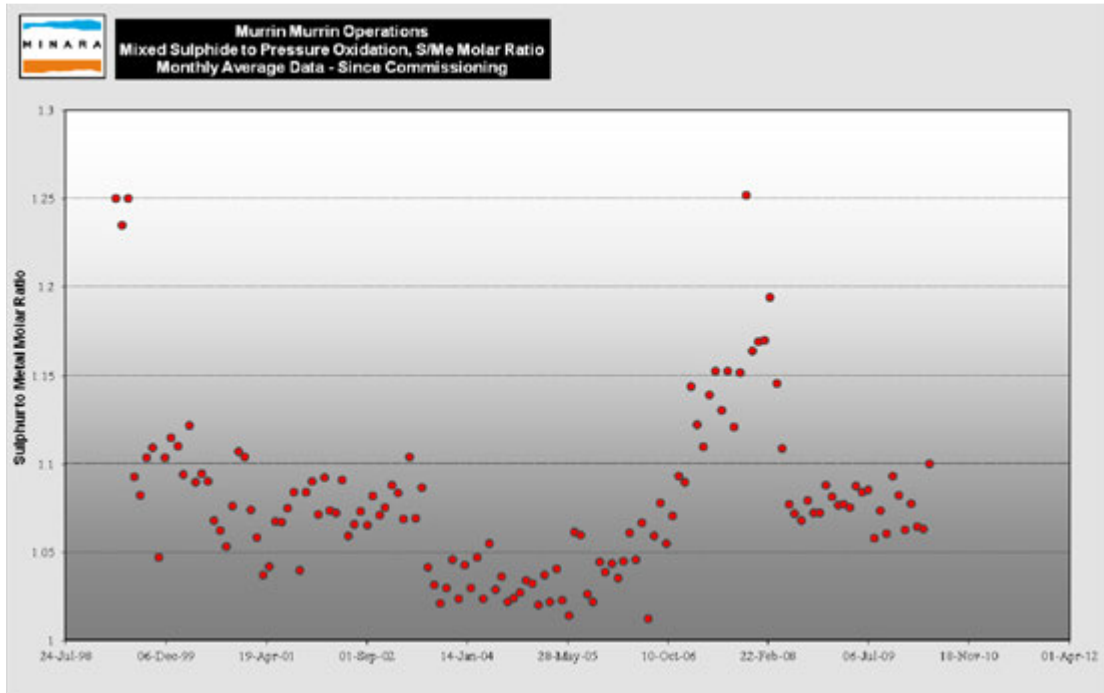
3500 – Mixed Sulphide Precipitation
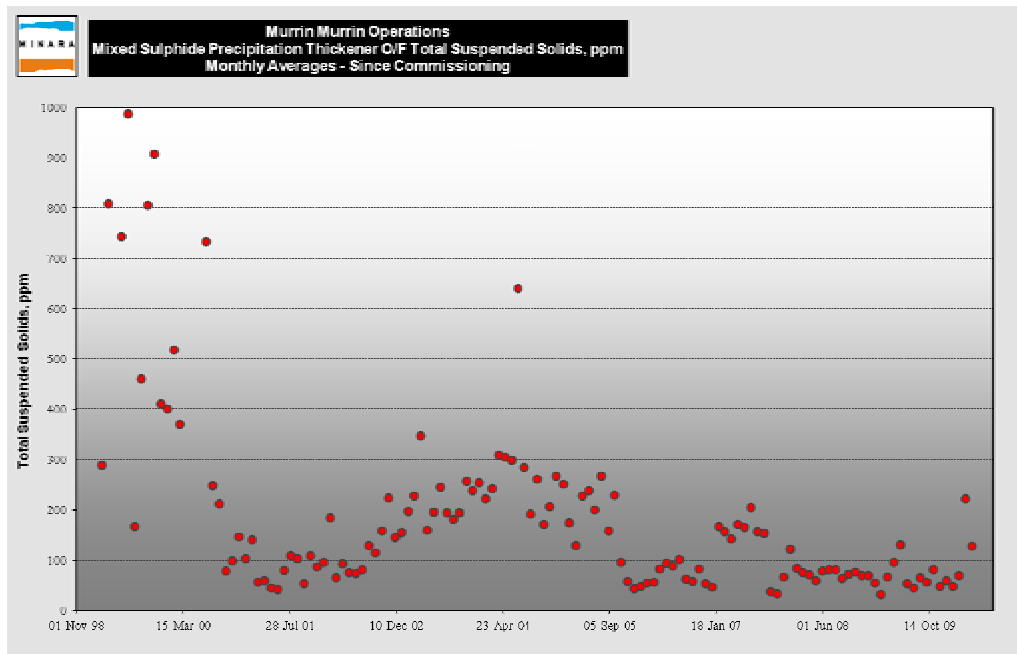
3600 – Oxygen Leach Autoclave

3600 - Mixed Sulphide O$_2$ Pressure Leach & Fe/Cu Removal
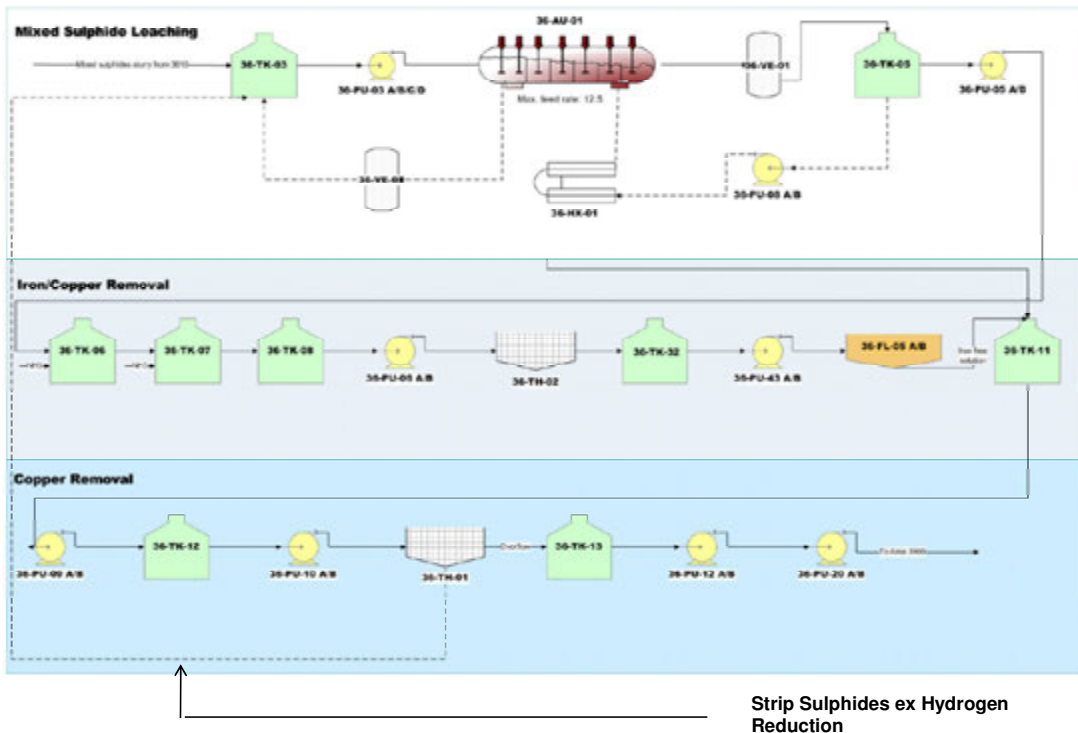
3600 –Sulphide Oxidation & Fe/Cu Removal Process Objectives

- To maximise re-leach of MSP (>99.5% Ni extraction)
- Minimise Fe in discharge solution. Need control of autoclave temperature.
- Fe removal via hydrolysis - pH control. Good pH control essential. Air added for Fe(II) oxidation. Peroxide sometimes used.
- Cu to be removed to low levels for on-spec cobalt.

Metathesis reaction with strip sulphides is used on their way back to autoclave for re-leach.

$$(Ni/Co)S + CuSO_4 \rightarrow CuS + (Ni/Co)SO_4$$
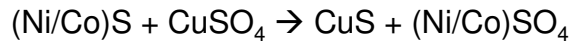
3900 - Solvent Extraction

3900 – Solvent Extraction – Process Objectives

Step 1 – Zn Removal

- Maximise Zn removal. Zn occupies sites on C272 in Co SX if recovery is not high.
- Minimise Co co-extraction in Zn SX. Good control of pH and organic flow is required.

Step 2 – Co Recovery

- Maximise cobalt recovery – although Ni H_2 reduction can tolerate some Co via molar ratio control
- Maximise organic loading in extraction to minimise scrub recycle Co.
- Scrub circuit to maximise Ni/Mg rejection while minimising Co recycle

3700 - Nickel Hydrogen Reduction

3700 - Nickel Hydrogen Reduction - Flowsheet
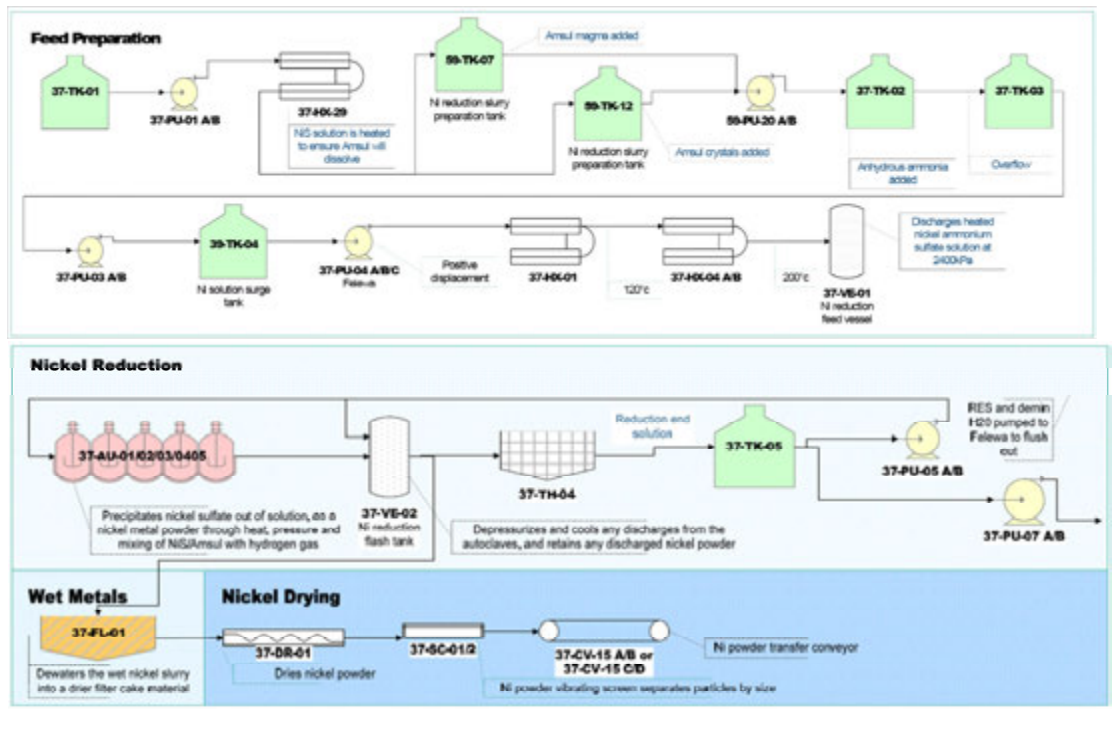
3700 – Nickel Hydrogen Reduction – Process Objectives

- Final metal winning step for nickel.

- Minimise residual nickel in Reduction End Solution

- Maximise reduction feed solution grade – batch process.   This maximises productivity

- Produce powder of approximate top size of 250-300 micron but must have variable size range for optimum briquetting performance

- Minimise reduction times.

- Minimise "non-reduction" parts of cycle. Eg rinsing, leaching, feed and discharge of solution, settling etc

3700 - Nickel Hydrogen Reduction – Nickel Powder
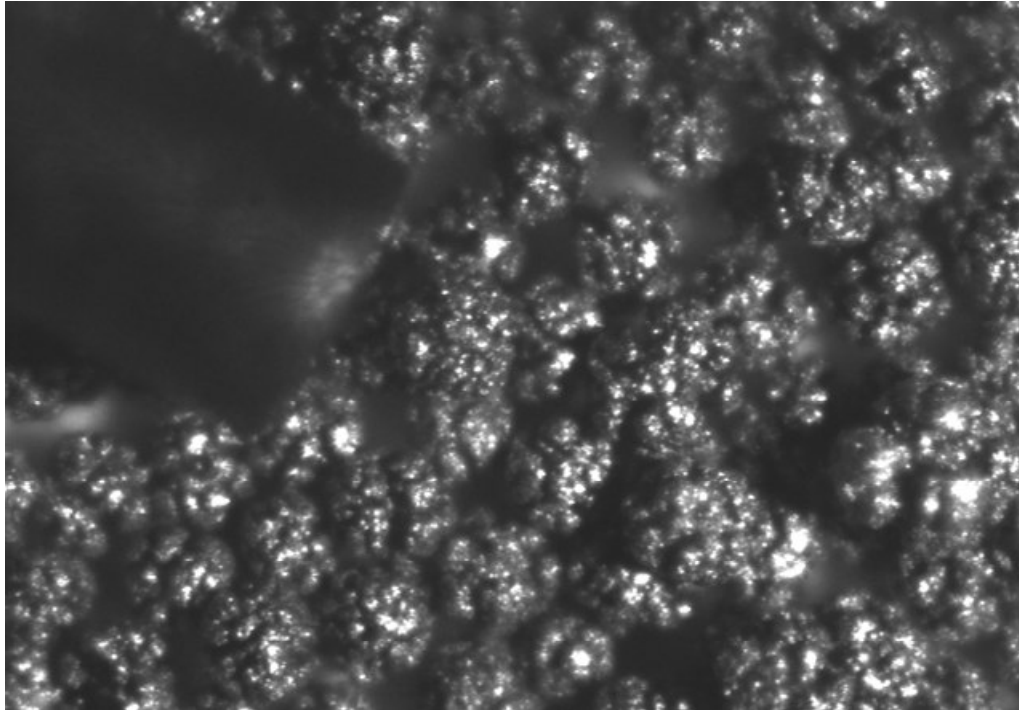
3700 - Nickel Hydrogen Reduction – Autoclave Plating

3700 - Nickel Sinter Furnace

3700 - Nickel Sinter Furnace – Ni Briquettes

Nickel and Cobalt Briquettes (ref $A1 coin)

3800 - Cobalt Hydrogen Reduction
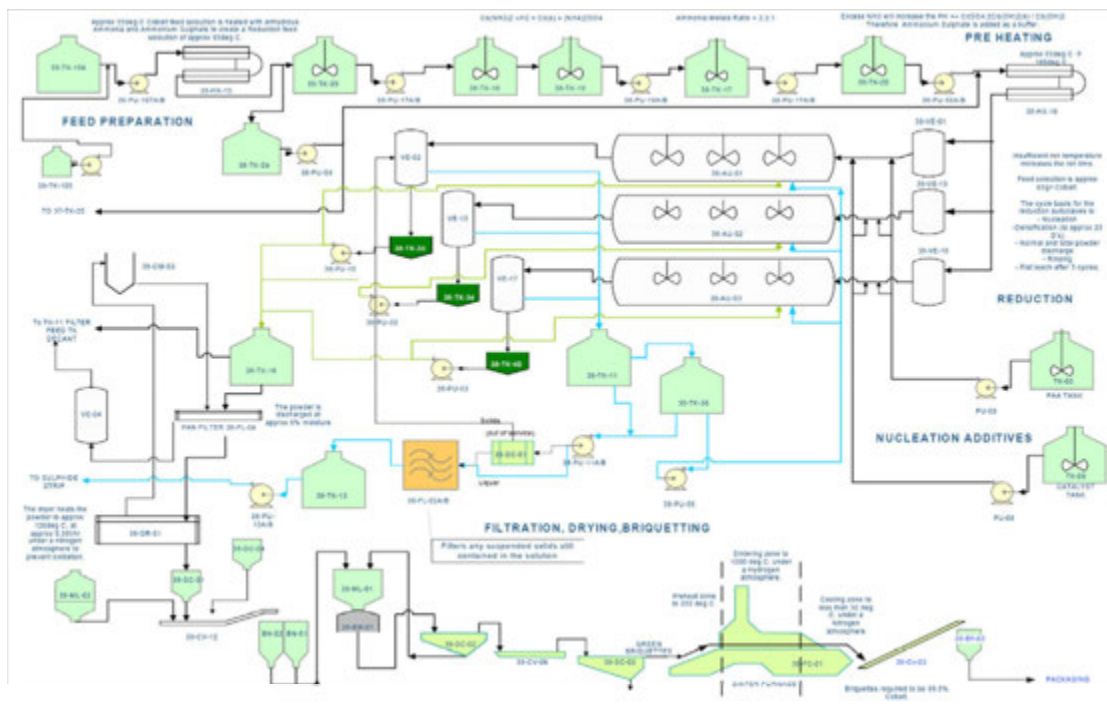
3800 – Cobalt Hydrogen Reduction – Process Objectives

- Effectively as per nickel hydrogen reduction

- Feed solution chemistry is slightly different to nickel in terms of NH_3/Co molar ratio and amsul levels but the process is very similar

5900 - Ammonium Sulphate

5900 - Ammonium Sulphate - Flowsheet

5900: AMMONIUM SULPHATE CRYSTALISATION
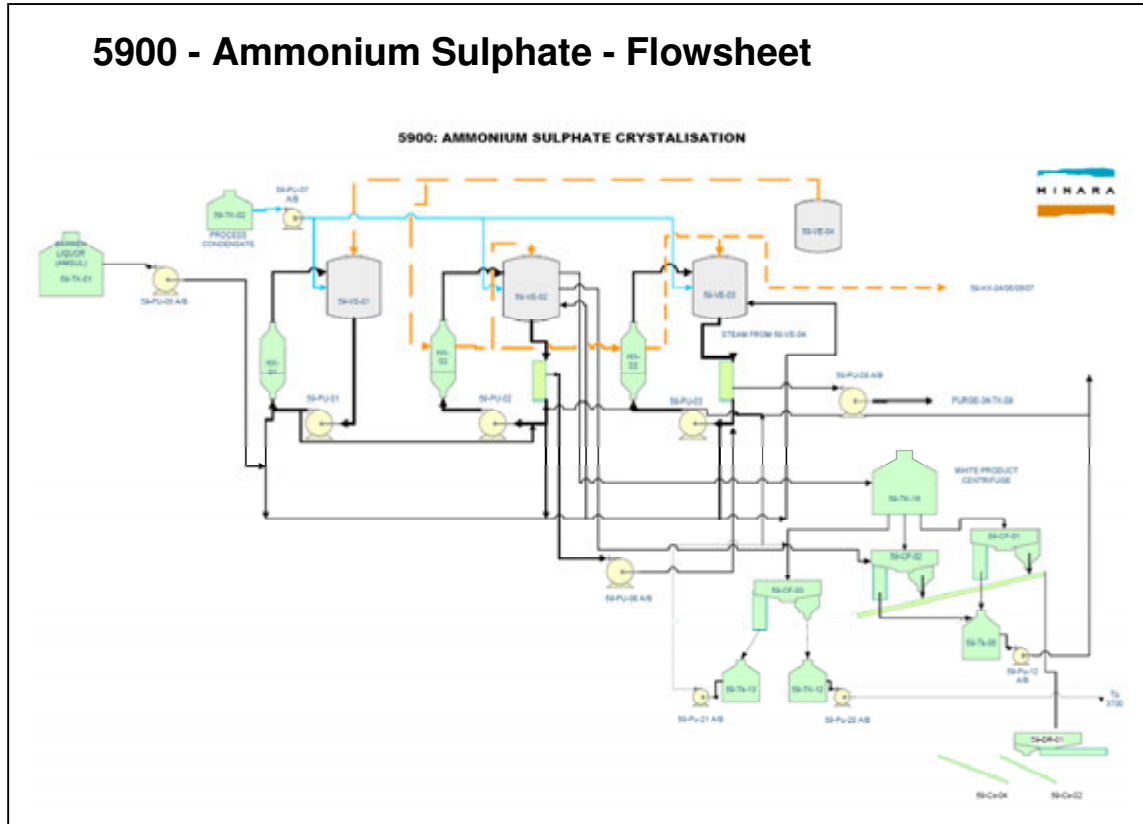
Water Treatment - Six RO Trains

Steam Turbine, 28MW Fully Condensing

Gas Turbine, 22MW with HRSG

Acid Plant, MECS 4400 tpd

**Sulfur
Handling**
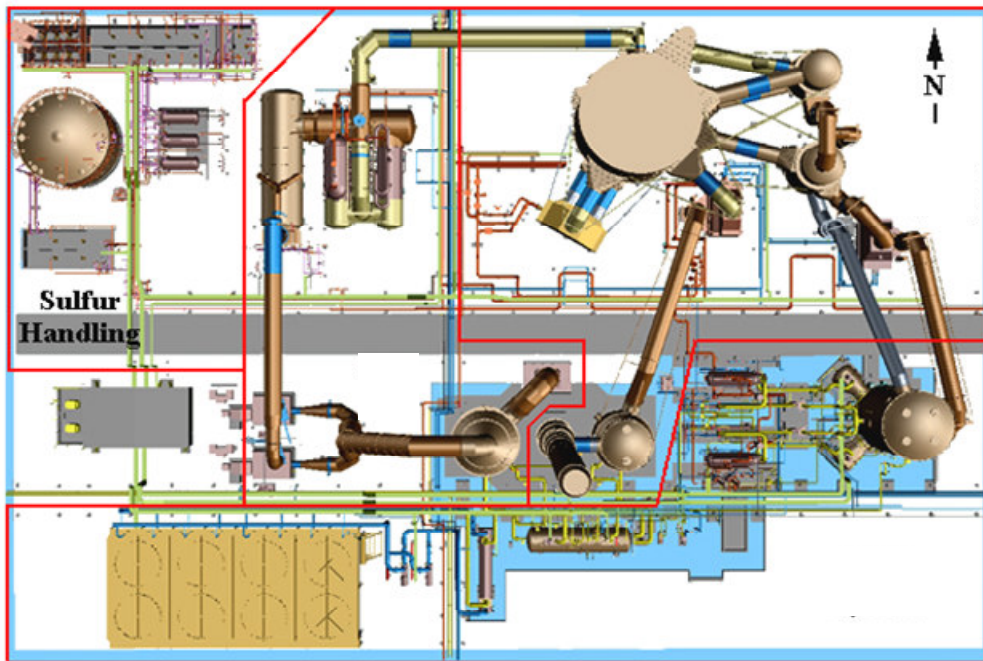
H₂S and Acid Plant

Acid Plant – Interpass Heat Exchangers

H$_2$S Plant – Two trains each ~2.8 tph H$_2$S

BOC Plants, H$_2$ and O$_2$/N$_2$

Package Boilers x 3

Plant Upgrade and Investment

2000-2003
Design Remediation

- Screening upgrade

- Slurry storage agitation

- HPAL flash system

- Nickel solution storage de-couples ore leach from refinery

- Second mixed sulphide train

🟥	Sustaining
🟦	Build in Redundancy
🟩	Enhance

Plant Upgrade and Investment

2004-2006
Reliability Focus

- Power system upgrade

- HPAL acid supply system

- Additional HPAL feed pumps

- Borefield development

- Secondary feed mill

- Murrin South ore-body development

🟥	Sustaining
🟦	Build in Redundancy
🟩	Enhance

Plant Upgrade and Investment

2007-2008
Utilities Upgrade and
Heap Leach

- Major acid plant upgrade
- Gas plant upgrades
- New hydrogen sulphide reactors
- Heap leach commences
- In-pit tailings commences

☐ (red)	Sustaining
☐ (blue)	Build in Redundancy
☐ (green)	Enhance

Plant Upgrade and Investment

2009-2011
Throughput Enhancement
and Redundancy

- HDS process debottlenecking
- 6th nickel reduction autoclave, 2nd flash vessel
- Murrin East ore-body development
- In-pit tailings continues

☐ (red)	Sustaining
☐ (blue)	Build in Redundancy
☐ (green)	Enhance
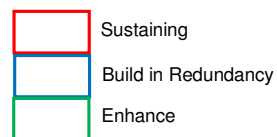
Plant Upgrade and Investment

10 Years of Investment

- Starting point: world's first integrated HPAL plant

- Addressed design flaws

- Built-in redundancy, reserve capacity, parallel processing

- Today: robust, long-term facility

Sustaining

Build in Redundancy

Enhance

Borefields Road – yes it does occasionally rain !!

Minara pastoral stations cover approximately 924,000 hectares

Goats sold for export market

Wild flowers after rain

Sturt desert pea

Rehabilitated pit 3-4 waste dump

Calcrete quarry – rehabilitated area

Statements related to Resources and Reserves

Resources

Murrin Murrin's Resources are based on a cut-off grade of 0.8% nickel and depletion of the geological block models using end of period surface surveys. The Resource classification is based on drill spacing, with the Measured category less than or equal to 50m x 50m, the Indicated category less than or equal to 100m x 100m and the Inferred category greater than 100m x 100m. The changes in Resource position are due to a combination of depletion of material from mining and processing activities and the updating of Resources with new Resource models. There is a significant increase in the Measured Resource from last year with a corresponding decrease in Indicated Resource due to the upgrading of the Resource with newer resource infill drilling that better defines the Resource and continued revision of modelling technique and parameters. Further change is related to normal mining activities and increased stockpile volumes.

Reserves

Murrin Murrin's Reserves are based on optimisations using long term assumptions of US$16,000 per tonne nickel, US$10.00 per pound cobalt and an exchange rate of US$0.70/A$. The 2010 Reserve optimisations consider the presence of project-to-date backfill, in-pit tailings deposition, public infrastructure and sites of cultural significance. During the preparation of the 2010 Reserve estimate it became apparent that a miscalculation had resulted in an overstatement of 15Mt in the 2009 Reserve estimate. This overstatement has been corrected in the 2010 Reserve. Additionally, the 2010 Reserve is net of all mining, milling and stockpiling activities completed during the period. As a result of the above there has been a net reduction in the reserve position from 2009.

The Measured and Indicated Mineral Resources include those Mineral Resources modified to produce the Ore Reserves. The process of deriving Ore Reserves uses the economic value of the ore blocks as the basis for inclusion in the Reserve, and is in accordance with the Australasian Code for the Reporting of Identified Mineral Resources and Ore Reserves (JORC, 2004). The economic value is based on metal grades and projected values, processing and associated operating costs. The above Resources and Reserves have been prepared in accordance with JORC requirements for public reporting.

Competent Persons Statement

The information in this presentation relating to Mineral Resources is based on information compiled by Mr Stephen King and Mr David Selfe, the information relating to Ore Reserves is based on information compiled by Mr Brett Fowler and the information relating to Metallurgical Results is based on information compiled by Mr David Readett.

Mr Selfe, Mr King, Mr Fowler and Mr Readett are all Members of the Australasian Institute of Mining and Metallurgy and at the time of compiling the information for this presentation were all full time employees of Minara Resources Limited. Mr Selfe, Mr King, Mr Fowler and Mr Readett all have sufficient experience which is relevant to the style of mineralisation and type of deposit under consideration and to the activity which they are undertaking in order to qualify as Competent Persons as defined in the 2004 Edition of the 'Australasian Code for Reporting of Exploration Results, Mineral Resources and Ore Reserves' and all consent to the inclusion in this release of the matters based on their information in the form and context in which it appears.

CORAL BAY NICKEL HPP-2 PROJECT IN PALAWAN, PHILIPPINES

By

Shinichiro Yumoto, Tozo Otani, Tadashi Nagai and Isao Ikeda

JGC corporation, Japan

Presenter and Corresponding Author

Shinichiro Yumoto
Yumoto.shinichiro@jgc.co.jp

ABSTRACT

Coral Bay Nickel HPP-2 Project (CBNH-2 PJ.) conducted by Coral Bay Nickel Corporation (CBNC) in the Philippines was mechanically completed on February, 2009. CBNC achieved the name plate capacity operation on April, 2009. Ramp-up period was only a couple of months. This paper presents the Project overview of CBNH-2 PJ and refers to a previous project, Rio Tuba Nickel HPP-1 Project (RTNH-1 PJ), and presents a discussion of the keys to success of completing the project on schedule, within budget, with high quality and with early ramp-up, in terms of validated design, reliable EPC execution, competent operator and maintenance staff, and an EPC lump sum contract scheme. Thanks to the success of these two HPAL projects, JGC was selected as a main contractor for Taganito PJ which is underway in Philippines now.

Coral Bay Nickel HPP-2 Project(CBNH-2 PJ) was conducted and operated by Coral Bay Nickel Corporation (CBNC), which is a joint venture of Sumitomo Metal Mining Co., Ltd.(SMM), Sojitsu Corp., Mitsui & Co., Ltd., and Rio Tuba Nickel Mining Corp. This project was an expansion of the Rio Tuba Nickel HPP Plant (RTNH-1 PJ), completed on 2006. This project was awarded to JGC Corporation (JGC), the EPC contractor, exclusively and was mechanically completed on February 20th 2009. Commissioning was completed in April 2009. CBNC achieved early start up in a couple of months.

Firstly, the characteristics of the CBNH-2 PJ will be reviewed in comparison with RTNH-1 PJ. Next the improvements and achievements in the stages of Engineering, Procurement and Construction (EPC) through the experience and Lessons learned in RTNH-1 will be presented.

Project Summary

Location

Palawan Island is located in the South China Sea and is 450 km in length and 50 km in width. Rio Tuba is located 250 km south of Puerto Princesa, which is the capital of Palawan Island (see Figure 1). Puerto Princesa has an international airport and is a 1 hour and 15 minute flight from Ninoy Aquino International airport in Manila.

Figure 1: Project location

Plot Plan

Expansion of CBNH-2 PJ was planned at an area adjacent to and surrounding RTNH-1 PJ (see Figure 2). One sulfuric acid tank (10,000 tons) is added in Pier site located near the sea shore and 8 km away from the Process Plant Site. Coal storage yard also expanded by client at Pier site.

This allocation of expansion area created the difficult constructability for the access to the new construction area and construction works beside the RTNH-1 plant in order to avoid the stoppage of the plant operation.

Many interconnection lines were planned for flexible operation of both plants. Total tie-in points came up to 168 points. All tie-in points were constructed during RTNH-1 plant shutdown (two times during construction: 45 points and 123 points). It was another constraint for the construction schedule.
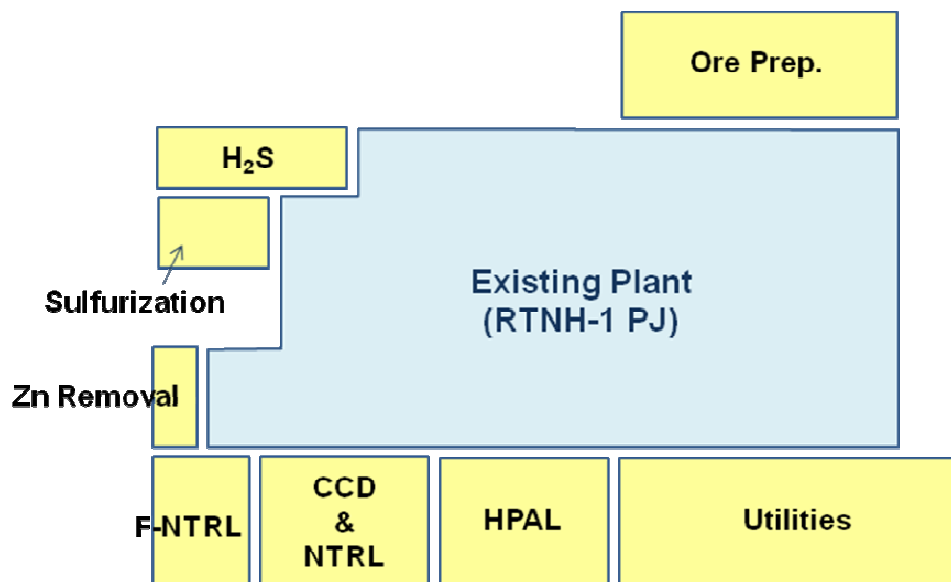

Figure 2: Plot plan for both plants

Process Description

The overall process comprises the following units, the same as RTNH-1 Plant (See Figure 3).
➢ Ore Preparation (Ore)
➢ High Pressure Acid Leach (HPAL)
➢ Counter Current Decantation (CCD)
➢ Neutralization (NTRL)
➢ Zinc Removal (De-Zinc)
➢ Sulfurization (MS)
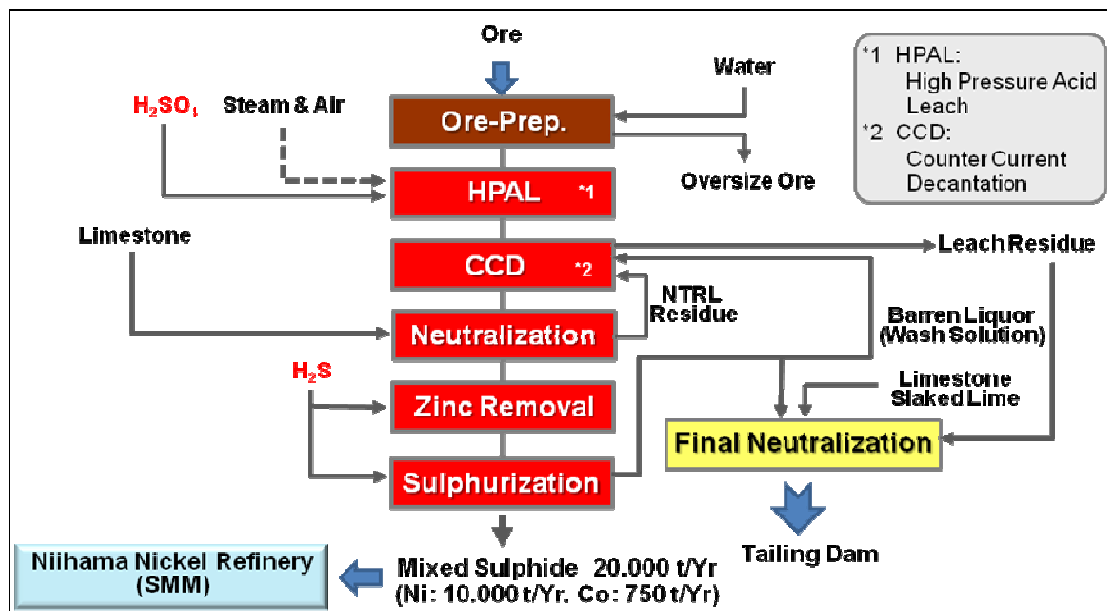➢ Final Neutralization (F-NTRL)

Figure 3: Process flow diagram

Project Overall

Construction contract was awarded in 2006. The construction boom started in the Middle East around the same time as CBNH-2 PJ., so that manpower for engineering was short, material cost was high and rising, vendors had become busy, and in addition, construction manpower was limited in the Philippines. We will discuss the detailed review later.

The increases in the bill of quantities (BOQ) for concrete, steel and piping were mainly affected by the extension of the Pipe Rack to connect each system in both plants. Tank/Thicker BOQ was decreased because Methanol tank was not constructed in CBNH-2 PJ. Acid proof lining area decreased caused by value engineering.

Table 1 shows the summary of both RTNH-1 PJ and CBNH-2 PJ overview.

Table 1 Project summary of RTNH-1 PJ & CBNH-2 PJ

		RTNH-1 PJ	RTNH-2 PJ
CLIENT		**Coral Bay Nickel Corporation** (Sumitomo Metal Mining Co., Ltd.: 54% ,Mitsui & Co., Ltd.: 18%,Sojitsu Corp.: 18%,Rio Tuba Nickel Mining Corp.: 10%)	Same as RTNH-1 PJ
PRODUCT		Mixed Sulfide (MS)	Same as RTNH-1 PJ
LOCATION		Rio Tuba, Palawan, Philippines	Same as RTNH-1 PJ
LOI		January 22, 2002	April 28, 2006
CONTRACTUAL DELIVERY DATE		October 15, 2004 (33 months)	May 31, 2009 (37 months)
MECHANICAL COMPLETION		August 31, 2004 (32 months)	February 20, 2009 (35 months)
MAJOR Bill of Quantities(BOQ)	CONCRETE	12,000 m3	13,600 m3
	STEEL STRUCTURE	1,800 tons	2,900 tons
	TANK / THICKENER	2,600 tons	2,400 tons
	PIPING	840 t Rubber Lined Pipe : 6,500 pcs	1,100 t Rubber Lined Pipe : 7,200 pcs
	RUBBER LINING	18,400 m2	18,300 m2
	ACID PROOF LINING	15,100 m2	11,900 m2

Overall Schedule

The difference in schedule between the projects came from the difference in the circumstances of the projects.

In engineering phase, total duration was longer than RTNH-1 PJ due to the shortage of manpower for the engineering work. Several huge projects were under way due to the construction boom in the Middle East, so that the arrangement of the workforce was very tight at that time. Basic design was completed rather quickly due to the experience and lessons learned in RTNH-1 PJ. The detailed design took more time and manpower than in RTNH-1 PJ.

In procurement phase, Purchase Order (PO) issue was started earlier based on BOQ of RTNH-1 PJ and data from the same vendors to gain the time.

In construction phase, the construction boom in the Middle East influenced the manpower supply. In addition, civil work started near the rainy season, so the duration of civil work was prolonged. In the last part of mechanical work, the rainy season affected the rubber lining work. Total duration was longer than in RTNH-1 PJ.

The construction boom in the Middle East influenced the material supply and the manpower supply in all of EPC phase. However JGC achieved early mechanical completion in CBNH-2 PJ.

RTNH-1
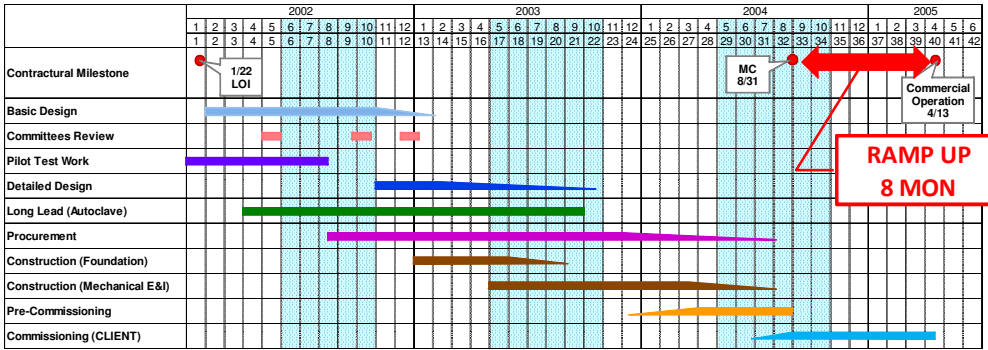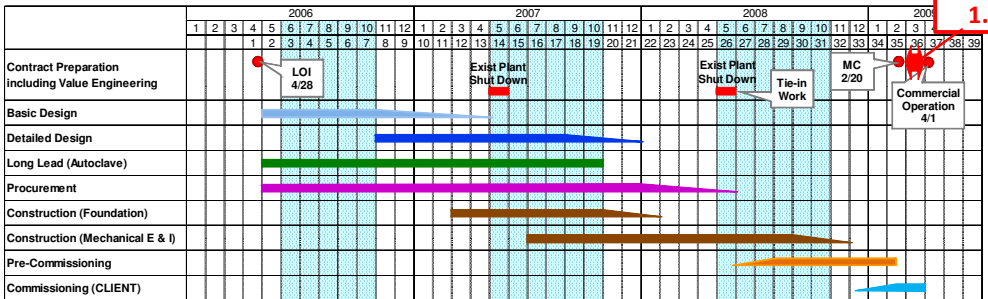
CBNH-2

Figure 4: Project schedule

Highlighted point was the 1.5 month Ramp-up period in CBNH-2 PJ. It is shorter than the other project (see Figure 5). We will discuss the reasons of this achievement later.
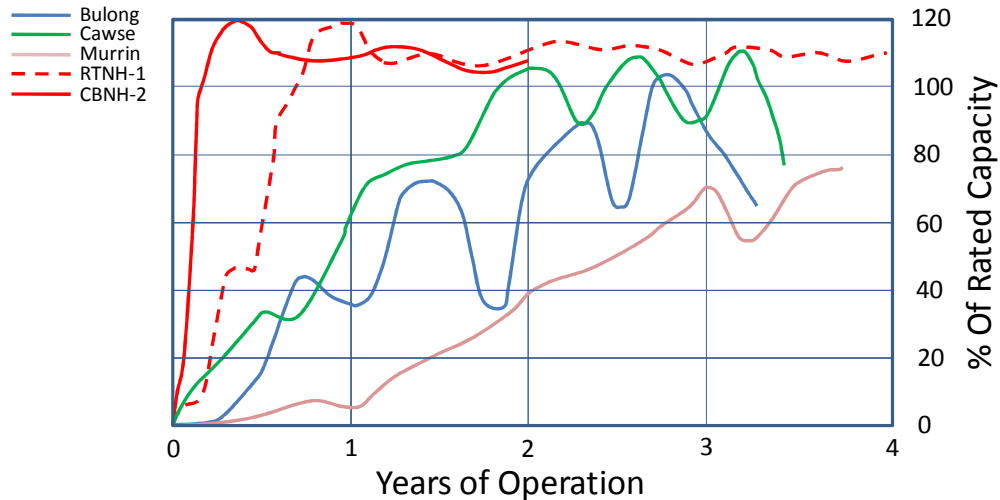
Figure 5: Ramp-up curve[1]

Engineering Review

Engineering works were implemented in JGC (in Japan) and JGC Philippines inc., (in Philippines). Total man hour (MH) spent in CBNH-2 was increasing in comparison with RTNH-1. The reason is the man power shortage both in Japan and in Philippines due to the construction boom in the Middle East. A lot of projects were going on in JGC and JGC Philippines at the time. It was difficult to assign senior engineer both in JGC and in JGC Philippines. So that total productivity was going down and total man hours were increasing.

Engineering MH and lessons learned (Engineering, Procurement, and Construction) in both RTNH-1 and CBNH-2 is summarized in table-2.

Table 2: Engineering man hour and lessons learned

	RTNH-1	CBNH-2
Basic Design Man Hour (hr)	29,000	26,000
Detailed Design Man Hour (hr)	320,000	450,000
Lessons learned (items)		
Engineering	340	220
Procurement (Fablication)	280	95
Construction	370	195
Total	990	510

Several design improvements were made as a result of the lessons learned in RTNH-1. Major improvements and alterations are described below.

HPAL Process Design

In the beginning of RTNH-1 Project, CBNC and JGC investigated existing HPAL plants with hydrometallurgical experts and several laboratory tests to verify the HPAL process. The basic design of HPAL process was done in cooperation with SNC-Lavalin. After the RTNH-1 project, CBNC developed its own operational know-how and improved the design philosophy. JGC did their original HPAL design based on the CBNC process design criteria and the lessons learned in RTNH-1 Project.

Machinery Design

➢ Ore preparation
In RTNH-1 project, several problems happened in the ore preparation area due to the larger mass of ore, the wet ore in rainy season and the mixed foreign matter. An ore feed stoppage caused a loss of plant operation and capacity. Design changes were made in the hopper and chute to avoid clogging with ore. Conveyor pulley was designed with a high safety factor to prevent damage, in CBNH-2 PJ.

➢ Rotary machinery
In RTNH-1 project, plant operation suffered from motor vibration on slurry pumps and agitators frequently. Supporting structure was strengthened during Pre-commissioning. In CBNH-2 project, prior to manufacturing the skid for pumps and agitators, vibration analysis was done by JGC and vendors to eliminate vibration problems after starting operation.

➢ Coal handling
The vertical bucket conveyor for the coal handling had many problems of stoppage and damage in RTNH-1 project because wet, cohesive and powdered coal was stuck inside bucket and casing of conveyor. Coal handling is also a critical facility for power generation in the utility system. Rubber type conveyor was selected and operated well in CBNH-2 project.

Material Design

➢ Rubber lining
Rubber lining work for tanks and thickeners is the one of the most critical construction items due to in-situ manual application over a huge area. Vulcanized material was selected to ensure the adhesion to the base metal in RTNH-1 Project. However steam curing was the most critical work, preparing temporary cover above the tank and keep it tight during steam curing, especially in the rainy season. Vulcanized material was selected in CBNHH-2 and adhesion was acceptable in comparison with the vulcanize type.

➢ Acid proof lining
Huge areas had to be lined with acid proof materials on the concrete pavement to maintain acidic process slurry. However the application timing was very limited between mechanical work and pre-commissioning work. The layered FRP was applied in RTNH-1. Many locations peeled off due to insufficient dryness of the concrete surface. Poly urea resin was applied by

spray in CBNH-2 PJ. The constructability was drastically improved to cope with the tight application schedule.

➤ Flake lining
We had the experience of the peeling off of the flake lining which was applied in the factory in RTNH-1 PJ. We found the damage after the installation of the vessels. The reason for the peeling off was over drying of the primer coat to prevent rust on the surface of metal. The application procedure was changed to the direct application of flake lining immediately after sand blasting at the site in CBNH-2.

Procurement Review

Major equipment was manufactured by the same vendors based on the operational results in RTNH-1 PJ (see table 3). The partnership between JGC and vendors was created by means of discussion to solve any problems and improve design of the equipment. Only a few systems were procured from different venders in order to widen the vendor selection.

Due to the construction boom in the Middle East, most of the material and equipment prices were rising and there were shortages. Vendor factories were busy all over the world.

JGC targeted early PO (Purchase Order) submission based on the data from RTNH-1 PJ. JGC also used new low cost suppliers for several steel structures and heat exchangers. JGC learned the quality control techniques for low cost vendors and acquired a wide selection of vendors in these categories for future construction.

In logistics, LCT (Landing craft transport) shortage occurred in 2007~2008 due to the boom in construction in the Middle East and many items of equipment were stuck in Manila port at one time. Long charter contracts with large vessels were let to overcome this critical situation. A large temporary stockyard was also arranged at Rio Tuba port for these shipments.

Table 3: Summary of Vendors

Project name	Location	Pre-heater	A/C Feed pump	Autoclave	A/C Agitator	Flash Tank	CCD Thickener	Boiler
RTNH-1	Philippine	Hitachi PT	GEHO	Hitachi PT	Lightnin(SPX)	Stebbins	Outotec	TBW (India)
CBNH-2	Philippine	Hitachi PT	GEHO	Hitachi PT	Lightnin(SPX)	Stebbins	Outotec	SEEN TEC (Korea)

Construction Review

Due to the difficult condition to build a new plant adjacent to and surrounding a live plant and the difficult economic circumstances caused by the construction boom in the Middle East, construction planning and safety management were major challenges in CBNH-2 project.

Due to the construction boom in the Middle East, construction manpower was short, especially skilled workers, in the Philippines. It created high risk for safety, schedule and quality. The increase of unskilled workers created another safety problem, and JGC strengthened safety measures, such as increasing safety supervisors and establishing stringent site rules. JGC mobilized its own expatriate supervisors and construction equipment to keep to schedule and ensure quality. Subcontractors increased their manpower to keep to the target productivities to comply with the schedule (see Table 4).

➤ Total direct man hour of RTNH-2 is 40% higher than RTNH-1 due to increase manpower to catch up total productivity.
➤ Due to the increase of Subcontractors direct manpower, JGC mobilized additional manpower for control the subcontractors. JGC indirect man hour increase 60% of RTNH-1.
➤ Especially Japanese Manpower was reinforced in CBNH-2.

Table 4: Summary of construction man hour records

	RTNH-1 PJ	CBNH-2 PJ	Ratio (CBNH-2 /RTNH-1)
Field Indirect MH (hr)	266,000	425,000	*1.60*
Japanese MH (hr)	33,000	69,000	*2.09*
Direct MH (hr)	3,533,000	5,031,000	*1.42*
Direct/Field Indirect	13.3	11.8	*0.89*

KEYS TO SUCCESS

Both, RTNH-1 PJ and CBNH-2 PJ were completed on schedule, within budget and with high quality. CBNH-2 project attained early completion of ramp-up operation to achieve the name plate capacity in a couple of months. Furthermore both CBNC plants are now operating steadily keeping the name plate capacity and now are trying to increase capacity to 120% of the name plate capacity.

We would like to discuss the empirical reasons for this successful achievement of CBNC project based on the following viewpoints. Keys to the success are a combination of them, not just one of them.

Highly Validated Design

Since the beginning of RTNH-1 PJ, CBNC and JGC made an effort to verify the process design by the pilot plant test and investigated the existing HPAL plants in design and maintenance viewpoints as follows:

➢ Pilot plant test for leaching test, CCD test, ore test.
➢ Organizing science committee with hydrometallurgical experts.
➢ Organizing engineering committee with the expertise from HPAL plant

After the completion of RTNH-1 PJ, CBNC made an effort during plant operation and developed its own operation know- how and validated the process design. JGC followed the engineering lessons learned in the RTNH-1 PJ and improved the design in CBNH-2 PJ.

The success of the project is derived from such validation of the process design and is the best knowledge at present. CBNH-2 project was based on the experience of the operation in RTNH-1 as a full scale test plant.

Reliable EPC Execution

After finalizing the validated process design, the next key point for the project success was how to materialize the process plant.

Project management capability was essential to achieve the reliable EPC execution. JGC has a long history to implement EPC turnkey projects in oil and gas industry. JGC has been cultivating the skill of project management.

The final goals of Project management must be complete the project on time, within budget and in good quality to ensure owners satisfaction. In order to achieve those objectives, effective use of resources (manpower, materials, machines, money, and methods) are essential for project management (see Figure 5).
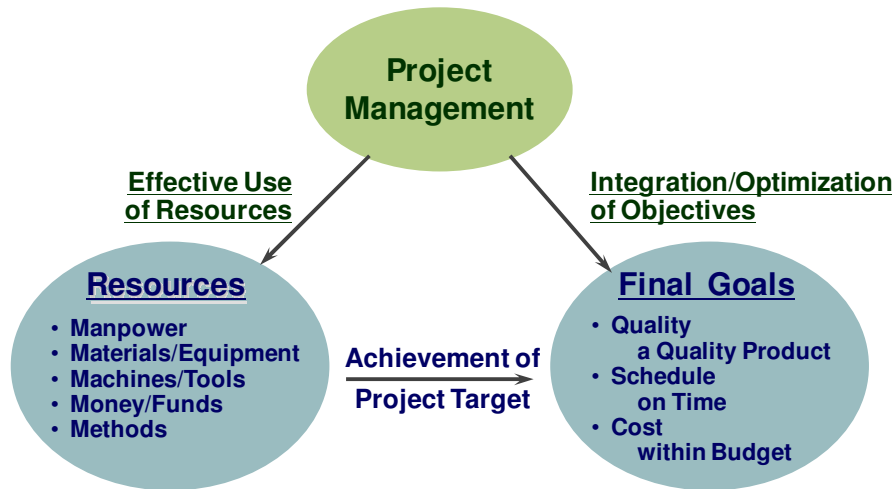
Figure 6: Project management

Project management comprises three control systems, schedule control, cost control and quality control. Each control system is functioning based on the monitoring and tracking of 5 resources in each phase, engineering, procurement and construction.

In both projects, JGC implemented project management based on the above philosophy.
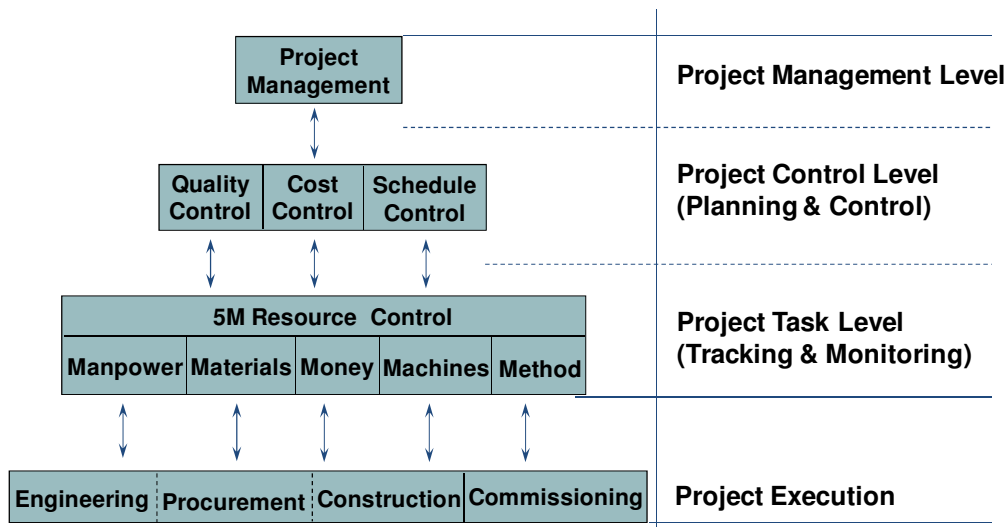
Figure 7: Project control

Competent Operator and Maintenance Staff

During pre-commissioning and commissioning after completing the construction work, it is important to collaborate between owner (operator) and contractor (maintenance) to achieve early completion of the ramp-up. Contractor (JGC) completed and handed over the plant system by system to enable CBNC to start operation at an early stage and fixed the mechanical problems which come up during operation as soon as possible.

CBNC made an effort to train thirty Philippino trainees in Japan at RTNH-1 PJ under the Company mission, "Exploiting limited natural resources efficiently with thanks to the earth and nature," and they acquired the experience to operate the first plant. Most of them joined the Commissioning team of CBNH-2 PJ. Thirty Japanese staff also joined in the commissioning team in CBNH-2 PJ.

JGC established a plant maintenance team (JMNT) in JGC Philippines Inc., at the beginning of RTNH-1 project. They started with 70 core members, dealing with the planning of the maintenance work and implementation of actual site work, such as scaffolding, welding, machining and so on. Now, core members have increased to around 150 for both plants. JMNT also mobilized over 200

"Shutdowners" (Workers mobilized only for Shut down) for Shut down maintenance twice a year. They had worked on the RTNH-1 plant maintenance. They had joined in commissioning stage to maintain the plant.

EPC Lump Sum Contract

Contract type shall be selected depending on the project nature. Generally lump sum contract is applied for a project being clearly defined in design, scope of work and work volume. Reimbursable contract is applied for the project being started before fixing the details for some reason or for a project based on newly developed technology or an experimental project.

Both of CBNC project completed within budget and schedule under EPC lump sum contract. Some other projects under reimbursable contract are over budget and schedule. In this case the merit of lump sum contract for client and contractor, as noted below, amplifies the success of the project. Lump sum contract is an incentive for reducing costs and keeping to the schedule, for both, Client and Contractor.

JGC is able to implement the largest GTL plant in Qatar under reimbursable contract with the mind of EPC bases and the performance of schedule and cost are appreciated by a client.

Client Merit

➢ Project budget is fixed in early stage of the project
➢ Encourage the contractor to cut costs and shorten the schedule in bidding stage
➢ Concentrate planning on commissioning and operation during construction

Contractor Merit

➢ Incentive for early completion to reduce cost
➢ Fast decision making in EPC control under single responsibility
➢ Minimum reporting to client to concentrate work

The comparison table shows typical features of lump sum and reimbursable contracts (see Table 5).

Table 5: Comparison of lump sum and reimbursable contracts[2]

	LUMP SUM	REIMBURSABLE
Project definition required in enquiry	✓ Complete	✓ Minimum-sufficient to enable tenderers to check that they have the resources
Advantage	✓ Purchaser knows his expenditure commitment ✓ Clarity of contractual risk and project management ✓ Allows fullest competition between potential contractors ✓ Bid evaluation is more straight forward	✓ Requires minimum enquiry definition ✓ Shortest possible bid time ✓ Complete flexibility-design development and purchaser participation practicable ✓ Purchaser/contractor conflict of interest is minimized ✓ Purchaser has control over costs incurred ✓ Purchaser can assess tenderers' rates
Disadvantage	✓ Purchaser/Contractor interests are more divergent ✓ Lengthy enquiry preparation time to prepare clear and complete specification and bid documentation ✓ Lack of flexibility-changes are difficult/expensive ✓ Purchaser participation in project is difficult	✓ Contractor has no monetary incentive to minimize cost to purchaser ✓ Purchaser has no assurance of final cost ✓ Purchaser has to check and verify contractor's man-hour and expense records ✓ Bid evaluation may be difficult

Comments	✓ Complete project definition is essential for a lump-sum contract ✓ Purchaser should minimize contracting industry tending costs by (a) not inviting bids until there is a high probability of the project proceeding(b) minimizing the number of tenderers (c) Pre-qualifying each tenderer so that he will not be rejected later on grounds that should have been known to Purchaser before the enquiry was issued and (d) considering reimbursing pre-qualified unsuccessful tenderers for their costs of bid preparation	✓ The most flexible type of contract, allowing a very rapid start. ✓ Flexibility may encourage purchaser to introduce design changes resulting in increased cost and longer programme. ✓ Contractor's profit/loss is limited ✓ Conversion of all or part of contract to a lump sum basis is possible during the project at the stage when scope of work becomes fully defined

CONCLUSION

Keys to success for these projects are firstly validating their process design by means of verification of the existing technology and pilot test, secondly implementing project under the advanced project management, thirdly training operators and maintenance staff, lastly considering contract scheme to encourage both parties to make an effort to minimize cost and schedule.

After completion of the two projects, JGC is now implementing another HPAL project named Taganito PJ in Philippines for Taganito HPAL Nickel Corporation which major share holder is Sumitomo Metal Mining Co.,Ltd. In addition, JGC has acquired remarkable experience and technologies in the non-ferrous metals field. JGC would like to make an effort to gain more advanced technology and project management skill in order to contribute to the growth in the non-ferrous metals industry.

Lastly JGC would like to extend our gratitude to the project owners, Sumitomo Metal Mining Co., and Coral Bay Nickel Corporation and to vendors and subcontractors who supported these projects for long time.

REFERENCES

1. T.Wilkinson, "Engineering of Coral Bay (Rio Tuba) Nickel Project; Second Generation HPAL?", ALTA 2006 Nickel/Cobalt conference, Perth, Australia, 2006.

2. "Table 1-Comparison of lump sum and reimbursable contracts" , International Form of Contract, Lump Sum contracts, The international Red Book, First edition 2007. Institution of Chemical Engineers

CORAL BAY NICKEL HPAL PLANT EXPANSION PROJECT

By

James Elson Llerin, Isao Nishikawa and Munekazu Kawata

Coral Bay Nickel Corporation (CBNC), Philippines

Presenter and Corresponding Author

James Elson Llerin

e.l.llerin@cbnc.com.ph

ABSTRACT

This Paper will present Coral Bay Nickel Corporation (CBNC) High Pressure Acid Leach (HPAL) Plant Project in the Philippines, mainly its Expansion activities. The original Plant was inaugurated on April 5, 2005 and has achieved its nameplate capacity of 10,000 Ni-Tons/Y in year 2007, where it produced 10, 078 Ni-tons. It was again achieved on the next year, where it produced 10,562 Ni-tons. The Expansion Plant was essentially designed to more than double the production capacity of CBNC HPAL Plant to 22,000 Ni-Tons and 1,500 Co-Tons in a year. Line-2 is basically a mirror-image of Line-1, where each major process circuit is duplicated. To increase Nickel throughput, the High Rate Ore Thickener type of Line-1 was replaced with a High Compression Thickener type in Line-2 to ensure higher %solids of ore slurry. Moreover, GEHO Pumps operation innovation was introduced by the use of Parallel method, which minimized operation down time. To achieve greater efficiency and high availability rate in the 2-Plant operation, tie-in lines were incorporated in the design, where vital solutions and slurries can be transferred from one Plant to another, depending on operational requirements.

The Construction of the Expansion plant was started in year 2006 and achieved its Mechanical Completion on February 20, 2009. After 6 months, Commissioning Completion was achieved on May 2009.

511

INTRODUCTION

Coral Bay Nickel Corporation (CBNC) was founded on April 2002, as a joint venture of four (4) companies namely, Mitsui Corporation (18%), Sojitz Corporation (18%), Rio Tuba Nickel (RTN) Corporation (10%) and Sumitomo Metal Mining (SMM) Corporation with a controlling stake of 54%. Aside from its capital share, RTN Corporation also supplies the Ore and Limestone for the High Pressure Acid Leach (HPAL) Plant located in Rio Tuba, Bataraza, Palawan, Philippines. The product of this Plant, a Mixed (Ni/Co) Sulphide is shipped to the SMM's Nickel Refinery in Niihama, Japan. SMM Corporation provides the Technology and Management personnel to the Plant, as well as the Sulfuric Acid, H_2SO_4, which is the main reagent for the HPAL process. Figure 1 below illustrates this relationship.
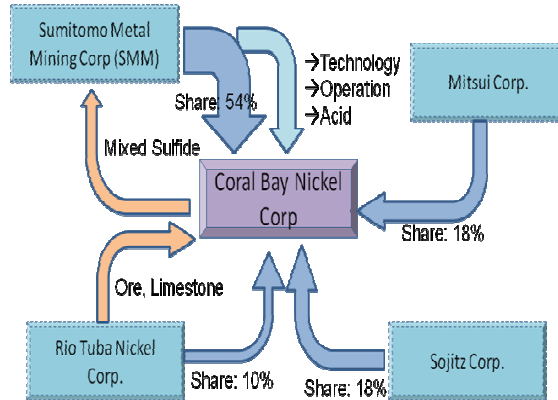
Figure 1: CBNC Shareholders Profile
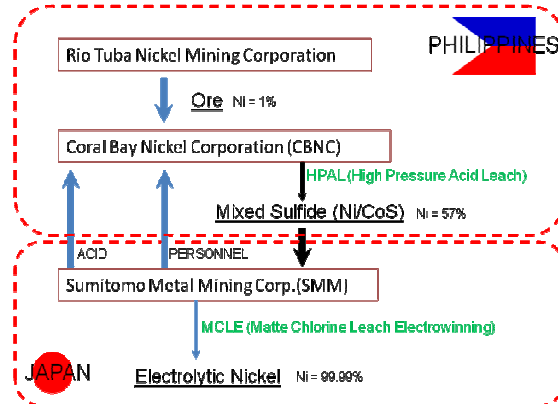
Figure 2: Geographical Relationship Profile

Figure 2 above shows the progression of Nickel metal from a low of 1% presence in Laterite ore mined by Rio Tuba Nickel Corporation, which is extracted and converted to an intermediate product by Coral Bay Nickel Corporation HPAL Plant to 57% concentration. The Niihama Nickel Refinery (NNR) in Japan refines this intermediate product to 99.99% of Nickel metal.

The nascent HPAL technology, combined with the proven Matte Chlorine Leach Electrowinning (MCLE) process of Sumitomo Metal Mining (SMM) has made this transformation of ore to pure metal possible.

In year 2000, SMM conducted the bankable feasibility study for the HPAL Plant in Rio Tuba, using the stockpiled Ore of Rio Tuba Nickel Corporation. RTN exports raw Nickel ore to Japan, and those that were below its cut-off grade were segregated into stockpiles and conveniently mapped.

512

By April 2002, CBNC was incorporated and construction of the Rio Tuba Plant started on January 2003. Mechanical Completion was achieved on August 2004.

Coral Bay Nickel Corporation's High Pressure Acid Leach (HPAL) Plant was inaugurated on April 5, 2005.

The Plant was designed to produce 10,000 tons of Nickel and 750 tons of Cobalt in a year. It achieved nameplate capacity in the year 2007, merely 2 years after its Mechanical Completion, where 10,078 Ni-Tons were produced. It was again achieved the next year, producing 10,562 Ni-Tons.

The Expansion Project of the HPAL Plant started in 2006 when the Engineering, Procurement and Construction (EPC) contract was awarded to Japan Gas Corporation (JGC) Philippines in April, the same Company that built Line-1. Basically, the expansion Plant design is just a mirror-image of the original Plant, duplicating its major Process circuits. In incorporating key improvements, such as tie-in lines of vital solutions and slurries, the Plant's overall Efficiency and availability was enhanced.

Mechanical Completion was achieved on February 20, 2009. Commissioning was completed on May 2009.

CBNC Profile

Location:	Barangay Rio Tuba, Bataraza, Palawan, SW of Manila, Philippines (about 250-km from Puerto Princesa, provincial capital)
Capital:	US$ 180 M + US$ 370 M
Product:	MS (NiS/CoS); Ni = 55 – 58 %; Co = 4 – 5%
Capacity:	22,000 Ni-T per year 1,500 Co-T per year
Resources:	2 Million DM Tons per year @ 1.26% Ni and 0.09% Co

Figure 3: CBNC HPAL Plant Location Map

CBNC is a major contributor to the country's economy, where it registered a net income of US$ 234 Million in the year 2009, which was about 10% of total income from metallic minerals mining in the Philippines on that year as shown in Figure 4 below[1]. The Company also employs directly and indirectly approximately 2,000 persons. Through the Social Development Management Program (SDMP), it is able to provide financial assistance to a school, hospital, road and other infrastructures building, housing, water and electrical supply and other supports to local government units.
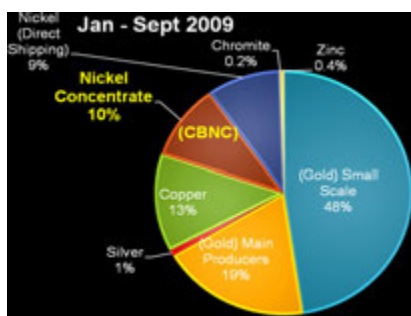

Figure 4: Philippine Metallic Mining Production in Jan – Sept 2009.
Source: Philippine Chamber of Commerce

513

CBNC Nickel Production

In its 3rd year of Operations, Coral Bay Nickel HPAL Plant was able to achieve its nameplate capacity of 10,000 Ni-tons in 2007. The Plant was able to sustain the production the next year, where it again produced 10,562 Ni-tons. Figure 5 below shows the annual production output of the Plant from 2005 where it started commercial operation up to year 2011 where it projects to produce more than 22,000 Ni-tons, its new nameplate capacity. However, since the Plant has been registering continuous annual growth; the Company is hoping to sustain it by actually targeting 23,000 Ni-tons in 2011. Furthermore, the target for year 2012 is 24,000 Ni-tons.

Notably, Coral Bay Nickel HPAL plant has breached the 2,000-Ni-ton per month for 6 months already. This monthly production Ni-ton quantity had been used as a benchmark on monthly achievements, which is based on nameplate capacity of each plant.

However, the highest monthly Production output thus far was registered on December 2010 with 2, 310 Ni-tons. With this milestone, 2,300 Ni-tons in a month has become the new benchmark of superior performance.
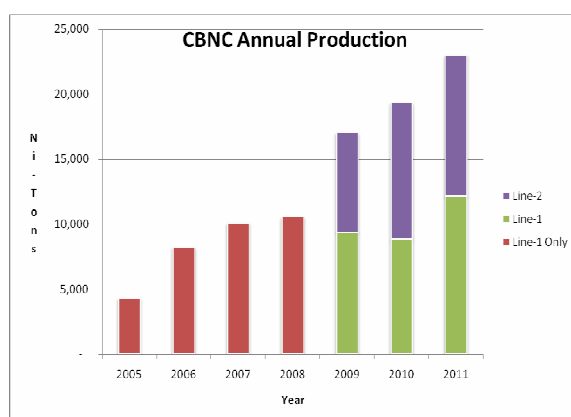
Figure 5: Coral Bay Nickel Corporation's Annual Nickel Production from 2005 to 2010

CBNC Flow Sheet

The stockpiled ores of Rio Tuba Nickel mines are delivered by trucks to the Plant site. The Coral Bay Nickel Plant processes this ore to produce Mixed (Ni/Co) Sulfides and sent to Niihama Nickel Refinery in Japan.

Figure 6 below shows the Process Flow Sheet of the Coral Bay Nickel HPAL Process. The flow sheet on the left shows the Line-1 and the flow sheet on the right is Line-2. As mentioned earlier, Line-2 is basically designed same as Line-1. Even the sizes of key equipments such as the Autoclave, CCD Thickeners, and Reactors are fundamentally the same.

514
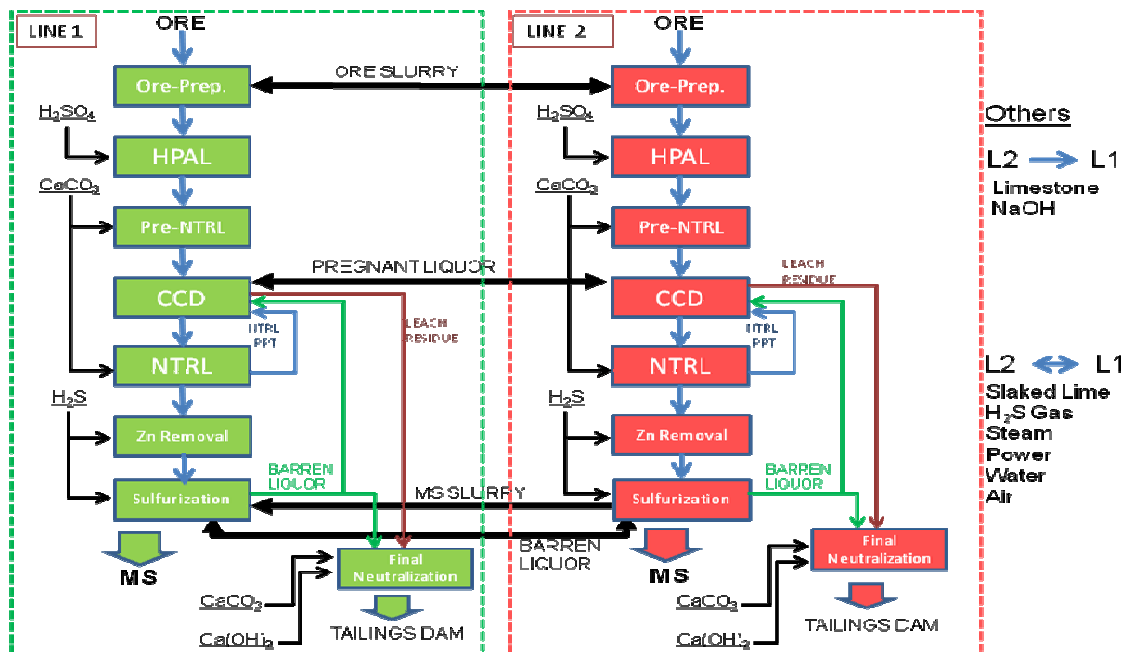
Figure 6: CBNC Process Flow sheet showing the tie-in lines.

Each major process circuit is briefly explained below:

1. Ore Preparation Circuit

    Laterite ores are screened in this circuit from +150-mm to -1.8-mm particles and pulped into 40 - 43% solids slurry. By blending of three different kinds of laterite ores, the resulting slurry has a typical assay of 1.26%Ni, 0.09% Co, 2.21% Mg, and 8.15% Si.

2. High Pressure Acid Leach

    The Ore slurry is pre-heated up to 200°C before pumping to the Autoclave using a Positive Displacement Pump. Using 99.8% H_2SO4 as lixiviant, the leaching reaction is carried out on 245°C and 4.0 MPa. The exiting leached slurry, which has a free acidity of 45 – 50 gpL is de-pressurized by a series of 3 flash tanks and sent to Pre-Neutralization Circuit. The recovered steam from the flash tanks is recycled back to the pre-heaters to heat the ore slurry prior to injection to the autoclave.

3. Pre-Neutralization

    The Leached slurry which has a pH of < 1 and free acid concentration of 45 – 50 gpL is neutralized to a pH of 2.7 – 3 using Limestone slurry. The reaction is carried out in 45 minutes and the neutralized slurry is sent to Counter Current Decantation circuit for washing.

4. Counter Current Decantation (CCD)

   Seven (7) thickeners are used in this circuit to wash the Leached slurry using Barren Liquor from Sulfurization Circuit. The resulting Pregnant Liquor overflow has a Nickel concentration of 4 – 4.5 gpL, which is sent to Neutralization circuit. The thickened solids of 40 – 45% Solids are sent to Final Neutralization circuit for treatment prior to disposal to Tailings Dam.

5. Neutralization

    The Pregnant Liquor from CCD circuit is neutralized using Limestone slurry to pH 3.2 – 3.4. The objective is to remove impurities such as Iron, Aluminum and Chromium by precipitating them as hydroxides. The resulting solids are thickened and sent back to CCD circuit and the clear neutralized overflow is sent to Zn Removal circuit.

6. Zn Removal

    The objective of this circuit is to remove Zinc from the Pregnant liquor using H_2S gas as it will co-precipitate with Nickel and Cobalt in the Sulfurization Circuit. Zinc is a major impurity of the final MS product as it will have adverse effects in the final refining process in Niihama Nickel Refinery in Japan. The precipitated ZnS solids are removed from the Pregnant Liquor using Polishing Filters.

515

7. Sulfurization

The Zn-free Pregnant Liquor is sent to Sulfurization circuit for the complete precipitation of Nickel and Cobalt to produce Mixed Sulfides. H_2S gas is used to recover over 99% of Nickel and Cobalt at a temperature of 63 – 70°C and pressure of 200 – 270 kPaG. The barren liquor, which contains 0.04 – 0.09 grams per Liter of Nickel, is sent to CCD circuit as wash water for Leach residue. Excess barren liquor is sent to Final Neutralization for treatment before disposal to Tailings Dam.

MS Product is bagged using flexible containers weighing 1,750 – 1,800 kilograms. The MS powder has a typical analysis as the following:

Table 1: Coral Bay Nickel MS Product profile

Component	Concentration	Unit
Ni	55 – 57	%
Co	4 – 5	%
Fe	0.2 – 0.5	%
S	30 – 35	%
Moisture	10 – 12	%
Particle Size (@50%D)	40 – 50	μm

8. Final Neutralization

The Leached residue thickened in CCD circuit and excess barren liquor from Sulfurization circuit are combined and treated in Final Neutralized circuit. The objective of this circuit is to remove the heavy metals such as Manganese, Iron and Chromium and adjust pH up to 8.5 – 9.0, using Limestone slurry in the first tank and Slaked Lime slurry in the succeeding tanks. The neutralized slurry is discharged to the Tailings Dam.

Most of the Supernatant in the Tailings Dam is recycled back to the Plant to be used in the production of Limestone and Slaked Lime slurries and feed water to Ore Preparation circuit. Excess Supernatant is discharged to the sea.

New Developments

1. Ore Thickener

Line 1 uses the Outokumpu's SUPAFLO® High Rate Thickener (HRT) type while Line-2 has the SUPAFLO® High Compression Thickener (HCT) type**.** SUPAFLO® High rate thickeners are suitable for all applications where flocculants can be used in the process and where the feed rate does not vary substantially over a short period of time. It has a short retention time and generates clear overflow. SUPAFLO® High compression thickeners provide consistently higher underflow density due to its extended high compression zone [2].

On July 2009, an FLSmidth's Dorr-Oliver® EIMCO® Deep Cone Paste Thickener (DCT) was added to Line-1. The EIMCO® Deep Cone® Paste Thickeners combine a proven system for optimizing flocculation with deep tankage design to allow maximum gravity reduction in the surface area and a substantial increase in underflow solids concentration. Settled solids can be brought to a density approaching consolidation and discharged at high viscosity[3].

The three thickener type's construction differences are shown in Figure 7 below. HCT has about 1.5 times the height of the HRT and the cone slope has 1.5 times the angle. On the other side, DCT has 2 times the height of HCT and the cone slope has 2 times the angle. This distinction in construction design spelled the difference of the three thickeners underflow slurry output.

516

			HRT	HCT	DCT
Tank	Diameter	m	20.0	20.0	14.0
	Depth	m	2.6	4.0	8.9
	Slope	°	9.5	14.0	30.0
Drum	Diameter	m			2.0
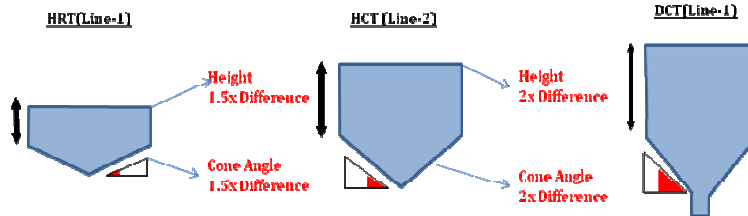
Figure 7: Difference of construction of three thickener types

Based on the latest CBNC Operations data a shown in Figure 8 below, HCT can generate about 1% more than the Solids % of the HRT with respect to Silica concentration. Furthermore, DCT can generate about 3% more than that of HCT. High %solids of ore slurry increase the Nickel throughput of the Plant, with optimal volumetric flow rate.
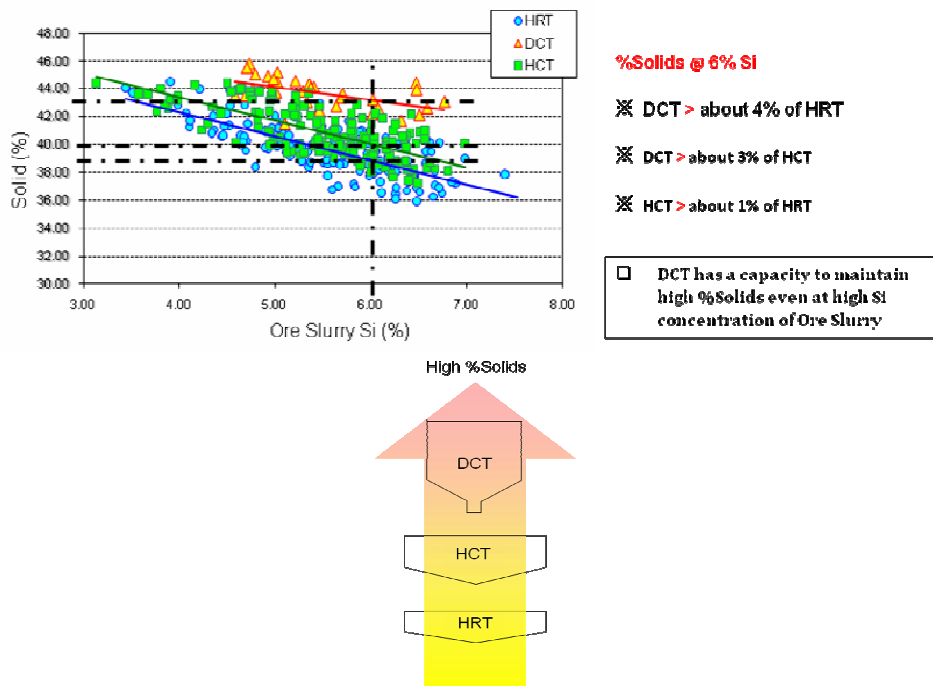
Figure 8: High Rate Thickener (HRT) and High Compression Thickener (HCT) comparison

517

2. Oversize Ore Removal
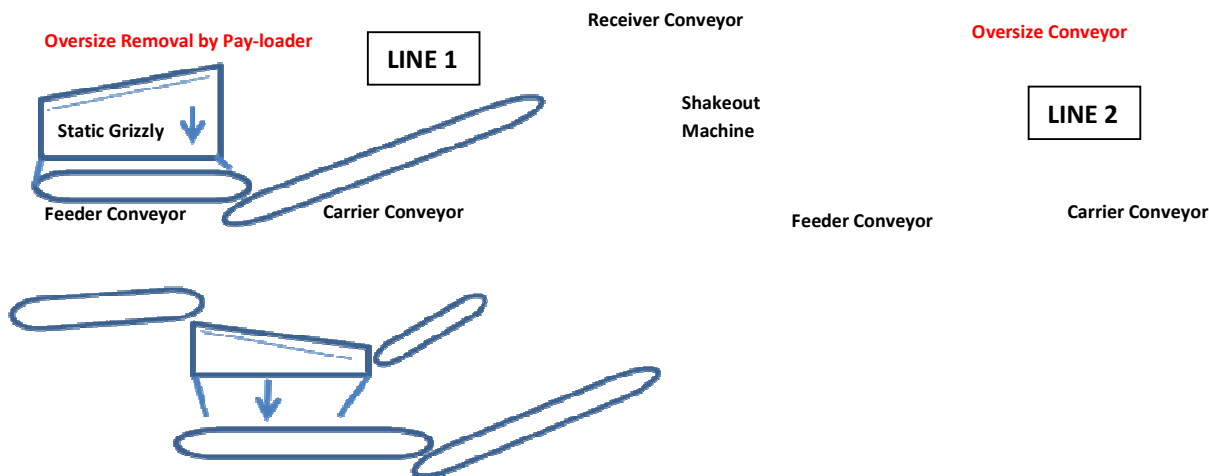
Figure 9: Line 1 and Line-2 Ore feeding circuits.

Payloaders are used in feeding ore for both lines. In Line-1, ore is dumped into a hopper with a 150-mm gap grizzly. Oversize ores that stay on top of the grizzly are removed by the same payloaders.

In Line-2 however, ore is dumped into a main conveyor. This conveyor feeds the ore to a Shakeout machine with a 150-mm mesh bars to separate oversize ores. The shakeout machine mesh bars has a slope of at least 5 degrees that allow the oversize to be removed at the other end due to continuous up and down movement of the machine to shake off ores. The oversize then drops onto a conveyor at the end of the shakeout machine that moves it to a depository awaiting transfer to another location using dump trucks.

This Line-2 new ore screening design added more efficiency as it eliminates human intervention in gathering the oversize ores. Continuous feeding of ore can then be achieved.

3. HPAL GEHO® Pumps Parallel Operation

Ore slurry is pumped into the Autoclave using a Positive Displacement Pump made by Weir Minerals, which is called GEHO® Pump. This is the most important pump in the Plant as it practically outlines the Plant Availability. In order for the Plant to operate continuously, the GEHO® pump must be available all the time.

The GEHO® Heatbarrier type design is used in CBNC HPAL plant. The design and model of the pumps of both lines is similar. This GEHO® Heatbarrier pump is a crankshaft driven two-cylinder double-acting and three-cylinder single-acting high temperature piston diaphragm pumps. The Heatbarrier design handles slurry up to 210°C. A drop-leg pipe connects the valves to the dead-headed diaphragm housing. The water jacket and oscillating separator sustain a low diaphragm temperature (below 100°C) with minimum heat loss. A free floating separator, which oscillates with the pump stroke speed, acts as a mechanical heat barrier to minimize heat transfer losses and equipment sizing. The poppet valves are the only wear parts[4].

The poppet valves or more commonly known as cone valves, being the only wear parts, hugely affect not only the Maintenance cost but also the availability of the GEHO® Pump, and consequently the HPAL operation. Without sacrificing operation rate, Coral Bay Nickel has been able to lengthen the life of its GEHO® cone valves by the use of Parallel Operation. Basically, all pumps in the Plant are available in two's to ensure continuous operation whereby one unit is spare while the other is in operation. The HPAL GEHO® pump is no exception; however, Coral Bay Nickel has been using the two pumps always in Parallel operation.

When two pumps having common Suction and Discharge lines are operated at the same time, they are said to be running in Parallel.

518

When in Single Operation, GEHO® Pump has to be operated at 83% to 100% output all the time and this takes a toll on the cone valves. The wear rate of the cone valves is caused by multiple factors such as particle size and abrasiveness of the materials, but it is enhanced by the amount of the material that passes through it. Parallel operation enables Coral Bay Nickel Plant to run the GEHO® Pump to a minimum of 50% to a maximum of 60% output per unit only.

The positive displacement of fluid and fixed volume is the result of the fluid being mechanically moved through their pump passage on a regular cycle. This means that regardless of the system they discharge into, the pressure and volume will remain constant. The power of the driving device and its speed, limit the volume and pressure.[5] Therefore, when two (2) GEHO® Pumps are running at 50% in Parallel, it has an equivalent output to a single-unit operation at 100%. This allowed Coral Bay Nickel Plant to operate its GEHO® pumps continuously in a longer period of time, and the result is illustrated in Table 2 below.

Table 2: Comparison of Single and Parallel GEHO® Pump Operation with respect to Cone Valve life

Year	Operation Method	GEHO® A	GEHO® B
2006	Single @ 100%	9.8 Days	7.5 Days
2010	Parallel @ 60%	19.5 days	21.8 days
• Longest cone valve life recorded was 68 days without replacement.			

Replacement of cone valves usually consumes about 5 hours of maintenance, and with the current currency exchange rates, it costs about US$ 32,000, excluding labor.

4. Supernatant Recycle

Coral Bay Nickel's neutralized waste slurry is discharged to the Tailings dam. The solids are allowed to settle and the Supernatant is recycled back to the Plant for the dilution of Chemicals such as Limestone and Slaked Lime. Excess Supernatant is discharged to the sea. This water contains high Calcium e.g. 400 – 600 mg/L, making it unusable for Ore Slurry preparation. Scaling of the pre-heaters depends on magnesium and <u>calcium</u> of the feed water[6].

To increase the recycle of Supernatant back to the Plant, Line-2 included Calcium Removal facilities to reduce calcium to less than 30 parts per million (ppm). This enables the Plant to conserve up to 200 m3/hr of raw water for Ore slurry preparation. This becomes handy especially during the dry months from March to July. Table 3 below shows the raw water, Supernatant and the Calcium-removed Supernatant water elemental analysis taken from the CBNC March 2010 Operations data.

Table 3: Raw water, Supernatant, and treated Supernatant components analysis (CBNC March 2010 Operations Average Data)

Water type	Si	Mg	Mn	Ca
Raw Water, gpL	0.02	0.03	< 0.001	< 0.01
Ca-removed Supernatant, gpL	< 0.01	0.03	< 0.001	0.02
Supernatant Water, gpL	< 0.01	0.09	0.001	0.57

5. Pipeline Tie-ins

To boost the efficiency of 2-Plant operation, tie-in lines were incorporated in the design. Ore slurry, Pregnant Liquor and Barren Liquor can be transferred from Line-1 to Line-2 and vice versa. Also, Slaked Lime, H_2S gas, and utilities such as water, steam and power can be interchanged by the two lines whenever needed. Moreover, the Limestone slurry preparation

519

and Caustic Soda (NaOH) dissolution facilities in Line-2 were upgraded 150% of Line-1; hence, it can supply Line-1 also. Excess MS Slurry of Line-2 is also transferred to Line-1 since the MS bagging facilities of the former is half of the latter.

Table 4: Summary of Tie-in Pipelines of Coral Bay Nickel HPAL Plant

Area	Material	Direction of Transfer
Ore Preparation	Ore Slurry	L1 ← → L2
CCD	Pregnant Liquor	L1 ← → L2
Sulfurization	MS Slurry	L1 ← L2
H_2S Plant	H_2S Gas	L1 ← → L2
Chemicals	Limestone	L1 → L2
	Slaked Lime	L1 ← → L2
	NaOH	L1 ← L2
	Calcium-Free Supernatant	L1 ← L2
Utilities	Air, Power, Water, Steam	L1 ← → L2

Table 4 above shows the Line-1 and Line-2 tie-in lines and direction of flow of vital process solution and slurry and other materials that allowed more flexibility to Plant Operations as the inventory holding capacities are practically enhanced. The Operation rates of the two lines can be adjusted accordingly. For example, if one train of Ore Preparation is shut down for maintenance repairs for more than 6 hours, HPAL operation rate need not be decreased because Ore slurry is available for transfer from another line. As a result, both lines can maintain its maximum operation rate. One train of Ore Preparation is designed to operate up to 80% of Plant Operations, and two trains are continuously operating in parallel.

Expansion Plant Commissioning

1. Overall Project Schedule
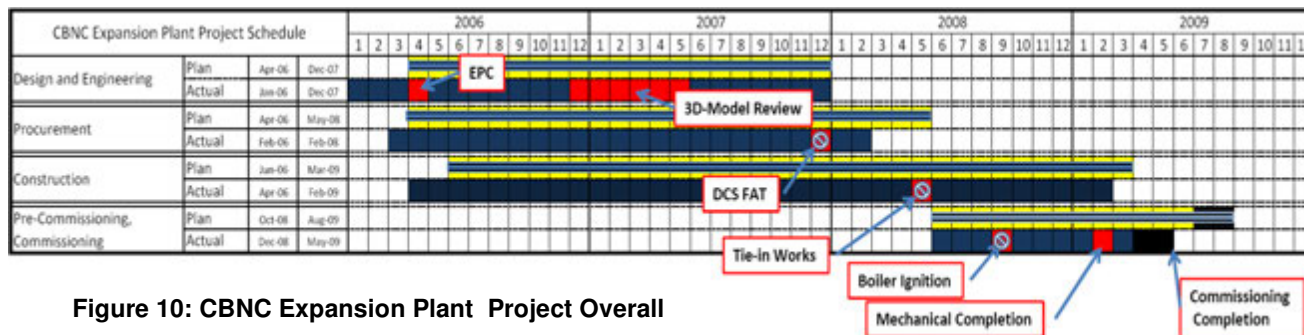
Figure 10: CBNC Expansion Plant Project Overall

Figure 10 above shows the overall schedule of Coral Bay Nickel HPAL Expansion project. The EPC Contract was signed on April 2006 and a total of six (6) months were spent to finish the 3D Model Review. The Engineering Design was completed on schedule.

Moreover, Procurement phase of the project was completed ahead as planned. The DCS Final Acceptance Test (FAT) was held on December 2007. Construction activities proceeded smoothly and it was completed just a month ahead of schedule. After the Tie-in activities with Line-1 common equipment on May 2008, Pre-Commissioning Activities started on June 2008, for the most part in Utilities area.

Expansion Plant's Boiler first Ignition took place on September 2008. By that time, Chemicals and other Auxiliary circuits were already in its pre-commissioning stages

Pre-commissioning of Process areas and its Commissioning proceeded accordingly.

520

2. Line-2 Commissioning
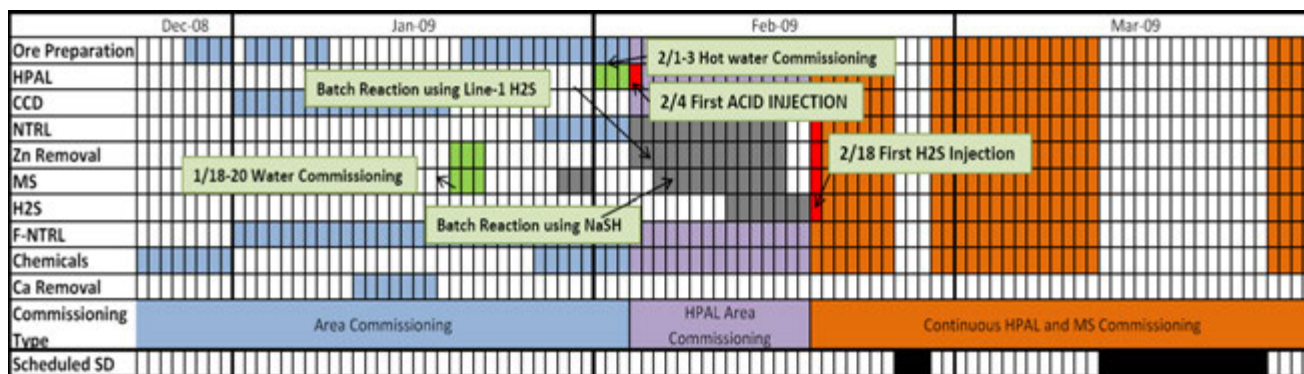
Figure 11: Line-2 Commissioning Schedule

Figure 11 above shows the Commissioning Schedule of Coral Bay Nickel's Line-2 Plant. Ore Preparation Circuit and Chemicals Preparation Circuit started its area commissioning on December 2008. Sulfurization Circuit had its Water Commissioning on January 18 – 20, 2009; while HPAL's Hot Water Commissioning was performed on February 1 – 3, 2009.

The Water Commissioning episodes served as training runs for the Operation team. While checking the interlocks and sequences, it also familiarized the Operators in the controls of the Line-2 equipment.

On February 3, High Pressure Acid Leaching operation was started when 99.8% H_2SO_4 was injected to the Autoclave for the first time. Ore Preparation, HPAL, Counter-Current Decantation (CCD) and Final Neutralization circuits were operated continuously. During this period, the Pregnant Liquor overflow solution of CCD circuits was transferred to Line-1 using the tie-in line since Zn Removal and Sulfurization circuits were not yet ready to receive it.

At that time, Zn Removal and Sulfurization circuits were undergoing 'batch' operations. Since Line-2 H_2S Plant construction was not yet completed, H_2S gas was 'borrowed' from H_2S Plant Line-1 to conduct initial tests on the Zn Removal equipment. Also, NaSH solution was prepared by dissolving NaSH flakes to start the batch reaction operation of Sulfurization reactors. Moreover, MS Slurry was 'borrowed' from Line-1 Sulfurization Circuit to test the MS Pressure Filter Equipment.

When Line-2 H_2S Plant produced its first H_2S gas on February 18, continuous operation of Zn Removal and Sulfurization circuits ensued. The two circuits were made online with other already running circuits making that phase of operation a full plant run. For the first time, Pregnant Liquor was continuously neutralized in the Neutralization circuit and fed to Zn Removal circuit in preparation for the Sulfurization reaction. Flow rate in the Sulfurization was at modest 200 m^3hr or about 50% design capacity yet, thus about 90 m3/hr of Pregnant Liquor was still being transferred to Line-1. This rate was continued until the first scheduled shutdown on that month.

After the 3-day scheduled shutdown on February 24 – 26 to make way for adjustments of the minor troubles encountered in Zn Removal and Sulfurization circuits, operation rate peaked up. One hundred percent (100%) Plant operation rate was achieved at this second continuous run until the next scheduled shutdown on March 14 – 26 to make way for a major modification of the Limestone Slurry Preparation equipment.

For the month of March 2009, 329 Ni-tons were produced. Line-2 Commissioning progressed quickly where it produced 845 Ni-tons in April and 798 Ni-tons in May.

Commissioning Completion was declared at the end of May 2009.

Another shutdown was scheduled after the Commissioning Completion on June 15 – 28 to make way for the JGC Construction Group to conduct repairs and adjustments on some equipment, which were encountered during the previous operation.

521

After the June scheduled major shutdown, Line-2 operations continued smoothly. In the month of August 2009, Line-2 helped Coral Bay Nickel HPAL Plant to record for the first time at least 2,000 Ni-tons a month. In that year, Line-2 produced 7,487 tons of Nickel overall.

In year 2010, Line-2 production improved to 10,424 Ni-tons. Figure 12 below shows the comparison of operation rate progress of Coral Bay Nickel Plant's two (2) Lines. In terms of design capacity, Line-2 achieved 100% in its 9th month of Operation only.
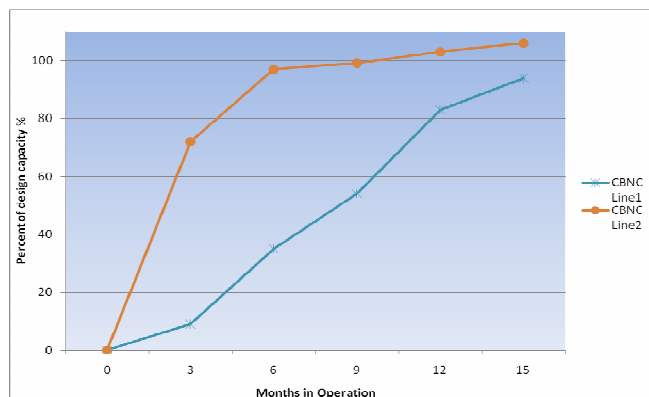
Figure 12: Comparison of Operation Rate Progress of Coral Bay Nickel's two Lines

The rapid pace of Line-2 Commissioning, among various contributing factors, was attributed to the following:

1. Strong Commissioning Team – from the start, Design stage, to Pre-Commissioning stage and finally to Commissioning, the Members are all the same. This set-up ensured efficient flow of information and knowledge because every step was done by the same persons. The Commissioning team had ample time to study the operations of the Plant since they were directly engaged on its design. By knowing even the minor details of the Plant, it became easier to operate.

2. Operators' Training – the Production Operators were previously working in the original Plant. Since the Expansion Plant is basically a mirror-image of Line-1, the Operators' skills and knowledge was top notch. They had most of their 'training' while in operating Line-1. Basically, Line-2 Commissioning became a simple Start-up from Long Shutdown mode for the Operators.

3. Experience in Line-1 Commissioning – the knowledge gained in Line-1 Commissioning and during its Commercial operation made a very significant contribution not only to Line-2's overall design but to its commissioning as well. The mistakes of the past were carefully avoided. Line-2 Commissioning became easier since Line-1 provided the basis – it became easier to imagine.

4. Use of Tie-in Pipelines – The inclusion of the Tie-in pipelines afforded a smoother Commissioning of Line-2 because it provided some flexibility. For instance, MS Slurry was 'borrowed' from Line-1 for the advance commissioning of LAROX Pressure Filter and for the use of MS Seed for start-up. Also, Pregnant Liquor was transferred back and forth between 2 lines depending on the requirements of the downstream Sulfurization Section. Moreover, there was no shortage of H_2S gas, Slaked Lime and other chemicals available in Line-1. As a result, much focus and attention was provided by the Commissioning team to major Line-2 circuits to achieve quick completion.

CONCLUSION

The experience in Line-1 commissioning and commercial operation brought about substantial skills and knowledge that enabled Coral Bay Nickel Corporation to complete the Commissioning of its Expansion Plant in record pace. The improvements made and the introduction of new technologies gave Line-2 an advantage to be more efficient and productive. The installation of tie-in lines between the 2 Plants provided greater flexibility and when properly harnessed, can increase the overall availability of the Plant. Line-1 and Line-2 can operate independently from each other;

522

therefore the Maintenance procedures can be easily planned out. And since most of the major equipments are similar, spare parts stocking and inventory is simplified.

Moreover, the experience in operating two (2) independent Plants in tandem have given Sumitomo Metal Mining and Coral Bay Nickel Corporation the skills and knowledge that will become valuable for the Commissioning and Operation of the upcoming Taganito HPAL Project in Surigao, Mindanao Island, Philippines. This Project, which has a capital expenditure of US$ 1.3 Billion, is scheduled to be commissioned in year 2012. Commercial operation is projected by year 2013.

Taganito HPAL Project will use CBNC's HPAL and MS technology to produce Nickel/Cobalt Mixed Sulfides, equivalent to 30,000 Ni-tons and 2,600 Co-tons per year. As a sign of good things to come, test operations using Taganito ore in CBNC Rio Tuba Plant conducted on May 2010 were remarkably successful.

Finally, the SMM's Philippine HPAL Project is a testament to a successful collaboration between Japanese and Filipino nations. Japan provided the Capital, Technology and technical knowledge to the project and the Filipinos' hard work and perseverance complemented it. Both peoples are looking forward to more successful collaborative efforts in the future.

REFERENCES

1. Mines and Geosciences Bureau, Department of Environment and Natural Resources, "Philippine Metallic Minerals Production", as of November 2010.

2. Outokumpu, "Leading-edge technologies for thickening and clarifying", Stainless/Copper/Technology, Helsinki, Finland, May 2004. Retrieved March 19, 2011, from http://www.outokumpu.com/files/Technology/Documents/New%20brochures/Thickeners_WEB .pdf.

3. FLSmidth Official Website, Industries, Light Metals, Alumina & Bauxite, Sedimentation, EIMCO Deep Cone Paste Thickeners, Retrieved March 19, 2011 from http://www.flsmidth.com/en-US/Products/Light+Metals/Alumina+and+Bauxite/Sedimentation/DeepConePasteThickeners/EI MCODeepConePasteThickeners.

4. Weir Minerals Official Website, GEHO® HeatBarrier Pumps, Features and Benefits, Retrieved March 19, 2011 from PumpBiz.Com Website, Home, Type, Positive Displacement Pumps, Retrieved May 9, 2011, from http://www.pumpbiz.com/shopping_product_list.asp?pcid=5225.

5. D.M. Muir et al, "Pressure Acid Leaching of Arid-Region Nickel Laterite Ore, Part 1: Effect of Water Quality", Hydrometallurgy, 70 (2003), 31 – 46.

RAMU NICKEL PROJECT UPDATE

By

James Wang

Ramu NiCo Management (MCC) Ltd, PNG

Presenter and Corresponding Author

James Wang
wangchun@mccgrd.com

Ramu Nickel Project-Key Data

- ➤ **Total resources:**
  143 million tons
- ➤ **Main components:**
  - ✓ **open-pit mining and progressive re-habitation**
  - ✓ **slurry pipeline transport**
  - ✓ **HPAL Process**
  - ✓ **Deep Sea Tailing Placement**

- ➤ **Construction cost:**
  1.4 Billion USD
- ➤ **Project Life:**
  Over 20 years
- ➤ **Annual output**
  Intermediate Hydroxide product
  Nickel: 31,280 t
  Cobalt: 3,220 t

Company History

February 2004, Framework Agreement signed; Technical, legal and economic due diligence launched

2004

Mine and Pipeline water commissioned, Refinery construction 90% completed Hot commissioning in 2011

2010

March 2005, Master Agreement signed; October 2005, JV Agreement Signed.

2005

2009

April 2006, Financing Agreement concluded; August 2006, Amendment MDC signed; November 2006, Foundation Ceremony held.

2006

2008

Mine construction completed. Refinery construction 70% completed

2007

April 2008, full construction began

July 2007, Amended Project Development Proposal approved by MRA; November 2007, Project Environmental Permit for construction and operation phase granted by DEC

Project Structure

After full repayment of the bank debt, 5% to be transferred to nominated PNG parties:

MCC Ramu: 80%; PNG Parties to 20% (RNL: 11.3%;MRRL: 5.2%; MRML:3.5%)

After exercise of the nominated PNG parties' option to acquire additional 15%:

Ramu Nickel Project Layout

Madang Headquarter

Kbk Mine

Basamuk Processing Plant

Ramu Nickel Project Headquarter in Madang

Madang Airport

Madang Resort

Madang Office Complex

Kurumbukari Mine

Water and slurry tested, ready for load Commissioning in June 2011

Ramu Nickel Site Update @ KBK

De-agglomeration Plant

- Slurry preparation and rock recovery and reuse
- Settling Ponds
- Trail Rehabilitation

Beneficiation Plant

- Chromite Removal and Recovery
- Slurry Pump Station
- Power Plant

Permanent Camp and Entertainment Facilities

- Accommodation for over 600 staff
- Western and Chinese Mess
- Sport and Entertainment Facilities

Pipeline Route

Buried : 68 km

On Ground: 67 km

Pipeline Control and Monitoring System

- Storage Tanks, Pump and Monitoring Stations
- Loop tests to measure slurry rheology
- Online monitoring of Pressure, flowrate & density

Basamuk Processing Plant

Water tested, HPAL trains ready, Utility Plants tested and certified, getting ready for load commissioning

---

Ramu Nickel Site Update @ Basamuk

Major Utilities

- Acid Plant/Backup Boiler
- Power Plant
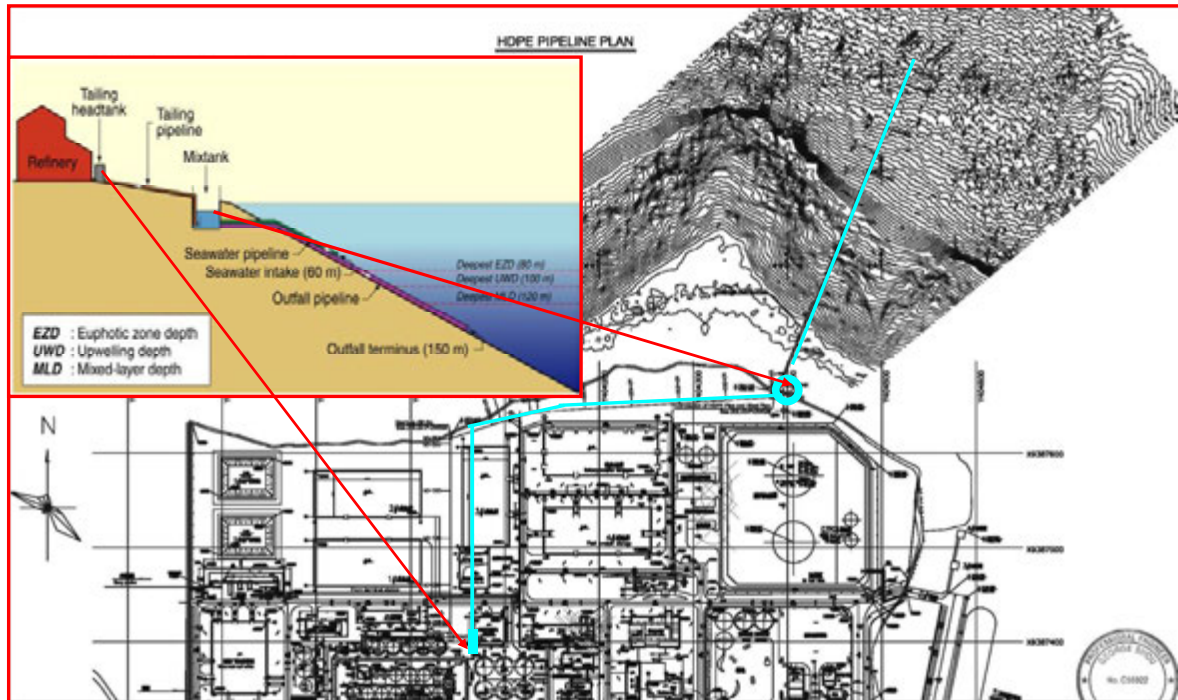- Lime Plant
- Water plant

Process Plant

- HPAL Plant and Central Control Room
- Al/Fe removal and Ni/Co Precipitation
- Tailing Neutralization
- DSTP System

Major Infrastructures

- 55,000 DWT wharf and tug boat Wharf
- Elemental Sulfur Stockpile
- HFO, diesel and caustic soda Storage Tanks

DSTP Engineering

DSTP and Emergency Response Configuration
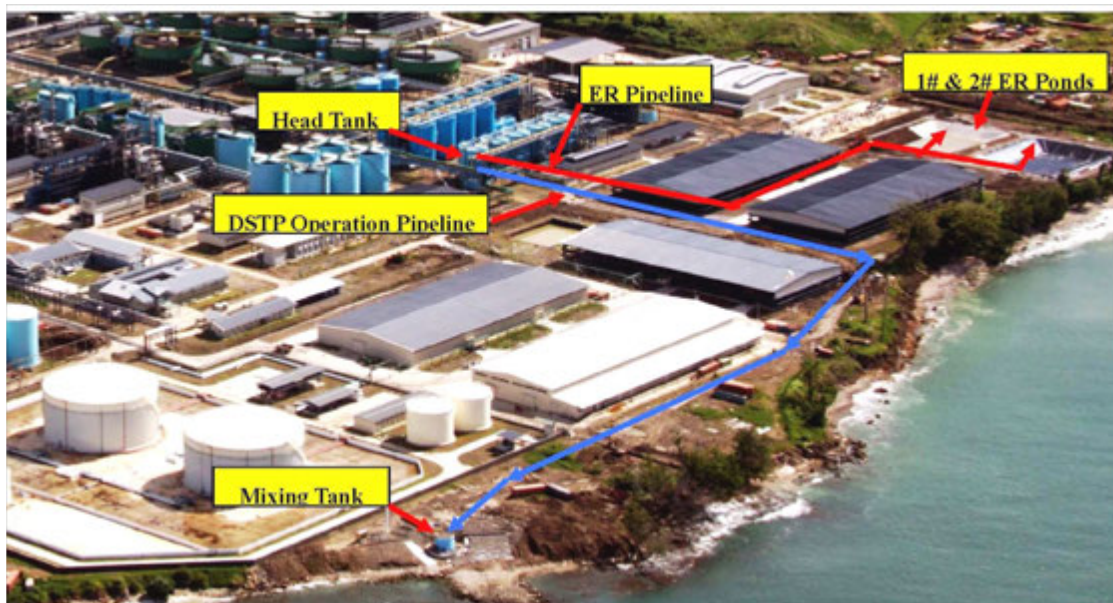
Unprocessed Slurry Emergency Response Mechanism
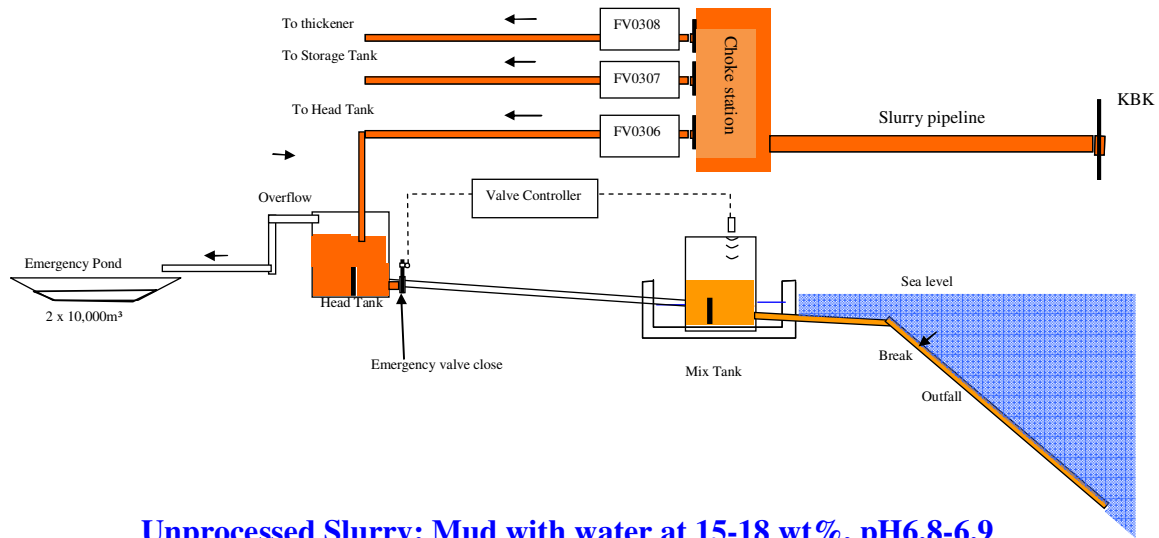
Unprocessed Slurry: Mud with water at 15-18 wt%, pH6.8-6.9
- Open Valve FV0307 to the Storage Tank;
- Open Valve FV0308, to Slurry Thickener.
- Open Value FV0306, the un processed slurry diverted to Head Tank then discharged via DSTP

DSTP and Emergency Response Mechanism

Scenarios (I)
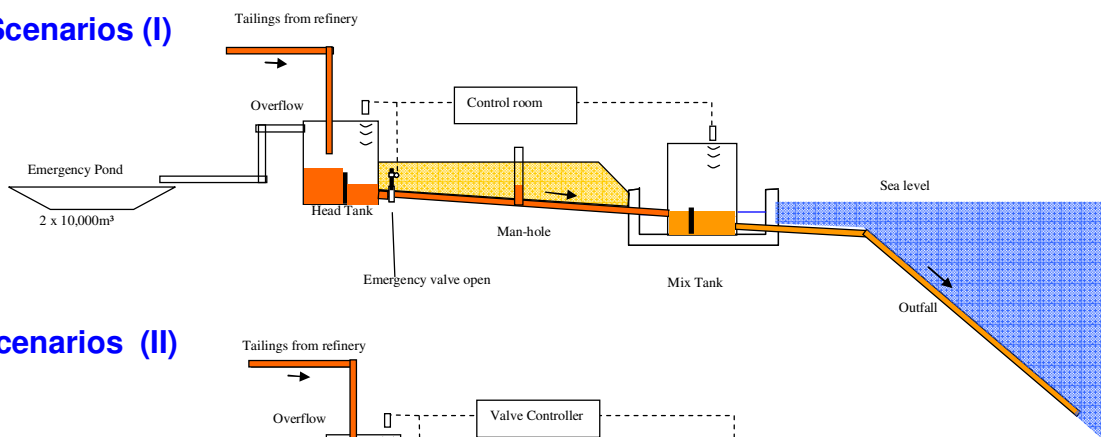
Scenarios (II)

Neutralized tailing of 9-13 wt%@ pH 8.0
- Discharged to the emergency pond via overflow pipe.
- Processing Plant shut down in planned sequence.

DSTP and Emergency Response Mechanism (III)

Scenarios (III)

Tailings from refinery

Overflow

Valve Controller

Emergency Pond

2 x 10,000m³

Head Tank

Emergency valve close

Mix Tank

Sea level

Break
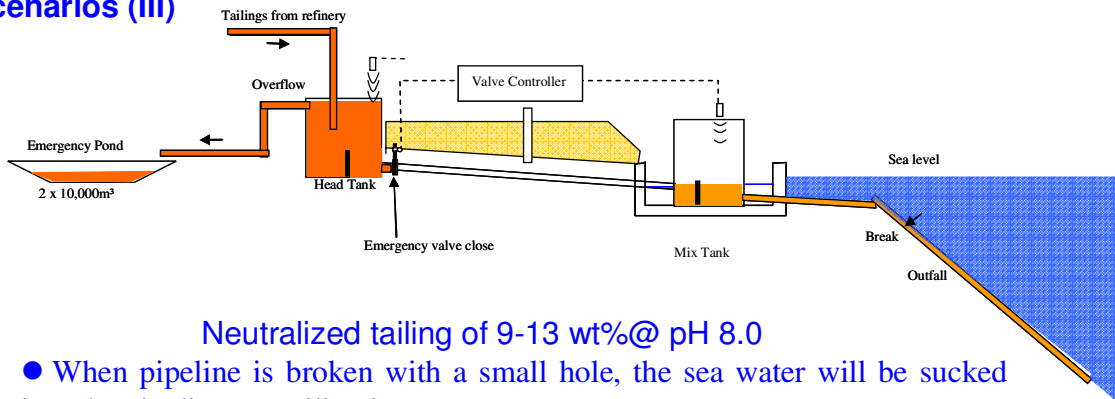
Outfall

Neutralized tailing of 9-13 wt%@ pH 8.0

● When pipeline is broken with a small hole, the sea water will be sucked into the pipeline, no tailing into sea.
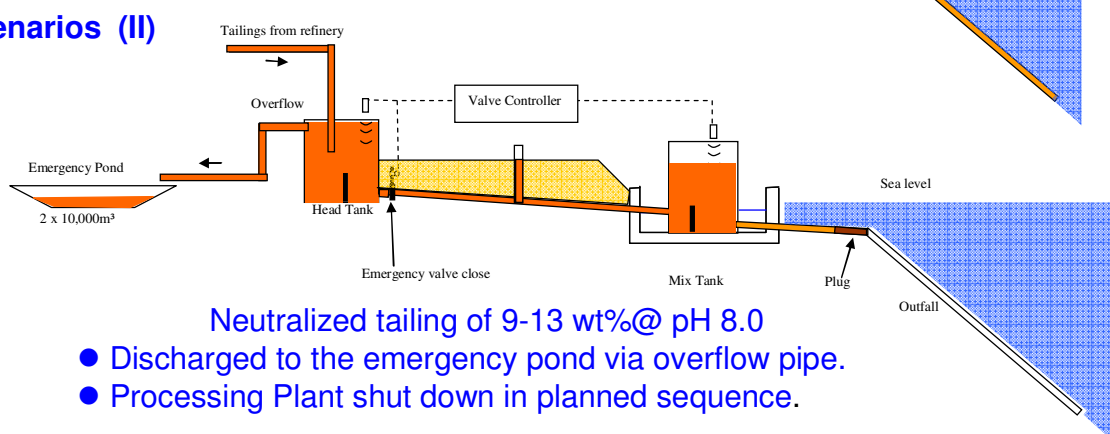
● If outfall pipeline is broken into halves suddenly, the mix tank level will change suddenly. The level transmitter will send the change signal to the valve controller. The emergency valve will be closed immediately. The tailings will be diverted to the emergency ponds through the overflow pipe.

● The neutralized tailing is benign to marine environment

Sustainable Development Strategy

One Ramu NiCo, One Community

Employees

Environment Health & Safety

Company Growth

Sustainable Development

Transparency

Community & People

Land – "Blood of life" for Papua New Guineans

Sustainable Development: Establishing Infrastructure

Infrastructures

Ramu River Bridge(247 m)
- Basamuk Wharf (55,000 DWT)
- Access Road (30 Km from Usino to Butua)

• Ramu River Bridge
December 2008

• Basamuk Wharf
November 2008

• Access road from Usino to Butua
November 2007

Environment Management & Monitoring

➢ Over 3.5 million US dollars directly invested in this field Since 2006.

➢ Transparent policy – project impacted area locals participated in environmental awareness programs

➢ 5 year extensive terrestrial and marine baseline survey to build Project environment database

➢ Water resource, liquid and solid waste management Plan
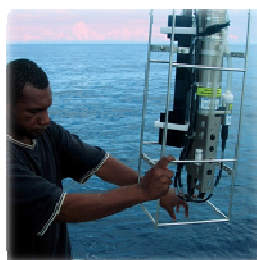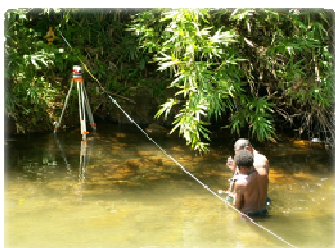
Land Rehabilitation Programs-Erosion Control

Land Rehabilitation Process
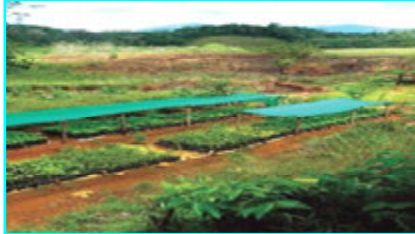
Vetiver & tress in open stand-out bed ready for planting.

Vetiver grass planted in de-agglomeration and settling ponds
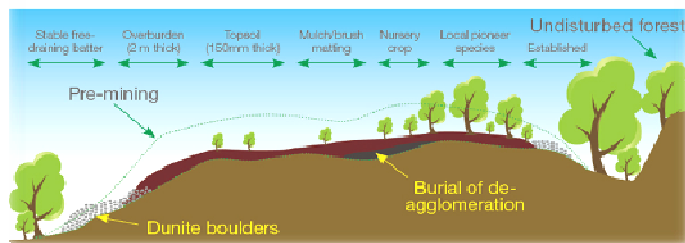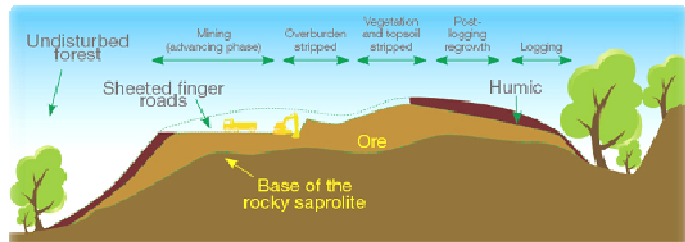
Agricultural Development Plan & Programs

Chinese agricultural experts invited as trainers for Community

- **Model Farms in the Project Area**
- **Seeds Fund Support Program**
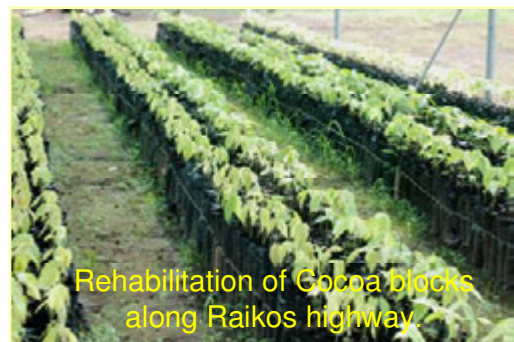
Rehabilitation of Cocoa blocks along Raikos highway.

Model Farm at Basamuk

Local residents harvest rice from a company-sponsored agriculture program

Experiences: What did we learn?

Lack of infrastructure and located at an isolated area

Different political & economic systems; language & cultural background

Lack of experienced and skillful employees in nickel laterite Operation

Management of technical, engineering, communities relation and social risks

---
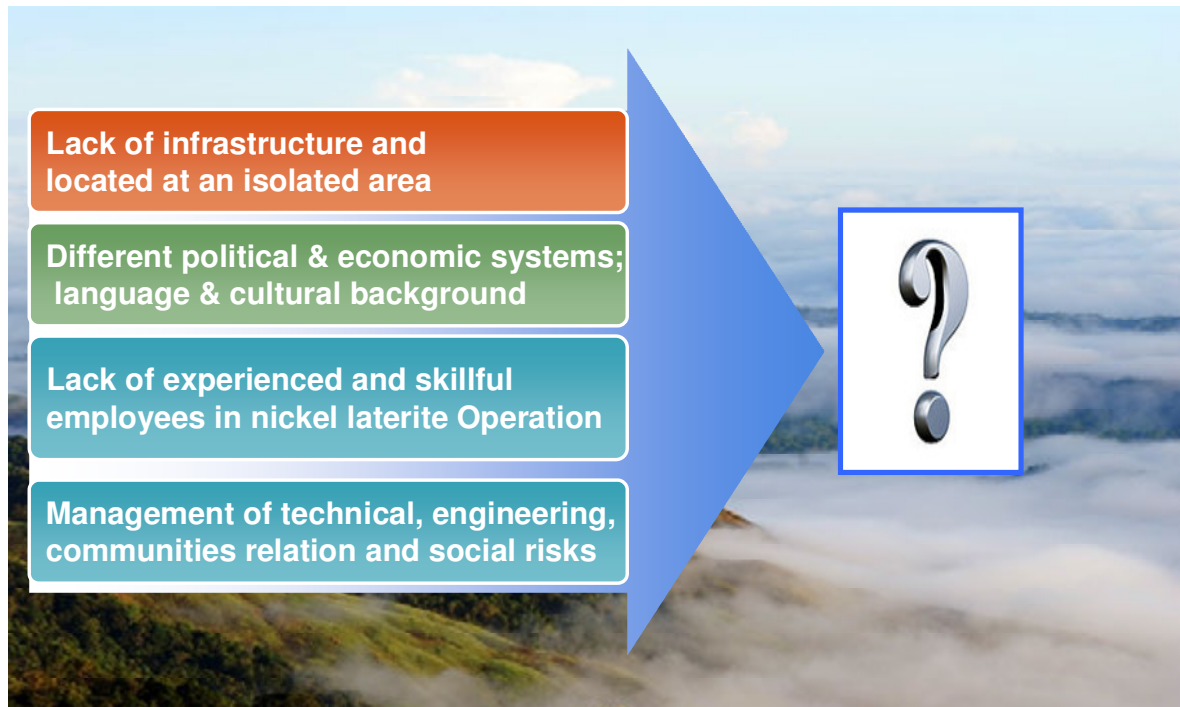
Construction & Commissioning: Ramu's Experiences

● Learn the experiences from other laterite PAL operations and integrate these lessons into the engineering at earlier stage.

● Materials of Construction – formalize the criteria of selection of materials under different process conditions and tropical humid and salty environment and integrate these criteria at Engineering and Procurement stage. On site QC and QA procedure is of importance to meet engineering criteria.

● Set up stock warehouse at early stage of construction phase. Protect, store and maintain properly the equipments and instruments during long construction period.

● Development of SOPs before commissioning and keep them updated to properly reflect the change and improvements within the process, integrate Emergency Response Procedures and Practices with key operating area based on risk analysis

Operating in PNG: Ramu's Experiences

● Learnt how to operate a mine from other mines operated in PNG in terms of cross-cultural Confrontation, HSE, HR recruitment and training management.

● To engage experienced staff and world class consultants to implement and improve HR, HSE, IT, training, accounting, maintenance and risk management systems

● To explore the balance between commercial competitiveness and social sustainability; to balance and share benefits in business and employment opportunities with local communities;

● To share the similarity and respect the difference in culture, reach inter and intra-organization mutual understanding to keep communication and awareness with all stakeholders, and work together to address issues in a timely and transparent manner.

2011 Mine Production Targets
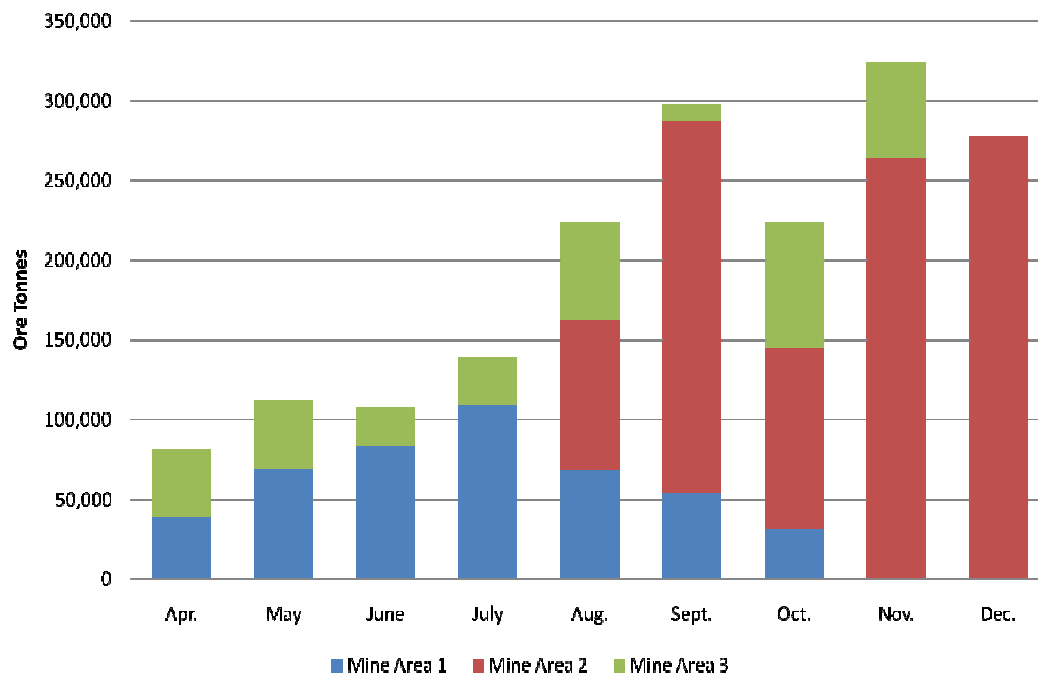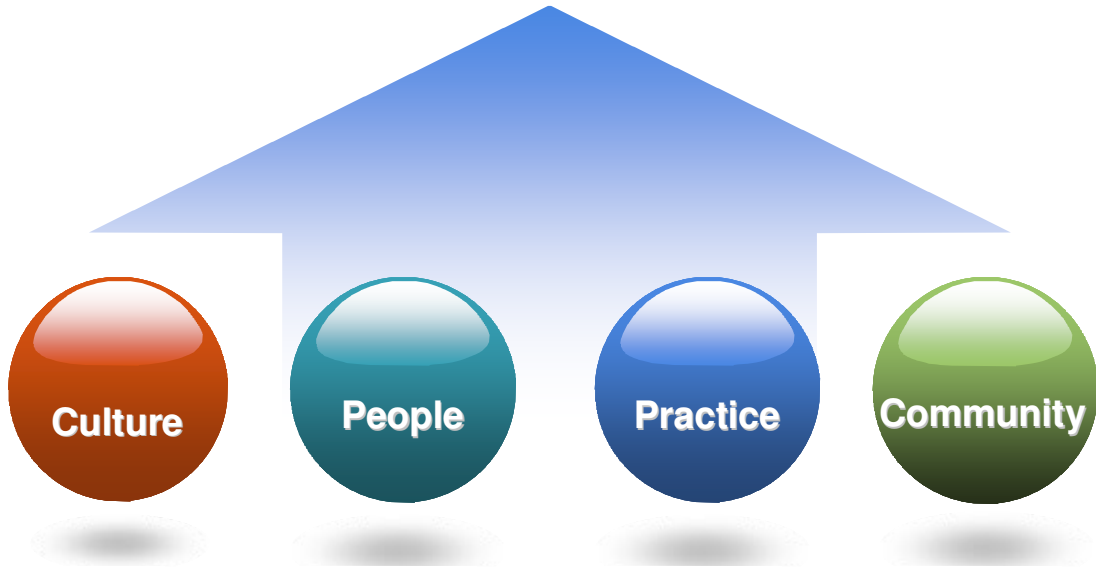
CARBON FRIENDLY NICKEL PROCESSING AND PRESSURE ACID LEACHING: REDUCED CARBON EMISSIONS AND MORE EFFICIENT ACID USE FOR HIGHER ECONOMIC RETURNS

By

S Willis, T Newton, and B Muller

Simulus Engineers, Australia

Presented by

Simon Willis
simon.willis@simulus.com.au

ABSTRACT

Simulus Engineers were awarded an AusIndustry grant in 2010 to co-fund the development of a novel process for the production of nickel metal from laterite ores. The Carbon Friendly Nickel Production (CFNP) process, involves membrane technology to recover sulphuric acid and reductive calcination to regenerate reactive magnesia from waste process liquor. The CFNP process is anticipated to reduce CO_2 emissions by over 60% from a base case conventional atmospheric leach / neutralisation / mixed hydroxide process (MHP) flowsheet. This is achieved through lower process emissions by avoiding the need for limestone and lime neutralisation of residual free acid, and reduced emissions from the transportation of reagents. Reagent costs for CFNP can be up to 75% lower than the base case flowsheet (including credits for excess magnesia and sulphuric acid production). The CFNP flowsheet can be applied to any sulphuric acid leach technology: PAL, atmospheric, or heap leach.

Operating costs are estimated to be 25 to 48% lower than the conventional flowsheet depending on the flowsheet scenario chosen. Capital costs are similar to the conventional atmospheric leach flowsheet, but can be 29% lower, or 24% higher, depending on the scenario. The optimum scenario will depend on the ore body and business strategy of any company seeking to implement the membrane and magnesia recovery technology.

Simulus Engineers will be operating a demonstration plant to showcase the new process in late 2011, in conjunction with further testwork to optimise two stage leach, iron removal, and magnesia recovery process parameters.

THE PROCESS

There are two key features of the CFNP flowsheet. The first centres on the recovery of residual sulphuric acid from free acid and also from hydrolysable metal sulphates for atmospheric leach processes, to reduce net acid consumption and neutralisation requirements.

The second key feature involves the recovery of magnesium sulphate from the waste liquor to produce magnesia and SO_2. The magnesia can be recycled to the process as a bulk neutralising agent, not just restricted to the first stage of MHP. The SO_2 evolved is the main sulphur source to the sulphuric acid plant. A simplified block flow diagram of the flowsheet as applied to PAL is in Figure 1.
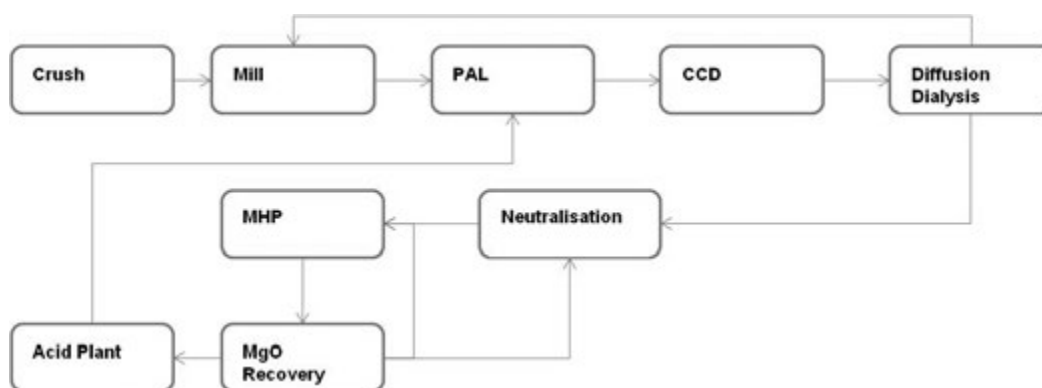
Figure 1: Simplified CFNP flowsheet for PAL

Traditionally in MHP flowsheets, any sulphate in solution following leach (except for $MgSO_4$, $NiSO_4$ and $CoSO_4$), is precipitated as gypsum by limestone and lime addition. This is wasteful for several reasons:

- Acid is wasted

- Limestone and lime is consumed

- CO_2 emissions are high

- Gypsum tailings must be processed and stored (1.8 ton of gypsum per ton of neutralised acid)

By reducing the amount of acid wasted, the size of the sulphuric acid plant can be reduced. The sulphur reagent costs, transport and handling costs are also reduced. Limestone and lime neutralisation can be replaced with magnesia neutralisation, depending on the economics of the project. Magnesia is a byproduct of the flowsheet, thus the reagent costs of imported magnesia are avoided.

Depending on the location of the project, emissions restrictions may prevent the release of magnesium sulphate effluent to the environment. In certain circumstances this alone could determine whether the project is viable or not. By recovering the magnesium sulphate from solution, not only are tailings emissions targets achievable, but magnesia and SO_2 recovered from what would otherwise be a tailings stream reduce the reliance of the project on imported reagents.

Acid Recovery

Residual free acid remaining in solution following the sulphuric acid leaching of ore, is recovered using diffusion dialysis membrane technology. The diffusion dialysis equipment consists of multiple banks of anionic exchange membrane stacks operating in parallel. Each membrane stack contacts PLS on one side of the membrane with a process water stream on the other side of the membrane. The PLS and water streams run counter-current to each other in the membrane stacks. An illustration of the diffusion dialysis process is in Figure 2.
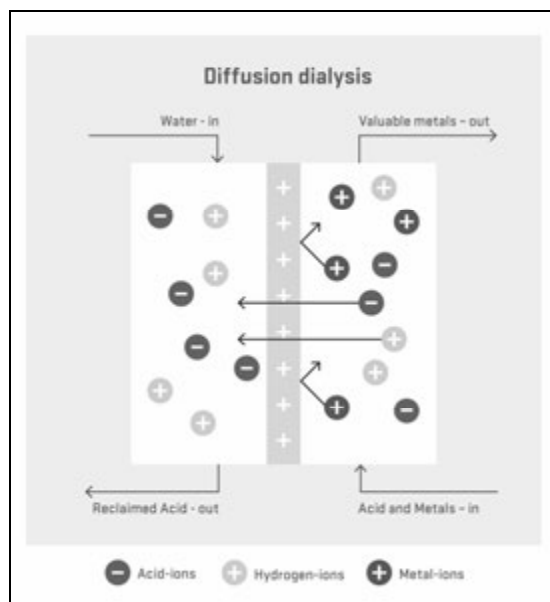
Figure 2: Diffusion dialysis for acid recovery

THE anionic exchange membrane is positively charged at its surface. Anions in solution (mainly sulphate and bisulphate) are attracted to the membrane, creating a high concentration gradient across the membrane. This results in increased anion diffusion rates through the membrane. For electoneutrality, cations must also permeate the membrane, however metal cations are strongly inhibited from passing the positively charged membrane. Hydrogen ions, which are strongly associated with water, can pass the membrane relatively uninhibited. Thus, sulphuric acid in the PLS diffuses through the membrane into the water stream, depleting the PLS of free acid. The flow of divalent and trivalent metal sulphates through the membrane is low in comparison to the flow of sulphuric acid.
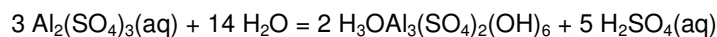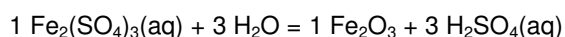
The PLS feed to each membrane stack is controlled for a target flux to each stack. Water is fed to each membrane stack at a separate target flux. It is possible to recover sulphuric acid from PLS into a water stream of flux low enough to result in an acid concentration higher than the initial PLS acid concentration. PLS depleted of free sulphuric acid is collected from each bank of membranes in a common launder. The recovered sulphuric acid is used as acidic ore beneficiation makeup water, to reduce the amount of net water addition to the flowsheet.

For atmospheric leach and heap leach flowsheets, the hydrolysable ions (mainly ferric and aluminium) can be precipitated in an autoclave at 200°C:

$$1 \; Fe_2(SO_4)_3(aq) + 3 \; H_2O = 1 \; Fe_2O_3 + 3 \; H_2SO_4(aq)$$

$$3 \; Al_2(SO_4)_3(aq) + 14 \; H_2O = 2 \; H_3OAl_3(SO_4)_2(OH)_6 + 5 \; H_2SO_4(aq)$$

Iron and aluminium solubility increases with acid concentration, so the final iron, aluminium and free acid equilibrium will depend on the feed iron and aluminium concentration. The upstream diffusion dialysis is necessary to first remove as much free acid as possible from the autoclave feed liquor to drive the hydrolysis precipitation reactions further. This liberates more free acid which is recovered in a second stage of diffusion dialysis.

For PAL flowsheets, the discharge from the first stage of diffusion dialysis is already low in hydrolysable ions due to their precipitation in the PAL autoclaves. The 200°C autoclave and second stage of diffusion dialysis is therefore not required and the acid depleted PLS can be neutralised directly for impurity removal and MHP precipitation.

Magnesia Recovery

The second key feature of the CFNP flowsheet involves recovering magnesium sulphate from the tailings liquor for the production of magnesia and SO_2. Magnesium sulphate is recovered from solution using a combination of reverse osmosis and evaporative crysallisation. Reverse osmosis is

used to increase the concentration of the MgSO$_4$ brine, prior to further concentration and crystallision by evaporation.

There are several hydrates of magnesium sulphate, but kieserite (MgSO$_4$.H$_2$O) is the stable phase provided the crystallisation temperature is over ~70°C. The kieserite slurry is centrifuged in a vibratory centrifuge to separate most of the saturated magnesium sulphate solution from the solids, with the liquor returned to the evaporators.

Evaporation of the unbound water from the centrifuge cake occurs at <110°C, but dehydration of the bound water requires heating the crystals to above 350°C. This is achieved by indirect heat exchange with hot combustion gases from a fuel burner. The anhydrous MgSO$_4$ is then reduced to MgO by counter current contact with gaseous elemental sulphur, evolving SO$_2$ gas according to:

$$4 \text{ MgSO}_4 + 1 \text{ S}_2(g) = 4 \text{ MgO} + 6 \text{ SO}_2(g)$$
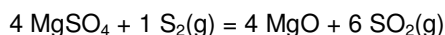
The reductive calcination temperature is maintained at ~800°C by indirect contact with hot combustion gases. The evolved SO$_2$ is ducted to post-combustion with a fan feeding additional combustion air, to fully oxidise any residual unreacted sulphur. The gas is then ducted to the sulphuric acid plant for the production of sulphuric acid.

TESTWORK

A laboratory testwork program was completed to evaluate the performance of diffusion dialysis, for the CFNP flowsheet. A sample of leach solution was supplied by an industry partner.

The lab unit has a total active membrane area of 0.0929 m² and a linear flow path of 1.22 m. The unit has two feed solution reservoirs, for water and for the leach liquor. It is equipped with two diaphragm metering pumps to control the flow through the membrane stack for the water/recovered acid and the leach liquor/acid depleted liquor. The performance of the diffusion dialysis unit was evaluated for the leach liquor supplied. The effect of the following process variables were to be assessed:

- total flux

- relative flux

- feed liquor acid concentration.

A summary of the diffusion dialysis testwork results is in Table 1.

Table 1: Summary of diffusion dialysis testwork results

Data point	Reject flux	Reclaim to reject flux	Acid recovery	Monovalent metal rejection	Divalent metal rejection	Trivalent metal rejection
	L/(m².h)	v/v	%	%	%	%
A	1.0	0.6	74.5	92.3	98.0	98.0
B	1.0	1.1	91.5	96.0	98.6	97.9
C	1.3	1.0	77.6	93.3	98.2	98.4
D	2.3	1.0	58.7	96.7	98.8	99.0
E	2.4	0.7	53.8	97.4	99.4	99.2
F	3.0	1.1	53.7	94.3	98.8	99.1

It is desirable to operate the diffusion dialysis equipment at the highest possible reject flux, as this decreases the number of membrane cells required to process the PLS. It is also desirable to operate at the lowest reclaim to reject flux ratio, as this minimises the amount of water addition to the process and increases the concentration of the recovered acid.

The diffusion dialysis test rig was operated continuously for a month, with no appreciable decrease in performance. The acid recovery performance was excellent, with over 90% of sulphuric acid

recovery achievable, with only 1-4 % of metals permeating through the membranes. In practice, the operating conditions for the diffusion dialysis units will depend on the water balance of the flowsheet, and the economic trade-off between the capital cost of the membrane units, and the costs associated with the wasted acid.

Reject flux may appear low in comparison to other membrane technologies such as reverse osmosis and nano-filtration, but pressure loss in diffusion dialysis is negligible, so high pressure feed pumps are not required. Simulus Engineers investigated the recovery of acid by nano-filtration, but the osmotic pressure of PLS is so high that no liquor permeates the membrane, even at > 60 bar membrane feed pressure. Diffusion dialysis performance does not deteriorate at elevated osmotic pressure. The common ion effect can even lead to improved acid recovery at higher salt concentrations.

DEMONSTRATION PLANT

The design of a demonstration plant for the CFNP flowsheet which incorporates magnesia recovery is currently underway. The demonstration plant, to be constructed at the newly opened Simulus Laboratories, will be predominantly manually operated, with 24 hour coverage during operational campaigns undertaken during over a six month period. The demonstration plant will be designed to process 50 kg/h of dry ore.

The magnesium sulphate dehydrator and reducer will be powered electrically rather than by hot combustion gases. The demonstration plant will not include a sulphuric acid plant, therefore the SO_2 evolved in magnesia recovery will be scrubbed out and discarded.

CARBON EMISSIONS

Simulus Engineers completed a feasibility study in 2010 for the CFNP flowsheet, comparing 7 flowsheet scenarios with a traditional atmospheric leach to MHP base case scenario. The carbon emissions for each flowsheet were compared, including emissions from the transportation of reagents and production of lime from limestone. The carbon emissions are compared in Table 2.

Table 2: Carbon emissions comparison for CFNP flowsheet scenarios

Scenario	Description	CO_2 emissions reduction
1	Base case atmospheric leach	-
2	Atmospheric leach CFNP without magnesia recovery	61%
3	Two stage atmospheric leach CFNP without magnesia recovery	55%
4	PAL CFNP without magnesia recovery	70%
5	Atmospheric leach CFNP with full magnesia recovery	36%
6	Two stage leach with full magnesia recovery	39%
7	Atmospheric leach CFNP with magnesia recovery for neutralisation	53%
8	Two stage atmospheric leach CFNP with magnesia recovery for neutralisation	55%

Scenarios 5 and 6 recover magnesia from the entire tailings liquor stream. This results in more magnesia being produced than the flowsheet consumes, even when all limestone and lime neutralisation duties are replace with magnesia. The excess magnesia is available for sale. Scenarios 7 and 8 recover only the amount of magnesia required for the neutralisation requirements of the flowsheet, with the remaining magnesium sulphate liquor bled to tailings.

Carbon emissions were estimated to be reduced by over 60% by incorporating diffusion dialysis for acid recovery. The recovery of magnesia from magnesium sulphate increases the carbon emissions (with respect to scenario 2) due to the energy intensity of the dehydration and reductive calcination reaction.

FINANCIAL EVALUATION

Capital Cost Estimate

Capital cost estimates were prepared during the 2010 feasibility study, for all flowsheet options, with the top 80% of the equipment costs sourced from vendor quotations. The comparative capital cost estimate is in Table 3.

Table 3: Capital cost estimate comparison for CFNP flowsheet scenarios

Scenario	Description	CAPEX change, %
1	Base case atmospheric leach	-
2	Atmospheric leach CFNP without magnesia recovery	1%
3	Two stage atmospheric leach CFNP without magnesia recovery	-23%
4	PAL CFNP without magnesia recovery	-29%
5	Atmospheric leach CFNP with full magnesia recovery	24%
6	Two stage leach with full magnesia recovery	5%
7	Atmospheric leach CFNP with magnesia recovery for neutralisation	18%
8	Two stage atmospheric leach CFNP with magnesia recovery for neutralisation	-4%

The most expensive additional capital in the CFNP flowsheets is the membrane stacks and the magnesia recovery equipment. For the feasibility study, indirect screw heat exchanger units were specified for the magnesium sulphate dehydration and reductive calcination, however Simulus Engineers are currently investigating lower cost alternative technologies.

The lowest capital cost scenarios are those which have low hydrolysable cations in the PLS. A two-stage atmospheric leach flowsheet which can take advantage of the neutralising capacity of fresh ore to reduce iron concentrations in solution, or a PAL flowsheet, avoids the need for downstream hydrolysis and secondary membrane acid recovery, keeping capital costs low.

Operating Cost Estimate

Operating cost estimates were prepared during the 2010 feasibility study, for all flowsheet options. The comparative operating cost estimate is in Table 4.

Table 4: Operating cost estimate comparison for CFNP flowsheet scenarios

Scenario	Description	OPEX change, %
1	Base case atmospheric leach	-
2	Atmospheric leach CFNP without magnesia recovery	-25%
3	Two stage atmospheric leach CFNP without magnesia recovery	-25%
4	PAL CFNP without magnesia recovery	-36%
5	Atmospheric leach CFNP with full magnesia recovery	-42%
6	Two stage leach with full magnesia recovery	-48%
7	Atmospheric leach CFNP with magnesia recovery for neutralisation	-27%
8	Two stage atmospheric leach CFNP with magnesia recovery for neutralisation	-32%

Magnesia credits for scenarios 5 and 6 are assumed. These scenarios produce excess magnesia that can be sold.

The operating cost for all CFNP scenarios is lower than the base case atmospheric leach flowsheet. This is predominantly due to extremely low reagent costs. As an example, scenario 5 benefits from the reagent consumption reductions specified in

Table **5**.

Table 5: Scenario 5 net reagent consumption relative to base case

Reagent	Change from base case, %
Sulphur	-81
Limestone	-100
Lime	-100
Magnesia	-100

Net water consumption is also much lower for CFNP flowsheets with magnesia recovery than traditional MHP flowsheets, due to the recovery of water from the magnesium sulphate waste liquor. This water is reused as feed water to the diffusion dialysis membranes, to recover acid. Recycling the acidic water back to the ore beneficiation plant decreases the requirements for fresh raw water addition.

CONCLUSIONS

The CFNP process provides an integrated method to reduce the environmental impact of nickel laterite acid leach flowsheets, by:

- reducing carbon emissions
- reducing net reagent consumption
- recycling waste effluents whenever possible
- minimising the tailings storage footprint
- minimising the net water consumption.

Simulus Engineers are continuing with engineering design, to be further refined during the operation of the demonstration plant. The opportunity exists for suitable industry partners to participate with Simulus Engineers in the demonstration of this valuable technology. The CFNP technology can be tailored to the ore body mineralogy and flowsheet constraints, so partnering with a resource owner early on makes good sense.

ALTA 2011
NICKEL/COBALT/COPPER

ADDITIONAL PAPER

(Not presented at conference)

RECENT DEVELOPMENTS IN NOVEL PHASE CONTACTING DEVICES/ASPECTS FOR HYDROMETALLURGICAL APPLICATIONS

By

Katragadda Sarveswara Rao

EEE, India

Presenter and Corresponding Author

Katragadda Sarveswara Rao
srvswr.rao@gmail.com

ABSTRACT

This paper attempts to provide an overview of novel phase contacting devices with regard to gas-liquid, liquid-liquid and solid-liquid systems including the effect of sonication as applicable to process intensification in hydrometallurgy. The leaching of complex materials by pressure autoclaves has led to benefits of having much more rapid reactions, more compact equipment, and a reduced environmental burden. However, designing of suitable pressure reactors is a difficult task because autoclave technology depends on factors like batch/continuous mode operation, suitable material of construction to withstand corrosive atmosphere at high temperature and pressure, ease of assembly and disassembly, provision for easy withdrawal of intermittent samples for process monitoring, and finally, overall safety management. The salient features associated with safety management of autoclave reactors are described with special emphasis on materials of construction. The challenges/limitations associated with the application of novel phase contacting devices for leaching of sulphide minerals are described as a case study.

INTRODUCTION

Process intensification (PI) is expected to gain increasing importance for its various advantages in process industry, viz. to improve manufacturing and processing by reducing equipment size, improving plant efficiency, saving energy, reducing capital costs and minimizing environmental impact, and increasing safety, remote control and automation. Similarly, in hydrometallurgy, leaching process intensification by pressure autoclaves has led to benefits of having much more rapid reactions, more compact equipment, and a reduced environmental burden. There is a strong nexus between energy and process intensification, and between process intensification and the move to sustainable processes. The attainment of autogenous steady-state temperature of autoclave and agitation/mixing of slurry, or use of external field like ultrasound will influence the energy saving measures[1]. However, designing of suitable pressure reactors is a difficult task because autoclave technology depends on factors like batch/continuous mode operation, suitable material of construction to withstand corrosive atmosphere at high temperature and pressure, ease of assembly and disassembly, provision for easy withdrawal of intermittent samples for process monitoring, and finally, overall safety management.

The application of ultrasound (sonication) is proving to be of considerable interest for intensifying the performance of leaching processes. Enhanced dissolution rates, improved metal recoveries, and reduced reagent consumption are some of the advantages claimed by this technique. The benefits were attributed to some of the various phenomena produced by ultrasound-like cavitation (bubble formation and implosion), microstreaming, radiation pressure and degassing. They contribute to chemical, physical, and hydrodynamic effects, which need to be discriminated for better understanding of sonication in any leaching process. Accordingly, this article addresses the importance of process intensification as relevant to application of ultrasound in leaching, safety aspects of autoclaves, novel phase contacting devices, and the limitations involved therein.

THE IMPORTANCE OF PROCESS INTENSIFICATION

Application of Ultrasound

Atmospheric aqueous ammonia leaching data for a lean grade copper oxide ore have been obtained using mechanical agitation as well as by a sonication technique. The study was conducted at ambient temperature (298 K) using a fixed range of particle size ($-300+150\mu m$) in 2M ammoniacal solution, solid/liquid ratio of 1/100 at a constant stirring speed. A maximum recovery of copper of about 70% was obtained with mechanical agitation. The recovery increased up to 90% by the application of ultrasound. It was shown that the use of ultrasound decreased the leaching time by a factor of nearly 6 times (from 120 to 20 minutes) and also decreased the reagent consumption compared to that during leaching using mechanical agitation. For the same particle size, ultrasound not only enhanced the extraction rate but also improved the metal recovery. Other conditions remaining the same, it was shown that intermittent use of ultrasound had a pronounced effect over the continuous use of ultrasound for extraction of copper. More details are available elsewhere[2].

A process intensification study was carried out for sono-chemical leaching of uranium[3]. This was aimed at determining the mechanism of uranium leaching in nitric acid and sulfuric acid media. The enhancement in the leaching rate observed in the presence of ultrasound was higher with low leach acid concentration of HNO_3, and was also high at high leach acid concentration in the case of H_2SO_4 being used as a leachant, when compared to conventional mechanical agitation. The basic reason behind this observed variation was explained on the basis of the reaction mechanism involving the oxidative conversion of acid insoluble tetravalent uranium form to the soluble hexavalent form of uranium in the presence of ultrasound at a faster rate. It was shown that the oxidative formation of Fe^{3+} [$Fe_2(SO_4)_3$] appears to be the rate controlling phenomena, and this step is speeded by the oxidizing conditions (OH radicals) produced during ultrasound cavitation under high acid medium conditions, i.e., chemical effects of ultrasound cavitation causing the enhancement in the leaching rate of uranium. Over the last few years, researchers have developed an interest in the application of power ultrasound for industrial use. A typical example is the ResonantSonics device to produce cavitation and acoustic streaming processes, as a very effective means, to disperse steam through the solution and/or slurry on a molecular level. This accelerates the leaching of trihydrate alumina from the bauxite ore[4].

Other Applications

The direct microwave heating of minerals appears to be highly promising for processing high pulp density slurries compared to the hydrothermal leaching of low pulp materials in CSTRs in terms of time, reactor capacity, and energy savings. The mechanochemical processing is a one step process of grinding-leaching. This avoids heat loss, mineral deactivation, and surface passivation while providing new surfaces, cracks, activated sites, etc. for selective leaching. This technique has been applied successfully by many early researchers for processing valuable and/or toxic materials of several complex sulfides as described[5].

SAFETY ASPECTS OF AUTOCLAVES

Pressure autoclaves have been increasingly used for effective utilization of refractory ores, recycling of resource materials, water purification management. Designing a suitable autoclave system with safety set standards is a difficult task owing to the scale and nature of the R&D activity involved. An ideal autoclave reactor should have many characteristic features including suitable materials of construction to withstand corrosive atmosphere, ease of assembly and disassembly etc. Safety management of autoclave systems include design of pressure vessels, design of pressure relief valves and rupture discs, corrosion aspects, design and construction of barricades, operation & maintenance of laboratory autoclaves, pilot plant autoclaves and process control modules as described in a safety manual[6]. This is a well documented work with an effort to list laboratory's experience in pressure hydrometallurgy. The safety management described is based on review of literature, catalogues of autoclave manufacturers and on a methodology developed for safe operation and maintenance of autoclaves. Recently, pressure leaching has proved promising for leaching of copper and zinc sulphides, and nickel laterites on a commercial scale as described in literature. For example, acid resistant brick lined vessels are utilized in pressure leaching and pressure oxidation for copper, nickel, gold and other metals. As lined vessels in hydrometallurgical processes continue to increase in scale to improve project economics, the maximum allowable size becomes a design consideration. The properties of the acid brick lining and the process must be considered when selecting the vessel size and configuration during the early design stages of a process plant as described[7].

Materials of Construction

Though corrosion exists in many faces/forms, there are several suitable stainless steel grades developed for hydrometallurgical applications. The most demanding application is in the leaching stages wherein the combination of sulfuric acid, metal ions, chlorides and elevated temperatures creates harsh conditions for stainless steel. Additionally, the oxygen solubility increases with temperature up to about 80^0C, then drops to zero at the boiling point of water. A low oxygen content in combination with hydrogen ions results in a very corrosive and reducing acid near the boiling point. In spite of those complications, stainless steels have many advantages from a design and process flexibility point of view in hydrometallurgical environments. Under the most severe conditions, there are possibilities to identify applications for the highest alloyed super austenitic and super duplex stainless steel grades while other steel grades find use in less severe environments. By performing laboratory corrosion tests and field-experiments to gather information about the performance of stainless steel in environments used within the hydrometallurgical industry, it is possible to choose appropriate materials of construction[8].

NOVEL PHASE CONTACTING DEVICES

There are many new concepts put forward for a better explanation of the improvement in the performance of leaching reactors. Because leaching forms a critical operation in hydrometallurgy, the performance of the leaching sections of a processing plant usually has a significant impact on the downstream processing and thereby overall performance of the plant. Moreover, leaching reactors are usually complex with multiple reactions associated with gas, liquid and solid phases. Especially, the design of continuous leaching reactors is poorly understood due to emphasis laid mainly on the leaching conditions and chemistry to generate data from batch leaching experiments, with scant regard for the reactor engineering, e.g. without accounting for the continuous feeding and removal of particles of different sizes from the system. It was also assumed that the particle size and particle size distribution have no influence on the performance of the reactor. To overcome such drawbacks/limitations, a dimensionless 'leaching number' was proposed for a better

interpretation of reactor performance/ comparison of process technologies, viz. BioCOP, AAC/UBC, Placer Dome/Phelps Dodge) for leaching of chalcopyrite ($CuFeS_2$) concentrate[9].

Another novel reaction system was attempted for direct leaching of zinc sulfide concentrates. The reaction system consists of a dispersion space and a reaction volume. The dispersion space is used to generate efficient interfacial heat and mass transfer, especially to dissolve oxygen into the liquid phase. Because the chemical reactions require longer residence time, they mainly occur in the reaction volume, where the dissolved oxygen takes part in reactions as described. It was concluded that the tests carried out in a semi-batch pilot plant indicate that the new reaction system is competitive to the conventional technology. Continuous stirred tanks used in industrial installations require residence times of many hours and have also large volumes. Modeling of the reaction system was reported to be successful as attributed to the appropriate research strategy[10].

Recently developed novel phase contacting devices include the high intensity jet reactors that provide significant improvement over conventional phase contacting equipment due to the impingement of high velocity feed streams upon each other in relatively small reactor volumes, resulting in a highly turbulent mixture of phases. Although scaling up may be a problem but the advantage of tube and jet reactor systems provide selective and fast dissolution and/or precipitation (viz. oxyhydrolysis) processes. The equipment was used to provide efficient mixing between phases in the capitation process. It was shown how transfer processes in this heterogeneous system have been intensified with this solid-liquid jet reactor to give very high mass transfer coefficients and interfacial areas (compared to conventional phase contacting systems) required to enhance gold leaching kinetics[11].

The limitations of intensive cyanidation conventionally carried out in a high-speed agitated tank or by vat leaching, are said to have been overcome by introducing an InLine Leach Reactor (ILR) to treat gravity concentrates from either batch type concentrators or continuous concentrators such as jigs or flotation. The use of the ILR has contributed to increased gravity gold recoveries; improved security by eliminating manual concentrate handling; eliminates smelting of metal sulfide concentrates and resultant toxic fumes; high shear agitation gives thorough mixing and increases reagent utilization; treats entire concentrate without removing gold bearing fines prior to leaching; flexible, up-gradable capacity (batch to continuous, expandable drum); fully integrated automation system; low installed power and less power consumption; low operating costs with inexpensive chemical reagents; low installed power of less than 10 kW; efficient clarification step producing clear electrowinning solutions suitable for metal recovery[12].

Solvent Extraction and Liquid Membranes

Solvent extraction (SX) has been routinely used for copper refining since its invention in the 1960s, and it is suggested that well over 10% of refined copper production from ores is obtained by solvent extraction, accounting for millions of tonnes of metal. It is even more popular for refining copper from scrap. In more recent years, the SX technology has been implemented for other base metals, precious metals, and specialty metals. While specific details of the SX refining steps remain closely guarded, several publications in the open literature give interesting insight to the clever chemistry and novel ideas that have been employed in the development of these processes as reviewed[13].

Membrane processes meet the requirements of PI because they have potential to replace conventional energy-intensive techniques, to accomplish the selective and efficient transport of specific components, and to improve the performance of reactive processes[14]. Liquid membranes offer new options for the design, rationalization and optimization of innovative production cycles. Because of their ability to combine both thermodynamic and kinetic partitioning, membranes represent an intrinsic paradigm of intensification. Emulsion liquid membranes (ELMs) as well as supported liquid membranes (SLMs) remove the equilibrium limitations of solvent extraction by combining extraction and stripping in a single operation, thereby achieving reduction of metal concentration in the feed stream to very low levels like low copper tenor leach liquors or mine run waters. Furthermore, they reduce the inventory of the organic solvent and metal extractant substantially[15].

CHALLENGES/LIMITATIONS OF PI

Those are, firstly, the difficulty to introduce unproven intensified equipment that any malfunction will compromise the output of the whole plant, secondly, the full benefits are likely to be realized only when the whole plant is intensified. Consequently, a very wide range of PI technology must be

developed which covers the major reactor types and separation duties in order to ensure that PI is readily accepted. Most plant managers are understandably conservative and require full-scale evidence of successful operation before they are prepared to take any risk. A good opportunity for the adoption of the new technology is when a new plant is being considered and where there are significant space or weight problems associated with conventional technology as described[16].

Further, a developing technology such as PI is not embodied in standard design codes. A very effective technique for PI involves the use of laminar flow in narrow channels so as to improve both heat and mass transfer coefficients and consequently the transfer area available per unit equipment volume. Unfortunately, small passages are notoriously prone to blockage if the system is liable to deposit scale or contain solids having a size greater than about 20% of the channel width. In some cases, such as with crystal scale or carbon deposition, the improved heat and mass transfer associated with PI may alleviate the problem by reducing surface supersaturations or surface temperature. Nevertheless, in general, a severe fouling environment may seriously limit the intensification potential for a given unit operation.

About design of leaching reactors including autoclaves, the main problem of PI appears to be in monitoring the interface heat and mass transfer effects and reaction progress in a single step. The concept of separating dispersion space from reaction volume appears to be an encouraging trend in that direction. In this context, tube digesters/reactors deserve another look. Sonication appears to be a typical example to reduce the relatively long contact time (residence time) required for the solubilization of metals in the existing hydrometallurgical leaching operations.

ELMs need be sufficiently stable and hence to be adequately formulated. In spite the limitations from the extractants and the membrane, the SLMs still work well. Consider the extractant – these are generally commercial compounds that have been optimized for solvent extraction equipment with its requirements for good loading and adequate kinetics, with a two or three-minute mixing time. Reagents for liquid membranes require the reverse of these parameters of adequate loading and fast kinetics. Also, in solvent extraction to improve metal extraction the reagent concentration can be increased with little difficulty. However, in liquid membranes this is not so easy because as the reagent concentration in the diluent increases, the viscosity of the organic phase also increases, which slows down the rate of membrane diffusion. Thus, there is an optimum concentration where maximum flux occurs. It is difficult to meet the requirements of the optimum properties for supported liquid membranes, so perhaps the configuration of the flowing membrane where the organic phase flows across the feed side of the membrane is the best compromise[17].

CONCLUDING REMARKS

During atmospheric aqueous ammonia leaching of a lean grade copper oxide ore, it was shown that ultrasound not only enhanced the extraction rate but also improved the metal recovery. Other conditions remaining the same, intermittent use of ultrasound had a pronounced effect over the continuous use of ultrasound for extraction of copper. Safety management of autoclave system indicated the possibility of choosing appropriate materials of construction for hydrometallurgical application. A critical analysis of the novel phase contacting devices include process technologies for leaching of chalcopyrite and zinc sulfide concentrates; tube and jet reactor, and InLine Leach Reactor for enhancing gold recovery. The challenges/limitations of PI during leaching, solvent extraction and liquid membranes were also briefly discussed.

REFERENCES

1. K. Sarveswara Rao, "On promoting energy conservation in hydrometallurgical processing of complex materials", In: Stanley M. Howard (Ed.), Proc. "EPD Congress 2008, TMS (The Minerals, Metals & Materials Society), New Orleans, Louisiana, March 2008, ISBN 978-0-87339-715-5, pp.77-82.

2. K. Sarveswara Rao, K.L. Narayana, K.M. Swamy, J.S. Murty, "Influence of ultrasound in ammonia leaching of copper oxide ore", Metallurgical and Materials Transactions B 28B, pp.721-723, 1997.

3. B. Avvaru, S.B. Roy, Y. Ladola, S. Chowdhury, K.N. Hareendran, A.B. Pandit, "Sono-chemical leaching of uranium", Chemical Engineering and Processing, pp.2107-2113, 2008.

4. S.F. McGrath, L.C. Farrar, Journal of Metals, pp.34-37, 1998.

5. K. Sarveswara Rao, S. Acharya, "Trends in non-ferrous hydrometallurgy – Solutions and challenges" In: Young, C.A., Taylor, P.R., Anderson, C.G., Choi, Y., (Eds.), Proc. Hydrometallurgy 2008, Sixth International Symposium Honoring Robert S. Shoemaker, Society for Mining, Metallurgy, and Exploration, Inc. (SME), Phoenix, Arizona, August 2008 ISBN 978-0-87335-266-6, pp. 416-424.

6. K. Sarveswara Rao, Manual for safe operation and maintenance of laboratory autoclaves, Report No. T/HM/177/NOV./1996, Regional Research Laboratory, Bhubaneswar.

7. Kevin Brooks, "Sizing considerations for acid brick lining systems for large hydromet process vessels", In: Young, C.A., Taylor, P.R., Anderson, C.G., Choi, Y., (Eds.), Proc. Hydrometallurgy 2008, Sixth International Symposium Honoring Robert S. Shoemaker, Society for Mining, Metallurgy, and Exploration, Inc. (SME), Phoenix, Arizona, August 2008 ISBN 978-0-87335-266-6, pp. 1024-1028.

8. S. Ekman, A. Bergquist, "Suitable stainless steel grades for hydrometallurgical applications", In: Young, C.A., Taylor, P.R., Anderson, C.G., Choi, Y., (Eds.), Proc. Hydrometallurgy 2008, Sixth International Symposium Honoring Robert S. Shoemaker, Society for Mining, Metallurgy, and Exploration, Inc. (SME), Phoenix, Arizona, August 2008 ISBN 978-0-87335-266-6, pp. 1038-1047.

9. F. Crundwell, Minerals Engineering, 18, pp. 1315-1324, 1998.

10. T. Haakana, M. Lahtinen, H. Takala, M. Ruonala, I. Turunen, Chemical Engineering Science, 62 pp. 5648 –5654, 2007.

11. L. Lorenzen, A.W. Kleingeld, Minerals Engineering, 13, pp. 1107-1115, 2000.

12. R.J. Longley, A. McCallum, N. Katsikaros, Minerals Engineering, 16, pp. 411–419, 2003.

13. K.C. Sole, A.M. Feather, P.M. Cole, Hydrometallurgy 78, pp. 52-78, 2005.

14. E. Drioli, E. Curcio, E. J Chem Technol Biotechnol, 82, pp. 223-227, 2007.

15. B. Sengupta, R. Sengupta, N. Subrahmanyam, Hydrometallurgy, 84, pp. 43-53, 2006.

16. D. Reay, C. Ramshaw, A. Harvey, (2008) Process intensification: engineering for efficiency, sustainability and flexibility, Elsevier/Butterworth- Heinemann, Oxford, UK, Burlington (MA), USA, ISBN: 978-0-7506-8941-0, pp.37-38.

17. M. Aguilar, J.L. Cortina, (2008) Solvent extraction and liquid membranes: fundamentals and applications in new materials, CRC Press, © 2008 by Taylor & Francis Group, LLC, ISBN 978-0-8247-4015-3, pp. 16-17.